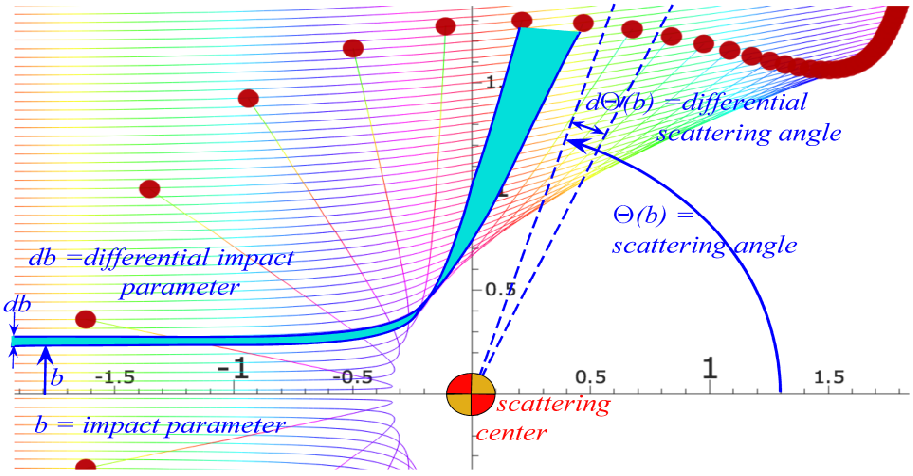

CLASSICAL MECHANICS

with a

BANG!..

A Geometric Introduction to Analysis of Classical Momentum, Energy, and Dynamics

W. G. Harter
University of Arkansas
Fayetteville

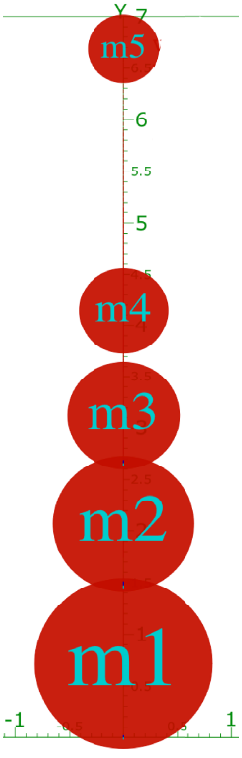

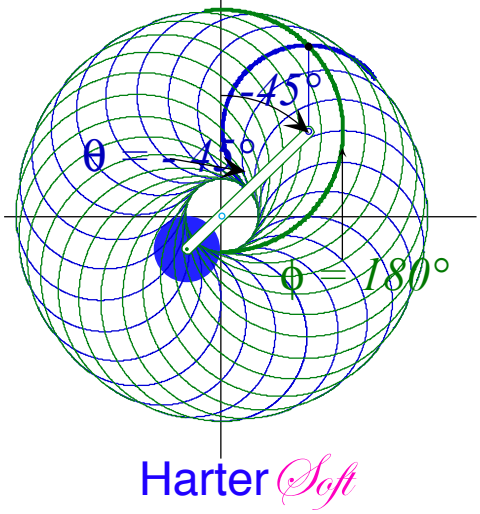

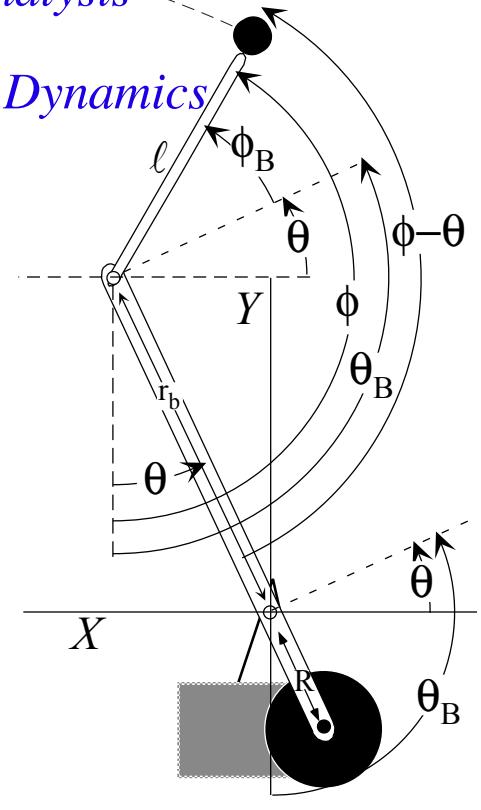

Harter Soft

Elegant Educational tools Since 2001

Physics 5103

Fall 2015

CLASSICAL MECHANICS with a BANG!.. ...(and a whimper)

Topics in Units 1-8

Unit 1. Review of velocity, momentum, energy, and fields

Introduction to geometry and algebra of mechanics fundamentals by plane geometry
Review of fields and their vector analysis by geometry and complex variables
Superball missile and neutron starlet dynamics. Coupled oscilllator and rotational motion.
Introduction to Hamiltonian, Estrangian, and Lagrangian contact mechanics of Action

Unit 2. Lagrangian and Hamiltionian mechanics

Generalized coordinate equations of motion. Pendulum and trebuchet motion
Sports kinematics vs. trebuchet dynamics. E&B Lagrangian and field orbits.

Unit 3. General Curvilinear Coordinate transformations

Riemann-Christoffel covariant tensor equations of motion and differential geometry
Effective potentials and geometry of constraints and Lagrange multipliers

Unit 4. Oscillation and waves

Lorentz resonance response and Fourier analysis
Normal modes and U(2) Euler angle geometry of pair resonance
Fourier and symmetry analysis of wave dispersion and parametric resonance

Unit 5. Orbits and scattering

Coulomb and central-force orbits and trajectory envelopes. Rutherford orbit geometry.
U(2) and R(4) geometry of oscillator and Coulomb dynamics
Rutherford, Stark, Zeeman, and 2-center orbits

Unit 6. Rigid and semi-rigid bodies

2-particle scattering.
Angular rotation and momentum of gyros, tops, spacecraft, and molecules
Euler-angle geometry and rotational energy surface analysis of soft rotors

Unit 7. Action and functional variation

Calculus of variation and Hamiltion-Jacobi equations
Geometry of contact transformations
Semiclassical action quantization by Davis-Heller phase color addition

Unit 8. Advanced Topics

Optical dispersion derivation of relativistic quantum mechanics
Chaotic motion. Optimal control theory

Introduction to text
Classical Mechanics with a BANG!

Preface: A back-to-the-future look at the classics

Before beginning a book on mechanics it should be noted that *classical* mechanics is out of date. For centuries, following work by Galileo and Newton, mechanics *was* physics. No *classical* descriptor was needed. Then along came the *quantum* revolution of the early 20^{th}-century. After that there arose the need to distinguish classical mechanics from quantum mechanics.

While classical mechanics may be out of date, it's not obsolete and never will be for things that go *Bang!* or *Click!* Our first examples, involving banging cars and balls, are easy *classical* problems but *very* difficult *quantum* problems. Detailed 21^{st}-century quantum mechanical solutions at even a Joule of energy would require impossible 10^{40} byte computers. Classical mechanics, on the other hand, permits solution by classical Greek computers, that is, a ruler and compass. Quantum mechanics may be more *fundamental* and *elementary* but it is not *easier* since it involves an astronomical increase in number of variables.

Our approach to classical mechanics combines Euclidian geometry and Newtonian calculus in ways that Newton did in his *Principia*. However, 21^{st}-century computer graphics are much better at exposing hidden power of geometry than Newton's tediously engraved 18^{th}-century figures. Old fashioned printing led authors to overlap multiple geometric steps into indecipherable spider-webs that obscured their logic. This in turn led to a modern impression that the logic of algebra and calculus *always* trumps that of geometry.

For example, consider the Bourbakian society that arose in 1930's in rebellion to Henri Poincare. (His work is used heavily throughout this book.) The Bourbakians were a group of French mathematical purists who practically forbade geometric figures. This led to a gulf in syntax and pedagogy for both mathematics and physics, an unfortunate one that this book tries to cross.

A distinguishing feature of this book is its use of geometry, both Euclidian and Riemannian. Two centuries of mechanics books include few if any that clearly apply analytic geometry to gain derivations, solutions, and most important, an *understanding* of mechanics. Some little-known lectures by Richard Feynman (*Six Easy Pieces (Persius 1997)*), and books by Vladimir Moser and Frank Crawford are among a few that begin to revive this ancient art.

We should note that many geometric constructions in this book were found using computer animations and simulations. This is another feature of this book and useful tool for any serious student of physics. Modern theory courses should have a computer graphics lab for comparing numerical experiments to real experiments with tools to show the geometry of both classical and quantum mechanics.

Most of physics is understood by analogies that expose underlying connections between seemingly disparate objects or phenomena. Mechanical analogies or analogs have been sources of understanding since the Hellenic period and are a large part of the development in this book. Analogies are often based on a shared mathematical description like a differential equation or symmetry algebra that reflects an underlying

shared geometry. It is such connections that we treasure and develop in this text. Most important are mechanical analogies that shed light on the relation of classical physics to modern physics. With this one gains a better understanding of both. The final Unit 8 contains a novel development of this.

Thumbnail sketches of Unit topics: Review-Preview Unit 1

A *geometric* approach to classical mechanics is used throughout. Geometry helps to clarify the calculus and physics of mechanics and show the symmetry principles behind classical theory that also underlie quantum theory. Unit 1 begins using Hellenic *plane geometry* of Thales (~600BC) and Euclid (~300BC) in Ch. 1-11 and introduces Teutonic *differential geometry* of Gauss and Riemann (1800-1900) in its final Ch. 12.

Between the Hellenic and Teutonic extremes lies *analytic geometry* of Galileo (1564-1642), Newton (1642-1727), and many others, that is the more familiar combination of geometry and algebra used throughout.

Ruler&compass constructions of collision mechanics and potentials start with 2-body collision (V_1, V_2) geometry of momentum lines and kinetic-energy ellipses . Ellipse secant-tangent-geometry elegantly clarifies axioms of classical mechanics (in Ch. 3 Unit 1 sketched↓below) and the role of momentum and energy.

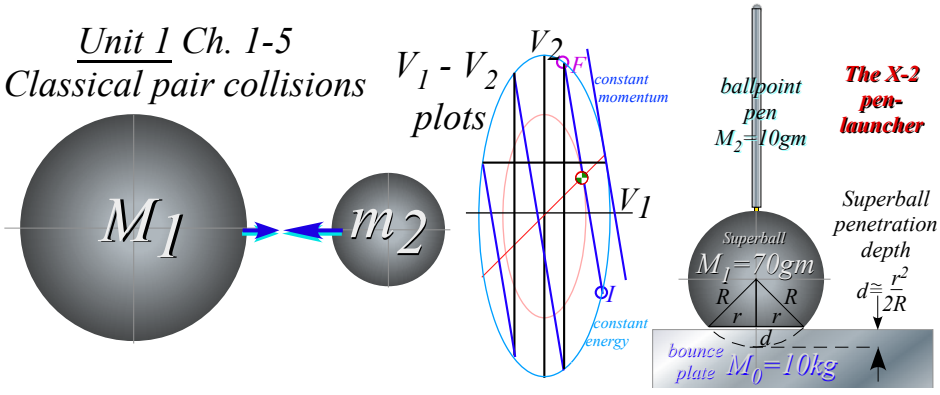

This is applied to a Superball pen-launcher from Ch. 4-5 of Unit 1 (above↑right: a spectacular and *real* experiment). Matrix operator geometry is introduced to solve multiple *n*-body collisions and related to supernovae dynamics, spinor-vector-tensor analyses, and potential theory applied in later Chapters 6-9.

Later in Ch. 12 of Unit 1, ellipse-tangent-line geometry is used to relate Lagrangian *L* to Hamiltonian *H* (sketched below↓left) and derive the Poincare action *Ldt=pdx-Hdt* (below↓right) for advanced mechanics.

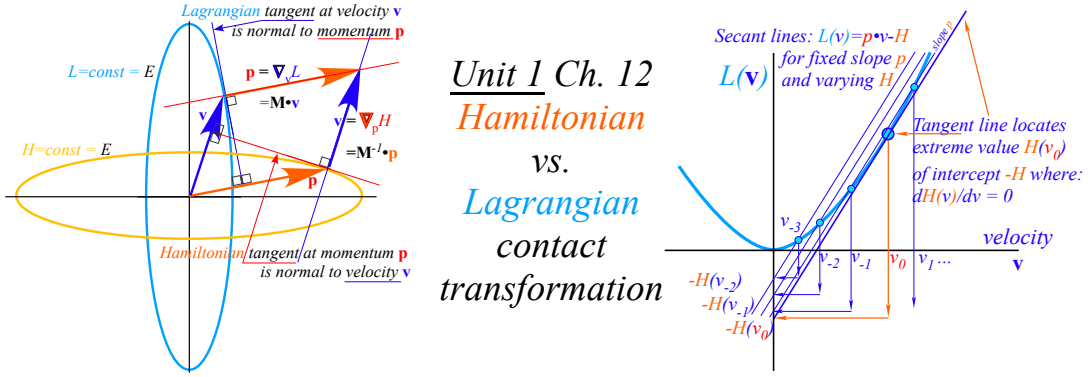

It is important to note that Unit 1 is both a geometric *re*view of undergraduate mechanics and a *pre*view of topics in Units 2 thru 8 that go on to graduate level applications. The geometry is so novel and powerful that one may jump outside the box and and derive advanced concepts in a fraction of the time they take without these graphical insights. For example, geometric oscillator and Coulomb potential models of Earth inside-and-out (sketched below from Ch. 9 of Unit 1) preview more detailed treatments in Unit 4-5.

Unit 1 Ch. 9 Sophomore physics Earth field model

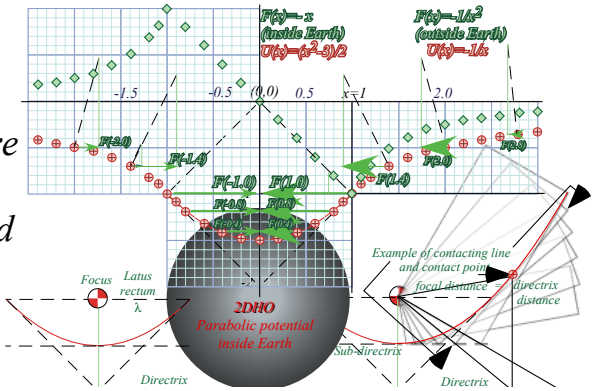

2-dimensional harmonic oscillator (2DHO) motion of "neutron-starlet" orbits inside Earth (sketched below from Ch. 9-11 of Unit 1) previews Unit 4 theory. It uses ellipse-tangent geometry (sketched below↓right).

Unit 1 Ch. 9 2DHO Orbits

Unit 1 Ch. 11 2DHO Orbit and tangent geometry

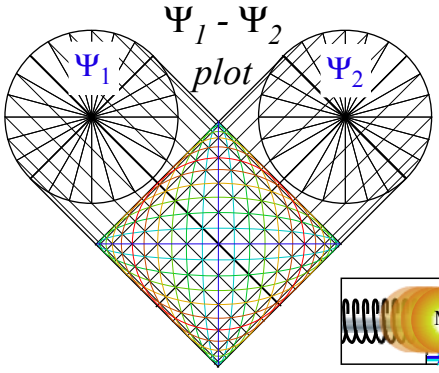

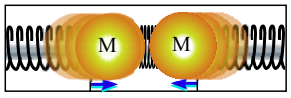

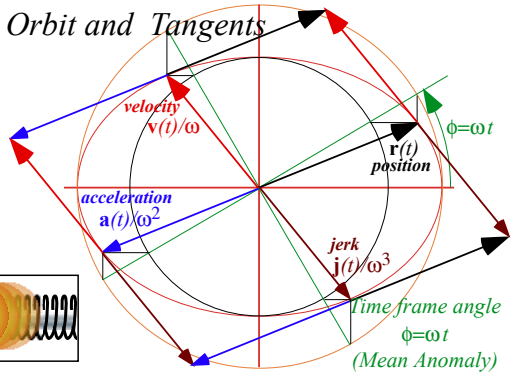

Identical masses coupled by identical springs (sketched above↑) are also 2DHO analogous to the inside-Earth orbiter. The 2DHO force fields provide classical analogs of quantum phenomena discussed Unit 4.

General 2-dimensional conservative-field vector calculus is done elegantly using complex variables $z=x+iy$ in Ch. 10 of Unit 1. Complex derivatives and integrals simplify field theory. Each function $f(z)$ such as z, $1/z$, z^2, $1/z^2$, $\sin z$, *etc*. defines a scalar-vector potential field, coordinate grid, mapping, and vector field. An example $f(z)=1/z^2$ from Ch. 10 (sketched below ↓) represents a 2D dipole field.

Unit 1 Ch.10 2D Dipole field and potential coordinate grid

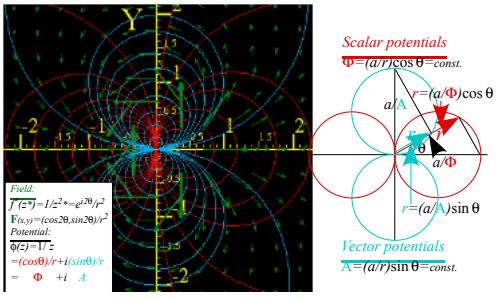

Thumbnail sketches of Unit topics: Advanced Mechanics Units 2 thru 8

One of the most important parts of advanced mechanics are its *Generalized-Curvilinear-Coordinate* (GCC) grids and their Jacobian transformation analysis, the main topics of Unit 2 and Unit 3. GCC theory has Unit 1 previews in Ch. 10 (sketched above↑) and in Ch. 12 that has a GCC grid made of a family of trajectories modeling the "*Volcanoes of Io*" or the "*Atomic Fountains of NIST*" (sketched below↓).

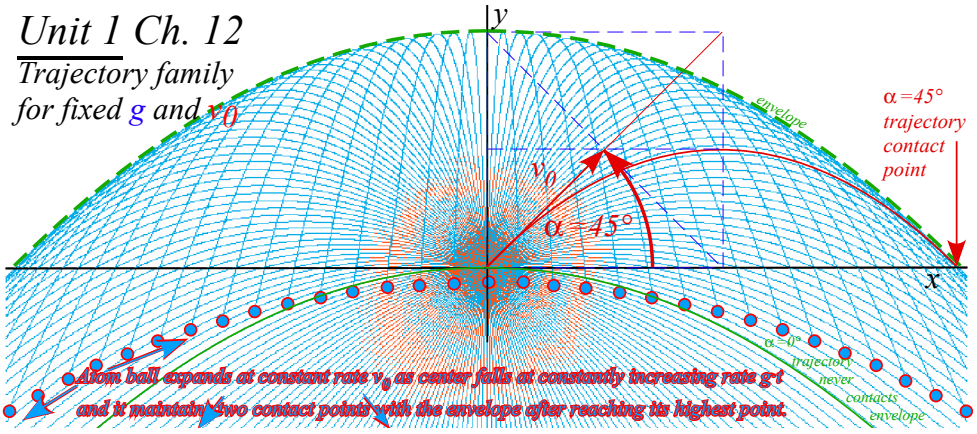

Unit 2 redevelops Lagrange and Hamilton mechanics using an ancient war machine called the *trebuchet* (sketched below ↓ left) as the object of study. The *trebuchet* or *ingenium*, used between 3000 BC and 1500 AD, duplicates human motions of throwing, reaping, chopping, and digging that built our culture. It also duplicates quite instructively motions used in modern sports of baseball, tennis, and golf and it is shown how one may improve one's swing in any such sport. (Also, it explains how to ring the bell at the fair! After all this, how could one *ever* claim that classical mechanics has become culturally irrelevant?)

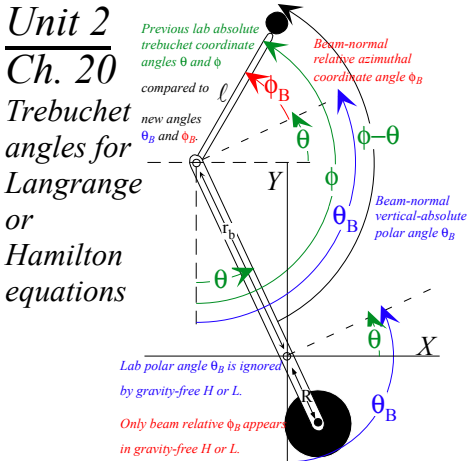

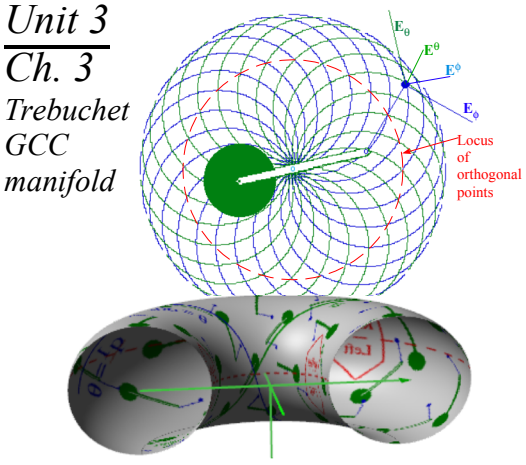

Unit 3 redoes Lagrange-Hamilton mechanics using GCC manifolds (sketched above ↑ right) with covariant tensor notation of Riemann-Christoffel differential geometry. This is used for relativistic mechanics and general relativity. The advantage of the Riemann equations for both numerical simulations and deeper understanding of "fictitious" forces and constraints is discussed.

Unit 4 begins oscillation and resonance with a forced damped harmonic oscillator and Lorentz-Green's functions (Lorentz geometry is sketched below↓left. It is similar to dipole geometry shown earlier.)

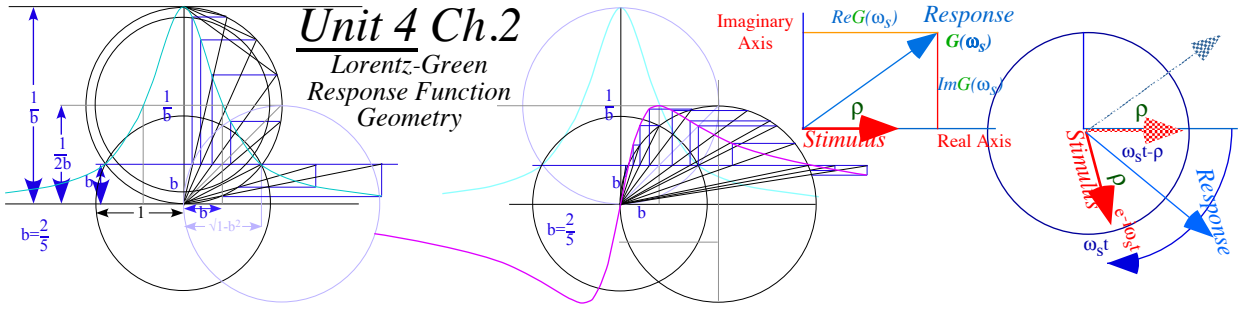

As in Unit 1, phasor clock geometry is used with complex algebra (sketched above↑right). Fourier wave mode analysis is done for discrete phasors (below↓left) and for continuum wave revivals (below↓right).

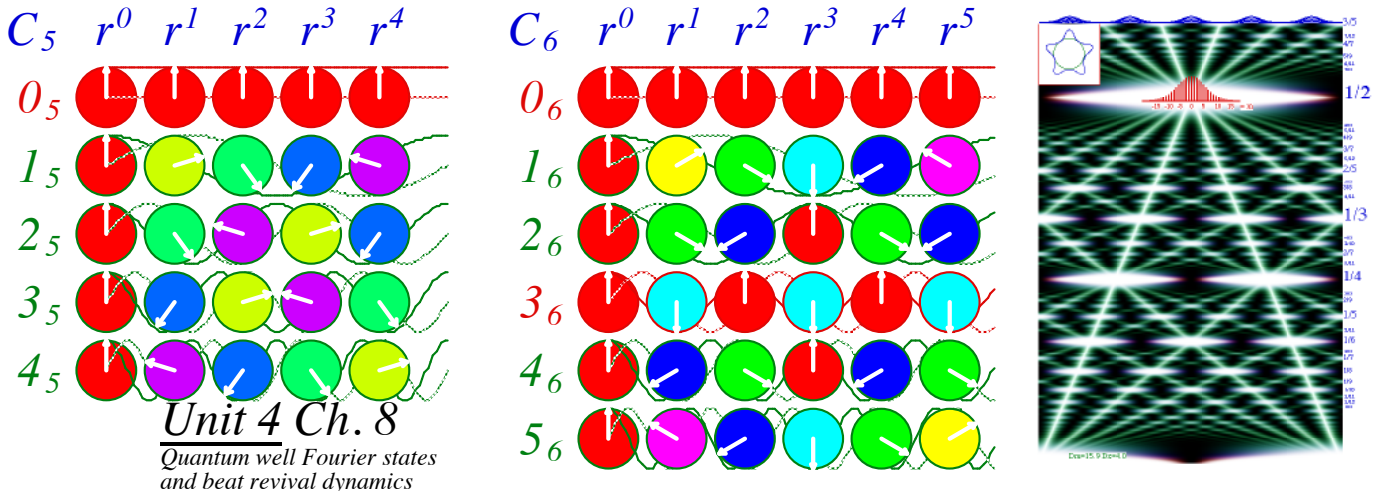

Two-dimensional harmonic oscillator (2DHO) motion is reintroduced in Unit 4 by merging calculus, U(2) algebra, and elliptic geometry. It is directly and precisely analogous to equations of motion for quantum mechanics, spectroscopy, and optical polarization, a powerful tool in modern physics and astrophysics based on Stokes 1867 real optical "spin" vector (below↓left) and its Poincare complex orbit space (below↓right).

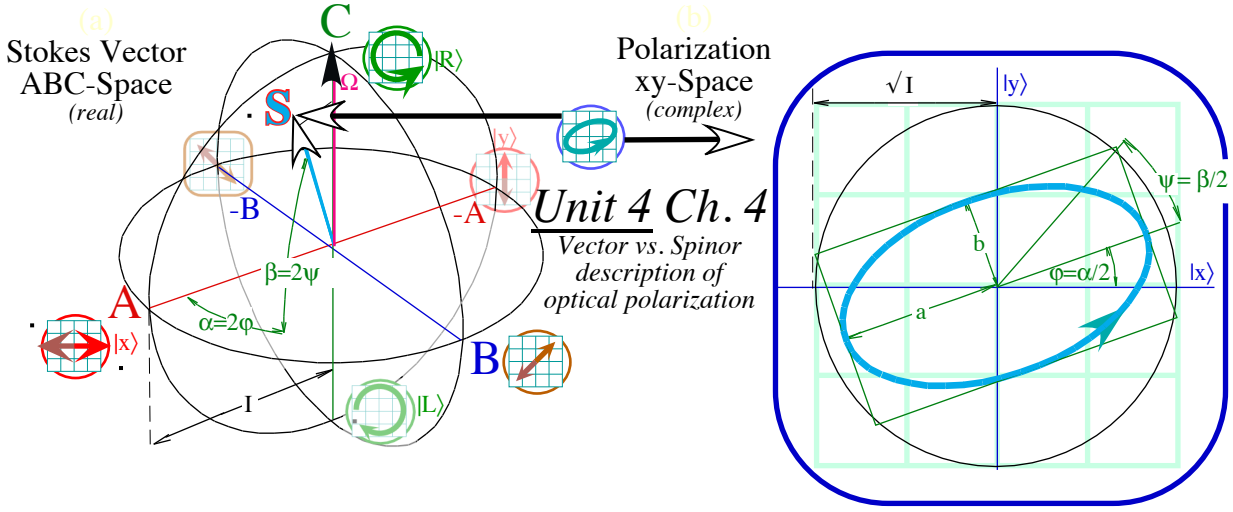

Unit 5 treats orbits in central fields including a continuation of Unit 4 geometry of 2D harmonic oscillation and Coulomb orbits. Here geometry is particularly powerful in analyzing whole families of orbits including geometry (sketched below↓left) of Rutherford scattering that showed atoms have nuclei.

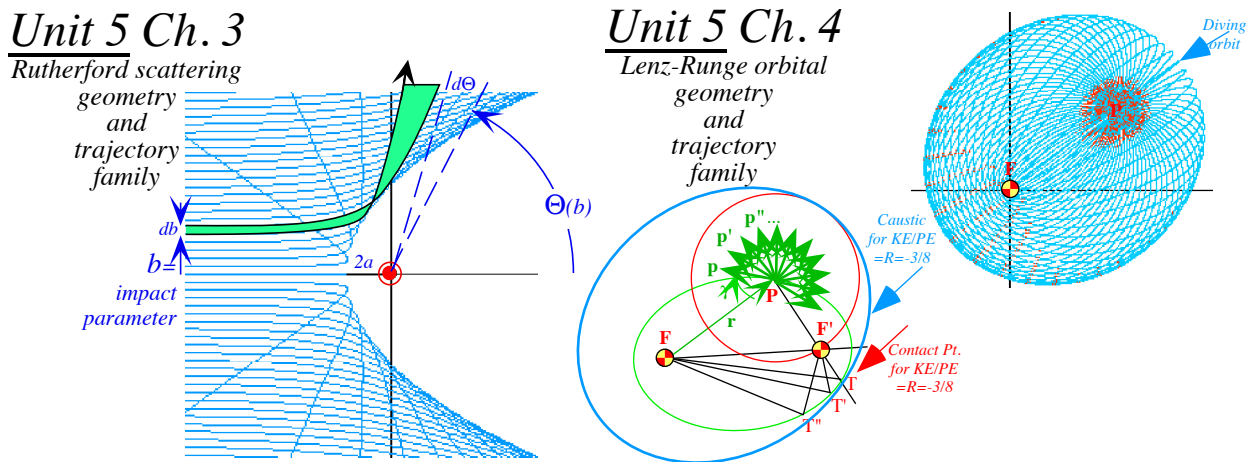

Ch. 12 orbits shown earlier generalize to constant energy Coulomb orbit geometry (sketched above↑right).

Unit 6 treats rotors and gyroscopic motion. The ellipse geometry of Unit 1 is again helpful and shows rotational mechanics from both Lagrangian and Hamiltonian viewpoints. A mechanical analog rotational computer (sketched below↓left) helps to visualize geometry and symmetry of Euler angle GCC.

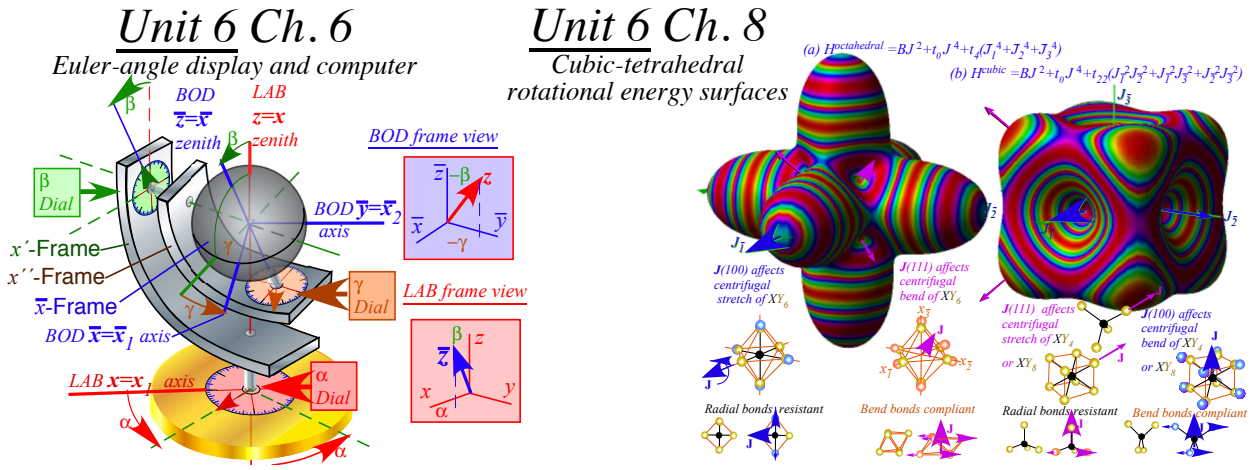

Rotational energy surfaces (above↑right) serve as a revealing phase space for non-rigid molecular rotors, common rigid rotors (below↓left) and very floppy systems like gyro-rotors (below↓right).

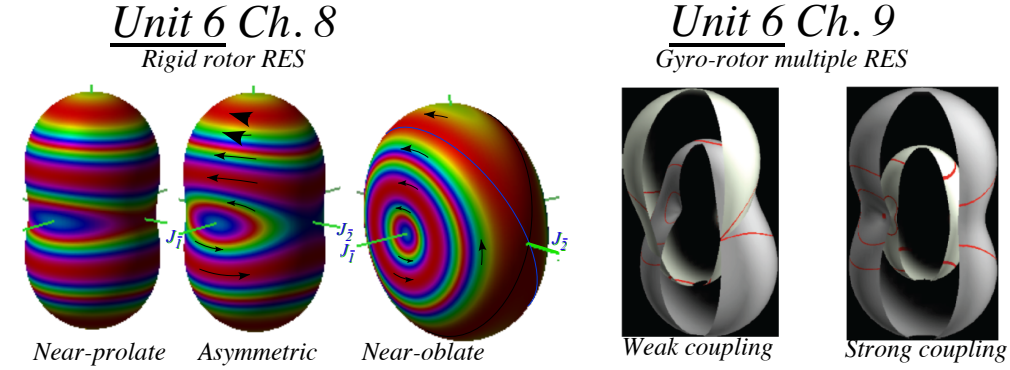

Unit 7 develops Poincare's invariant action introduced in Unit 1 into *Principal action*, *characteristic action*, and *Hamilton-Jacobi* equations. A numerical technique of coloring by action the 2DHO-trajectories of Unit 1 Ch.9 (below↓left) or "atomic-fountain" paths of Ch.12 (below↓right) gives quantum wave shapes.

Unit 7 Ch. 7
Color quantized 2DHO action

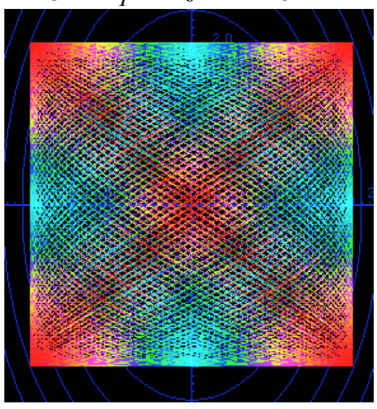

Unit 7 Ch. 7
Color quantized fountain

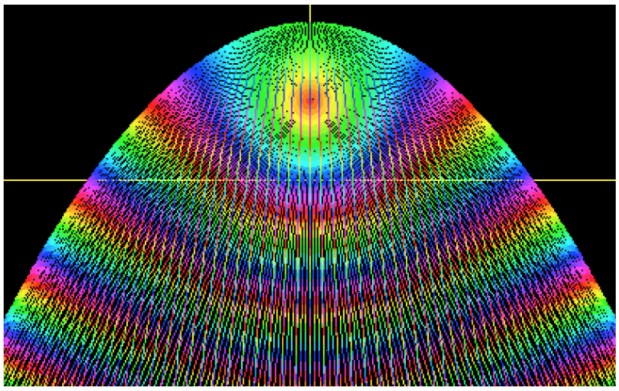

This technique is known as Davis-Heller classical chromodynamics. This colorful wave geometry provides new viewpoints. One example, a colorful way in Unit 8 to get special relativity (SR) and quantum mechanics (QM) from wave interference geometry, uses thought experiments involving colliding *Continuous Wave* (CW) laser beams (sketched below↓left). This derivation of SR and QM takes a few strokes with a ruler&compass to construct relativistic dispersion in per-space-time ((ω,k)-dispersion plot below↓right) and reduces advanced mechanics of Lagrange, Hamilton, and Poincare action to a wavelike child's play!

Unit 8 Ch. 1
laser continuous wave (CW) pair

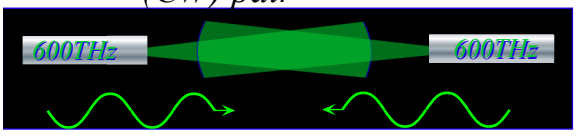

Unit 8 Ch. 3
$\vec{K} - \vec{K}$
dispersion plot

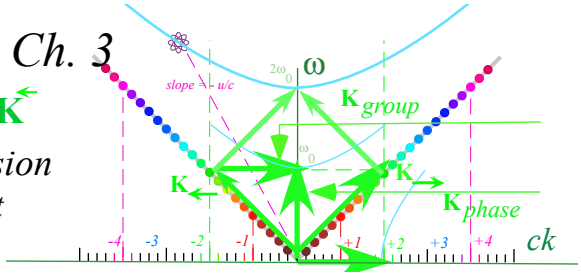

(The common acronym CW also stands for *Colored Wave*, *Coherent Wave*, and *Cosine Wave*, each representing important principles.) Both SR and QM are (1900-1905) theories about light waves, but it seems incredible that CW wave interference leads to such a simple reformulation with a theory of massive matter arising from simple properties of zero-mass or "light-matter" waves. But, there is that famous 1939 experiment by Carl Anderson *(1905-1991)* where γ-photon-pairs undergo electron-positron pair-creation!

e^+-e^- *pair-production*

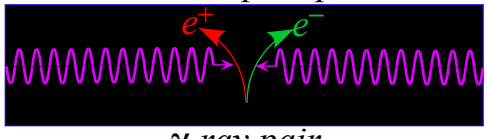

γ-ray pair

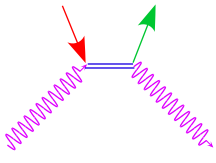

Unit 8 Ch. 7
Feynman graphs and dispersion plots

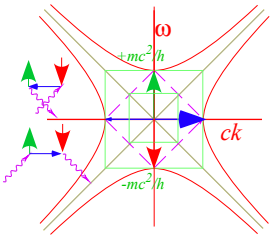

Feynman graphs (above↑right) for this incredible creation and related Compton effects appear in Unit 8.

The Unit 8 development uses a simple effect wherein a pair of counter-moving green CW beams make a space-time coordinate grid (below↓left) from real zeros (white lines) of the em-field.

Unit 8 Ch. 2 CW Rest frame vs. CW Lorentz Frame

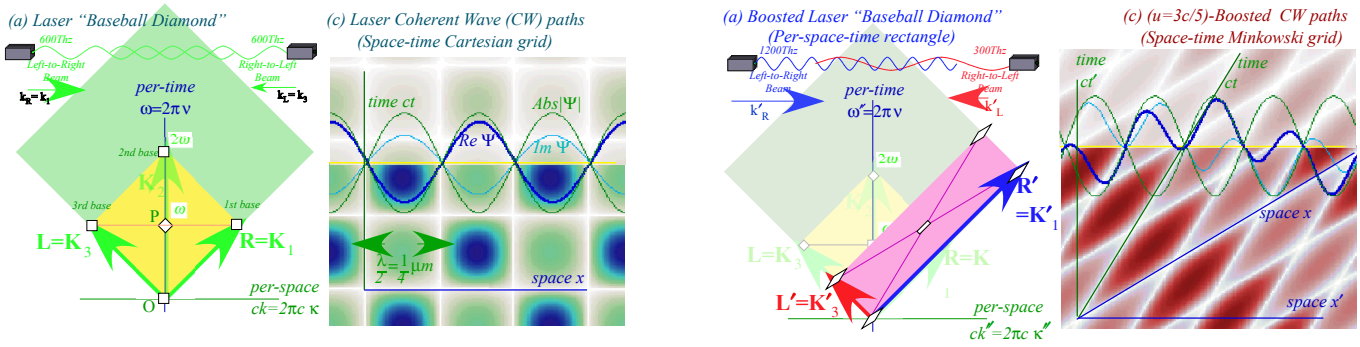

Moving atom sees ↑green CW beams Doppler shifted to (infra)↑red or(ultra)↑blue making Lorentz grid. A "baseball diamond" ↑ (above left) appears in per-space-time plot for rest frame. Space-time can also be mapped using pulse wave (PW) frequency comb structure shown below.

Unit 8 Ch. 2 PW Rest frame vs. PW Lorentz Frame

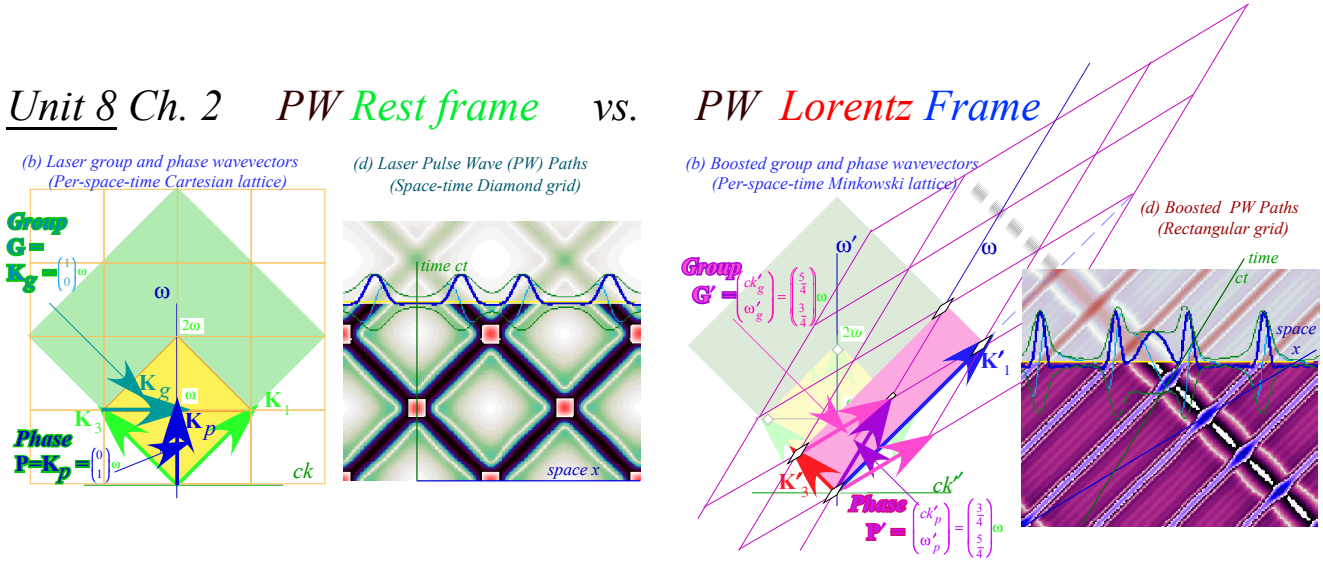

Cartesian square grids ↑ appear in per-space-time plot while "baseball diamonds" appear in space-time.

With wave-like intuition the science of mechanics begins to make more sense. The strange quantities given us by the classical masters such as momentum, energy, action, Lagrangian, Hamiltonian, force, and mass with all their rules of engagement can be reduced to simple relations of time and frequency (per-time) versus space and wave-vector (per-space) involving light waves constrained to travel at an invariant speed *c*.

That last "constraint" or axiom is a big deal! Much of the first part of Unit 8 is devoted to parsing the Einstein pulse wave (PW) axiom: *"All light flashes go c."* using Occam's Razor (See p. 16) to produce the Evenson laser wave (CW) axiom: *"All colors go c."* Ch. 1 of Unit 8 compares these axioms. (sketch below)

Unit 8 Ch. 1

Einstein PW Axiom

vs.

Evenson CW Axiom

(a) Einstein Pulse Wave (PW) Axiom: *PW speed seen by all observers is c*

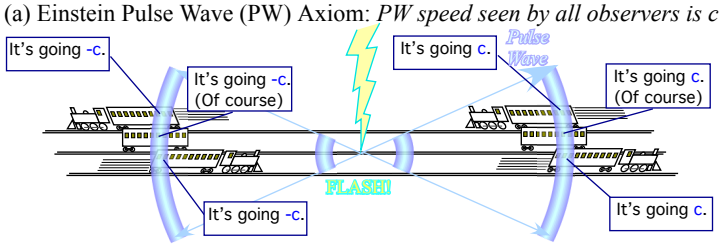

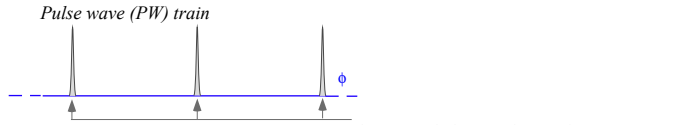

PW peaks precisely locate places where wave is.

CW zeros precisely locate places where wave is not.

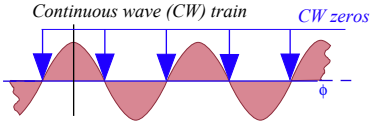

(b) Evenson Continuous Wave (CW) axiom: *CW speed for all colors is c*

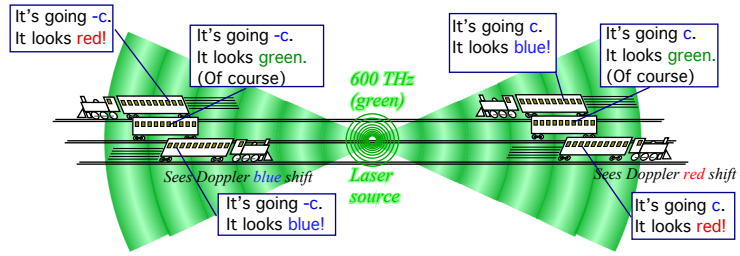

The simpler axiom gives a per-space-time geometry [*energy E=hυ(per-time) vs. momentum cp=hκ (per-space)*] (sketch below). So in summary: All of mechanics results from light whose colors march in lockstep.

Unit 8 Ch. 5

Energy-momentum (per-space-time) geometry

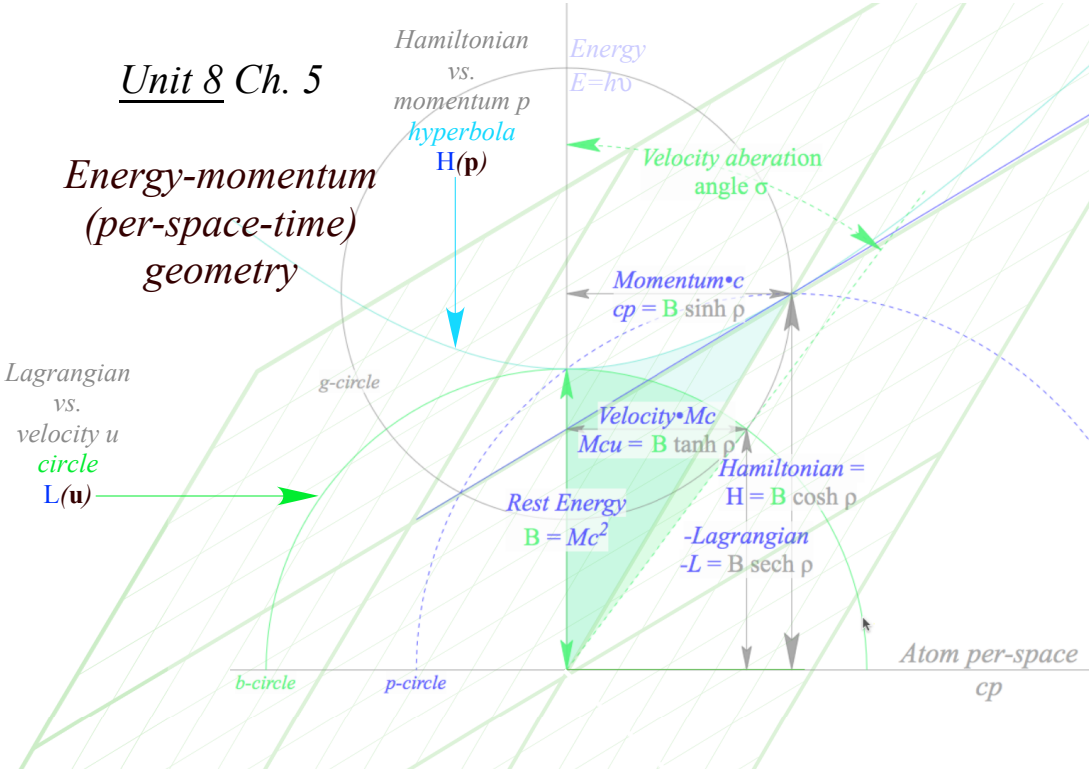

Mechanics begins and ends not so much with a Bang!, but with a whimper. (*after Robert Frost*)

The weapons of math instruction

When your physics fails (as in String theory) it could be you have lousy axioms. If so, it's back to the drawing board. That's how we start this course. It goes *wa-aaay* back to geometry of Thales *(600BCE)* and Euclid *(300BCE)*. You should always ask what tools have survived the test of time and check them out.

Toolbox 1: Euclidian plane geometry (Rule and compass)

Note that Toolbox 1 has a *rule* not the rul*er.* That's in Toolbox 2. A *rule* is just a *straightedge*, a ruler without its inch or *mm* scale. Euclid's pretty strict about this. Formal plane geometry is kind of a game to see how much you can do drawing lines and circles with just these tools. And a pencil…did I forget the *eraser*?

Toolbox 1 has limitations, at least by formal rules of Mr. Euclid. You may have heard that you can't trisect an angle as Mr. Euclid wants it done, formally and *exactly* in a *finite* number of steps. That won't stop us. We'll do that and other "illegal" moves *approximately* and in as few steps as possible using tools below.

Toolbox 2: Navigational geometry (Set 1+ protractor, ruler, divider, parallel rule)

These were the tools used by the Portuguese, Spanish, Dutch, French, and English navigators who were at least indirectly responsible for many of us living in the American continent. These tools were also used by weekend sailors until the Global Positioning System made obsolete all but six-packs of beer.

Toolbox 3: Analytic geometry (Set 2+ graph paper, algebra, calculus, calculator)

The idea is not to discard algebra and other such formalisms but to *understand* them better. So one of the first things we do with each geometric graph is figure it out using algebra. This is called *analytic geometry* and is one of the quickest ways to understand calculus and its application to physics. This leads to complex algebra and geometry that is very important to physics. As a crutch for the arithmetically and algebraically challenged we include scientific calculators. (Most of these have complex algebra capability.)

Toolbox 4: Computer geometry (Set 3+ high resolution graphics, C++ etc.)

This is the "open" class of geometric analysis, and anything goes. A modern scientist without graphics programming is at a disadvantage. Current languages of greatest general usage, speed, and power are C++ and *Objective C* used to write simulations *BounceIt*, *BandIt*, etc. for this book. High-level languages such as Maple™, Mathematica™ are fine, too. But, by being jacks-of-all-trades they can become masters-of-few.

Toolbox 5: You

This is challenging stuff. Doing it will seem hard sometimes. Rome was not built in a day and neither was any understanding of Nature. So this book depends most on how much *you* like thinking and *doing*.

Ignorance about science is not a burden you must accept. It is a challenge you should overcome.

The Weapons of Math Instruction

(a) Toolbox 1. Euclidian Geometry

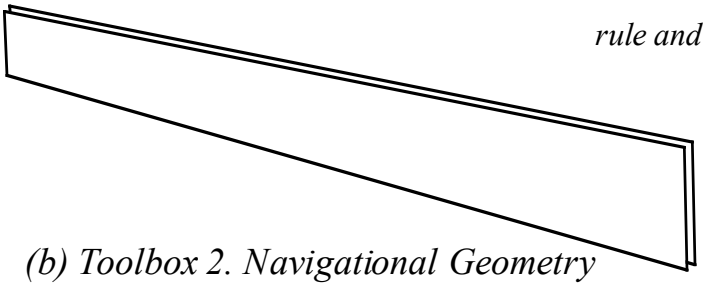

rule and compass

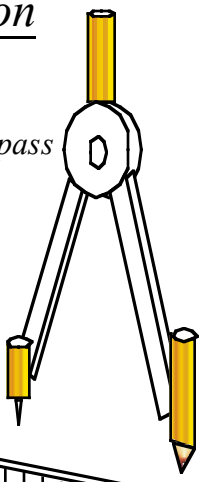

(b) Toolbox 2. Navigational Geometry

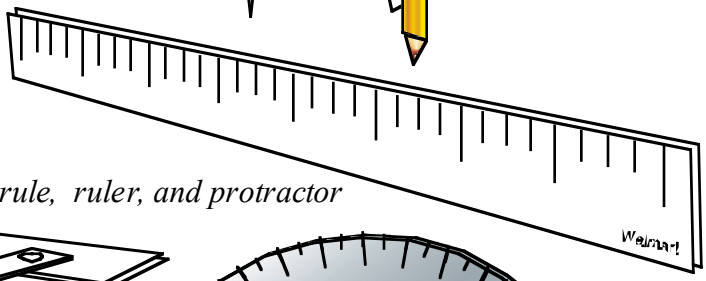

parallel rule, ruler, and protractor

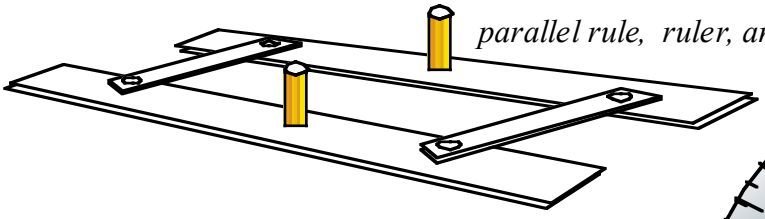

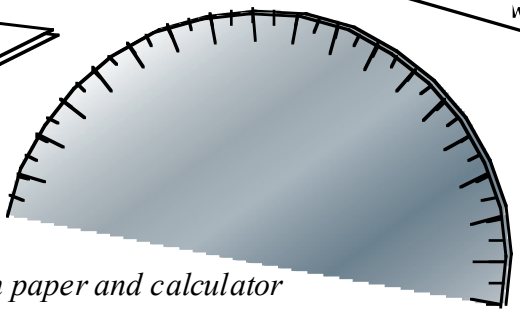

(c) Toolbox 3. Analytical geometry

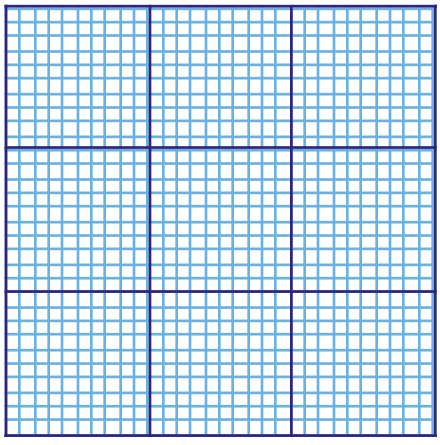

Graph paper and calculator

Complex algebra and calculus

$$1/z = r^{-1} e^{-i\theta}$$

$$\int 1/z \, dz = \ln z$$

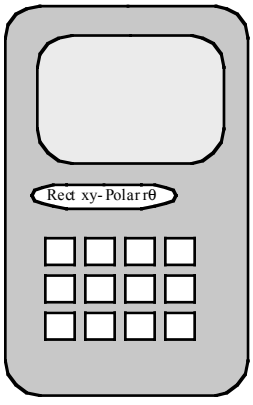

(d) Toolbox 4. Computer geometry...Anything goes!

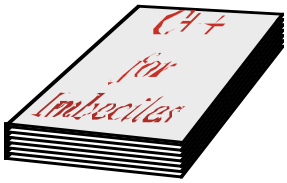

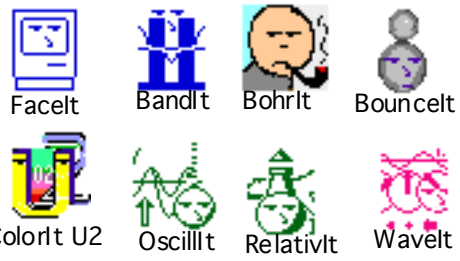

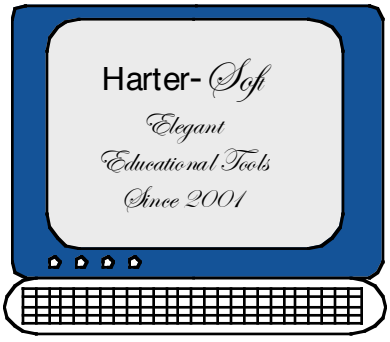

About the computer simulations: LearnIt and CodeIt

The first tier of computer programs used to make figures in this book and provide animated visualizations of physical phenomena or analogies thereof in this book is *LearnIt* series consisting of *BounceIt*, *OscillIt*, *QuantIt*, *WaveIt*, etc. listed in the table below. The idea was to make them like are analog computers that allow text figures to become dynamic thought experiments.

The suffix *"It"* attached to most of these programs is derived from the *FaceIt* interface invented by Dan Kampemier of *FaceWare* in Urbana, IL a worldwide programming project I joined in 1985 to 1993. A lot has changed since then! Now with T.C. Reimer begins re-application using *X-Code*, IOS, HTML5, *Mathematica*, and others. One needs a graphical user/programmer interface (GUI or GPI) that can be easily updated with new menus, dials, text editors, spreadsheets, OpenGL, 3D stereo windows, *etc*.

Academic application needs GPI to keep model, control, and view separate to avoid wasting time reinventing the wheel or debugging buttons in class. Teaching *useful* root-level object oriented programming along with physics is possible. Mixing serious academics with coding is coming of age.

GPI's facilitate a tree of programming projects for a given course. Such project trees make up a *CodeIt* system. Eventually, students can use one or more branches of *CodeIt* trees to build their own applications as homework or lab projects, leading to applications of sufficient complexity to aid in their thesis or dissertation research projects. Also, select *CodeIt* applications may be added to the *LearnIt*. Ideally, each *LearnIt* program has an accompanying expository text and/or on-line help hypertext.
Listed below are Units 1-8 with some *LearnIt* and *CodeIt* programs that apply to each.

Unit 1 Review of elementary mechanics of velocity, momentum, energy, and fields.
BounceIt , *AnalyIt*, and *BoxIt* with help from *CoulIt* and *ColorU(2)*.
Unit 2 Lagrange and Hamiltonian mechanics.
TrebuchIt and *BoxIt* with help from *Pendulum* and *Cyclotron*.
Unit 3 Coordinates and transformations.
CoordinIt and *AnalyIt* with help from *TrebuchIt*.
Unit 4 Oscillation and waves.
OscillIt , *WaveIt, ColorU(2), JerkIt*, and *BoxIt* with help from C_{nv}*MolVibes*.
Unit 5 Orbits and scattering.
CoulIt and *AnalyIt* with help from *CoulombOrbits*.
Unit 6 Rigid and semi-rigid bodies.
RotateIt (Others under development.)
Unit 7 Action , functional variation, and semi-classical mechanics.
ColorU(2) and *CoulIt*. (Others under development.)
Unit 8 Relativitic mechanics and advanced topics. https://www.uark.edu/ua/pirelli/php/title_page.php
or: https://www.uark.edu/ua/pirelli/php/pirelli_trail_map.php

The following are listings as of August 20, 2013 of web/browser based HTML5 applications that are built from the old Fortran, Pascal, C++ *FaceIt* applications for Classic Mac that are listed above. Most of these do not yet have all the features of the originals but are much finer in resolution.

Links to the current Harter-Soft LearnIt web apps for Physics

Bold links have default redirect pages. *Italics* are not yet meant for production.Red: the final stages of testing.

Production Links - *For the students & general public*

BohrIt - Production; URL is "http://www.uark.edu/ua/modphys/markup/BohrItWeb.html"
BounceIt - Production; URL is "http://www.uark.edu/ua/modphys/markup/BounceItWeb.html"
BoxIt - Production; URL is "http://www.uark.edu/ua/modphys/markup/BoxItWeb.html"
CoulIt - Production; URL is "http://www.uark.edu/ua/modphys/markup/CoulItWeb.html"
Cycloidulum - Production; URL is "http://www.uark.edu/ua/modphys/markup/CycloidulumWeb.html"
LearnIt - Production; URL is "**http://www.uark.edu/ua/modphys**" or "http://www.uark.edu/ua/modphys/markup/LearnItWeb.html"
JerkIt - Production; URL is "http://www.uark.edu/ua/modphys/markup/JerkItWeb.html"
MolVibes - Production; URL is "http://www.uark.edu/ua/modphys/markup/MolVibesWeb.html"
Pendulum - Production; URL is "http://www.uark.edu/ua/modphys/markup/PendulumWeb.html"
QuantIt - Production; URL is "http://www.uark.edu/ua/modphys/markup/QuantItWeb.html"
Relativity - Pirelli Entrant - Production; URL is "**http://www.uark.edu/ua/pirelli**" or "http://www.uark.edu/ua/pirelli/html/default.html"
Trebuchet Production; URL is "http://www.uark.edu/ua/modphys/markup/TrebuchetWeb.html"
WaveIt Production; URL is "http://www.uark.edu/ua/modphys/markup/WaveItWeb.html"

About Logic: Some philosophy and neurophysiology concerning axioms

This book is a *geometric* approach to classical mechanics. By geometry we mean both the Greek and German kind, that is, both the plane geometry of Euclid *(~300BC)* and the differential geometry of Gauss and Riemann *(1800-1900)*. We begin with ruler&compass constructions of collision mechanics and potentials. Geometry helps clarify the *logic* of calculus and physics of mechanics and show the symmetry principles behind classical theory that underlie quantum theory. Then we we'll do relativity and QM the same way.

From the earliest Euclidean geometry through modern mathematics and physics we encounter *axioms* at the very beginning of each development. These are *a priori* assumptions that underlie all subsequent logical development. Logic relies on an axiom set. We hope to produce maximum *truth*, that is, ideas that will longest survive the test of time and *experiment*. We need to choose the best axioms to do that. But, how?

To parse this let us consider two extremes each written by a friar (churchman) who sought truth during the *1300-1400* late medieval period when there was precious little. On one hand we have *William of Ockham (~1285-1349)* now known for *Occam's razor*. He wrote, *"Pluralitas non est ponenda sineneccesitate"* trans: *(Plurality should not be assumed without necessity)*. The other is Martin Luther who wrote the following in *The Lies of the Jew (1433)*. "*Die verfluchte hure, vernunft.*" trans: (*That damned whore, reason.*)

Martin was angry at Jews who refused to convert to his axiom set. He was also angry at Copernicus who was proposing a non-geocentric solar system that he thought contradicted his scriptural axiom set. *"The fool wants to turn the whole art of astronomy upside-down. However, as Holy Scripture(*Joshua 10:10-15*.) tells us, so did Joshua bid the sun to stand still and not the earth....."(Copernicus is)... "a fool who went against Holy Writ"*

So whose axiom set produced the most lasting truths?

Here we are comparing two parts of human neurophysiological anatomy, the cerebral cortex *(CC)* and the lower limbic lobes *(LLL)* that include what we call *reptilian* "lizard-brain" and *mammalian* " rat-brain" lobes. For most of history, humans are totally *LLL*-dependent. It's our evolutionary residual unconscious operating system (Human DOS 1.0). *LLL* "boots-up from the box" while *CC* requires difficult education.

Humans attempts to develop the *CC* are so sporadic at first it is impossible to label its emergence. Traditionally one points to the *Seven Liberal Arts* as our break with pre-medieval superstition. The seven consisted of the *Trivium*: (*Grammar*, *Logic*, and *Rhetoric*), and the *Quadrivium*: (*Arithmetic*, *Geometry*, *Astronomy*, and *Music*). The term *Liberal* is interchangeable with *Liberating* and probably was used to designate a pathway to avoid slavery. It appears that the *Trivium* contains *drivers* of the creative results in the *Quadrivium*. Indeed the latter has grown to more like *Seven Thousand* Liberal Arts *and Sciences* in just a few centuries. It's an explosion! You'll have to excuse physics and chemistry for not making the first cut. Those alchemists were busy distilling gold from horse urine. (Nice try, but a little too stinky for polite liberal company.)

Occam was a *CC* user who studied all the ancient texts he could find. (A lot got burned when Bishop Cyril (later a saint) ordered Coptic Christians to destroy the Alexandrian Libraries and brutally murder the famous lady mathematician Hypatia in 415AD. (This is mentioned in Edward Gibbon's "The Decline and Fall of the Roman Empire." Less reliable accounts say Caesar accidentally destroyed the library in 48 BCE.)

Luther, on the other hand, was more anti-scholarly, at least with regard to Copernicus. His *LLL* attitude was less *Seven Liberal Arts* and more *Seven Deadly Sins*. These may also be divided into a *Trivium* and a *Quadrivium*, however now the latter (*Greed*, *Envy*, *Lust*, and *Gluttony*) are drivers of the former (*Pride*, *Wrath*, and *Sloth*), that is, *Pride* or *"Gloating"* if your *Greed*, *Envy*,..etc. yields success, or else *Wrath* or *"Rage"* if you are unsuccessful, followed by *Sloth* or *"Depression."* These are just drives and responses of *LLL* acquisition processes involving short-term ebb and flow of our small 3-to-5-ring molecules called *neurotransmitters*.

So how creative is the *LLL* approach of Luther with its enormously complex and rigidly cumbersome axiom set? Can *LLL*'s claim thousands of new sins? Well, perhaps we can credit modern *LLL* users (known as the *rabid right*) with two new sins, namely *Torture* and *Terror* that were recently declared quite legal.

However, these two are hardly new. The ancient churches have had them all along. They just did not classify them as sins *per se*, but rather as *"parishioner management."*

In conclusion, let me argue in favor of the Occam Razor approach to logical quests and paraphrase it with the common suggestions *"Keep it simple and make it powerful!"* or *"Assume the least, prove the most."* Occam's razor is supposed find ways to cut down any axiom set or *sine qua non* (without which there is nothing). It is amazing that such a "cutting" idea actually works! Perhaps, by reducing logical clutter, we hack away unknowns and clear the way for new stuff. But, there is more to it than that.

Thought driven by *a desire to undermine its own premises* leads to a thought path that grows geometrically as the *CC* harnesses the *LLL*. It's *mind* over *matter*! An exponential explosion of mathematics, science, and technology results. The *CC*'s "faith" in its axioms *must* be a temporary one. All logical laws are made to be eventually broken. (Including, presumably *this* one. Maybe, there *is* a TOE!)

Of course, Occam's idea was *heresy* and he was nearly *"fired."* as were Copernicus, Galileo, Bruno, and most other *CC* pioneers following such thought progressions. (Bruno had to go to a *1600* church barbecue where he was the charcoal.) Hacking sacred Churchly axioms or *mythos* is always trouble. Occam's idea is to always, *"Hack the axioms to save man."* The Church says, *"Hack the man to save axioms."* I'll vote for Occam!

I hope these words (and equations combined with geometry) will serve you creatively.

William G. Harter

Fayetteville, Arkansas

August 2012

Unit 1 Classical Velocity, Momentum, Energy and Fields

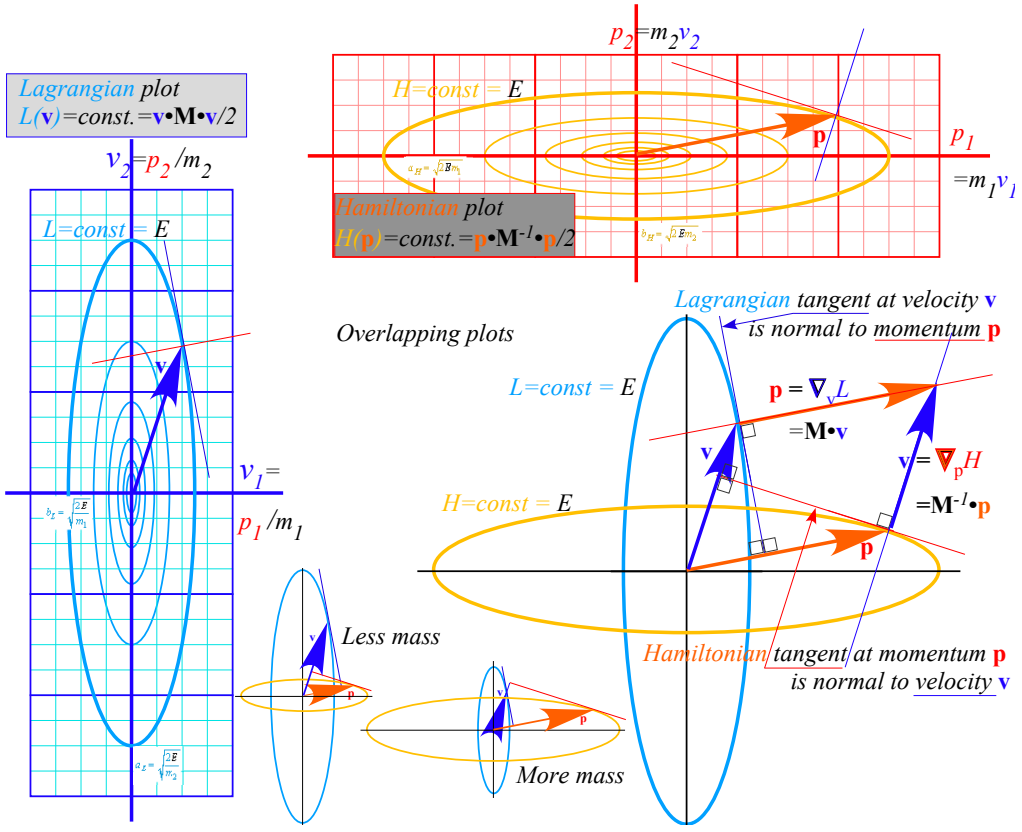

W. G. Harter

Basic ideas of classical velocity, momentum, and kinetic energy (KE) are reviewed and previewed using geometry and super-ball collision experiments involving two different masses. The idea of potential energy (PE) and force is introduced by defining PE as the KE of “idler” balls that provide force fields for others. The two most famous PE functions, those of Coulomb and of a harmonic oscillator or linear (Hooke-Law) force are introduced. Elliptic orbit geometry in the latter serves to introduce quadratic forms and rotational Coriolis-centrifugal forces. This helps introduce more advanced ideas of Lagrange, Hamilton, and Poincare and generalized curvilinear coordinates for classical mechanics. A review of complex analysis of functions and fields shows how 2D vector calculus may be done with elementary calculus and applied to conformal potential field coordinates sets for use in later Units.

-Unit 1 - Review of Velocity, Momentum, Energy, and Fields

Perhaps the most common fundamental physics experiment is to collide particles against each other. That's *all* they do at LHC (Large Hadron Collider) where protons are rammed head-on at speeds above *0.999999c* at several *TeV* (*Trillion* or *Tera*-electron Volts). Electron microscopes and laser spectral experiments are just particle crashes, too, involving molecules, atoms, electrons, and photons at intermediate energies ranging from *keV* (*Thousand* or *kilo-eV*) to about *1eV* for one green light photon down to ultra-low energies measured in *neV* (*Billionths* or *nano-eV*) for collisions in BEC experiments. To study momentum and energy we make classical analogies to common (Let's hope not for us!) freeway car crashes.

Chapter 1. Collision velocity change and slope geometry

Ka-runch! A 4-ton SUV going *60mph* rear-ends a 1-ton VW going *10mph*. See Fig. 1.1a. The SUV driver was busy texting a cell-phone and not watching the road. Both vehicles abruptly change speeds as seen in Fig. 1.1b-c. In order to calculate the speed changes we need to decide whether our collision is a *"ka-runch!"* where the cars get welded into a single mass as in the top right of Fig. 1.1(c) or a *"ka-bong!"* where they bounce off with no damage (very unlikely) as in center Fig. 1.1b or else quite likely intermediate *"ka-whump!"* collisions to be detailed later on. The technical term for *ka-runch* is a *totally inelastic collision*. We'll study it first followed by *ka-bong*, or technically a *perfectly elastic collision,* and finally the generic range of *ka-whumps* or *inelastic collisions* that lie between the first two ideals or extremes.

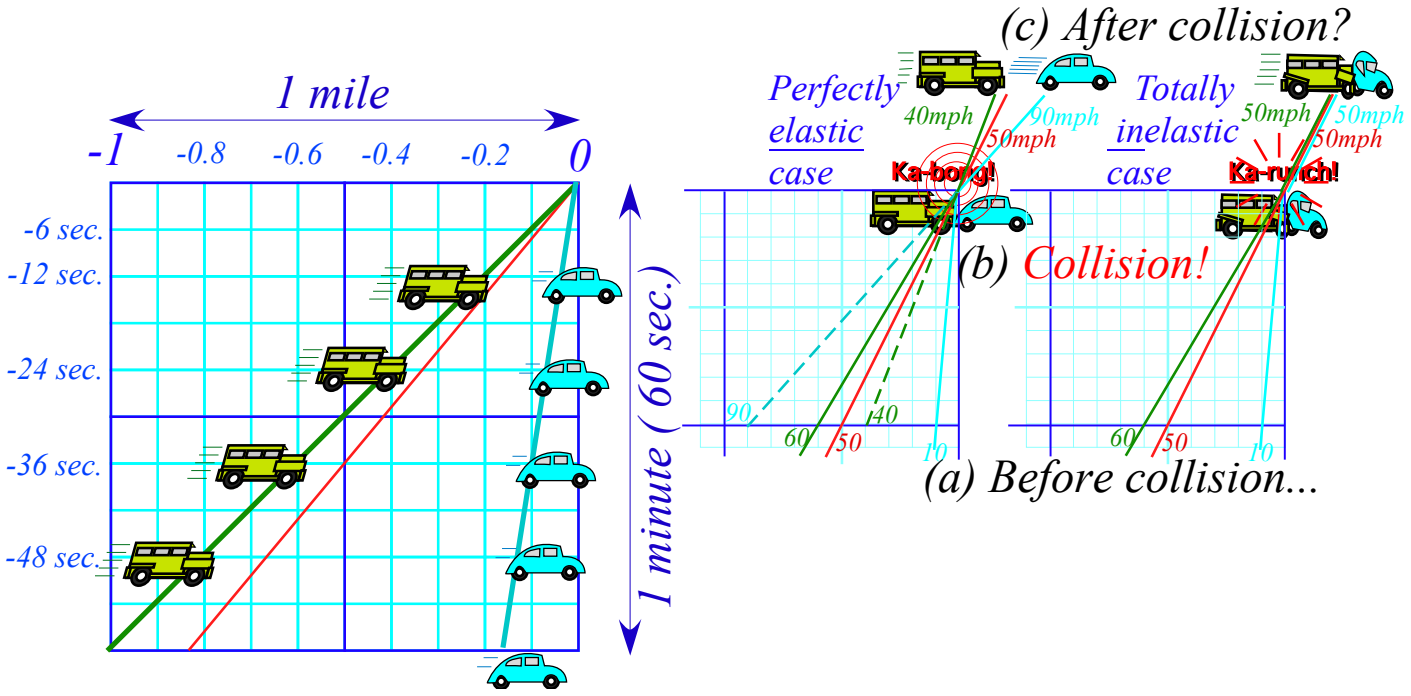

Fig. 1.1 Time vs. space graphs of (a) SUV (going 60mph) and VW (going10mph), (b) collision, and (c) possible outcomes of two extreme cases: the inelastic "ka-runch!" and perfectly elastic "ka-bong!"

This text uses of geometry to get quicker results and expose logic. First, let's review some conventions regarding slope on graphs. Our first graph (Fig. 1.1 or Fig. 1.2a below) is a *time vs. distance plot* and speed is *slope-from-vertical* as favored in relativity theory and by Einstein's math teacher, Herman Minkowski. In contrast, Newtonian calculus favors *distance vs. time plots* like Fig. 1.2b and speed is *slope-from-horizontal*. Both our plots are scaled so a 1:1 ratio *(45°slope=1/1)* represents *60 mph = 1 mile/min.* in Fig. 1.2a or *1 min./mile* in Fig. 1.2b. Plot (a) *compliments* (b). One becomes the other by doing a mirror-reflection across the 45° diagonal (1:1)-"SUV-line" that is the same in (a) and (b). Plot (a) is best for car motion since cars go horizontally. For (b) one might ask, "Do cars climb walls?!" (See review of slope.)

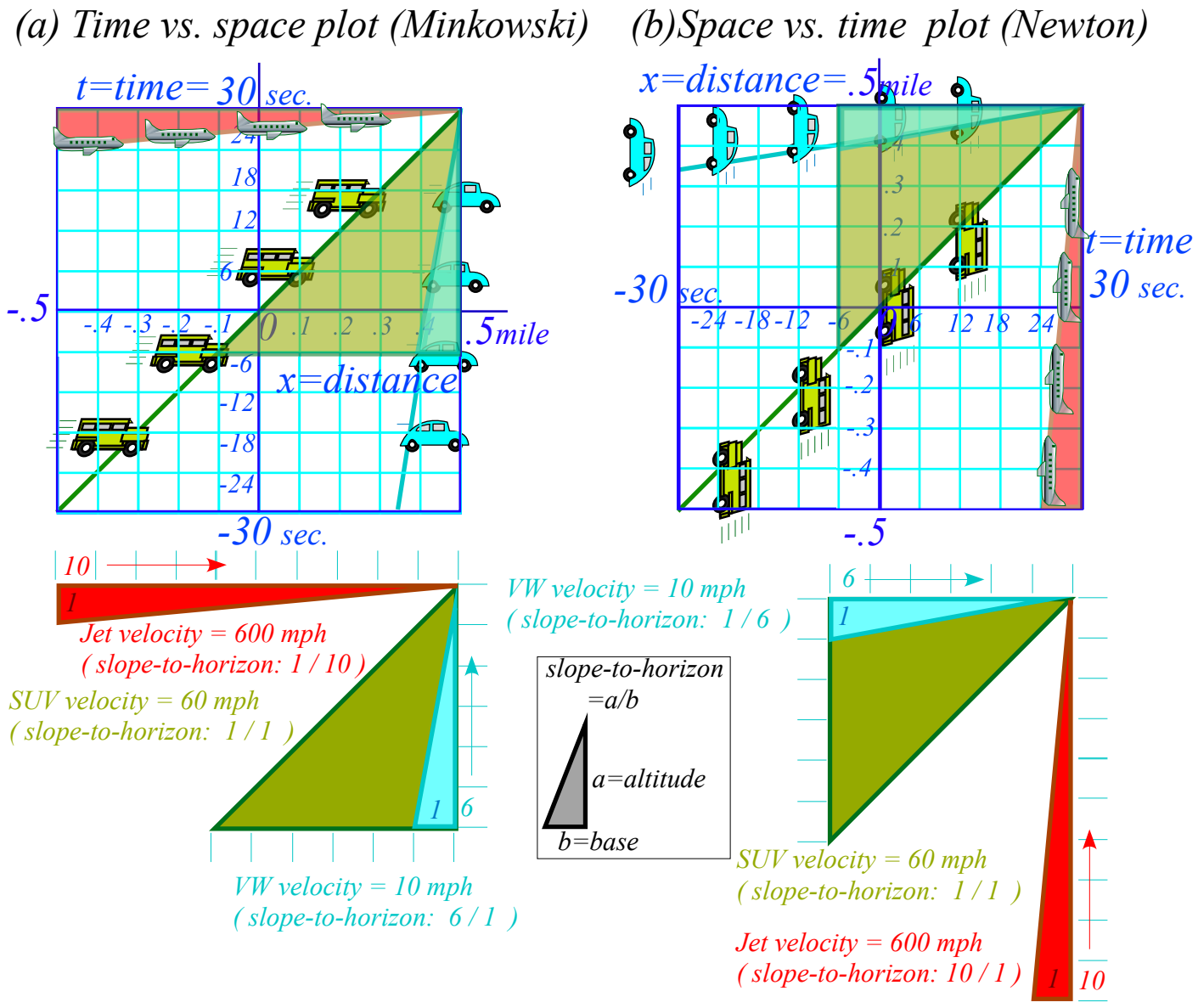

Fig. 1.2 Complimentary plots (a) Minkowski time vs. space plots vs. (b) Newton's space vs. time plots.

Before proceeding with car-crash analysis, it is required we give full disclosure of an important part of physics that concerns its idealization and model building.

Idealization and model building

Landscape 1.1 below applies explicitly to this Unit 1 but implicitly to this entire text and to all other physics texts. Scientific theory always requires an idealized model in which to develop its axioms and logic for its qualitative and quantitative *thought (Gadaken) experiments*. It's an ancient tradition for physics.

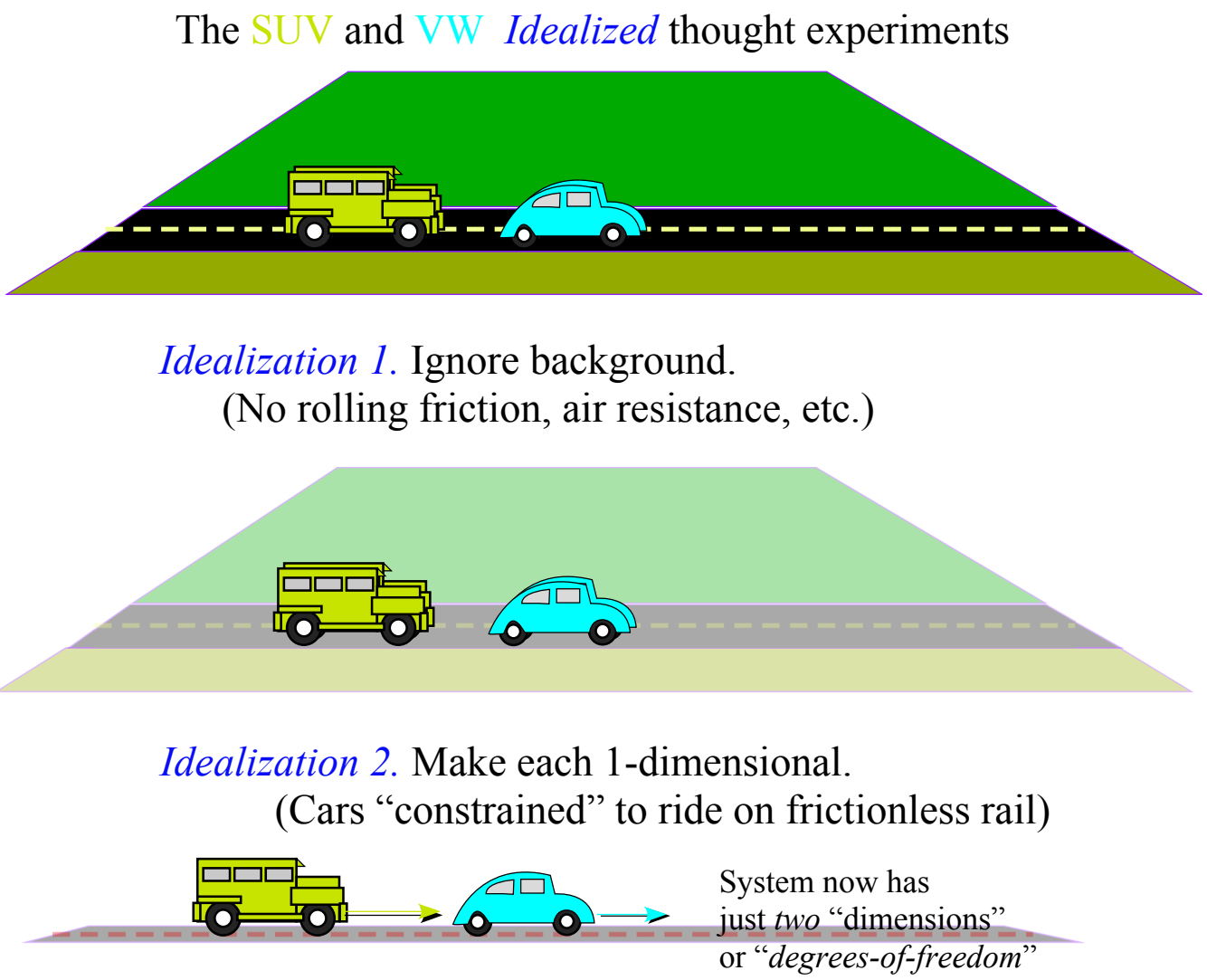

Landscape 1.1 Idealized model for collision model and thought experiments

Here is where we play "Let's pretend." We ignore most of the reality of the open road, most notably friction of the road surface-tire interface and air resistance. Also, we restrict the number of independent variables or *dimensions*. They are also called *degrees of freedom*. Here there is only one dimension for each car or two dimensions in all. It is as though we have re-framed the car crash as a perfect air-track with two bumper-cars floating on it. Models like this one are meant to be expanded. The next Landscape 1.2 begins this process by listing the most important classical degrees of freedoms for AMO physics.

Summary of Classical Mechanical Degrees of Freedom

Translation (Each body has 3 translational degrees of freedom) (Intoduced in Units 1 and 2)

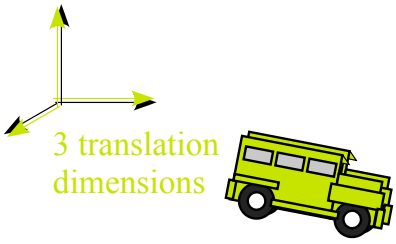

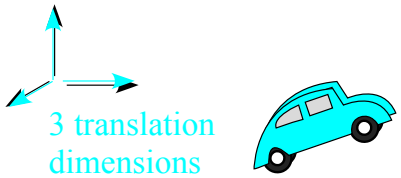

6 translational degrees of freedom for SUV and VW.

Rotation (Each body has 3 rotationaldegrees of freedom) (Intoduced in Units 3 and 7)

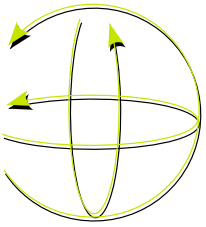

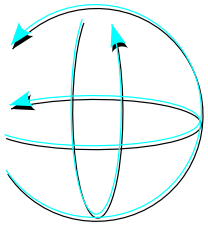

6 rotational degrees of freedom for SUV and VW.

SUV and VW system involves
12 rigid-body degrees of freedom

Vibration (Each body has many vibrational degrees of freedom) (Intoduced in Units 3-8)

An N-atom molecule has 3N-6 vibrational degrees of freedom

Landscape 1.2 Some idealized classical model degrees of freedom

Models of molecules, atoms, and even nuclei begin with classical models having 3 translational, 3 rotational, and *N* vibrational degrees of freedom for every nucleon or nucleus and every electron in them.

Classical translation-rotation-vibration degrees of freedom may be expressed in coordinates that are more convenient than the Cartesian coordinates (CC). These are known as *Generalized Curvilinear Coordinates (GCC)* and are essential in general relativity theory. A simple example, polar coordinates, are used to introduce GCC in Chapter 12. Other examples of Orthogonal Curvilinear COordinates (OCC) are derived in Chapter 10 in connection with complex field coordinates.

In quantum mechanics, we find for each classical degree of freedom an *infinite* number (∞) of degrees of freedom. In fact, it's two infinities (2∞) for each since they are complex dimensions.

Now if you know everything about slope, you may proceed to Ch. 2 for more news on the car crash. But, there are some tricky and subtle things in this *Review of slope...* section that follows. These could bite you later! So it is definitely recommended reading. See if you can do exercises without peeking at answers.

Review of slope geometry, sin, sec, tan and complimentary trig functions

Slope is defined as the ratio $\Delta y/\Delta x$ of vertical altitude Δy per horizontal base Δx. This equals velocity $v=\Delta x/\Delta t$ for a horizontal time-*t*-axis and vertical space-*x*-axis like Fig. 1.2b. So horizontal *x*-axis and vertical time-*t*-axis of Fig. 1.2a has $slope=\Delta t/\Delta x=1/v$ inverse to Fig. 1.2b slope. The lowest $slope=1/10$ in Fig. 1.2a belongs to jet velocity $v=600mph$ that is the highest $slope=10/1$ in Fig. 1.2b, and a low VW velocity of $v=10mph$ has a steep triangle of $slope=6/1$ in Fig. 1.2a but in Fig. 1.2b that VW line is a low $slope=1/6$.

Each unit graph square in Fig. 1.2a has a *horizontal scale factor* of $s_x=0.1mile$(per square) and a *vertical scale factor* of $s_y=6sec.$(per square) and *vice versa* for Fig. 1.2b. If you multiply scale s_x by factor f_x and s_y by f_y then each graph slope $\frac{\Delta y}{\Delta x}=(n_y \text{ vert. squares})/(n_x \text{ horiz. squares})$ changes to $(f_x/f_y)\frac{\Delta y}{\Delta x}$.

We do rescaling of dimensions to change units. For example, changing miles to feet in Fig. 1.2a uses factor $f_x=5{,}280\,ft.\,per\,mile$ (or) and changing minutes to seconds uses $f_y=60$. The scale ratio (f_x/f_y) is 88, that is, 60*mph* equals 88 . SUV slope of *1* in Fig. 1.2b is *88* in a *ft. vs. sec.* plot. That's too high to plot 60*mph* accurately but a *ft. vs. sec.* or *ft. vs. min.* plot will be more appropriate for parking lot speeds.

Slope angles, ratios, and areas

Most of us learn to measure slope by *degrees(°)* of a *slope angle* σ. Greek "s" or *sigma* σ stands for sector slope. (We also use *theta* (θ) or *phi* (ϕ).) But, degrees are an *arbitrary* choice of 180° per (1/2)-turn or 360° per full turn. A better unit is $1\ radian=180/\pi\sim57.3°$. A $\sigma=1radian$-sector on unit circle ($r=1$) (Fig. 1.3a) has *unit arc-length* ($\ell=\sigma\cdot r=1$) and *unit sector area* ($A=\sigma\cdot r^2=1$) based on $\pi=3.14159...$(pi), *not* an arbitrary number.

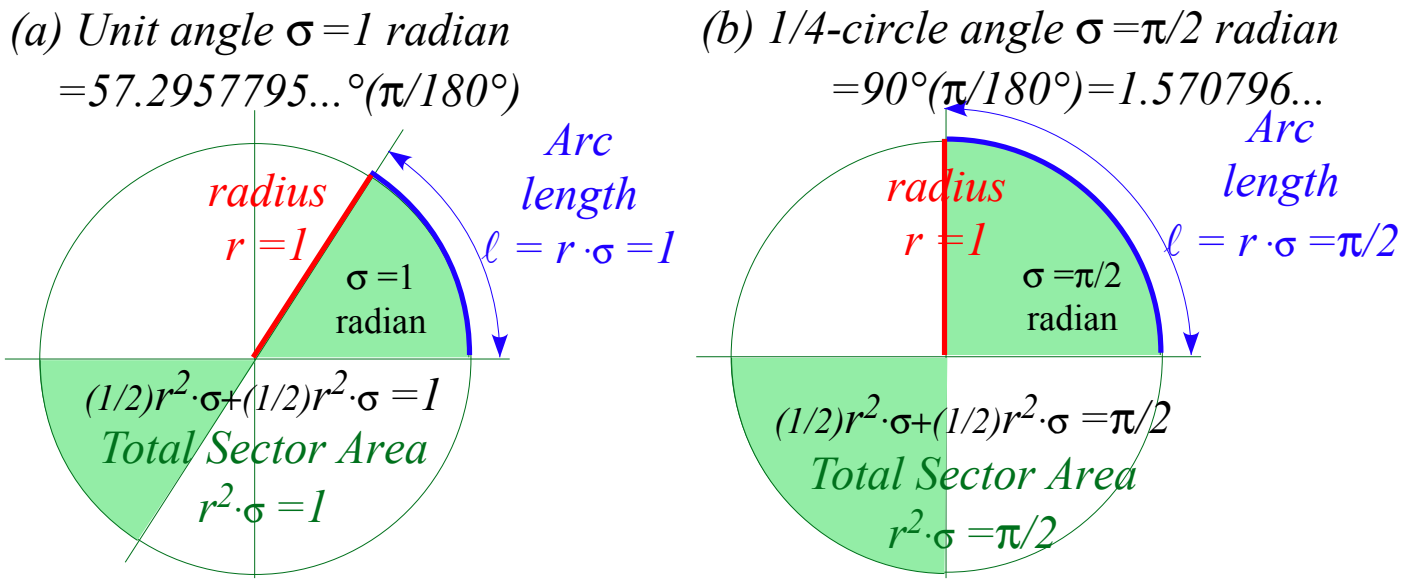

Fig. 1.3 (a) Definition of unit angle (σ =1) on unit circle (r =1) (b) A quarter turn sweeps half the area.

The trick here is that the sector slope line sweeps out *two* pieces of the pie to make a whole pie or area $pi=\pi$ if angle σ is π or *180°*. The 1/4-circle angle $\sigma=\pi/2$ in Fig. 1.3b sweeps area $\pi r^2/2=\pi/2$ of half a pie. It may not be how *you* serve pie, but it's how mathematicians serve π. (There (or their) pie (or pi) *are* squared!)

Actual slope is the *tangent of angle* σ written tanσ and so called since it is the *length* of a line tangent to or *"touching"* a unit circle from angle σ to *x*-axis. (See Fig. 1.4b.) Another triangular ratio is the *sine* or sinσ that stands (*I'm guessing*) for "slope over incline." The *tangent* in Fig. 1.4 is an *a:b* ratio (a/b), but the *sine* is an *a:r* ratio (a/r) that civil engineers use to "grade" roads.

$$\text{percent-grade} = 100 \cdot (\text{altitude } \Delta y \text{ gained}) / (\text{distance } \Delta r \text{ traveled}) = 100 \sin\sigma$$

High grades are *good* in school but *bad* for roads. An interstate highway would "flunk" anywhere its grade was above 5%. This changed in 2001 with the Bush administration's *"No Road Left Behind"* policy.

Each triangle ratio switches places with its *codependent ratio* if you switch *x*-and-*y*-axes (or altitude-and-base) or switch Fig. 1.2a Minkowski plots to Fig. 1.2b Newton plots. For example, a *cotangent* ratio is codependent to tan σ, and *cosine* ratio $\frac{base}{radius} = \frac{b}{r} = \frac{\Delta x}{\Delta r} = \cos\sigma$ is codependent to sin σ.

In comparing (a) *vs.* (b) in Fig. 1.2 we saw that a slope (like *6/1*) in (a) is inverse slope (*1/6*) in (b). (That was for the *10mph* VW.) In other words, any slope $\frac{a}{b} = \tan\sigma$ in (a) becomes $\frac{b}{a} = \cot\sigma = 1/\tan\sigma$ in (b). Also any slope angle σ in (a) becomes a *compliment* $\sigma_c = \frac{\pi}{2} - \sigma$ *to angle* σ in (b). (See Fig. 1.4a.)

From the two preceding paragraphs we deduce that any ratio like sinσ or tanσ for angle σ must equal its co-ratio for the compliment $\sigma_c = \pi/2 - \sigma$, and *vice versa*.

$$\sin\sigma = \cos\sigma_c\,, \quad \sin\sigma_c = \cos\sigma\,, \quad \tan\sigma = \cot\sigma_c = 1/\tan\sigma_c\,, \quad \tan\sigma_c = \cot\sigma = 1/\tan\sigma$$

Two other ratios use secant (or "*sword-like*") lines that pierce the circle in Fig. 1.4b. The horizontal line is a *secant* ratio $\frac{radius}{base} = \frac{r}{b} = \frac{\Delta r}{\Delta x} = \sec\sigma = 1/\cos\sigma$ and its co-ratio is a *cosecant* ratio $\frac{radius}{altitude} = \frac{r}{a} = \frac{\Delta r}{\Delta y} = \csc\sigma = 1/\sin\sigma$.

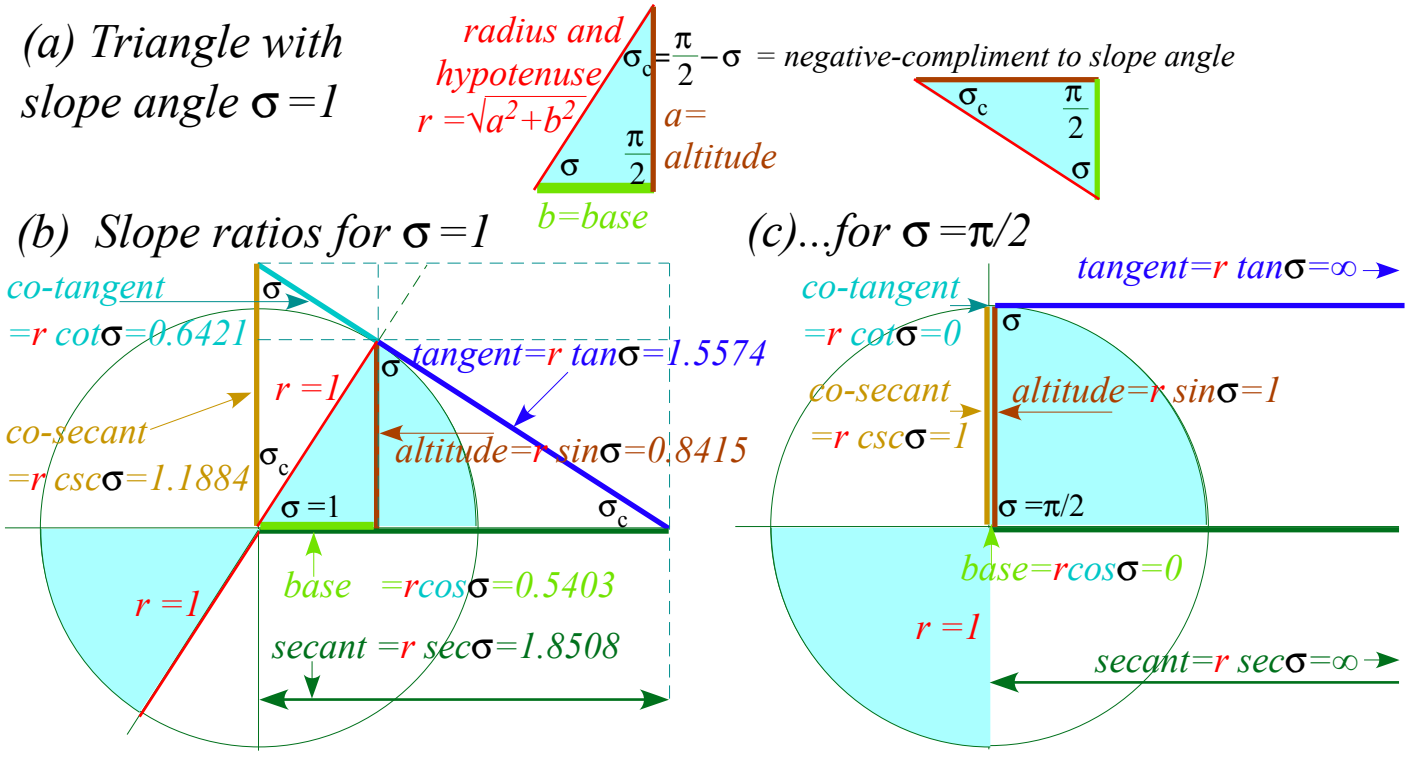

Fig. 1.4 (a) Right triangle geometry for σ=1 slope (b) Triangle ratios for σ=1 and (c) σ=π/2.

Right-handed Cartesian coordinates

Rene Descartes (1596-1650) is said to have invented (or discovered) the Cartesian graph and coordinate system. We usually call the two-dimensional (2D) version "XY-coordinates" and three-dimensional (3D) versions are "XYZ-coordinates."

Four-dimensional (4D) space-time *(xyzt)-Minkowski coordinates* after Herman Minkowski (who was Einstein's math professor)†came later (1905-1908). The 2D projection of one space dimension (*x* or *y* or *z*) and time scale-by-lightspeed (*ct*) is called a *Minkowski graph*. Lightspeed $c=2.99792458\ m/s$ has velocity units so *ct* has distance units like *x* or *y* or *z*.

Two-dimensional (2D) XY-graphs often draw the primary X or *x*-axis along the horizontal direction with *x* increasing to the right, and then place the secondary Y or *y*-axis perpendicular or *normal* to the X-axis with *y* increasing vertically.

What (or which) physics variables should be "primary?" Well, that's up to you. The choice between Minkowski(a) and Newton(b) in Fig. 1.2 is a matter of taste.

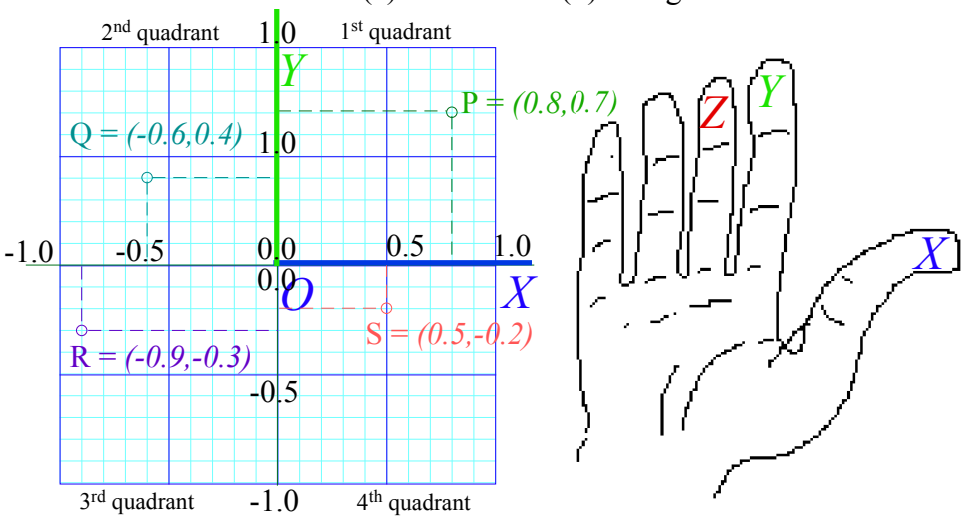

The graph above is called a *right-handed coordinate system* since it points like your thumb (*X*) and forefinger (*Y*) of your right hand as you extend to shake hands or hand someone a plate of *escargot*. (Descartes' French cuisine is respected here.)

A toothpick sticking up from the *escargot* points in the *Z* or *z*-axis direction of a right-handed 3D Cartesian coordinate system as shown below.

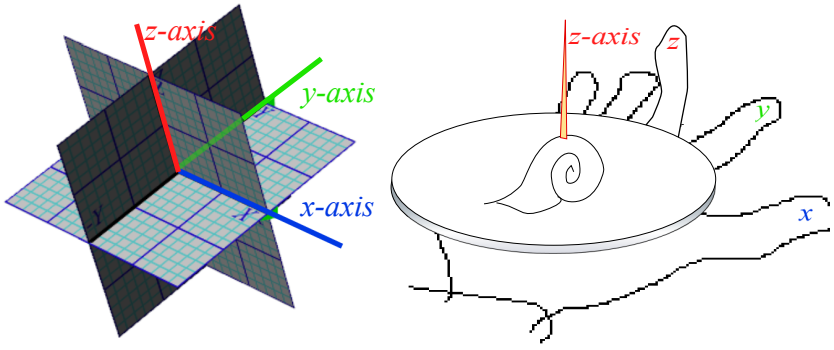

† *Minkowski (who was Polish) told Einstein (who was Swiss) that he was a "fat lazy boy." Einstein was so insulted that he never used Minkowski plots. It is sad story since Herman's graphs could have helped many more to visualize relativity by exposing its geometric structure. Eventually, we hope to make up for that sad mistake!*

A. Einstein, *Annalen der Physik* 17, 891(1905).

H. Minkowski, *Mathematisch-Physikalische Klasse*, vol. 1, 53 (1908).

Change and delta variables

The *delta notation*, such as Δx, Δv, Δt, and so forth, is confusing to one who has not had a calculus course (or has forgotten that stuff). Roughly speaking, the Greek upper case "*D*" or *delta* (Δ) stands for "difference" or *differential*, and Δx should be read as "change of x" or *differential of* x and thought of as a single entity.

It is a common mistake to read Δx as "Δ multiplied by x" or "Δ times x" since, after all, product p of quantities a and x is written $p=ax$ or better $p=a\cdot x$. Instead, the mathematical *cognescenti* think of Δ as an *operation* that acts on a variable x or whatever to give whatever change has occurred in that variable.

When the letter Δ is used to denote an actual number or variable one should take care to write its product with another variable x as $\Delta\cdot x$ or (better) $x\cdot\Delta$ to avoid confusing it with Δx.

Slope and delta ratios

Slope ratio $\Delta y/\Delta x$ of a line or of a triangular hypotenuse is a key concept that is common to mathematics and physics beginning with Babylonian and Greek plane geometry of Euclid (300 BCE), and progressing through analytic geometry of Descartes (1620), the complex trigonometry of Euler (1700), the calculus of Newton (1720), the relativity of Einstein (1905), and the quantum mechanics of Planck (1900), Bohr (1920), Schrodinger (1925), and Dirac (1930). (That's a short list. A full one could take pages.) Physics uses slope like soup uses water. It's all based on slope and related triangular angles, areas, and ratios. *We must study slope!*

So far we have only talked about slope of straight lines in Fig. 1.1-2. For them triangle size or location makes no difference to ratio $\Delta y/\Delta x$. All triangles in the figure (a) below are *similar triangles*, but triangles hanging on a curve in figure (b) are not.

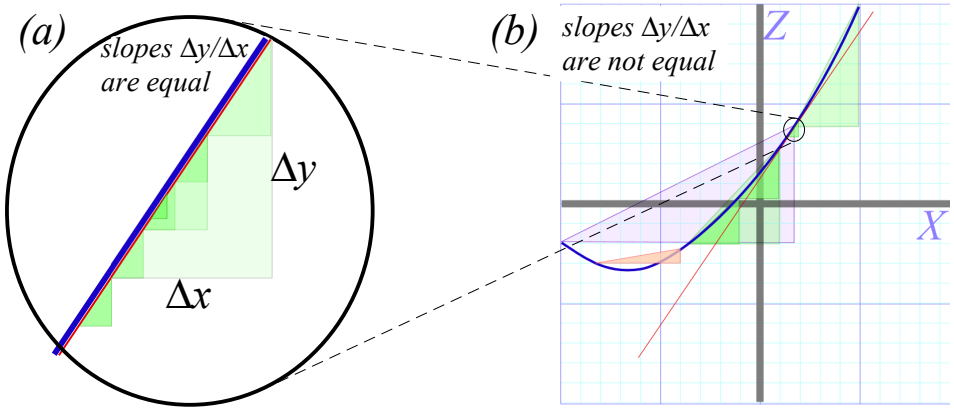

Slope of a triangle hanging on a curve depends on location x and base segment size Δx. Soon we will define slope of a *tangent line* to a curve in (b) by making its base segment Δx so small that the curve over it looks straight as in (a). Then tangent slope (to graph accuracy) only depends on location x on the curve and not on tiny Δx.

Fig. 1.4b has *eight* different but *similar* triangles with the same angles ($\sigma,\pi/2,\sigma_c$) as the triangle in Fig. 1.4a. Can you spot them? Whether big or small, similar triangles share ratios (sine, cosine, or tangent) if (and *only* if) they share angles. To do geometry problems we look for "hidden" similar triangles and hidden *right* triangles that form similar *rectangles*. Right triangles have relation $a^2+b^2=r^2$ of Pythagoras (~570 BC).

One secret is to visualize sequences of scale change or rotation transformation as in Fig. 1.5 where each rectangle is rotated by *90°* and shrunk by a factor $\cot\sigma=64.2\%$. Rectangle diagonals in Fig. 1.5a (and sides in Fig. 1.5b) give a *power sequence* ($\ldots\tan^1\sigma,\tan^0\sigma=1,(\tan\sigma)^{-1}=\cot^1\sigma,(\tan\sigma)^{-2}=\cot^2\sigma,(\tan\sigma)^{-3}=\cot^3\sigma,\ldots$).

A power sequence is also called a *geometric sequence* since it is suggested by geometry. A rectangle sequence in Fig. 1.5a is lined up with the XY coordinates of the page, that is, each side has zero or infinite slope but the first diagonal ($\tan\sigma$) has a negative slope angle of $-\sigma_c = -1$-radian or *–57.3°*. The sequence in Fig. 1.5b begins with a rectangle side ($\tan\sigma$) at angle *–57.3°*. Each sequential rotation in either figure is *90°* clockwise around the original tangent point with rectangle size shrunk by factor $\cot\sigma=64.21\%$ each time.

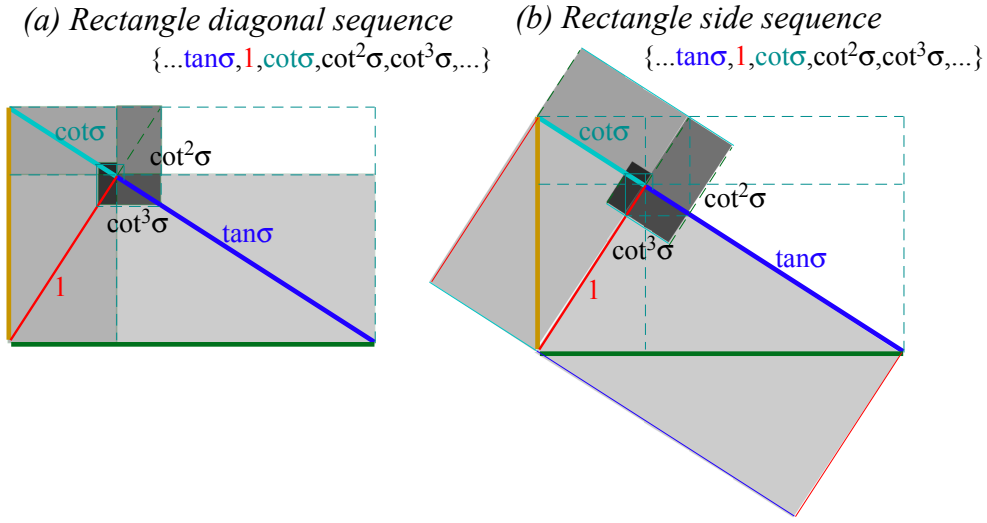

Fig. 1.5 Geometric $\cot\sigma=0.6241$ sequences of whirling rectangle segments based on slope angle $\sigma=1$.

Exercises for study of slope and trigonometry

1. Construct whirling square diagrams for *60°* slope angle $\sigma=\pi/3$ *without using protractor*. First compare the precision of graph-derived values of $\sin\sigma$, $\cos\sigma$, $\tan\sigma$, etc. with algebraic $^{\text{and}}/_{\text{or}}$ calculator-derived numbers.

Solution Hints:

Only certain angles have exact Euclid rule&compass construction and $\sigma=60°$ is one of them. (But, $\sigma=1$ isn't!) If you could "straighten" the ($\ell=1$)-arc of a ($\sigma=1$)-sector (Fig. 1.3a) to one ($r=1$)-side of an equilateral triangle, its slope angle would grow from $\sigma=1=57.3°$ to $\sigma=\pi/3=60°$ as shown in Fig. 1.6b.

To construct a *60°* slope *a' la* Euclid, draw a radius-($r=1$) circle by compass and use the same radius-*r* setting to strike an arc from X point-($x=1,y=0$) to locate R as in Fig. 1.6b. So now, theoretically, *arc*-RX is $\ell=\pi/3=1.0472\ldots$long *approximately* but *line*-RX has length-($r=1$) *exactly*. At 2-figure precision both have length *1.0*, but at 3-figure precision, *arc*-RX length is *1.05*, 5% greater than *line*-RX length *1.00*.

Whether a math or physics theory is "correct" or not depends on our level of precision. As we will see, it is pretty tough to get order-3 absolute precision (1 part in 1,000) with ruler and compass construction but order-2 is pretty easy. By taping fishing line onto *arc*-RX, we can see that it is about 5% shorter than a unit line, but measuring 4.7% is challenging and 4.72% requires tools most don't have.

We easily get level-9 precision by poking $\sin(\pi/3)$ into a calculator (or $\sin 60°$ if set for degrees) to get $\sin(\pi/3)=0.866025403\ldots$ but only can estimate 0.86 or 0.87 in Fig. 1.6b graph as indicated by ??? marks.

To construct the tangent declination by compliment angle $\sigma_c = \pi/2-\pi/3 = \pi/6$ (or $90°-60°=30°$) we strike a unit arc off the –Y point to intersection point Q on the 4th quadrant-YQX of unit circle in Fig. 1.6c. The line OQ thru point Q is perpendicular or *normal* to original slope line OR since $\sigma_c+\sigma$ is $\pi/2(90°)$ for any σ.

This line OQ drawn thru point R is the tangent decline we need for this problem. Just redo arc inter-sector -YQO to make sector NPR centered at R instead of O. Then draw tangent line PR so it extends down to secant point S on the X axis and up along the cotangent line to the cosecant point on the Y axis.

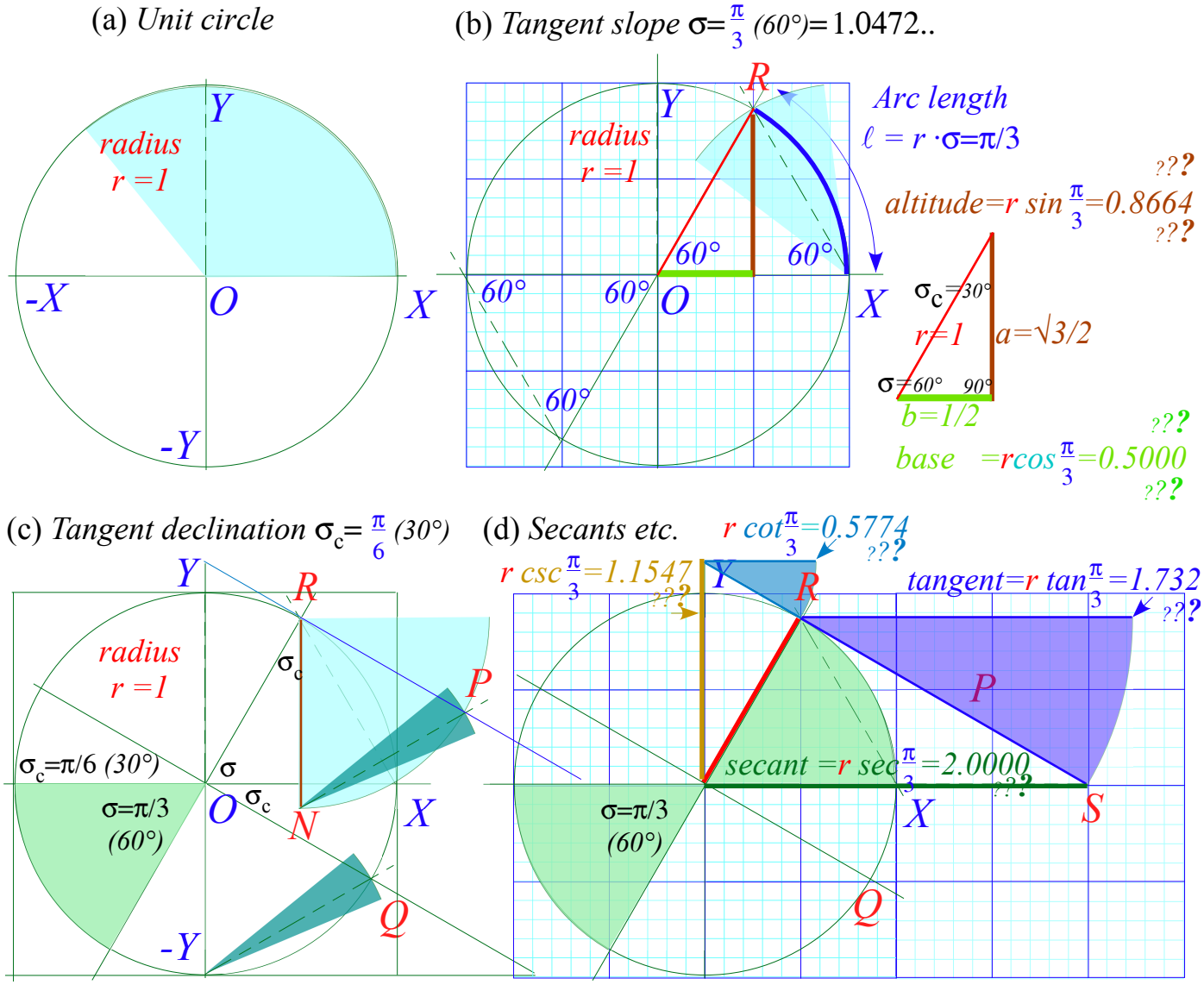

Fig. 1.6 Details of a geometric construction of Fig. 1.5 for slope angle σ=π/3 (60°)

Segments OS and YR provide numerical estimates of calculated values $\sec(\pi/3)=2.000$ and $\csc(\pi/3)=1.155$ along X and Y axes, respectively, in Fig. 1.6d. The value $\sec(\pi/3)=2$ like its inverse $\cos(\pi/3)=1/2$ is exactly rational, a nice feature of a *(30°,60°,90°)*-triangle with side ratios *(b:a:r)=(1:√3:2)* (It is a right triangle, so: $a^2+b^2=r^2$.) The "*30-60*" is a famous right triangle students must learn. Others are "*3-4-5*" (*(a:b:r)=(3:4:5)*) and the "*45*" (*(45°,45°,90°)*or*(a:b:r)=(1:1:√2)*). A "Golden" ratio $G=\frac{1}{2}(1+\sqrt{5})$ triangle is very cool *(and rich)*.

Arc functions

So far we give an angle or unit-circle arc σ and construct or calculate trigonometric functions of σ including $a=\sin\sigma$, $b=\cos\sigma$, $t=\tan\sigma$, $1/a=\csc\sigma$ or their co-functions. Now consider the reverse or inverse case: we are given *a*, or *b*, or *t etc.* and must come up with an arc σ (or arcs σ_1,σ_2...) that gives *a*, *etc*. To do this we find *arc-functions arc-sine, arc-cosine…* or *inverse trig functions* $\sin^{-1}$, $\cos^{-1}$…as follows.

$\sigma=\arcsin(a)=\sin^{-1}(a)$, $\sigma=\arccos(b)=\cos^{-1}(b)$, $\sigma=\arctan(t)=\tan^{-1}(t)$,…

The exponential $(^{-1})$-notation seems to confuse $\sin^{-1}(a)$ with $(\sin(a))^{-1}=1/(\sin(a))$ that we do *not* want here. (However, it is conventional to write $(\sin(a))^n=\sin^n(a)$ or any power but $(^{-1})$.)

Algebra of arc-functions is trickier than algebra of functions themselves. Geometric constructions of $\sin^{-1}$, $\cos^{-1}$…*etc.* are not so tricky but quite simple and revealing. To find $\sin^{-1}(0.5)$, for example, we draw a horizontal line at *y=0.5* and see where it intersects the unit circle. (Fig. 7a) Nothing to that! Except, we see there are *two* angles $\sigma_1=\pi/3$ and $\sigma_2=2\pi/3$ that give $\sin\sigma_1=0.5=\sin\sigma_2$. The same applies to $\cos^{-1}(0.5)$ except now the angles are $\pm\pi/3$. (Fig. 1.7b) Note the *antipodal (±180°)* angles that equal $\tan^{-1}(0.5)$. (Fig. 1.7c)

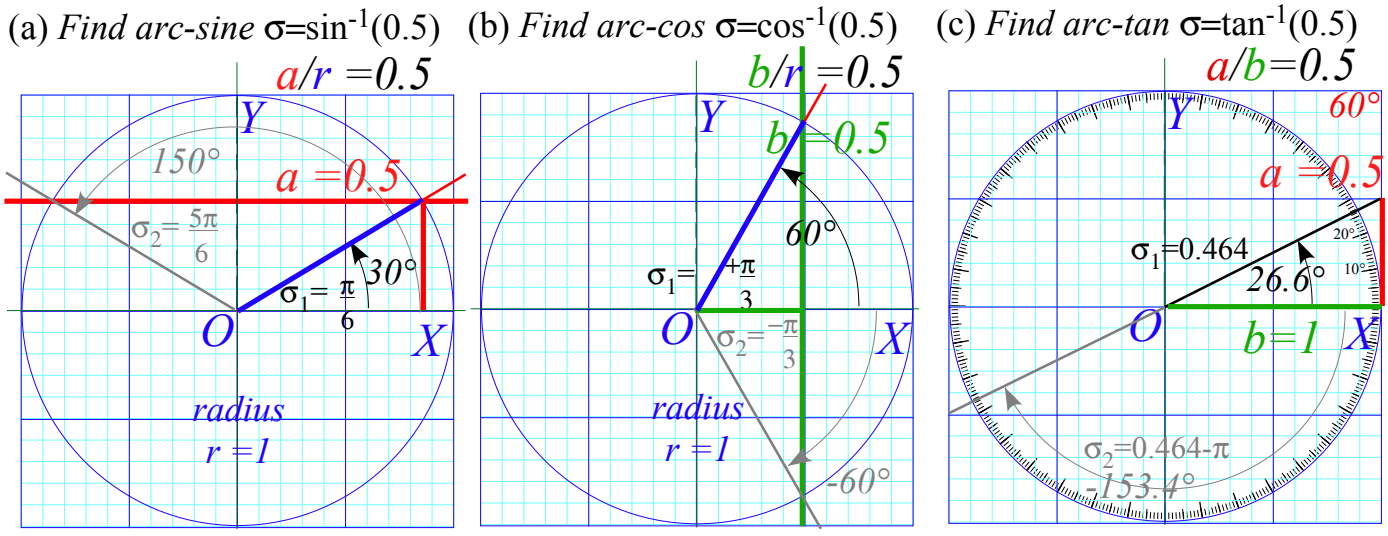

Fig. 1.7 Geometric construction of arc-trig functions of 0.5=½. (a) $\sin^{-1}(\frac{1}{2})$ (b) $\cos^{-1}(\frac{1}{2})$ (c) $\tan^{-1}(\frac{1}{2})$

2. Find *arc-secant* (say, $\sec^{-1}3.0$) by geometry. Try it first without looking at the answer.

Solution Hints:

We need to find the tangent that goes from 3.0 to touch the circle. A circle of radius *r=3.0* concentric to the unit circle has rectangle tangents of that size that we copy from *x=3.0* to touch unit circle.

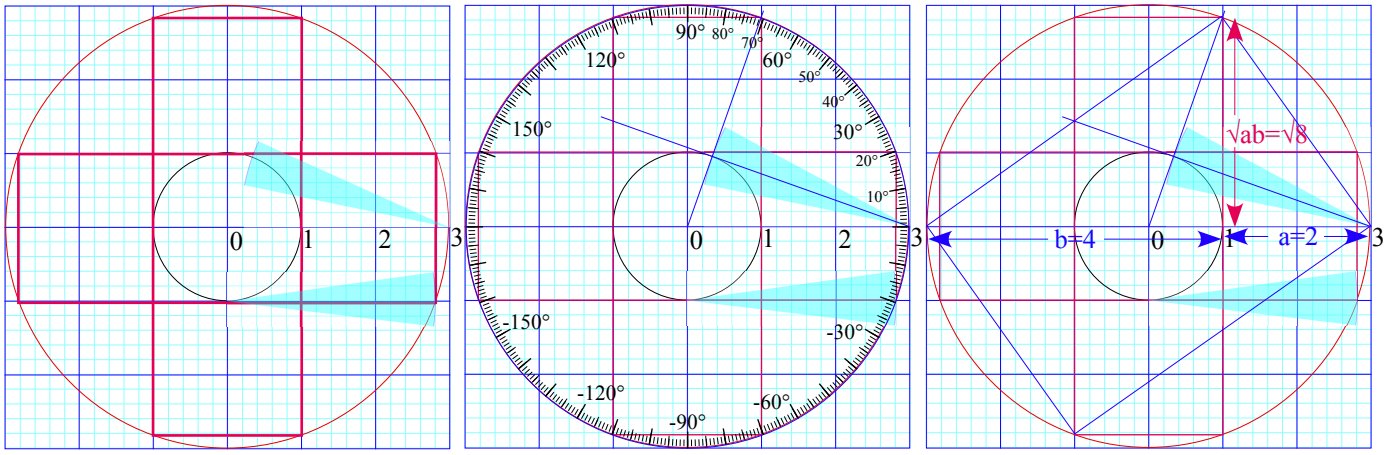

Fig. 1.8 Geometric construction of arc tangent, arc secant, and geometric-mean square-root.

Or else we simply draw rectangle diagonal thru unit circle. This involves *Thales's Geometric Mean (GM)* construction in Fig. 1.9a of a product square root $\sqrt{(a \cdot b)}$. In Fig. 1.8 it is $\sqrt{8}=2.82...$ the desired tangent. The special case of the Golden Mean is shown in Fig. 1.9b. The whirling rectangle in Fig. 1.5 is a whirling square in Fig. 1.10 if the rectangle tangent and cotangent are Golden Means 1.618.. and -0.618.., respectively.

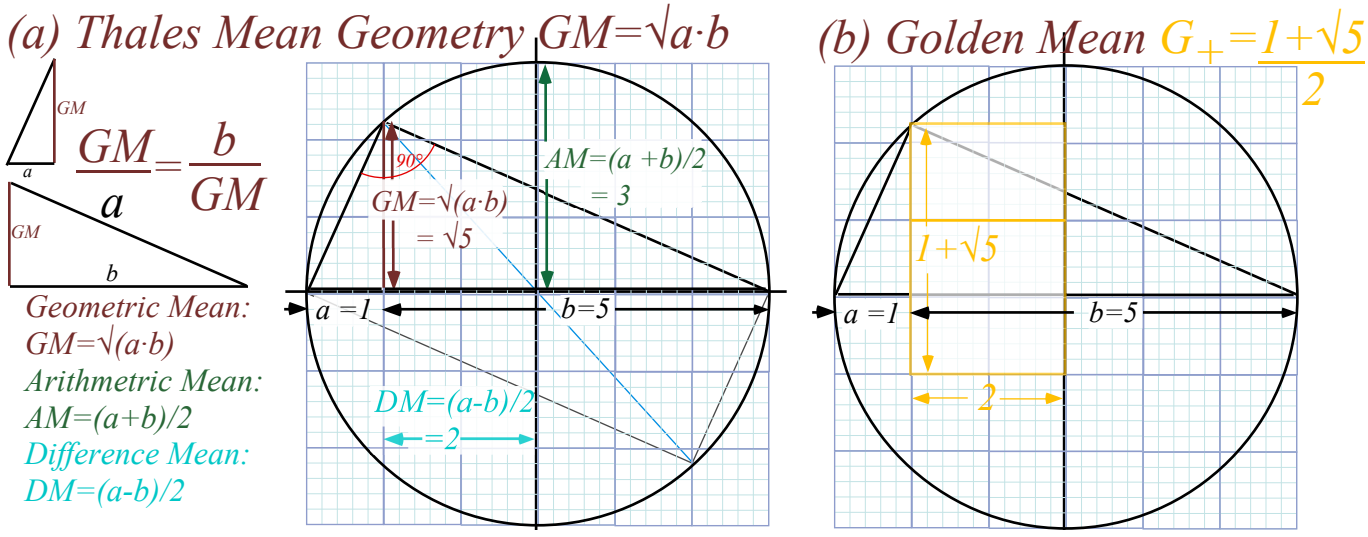

Fig. 1.9 Thales construction of geometric-mean, square-root, and Golden Mean.

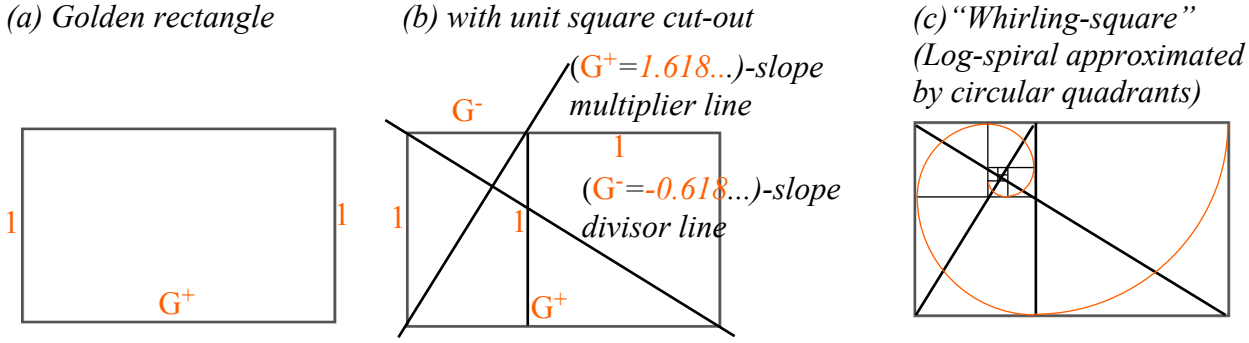

Fig. 1.10 (a) Golden Rectangle, (b) Golden slope geometry, and (c) Whirling Square like Fig. 1.5.

Know your calculator and ATAN, too! (atan2*(y,x)*)

Scientific calculators do not always give the solution you want for arc-function $\sin^{-1}(a)$, $\cos^{-1}(b)$, or $\tan^{-1}(b/a)$. For one thing, they never give an angle in the *3rd* quadrant *(minus-x,minus-y)* so you could be wrong at least 25% of the time.

But it is worse than that. "Blind" arc-calculations are wrong *half* the time.

As you vary altitude $a=y$ from (+1) to (–1) values in Fig. 1.7a the *1st* arc-solution $\sigma_1 = \sin^{-1}(a/r)$ sweeps the unit circle in the right-half plane while its *x*-reflection is the *2nd* solution σ_2 is in the left-half plane. The calculator ignores σ_2.

As you vary base $b=x$ from (+1) to (–1) values in Fig. 1.7b the *1st* arc-solution $\sigma_1 = \cos^{-1}(b/r)$ sweeps the unit circle in the upper-half plane while its *y*-reflection is the *2nd* solution σ_2 is in the lower-half plane. Again, the calculator ignores σ_2.

Varying either altitude $a=y$ or base $b=x$ from (+1) to (–1) in Fig. 1.7c gives a full range of solutions $\sigma_1 = \tan^{-1}(a/b)$ but a calculator cannot distinguish between the first solution and the *2nd antipodal* solution $\sigma_2 = \tan^{-1}(-a/-b)$ since $a/b=-a/-b$.

So the calculator plays it safe and gives the *acute angle* solution in the arc-range *–90°* and *+90°*, that is $(-\frac{\pi}{2} \le \sigma \le +\frac{\pi}{2})$. The *obtuse angle* solution is ignored for ranges *+90°* to *+180°* (2^{nd} *quadrant* $: +\frac{\pi}{2} < \sigma \le +\pi$) or *-90°* and *-180°* (3^{rd} *quadrant* $: -\frac{\pi}{2} > \sigma \ge -\pi$)

A correct solution is the sure-fire **atan2***(y,x)* function that requires you to give both the altitude $a=y$ and the base $b=x$ (with correct signs, of course) so it knows which quadrant you're in. The **atan2**, built into calculators gives what is called the *rect-to-polar coordinate conversion* often labeled by a $(x,y) \to (r,\theta)$ -button.

Plug in *x* and *y* and out comes $r = \sqrt{x^2 + y^2}$ and $\theta = \tan^{-1}\frac{y}{x}$. The θ is our σ.

Trig function plotting exercises (And, how we trisect angles)

3. Use ruler&compass to plot *y=cos(x)* and *y= cos-1(x)=arccos(x)*. Do *y=sin(x)* and *y=sin-1(x)*. Begin by constructing a 12-pt "clock" circle. Repeat using 45° diagonals to make a 24-hr clock and project the 24 points horizontally for *y=cos(x)* and vertically *y=cos-1(x)=arccos(x)*. Shift plot by 3 hours (90°) for sine and arc-sine functions. Each "hour" is angle 15° or π/6. Sine curves allow "forbidden" constructions such as cycloids and angle-*n*-sections. In quantum physics sinusoidal waves are *really* important curves!

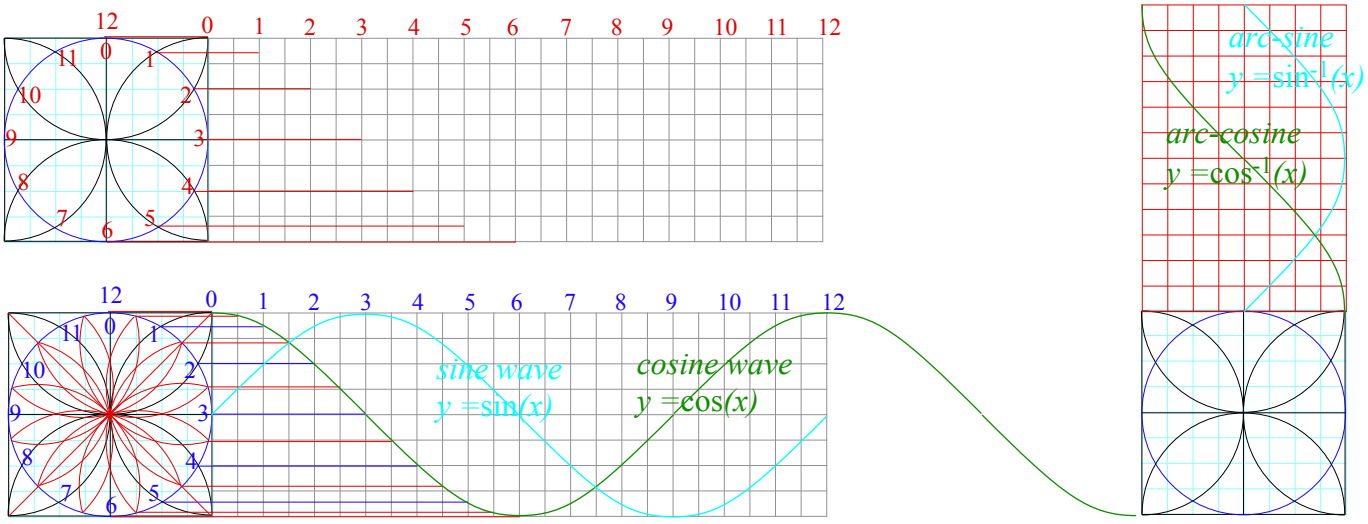

Exercise 1.1.4
Construct both Golden *angles* associated with the *Golden Ratios* G_+ and G_- and measure their slopes in degrees on protractor graph paper below. (Also available online.) Can you find a simpler (Pythagorean) construction of √5 ?

Exercise 1.1.5
Construct whirling rectangle diagram like Fig. Fig. 1.5 but for Golden slope angle to give whirling square sketched in Fig. 1.10. Use protractor graph from Ex. 1.1.3 to measure angles of slopes obtained this way.

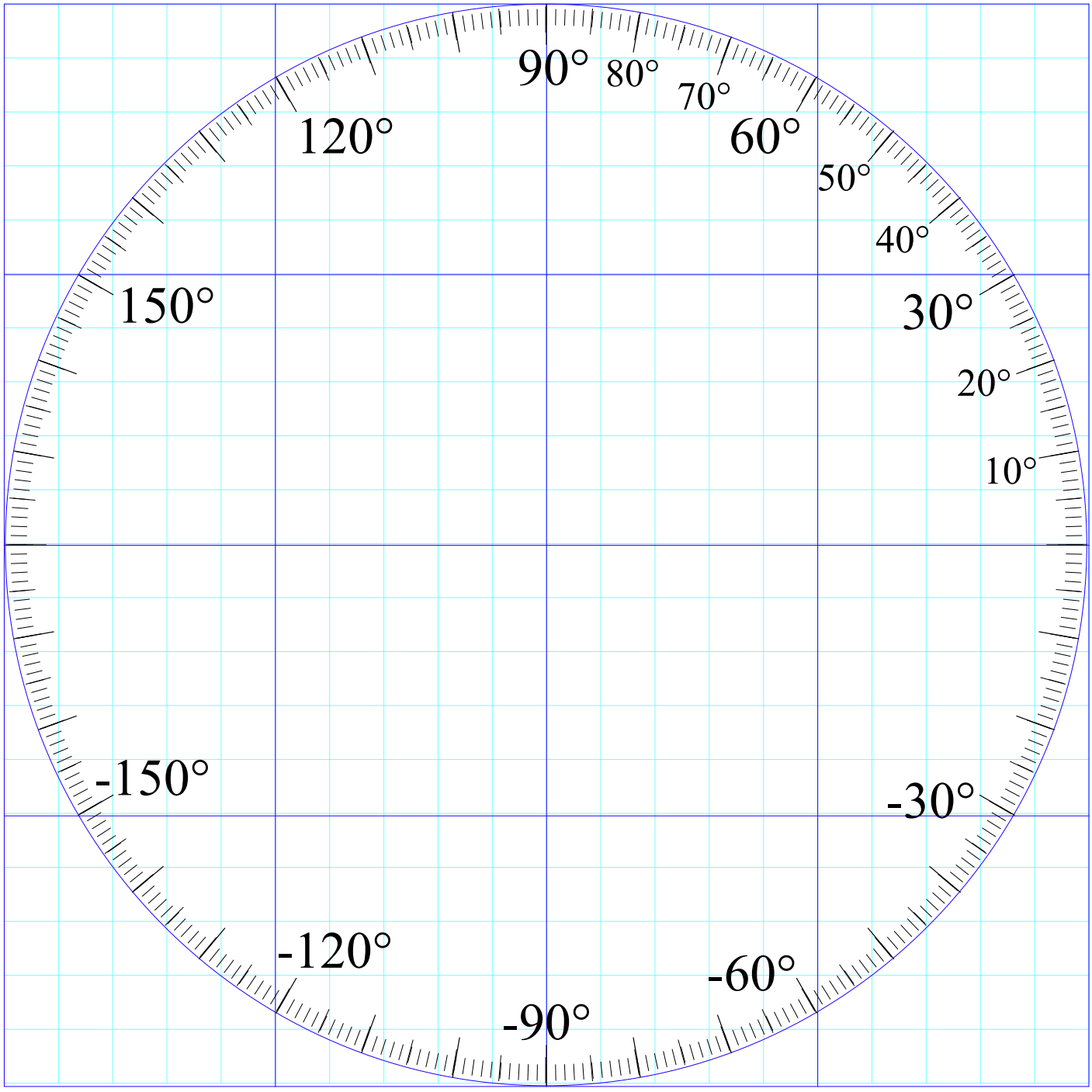

Chapter 2. Velocity and momentum

Recall the car-crash problems discussed first in Chapter 1 regarding Fig. 1.1. The first one involves a text-messaging driver of 4-ton SUV going *60mph* SUV rear-ending a dawdling 1-ton VW going *10mph*. (Fig. 1.1b.) What final velocity or velocities do the cars have? You may have been taught to analyze collisions by solving momentum and energy formulas in a resulting quadratic equation. Fig. 2.1 shows an easier geometric solution using a single line on graph paper. Moreover, its logic is clear enough to *derive* those formulas!

As sketched in Fig. 1.1b, the answer depends on whether it's *"Ka-Runch"* or *"Ka-Bong"* or some more generic noise like *"Ka-whump"*. By *"Ka-Runch"* we mean the cars crumpled enough to become crunched into one hunk of metal weighing 5 tons. *(4+1=5)* This is a simple problem that is solved by drawing a line of slope *(–4/1)* on a velocity *vs.* velocity graph from before-crash-point $(V_{SUV}^{INITIAL}=60,\ V_{VW}^{INITIAL}=10)$ to where that line intersects the red 45° $(V_{SUV}=V_{VW})$-line at the after-crash-point $(V_{SUV}^{FINAL}=50,\ V_{VW}^{FINAL}=50)$. (Fig. 2.1)

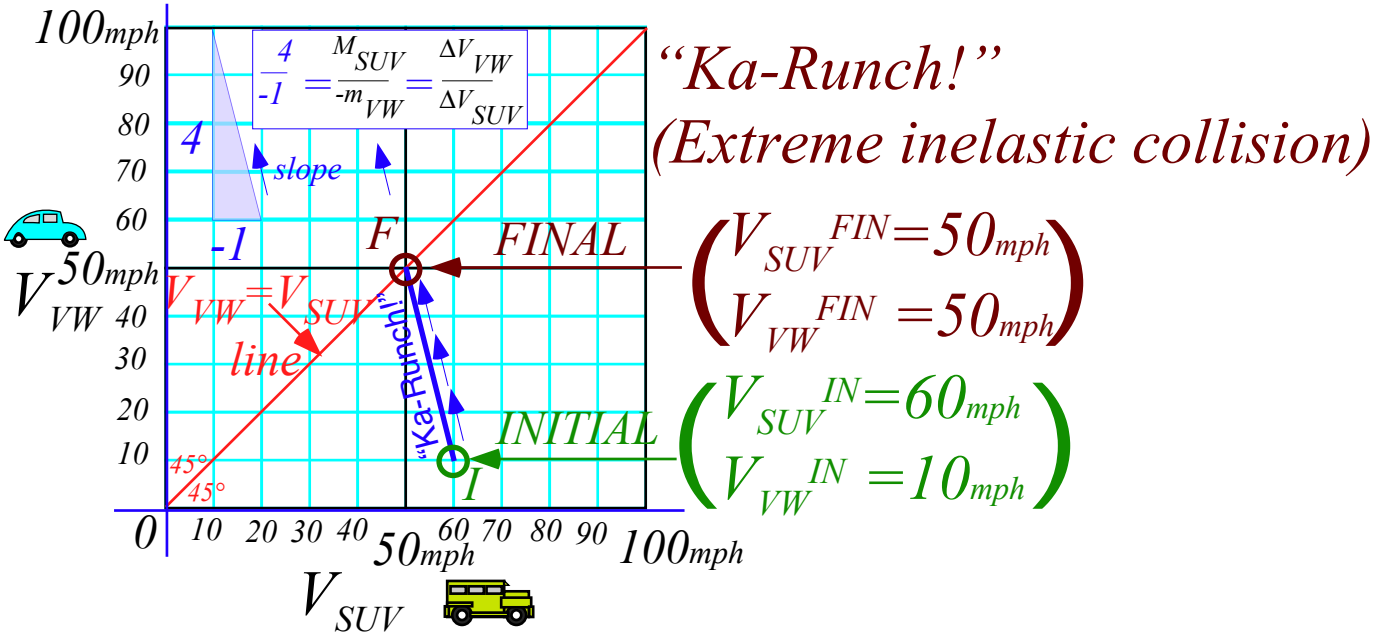

Fig. 2.1 Anatomy in velocity space of a "Ka-runch!" that is an extreme inelastic collision.

The logic behind a $(V_{SUV}=V_{VW})$-line is that crunched vehicles have equal velocity. The logic behind a *Ka-Runch*-line of slope *(–4/1)* is subtler. It is due to *Newton's 1st axiom* or "law" that says Nature conserves so-called *momentum*, a sum of products of each mass with its velocity. It's a law we can live with but, why?

Momentum exchange: a zero-sum game

During the car crash the velocity coordinate pair (V_{SUV}, V_{VW}) change very rapidly in moving from initial point *I* at *(60,10)* to final point *F* at *(50,50)* in Fig. 2.1. The *Ka-Runch* takes less than a second. In that time, SUV is losing only *one* unit of velocity for every *four* units gained by VW since SUV is *four* times heavier than VW. Newton writes this as a *total momentum conservation* equation.

$$P_{SUV} + P_{VW} = M_{SUV}\cdot V_{SUV} + m_{VW}\cdot V_{VW} = P_{Total} = constant \qquad (2.1)$$

Checking (2.1) with Fig. 2.1 gives a total momentum $P_{Total}=250$ that SUV and VW have together.

$$4{\cdot}60+1{\cdot}10 = 4{\cdot}V_{SUV}+1{\cdot}V_{VW} = 4{\cdot}50+1{\cdot}10 = P_{Total} = 250 \qquad (2.2)$$

The *change* of P_{Total} must be zero ($\Delta P_{Total}=0$) before, during, and after the crash. It's a zero-sum game.

$$M_{SUV}{\cdot}\Delta V_{SUV} + m_{VW}{\cdot}\Delta V_{VW} = \Delta P_{Total} = 0 \qquad (2.3)$$

Dividing by SUV change-of-velocity (ΔV_{SUV}) and VW mass (m_{VW}) gives the slope relation in Fig. 2.1.

$$\frac{M_{SUV}}{m_{VW}} + \frac{\Delta V_{VW}}{\Delta V_{SUV}} = 0 \quad \text{or:} \qquad \frac{\Delta V_{VW}}{\Delta V_{SUV}} = -\frac{M_{SUV}}{m_{VW}} \qquad (2.4)$$

P_{Total} is also conserved in an ideal *Ka-Bong* of Fig. 2.2. Here cars bounce off each other without damage. That's unlikely at *60mph* speeds! So Fig. 2.2 is rescaled to units of *feet per minute*. Then initial V_{SUV}^{IN} *=60 feet per minute=1ft. per sec.* is more like a parking lot speed. (Insurance claims are a lot less!) The VW is bumped from an initial V_{VW}^{IN} *=10 ft per min* to V_{VW}^{FIN} *=90 ft per min=1.5 fps=1.02 mph*. To find V_{VW}^{FIN} in Fig. 2.2, draw an arc from initial *I*-pt *(60,10)* to hit final *F*-pt *(40,90)*. Arc-center is *Center of Momentum COM pt-(50,50)* on the *45°* line. (It's the *final* point if cars get "stuck" to each other as in a *Ka-Runch* like Fig. 2.1.)

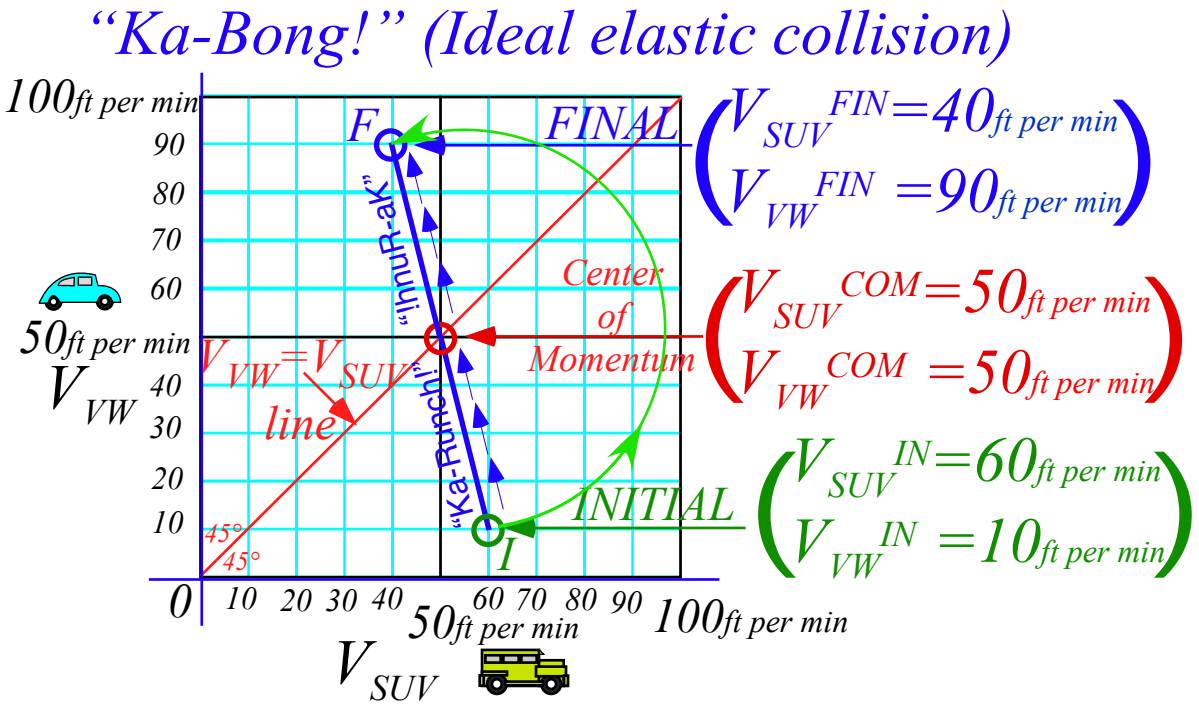

Fig. 2.2 Anatomy in velocity space of a "Ka-Bong!" that is an extreme or ideal elastic collision.

The *Ka-Bong* in Fig. 2.2 is like the *Ka-Runch* in Fig. 2.1 followed by an equal but opposite rebound or *hcnuR-aK (un-crash)* that undoes the "damage" by the *Ka-Runch*. Now you might ask, "Is this possible outside of the cartoon world or a video game?" Well, *certainly not* at high speeds and *not quite* at low speeds.

Only in a quantum nano-world do *perfectly* elastic processes exist. Any classical collision, however gentle, is audible, visible, and disturbs or exchanges many atoms, electrons, and photons. This is called *"wear&tear"* or *entropy growth.* (Usually one ignores it until it has gone too far. Then it fills landfills!)

Even gentle bumps like the one starting at initial *pt-I* in Fig. 2.2 cannot quite go *exactly* to final *pt-F* on the *COM* circle, but collisions with no appreciable damage pass as *(almost) elastic* or *time reversible* bumps. A video of the Fig. 2.2 $I \to F$ bump played backwards looks like an $F \leftarrow I$ bump that is quite ordinary. But reversed video of the Fig. 2.1 crash looks like a crazy *"un-crash"* as ruined cars get reborn like new.

Deducing (perfect?) conservation from (ideal?) symmetry

Newton's momentum or *P*-conservation axiom or "law" is one of the most strictly enforced laws in classical physics. (It's also quasi-conserved in quantum physics that so often seems to get away with utter mayhem!) Momentum is like some kind of fluid that you might buy and sell but cannot create or destroy. In our car bumps or crashes the zero-sum-rule says, "Whatever *P* the VW gains (or loses) the SUV loses (or gains.)"

A classical law without classical proof remains an axiom until deeper theory may rule on it. Quantum theory has ruled and can shed some light on origin and properties of this mysterious "*P*-fluid." It also shows how to cheat *P*-conservation and other classical "laws" a little. This will be discussed in later units.

In the meantime it is possible to relate *P*-conservation to more fundamental axioms that are called *symmetry principles*. Symmetry is a grown-up geometry that is also *very* useful in the quantum world. Most immediately, symmetry helps deduce principles of energy *E* and *E*-conservation as discussed below.

Symmetry means *"same-etry"* or *"similarity"* or *"smoothness"* and other *"s"* words like *simplicity*. One fancy technical term is *isotropy* or *isometry* with *iso* meaning *same*. For example, the most *symmetric* ball would be a *sphere* that is *isotropic* by having the *same* radius everywhere. A most-isotropic (or most-symmetric plane) is *flat* and *bump-free*. Some would say *symmetry* means *Beauty*, but others might say it means *Boring*. Think of a seemingly endless *Kansas* prairie for either response.

Symmetry can refer to *sameness* in time as well as in space and often the two are related. (Think of *driving* across Kansas.) The idea of being *time reversible* is an example from the preceding page. Another is Galileo's relative-velocity symmetry or *Galilean relativity*. Both are involved in Fig. 2.2 and Fig. 2.4 below.

Galilean time-reversal symmetry

Suppose a traffic cop is going *50mph* in a lane adjacent to the one occupied by the SUV and VW. He or she records (using radar) the SUV coming up at *60mph*, and puts on the blue-light to stop it for exceeding the *20mph* limit in a school zone. Then *Ka-Runch!* as SUV+VW become a single 5-ton hunk going *50 mph*, the same speed as the cop. (The cop can just reach across to hand SUV a cyber-ticket for (1) speeding in a school zone, (2) improper following, and (3) driving while faxing. c-tickets are *costly* even for rich SUV-ites!)

The V_{VW} *vs.* V_{SUV} graph for the *Ka-Runch* is shown in Fig. 2.3 as viewed by the *50mph* cop. It is the same as Earth-frame-view in Fig. 2.1 except the cop's speed of *50mph* is subtracted from both *V*-scales. The cop sees a final 5-ton SUV-VW hunk going *0 mph* relative to cop-frame or *COM frame* of SUV+VW.

The V_{VW} *vs.* V_{SUV} graph for the *Ka-Bong* in Fig. 2.4 is also viewed in the *50mph* cop-frame or *COM*-frame. Again, it's just Fig. 2.2 with *50mph* subtracted off *V*-scales. Cop or *COM*-frame view shows *simplicity* and *symmetry*. Velocity values simply change sign as the *Ka-Bong* crosses the whole *COM*-circle diameter.

Initial I-pt (10,-40) $\to$ *(reflection thru COM pt-(0,0))* $\to$ *final F-pt (-10,40)*

Reversing time $(\Delta t \to -\Delta t)$ makes *(-)*velocity $(V = \frac{\Delta x}{\Delta t} \to \frac{\Delta x}{-\Delta t} = -V)$ and reflects *I-pt* and *F-pt* into each other.

Initial I-pt (-10,40) → *(reflection thru COM pt-(-0,-0))* → *final F-pt (10,-40)*

That is just Fig. 2.4 with blue time-direction arrows reversed. (*INITIAL I* switches places with *FINAL F*.)

Elastic collisions (Fig. 2.4) are *symmetric* and *balanced* to *t*-reversal, but inelastic *Ka-whump*'s are *un*balanced if they stop short of the *COM* circle. A *Ka-Runch* (Fig. 2.3) is *unbalanced to the extreme*.

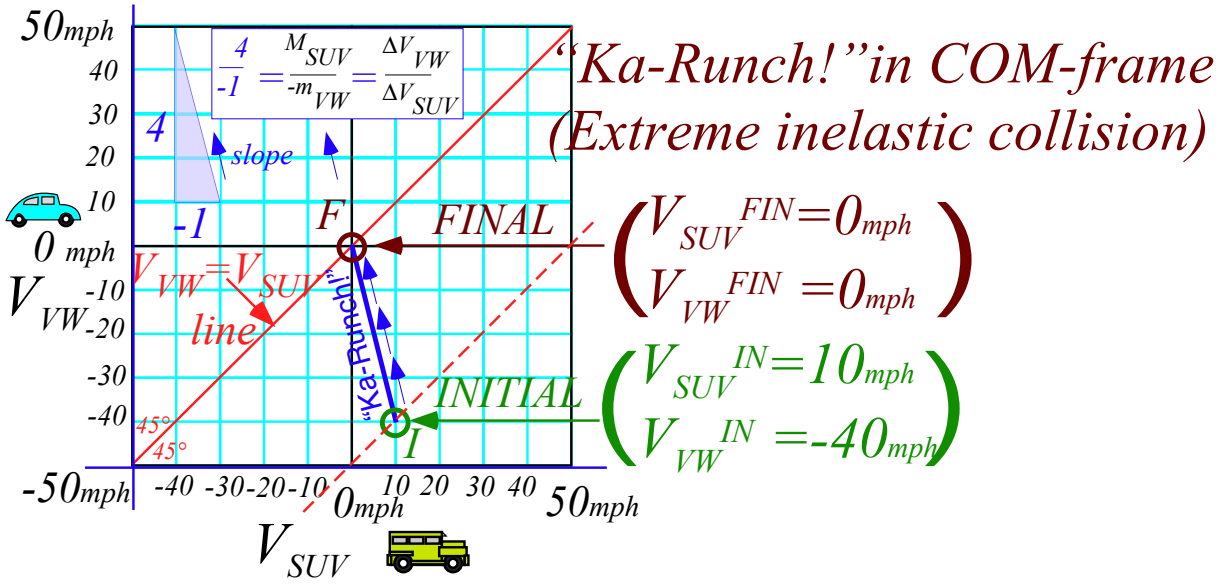

Fig. 2.3 COM-frame or 50mph cop-frame view of a "Ka-runch" inelastic collision of Fig. 2.1.

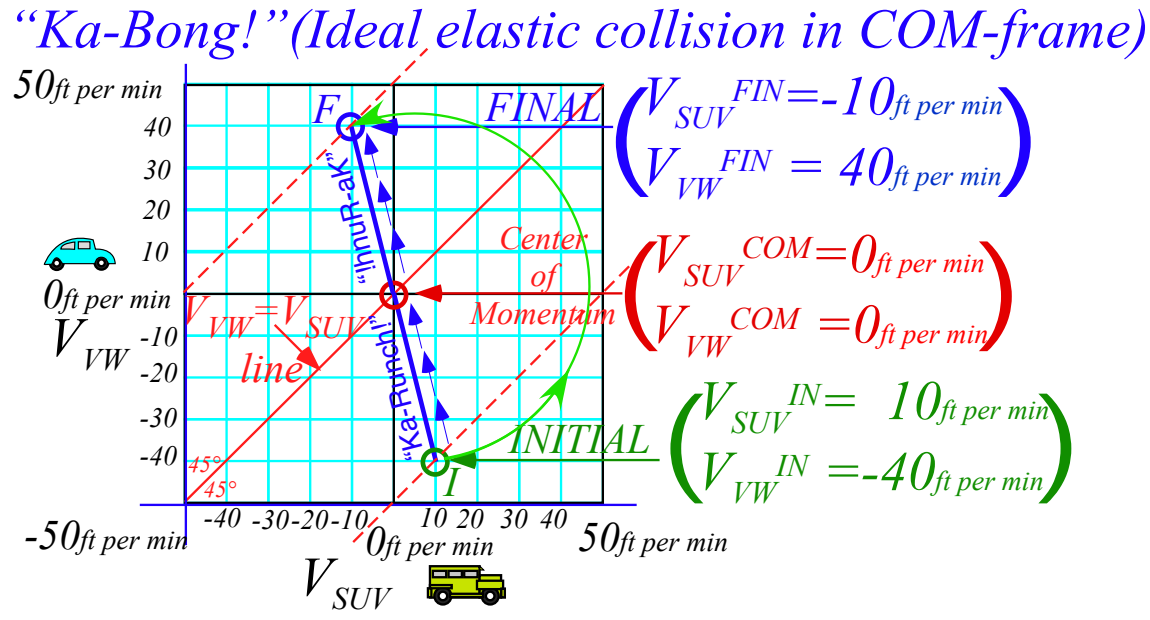

Fig. 2.4 COM-frame or 50mph cop-frame view of a "KaBong" elastic collision of Fig. 2.2.

This is a common situation in physics. The real (or *generic*) world lies between extreme ideals that are easiest to quantify. On one hand, we'll say a *Ka-whump* that ends up close to its inital *COM*-circle is *elastic* or *Ka-Bong-like* and, on the other hand, a *Ka-whump* that stops near its *COM*-point is *inelastic* or *Ka-Runch-like*.

Galilean relativity and spacetime symmetry

Galileo grew up in Renaissance Italy as it flourished from its sea trade. Perhaps, watching ships of trade glide smoothly in the harbor led him to ideas about relativity of velocity. In any case he wrote about comparing what a sailor sees in a ship-frame with what is seen in the Earth-frame. He noted how apparent velocity of an object decreases by subtracting the velocity of the observer's frame.

Subtraction of the cop's velocity $V_{cop}=50$ from Earth-frame velocity $(V_{SUV},V_{VW})=(60,10)$ of SUV and VW in Fig. 2.2 gives their initial velocity $(60,10)-(50,50)=(10,-40)$ in cop-frame. (Fig. 2.4) Such a subtraction (or addition if the cop goes the other way) is a *Galilean relativity transformation*. Fig. 2.4 is a redrawing of Fig. 2.2 with new (V_{SUV},V_{VW}) scales, each reduced by *50mph*. Or else, start with Fig. 2.2 and slide each velocity point down 45°-line by *50mph*, (*COM* /cop-frame Earth-relative velocity) as in Fig. 2.5a.

It is a kind of "slide-rule" in Fig. 2.5b that quantifies several Galilean frames. The initial VW frame (*VW(I)*) is found where the *45°-I-line* hits the horizontal ($V_{VW}=0$) axis. VW starts in frame-*VW(I)* and is hit by a ($V_{SUV}=50$)-SUV that knocks VW into a new frame-*VW(F)* of final $V_{VW}=80$ as SUV slows to a final $V_{SUV}=30$.

Next a final SUV frame (*SUV(F)*) intersects the *45°-F-line* on the vertical ($V_{SUV}=0$) axis where a final *point-*$F_{SUV(F)}$ $(V_{SUV},V_{VW})=(0,50)$ results if initially a ($V_{SUV}=20$)-SUV *Ka-Bongs* a $(V_{VW}=-30)$-VW at *point-*$I_{SUV(F)}$.

Note that seven *Ka-Bong* lines in Fig. 2.5 *show seven different-frame views of the same Ka-Bong*. In four frames, one car has $V=0$ either before *or* after the *Ka-Bong*. One frame, the *COM* has $V_{COM}=0$ before *and* after. That *COM*-frame is balanced to velocity reversal $(+V \leftrightarrow -V)$. Other frames have distinct V-reversed twins with *INITIAL I* and *FINAL F* switched, such as symmetry twins $I_{SUV(F)} \leftrightarrow F_{SUV(I)}$ and $F_{SUV(F)} \leftrightarrow I_{SUV(I)}$ on each side of the central *COM*-frame in Fig. 2.5b.

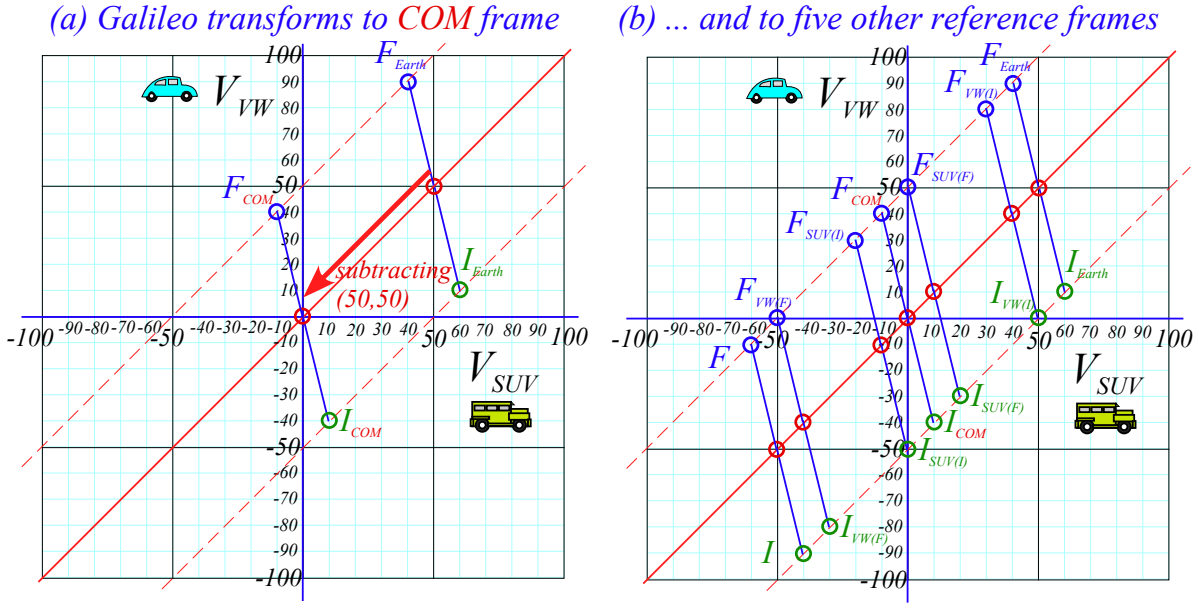

Fig. 2.5 Galilean transform of "KaBong" in Fig. 2.2 to (a) COM-frame and (b) to other frame views.

Geometry of Balance: Center of Momentum (COM) and Center of Gravity (COG)

The uniqueness and constancy of a *COM* for the SUV and VW is connected with underlying space-time symmetry or geometry of spatial balance in Newton's equation (2.1) repeated here in different forms.

$$P_{Total} = P_{SUV} + P_{VW} = M_{SUV} \cdot V_{SUV} + m_{VW} \cdot V_{VW} = M_{TOTAL} \cdot V_{COM} = constant \qquad (2.5a)$$

Total momentum is a product of V_{COM} and total mass $M_{TOTAL}=M_{SUV}+m_{VW}$ of a 5-ton SUV-VW "hunk". This holds whether the "hunk" forms permanently in a *Ka-Runch* or the cars bounce off in a *Ka-Bong* or *Ka-whump*. Both $P_{Total} = M_{TOTAL} \cdot V_{COM}$ and V_{COM} are constant throughout the collision regardless of "auto-elasticity."

$$V_{COM} = \frac{M_{SUV} \cdot V_{SUV} + m_{VW} \cdot V_{VW}}{M_{SUV} + m_{VW}} = \underset{\text{weighted average of } V_{SUV} \text{ and } V_{VW}}{M_{SUV}:m_{VW}} = \frac{constant}{M_{TOTAL}} \qquad (2.5b)$$

Weighted average V_{COM} of (V_{SUV}, V_{VW}) is fixed as V go from *initial* to *in-between* to *final* values. Collisions in Fig. 2.1 thru Fig. 2.5 all have $V_{COM}=50$ in the Earth frame. The *4:1*-weighted average of each coordinate pair *(40,90)*, *(50,50)*, *(60,10)*, *(70,-30)*,*etc.* on the slope-*(-1:4)*-line (in Fig. 2.6a below) is $V_{COM}=50$.

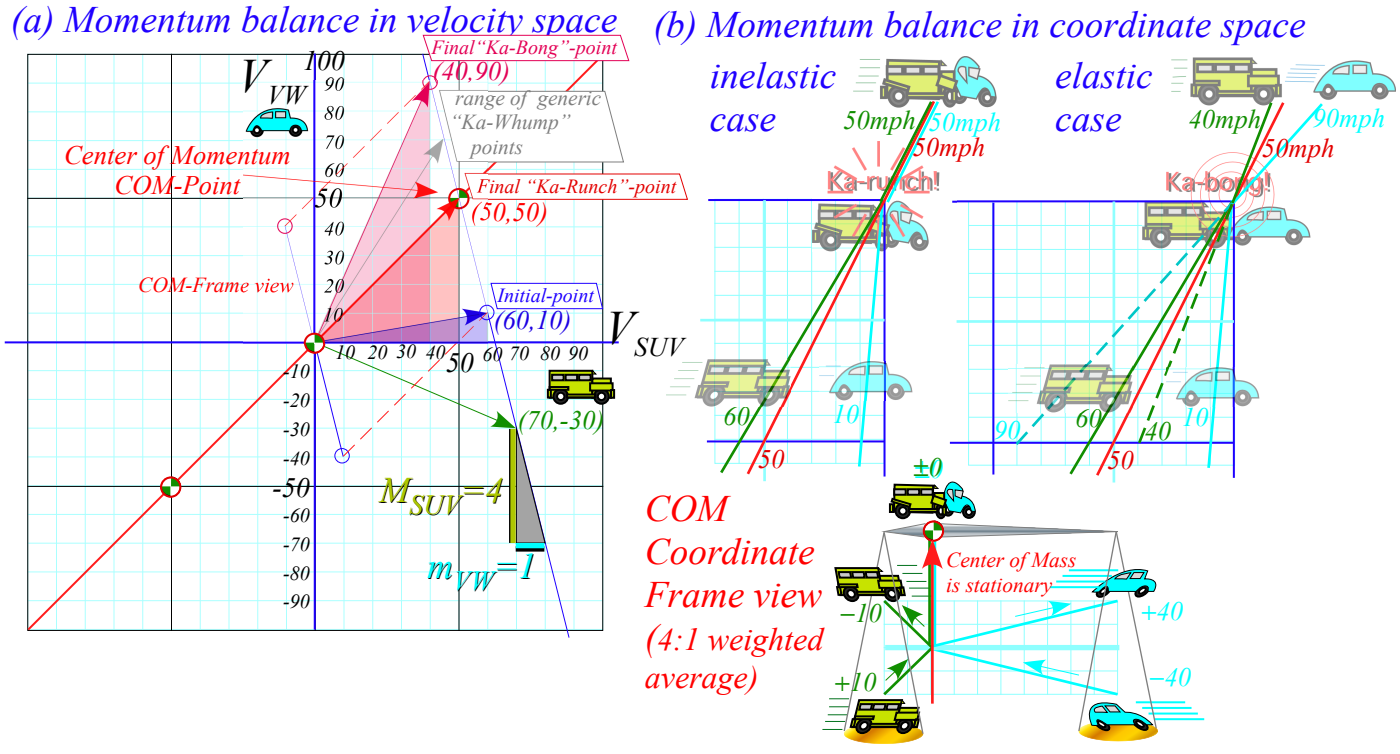

Fig. 2.6 Geometry of (a) 4:1-weighted velocity average (b) 4:1-weighted coordinate average.

Balance between *velocity* V_{SUV} and V_{VW} in (2.5b) relates to balance between *position* x_{SUV} and x_{VW}.

$$x_{COM} = \frac{M_{SUV} \cdot x_{SUV} + m_{VW} \cdot x_{VW}}{M_{SUV} + m_{VW}} = \underset{\text{weighted average of } x_{SUV} \text{ and } x_{VW}}{M_{SUV}:m_{VW}} \qquad (2.5c)$$

As SUV and VW close, collide, bounce, or stick, the *Center of Mass* x_{COM} stays at a constant velocity V_{COM}. In the *COM* frame that velocity is zero as sketched in the lower part of Fig. 2.6b. The weighted average x_{COM} in (2.5c) of coordinates x_{SUV} and x_{VW} is also a *Center of Gravity* and is cartooned by a 4:1 Greek balance.

Exercise 1.2.1

Redraw Fig. 2.5 for initial speeds $(V_{SUV}=40, V_{VW}=10)$ with the SUV only twice the mass of the VW. (Hummer-Lite) Include also a line describing the frame in which the SUV is initially stationary and another for which the SUV is finally stationary.

Chapter 3. Velocity and energy

We noted that reflection symmetry or balance in *space* is connected with *momentum* or $P=m\cdot V$ conservation. Uniformity or "sameness" of coordinate and velocity space means the SUV can lose a unit of momentum only if the VW gains that unit, and *vice versa*. Momentum is a zero-sum game that does not depend on whether the two protagonists bounce elastically or crumple in-elastically during their collisions.

Time symmetry and energy conservation

Now we consider symmetry or balance in *time*. This is connected with a something called *energy* that also plays a conservation zero-sum game but, unlike momentum, requires elastic *(Ka-Bong!)* collisions. While momentum conservation is *axiomatic*, energy conservation is *derived* by algebra or geometry. Let's do that.

Time symmetry

Symmetry balance in Fig. 2.6 is between pairs of velocity values (V_{SUV},V_{VW}) or spatial coordinates (x_{SUV},x_{VW}) of the colliding SUV and VW. Weighted average (2.5b) equals the same V_{COM} for the initial pair $(V_{SUV}^{IN},V_{VW}^{IN})$, the final pair $(V_{SUV}^{FIN},V_{VW}^{FIN})$, or a pair $(V_{SUV}(t),V_{VW}(t))$ at anytime t. (*Recall (2.1) and (2.5), too.*)

$$P_{Total}=M_{Total}V_{COM}=M_{SUV}V_{SUV}^{IN}+M_{VW}V_{VW}^{IN}=M_{SUV}V_{SUV}^{FIN}+M_{VW}V_{VW}^{FIN}=etc. \qquad (3.1)$$

We subtract *IN*'s from *FIN*'s to isolate SUV terms from VW terms and redo *zero-sum relation* (2.3).

$$0=P_{Total}-M_{SUV}V_{SUV}^{IN}-M_{VW}V_{VW}^{IN}=M_{SUV}(V_{SUV}^{FIN}-V_{SUV}^{IN})+M_{VW}(V_{VW}^{FIN}-V_{VW}^{IN}) \qquad (3.2a)$$

$$0=M_{SUV}\cdot(\Delta V_{SUV})\qquad +M_{VW}\cdot(\Delta V_{VW}) \qquad (3.2b)$$

(Ch.1 reviews *Delta* notation $\Delta V=V^{FIN}-V^{IN}$.) Here is another way to write the zero-sum relation.

$$M_{SUV}(V_{SUV}^{FIN}-V_{SUV}^{IN})=M_{VW}(V_{VW}^{IN}-V_{VW}^{FIN}) \qquad (3.3)$$

Now consider balancing *IN vs. FIN* pair $(V_{SUV}^{IN},V_{SUV}^{FIN})$ for SUV or $(V_{VW}^{IN},V_{VW}^{FIN})$ for VW. Elastic *(Ka-Bong!)* cases in Fig. 2.2 or Fig. 2.6 show how V_{COM} is a balanced *IN-vs.-FIN* pair-average of *both* SUV *and* VW.

$$V_{COM}=\tfrac{1}{2}(V_{SUV}^{FIN}+V_{SUV}^{IN})=\tfrac{1}{2}(V_{VW}^{FIN}+V_{VW}^{IN}) \qquad (3.4)$$

This is an algebraic statement of a *time reversal symmetry* axiom or *IN vs. FIN balance* mentioned earlier. For ideal elastic *(Ka-Bong!)* collisions, *IN* and *FIN* points balance around the *COM* point. Switching past and future gives a similar *Ka-Bong* and not a miraculous "*un-crash*" where V^{FIN} ends up further from V_{COM} than V^{IN} was.

Kinetic Energy conservation

A definition of energy emerges from multiplying *space and time balance equations* (3.3) with (3.4)

$$\tfrac{1}{2}(V_{SUV}^{FIN}+V_{SUV}^{IN})M_{SUV}(V_{SUV}^{FIN}-V_{SUV}^{IN})=\tfrac{1}{2}(V_{VW}^{FIN}+V_{VW}^{IN})M_{VW}(V_{VW}^{IN}-V_{VW}^{FIN})$$
$$\tfrac{1}{2}M_{SUV}(V_{SUV}^{FIN})^2-\tfrac{1}{2}M_{SUV}(V_{SUV}^{IN})^2=\tfrac{1}{2}M_{VW}(V_{VW}^{IN})^2-\tfrac{1}{2}M_{VW}(V_{VW}^{FIN})^2 \qquad (3.3)\cdot(3.4)$$

Then adding the *(-)*-terms to both sides isolates *IN*-terms. A *FIN*-sum is proved to equal an *IN*-sum.

$$\tfrac{1}{2}M_{SUV}(V_{SUV}^{FIN})^2+\tfrac{1}{2}M_{VW}(V_{VW}^{FIN})^2=\tfrac{1}{2}M_{VW}(V_{VW}^{IN})^2+\tfrac{1}{2}M_{SUV}(V_{SUV}^{IN})^2 \qquad (3.5a)$$

This derives a second quantity $1/2M\cdot V^2$ (or just $M\cdot V^2$) whose conserved sum is assured by the axiom (2.5a) (conserved sum of momentum $M\cdot V$) and *t*-reversal axiom (3.4). ($M\cdot V$ is conserved by *x*-reversal symmetry.)

This $1/2M\cdot V^2$ is *kinetic energy (KE)* and it is conserved by a relation like (2.5a) for *momentum* $P=M\cdot V$.

$$constant = KE_{Total} = KE_{SUV}^{FIN} + KE_{VW}^{FIN} = KE_{SUV}^{IN} + KE_{VW}^{IN} \quad \text{where: } KE = \tfrac{1}{2} M\cdot V^2 \qquad (3.5b)$$

$$constant = P_{Total} = P_{SUV}^{FIN} + P_{VW}^{FIN} = P_{SUV}^{IN} + P_{VW}^{IN} \quad \text{where: } P = M\cdot V \qquad (2.5a)_{repeated}$$

Conservation holds for any overall factor so the factor-$1/2$ in (3.5a) looks fortuitous. But, KE is defined later by integral $KE=\int V\cdot dP$ or area $KE=1/2\ P\cdot V=1/2M\cdot V^2$ of a triangle with base $P=M\cdot V$ and altitude V. Thus $(3.3)\cdot(3.4)$ is product $\bar{V}\cdot\Delta P=\int V\cdot dP=1/2M\cdot V^2$ of Δp and V-average $\bar{V}=(V^{IN}+V^{FIN})/2$. Fig. 3.1 below also verifies the $1/2$.

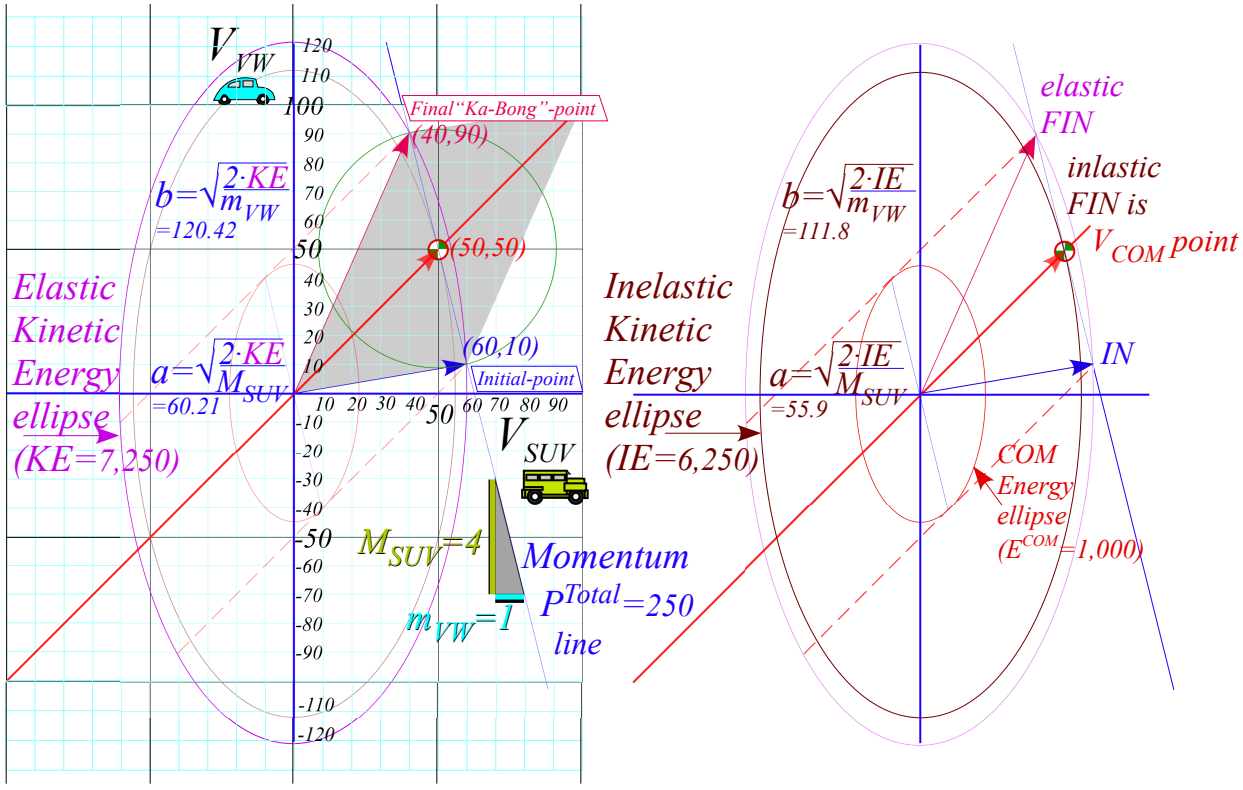

Fig. 3.1 Elastic KE-ellipse hits (P^{Total})-line at IN and FIN pts. Inelastic IE-ellipse hits only at V_{COM} pt.

Geometry of kinetic energy ellipse and momentum line

First, P-conservation relation (2.5a) is rearranged to show its geometry.

$$m_{VW}\cdot V_{VW}+M_{SUV}\cdot V_{SUV}=(M_{SUV}+m_{VW})\cdot V_{COM} \quad becomes: \quad V_{VW}-V_{COM}=-\frac{M_{SUV}}{m_{VW}}(V_{SUV}-V_{COM}) \qquad (3.6a)$$

The V_{SUV}-vs-V_{VW}-plot of (3.6a) in Fig. 3.1 is a line of slope $-M_{SUV}/m_{VW}$ thru the *COM*-point (V_{COM},V_{COM}).

$$y-y_0=m\cdot(x-x_0) \quad \text{where: } \begin{cases}(x,y) = (V_{SUV},V_{VW})\\ (x_0,y_0)=(V_{COM},V_{COM})\end{cases} \text{ and: } m=-\frac{M_{SUV}}{m_{VW}} \qquad (3.6b)$$

Then KE conservation relation (3.5a) is rearranged by placing KE and masses into denominator.

$$\tfrac{1}{2}M_{SUV}\cdot V_{SUV}{}^2+\tfrac{1}{2}m_{VW}\cdot V_{VW}{}^2=KE \qquad becomes: \qquad \frac{V_{SUV}^2}{\left(\frac{2\cdot KE}{M_{SUV}}\right)}+\frac{V_{VW}^2}{\left(\frac{2\cdot KE}{m_{VW}}\right)}=1 \qquad (3.7a)$$

The V_{SUV}-vs-V_{VW}-plot (3.7a) in Fig. 3.1 is *KE*-ellipse (3.7b) of x-radius a and y-radius b to match (3.7a).

$$\frac{x^2}{a^2}+\frac{y^2}{b^2}=1 \qquad \text{where: } \begin{cases}(x,y)= & (V_{SUV},V_{VW})\\ (a,b)=(\sqrt{\frac{2\cdot KE}{M_{SUV}}},\sqrt{\frac{2\cdot KE}{m_{VW}}}) & \end{cases} \qquad (3.7b)$$

Fig. 3.1 also shows an inelastic *Ka-runch-IE*-ellipse inside and a small *KE*-ellipse seen in the *COM*-frame. Elastic $KE\ (V_{SUV}=60,\ V_{SUV}=10)$, inelastic $IE(50,\ 50)$, and $E^{COM}(10,\ 40)$ in *COM* frame is worked out for Fig. 3.1.

$$\tfrac{1}{2}4\cdot 60^2+\tfrac{1}{2}\,1\cdot 10^2=7{,}250 \qquad \tfrac{1}{2}4\cdot 50^2+\tfrac{1}{2}\,1\cdot 50^2=6{,}250 \qquad \tfrac{1}{2}4\cdot 10^2+\tfrac{1}{2}\,1\cdot 40^2=1{,}000 \qquad (3.8)$$

The difference in energy between the two extreme types of collision, *Ka-Bong* and *Ka-runch*, is *1,000* units in the Earth frame and *1,000* units in the *COM* frame. But, only in the *COM* frame does the *Ka-runch!* take *all* the kinetic energy and leave both cars standing still. Galilean symmetry has "cost" of damage be the same in all frames. A generic *Ka-whump* will only lose some fraction of $E^{COM}=1{,}000$ inelastic crumpling.

A fine point of Fig. 3.1 geometry deserves notice. The tangent slope to the *IE*-ellipse at pt-*(50, 50)* on the *45°(slope-1)-COM*-line is that of the momentum line, namely $-M_{SUV}/m_{VW}=-4$. Conversely, slope of dashed tangent lines to the $E^{COM}(10,\ 40)$-ellipse on $(slope=-M_{SUV}/m_{VW})$-line is that of the *COM*–line, namely *slope-1*. This beautiful duality is an important part of mechanics, both classical and quantum. Here it has *IN* and *FIN* points stay on a $(slope=-M_{SUV}/m_{VW})$-line *even as they coalesce to a tangent point of non-collision!* Head-on $(V^{IN}_{SUV}=3, V^{IN}_{VW}=-4)$ collisions are plotted in Fig. 3.2 below showing increasing inelasticity in parts (b) and (c). (These involve a $M_1=6$*ton SUV* satisfying Bush gas-hog entitlement.) The final KE-ellipse shrinks from the initial elastic *Ka-Bong* ellipse to a smaller inelastic *Ka-whump* ellipse ($E^{whump}=23\,1/3$ in Fig. 3.2b is chosen arbitrarily) and to the totally inelastic *Ka-runch*-ellipse ($IE=14$ in Fig. 3.2c).

The generic "in-between-ideals" or *Ka-whump* cases will each have *two* possible final *F*-points where the momentum line cuts the *Ka-whump* ellipse. The top F_{whump} point represents the partial rebound. Below is its symmetry point $F_{Pass\text{-}thru}$ that represents cars *passing through each other*. Fortunately, that's not a usual highway event (and not very survivable). But in a quantum wave world it is the most common case.

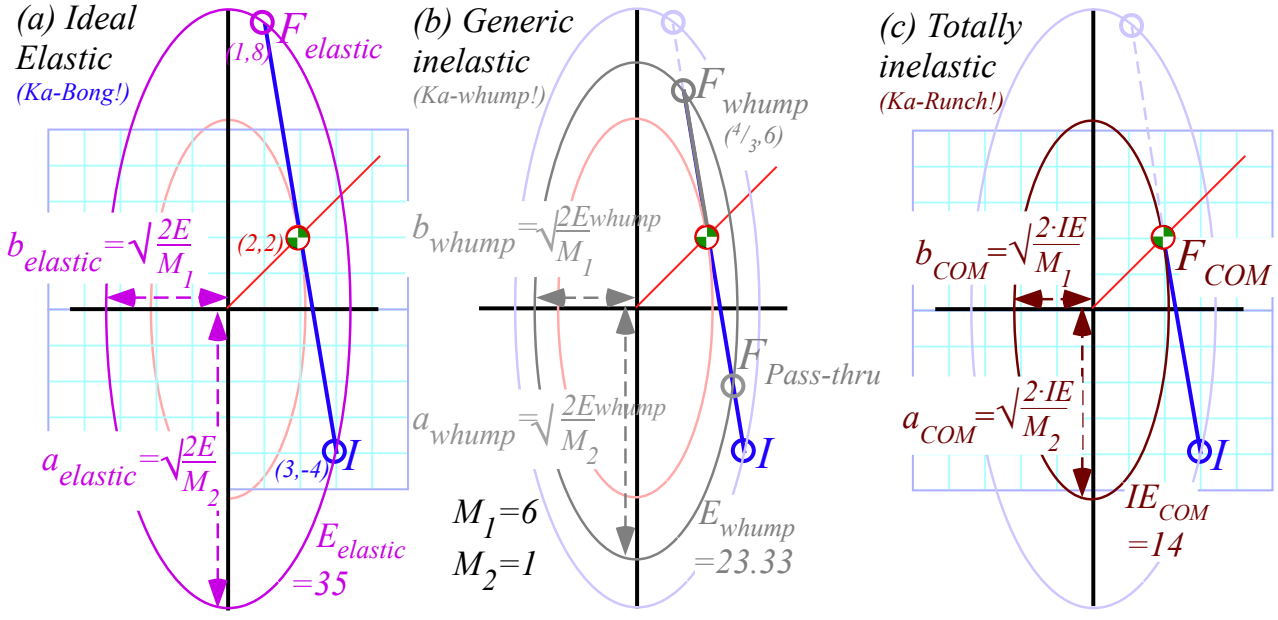

Fig. 3.2 ($V_1=3$, $V_2=-4$) collisions. (a) Elastic ($E^{loss}=0$). (a) Generic ($E^{loss}=11\,2/3$). (a) Inelastic ($E^{loss}=21=E^{COM}$).

Introducing vector and tensor geometry of momentum-energy conservation

We now introduce a generalization of classical energy-momentum using vector-tensor or matrix notation prevalent in the modern physics. Equations (3.1) thru (3.8) are dressed up in matrix notation starting with $P=M\cdot V$ definitions. Modern physicists use *inertia* **M**-*tensors* to hold mass coefficients M_1, M_2...etc.

$$\left.\begin{aligned} P_{SUV} &= M_{SUV}V_{SUV} \\ P_{VW} &= M_{VW}V_{VW} \end{aligned}\right\} denoted: \vec{\mathbf{P}} = \ddot{\mathbf{M}}\cdot\vec{\mathbf{V}} \quad or: \begin{pmatrix} P_{SUV} \\ P_{VW} \end{pmatrix} = \begin{pmatrix} M_{SUV} & 0 \\ 0 & M_{VW} \end{pmatrix}\begin{pmatrix} V_{SUV} \\ V_{VW} \end{pmatrix} \tag{3.9a}$$

Later we will need to upgrade to a full matrix of n^2 inertial coefficients M_{jk} for any dimension n.

$$\left.\begin{aligned} P_1 &= M_{11}V_1 + M_{12}V_2 \\ P_2 &= M_{21}V_1 + M_{22}V_2 \end{aligned}\right\} \quad denoted: \vec{\mathbf{P}} = \ddot{\mathbf{M}}\cdot\vec{\mathbf{V}} \quad or: \begin{pmatrix} P_1 \\ P_2 \end{pmatrix} = \begin{pmatrix} M_{11} & M_{12} \\ M_{21} & M_{22} \end{pmatrix}\begin{pmatrix} V_1 \\ V_2 \end{pmatrix} \tag{3.9b}$$

Fig. 3.3 plots (3.10) below. (Recall Fig. 3.1 plot of (3.1) with 45° diagonal $\mathbf{V}^{COM}$ so: $V_1^{COM} = V_2^{COM} = V^{COM}$.)

$$P_{Total} = M_1V_1^{IN} + M_2V_2^{IN} = M_1V_1^{FIN} + M_2V_2^{FIN} = M_1V^{COM} + M_2V^{COM} = M_{Total}V^{COM} \tag{3.10}$$

A product of total momentum P_{Total} and V^{COM} is expressed by *tensor quadratic forms* **v•M•u** as follows.

$$V^{COM}P_{Total} = \vec{\mathbf{V}}^{COM}\cdot\ddot{\mathbf{M}}\cdot\vec{\mathbf{V}}^{IN} = \vec{\mathbf{V}}^{COM}\cdot\ddot{\mathbf{M}}\cdot\vec{\mathbf{V}}^{FIN} = \vec{\mathbf{V}}^{COM}\cdot\ddot{\mathbf{M}}\cdot\vec{\mathbf{V}}^{COM} = V^{COM}M_{Total}V^{COM} \tag{3.11a}$$

It helps to write this out with the numbers appearing in the original Fig. 3.1 starting with $V^{COM} = 50$.

$$\begin{aligned} 50P_{Total} &= \begin{pmatrix} 50 & 50 \end{pmatrix}\cdot\begin{pmatrix} 4 & 0 \\ 0 & 1 \end{pmatrix}\cdot\begin{pmatrix} 60 \\ 10 \end{pmatrix} = \begin{pmatrix} 50 & 50 \end{pmatrix}\cdot\begin{pmatrix} 4 & 0 \\ 0 & 1 \end{pmatrix}\cdot\begin{pmatrix} 40 \\ 90 \end{pmatrix} = 50M_{Total}50 = 12{,}500 \\ &= 100\cdot125 = 100\cdot125 = 50\cdot250 \end{aligned} \tag{3.11b}$$

(3.11) says momentum $P_{Total}=250$ is the same at IN, FIN, and COM. Now use T-symmetry: $\vec{\mathbf{V}}^{COM}=(\vec{\mathbf{V}}^{FIN}+\vec{\mathbf{V}}^{IN})/2$

$$\begin{aligned} V^{COM}P_{Total} &= \frac{\vec{\mathbf{V}}^{FIN}+\vec{\mathbf{V}}^{IN}}{2}\cdot\ddot{\mathbf{M}}\cdot\vec{\mathbf{V}}^{IN} = \frac{\vec{\mathbf{V}}^{FIN}+\vec{\mathbf{V}}^{IN}}{2}\cdot\ddot{\mathbf{M}}\cdot\vec{\mathbf{V}}^{FIN} = \frac{\vec{\mathbf{V}}^{FIN}+\vec{\mathbf{V}}^{IN}}{2}\cdot\ddot{\mathbf{M}}\cdot\frac{\vec{\mathbf{V}}^{FIN}+\vec{\mathbf{V}}^{IN}}{2} \\ V^{COM}P_{Total} - \frac{\vec{\mathbf{V}}^{FIN}\cdot\ddot{\mathbf{M}}\cdot\vec{\mathbf{V}}^{IN}}{2} &= \frac{\vec{\mathbf{V}}^{IN}\cdot\ddot{\mathbf{M}}\cdot\vec{\mathbf{V}}^{IN}}{2} = \frac{\vec{\mathbf{V}}^{FIN}\cdot\ddot{\mathbf{M}}\cdot\vec{\mathbf{V}}^{FIN}}{2} = \frac{\vec{\mathbf{V}}^{IN}\cdot\ddot{\mathbf{M}}\cdot\vec{\mathbf{V}}^{IN}}{4} + \frac{\vec{\mathbf{V}}^{FIN}\cdot\ddot{\mathbf{M}}\cdot\vec{\mathbf{V}}^{FIN}}{4} \end{aligned} \tag{3.12a}$$

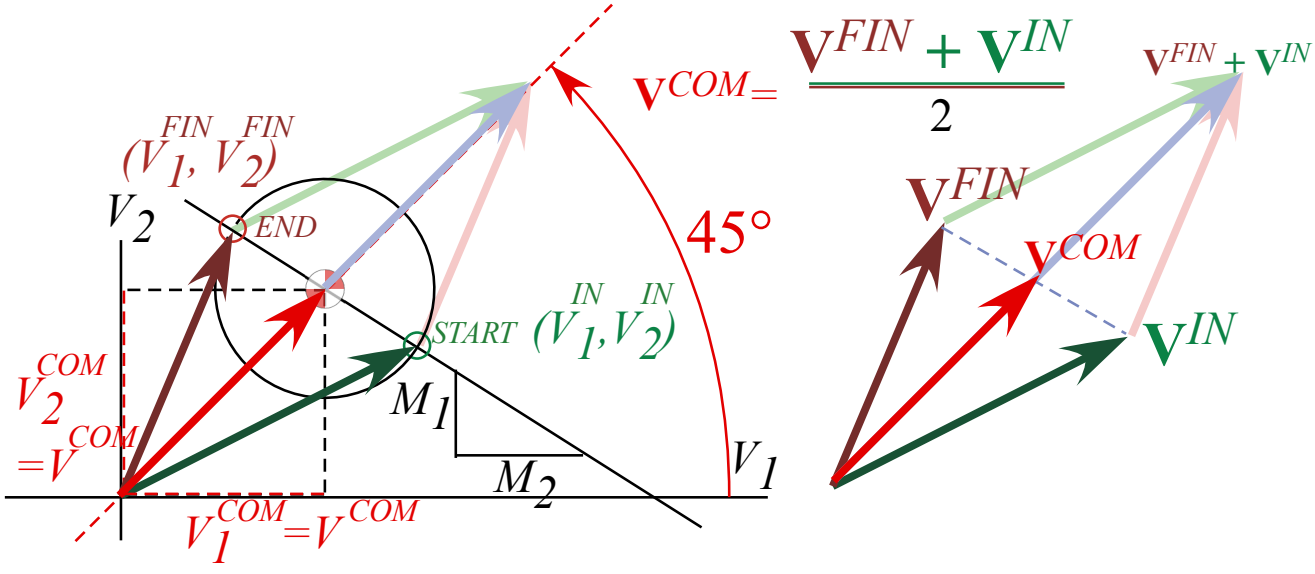

Fig. 3.3 Generic collision geometry. (Recall Fig. 3.1.)

Line-2 of (3.12a) uses *transpose symmetry* ($M_{jk}=M_{kj}$) of the **M**-matrix so that $\vec{V}^{FIN}\cdot\vec{\mathbf{M}}\cdot\vec{V}^{IN}=\vec{V}^{IN}\cdot\vec{\mathbf{M}}\cdot\vec{V}^{FIN}$.

$$\begin{array}{ccc} \vec{V}^{FIN}\cdot\vec{\mathbf{M}}\cdot\vec{V}^{IN} & = & \vec{V}^{IN}\cdot\vec{\mathbf{M}}\cdot\vec{V}^{FIN} \\ \begin{pmatrix}40 & 90\end{pmatrix}\cdot\begin{pmatrix}4 & 0\\ 0 & 1\end{pmatrix}\cdot\begin{pmatrix}60\\ 10\end{pmatrix} & = & \begin{pmatrix}60 & 10\end{pmatrix}\cdot\begin{pmatrix}4 & 0\\ 0 & 1\end{pmatrix}\cdot\begin{pmatrix}40\\ 90\end{pmatrix} \\ = \quad 100\cdot 105 & = & 100\cdot 105 \quad = 10{,}500 \end{array} \tag{3.12b}$$

In our case ($M_{12}=0=M_{21}$) and that implies kinetic energy $KE_{Elastic}=\frac{1}{2}\vec{V}\cdot\vec{\mathbf{M}}\cdot\vec{V}$ is the same at IN and FIN.

$$\begin{array}{ccccccc} V^{COM}P_{Total} & - & \frac{\vec{V}^{FIN}\cdot\vec{\mathbf{M}}\cdot\vec{V}^{IN}}{2} & = & \frac{\vec{V}^{IN}\cdot\vec{\mathbf{M}}\cdot\vec{V}^{IN}}{2} & = & \frac{\vec{V}^{FIN}\cdot\vec{\mathbf{M}}\cdot\vec{V}^{FIN}}{2} \quad = KE_{Elastic} \\ 12{,}500 & - & \frac{10{,}500}{2} & = & \frac{\begin{pmatrix}60 & 10\end{pmatrix}\cdot\begin{pmatrix}4 & 0\\ 0 & 1\end{pmatrix}\cdot\begin{pmatrix}60\\ 10\end{pmatrix}}{2} & = & \frac{\begin{pmatrix}40 & 90\end{pmatrix}\cdot\begin{pmatrix}4 & 0\\ 0 & 1\end{pmatrix}\cdot\begin{pmatrix}40\\ 90\end{pmatrix}}{2} \quad = KE_{Elastic} \\ 12{,}500 & - & 5{,}250 & = & 7{,}250 & = & 7{,}250 \end{array} \tag{3.12c}$$

However, kinetic energy $IE=\frac{1}{2}\vec{V}\cdot\vec{\mathbf{M}}\cdot\vec{V}$ in Fig. 3.1 is reduced by *1,000* at COM. That is calculated from (3.12c).

$$\begin{array}{ccccccccc} KE_{Inelastic}=\frac{1}{2}V^{COM}P_{Total}=\frac{\vec{V}^{COM}\cdot\vec{\mathbf{M}}\cdot\vec{V}^{COM}}{2} & = & \frac{\vec{V}^{IN}\cdot\vec{\mathbf{M}}\cdot\vec{V}^{IN}}{4} & + & \frac{\vec{V}^{FIN}\cdot\vec{\mathbf{M}}\cdot\vec{V}^{IN}}{4} & = & \frac{1}{2}KE_{Elastic} & + & \frac{\vec{V}^{FIN}\cdot\vec{\mathbf{M}}\cdot\vec{V}^{IN}}{4} \\ \frac{12{,}500}{2} & = & 6{,}250 & = & 3{,}625 & + & 2{,}625 & = & IE \end{array} \tag{3.13}$$

That difference is inelastic "crunch" energy $KE-IE$ or, for elastic cases, potential energy of compression.

$$\begin{array}{ccccc} KE_{Elastic}-KE_{Inelastic} & = & \frac{\vec{V}^{IN}\cdot\vec{\mathbf{M}}\cdot\vec{V}^{IN}}{4} & - & \frac{\vec{V}^{FIN}\cdot\vec{\mathbf{M}}\cdot\vec{V}^{IN}}{4} \\ 1{,}000 & = & 3{,}625 & - & 2{,}625 \quad = KE-IE \end{array} \tag{3.14}$$

Potential energy is given by *spatial* tensor quadratic forms such as $PE_{Elastic}=\frac{1}{2}\vec{r}\cdot\vec{\mathbf{K}}\cdot\vec{r}=V(r)$ detailed later. *Tensors* probably get their name from this application to tension and stress energy.

You should note that the less motivated development between (3.1) and (3.5) is improved by a tensor development from (3.11) thru (3.14). The former does not suggest the *(3.3)·(3.4)* product as easily as the latter suggests the rearrangements going from (3.11) to (3.12) or (3.13). Also arithmetic is displayed clearly and is easier to enter in a computer program involving a full *M* matrix of any dimension. Finally, (3.12) shows clearly that kinetic energy is conserved if and only if *M* is transpose-symmetric ($M_{jk}=M_{kj}$).

Tensor forms describe quadratic curves such as ellipses in Fig. 3.1 and the following.

$$1=\vec{r}\cdot\vec{\mathbf{M}}\cdot\vec{r}=\begin{pmatrix}x & y\end{pmatrix}\cdot\begin{pmatrix}1/a^2 & 0\\ 0 & 1/b^2\end{pmatrix}\cdot\begin{pmatrix}x\\ y\end{pmatrix}=\frac{x^2}{a^2}+\frac{x^2}{b^2} \tag{3.15}$$

Geometry of tensor operator forms is beautiful and powerful for mathematics and physics as will be shown in later chapters. In quantum theory they define expectation $\langle r|M|r\rangle$ and transition $\langle r|M|s\rangle$ amplitudes.

Momentum vs. energy (Bang! for the $buck$!): Standard (mks) units

What are *momentum P* and *energy E*, really? A flippant answer is *Bang!* for the *$Buck$*. We pay a lot of bucks in order to get some bangs in our autos, for example. A less flippant answer based on space-time relativity and quantum wave theory must wait until later. But, we can discuss relations involving $P=M\cdot V$ and $E=M\cdot V^2/2$ and review proper *meter-kilogram-second (mks)* units to replace haphazard geometrical units used so far. Velocity is *V meters per second* ($m\cdot s^{-1}$) and Momentum is $P=M\cdot V$ *kilogram meters per second* ($kg\cdot m\cdot s^{-1}$).

Energy is $E=M\cdot V^2/2$ *kilogram (meters per second)*^{2} $(kg\cdot m^2\cdot s^{-2})$. The E unit is such a mouthful that there is a famous name for it: $1\ (kg\cdot m^2\cdot s^{-2}) = 1$ *Joule* $= 1\ J$.

Our collision analysis did not mention the *Force F* that SUV or VW feel during their encounters. Force is the *rate* of being banged in *bangs per second*, or units of momentum delivered per second, or in (*mks*), *F kilogram meters per second per second* $(kg\cdot m\cdot s^{-2})$. The F unit is another mouthful with a *very* famous name: $1\ (kg\cdot m\cdot s^{-2}) = 1$ *Newton* $= 1\ N$. *Note:* 1 *Joule* $= 1$ *Newton* $\cdot$*meter* $= 1\ N\cdot m$ is a common unit of *Work*, that is, "*Force-times-Distance.*" Also, 1 *Joule per meter* $= 1\ J\cdot m^{-1} = 1$ *Newton* is a "*potential force*" unit.

Another important unit is that of *power* Π, the *rate* of *$bucks$ paid per second*, or in (*mks*), Π *Joule per second*. The famous-name power unit is 1 *Watt* $= 1$ *Joule per second* $= 1\ J\cdot s^{-1}$.

Here is a list of geometric slope and area definitions of important classical mechanical quantities.

Velocity V is slope $V=\frac{\Delta x}{\Delta t}$ on graph *x(t)* of *position x vs.* time *t*. *Position x(t)* is area $\int V\,dt$ of *V(t) vs. t*.

Force F is slope $F=\frac{\Delta P}{\Delta t}$ on graph *P(t)* of *momentum P vs.* time *t*. *Momentum P(t)* is area $\int F\,dt$ of *F(t) vs. t*.

Force F is slope $F=\frac{\Delta E}{\Delta x}$ on graph *E(x)* of *energy E vs.* position *x*. *Energy E(x)* is area $\int F\,dx$ of *F(x) vs. x*.

Power Π is slope $\Pi=\frac{\Delta E}{\Delta t}$ on graph *E(t)* of *energy E vs.* time *t*. *Energy E(t)* is area $\int \Pi\,dt$ of $\Pi(t)$ *vs. t*.

These and other relations (in calculus form) are collected below in preparation for discussion later on.

Quick review of kinetic relations and formulas

The suffix *kinetic* refers to energy connected directly to velocity of motion ("*kinos*" means *moving*). Kinetic energy *KE* is distinct from *potential energy* (*PE* is "stored" energy) or entropic energy (*entropy* is chaotic or "trashed" energy like *heat*) that is reviewed later in Ch. 6 and Ch. 7.

We now give a quick algebraic run-down of energy-related formulas to be introduced with more detail and geometry in Ch. 7. (See (7.5a) to (7.5d) in particular.) Readers with calculus or physics knowledge may use this to review to connect our geometrical developments with the more conventional ones.

Relations of energy W and space x

Energy or *work* may be defined by a delta-*work* product $\Delta W=F\cdot\Delta x$ of force F and *distance*-Δx-pushed. More precisely, W is an integral $\int_0^{\Delta x} F\cdot dx$, the area of a *Fvs.x* work-plot. *Power*, a time rate $\Pi=\frac{\Delta W}{\Delta t}$ of energy production, is the product $\Pi=F\cdot V$ of force and velocity $V=\frac{\Delta x}{\Delta t}=\frac{dx}{dt}$. So, $\Delta W=\Pi\cdot\Delta t$ or $W=\int_0^{\Delta t}\Pi\cdot dt=\int_0^{\Delta t} F\cdot V\cdot dt=\int F\cdot dx$.

Relations of momentum P and time t

Momentum may be defined by a delta-*momentum* product $\Delta P=F\cdot\Delta t$ of force F and *time* interval Δt. More precisely, P is an integral $\int_0^{\Delta t} F\cdot dt$, the area of a *Fvs.t* plot. *Force*, a time rate $F=\frac{\Delta P}{\Delta t}=\frac{dP}{dt}$ of momentum production, is a product $F=M\cdot a$ of mass and *acceleration* $a=\frac{\Delta V}{\Delta t}$. ($F=M\cdot a$ is called *Newton's "2nd Law."*)

With $F=\frac{dP}{dt}$, energy integral $W=\int_0^{\Delta t}\Pi\cdot dt=\int_0^{\Delta t} F\cdot V\cdot dt$ is $W=\int_0^{\Delta t} F\cdot V\cdot dt=\int_0^{\Delta t}\frac{dP}{dt}\cdot V\cdot dt=\int V\cdot dP$, the area under a *V vs.P* plot where $P=M\cdot V$ is momentum. For a single mass M this area is kinetic energy: $\frac{1}{2}M\cdot V^2$.

Table 3.1 of kinetic relations

Position or space	*Velocity or time-rate*	*Acceleration or time-rate*
$x = \int V \cdot dt$	*of position* $: V = \frac{dx}{dt}$	*of velocity* $: a = \frac{dV}{dt}$

Work or Energy	*Power or time-rate*	*Impulse or momentum*	*Force or time-rate*
$E = \int \Pi \cdot dt = \int F \cdot dx$ $= \int F \cdot V \cdot dt$ $= \int V \cdot dP = \frac{1}{2} M \cdot V^2$	*of Energy* $: \Pi = \frac{dE}{dt}$	$P = \int F \cdot dt \simeq M \cdot V$	*of momentum* $: F = \frac{dP}{dt} = M \cdot a$
(3.16a)	(3.16b)	(3.16c)	(3.16d)

Exercise 1.3.1

Plot a $(V_{SUV\text{-}1}, V_{SUV\text{-}2}) = (60,10)$ collision like Fig. 3.1 but with an identical $M=4$ SUV replacing the VW.

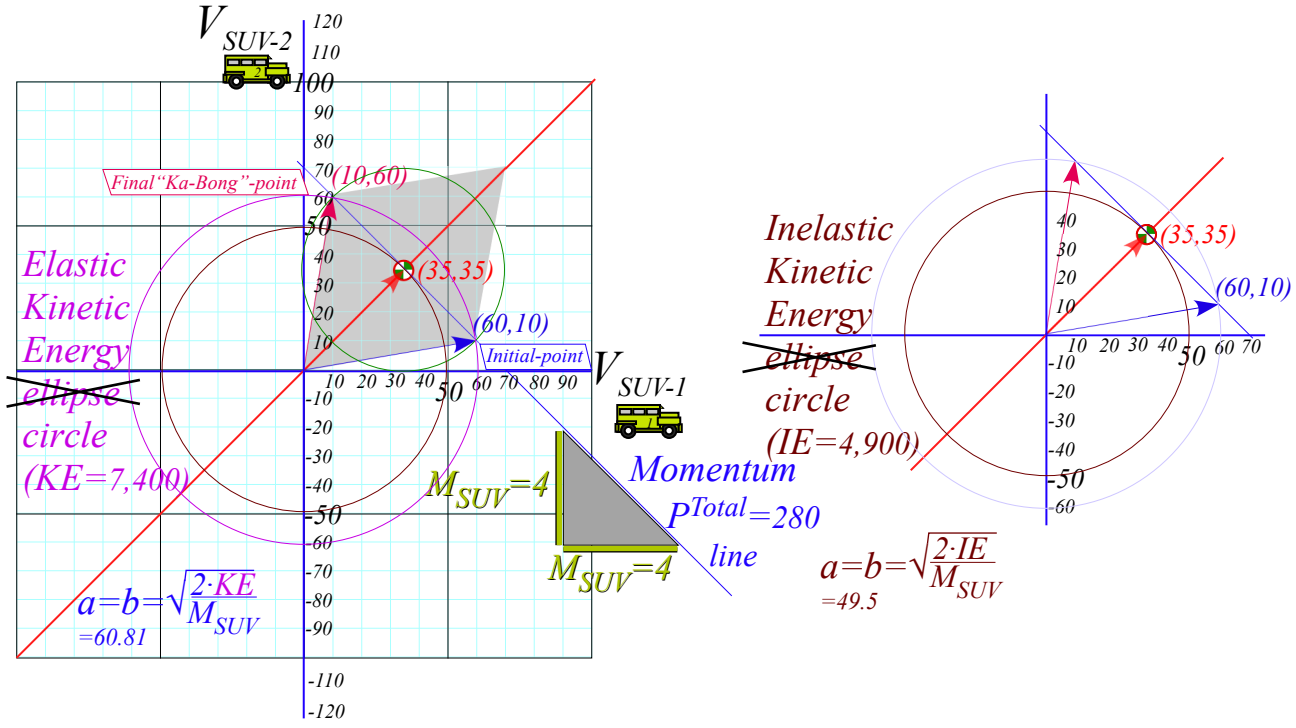

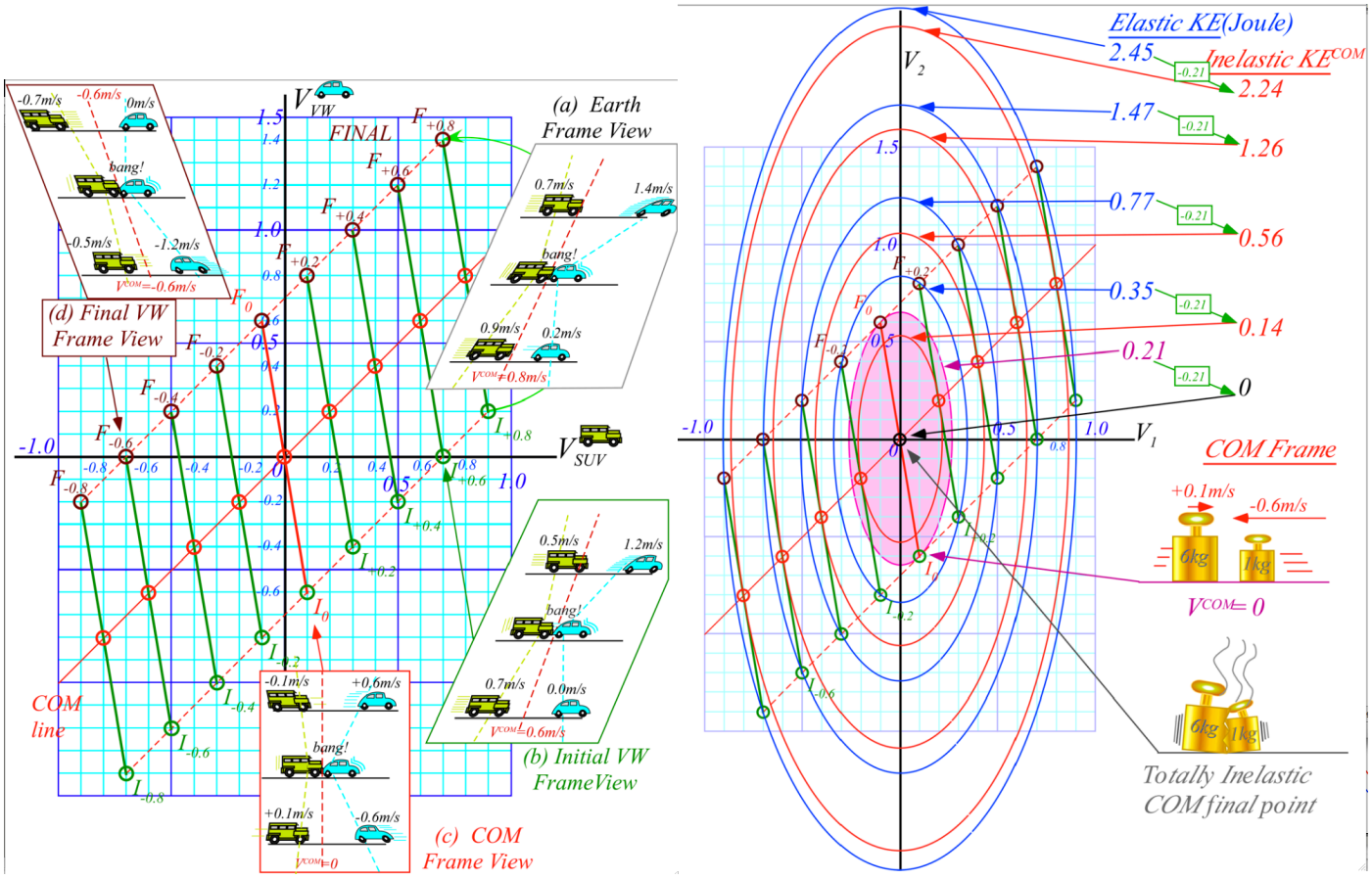

Fig. 3.4 Galilean Frame Views of collision like Fig. 2.5 or Fig. 3.1 with Bush SUV. (a) Earth frame view (b) Initial VW frame (VW initially fixed) (c) COM frame view (d) Final VW frame (VW ends up fixed)

Fig. 3.5 Momentum (P=const.)-lines and energy (KE=const.)-ellipses appropriate for Fig. 3.4.

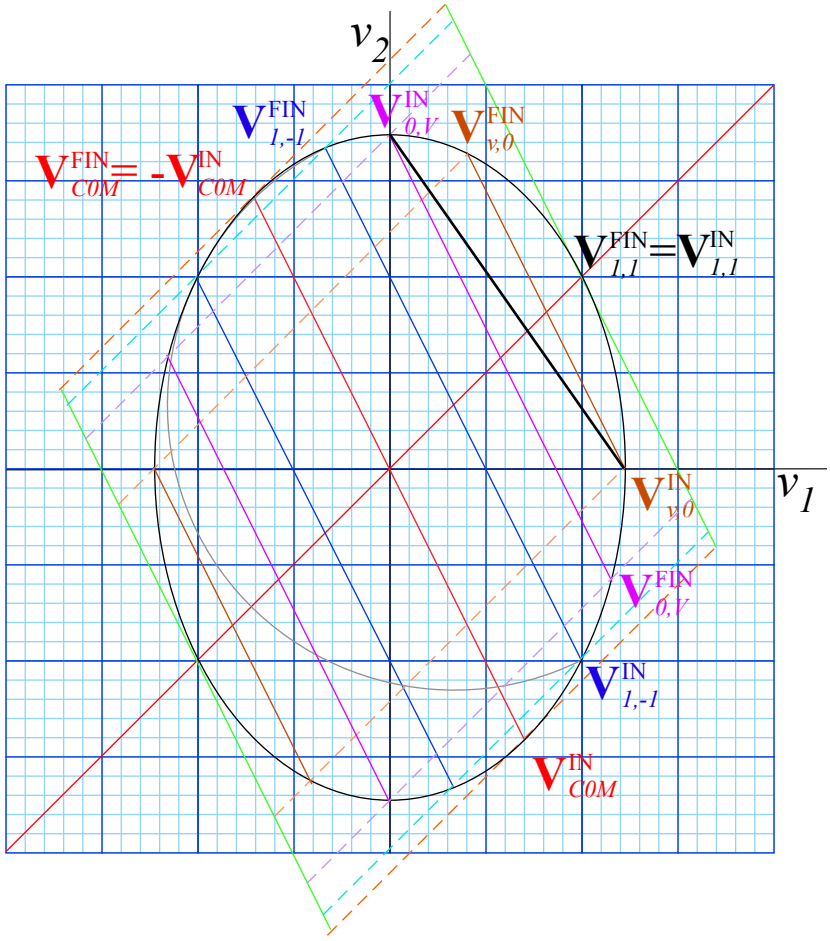

Exercise 1.3.2. Ch. 1-5 contains geometric description of 1D-2-body collisions. Most examples originate from initial velocity vectors $\mathbf{V}^{IN}_{1,-1} = (1,-1)$ for which m_1 and m_2 have equal speeds (in this case *unit* speed).

This exercise is intended to help match algebra and geometry by asking for the simplest formulas for the various velocities in a figure above that are final elastic results of the following initial velocity vectors.

a. $\mathbf{V}^{IN}_{1,-1} = (1,-1)$ b. $\mathbf{V}^{IN}_{v,0} = (v,0)$ c. $\mathbf{V}^{IN}_{0,V} = (0,V)$ d. $\mathbf{V}^{IN}_{COM} = (v_x^{COM}, v_y^{COM})$

Derive the IN and FIN components of all vectors in terms of masses m_1 and m_2 only assuming the same total KE as $\mathbf{V}^{IN}_{1,-1} = (1,-1)$ has. (Check your results against figure in which ratio $2=m_1/m_2$ holds.)

Indicate where the time reversed vector $\mathbf{T}\cdot\mathbf{V}^{IN}$ of each $\mathbf{V}^{IN}$ lies.
Give a formula for the orange (dashed) and green (solid) tangent line slopes in terms of m_1 and m_2.
…and compare to slope of the black line connecting major and minor radii in terms of m_1 and m_2.

Exercise 1.3.3. Quick construction of Energy ellipses

Graph paper facilitates construction of energy ellipses given the two radii *a* and *b* in (3.7). The first step is to draw concentric circles of radius *a* and *b*. Then any radial line OBA "points" to a point E on the ellipse. Ellipse point E lies at the intersection of a vertical line AE thru radial intersection A with circle *a* and a horizontal line BE thru radial intersection B with circle *b*.

Graph grid "finds" E for a radius OBA, no need to draw AE or BE. You can pick *x* and find *y* or *vice-versa*.

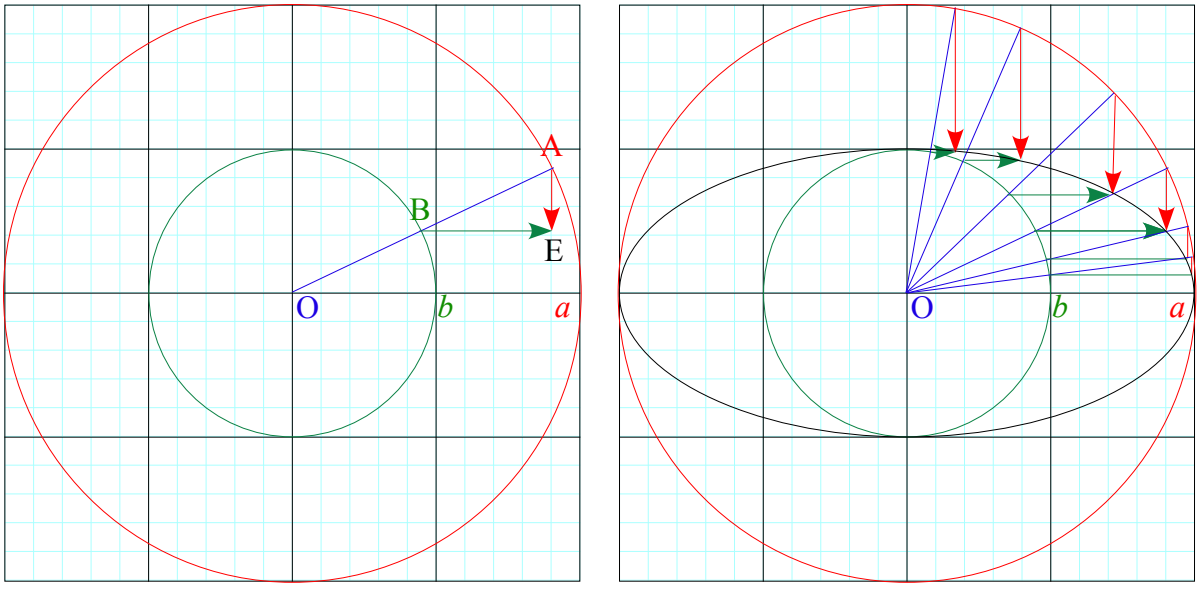

Exercise Fig. 3.6 Ellipse construction

Ellipse coordinates ($x_E=a\cdot\cos\sigma$, $y_E=b\cdot\sin\sigma$) are rescaled base and altitude ($x_r=r\cdot\cos\sigma$, $y_r=r\cdot\sin\sigma$) of Fig. 1.4.

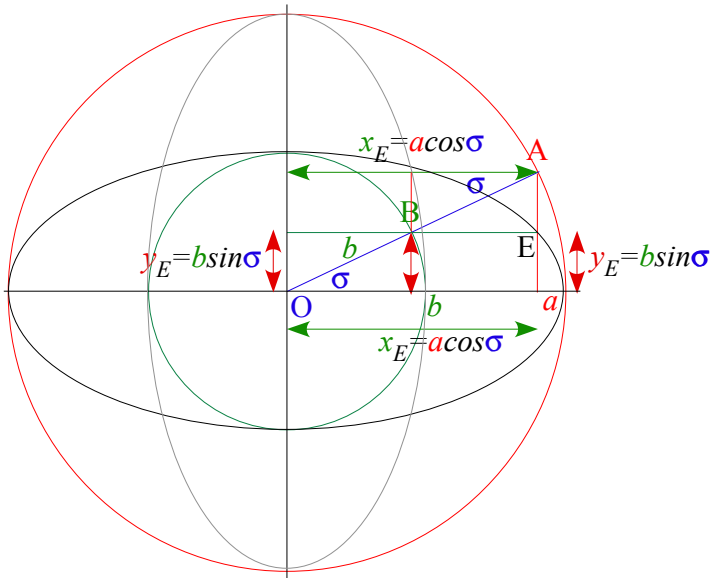

Exercise Fig. 3.7 Complimentary analytic ellipse geometry

Verify that the values ($x=a\cdot\cos\sigma$, $y=b\cdot\sin\sigma$) satisfy an ellipse equation (3.7b).

A dual or complimentary (gray) ellipse results if compliment angle $\sigma_c=\pi/2-\sigma$ is used so *x* and *y* values switch.

Chapter 4. Dynamics and geometry of successive collisions

Mechanics gets difficult for many collisions, dimensions, or masses. A single one-dimensional two-mass (1D-2-body) collision occupies Ch. 2-3. Now we do more dangerous things such as an X2-super bouncer from *Project Ball*, a 1969 class project. (*Am. J. Phys.* **39**, 656 (1971)) See product liability disclaimer in Fig. 4.1.

Caution: Product Liablility Disclaimer
This ballpoint pen could be hazardous to your health! The experiments which are the subject of this discussion are both spectacular and potentially dangerous, and care to protect one's eyes should be taken. The simplest experiment involves sticking a ball point pen into a superball or other hard rubber ball and dropping the two onto a hard floor. If done correctly the pen will eject the ball with such force it may stick in the ceiling of the room. Obviously you want to be careful with this weapon. And, this goes doubly and triply for the more advanced models that may be developed in the course of studying this stuff. It is recommended that experimenters wear safety glasses when doing these experiments with pens. (We could just say don't use pens, but that's an easy way to do this experiment and probably the way most people will go about it.) Some of the tangential experiments associated with this development are less hazardous. To measure the potential force function of a ball one may simply paint the ball and measure the spot size as a function of drop height *h*.

The saggital approximation $d=r^2/2R$ allows one to quickly convert spot radius *r* to penetration depth *x* for a superball of radius *R* as shown in the figure. Equating this to *Mgh* gives the ball potential energy function *V(x)*.

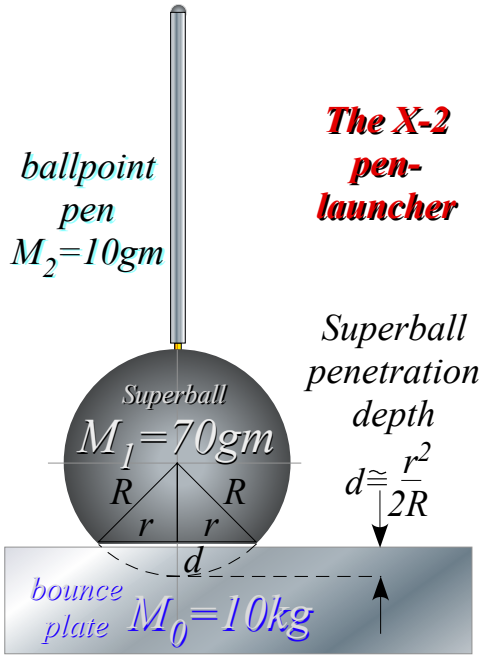

Fig. 4.1 The X2-pen launcher with product liability disclaimer.

At first, the X2 looks like a 1D-2-body device. A *superball*(©™*Whammo Corp.*) of mass $M_1 = 70gm$ launches a ballpoint pen of mass $M_2 = 10gm$. But, it has a 3rd body, bounce plate mass-$M_O = 10kg$ shown by a rectangle in Fig. 4.1. Actually the third body most responsible for this experiment is good old Mother Earth of mass $M_\oplus = 6{\cdot}10^{24}\,kg$. (Earth mass $M_\oplus$ and solar mass $M_\odot = 2{\cdot}10^{30}\,kg$ are good-to-2-figure numbers for astrophysicists to remember. More precisely: $M_\oplus = 5.9742{\cdot}10^{24}\,kg$ and $M_\odot = 1.9891{\cdot}10^{30}\,kg$.)

Collisions of very large with very small masses beg thorny questions (Like, *"What IS mass?"* or how do we deal with it?) As a mass ratio M_1/M_2 approaches zero or infinity the slope of the *P*-conservation line in (V_1,V_2)-space *(Recall Fig. 3.2.)* approaches infinity or zero, respectively, as drawn in Fig. 4.2(a-b).

Geometric construction in Fig. 4.2a of final velocity for an elastic collision is a vertical reflection thru the *COM* point ($V_1=V_2$) on the *P*-line if $M_1 >> M_2$ or else a horizontal reflection in Fig. 4.2b if $M_1 << M_2$. Inelastic final points approach the *COM* point more closely if inelasticity is significant. (Recall Fig. 3.2.)

You should understand how a relatively large mass may give huge momentum to a smaller one but transfer only tiny amounts of energy. Each *P*-line in Fig. 4.2 is part of a KE-ellipse. In the *COM* frame (where the *COM* point is at origin) the *P*-line sits on top of an entire *E*-ellipse as the ratio M_1/M_2 approaches *(a)*

infinity or *(b)* zero. I visualize COM *P*-lines as ultra-thin ellipses between I_0 and F_0 and other *P*-lines in Fig. 4.2 as segments of a KE-ellipse that has *(a)* a huge V_2-axis $\sqrt{2E/M_2}$ or *(b)* a huge V_1-axis $\sqrt{2E/M_1}$.

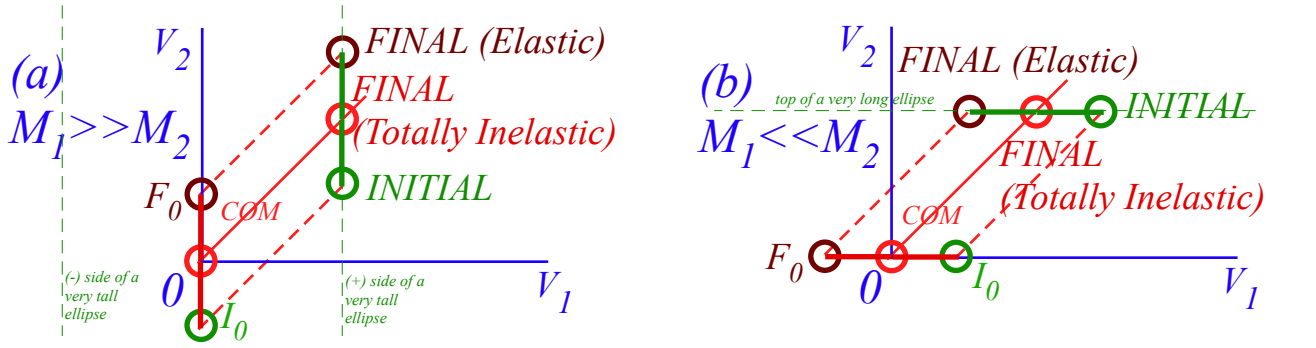

Fig. 4.2 Extreme mass-ratio collisions (a) M_1/M_2 approaches infinity. (b) M_1/M_2 approaches zero.

Fig. 4.2a reflects our common experience of a bouncy ball of mass M_2 hitting the Earth of mass $M_\oplus$ with velocity $-V_0$*(point* I_0*)* and being reflected with velocity $+V_0$*(point* F_0*)*. While standing in the Earth frame, one is very nearly in the COM frame, too. Earth's COM velocity is a tiny fraction $M_2/M_\oplus$ of the apparent ball velocity V_0. For super-balls of mass M_2=60*gm*, the fraction $M_2/M_\oplus$ is $0.06/(6\cdot10^{24})=10^{-26}$.

Bounce momentum absorbed by Earth is $2\,M_2V_0$ (or M_2V_0 if the ball goes *"Ka-runch!"*) but Earth absorbs at most a tiny KE of $\frac{1}{2}M_\oplus(V_0M_2/M_\oplus)^2$, that is, a fraction 10^{-26} of ball KE: $\frac{1}{2}M_2(V_0)^2$. Moreover, for elastic collisions, Mother Earth returns *all* the *KE* to M_2 but she absorbs *double* momentum $P=2\,M_2V_0$.

However, common experience does not prepare us for X2 easily rebounding M_2 with more than *twice* its drop velocity in Fig. 4.3. (As we'll see that means M_2 rises to more than *four* times its drop height!)

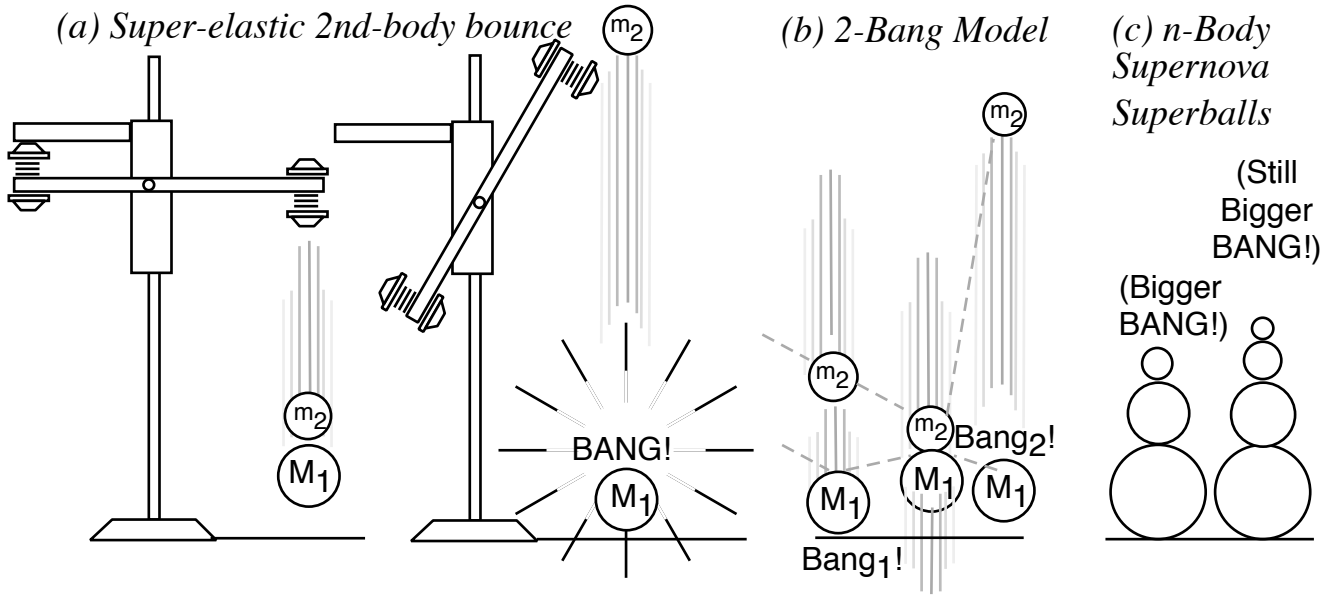

Fig. 4.3 n-Body collision experiments. (a) X-2 drop. (b) Independent collision model. (c) Ball towers.

Independent collision models (ICM)

To compute final velocities of M_1 and M_2 it helps to idealize the collision of three bodies M_1, M_2, and $M_\oplus$ as a sequence of two separate 2-body collisions that are completely determined by P and KE conservation. First M_1 bounces off Earth $M_\oplus$. Only then does M_1 knock M_2 to a faster speed as in Fig. 4.3b. The first collision is labeled *Bang-1*$_{(01)}$ in Fig. 4.4a followed by *Bang-2*$_{(12)}$ in Fig. 4.4b. The first *Bang-1*$_{(01)}$ between Earth $M_\oplus$ and M_1 has a horizontal line like the I_0F_0 line in Fig. 4.2b. The second *Bang-2*$_{(12)}$ between mass M_1 and M_2 has a line of slope $-M_1/M_2 = -7$ for a $M_1 = 70gm$ and $M_2 = 10gm$ (that of a superball and pen, respectively). The *Bang-2*$_{(12)}$ line is like the *IF* line in Fig. 3.1 or Fig. 3.2.

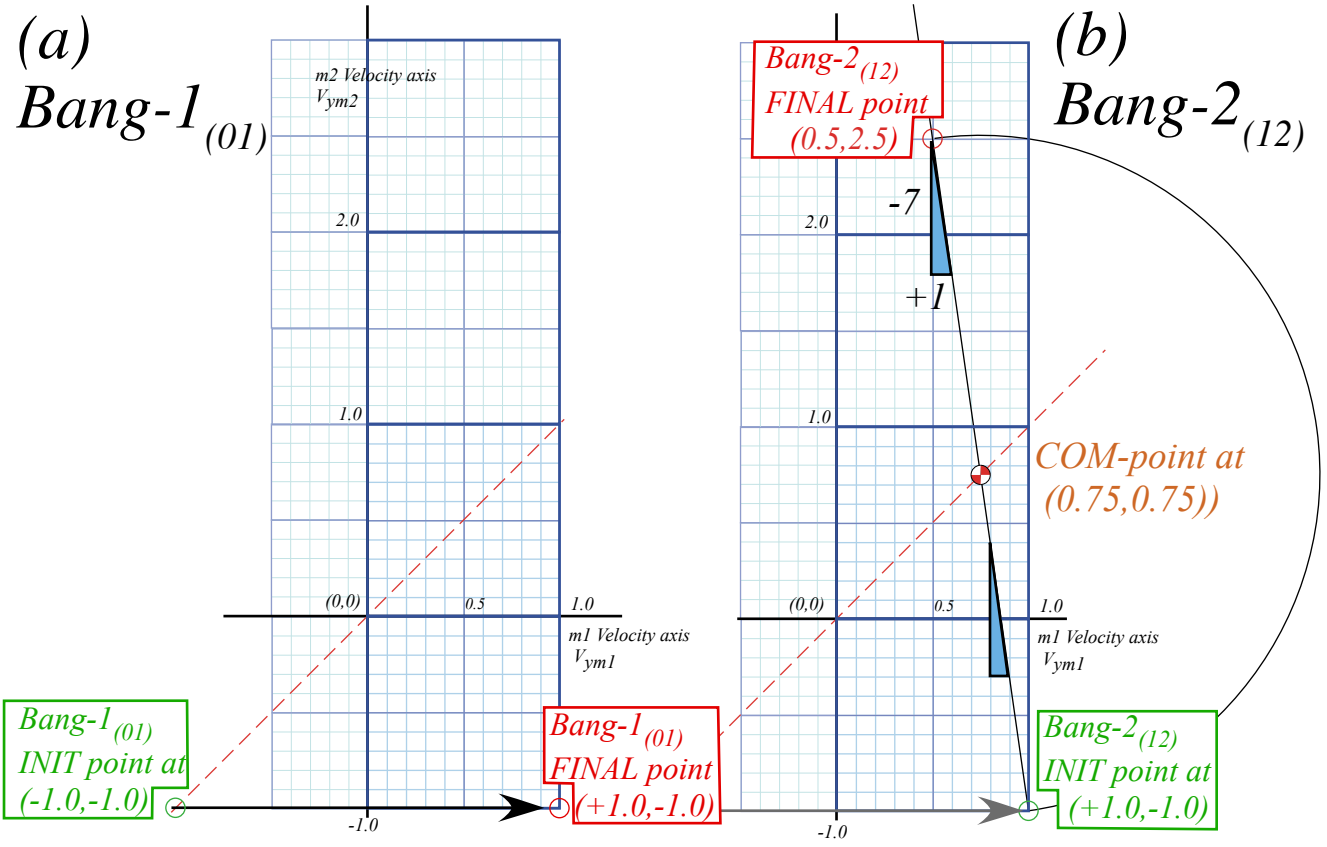

Fig. 4.4 (V_1-V_2)-plot of 2-Bang collision. (a) M_1 bounces off floor. (b) M_1 hits M_2 head-on.

This approximation is called an *independent collision model* (ICM) and is one secret to analyzing such 1D-3-body bang-up that otherwise has too many unknown velocities to be found by just two equations $\Delta P=0$ and $\Delta KE=0$ alone. ICM is exactly true if we initially separate M_1 and M_2 so three M_1, M_2, and $M_\oplus$ never *collectively* bargain for available momentum and energy. ICM also applies to n-ball towers in Fig. 4.3c. They give very high-energy ejections and serve as classical models for supernovae. (N-body bangs are in Ch.8.)

Velocity geometry suggests a family of X2 solutions as shown in Fig. 4.5 for a range of mass ratio M_1/M_2. This is an advantage of geometric solutions. Just a few points in Fig. 4.5a show all elastic $(V_1$-$V_2)$ points lie on the 45°-line *CPL*. Extreme or optimal cases are located in Fig. 4.5b.

Extreme and optimal cases

First, the upper limit for elastic final velocity is $V_2=3\cdot V_0$ at pt-***I*** for infinite mass ratio $M_1/M_2\rightarrow\infty$. If no energy is lost, a particle of dust on a superball could be ejected three times the speed that the ball hits the floor. (And, it could go *nine* ($9=3^2$) times the drop height. However, the elastic ICM model is not so good for tiny M_2 due to weak molecular forces. So bouncing balls don't embed dust in ceilings. (But in a vacuum...!)

Second, an optimal performance case is shown by pt-***M*** where the collision achieves a 100% transfer of energy to projectile M_2. The ***M***-point is the intersection of the *CPL* line with the V_2-axis on which the M_1-ball velocity is zero. ($V_1=0$) There mass ratio is $M_1/M_2=3.0$, the slope of the ***M***-line.

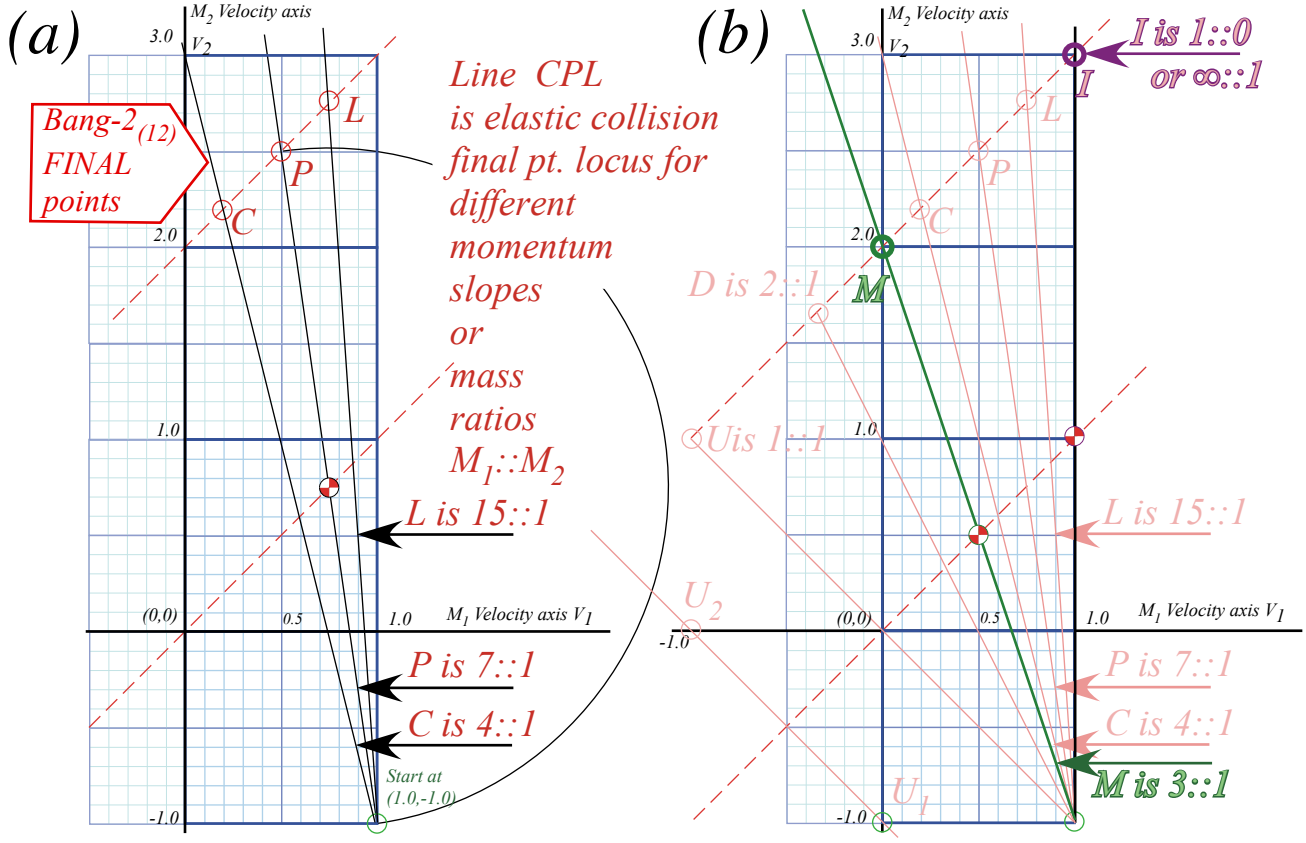

Fig. 4.5 X2-Final (V_1,V_2) (a) Final point locus. (b) Infinite ratio pt. I and maximum transfer pt. M.

Another singular point ***U*** is for unit ratio $M_1/M_2=1$, a familiar ratio for players of billiards or pool. ***U*** undergoes inversion of velocities *(+1,-1)->(-1,+1)*. (Its COM point lies at origin.) If the ***U***-line is boosted by (-1) to *(0,-2)->(-2,0)* it is like a straight elastic pool shot. A 100% of *KE* transfers from a moving ball to an equal sized ball that was stationary. The same process at half that speed is *(0,-1)->(-1,0)* shown by the Galileo-shifted line $\boldsymbol{U}_1\text{->}\boldsymbol{U}_2$ in the lower left hand side of Fig. 4.5b.

Points ***D*** between ***U*** and ***M*** have ball M_1 knocked to negative velocity by the down-coming M_2. Then M_1 hits the floor (Earth) at velocity $-v$ to rebound at $+v$. For unit ratio case ***U***, M_1 and M_2 rebound quite like a rigid body. Below ***U***, ball M_1 rebounds at a speed faster than M_2 to hit M_2 again. In cases of low mass ratio, $(M_1/M_2<<1)$ mass M_1 must hit M_2 many times to turn it around. We will study this effect shortly.

Integrating velocity plots to find position

It is important to see how velocity values of Fig. 4.4b are turned into space-time position plot lines. Consider the first collision (*Bang-1*$_{(10)}$) in Fig. 4.6a and corresponding space-time paths in Fig. 4.6b. Initial velocity $V_{y1}(0)=-1.0$ gives a slope *(distance)/(time)* of an M_1 path but doesn't tell *where* is the path or particle. The same for velocity $V_{y2}(0)=-1$ of M_2 in Fig. 4.6a. The paths need location, location,…

Initial position values such as ($y_1(0)=1$, $y_2(0)=3$) locate the paths as shown in Fig. 4.6b. Each path keeps its slope until a collision (*Bang-1*$_{(10)}$) between M_1 and the floor occurs at $y_1(t=1)$ where its path and the floor intersect. Then, according to Fig. 4.6a, M_1 bounces its slope from $V_{y1}=-1$ up to $V_{y1}=+1$. Meanwhile, the upper path (M_2) maintains its down slope of $V_{y2}=-1$ until it intersects the rising path of M_1.

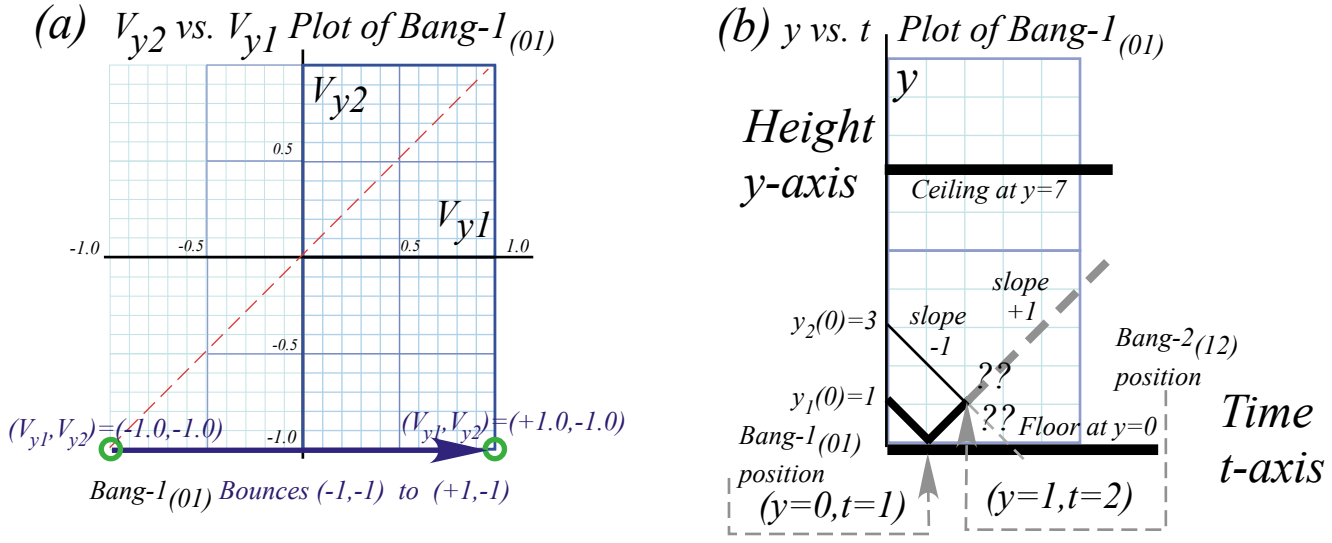

Fig. 4.6 Plots of 1st collision (Bang-1$_{(10)}$*). (a) Velocity-velocity plot. (b) Space-time plot.*

At time *(t=2)* there is an intersection of paths and the 2nd collision (*Bang-2*$_{(12)}$) between M_1 and M_2 at space-time point ($y_1(2)=1$, $y_2(2)=3$). This gives $V_{y1}=0.5$ and $V_{y2}=2.5$ in Fig. 4.4b or in Fig. 4.7a-b below. Then to keep M_2 from flying away we install an elastic ceiling at $y=7$.

The game becomes more interesting as *Bang-3*$_{(20)}$ between the ceiling (part of Earth $M_\oplus$) is shown in Fig. 4.7b by a vertical arrow (like an *IF* line in Fig. 4.2a) reflecting M_2 to speed $V_{y2}=-2.5$. Then M_2 has *Bang-4*$_{(12)}$ between M_1 and itself that sends it back to the ceiling at a blistering speed of $V_{y2}=+2.7$ as M_1 returns more slowly toward the floor with velocity $V_{y1}=-0.5$.

The high speed of M_2 lets it go to the ceiling for *Bang-5*$_{(20)}$ and return to knock M_1 down once more (*Bang-6*$_{(12)}$) before M_1 hits the floor at $V_{y1}=-0.9$. (*Bang-7*$_{(10)}$) Then M_2 having lost speed to $V_{y2}=+1.5$ hits the ceiling (*Bang-8*$_{(02)}$) and returns for *Bang-9*$_{(12)}$ with M_1 rising at $V_{y1}=+0.9$.

Masses are treated as point-masses moving along straight lines between collisions in space-time plots. This is an ideal gravity-free ICM approximation with only straight lines in *VV*-plots. So we may derive motion without having to integrate the kinetic equations at the end of Ch. 3.

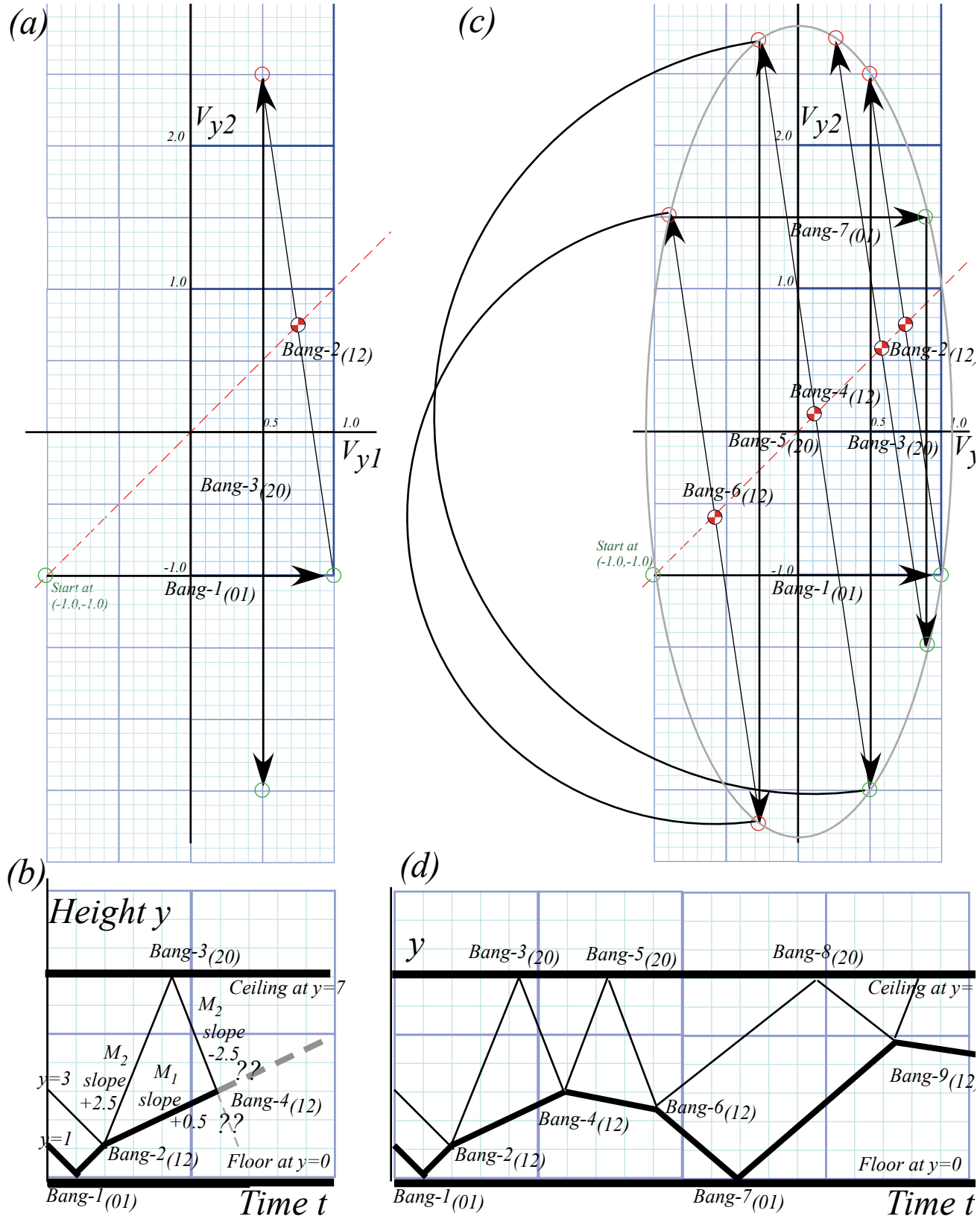

Fig. 4.7 Collision sequence. (a-b) Up to Bang-4(12). (c-d) Up to Bang-9(12).

For comparison, a force-law simulation using *BounceIt* of the bang sequence of Fig. 4.7 is shown in Fig. 4.8. It has finite radius balls instead of ideal point particles, yet compares quite well. (So far as it goes.)

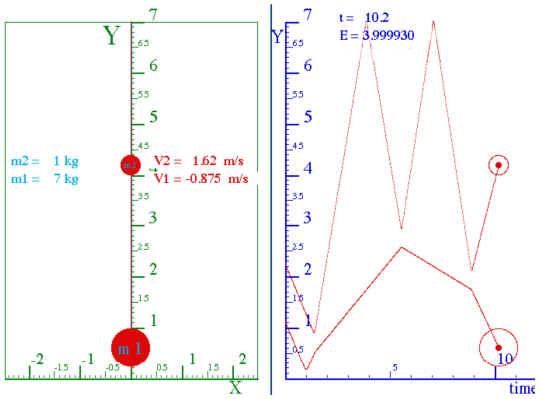

Fig. 4.8 BounceIt x-vs.-t simulation to compare with Fig. 1.4.7d up to Bang-6. (V_1/V_2 =7/1.)

Fig. 4.7c and *BounceIt* V_1-V_2 simulations in Fig. 4.9 build an ellipse out of multiple *IF* lines. (This is a quite *non*-traditional ellipse construction!) Ellipse radii *(a,b)* follow from *KE conservation* equation (3.7b).

$$KE(unit V_1,V_2)=\tfrac{1}{2}M_1 1^2+\tfrac{1}{2}M_2 1^2=\tfrac{1}{2}\cdot 8 \begin{cases} M_1=7 & \text{minor radius } a=\sqrt{2\cdot KE/M_1}=\sqrt{8}=2.828 \\ M_2=1 & \text{major radius } b=\sqrt{2\cdot KE/M_2}=\sqrt{8/7}=1.069 \end{cases}$$

As time increases (Fig. 4.9a to Fig. 4.9c) the ellipse may fill with *IF*-lines that are dense *(ergodic)* or else just retrace sets of paths as in Fig. 4.9b. (Ch. 5 treats non-ergodic paths.) High *sensitivity-to-initial-conditions-or-parameters (STICOP)* means tiny *ICOP* variation has big effects. Extreme *STICOP* gives *stochasticity* or *chaos*.

Vector notation and space-space plots

Balance equation (3.4) concisely sums up preceding constructions or plots of elastic collisions.

$$\begin{aligned} \left(V_1^{FIN}+V_1^{IN}\right)/2=V^{COM} \\ \left(V_2^{FIN}+V_2^{IN}\right)/2=V^{COM} \end{aligned} \quad \text{or:} \quad \begin{aligned} V_1^{FIN}=2V^{COM}-V_1^{IN} \\ V_2^{FIN}=2V^{COM}-V_2^{IN} \end{aligned} \qquad (3.4)_{repeated}$$

More concise notation uses *vector* equations or arrays.

$$\begin{aligned} v_1^{FIN}=2V^{COM}-v_1^{IN} \\ v_2^{FIN}=2V^{COM}-v_2^{IN} \end{aligned} \quad \text{is written:} \quad \begin{pmatrix} v_1^{FIN} \\ v_2^{FIN} \end{pmatrix}=\begin{pmatrix} 2V^{COM}-v_1^{IN} \\ 2V^{COM}-v_2^{IN} \end{pmatrix}=2\begin{pmatrix} V^{COM} \\ V^{COM} \end{pmatrix}-\begin{pmatrix} v_1^{IN} \\ v_2^{IN} \end{pmatrix} \qquad (4.1)$$

It saves writing two (=)'s and two (-)'s. Also, each *column vector* may be labeled by a "fat" letter.

$$\mathbf{v}^{FIN}=\begin{pmatrix} v_1^{FIN} \\ v_2^{FIN} \end{pmatrix}=\vec{\mathrm{v}}^{FIN}, \qquad \mathbf{V}^{COM}=\begin{pmatrix} V^{COM} \\ V^{COM} \end{pmatrix}=\vec{\mathrm{V}}^{COM}, \qquad \mathbf{v}^{IN}=\begin{pmatrix} v_1^{IN} \\ v_2^{IN} \end{pmatrix}=\vec{\mathrm{v}}^{IN}. \qquad (4.2)$$

The *Gibbs vector form* of equation (3.4) or (4.1) uses fat-**v** and/or over-arrow-$\vec{\mathrm{v}}$.

$$\mathbf{v}^{FIN}=2\,\mathbf{V}^{COM}-\mathbf{v}^{IN}, \qquad \text{or:} \qquad \mathbf{V}^{COM}=\frac{\mathbf{v}^{IN}+\mathbf{v}^{FIN}}{2}. \qquad (4.3)$$

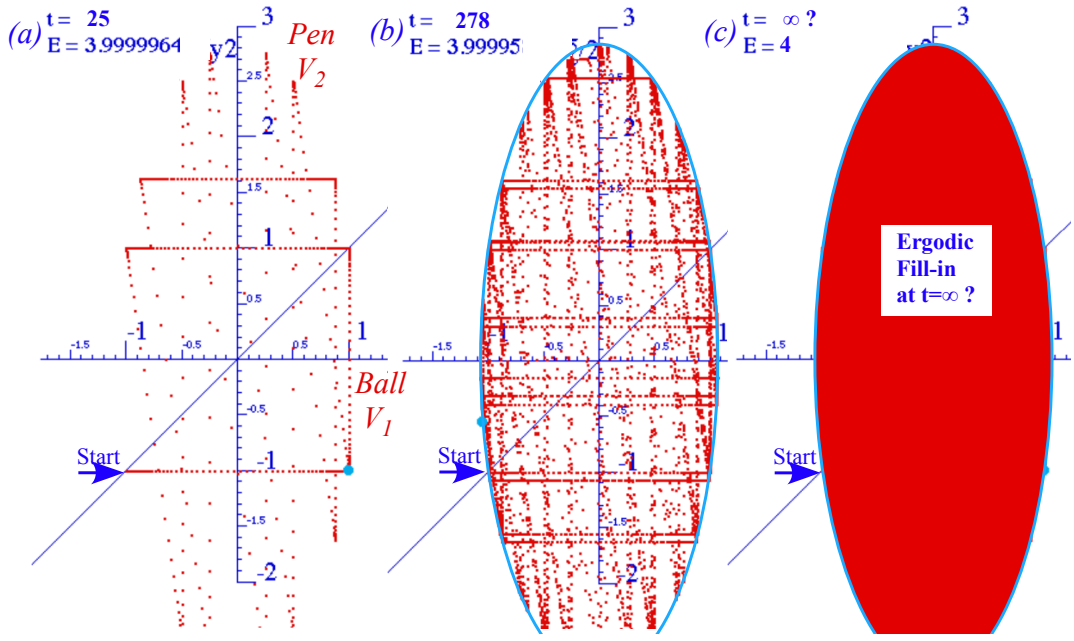

Fig. 4.9 BounceIt V_1-V_2 simulation up to (a) Bang-15 (b) Bang-150 and (c) beyond.

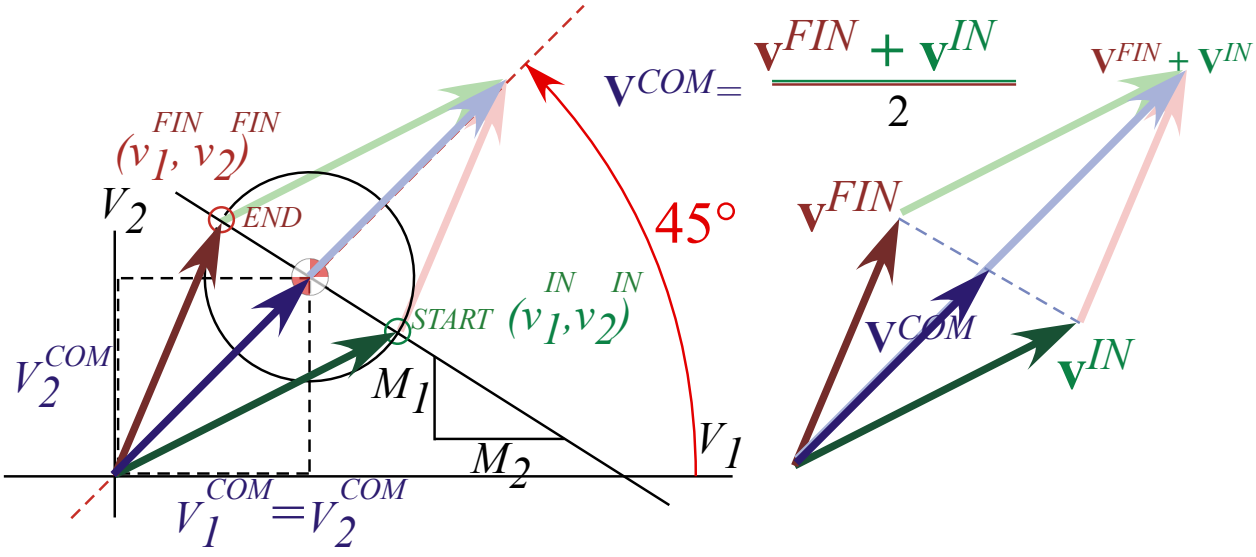

Fig. 4.10 Vector collision velocity diagrams (After equation (4.3) and virtually identical to Fig. 3.3.)

Note vector $\mathbf{V}^{COM}$ bisecting the ($\mathbf{v}^{IN}$+ $\mathbf{v}^{FIN}$)-parallelogram diagonal as per T-symmetry relation from (3.12a) and Fig. 3.3. Here vectors $\mathbf{v}=(v_1, v_2)$ denote *two* particles each in *one*-dimension. More common is vector $\mathbf{v}=(v_x, v_y)$ (or $\mathbf{v}=(v_x, v_y, v_z)$) for *one* particle in *two*-dimensions (or three dimensions).

Fig. 4.11 shows how velocity **v(n)** vectors find results of *Bang-1*$_{(01)}$ and *Bang-2*$_{(12)}$ collisions in Fig. 4.7. What's new is a *space-space* y_2 *vs.* y_1 or *position-vector* **y(n)**-plot whose paths are *spatial-trajectories* or just plain *trajectories*. Space-time paths are found in Fig. 4.6 and Fig. 4.7 by transferring velocity slopes over to the space-space or space-time plot, but vectors in Fig. 4.11 simplify this process. Again, ideally small masses called *point masses* are assumed.

As the construction steps in Fig. 4.11 show, one easily transfers each velocity vector **v(n)** from the V_2 *vs.*V_1 plot so it points away from start point **y(n)** in the y_2 *vs.* y_1 plot. *Step-0* does this by drawing initial velocity **v(0)**=*(-1,-1)* to point away from our given initial position **y(0)**=*(1,3)*. Then you extend that **v**-vector until it hits the floor (as **v(0)** does at **y(1)**=*(0,2)*), or else hits the collision line $(y_2=y_1)$ (as **v(1)** does at **y(2)**=*(1,1)*), or else hits the ceiling (as **v(2)** does at **y(3)**=*(2.2,7)*.). Each such "hit" is a Bang, *Bang-1*$_{(01)}$ at **y(1)**, *Bang-2*$_{(12)}$ at **y(2)**, or *Bang-3*$_{(20)}$ at **y(3)**. Then from each *Bang-n* position point **y(n)** is drawn the next **v(n)**-velocity vector from the V_2 *vs.*V_1 plots. This process continues in exercises that lead to Fig. 4.12 and beyond.

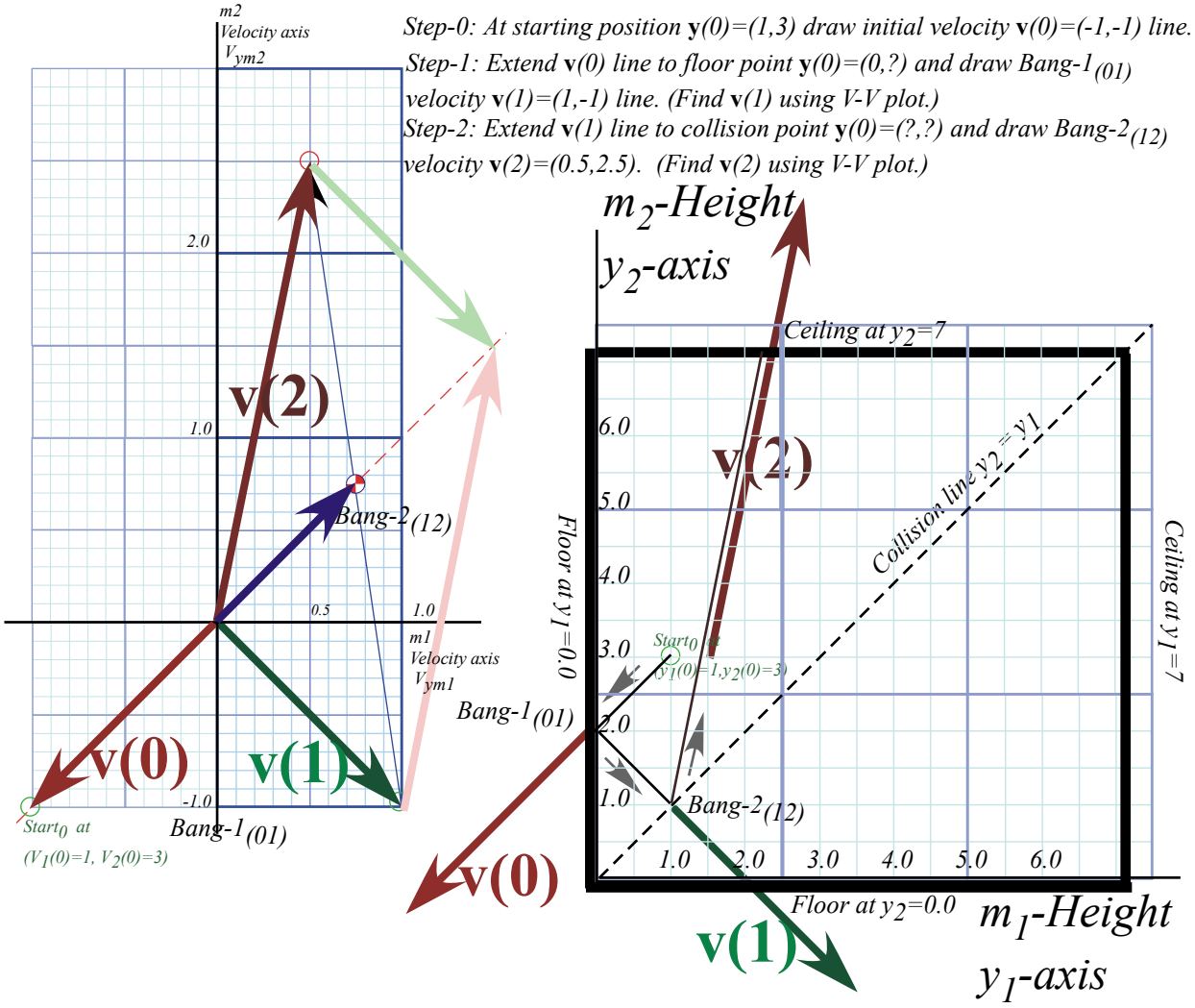

Fig. 4.11 Vector collision velocity diagrams with Velocity-Velocity space and space-space.

Step-2: Extend **v**(2) *line to ceiling point* **y**(3)=(?,7.1) *and draw Bang-3*$_{(20)}$ *velocity* **v**(3)=(1,-1) *line. (Find* **v**(3) *using V-V plot.)*
Step-3: Extend **v**(3) *line to collision point* **y**(4)=(?,?) *and draw Bang-4*$_{(12)}$ *velocity* **v**(4)=(0.5,2.5). *(Find* **v**(4) *using V-V plot.)*
Step-4: Extend **v**(4) *line to ceiling point* **y**(4)=(?,7.1) *and draw Bang-5*$_{(20)}$ *velocity* **v**(5)=(1,-1) *line. (Find* **v**(5) *using V-V plot.)*
Step-5: Extend **v**(5) *line to collision point* **y**(6)=(?,?) *and draw Bang-6*$_{(12)}$ *velocity* **v**(6)=(0.5,2.5). *(Find* **v**(6) *using V-V plot.)*

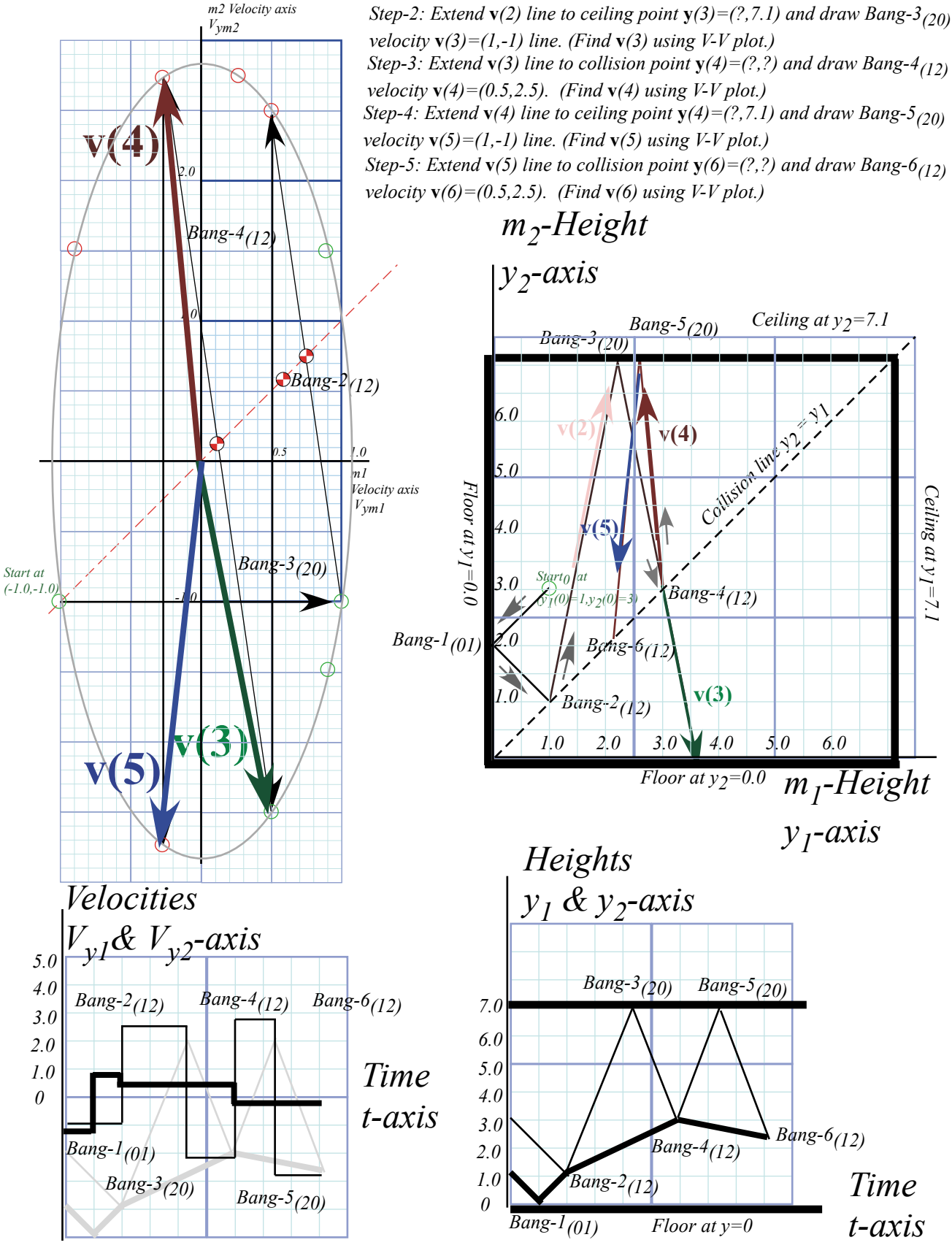

Fig. 4.12 Vector collision diagrams continued with velocity-time and space-time plots added.

Help! I'm trapped in a triangle.

The trajectory in these figures is confined to the triangle above the *45°*-collision line. Our model keeps m_2 above m_1. The right-hand "ceiling" in the figures never is hit because m_1 always is knocked down by m_2 before it touches the ceiling, and m_2 never sees the floor because m_1 is in the way. (Modern physicists beware! Quantum theory doesn't encourage this feature. Quantum objects pass easily through each other!)

Two balls in 1D vs. one ball in 2D

For ball-Earth collisions involving ceiling or floor, the paths bounce in the space-space plot as though they're inside a box. Only one component V_1 or V_2 changes each time and only by changing ±sign. Off the floor: (V_1, V_2) changes to $(-V_1, V_2)$, off of ceiling: (V_1, V_2) changes to $(V_1, -V_2)$. It is like a *single* particle bouncing around a pool table. Here (V_1, V_2) acts like (V_X, V_Y) in *two* dimensions, so *two* particles in *one*-dimension use graphs similar to *one* particle in *two* dimensions, an interesting analogy in quantum theory.

Angle of incidence=Angle of reflection (or NOT)

When paths bounce off the floor and ceiling in the space-space plot, the angle of incidence equals the angle of reflection just as light rays reflect off mirrors. (Newton imagined little light *corpuscles* bouncing around.) It is customary to measure path angles from the *normal* or perpendicular to a mirror so a normal bisects the angle between the incident and reflected paths.

For m_1-m_2 *Bangs* off the *45°*-collision line, the bisecting line has the slope $-M_1/M_2=-7$. It is like having mirror facets at slope $M_2/M_1=1/7$ along the *45°*-collision line. For equal-mass-$(M_1=M=M_2)$ balls, or *one* ball in *two* dimensions, the bisecting line slope at the *45°*-collision line is *–1* or *-45°* and the collision line acts like a unit-slope mirror on a triangular billiard table. It is not quite that simple if $M_1/M_2 \neq 1$.

Consider the two collisions *Bang-3*$_{(20)}$ and *Bang-4*$_{(12)}$ in Fig. 4.12. Velocity **v(2)** bounces off the ceiling in *Bang-3*$_{(20)}$ into **v(3)**, whose velocity slope is close to the mass-ratio M_1/M_2 which is *7:1* here. So the next collision *Bang-4*$_{(12)}$ bounces **v(3)** off the diagonal into **v(4)** which is close to **–v(3)**. It's followed by another ceiling bounce *Bang-5*$_{(20)}$ into **v(5)** heading down for another collision *Bang-6*$_{(12)}$.

Bang force

Lower Fig. 4.12 has a *velocity vs. time* plot next to a space-time plot. (A *y-t* plot in gray is under the *V-t* plot, too.) Each *Bang* means a change in velocity for any particle involved in the collision. By *Newton's 2nd law* (3.10c) each change in velocity, **v** to **v**+Δ**v**, or better, each change in *momentum*, *m***v** to *m*(**v**+Δ**v**), requires a force impulse $\mathbf{F}\cdot\Delta t = m(\Delta\mathbf{v})$ on each mass that changes. Shortly, we study ways to deal with this **F**.

Kinematics versus Dynamics

The velocity-velocity (v_1,v_2) plots, such as the left side of Fig. 4.12, fall in a category known as *kinematics*, or *momentum analysis*, which is concerned with how things are going, where they're headed, or what is their *velocity* or *momentum* and *energy*. (*kinos* means movement.)

In contrast, the space-time plots, such as the right side of Fig. 4.12, fall in a category known as *dynamics*, or *coordinate analysis*, which is concerned with how things are located, where they are, or what are their *coordinate* or *position* and *time* schedules. (*dynos* means change.) We introduced the *space-space* (x_1,x_2) *plot*, another geometric or *trajectory* representation of dynamics.

Before going on, let's compare how *kinos* and *dynos* play out in classical Newtonian physics versus their corresponding roles in quantum physics. This is a preview for later Unit 4, Unit 7, and Unit 8.

Dynos and Kinos: Classical vs. quantum theory

In Newtonian physics, a precise position plot (y_k *vs.* time) lets you find a precise velocity plot, too, and, a velocity plot (V_k *vs.* time) lets you find a position plot if you know starting position values. (We did just that in Fig. 4.7 and Fig. 4.11.) In calculus, finding position from velocity values is called *integration*, and finding velocity from position values is called *differentiation*. Of the two, the latter is formally easier but numerically and experimentally more sensitive to imprecision and noise.

In quantum physics, having a precise velocity plot renders a position plot meaningless and *vice-versa*! Werner Heisenberg was the first to state this quantum idea, now known as Heisenberg's Principle. If you know momentum exactly, that means a uniform wave is everywhere, and all positions are equally possible. If you know position exactly, that means every momentum is possible, implying a "wave-bomb" about to blow up the universe! (Neither of these extremes really exist and fortunately so for the last one.)

All this sounds crazy to most of us who are born-and-bred Aristotelean-to-Newtonian students. It is difficult enough to go from Aristotle's what-you-see-is-what-you-get *(WYSIWYG)* universe to Newton's corpuscular one. A quantum universe is yet another step removed on the *WYSIWYG* scale.

A way to see the quantum universe (Perhaps, it is *the* way.) is to learn about *wave* kinematics and dynamics without Newtonian corpuscles and see how waves *mimic* corpuscles and do so quite cleverly. The quantum universe is a W*YDA*W*YG* (*waves*-you-*don't* see-*are*-what-you-get) world!

So our plan is to cast classical Newtonian kinematics and dynamics in a form that carries over into vibration and wave kinematics and dynamics. It is done by *analogy* with classical waves such as sound waves, water waves, and (most important) light waves. Many classical wave analyses invoke corpuscles

(including, for Newton, light waves) so these analogies, like any analogy, need critical use of an Occam's razor that must be sharpened. Above all, symmetry (and *same*-try) principles must be taken seriously.

IF-ellipse geometry of Ch. 3 relates velocity, momentum and energy, and Ch. 4 derives space-time paths. Later this relates Lagrangian and Hamiltonian mechanics and finally leads to geometries of relativity and quantum mechanics. Then space-space and space-time plots relate to modern physics in subtle ways.

Exercise 1.4.1: Construct a history of a 4:1 mass ratio bounce. $x_1(0)=1.5$, $x_2(0)=3.0$, $v_1(0)=-1$, $v_2(0)=-1$ *Ceiling height=7.0.(For bottom row: Ceiling height=6.0) The 4:1 mass ratio case is surprisingly periodic.*

Exercise 1.4.2: Complete Fig. 4.7 and Fig. 4.11 by constructing more steps using same ceiling height=7.0. Continue until you reach the "gameover" point of last possible M_1-M_2 *collision assuming the floor is open after Bang-1 so both masses fall thru indefinitely. When and where do they last collide?*

Note, position **y(n)**-vectors of the *Bang-n* points are not drawn in Fig. 4.12 to avoid clutter.

Chapter 5 Multiple collisions and operator analysis

Analysis of many collisions with very different masses requires an advanced kind of geometry and algebra involving matrices and symmetry operators. Similar analysis is needed for quantum theory so this is a good opportunity to learn about these concepts using a more "down-to-Earth" classical bang physics.

Doing collisions with matrix products

Fig. 5.1 shows a big mass $m_1=49$ bang a little mass $m_2=1$ more than ten times off the ceiling before being halted. This tests our collision precision! To check our results we use our previous vector equation (4.1) to make a *matrix equation* in (5.1) with $V^{COM}=(m_1v_1+m_2v_2)/M$ and total mass $M=m_1+m_2$.

$$\begin{pmatrix} v_1^{FIN} \\ v_2^{FIN} \end{pmatrix} = \begin{pmatrix} 2V^{COM}-v_1^{IN} \\ 2V^{COM}-v_2^{IN} \end{pmatrix} (4.1)_{repeated} \begin{pmatrix} v_1^{FIN} \\ v_2^{FIN} \end{pmatrix} = \begin{pmatrix} 2\dfrac{m_1v_1+m_2v_2}{m_1+m_2}-v_1 \\ 2\dfrac{m_1v_1+m_2v_2}{m_1+m_2}-v_2 \end{pmatrix} = \frac{1}{M}\begin{pmatrix} m_1v_1-m_2v_1+2m_2v_2 \\ 2m_1v_1+m_2v_2-m_1v_2 \end{pmatrix} \quad (5.1a)$$

(Let $v_1^{IN}=v_1$ and $v_2^{IN}=v_2$ here.) Vector equation (5.1a) is converted to matrix equation $\mathbf{v}^{FIN}=\mathbf{M}\bullet\mathbf{v}$ in (5.1b).

$$\begin{pmatrix} v_1^{FIN} \\ v_2^{FIN} \end{pmatrix} = \frac{1}{M}\begin{pmatrix} m_1-m_2 & 2m_2 \\ 2m_1 & m_2-m_1 \end{pmatrix}\begin{pmatrix} v_1 \\ v_2 \end{pmatrix} \quad (5.1b)$$

Each *IN*-to-*FIN* bang is a $\mathbf{v}^{FIN}=\mathbf{M}\bullet\mathbf{v}^{IN}$ operation (5.2a). Matrix product $\mathbf{M}\bullet\mathbf{N}$ (5.4b) is bang-**M** *following* bang-**N**.

$$\mathbf{M}\bullet\mathbf{v} = \begin{pmatrix} A & B \\ C & D \end{pmatrix}\begin{pmatrix} a \\ b \end{pmatrix} = \begin{pmatrix} Aa+Bb \\ Ca+Db \end{pmatrix} \quad (5.2a) \qquad \mathbf{M}\bullet\mathbf{N} = \begin{pmatrix} A & B \\ C & D \end{pmatrix}\begin{pmatrix} a & c \\ b & d \end{pmatrix} = \begin{pmatrix} Aa+Bb & Ac+Bd \\ Ca+Db & Cc+Dd \end{pmatrix} \quad (5.2b)$$

Matrix **M** operates column-by-column on another matrix **N** as it does on a vector **v**. The off-the-ceiling matrix $\mathbf{C}=\left(\begin{smallmatrix} 1 & 0 \\ 0 & -1 \end{smallmatrix}\right)$ changes (v_1, v_2) to $(v_1, -v_2)$ (Odd-*n* *Bang-n(02)*) A 2-ball collision matrix **M** (Even-*n* *Bang-n(12)*) and ceiling bang **C** act *p*-times in matrix products $\mathbf{v}^{FIN-p}=(\mathbf{C}\bullet\mathbf{M})^p\bullet\mathbf{v}=(\mathbf{C}\bullet\mathbf{M})\bullet(\mathbf{C}\bullet\mathbf{M})\bullet(\mathbf{C}\bullet\mathbf{M})\bullet\ldots(\mathbf{C}\bullet\mathbf{M})\bullet\mathbf{v}$ to give Fig. 5.1.

$$\mathbf{C}\bullet\mathbf{M} = \begin{pmatrix} 1 & 0 \\ 0 & -1 \end{pmatrix}\frac{1}{M}\begin{pmatrix} m_1-m_2 & 2m_2 \\ 2m_1 & m_2-m_1 \end{pmatrix} = \frac{1}{M}\begin{pmatrix} m_1-m_2 & 2m_2 \\ -2m_1 & m_1-m_2 \end{pmatrix} = \begin{pmatrix} 1 & 0 \\ 0 & -1 \end{pmatrix}\begin{pmatrix} 0.96 & 0.04 \\ 1.96 & -0.96 \end{pmatrix} = \begin{pmatrix} 0.96 & 0.04 \\ -1.96 & 0.96 \end{pmatrix} \quad (5.3)$$

(5.4) shows *(p=5)* double-bangs $\mathbf{C}\bullet\mathbf{M}=\begin{pmatrix} 0.96 & 0.04 \\ -1.96 & 0.96 \end{pmatrix}$ *following* a floor-bounce $\mathbf{F}=\begin{pmatrix} -1 & 0 \\ 0 & +1 \end{pmatrix}$ or *11* bangs in all.

$$\begin{pmatrix} v_1^{FIN-11} \\ v_2^{FIN-11} \end{pmatrix} = \begin{pmatrix} 1 & 0 \\ 0 & -1 \end{pmatrix}\cdot\begin{pmatrix} 0.96 & 0.04 \\ 1.96 & -0.96 \end{pmatrix}\cdot\begin{pmatrix} 1 & 0 \\ 0 & -1 \end{pmatrix}\cdot\begin{pmatrix} 0.96 & 0.04 \\ 1.96 & -0.96 \end{pmatrix}\cdot\begin{pmatrix} 1 & 0 \\ 0 & -1 \end{pmatrix}\cdot\begin{pmatrix} 0.96 & 0.04 \\ 1.96 & -0.96 \end{pmatrix}\cdot\begin{pmatrix} 1 & 0 \\ 0 & -1 \end{pmatrix}\cdot\begin{pmatrix} 0.96 & 0.04 \\ 1.96 & -0.96 \end{pmatrix}\cdot\begin{pmatrix} -1 & 0 \\ 0 & +1 \end{pmatrix}\begin{pmatrix} v_1^{IN}=-1 \\ v_2^{IN}=-1 \end{pmatrix}_{(\text{INITIAL }(0))}$$

$$\begin{pmatrix} v_1^{FIN-11} \\ v_2^{FIN-11} \end{pmatrix} = \begin{pmatrix} 0.96 & 0.04 \\ -1.96 & 0.96 \end{pmatrix}\cdot\begin{pmatrix} 0.96 & 0.04 \\ -1.96 & 0.96 \end{pmatrix}\cdot\begin{pmatrix} 0.96 & 0.04 \\ -1.96 & 0.96 \end{pmatrix}\cdot\begin{pmatrix} 0.96 & 0.04 \\ -1.96 & 0.96 \end{pmatrix}\cdot\begin{pmatrix} 0.96 & 0.04 \\ -1.96 & 0.96 \end{pmatrix}\begin{pmatrix} v_1=1 \\ v_2=-1 \end{pmatrix}_{(\text{after Bang-1})} \quad (5.4)$$

$$\begin{pmatrix} v_1^{FIN-11} \\ v_2^{FIN-11} \end{pmatrix} = \begin{pmatrix} 0.96 & 0.04 \\ -1.96 & 0.96 \end{pmatrix}\cdot\begin{pmatrix} 0.96 & 0.04 \\ -1.96 & 0.96 \end{pmatrix}\cdot\begin{pmatrix} 0.96 & 0.04 \\ -1.96 & 0.96 \end{pmatrix}\cdot\begin{pmatrix} 0.96 & 0.04 \\ -1.96 & 0.96 \end{pmatrix}\begin{pmatrix} v_1=0.92 \\ v_2=-2.92 \end{pmatrix}_{(\text{after Bang-3})} \quad \text{Note: } \begin{pmatrix} 0.92 \\ -2.92 \end{pmatrix} = \begin{pmatrix} 0.96 & 0.04 \\ -1.96 & 0.96 \end{pmatrix}\begin{pmatrix} 1 \\ -1 \end{pmatrix}$$

$$\begin{pmatrix} v_1^{FIN-11} \\ v_2^{FIN-11} \end{pmatrix} = \begin{pmatrix} 0.96 & 0.04 \\ -1.96 & 0.96 \end{pmatrix}\cdot\begin{pmatrix} 0.96 & 0.04 \\ -1.96 & 0.96 \end{pmatrix}\cdot\begin{pmatrix} 0.96 & 0.04 \\ -1.96 & 0.96 \end{pmatrix}\begin{pmatrix} v_1=0.7664 \\ v_2=-4.606 \end{pmatrix}_{(\text{after Bang-5})} \quad \text{Note: } \begin{pmatrix} 0.7664 \\ -4.606 \end{pmatrix} = \begin{pmatrix} 0.96 & 0.04 \\ -1.96 & 0.96 \end{pmatrix}\begin{pmatrix} 0.92 \\ -2.92 \end{pmatrix}$$

$$\begin{pmatrix} v_1^{FIN-11} \\ v_2^{FIN-11} \end{pmatrix} = \begin{pmatrix} 0.96 & 0.04 \\ -1.96 & 0.96 \end{pmatrix}\cdot\begin{pmatrix} 0.96 & 0.04 \\ -1.96 & 0.96 \end{pmatrix}\cdot\begin{pmatrix} v_1=0.5515 \\ v_2=-5.924 \end{pmatrix}_{(\text{after Bang-7})} \quad \text{Note: } \begin{pmatrix} 0.5515 \\ -5.924 \end{pmatrix} = \begin{pmatrix} 0.96 & 0.04 \\ -1.96 & 0.96 \end{pmatrix}\begin{pmatrix} 0.7664 \\ -4.606 \end{pmatrix}$$

$$\begin{pmatrix} v_1^{FIN-11} \\ v_2^{FIN-11} \end{pmatrix} = \begin{pmatrix} 0.96 & 0.04 \\ -1.96 & 0.96 \end{pmatrix}\cdot\begin{pmatrix} v_1=0.2925 \\ v_2=-6.768 \end{pmatrix}_{(\text{after Bang-9})}$$

Even after 9 bangs, big m_1 still has a small upward velocity $v_1=0.2925$.
After *Bang-11(02)* big m_1 is nearly stopped and little m_2 is coming down at $v_2=-7.071$ with *all the energy*!

$$\begin{pmatrix} v_1^{FIN-11} \\ v_2^{FIN-11} \end{pmatrix} = \begin{pmatrix} v_1 = 0.0100 \\ v_2 = -7.071 \end{pmatrix}_{(\text{after Bang-11})} \tag{5.5}$$

Look out below! As m_1 turns back it crosses $v_1=0$ axis in Fig. 5.1a. The greatest curvature (acceleration and force) for the path of m_1 is between *Bang-8* and *Bang-14* in Fig. 5.1b just when m_2 is busiest.

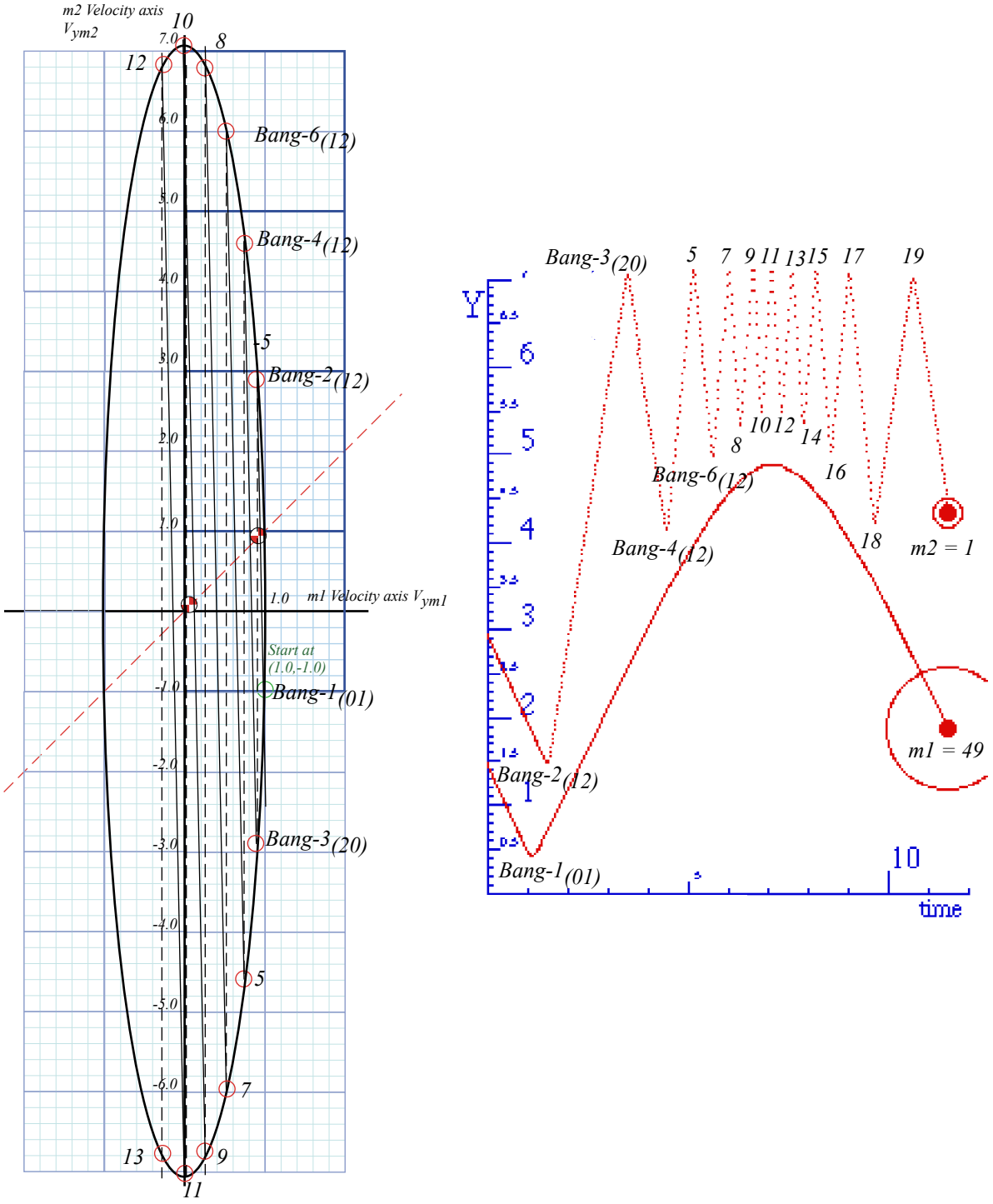

Fig. 5.1 Multiple Bangs of the $m_1=49$ and $m_2=1$ superball system. (a) V vs V plot. (b) Y vs time.

Big m_1 is repelled down by repeated m_2 hits and gains speed as m_2 loses it. If no floor intervenes to rebound m_1 there comes a final bang that leaves m_2 slower than m_1 who falls away so m_2 can't hit it again. (Exercises 5.1 and 5.2, ask you to find this a *game-over* point for various cases.)

However, if a floor intervenes, then a 2nd floor-bounce matrix $\mathbf{F}=\begin{pmatrix}-1 & 0\\ 0 & +1\end{pmatrix}$ changes (v_1, v_2) to $(-v_1, v_2)$ and bounces ball-m_1 back up to start the whole process over again. Ball-m_1 does another similar up-down trip but not exactly the one shown in Fig. 5.1. Below we consider how such processes may be perfectly periodic.

Except for floor bounces, the m_1-ball in Fig. 5.1 experiences a smoother flight than in Fig. 4.7 where a more massive m_2-ball jerks it severely. A smaller mass m_2 has less momentum-per-bang and gives a quasi-continuous force field for m_1. We will derive a funny kind of force and potential field theory from this.

Rotating in velocity space: Ticking around the clock

Here is an example of geometry and slope ratios being helpful. If you view the ellipse in Fig. 5.1a lower-edge-on (and do the exercise to finish it!) you may see it as a circular clock with each double-bang (*odd*-bangs *1,3,5,…*) rotating the **v**-vector like a clock hand ticking equal-angle jumps around a dial.

You can make an energy ellipse $(2E=m_1v_1^2+m_2v_2^2)$ like Fig. 5.1(a) sketched in Fig. 5.2(a) into an energy *circle* $(2E=\mathsf{V}_1^2+\mathsf{V}_2^2)$ like Fig. 5.2(b) by rescaling velocity (v_1, v_2) to $(\mathsf{V}_1 = v_1\cdot\sqrt{m_1}, \mathsf{V}_2 = v_2\cdot\sqrt{m_2})$.

$$\mathsf{V}_1=v_1\cdot\sqrt{m_1}, \qquad \mathsf{V}_2=v_2\cdot\sqrt{m_2} \qquad \text{where: } 2E=m_1v_1^2+m_2v_2^2=\mathsf{V}_1^2+\mathsf{V}_2^2 \tag{5.6}$$

Big-V variables replace little-v's by setting $(v_1=\mathsf{V}_1/\sqrt{m_1},\ v_2=\mathsf{V}_2/\sqrt{m_2})$ in matrix relation (5.1).

$$\begin{pmatrix} v_1^{FIN_1}\\ v_2^{FIN_1}\end{pmatrix}=\frac{1}{M}\begin{pmatrix} m_1-m_2 & 2m_2\\ 2m_1 & m_2-m_1\end{pmatrix}\begin{pmatrix} v_1\\ v_2\end{pmatrix} \text{(5.1)}_{\text{repeated}} \qquad \begin{pmatrix} \mathbf{V}_1^{FIN_1}/\sqrt{m_1}\\ \mathbf{V}_2^{FIN_1}/\sqrt{m_2}\end{pmatrix}=\frac{1}{M}\begin{pmatrix} m_1-m_2 & 2m_2\\ 2m_1 & m_2-m_1\end{pmatrix}\begin{pmatrix} \mathbf{V}_1/\sqrt{m_1}\\ \mathbf{V}_2/\sqrt{m_2}\end{pmatrix} \tag{5.7}$$

Clearing scale factors $\sqrt{m_k}$ gives the following big-V matrix relations to replace (5.1) above.

$$\mathsf{V}^{FIN_1}=\begin{pmatrix} \mathsf{V}_1^{FIN_1}\\ \mathsf{V}_2^{FIN_1}\end{pmatrix}=\frac{1}{M}\begin{pmatrix} m_1-m_2 & 2\sqrt{m_1m_2}\\ 2\sqrt{m_1m_2} & m_2-m_1\end{pmatrix}\begin{pmatrix} \mathsf{V}_1\\ \mathsf{V}_2\end{pmatrix}=\mathsf{M}\bullet\mathsf{V} \tag{5.8}$$

$$\mathbf{V}^{FIN_2}=\begin{pmatrix} \mathbf{V}_1^{FIN_2}\\ \mathbf{V}_2^{FIN_2}\end{pmatrix}=\frac{1}{M}\begin{pmatrix} m_1-m_2 & 2\sqrt{m_1m_2}\\ -2\sqrt{m_1m_2} & m_1-m_2\end{pmatrix}\begin{pmatrix} \mathbf{V}_1\\ \mathbf{V}_2\end{pmatrix}=\mathbf{C}\bullet\mathbf{M}\bullet\mathbf{V} \tag{5.9}$$

The trick is to notice a Pythagorean relation $x^2+y^2=1$ for the circular bang-matrix components.

$$\left(\frac{m_1-m_2}{M}\right)^2+\left(\frac{2\sqrt{m_1m_2}}{M}\right)^2=\frac{m_1+m_2}{m_1+m_2}=1 \tag{5.10a}$$

The matrix can be defined using $\sin\theta$ and $\cos\theta$ shown for $m_1=49$ and $m_2=1$ and angle $\theta=16.26°$ in Fig. 5.2(c).

$$\textit{Define}:\ \cos\theta\equiv\left(\frac{m_1-m_2}{M}\right)\quad \textit{and}:\ \sin\theta\equiv\left(\frac{2\sqrt{m_1m_2}}{M}\right) \tag{5.10b}$$

A *1-Bang* matrix is a *reflection* by θ. Our *2-Bang* matrix is a *rotation* by angle $-\theta=-16.26°$ in V space.

$$\begin{pmatrix} \mathsf{V}_1^{FIN_1}\\ \mathsf{V}_2^{FIN_1}\end{pmatrix}=\begin{pmatrix} \cos\theta & \sin\theta\\ \sin\theta & -\cos\theta\end{pmatrix}\begin{pmatrix} \mathsf{V}_1\\ \mathsf{V}_2\end{pmatrix} \tag{5.11}$$

$$\begin{pmatrix} \mathbf{V}_1^{FIN_2}\\ \mathbf{V}_2^{FIN_2}\end{pmatrix}=\begin{pmatrix} \cos\theta & \sin\theta\\ -\sin\theta & \cos\theta\end{pmatrix}\begin{pmatrix} \mathbf{V}_1\\ \mathbf{V}_2\end{pmatrix}=\begin{pmatrix} 0.96 & 0.04\\ -1.96 & 0.96\end{pmatrix}\begin{pmatrix} \mathbf{V}_1\\ \mathbf{V}_2\end{pmatrix} \tag{5.12}$$

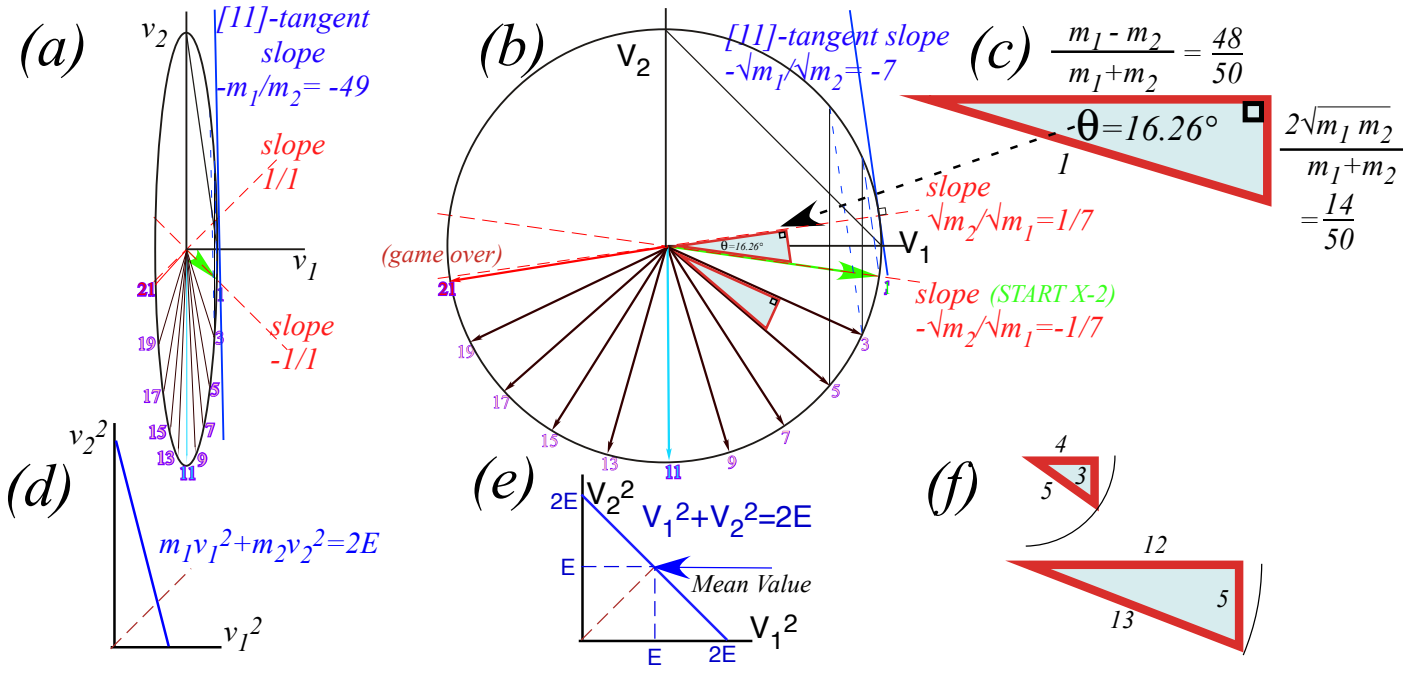

Fig. 5.2 Velocity-velocity clocks. (a) Energy ellipse (As in Fig. 5.1) (b-c) Energy bang-clock angles (d) Velocity-squared E-plot. (e) Mass-scaled V-squared E-plot. (f) Integral right triangles

Matrix (5.12) reduces N-double-bang chains like (5.4). N products of matrix (5.9) are done if $\theta = 16.26°$ in (5.12) is replaced by $N\theta = 81.30°$ to give (5.13) below. (We take $N=5$ double-bangs to check against (5.5).)

$$\begin{pmatrix} \mathbf{V}_1^{FIN\,2N} \\ \mathbf{V}_2^{FIN\,2N} \end{pmatrix} = (\mathbf{C}\cdot\mathbf{M})^N \cdot \mathbf{V} = \begin{pmatrix} \cos N\theta & \sin N\theta \\ -\sin N\theta & \cos N\theta \end{pmatrix} \begin{pmatrix} \mathbf{V}_1 \\ \mathbf{V}_2 \end{pmatrix} = \begin{pmatrix} \cos 5\theta & \sin 5\theta \\ -\sin 5\theta & \cos 5\theta \end{pmatrix} \begin{pmatrix} \mathbf{V}_1 \\ \mathbf{V}_2 \end{pmatrix} = \begin{pmatrix} 0.1512 & 0.9885 \\ -0.9885 & 0.1512 \end{pmatrix} \begin{pmatrix} \mathbf{V}_1 \\ \mathbf{V}_2 \end{pmatrix} (for: N = 5) \qquad (5.13a)$$

Relating $\mathbf{V}$'s to v's by ($\mathbf{V}_1 = v_1\sqrt{m_1}$, $\mathbf{V}_2 = v_2\sqrt{m_2}$) gives (5.5). Note $(\mathbf{C}\cdot\mathbf{M})^N$ *follows* initial floor **F**: $(v_1, v_2) = (1, -1)$.

$$\begin{pmatrix} v_1^{FIN\,2N} \\ v_2^{FIN\,2N} \end{pmatrix} = \begin{pmatrix} \cos N\theta & \sqrt{\frac{m_2}{m_1}}\sin N\theta \\ -\sqrt{\frac{m_1}{m_2}}\sin N\theta & \cos N\theta \end{pmatrix} \begin{pmatrix} v_1 \\ v_2 \end{pmatrix} = \begin{pmatrix} \cos 5\theta & \frac{1}{7}\sin 5\theta \\ -7\sin 5\theta & \cos 5\theta \end{pmatrix} \begin{pmatrix} v_1 \\ v_2 \end{pmatrix} = \begin{pmatrix} 0.1512 & 0.1412 \\ -6.9194 & 0.1512 \end{pmatrix} \begin{pmatrix} 1 \\ -1 \end{pmatrix} = \begin{pmatrix} 0.010 \\ -7.071 \end{pmatrix} for: \begin{cases} N = 5 \\ \frac{m_1}{m_2} = 49 \end{cases} \qquad (5.13b)$$

Without 2nd floor-bounce-back operation **F**, this sequence ends at "game-over" point near bang-*21*. (See exercise 5.1.) Matrix group products clarify collision sequences so they may be "engineered."

Statistical mechanics: Average energy

If two balls of mass $m_2=1$ and $m_1=7$ bounce back and forth between wall the small ball goes faster on the average than the bigger one. How much faster? Let's assume that arrows on the scaled velocity clock in Fig. 5.2(b) get uniformly distributed around its circle after many collisions. (Fig. 5.2(b) shows only m_1-m_2-bounce arrows. m_2-ceiling-bounce-arrows fill up the upper half.) A ball's velocity and momentum must sum and average to zero otherwise it will not stay in the region between the floor and the ceiling.

But, what is average squared-velocity v^2 of each ball? An energy plot in the space $(V_1)^2$ *vs* $(V_2)^2$ of scaled velocity-squared helps to answer this. The result is a *45°* line shown in Fig. 5.2(e). In other words points on the circle in Fig. 5.2(b) get mapped onto the *45°* line in Fig. 5.2(e) by KE conservation.

$$(V_1)^2 + (V_2)^2 = 2\,KE = m_1(v_1)^2 + m_2(v_2)^2$$

The average of all points on the *45°* line is its bisector.

$$(V_1)^2 = KE = (V_2)^2 \qquad \text{or:} \qquad m_1(v_1)^2 = KE = m_2(v_2)^2$$

This gives the average velocities or *root-mean-square-speeds* v_1^{rms} and v_1^{rms} of m_1 and m_2.

$$v_1^{rms} = \sqrt{KE/m_1} \qquad v_2^{rms} = \sqrt{KE/m_2} \qquad (5.14)$$

Each ball, regardless of mass, gets equal share (50% if there are just two) of the total energy. So, if m_1 is 7 times m_2 then the mean speed of m_2 is $\sqrt{7}=2.65$ times faster than that of m_1. The 1st bang in Fig. 4.4 gives *2.5*.

Bonus: Rational right triangles

Geometry often offers interesting numerics. In this case, the general right triangle in Fig. 5.2(c) makes integer or rational fraction solutions to the Pythagorean sum $a^2+b^2=c^2$ such as the famous *(a=3,b=4,c=5)* right triangle. Perfect-square mass values (m_1 and m_2=*1, 4, 9, 16, 25, 36, 49, 81, 100,…*) will give integral valued right triangle altitude $a=\sqrt{(4\,m_1 \cdot m_2)}$, base m_1-m_2, and hypotenuse m_1+m_2. Examples in Fig. 5.2 are *(a=14,b=48,c=50)* for (m_1=*49, m_2=1*) and *(a=12,b=5,c=13)* for (m_1=*9, m_2=4*).

Reflections about rotations: It's all done with mirrors

In 1843 Hamilton discovered his *quaternion algebra* {**1**,**i**,**j**,**k**}, a mathematical jewel. In 1930 Pauli found related *spinor matrices* {1,σ_X, σ_Y, σ_Z}. We label Pauli matrix σ_Z as *sigma-A*=σ_A (*A for Asymmetric*) and σ_X as *sigma-B*=σ_B (*B for Balanced*). They are Hamilton's **k** and **i** with an imaginary factor $i=\sqrt{-1}$ attached.

$$\boldsymbol{\sigma}_A = \begin{pmatrix} 1 & 0 \\ 0 & -1 \end{pmatrix} = \sigma_Z = i\mathbf{k} \qquad (5.15a) \qquad \boldsymbol{\sigma}_B = \begin{pmatrix} 0 & 1 \\ 1 & 0 \end{pmatrix} = \sigma_X = i\mathbf{i} \qquad (5.15b)$$

Other matrices, *sigma-C*=σ_C (*C for Circular*) and *sigma-0*=σ_0(*0 for "Origin"*) are products like $\sigma_A\sigma_B$ or σ_A^2.

$$\boldsymbol{\sigma}_A\boldsymbol{\sigma}_B = \begin{pmatrix} 1 & 0 \\ 0 & -1 \end{pmatrix}\cdot\begin{pmatrix} 0 & 1 \\ 1 & 0 \end{pmatrix} = \begin{pmatrix} 0 & 1 \\ -1 & 0 \end{pmatrix} = i\boldsymbol{\sigma}_C = i\sigma_Y = -\mathbf{j} \quad (5.15c)$$

$$\boldsymbol{\sigma}_A\boldsymbol{\sigma}_A = \boldsymbol{\sigma}_B\boldsymbol{\sigma}_B = \boldsymbol{\sigma}_C\boldsymbol{\sigma}_C = \begin{pmatrix} 1 & 0 \\ 0 & 1 \end{pmatrix} = \boldsymbol{\sigma}_0 = \mathbf{1} = 1 \qquad (5.15d)$$

Hamilton's {**i**,**j**,**k**} square to **-1**. *(*$\mathbf{i}^2=\mathbf{j}^2=\mathbf{k}^2=\mathbf{-1}$*)* That is like $i^2=-1$. But, Pauli-σ's square to +1. *(*$1=\sigma_X^2=\sigma_Y^2=\sigma_Z^2$*.)*

We now relate σ-matrices to simple super-ball collision reflections and rotations shown in Fig. 5.2. For example, the σ_A is our "ceiling bounce" **C** in (5.3) and our "floor bounce" **F** in (5.3) is just $-\sigma_A$.

$$\boldsymbol{\sigma}_A = \begin{pmatrix} 1 & 0 \\ 0 & -1 \end{pmatrix} = \mathbf{C} \qquad (5.15a) \qquad\qquad -\boldsymbol{\sigma}_A = \begin{pmatrix} -1 & 0 \\ 0 & 1 \end{pmatrix} = \mathbf{F} \qquad (5.15b)$$

A geometric view of σ_A (or $-\sigma_A$) is *mirror reflection* thru Cartesian x (or y) axes in Fig. 5.3a while σ_B (or $-\sigma_B$) is reflection thru mirror planes tilted at angle $\pi/4$ (or $-\pi/4$) *between* x-y axes in Fig. 5.3b. General reflection σ_ϕ thru a mirror plane tilted at angle $\phi/2$ (Fig. 5.3c) is a sum (5.15c) of $\sigma_A \cos\phi$ and $\sigma_B \sin\phi$. We now verify this.

$$\boldsymbol{\sigma}_\phi = \boldsymbol{\sigma}_A \cos\phi + \boldsymbol{\sigma}_B \sin\phi = \begin{pmatrix} 1 & 0 \\ 0 & -1 \end{pmatrix}\cos\phi + \begin{pmatrix} 0 & 1 \\ 1 & 0 \end{pmatrix}\sin\phi = \begin{pmatrix} \cos\phi & \sin\phi \\ \sin\phi & -\cos\phi \end{pmatrix} \qquad (5.15c)$$

Like all reflections, σ_ϕ must square-to-one. *($\sigma_\phi^2=\mathbf{1}$)* It does so because $\sigma_A^2=\mathbf{1}=\sigma_B^2$ and $\sigma_A\sigma_B = -\sigma_B\sigma_A$. We test σ_ϕ on unit vectors $\hat{\mathbf{x}} = \begin{pmatrix} 1 \\ 0 \end{pmatrix}$ and $\hat{\mathbf{y}} = \begin{pmatrix} 0 \\ 1 \end{pmatrix}$ and see that matrix algebra checks with geometry in Fig.5.3c.

$$\boldsymbol{\sigma}_\phi \cdot \hat{\mathbf{x}} = \begin{pmatrix} \cos\phi & \sin\phi \\ \sin\phi & -\cos\phi \end{pmatrix}\bullet\begin{pmatrix} 1 \\ 0 \end{pmatrix} = \begin{pmatrix} \cos\phi \\ \sin\phi \end{pmatrix} \qquad (5.16a) \qquad\qquad \boldsymbol{\sigma}_\phi \cdot \hat{\mathbf{y}} = \begin{pmatrix} \cos\phi & \sin\phi \\ \sin\phi & -\cos\phi \end{pmatrix}\bullet\begin{pmatrix} 0 \\ 1 \end{pmatrix} = \begin{pmatrix} \sin\phi \\ -\cos\phi \end{pmatrix} \qquad (5.16b)$$

Geometry Fig. 5.3d also shows that a product $\sigma_2\sigma_1$ of any two reflection matrices is a *rotation matrix R*.

In Fig. 5.3d $\sigma_\phi\sigma_A$ is right-hand rotation $\mathbf{R}_{+\phi}$ but $\sigma_A\sigma_\phi=\mathbf{R}_{-\phi}$ in Fig. 5.3e is left-handed. Rotation angle ϕ is *twice* the angle $\phi/2$ between mirrors. Direction of rotation $\sigma_2\sigma_1$ is from 1st mirror (of σ_1) to 2nd mirror (of σ_2).

$$\boldsymbol{\sigma}_\phi \cdot \boldsymbol{\sigma}_A = \begin{pmatrix} \cos\phi & \sin\phi \\ \sin\phi & -\cos\phi \end{pmatrix}\bullet\begin{pmatrix} 1 & 0 \\ 0 & -1 \end{pmatrix} = \begin{pmatrix} \cos\phi & -\sin\phi \\ \sin\phi & \cos\phi \end{pmatrix} \qquad (5.17a) \qquad\qquad \boldsymbol{\sigma}_A \cdot \boldsymbol{\sigma}_\phi = \begin{pmatrix} 1 & 0 \\ 0 & -1 \end{pmatrix}\bullet\begin{pmatrix} \cos\phi & \sin\phi \\ \sin\phi & -\cos\phi \end{pmatrix} = \begin{pmatrix} \cos\phi & \sin\phi \\ -\sin\phi & \cos\phi \end{pmatrix} \qquad (5.17a)$$

For example, rotation $\sigma_B\sigma_A$ is by $+90°$ and $\sigma_A\sigma_B$ is by $-90°$. Rotation $\sigma_A(-\sigma_A)=(-\sigma_A)\sigma_A$ is by $\pm 180°$.

Through the clothing store looking glass

The rotation in V_1 *vs* V_2 space of Fig. 5.2b is a product of ceiling bounce and m_1-m_2 collision that are each a reflection. An even simpler example of paired-reflection rotation is a clothing store mirror in Fig. 5.4a. It lets you swing two mirrors like doors to view multiple images of yourself. If you set the angle between mirrors to $\phi/2=30°$ as in Fig. 5.3 d-e or to $60°$ as in Fig. 5.4a then you see yourself rotated by twice that angle. Images are turned $120°$ counter-clockwise in the right mirror and clockwise ($-120°$) in the left mirror of the latter.

The sketches in Fig. 5.4a oversimplify the actual images shown by photos of a real mirror pair. The single reflections for σ_A are not shown in the sketch but clearly visible in photos where the σ_A and σ_ϕ images both have backwards text and a left hand image of the original right hand. This is corrected in the ($-120°$)-rotated $\sigma_A\sigma_\phi$ image and the ($+120°$)-rotated $\sigma_\phi\sigma_A$ image.

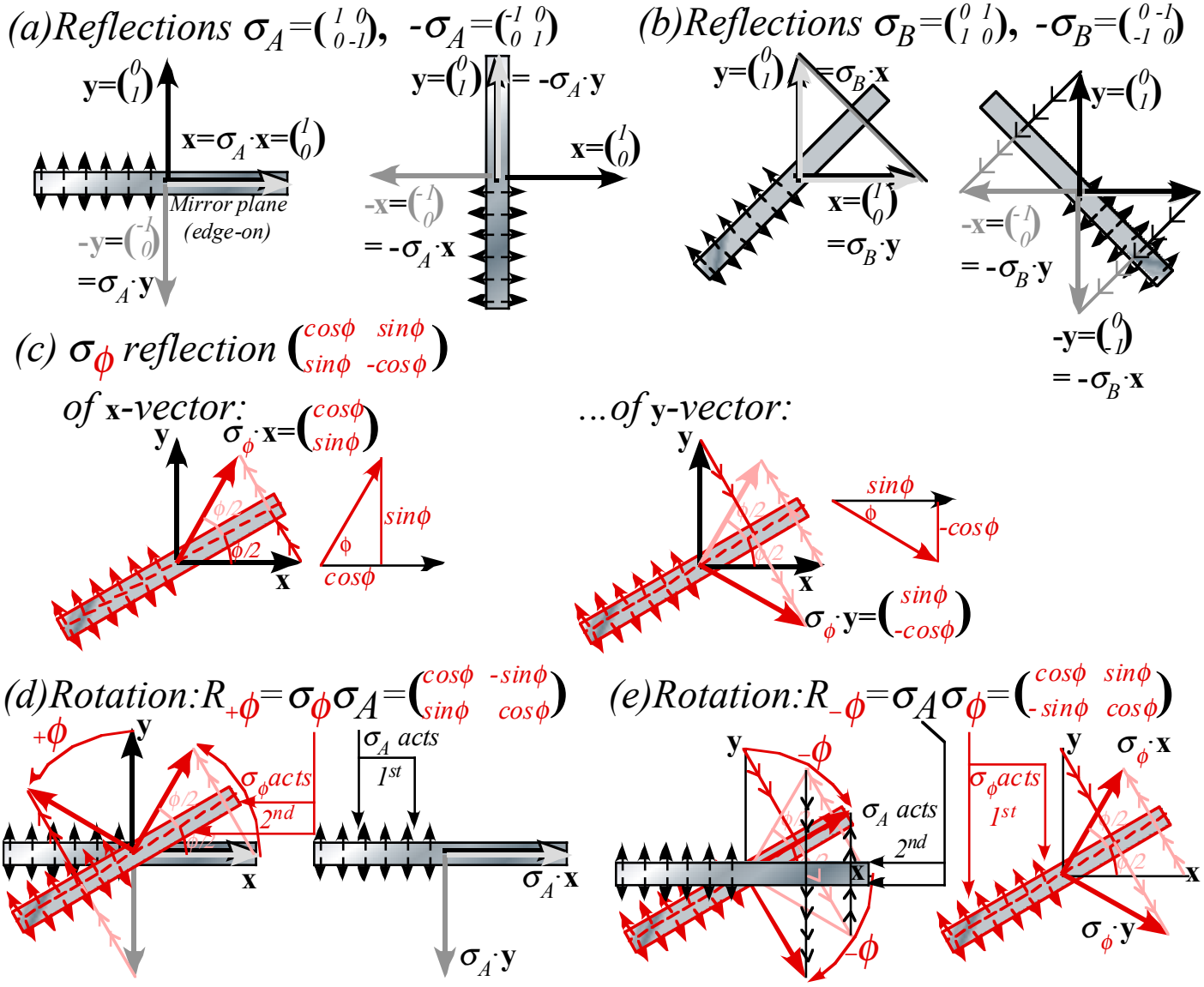

Fig. 5.3 Mirror-reflection geometry (a)±σ_A, (b) ±σ_B, (c) σ_ϕ. Right-and-left-handed rotation (e) $\sigma_\phi\sigma_A$ (f) $\sigma_A\sigma_\phi$.

A special case is rotation $\sigma_A(-\sigma_A)=(-\sigma_A)\sigma_A$ by $\pm 180°$ due to setting mirrors at exactly $\phi/2=90°$ as in Fig. 5.4b. The result is known as a *corner-reflector image*. Wherever you stand while viewing a $90°$ corner you see your image centered and rotated$\pm 180°$ to face you but it is *not reflected*. A $90°$ corner image is as others see you, complete with a readable monogram on your jacket and your right hand on the right side.

How fundamental are reflections?

A product of two reflections is a rotation $\mathbf{R}_\phi=\sigma_2\sigma_1$, but two rotations just give another rotation $\mathbf{R}_{\phi+\theta}=\mathbf{R}_\phi\mathbf{R}_\theta$ and never a reflection. This makes reflections more basic and *productive* than rotations.

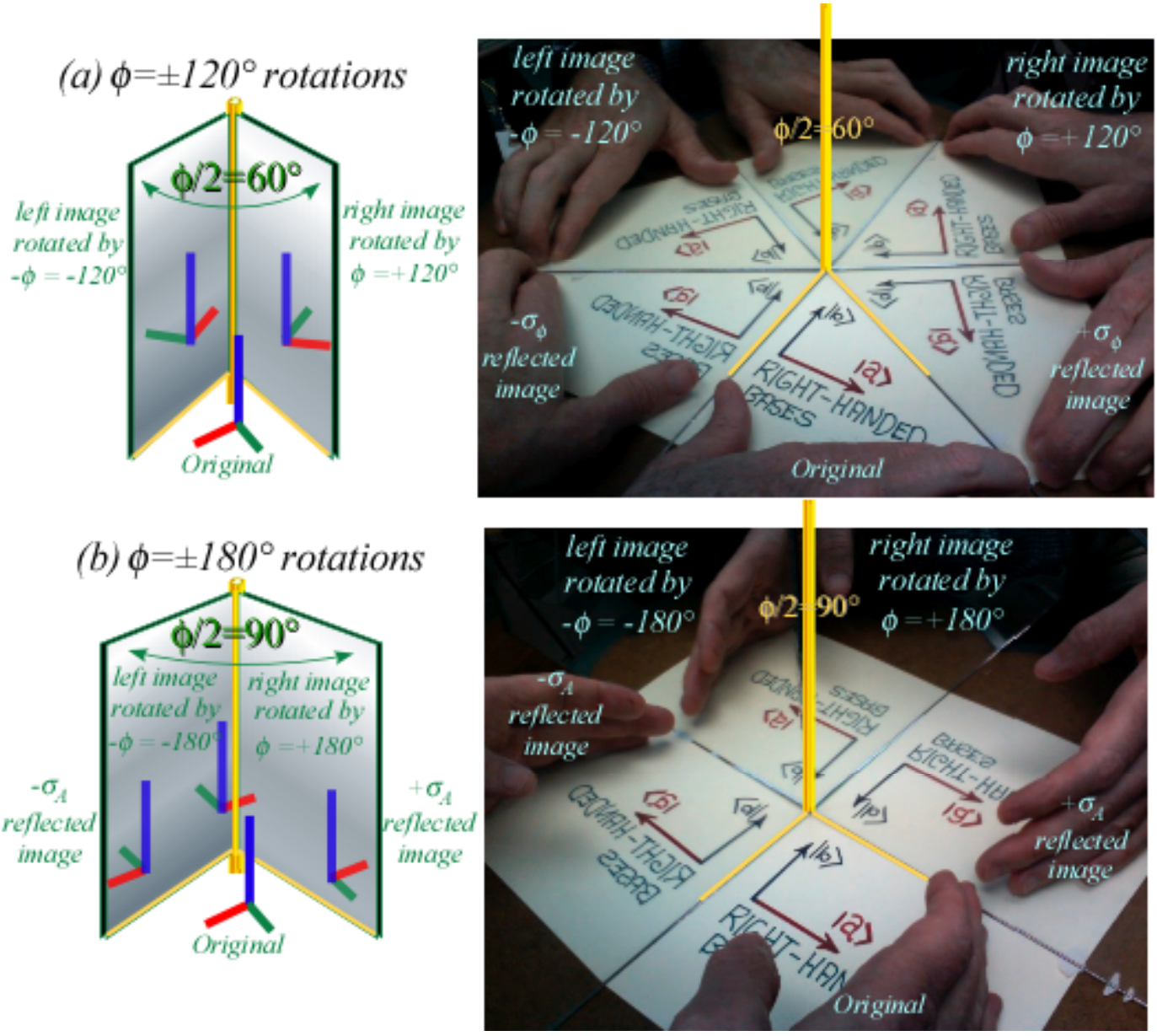

Fig. 5.4 Mirror reflections and their rotations with relative angle: (a) 60° (b) 90° (corner reflector images).

On the other hand, you cannot do a reflection of a real solid object without entering an Alice-in-Wonderland looking-glass-world. Moving every atom in a classical object to a reflected position (without destroying it) is unthinkable! Yet, we easily rotate semi-solid objects (like your eyeballs while reading this).

Waves, on the other hand, are very *un-solid* and do reflection effortlessly. Rotation takes twice the effort as seen in the looking glass images of Fig. 5.4. This is one reason reflection operations are so basic to the study of wave mechanics, quantum theory, and relativistic symmetry as we will see in later Units. They are elementary symmetry generators in a 1D world. A 1D translation by distance a is two reflections by 1D mirrors separated by distance $a/2$.

Symmetry operation **R** or σ is defined by what it does to unit vectors $\hat{\mathbf{x}}=\begin{pmatrix}1\\0\end{pmatrix}$ and $\hat{\mathbf{y}}=\begin{pmatrix}0\\1\end{pmatrix}$ as σ_ϕ (5.16) is done in Fig. 5.3c. That matrix does that same operation to any and all vectors $\mathbf{v}=\begin{pmatrix}v_1\\v_2\end{pmatrix}=v_1\hat{\mathbf{x}}+v_2\hat{\mathbf{y}}$ in the space.

$$\boldsymbol{\sigma}_\phi\bullet\mathbf{v}=v_1\boldsymbol{\sigma}_\phi\bullet\hat{\mathbf{x}}+v_2\boldsymbol{\sigma}_\phi\bullet\hat{\mathbf{y}}=v_1\begin{pmatrix}\cos\phi\\\sin\phi\end{pmatrix}+v_2\begin{pmatrix}\sin\phi\\-\cos\phi\end{pmatrix}=\begin{pmatrix}\cos\phi & \sin\phi\\\sin\phi & -\cos\phi\end{pmatrix}\begin{pmatrix}v_1\\v_2\end{pmatrix} \tag{5.18}$$

A way to distinguish rotation and reflection operators is by the *determinant* det|M| of their matrices.

$$\det|\mathbf{M}|=\det\left|\begin{pmatrix}a & b\\c & d\end{pmatrix}\right|=a\cdot d-b\cdot c \qquad \det\left|\begin{pmatrix}u_x & v_x\\u_y & v_y\end{pmatrix}\right|=u_x\cdot v_y-v_x\cdot u_y=|\mathbf{u}||\mathbf{v}|\sin\angle_{\mathbf{u}}^{\mathbf{v}}$$

A determinant of matrix M quantifies the space (area in this case) enclosed by vectors in M's rows or columns (**u** and **v** enclose a parallelogram in this case).

A rotation determinant is *+1*, but a reflection determinant is *–1*. Reflected area or angle in Fig. 1.3 is negative.

$$\det|\mathbf{R}_\phi|=\det\left|\begin{pmatrix}\cos\phi & \sin\phi\\-\sin\phi & \cos\phi\end{pmatrix}\right|=\cos^2\phi+\sin^2\phi=+1 \qquad \det|\boldsymbol{\sigma}_\phi|=\det\left|\begin{pmatrix}\cos\phi & \sin\phi\\\sin\phi & -\cos\phi\end{pmatrix}\right|=-\cos^2\phi-\sin^2\phi=-1$$

Determinants track the multiplication of matrices. The determinant of a product is a product of determinants.

$$\det|\mathbf{M}\cdot\mathbf{N}|=(\det|\mathbf{M}|)(\det|\mathbf{N}|)=\det|\mathbf{N}\cdot\mathbf{M}|$$

Thus, two reflections each with $det|\sigma|=-1$ form a product of $det|\sigma_1\sigma_2|=(-1)(-1)=+1$, that of a rotation. This also shows a product of rotations cannot make a negative-det-matrix and so cannot be a reflection.

Exercise 1.5.1 Gameover 49:1
Complete Fig. 5.1 (for $m_1:m_2=49:1$) up to the gameover point where sequence would end without 2nd floor bounce. Compare geometric results to analytic matrix analysis.
If the floor is open after the initial bounce of m_1, what mass-ratio near that of Fig. 5.1($m_1:m_2=49:1$) would cause m_1 and m_2 to drop away with the same final velocity.

Exercise 1.5.2 Bigger bangs 100:1
(a) Construct a plot for $m_1:m_2=100:1$ to the "gameover" point after which the bigger ball would need a floor bounce to continue hitting the small one. Such a large mass-ratio favors a rescaled *(Estrangian)* $\sqrt{m_1}v_1$ *vs.* $\sqrt{m_2}v_2$ *circle*–plot. You may use that instead of a plot like Fig. 5.1.
(b) Compare the accuracy of your geometric results with an analytic calculation like (5.2) or (5.13).

Solutions to 1.5.1

Chapter 6 Introducing Force, Potential Energy, and Action

Analysis of *force* is one of the trickier parts of Newtonian mechanics and one that Aristotle seems to have not done so well. We, like Aristotle, feel we know force after being pushed and pulled around by it most of our conscious lives. Aristotle related force directly to mass and its motion. If he ever wrote equations then, perhaps, Aristotle's equation would be $F=MV$.

NOT! MV is *momentum*, not force. Galileo and Newton may be the first to realize that force should be equated to a *change* in momentum. A famous equation $F=Ma$ equates force to mass or *inertia* M times *acceleration* a, the *rate of change* of velocity. (It is called *Newton's 2nd law* or *NEWTON-TWO*. Recall (3.16d).)

$$F = \frac{dP}{dt} = M\frac{dV}{dt} = M\cdot a \qquad (6.0)$$

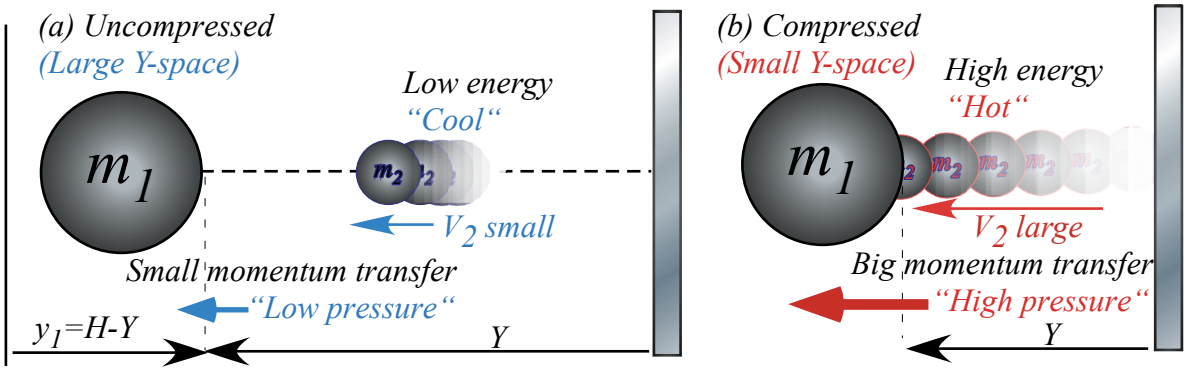

Fig. 6.1 Big mass m_1 feels "force field" or "pressure" of small ball rapidly bouncing to and fro.

MBM force fields and potentials

Motion of m_1 in Fig. 5.1b suggests a *kinetic model* and a *potential force field*. Boltzman uses this to derive gas force laws for volume, temperature, and pressure. As a big m_1-ball squeezes space (*volume*) for a tiny m_2-ball in Fig. 6.1, the speed v_2 and energy $^1/_2\, m_2v_2^2$ of m_2 increases. So does the *momentum transfer rate* or *bang-force* on m_1. Energy is related to *temperature* and bang-force is related to *pressure*. A furiously bouncing m_2 is like a single-atom gas getting hot when its Y-space is compressed as in Fig. 6.1b.

Fig. 6.1 Big mass-m_1 ball feeling "force-field" or "pressure" of small ball rapidly bouncing to-and-fro.

A "double-whammy" hits the m_1-ball as it closes in with velocity v_1 toward m_2 and wall *(Y=0)*:

(1) Bang rate B with m_2 increases with shrinking distance $2Y$ traveled by m_2 between m_1 and wall.

(2) Increased velocity v_2 (due to v_1) increases momentum m_2v_2 and ΔP transferred to m_1 by each bang.

(3) Increased velocity v_2 (due to v_1) increases bang rate even more. It's really a *triple* whammy!

If m_1 is huge (say *1kg*) compared to atom or molecule m_2 (say $(2/3)\cdot 10^{-27}kg$ for an H-atom), the speed v_1 of the macro-mass m_1 may be negligible compared to typical atomic speeds v_2 of 10^3 *m/s*. Then we ignore effects (2) and (3) due to tiny v_1 in a so-called *isothermal* model. An *adiabatic* model includes them.

Isothermal model force laws

Atom m_2 in Fig. 6.1 travels distance $2Y$ back & forth between m_1 and ceiling at Y for each bang m_1. If v_1 is slow, the time Δt between bangs is $2Y$ divided by velocity v_2 of m_2. *Bang rate B* is the inverse: $B=1/\Delta t$.

$$\Delta t = 2Y/v_2 \text{ (seconds per bang)} \quad (6.1a) \qquad B = 1/\Delta t = v_2/2Y \text{ (bangs per sec)} \quad (6.1b)$$

Each head-on bang of big m_1 on small m_2 changes velocity of m_2 from $-v_2$ to $+v_2^{FIN}$ as shown in Fig. 6.2.

$$(for: m_1>>m_2): \qquad v_2^{FIN} = v_2+2v_1 \qquad (\approx v_2 \text{ for: } v_2>>v_1) \quad (6.2)$$

Added speed for m_2 is $2v_1$, twice that of incoming m_1. (V-V-plot Fig. 6.2 assumes large-m_1.) The change ΔP of momentum m_2v_2 is the difference between *FIN* value $+m_2v_2^{FIN}$ and *IN* value $-m_2v_2$.

$$\Delta P = (+m_2v_2^{FIN})-(-m_2v_2)=2m_2v_2+2m_2v_1 \qquad (\approx 2m_2v_2 \text{ for: } v_2>>v_1) \quad (6.3)$$

So, if "atomic" velocity v_2 is large compared to v_1 it gives a *bang-force* $F=B\cdot\Delta P = \Delta P/\Delta t$ on m_1.

$$BP=\Delta P/\Delta t = F = 2m_2v_2(v_2/2Y) = m_2v_2^2/Y \quad (6.4)$$

So a *force field F=2·KE/Y* on m_1 due to m_2 is proportional to $KE={}^1/_2m_2v_2^2$ or *temperature T* of m_2. *Boltzman's constant k* of proportionality ($KE=kT$) gives an *isothermal* force law $FY=2kT$. It is a 1-D version of *Boyle's ideal gas law: PV=2kT*. Here a ceiling tries to keep energy or "temperature" of m_2 constant in spite of m_1.

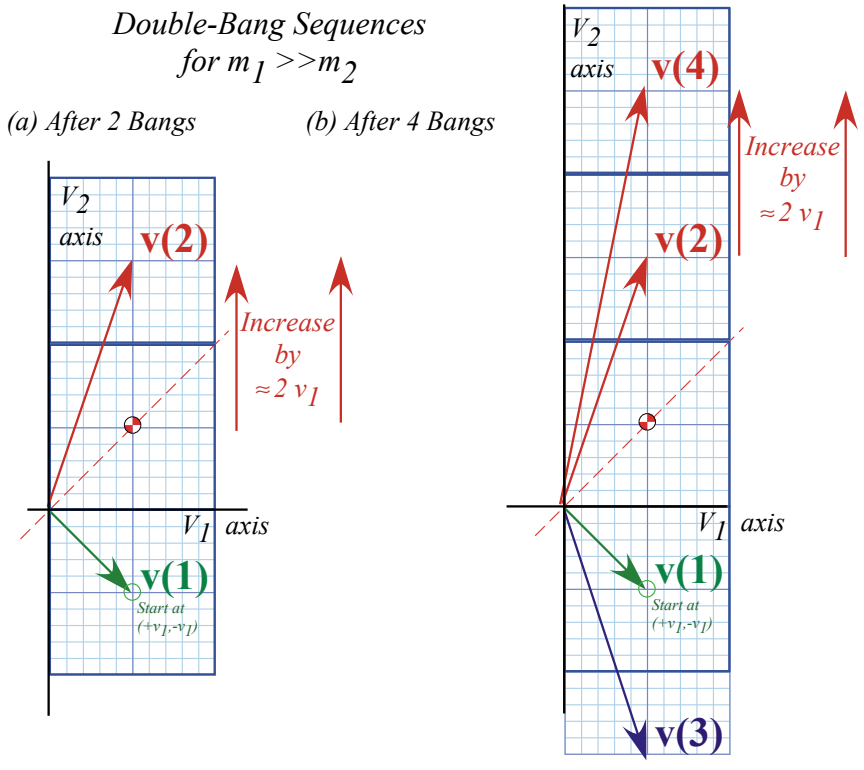

Fig. 6.2 Large mass-ratio ($m_1/m_2>>1$) bounce sequence. (Compare to Fig. 4.2a.)

Adiabatic model force laws

An elastic ceiling can't give or take energy so each m_1 bang adds velocity $2v_1$ to v_2 at rate $B=v_2/2Y$ (6.1). As m_1 closes at speed v_1 it reduces distance $2Y$ that m_2 travels. So bang rate B grows due to more v_2 *and* less Y.

$$\frac{dv_2}{dt}=2v_1B \qquad =2v_1\frac{v_2}{2Y}, \qquad y=v_1t=H-Y, \qquad \frac{dy}{dt}=v_1=-\frac{dY}{dt} \qquad (6.5a)$$

We cancel time and v_1 to show this force is inverse-Y- *cubed*, a lot "harder" than inverse-Y in (6.4).

$$\frac{dv_2}{dt}=\left(\frac{dY}{dt}\frac{dv_2}{dY}=-v_1\frac{dv_2}{dY}\right)=2v_1\frac{v_2}{2Y}, \qquad \frac{dv_2}{v_2}=-\frac{dY}{Y}, \quad v_2=\frac{const.}{Y}=\frac{v_2^{IN}Y(t=0)}{Y}, \qquad F=\frac{m_2v_2^2}{Y}=m_2\frac{(const.)^2}{Y^3} \quad (6.5b)$$

This is called an *adiabatic* or "fast" force law. Collisions are so fast that an isothermal-seeking "Robin Hood" in the ceiling hasn't time to steal m_2's energy when it's judged too energy-rich or give energy back when m_2 becomes energy-poor. So m_2 can get hotter and hit m_1 harder and more often as gap Y shrinks.

Conservative forces and potential energy functions

Either force law (5.9) and (6.5) actually conserves the energy of the big-m_1 ball in the long run. By that we mean that m_1 will come out with practically the same energy that it had when it went in.

The adiabatic case is easier to see. Each bang conserves energy as demanded by the kinetic energy *(KE)* conservation relation (3.5a). Little-ball velocity $v_2=const./Y$ from (6.5b) is used here.

$$E=\frac{1}{2}m_1v_1^2+\frac{1}{2}m_2v_2^2=\frac{1}{2}m_1v_1^2+\frac{1}{2}m_2\left(\frac{const.}{Y}\right)^2=const. \qquad (6.6)$$

The first term is m_1's *kinetic energy* KE_1. The second term, which is really m_2's kinetic energy, is called m_1's *potential energy* PE_1 or just plain *PE*, and it is labeled $U(Y)$ since it varies according to height Y of m_1 only.

$$E=KE_1+PE=\frac{1}{2}m_1v_1{}^2+U(Y) \qquad \text{where:} \quad PE=U(Y)=\frac{1}{2}m_2\left(\frac{const.}{Y}\right)^2 \qquad (6.7)$$

The *PE* is energy that m_1 lends to m_2 each time m_1 moves a distance ΔY closer so m_1 does a little bit of *work* ΔW on m_2. *Work* is defined as *force times distance*. *($\Delta W=F\cdot\Delta Y$) Power*, the rate of work done, is defined as *force times velocity*. Here distance is a small ΔY and the force F in (6.5b) is $m_2\,const.^2/Y^3$. But "work" force might be plus-or-minus $(\pm)m_2\,const.^2/Y^3$. Which sign? (+) or (−)? Conflicting sign conventions make force-physics confusing. The sign depends on how *force* and *direction* are defined. (It's all relative!)

Is it +or-? Physicist vs. mathematician and the 3rd law

A physicist's force F^{phys} is what is felt by a free object (Here that's m_1.) whose motion is driven by force field $F=F^{phys}$. A mathematician's force F^{math} is what is needed to *hold back* the object in the force field. (How *apropos*! A physicist lets it *go* but a constipated mathematician holds it *back*!) They differ by (±) sign only, that is, $F^{math}=-F^{phys}$, and F^{math} is the equal-but-opposite force by an object (m_1 here) on its field or force agent(s) (m_2 here). (This is essentially *Newton's 3rd law*. *(NEWTON-THREE)*)

Force is momentum flow. Momentum is stuff that's conserved, so the flow rate F^{phys} of this stuff *into* an object m_1 must be balanced by an equal-but-opposite negative flow, $F^{math}=-F^{phys}$, *out of* the forcing agent (s) (m_2 here), and, *vice versa*, whatever flows *out of* m_1 flows *into* m_2. Momentum $\mathbf{p}=m\mathbf{v}$ and force $\mathbf{F}$ are both vector quantities and a ±sign gives direction to-or-fro, another confusing (±) sign to bother us. But, whatever the flow rate F^{phys} seen by m_1, then m_2 sees the opposite rate $F^{math}=-F^{phys}$.

Let's define positive Y and F direction to be *away* from the wall in Fig. 6.1. So incoming m_1 has negative velocity $v_1=-\Delta Y/\Delta t$, but after m_1 reverses $V=\Delta Y/\Delta t$ is positive. Positive $V=-v_1$ (increasing Y) and positive F^{phys} means both momentum and energy of m_1 are being *increased* by force F^{phys}. Each bit of energy or work $\Delta W=F^{phys}\Delta Y$ gained by m_1 is energy lost by the force-field's potential "bank" that is m_2. *($\Delta U=-\Delta W$)*

$$\Delta W=F^{phys}\cdot\Delta Y=-\Delta U \qquad where:\ F^{phys}=F(Y)=m_2\frac{(const.)^2}{Y^3} \tag{6.8}$$

In other words, power $\Pi=F^{phys}\cdot V$ *into* m_1 is power $(-\Delta U/\Delta t)$ *out of* the field. ($V=\Delta Y/\Delta t$ is velocity of m_1.)

$$\Pi = F^{phys}\cdot V=-\frac{\Delta U}{\Delta t}=-\frac{\Delta U}{\Delta Y}\frac{\Delta Y}{\Delta t}=-\frac{\Delta U}{\Delta Y}V \qquad where:\ F^{phys}=-\frac{\Delta U}{\Delta Y} \tag{6.9}$$

But is this consistent? Does force F^{phys} in (6.8) really equal minus the slope of potential (6.7)?

$$F^{phys}=m_2\frac{(const.)^2}{Y^3} \qquad \begin{matrix}consistent\\ with:\end{matrix} \qquad F^{phys}=-\frac{\Delta U}{\Delta Y}=-\frac{d}{dY}\frac{1}{2}m_2\left(\frac{const.}{Y}\right)^2=m_2\frac{(const.)^2}{Y^3} \tag{6.10}$$

It *checks!!* Note that $F=-\Delta U/\Delta Y$ needs that $^1/_2$ on kinetic energy $^1/_2\, m_2v_2^2$. (Recall discussion of (3.5).)

Isothermal "Robin Hood"and "Fed rules"

The isothermal case is a weird one. The little "force-field agent" m_2 maintains it kinetic energy at around the same initial value $^1/_2\, m_2v_2^2$ no matter how much the big mass m_1 loses or gains kinetic energy.

It's as though a "Robin-Hood" in the ceiling acts like a big Federal Reserve Bank. (*"The Fed."*) Whatever energy m_2 earns from m_1 is taken and stored away if its over initial deposit $\frac{1}{2}(m_2v_2^2)=T$, but if m_2

deposits falls below that value, the Fed makes up the difference. This energy or deposit limit is determined by a prevailing allowed "temperature" of the ceiling or the current money supply. (I'm not making this up. It's what happens in nature and very roughly what happens in our economy. It becomes a problem if the Fed stops being a Robin Hood and becomes a robbing hood!)

Under ideal conditions, force agent m_2 makes a much "softer" $1/Y$ force field $F=m_2v_2^2/Y$ given by (5.9). Definition (6.9) of force F as negative-U-slope $-\Delta U/\Delta Y$ then gives a $log_eY=lnY$ potential.

$$F^{phys} = m_2\frac{v_2^2}{Y} = -\frac{\Delta U}{\Delta Y} \qquad implies: \qquad U = -m_2v_2^2\ln(Y) \qquad (6.11)$$

It may seem weird that we can define a useful potential while energy-funds are being siphoned in and out. Nevertheless, the ceiling "Robin Hood" is true to his word. (Analogy with "The Fed" ends here!) He puts back all the energy that m_1 gave up to m_2 (the potential U) on the way in, so that, except for small-change or "tips" left with m_2 after the final parting collision, m_1 recovers the energy it originally had. Such a force field, if determined by such a reliable potential, is also a *conservative* one. We discuss later the details of what is needed for general multi-dimensional fields to be labeled "conservative."

Oscillator force field and potential

Consider a mass m_1 between two walls and two little speeding m_2 masses as in Fig. 5.5. m_1 feels a force like that of an oscillator. As m_1 moves distance x off center the left wall space expands to $Y+x$ and the right wall space shrinks to $Y-x$. Two opposing forces (6.11) then are unbalanced. (Only $x^2, x^4, \ldots$ terms cancel.)

$$F^{total} = \frac{f}{1+x} - \frac{f}{1-x} = f\left[1-x+x^2-x^3\ldots\right] - f\left[1+x+x^2+x^3\ldots\right] = -2f\cdot x - 2f\cdot x^3 -$$

Here we let $Y=1$ be a unit interval and assume an isothermal kinetic constant $k \equiv 2f = 2m_2v_2^2$ for each side. For small x $(x<<1)$ the force F^{total} has a *linear* or *Hooke's law* form, and the potential U^{total} is *quadratic*.

$$F^{total} \simeq -k\cdot x = -\frac{\partial U^{total}}{\partial x} \qquad U^{total} \simeq \frac{1}{2}k\cdot x^2 = -\int F^{total}dx \qquad (6.12)$$

Harmonic oscillator (HO) linear forces and *quadratic* potentials are, perhaps, the most useful ones in AMO physics because they approximate any stable system. Normally, they are analogized by a mass on a spring, rubber band, or pendulum, only rarely (if ever) in a context like Fig. 6.3. *HO* motion is sinusoidal $y(t)=A\sin(\omega t+\varphi)$ with *angular frequency* $\omega=\sqrt{k/m_1}$ and period $\tau=2\pi/\omega$ independent of the oscillator amplitude A or phase φ. The calculation of period for Fig. 6.3c is left as an exercise.

The 2nd most useful field is probably the Coulomb potential $U=-k/r$ and force $F=k/r^2$. (See Ch. 7 for electrostatics and Earth gravity, which also have 2D *HO* potentials at their cores.) After that, the 2D Coulomb $U=k\cdot ln(r)$ and $F=k/r$ is an important field shown in Unit 10. (The latter is like (6.11). A pair of them underlies Fig. 6.3 for the isothermal case.)

You should be warned that an oscillator like Fig. 6.3 is not as simple as it might appear, and as we will see, neither are springs, rubber bands, or pendulums. Also, balls bouncing against moving objects are

particularly dicey devices. A simple model with one ball and one oscillating wall is called a *Fermi oscillator*, and is quite chaotic. The thing in Fig. 6.3 can be even more devilish if m_2 is not very small. *Caveat emptor!*

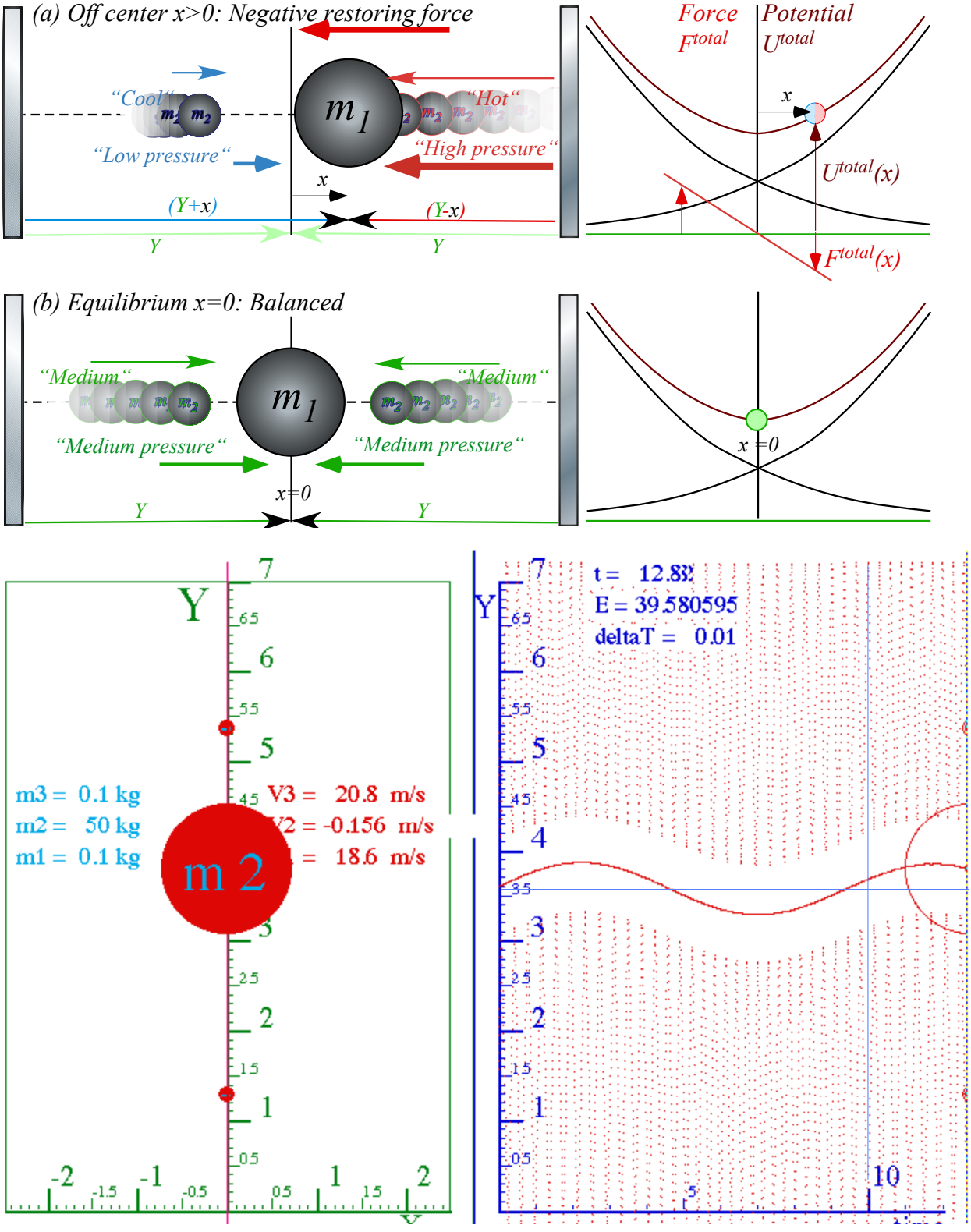

Fig. 6.3 Oscillator force and potential (a) Off center with (-)force (b) On center at equilibrium. (c) Quasi-harmonic oscillation of M=50 in adiabatic force of two m=0.1 masses of speed v_0=20 and range Y_0=3.

The simplest force field F=const.

We have mentioned power-law forces $F_{adiab}=k/y^3=ky^{-3}$ (6.5), $F_{Coul}=k/y^2=ky^{-2}$, $F_{isoT}=k/y=ky^{-1}$ (6.4), and lastly $F_{osc}=-ky$ (6.12), but have forgotten the simplest, namely *zero* power law $F_{const}=k=ky^0$. This last one is like a constant near-Earth-surface gravity force $F_{\odot}=-\frac{\partial U}{\partial y}=mg=-m|g|$ on a mass *m*. ((-) sign for *down*ward.) Acceleration of gravity near Earth's surface is nearly *-10* meters per second per second and *very* nearly *–9.8*. $(g=-9.7997 m/s^2)$ Terrestrial objects experience this whether they are bundled together or not.

All power-law forces $F=ky^p$ have power-law potentials $U=-\int F\cdot dy=-ky^p/(p+1)$, except for $p=-1$ where $F_{isoT}=k/y$ has a logarithmic $U_{isoT}=-k\ ln(y)$. (6.11) Earth-surface potential $U_{\odot}=mgh$ is *linear* in height $y=h$. This we use to compute height of a superball toss by equating its floor level $KE=1/2mV^2$ to maximum $PE=mgh$.

$$gh_{max}=\tfrac{1}{2}V_{floor}^2 \quad (6.13a) \qquad V_{floor}=\sqrt{2gh_{max}} \quad (6.13b)$$

Ejection height goes as the *square* of ejection velocity. A *3*-fold velocity gain means $3^2=9$-fold height gain.

Introducing Action. It's conserved (sort of)

It is remarkable that a bouncing mass has a physical property called *action* $S=\oint P\cdot dx$ that is more or less constant even if its position *x* momentum *P* and kinetic energy *KE* are driven crazy. Action is defined by the area of a one-cycle loop swept out in a momentum *vs* position *phase-plot (P vs x)*. That is analogous to an energy or *power-plot* of force *vs* position *(F vs x)* whose loop area $\oint F\cdot dx$ is work per cycle.

Conservation of momentum and conservation of energy are each a rigorously obeyed axiom or theorem for an isolated classical system. However, conservation of action is "more or less" or "sort of" and "it depends" *for a driven system*. The concept of action is both subtle and deep and it lies at the heart of quantum theory and accounts for a lot of how we affect and are affected by the world around us.

Here we use a geometric construction of a bouncing ball trajectory to quantify action conservation or lack thereof. We suppose the little mass m_2 is caught as before in Fig. 5.1 and Fig. 6.1 between a rock and a hard place, that is, bouncing between a big mass m_1 (moving in at a constant velocity $v_1=1$ from the left) and a hard elastic wall. The big ball path is indicated in Fig. 6.4 by a line of slope=1=v_1 that hits an initially fixed m_2 following a vertical line (slope=0=v_2) that then gets knocked up to a line of slope=2=v_2 (after Bang (1)). Throughout the imagined collision sequence we suppose the big ball is so much more massive that its change in velocity is not noticeable. This is in spite of the fact that it is absorbing more and more momentum from the little ball with each bang. (Surely, *something* in it is going to break eventually!)

Each time the small ball is banged elastically by the big one it picks up two more units of velocity v_1 that it maintains, apart from change in sign, through its subsequent bang with the elastic wall. Each time it returns for more, is banged again, and increases its speed by two units. (Recall Fig. 6.2.)

The horizontal dashed lines in Fig. 6.4 indicate the range Δx available to the small ball at each instant of its bang with the wall. Note that the product of the range Δx and the speed v_2 is a constant three units even as spatial range Δx rapidly decreases and the velocity range $\Delta v=2|v_2|$ increases just as rapidly.

$$\Delta x\, v_2 = 3.0 = \Delta x\, \Delta v/2$$

This is an example of conservation of action mentioned before. If we define the small ball's "range of velocity" by $\Delta v=2|v_2|$ then this relation takes the form of a weird kind of uncertainty relation, that is, it looks like Heisenberg's famous *minimum uncertainty relation* $\Delta x\, \Delta p = \hbar = (constant)$ for position and momentum. It happens that the two are related even though the constant used by Heisenberg is an unimaginably tiny Planck constant $(\hbar \sim 10^{-34} Js)$ compared to a constant 3.0 appearing above. (Ours has *gadzillions* of wave quanta!)

The geometry behind this relation is exposed in Fig. 6.4 (b). It is obtained by considering intersections between lines of integral speeds or slopes $v_2 = \pm 1, \pm 2, \pm 3, \pm 4, \pm 5, \pm 6, \pm 7, \ldots$ that are relevant to the bang sequence. They are also relevant to quantum theory where the speeds of a particle in a box are indeed quantized to integers times a tiny number. (This is where that tiny $\hbar$ comes in.) That is simply a reflection (pun intended) of the fact that mutually reflecting waves require that an integral (or half-integral) number of the wavelengths fit perfectly between mirroring containment walls or cavities.

Now we might ask if the action area $\Delta x\, \Delta v$ in Fig. 6.4c-e stays the same if the big-ball speed v_1 varies. Action variance was argued hotly by Einstein and the "quantum gang" at the1920 Solvay Conference. They imagined a hotel chandelier being dragged up or down by a clerk holding its support cable upstairs. They concluded that if the clerk could not detect the swinging pendulum phase or frequency, then he would seldom be able to change its action. However, if he could synchronize his oscillations then he could drive the chandelier exponentially to destruction. We shall review this important and explosive process known as *parametric resonance* in later units. It is fundamental to mechanics and particularly quantum wave mechanics. Action and its wiggly antics deserve our attention.

Monster mass M_1 and Galilean symmetry (It's deja vu all over, again.)

"Monster mass" M_1 bongs hapless m_2-atoms in Fig. 6.4 using Galilean symmetry. To show symmetry we imagine two head-on monster M_1's going at $\pm V_1 = \pm 1$ in Fig. 6.5. A mirror image of Fig. 6.4 lies in extended m_2-path lines. The red paths of even integral velocity $v_2 = 0, \pm 2, \pm 4, \ldots$ are copies of Fig. 6.4 paths. Odd integral velocity $v_2 = \pm 1, \pm 3, \ldots$ paths mesh with even ones to make a full grid. Any initial v_2 between $\pm V_1$ has a path on the grid. A blue path is drawn thru a series of bongs with $v_2 = -0.2, +2.2, -4.2, +6.2, \ldots$ in Fig. 6.5.

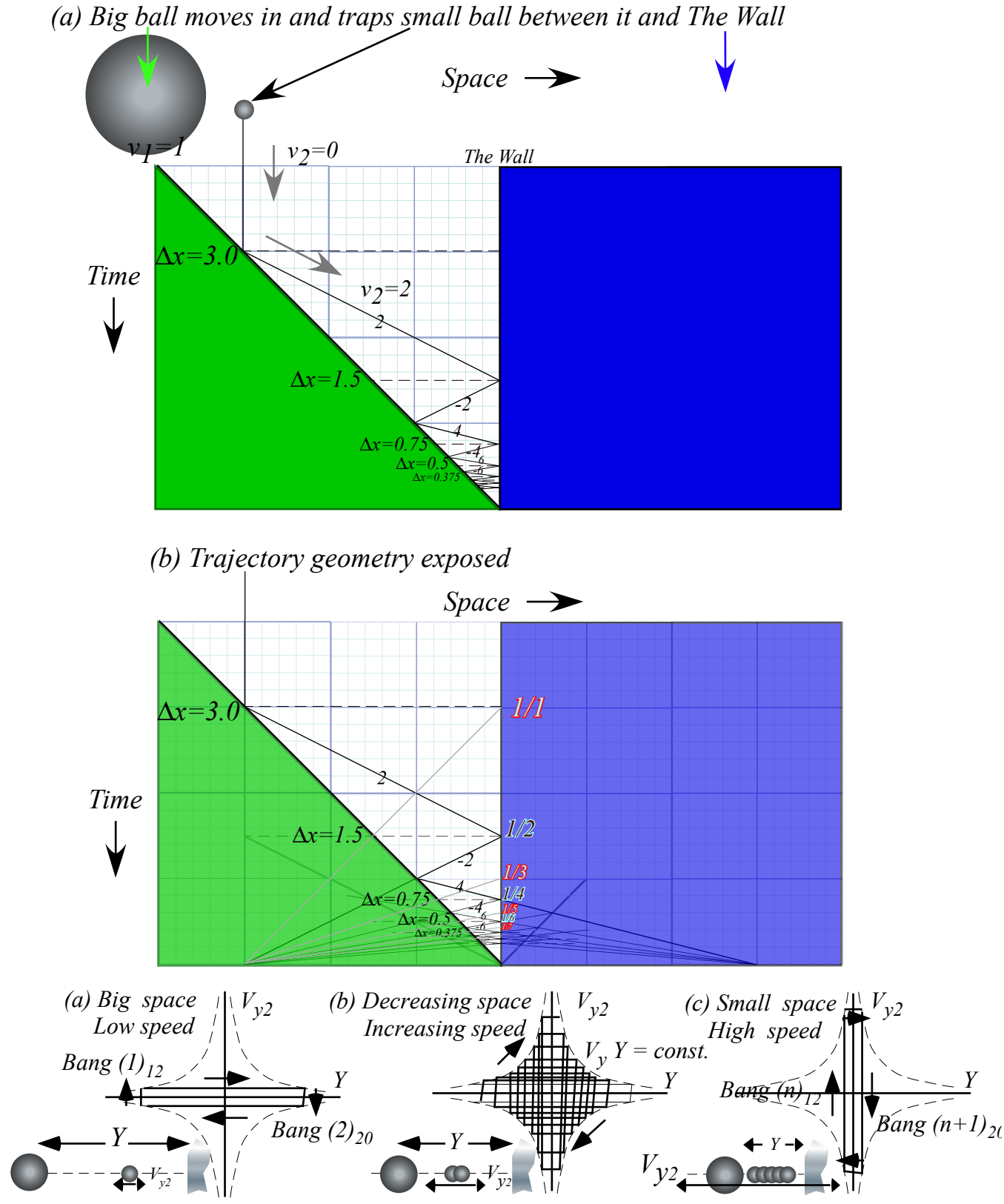

Fig. 6.4 Bang sequence for small ball between big ball and wall. (a) Spacetime paths. (b-c) Geometry of constant product $Y \cdot V_Y$ of velocity and coordinate ranges.

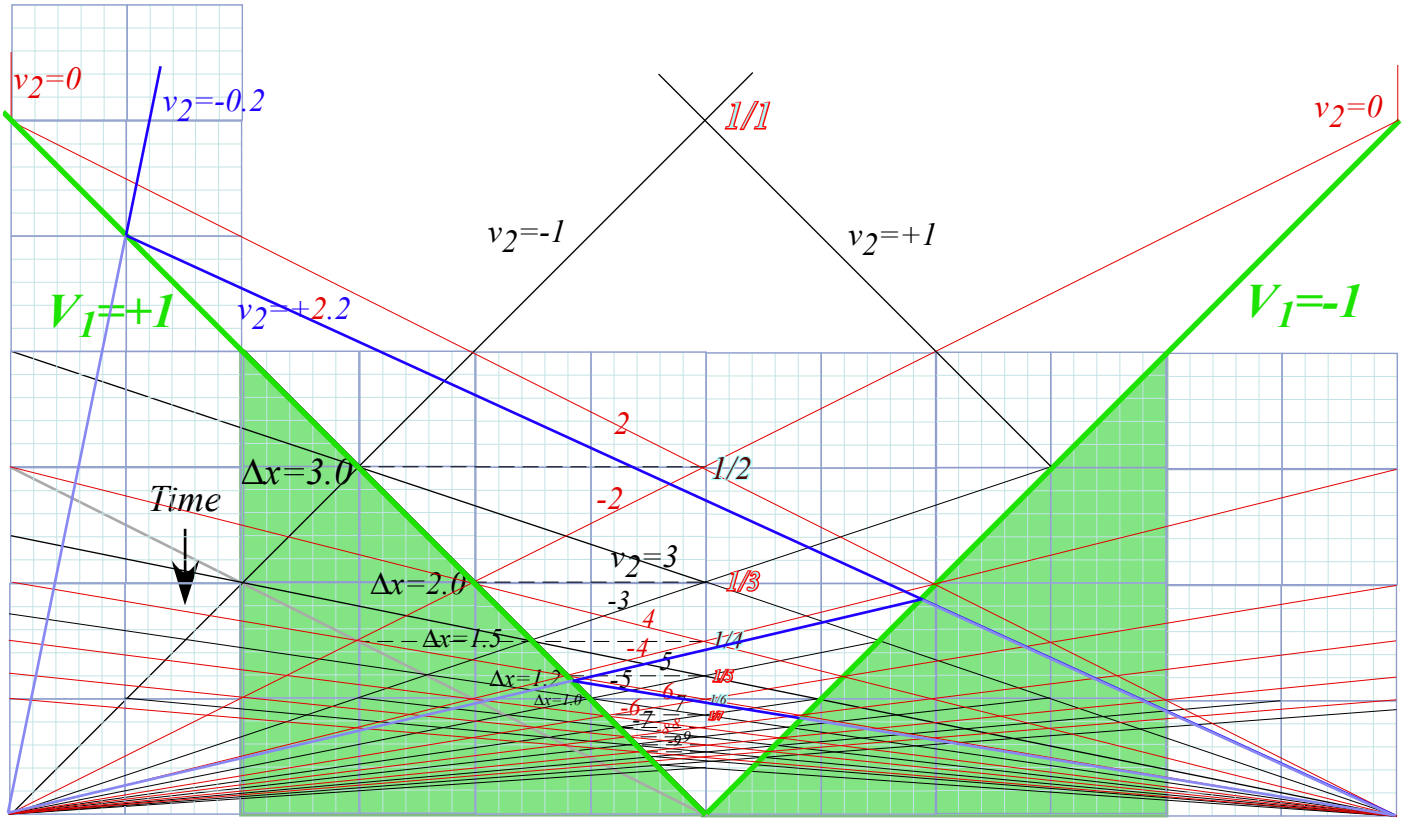

Fig. 6.5 Symmetric pair of head-on $V_1=\pm1$ monster-m_1-masses pong tiny-m_2-atoms to higher speeds.

Monster M_1/m_2-ratios have simple V_1-v_2-plots shown in Fig. 6.6a. (Recall Fig. 6.2.) Wall M_1 simply adds twice its speed ($2V_1$) to incoming speed v_2 of atom m_2 as M_1 bounces m_2 out at that speed $v^{FIN}{}_2=v^{IN}{}_2+2V_1$. Monster M_1 *is* the COM so its path bisects in-and-out paths as it balances v^{IN} and v^{FIN} paths of atom m_2. (In its COM frame each bong is simply a change of sign for velocity. Recall balance in Fig. 2.6.)

The geometry of adding slope $2V_1$ to speed v_2 is shown if Fig. 6.6a. It is based on the unit square and unit velocity $V_1=1$. Incoming $-v^{IN}{}_2$ is an altitude of a right triangle with vertical base $V_1=1$, and it is reflected thru the square diagonal to $+v^{IN}{}_2$ then added to $2V_1$ to give sum $v^{FIN}{}_2=v^{IN}{}_2+2V_1$ as long side of the triangle with right side vertical base $V_1=1$ in Fig. 6.6a. The hypotenuse is the final path with final slope $v^{FIN}{}_2$. Each m_2-path and slope originates or terminates at base $pt\text{-}B_-$ or else $pt\text{-}B_+$. These are ends of the double-unit square bisected by unit slope path of M_1 terminating at B_0. Fig. 6.6.c shows quadrilateral $B_-B_+A_+A_-$ bisected by M_1 path B_0CA_0. Similar triangles explain multiple coincidences.

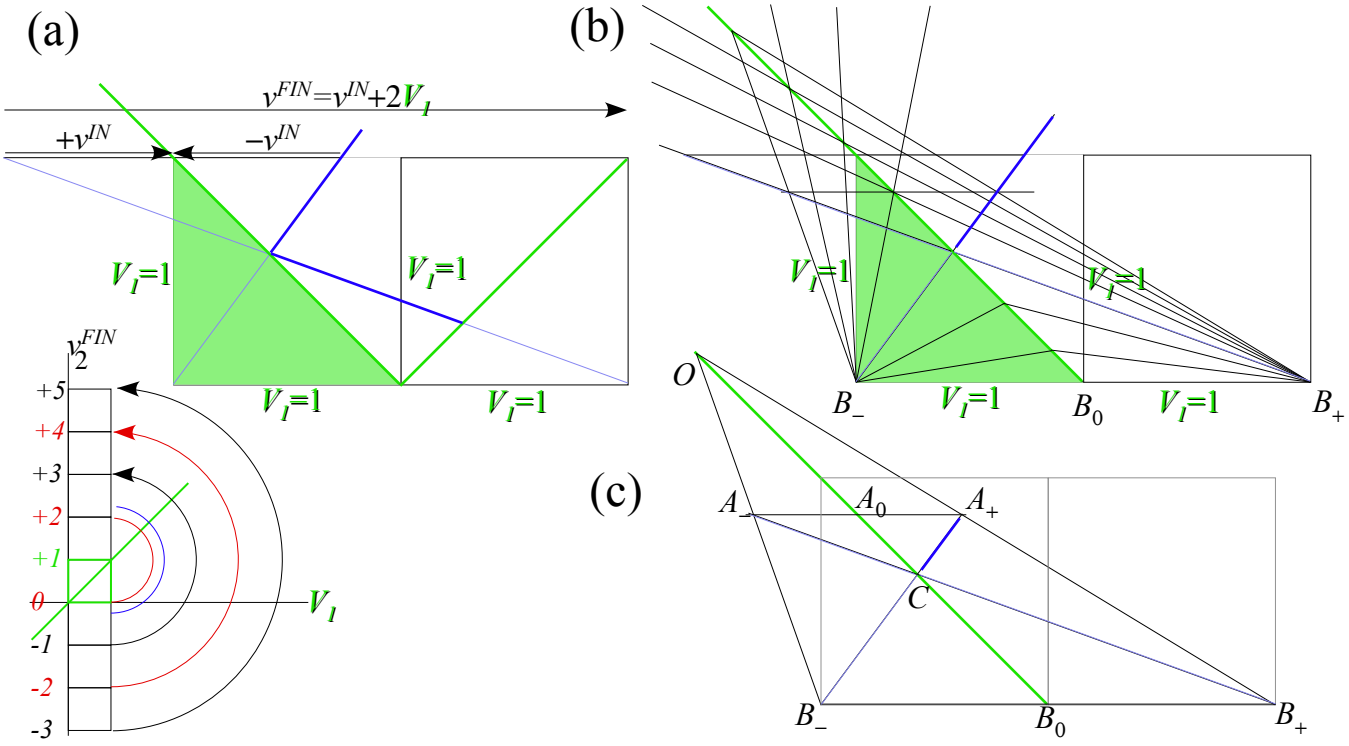

Fig. 6.6 Bisection geometry of Fig. 6.5.

Fig. 6.7 contains time plots for paths in different Galilean reference frames. An excerpt plot in Fig. 6.7a shows how Fig. 6.4 (copied in Fig. 6.7b) appears to a frame traveling at *V=1* with each velocity in Fig. 6.7b reduced by *V=1* in Fig. 6.7a. Also shown in Fig. 6.7a is the extension of lines connecting the two plots and this highlights this remarkable symmetry. All collision times in Fig. 6.7a match perfectly with ones in Fig. 6.7b though all velocities are shifted. Galileo's symmetry wouldn't have it any other way.

(a) *Galilean shift by V=1*

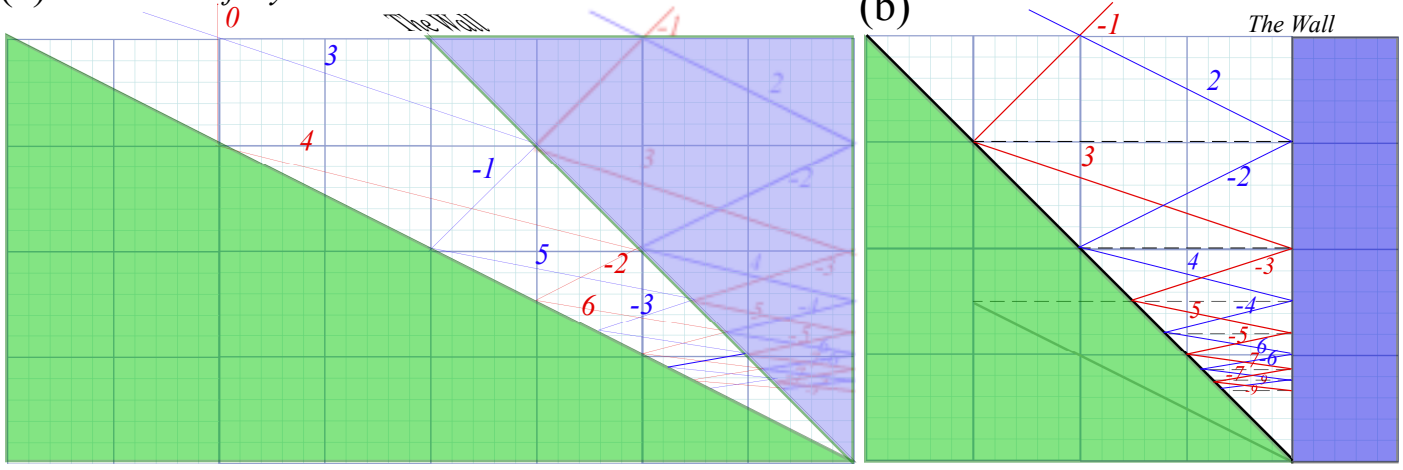

Fig. 6.7 (a) Galilean frame shift by frame velocity V=1 of collision sequence in Fig. 6.4 (shown in (b)).

Exercise 1.6.1 Suppose Fig. 6.3 shows a mass $m_1=1kg$ ball trapped between two smaller mass $m_2=1gm$ balls of high speed ($v_2(0)=1000m/s$ for $x=0$) that provide m_1 with an effective force law $F(x)$ based on isothermal approximation (6.11) while assuming m_1 moves only moderately far or fast from equilibrium at $x=0$.

(a) A further approximation is the one-Dimensional Harmonic Oscillator (1D-HO) force and PE in (6.12). If each mass m_2 start in an interval $Y_0=1m$, derive approximate 1D-HO frequency and period for mass m_1.

(b) What if the adiabatic approximation is used instead? Does the frequency decrease, increase, or just become anharmonic? Compare isothermal and adiabatic quantitative results for $m_1=1kg$ ball being hit by two $m_2=1gm$ balls each having speed of $v_2(0)=1000m/s$ as each starts bouncing in a space of $Y_0=1m$ on either side of the equilibrium point $x=0$ for the $1kg$ ball.

(c) How does the frequency decrease or increase in isothermal case *versus* the adiabatic case if we shorten the run interval $Y_0=1m$ to one-quarter meter?…What if we reduce the mass ratio m_1/m_2 by one-quarter?

(d) Derive the adiabatic frequency for the case $M=50kg$ in adiabatic force of two $m=0.1kg$ masses of initial speed $v_0=20m/s$ and range $Y_0=3m$. Compare with Fig. 1.6.3c.

Exercise 1.6.2 The moving ballwall-trapped-ball constructions in Fig. 6.4 involves a plot of a ballwall coming in with unit slope (velocity). Consider a construction where it has a velocity of $1/2$ and intercepts a trapped ball of velocity -1 at space-time point $(x=-2, t=4)$ that is 2 units from the fixed wall. Construct five or more back-and-forth collisions and comment on what, if any, differences exist with Fig. 6.4. If you can, also construct one or two *prior* collisions (before $t=4$).
Evaluate approximate or average action values as described in class or after Fig. 6.4 in Unit 1.

Chapter 7 Interaction Forces and Potentials in Collisions

Derivation of force field potentials in Ch. 6 used elementary bangs by tiny m_2's on a big M_1. (Ch.5) We predicted elementary bangs between a ball and floor, ceiling, or another ball without knowing potentials. However, three (or more) objects having a *ménage a trois* are not so easy to predict, and outcomes of *3-body interactions* depend more sensitively on whatever interaction potential or force law couples the participants.

Geometry of superball force law

When a superball or any elastic sphere hits the floor or ceiling it dents itself and, maybe it dents the surface it's hitting a little bit, too. But, if the floor, wall, or ceiling is much harder than the ball, we might assume only the ball develops a "flat-tire" as shown in the Figure 7.1a below.

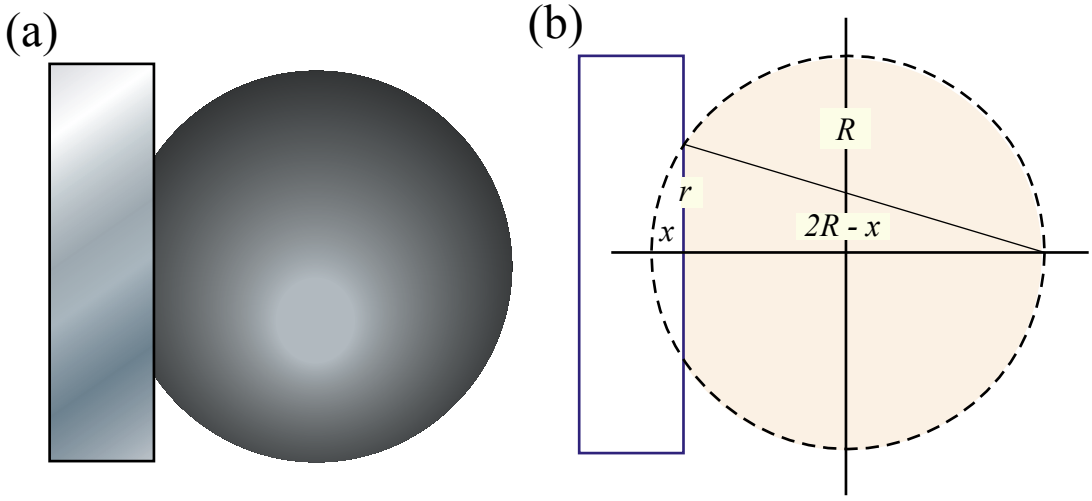

Fig. 7.1 Superball collides with solid wall. (a) "flat" (b) Saggital ("Bow") mean geometry

The radius r of the ball's "flat" is indicated by an altitude in Fig. 7.1b and is the geometric mean of the depression distance x and the remainder $2R$-x of the ball diameter. (Recall Thales geometry in Fig. 1.9a.)

$$r = \sqrt{x(2R-x)} \quad \left(\approx \sqrt{2Rx} \quad for: \quad x << R\right) \qquad (7.1a)$$

Solving approximately for depression x gives the Saggital ("bow") formula. (It's used for thin arc lenses.)

$$x \approx \frac{r^2}{2R} \qquad for: \quad x << R \qquad (7.1b)$$

How much force $F(x)$ is needed to depress the ball by distance x?

The answer is, "It depends." A hollow rubber ball or balloon with pressure P pushes back with force equal to product $P{\cdot}A$ of pressure and area of contact $A{=}\pi r^2$. It is a *linear (Hooke) force law* of a spring.

$$F_{balloon}(x) = P{\cdot}A = P\,\pi r^2 \approx 2\pi PRx \qquad (7.2)$$

(Recall (6.12) and Fig. 6.3.) Another example is gravity inside the Earth. (See (9.4) or Fig. 9.6 in Ch. 9.)

However, the pressure and force in a solid ball varies non-linearly with x. Even if force varies only linearly with volume of the x-dent in Fig. 7.1b, it's still non-linear in x. As seen in (7.4) below, sector volume varies roughly as quadratic x^2 function. Superballs involve even higher power laws. (Superpower!)

$$Volume(X) = \int_0^X \pi r^2 dx = \int_0^X \pi x\left(2R - x\right)dx$$

$$= \int_0^X 2R\pi x dx - \int_0^X \pi x^2 dx = R\pi X^2 - \frac{\pi X^3}{3} \approx \begin{cases} R\pi X^2 & \left(for: X << R\right) \\ \frac{4}{3}\pi R^3 & \left(for: X = 2R\right) \end{cases} \qquad (7.4)$$

(Here we check that our integral gives the whole ball volume $4\pi r^3/3$ for $x=2R$. That's the equivalent of crushing the superball into a black hole (or black spot). It's likely to complain before we get that far!)

Dynamics of superball force: The Project-Ball story

One of the interesting things to come out of *Project Ball* was the superball's peculiar force law behavior. The USC mechanical engineering department took an interest in this crazy project when it showed up on NBC News "Ray Duncan Reports." They offered to measure the superball force curve on a precise tension meter. But, that curve never worked. It didn't predict the bounces the students were observing. Nothing was making any sense even though we had a big analog computer working it all out.

That was a low point in the project. Even with all this fancy experiment, computers, and theory, I looked like I didn't know what the heck I was doing. So, what's new? That's science most of the time! But, to make things worse we got kicked out of the Project Ballroom, the old basement Lab 69 that we'd squatted in. It was up to be repainted so we had to drag all our stuff out of there and store it down the hall.

Well, after that I had to do something with the students so I arranged for a visit to Whammo Mfg. Co. in San Gabriel, California, where superballs and other goofy stuff was made. The Whammo man said maybe we could talk business about selling our super-elastic toy. So, a day or so later, with $$-signs in our eyes, we piled into our cars and drove down to the plant.

The trip to Whammo

By the time we got there, the inventors were on an all-day "alpha-wave break." That's a 60's fad where you try to increase your creativity by looking at your brain waves. I said, "Maybe, I could use some of that stuff!" But, the company lawyer wanted to show us around. After awhile, he said he thought our invention was cool, but its product liability potential looked too high to make a commercial toy.

We all must have looked pretty sad after hearing that. So he went in a back room and dragged out a big collection of superballs that had been rejected for one reason or another. "Here, take as many as you want!" We thanked him and loaded the balls into some boxes and headed back to USC.

When we got back to Rm 69, the painters were done but the paint wasn't quite dry. So I said, "Let's drop off our new balls so we're ready for tomorrow." The students took "drop" to mean literally and dumped them out of the boxes into the empty room. Right away the balls bounced into the wet paint and made lots of little polka-dot spots all over the floor and wall. What fun! What a mess.

Eureka! Polka-dots save Project Ball

But, suddenly, it occurred to me what was wrong with our force analysis and how we might fix it. The engineers had carefully and slowly produced a static or *isothermal* force curve, but what we *really*

needed was a fast-response or *adiabatic* force curve. I thought, *"Maybe that force law can be told by the polka-dots!"*

From a polka-dot radius r made by a superball of mass M and radius R dropped from a height h we could relate gravitational potential energy Mgh to an *adiabatic* superball potential energy U, and then find a $U(x)$ curve for each value of $x=r^2/2R$ in formula (7.1b) by plotting height h against x given by dot radius r. Then the adiabatic force curve $F(x)$ can be found from the slope $dU(x)/dx$ of a $U(x)$ curve.

Just as the adiabatic $F=1/Y^3$ in (6.5) force curve is steeper and curvier than the isothermal $F=1/Y$ in (6.4) so was the polka-dot bounce curve steeper than what we had been using. We stuck our new $F(x)$ on the analog computer's diode function generator and started getting good predictions. Now we could work out the deadly *Model-X3*, a *3*-ball super tower! (This is described later in Chapter 8.)

The "polka-dot" potential

First, let's look carefully at this "polka-dot" potential theory. What we did, like most of physics, was an approximation. Using gravitational potential to estimate superball $U(x)$ is a neat trick only if the superball forces are large and quick compared to the gravitational force or weight mg of the ball.

Fig. 7.2a shows a massive (Bowling-ball sized) superball at its $(V=0)$ drop point h, where potential energy is mgh. Kinetic energy rises from zero as the ball falls and flattens on the floor until it passes a point where the upward floor force cancels the ball's downward weight mg. That point-x_{static} of *static equilibrium* is at the bottom of the total potential energy curve in Fig. 7.2b. The ball would sit still if put gently at x_{static} with no kinetic energy. It's a point of zero slope since total force $F(x_{static})$ is zero there.

After passing x_{static} the ball slows down due to upward force. (That's positive $F(x)$ for $x<x_{static}$.) Finally it stops at its maximum penetration point x_{max} where the total energy line intersects the total potential line in Fig. 7.2c. Now the ball's initial gravity potential mgh_0 has been converted completely into potential energy $U(x_{max})$ due to compressing rubber a distance x_{max}. (We're ignoring tiny frictional heat.)

In the example, the ball's weight is almost as large as the inertial bang-force driving the ball into the floor. An indication of this is how flat the ball is in Fig. 7.2 b when its weight and compressive force are equal. A standard superball sits stiffly on a table with no noticeable depression, and mg is a tiny part of the total force. It's so stiff that its bang force is several times its weight and lasts only a few hundredths of a second. Very stiff rebounding potentials are shown in the later Fig. 7.3 and Fig. 7.4 b in which gravity is a negligible force and stiff rebound forces dominate during the collision.

By comparison, the ball in Fig. 7.2 is heavy and its potential is not so stiff. Instead it is so soft it has a big "flat" if sits still with zero KE at x_{static} just as it does when passing that point in Fig. 7.2 b. The collision shown in Fig. 7.2 a-c is less like a bang and more like a lingering smooch! Similarly soft collision energy for a linear rebound force and quadratic potential is shown in parts (d) and (e) of Fig. 7.4.

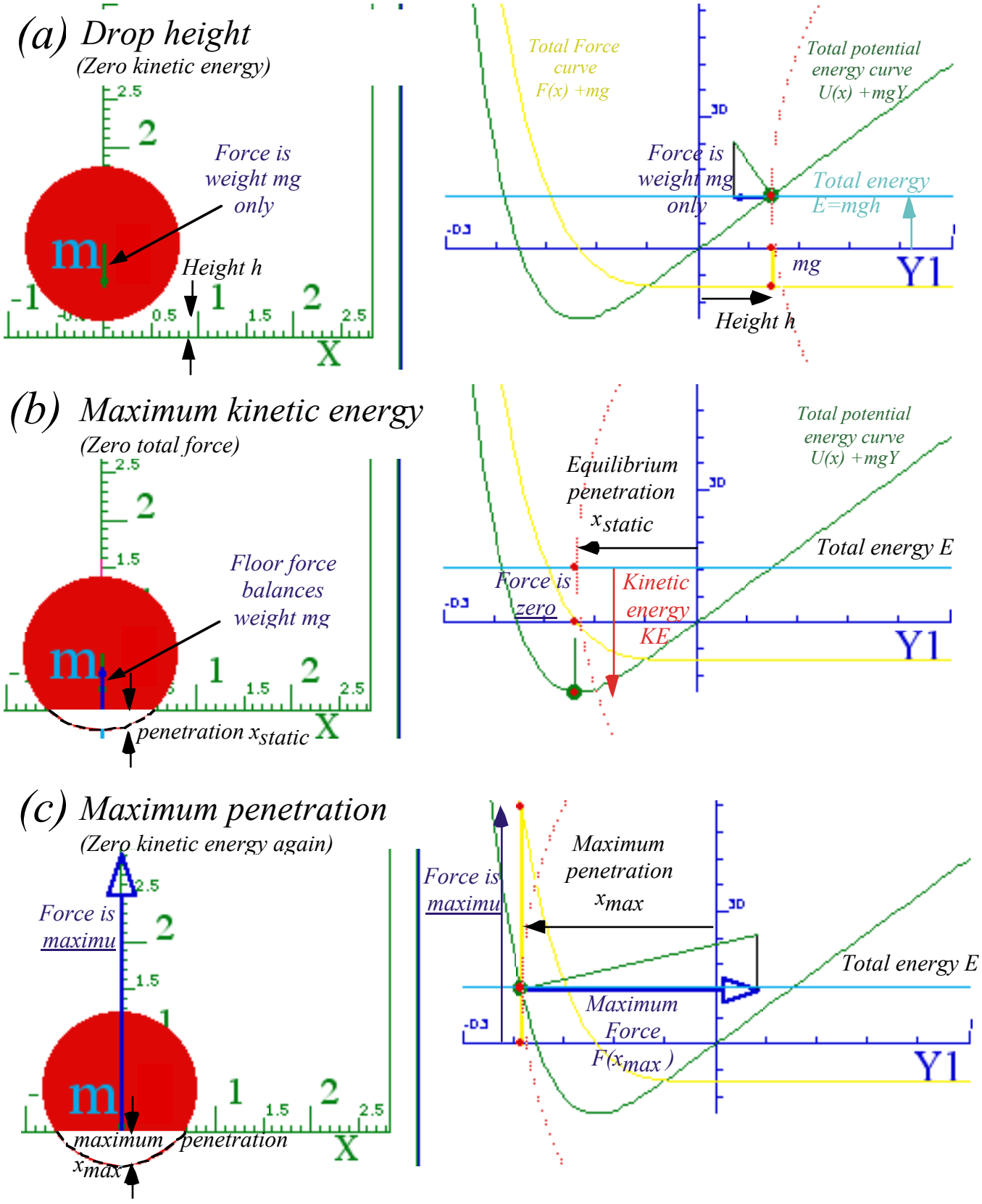

Fig. 7.2 Geometry of ball hitting floor (a) Ball is dropped. (b) Ball at max speed. (c) Ball at low point.

Force geometry: Work and impulse vs. energy and momentum

TV daredevils jump off *30*-meter towers and belly-flop into kiddy-pools that are less than 1 meter deep. What a way to earn a buck! And, how do they ever survive such stunts?

Two important physical quantities tell about survival chances. The first is the product $F\cdot x$ of force-times-distance, or, more precisely, the integral $\int Fdx$ of force over distance. The second is the product $F\cdot t$ of force-times-time, or, more precisely, the integral $\int Fdt$ of force over time. (Recall the fundamental Galileo-Newton relations (3.16) and (6.0).)

The first quantity $\int Fdx$ is *work* done or *energy* $-U(x)$ acquired. $U(x)$ is area under an $-F$ *vs.* x plot.

$$Work = W = \int F(x)\,dx = Energy\ acquired = Area\ of\ F(x) = -U(x) \qquad (7.5a)$$

If energy is stored as potential energy $U(x)$, then force $-F(x)$ is the slope of a $U(x)$ plot at point x.

$$F(x) = -\frac{dU(x)}{dx} \qquad (7.5b)$$

(Recall the discussion of force and potential leading up to (6.10).)

A second quantity $\int Fdt$ is *impulse* done or *momentum* $P(t)$ acquired and area under an F *vs.*t plot.

$$Impulse = P = \int F(t)\,dt = Momentum\ acquired = Area\ of\ F(t) = P(t) \qquad (7.5c)$$

If momentum is stored in kinetic velocity $V(t)= P(t)/M$ then force $F(t)$ is slope of the $P(t)$ plot at time t.

$$F(t) = \frac{dP(t)}{dt} \qquad (7.5d)$$

The time equation (7.5c-d) is just Newton's 2nd law given by (6.0). The space force law (7.5a-b) is just the slope rule first stated (with the physicist's minus-sign) in (6.9). Both laws deal with conserved stuff. If you, a daredevil, acquire x of this stuff (energy or momentum) sooner or later you are going to have to find something or someone help you get rid of x. Or else!

A daredevil falling *30* meters acquires energy equal to gravity force (body weight Mg) times *thirty* meters. Fig. 7.3a-b plots a constant $F=-Mg$ and a linear potential $U(y)=Mg\,y$ from $y=30$ to $y=0$. The *1m* kiddy-pool must get rid of the $30Mg$ (*Newton meters*) of energy in *one* meter, by applying a force of $30Mg$ (*Newtons*) *steadily* over the *entire meter* from $y=0$ to $y=-1$. (That's a $30g\sim300ms^{-2}$ deceleration. Human survivability is somewhere around *50g*.) An alternative is to get rid of that energy in the concrete below the pool in about *1millimeter*, a *30 thousand* g deceleration. (That is *not* survivable!)

Kiddy-pool versus trampoline

Suppose the daredevil falls onto a special trampoline that applies exactly the same constant force as the kiddy-pool, but stores the energy as potential instead of dissipating it all by dousing the audience with a huge splash. (Recall *Ka-Bong!* versus *Ka-Runch!* in Ch. 1.) The trampoline could then toss the daredevil back up to the *30 m* tower to do the fall over again. (My gosh! What a daredevil has to do to satisfy a sated TV audience these days!) Such a potential is plotted by a steep-slope line $U(y)=-30y$ in Fig. 7.3b.

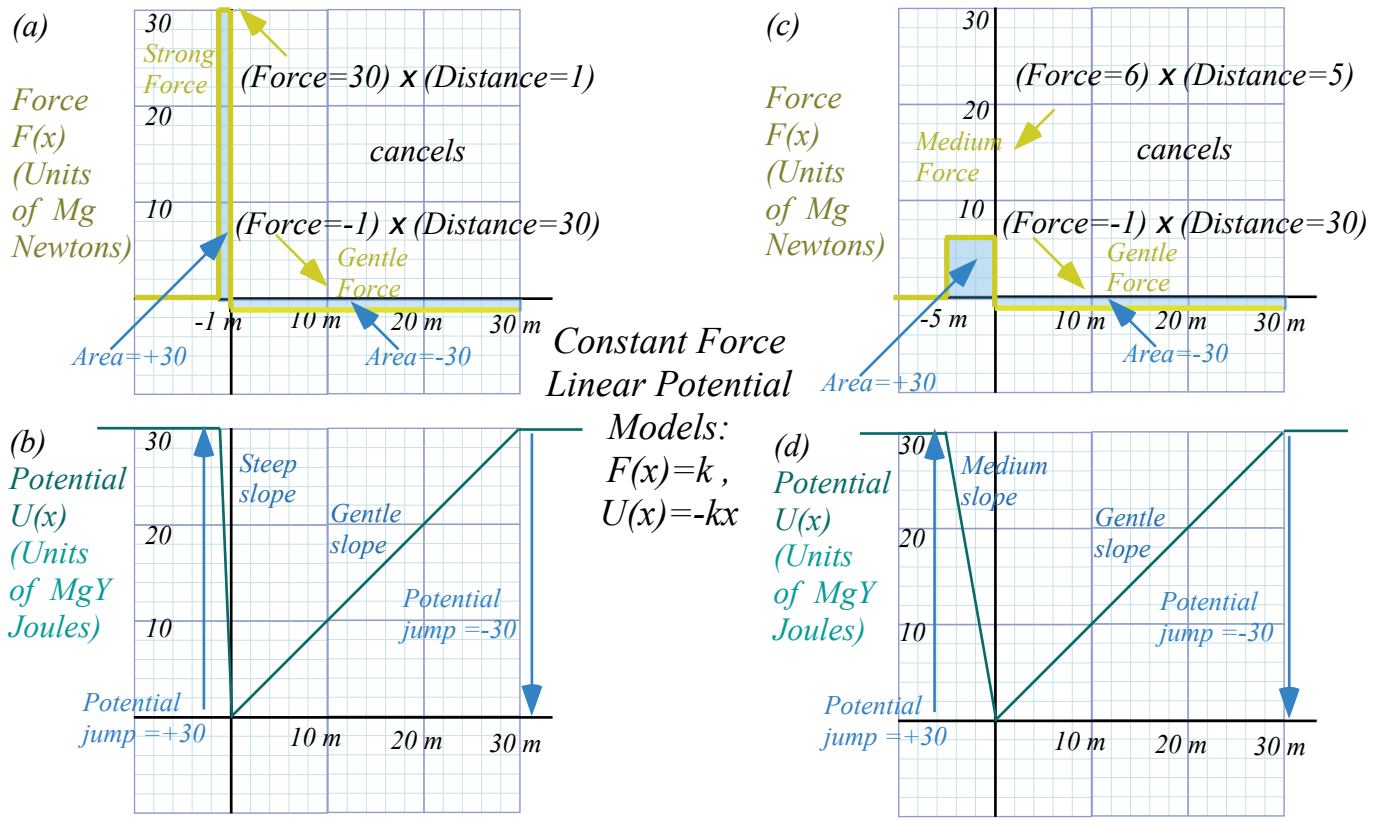

Fig. 7.3 Force and potential plots. (a-b) Strong (30g) deceleration. (c-d) Medium (6g) deceleration.

Suppose the Americans for Humane Daredevilry (AHD) demand that the deceleration distance be increased from 1 meter to 5 meters. (That's what Olympic divers get for a *10 m* fall.) As shown in Fig. 7.3c this reduces the deceleration by a factor of 5 from *30g* to only *6g*. (A walk in the park!) The sloping *U(x)* lines are tallying the area-accumulation under the *F(x)* lines. Starting on the right hand side, *U(x)* drops by *30* units in *30* meters in Fig. 7.3b to correspond to the *–30* units of area under the gravitational *F=-1* unit line for the same distance in Fig. 7.3a. The daredevil's kinetic energy must increase by *30* units to conserve total energy. So trampoline or pool is hit at *24* meters per sec. or 55 mph. (Recall (6.13).)

$$^1/_2\, M\, V^2 = 30\, Mg \qquad or:\ V=\sqrt{(60g)} = \sqrt{588} = 24.2 m/sec.$$

Getting rid of this *30 J* potential deficit means climbing a steep *30 J* high slope between *y=0* and *-1* in Fig. 7.3b or a medium slope of the same height between *y=0* and *–5* in Fig. 7.3d. Both cases have the same *+30 J* area under a force line, but having 5 meters instead of just one reduces the force to $^{30}/_5=6$.

Time functions *F(t)* and *MV(t)=P(t)* relate to *F(x)* and *U(x)* using *Newton II:* $F=M^{dV}/_{dt}$ in (7.5d).

$$-U(x) = \int F(x)\,dx = \int M\frac{dV}{dt}dx = \int M\frac{dx}{dt}dV = \int MV dV = M\frac{V^2}{2} - const. \quad \text{or: } M\frac{V^2}{2} + U(x) = const. \qquad (7.6a)$$

$$P(t) = \int F(t)\,dt = \int M\frac{dV}{dt}dt = \int M dV = MV + const. \qquad \text{or: } P(t) - MV(t) = const. \qquad (7.6b)$$

The first relation is *total energy conservation* (*KE+PE=const.*) first stated in (6.6) and (6.7).

Linear force law, again (But, with constant gravity, too)

Let's imagine the AHD demands further protection of daredevils from themselves by outlawing constant-force targets that turn on a full force suddenly upon entry. Claiming that "high-jerk" is bad, the AHD requires *linear-force* targets, instead. Physicists comply happily since a harmonic-oscillator linear-force-quadratic-potential (6.12) is the favorite force law. It also describes inside-Earth oscillation in Chapter 9.

Plots of linear-force-quadratic-potentials are shown in Fig. 7.4. Just like the preceding Fig. 7.3, a constant gravitational force $F_{grav}=-Mg$ is present both in and out of the $(y<0)$-region where the linear $F=-ky$ force and the $U(y)=\frac{1}{2}ky^2$ potential exist as a sum of constant and linear forces for $(y<0)$.

$$F^{Total}=F^{grav}+F^{target}=\begin{cases}-Mg & (y\ge 0)\\ -Mg-ky & (y<0)\end{cases} \qquad (7.7a)$$

$$U^{Total}=U^{grav}+U^{target}=\begin{cases}Mg\,y & (y\ge 0)\\ Mg\,y+\frac{1}{2}ky^2 & (y<0)\end{cases} \qquad (7.7b)$$

If a linear potential $b\cdot y$ is added to a quadratic $a\cdot y^2$ potential we get the same parabolic curve $U=a\cdot y^2$, but that curve is shifted to the left by $y_{shift}=-b/2a$ and down by $U_{shift}=-b^2/4a$ as follows.

$$U^{Total}(y)=ay^2+by=a\left(y+\frac{b}{2a}\right)^2-\frac{b^2}{4a}=a\left(y-y_{shift}\right)^2+U_{shift} \qquad (7.8a)$$

$$y_{shift}=-\frac{b}{2a}, \qquad U_{shift}=-\frac{b^2}{4a}=-a\left(\frac{b}{2a}\right)^2=-U\left(y_{shift}\right) \qquad (7.8b)$$

The nose or tip of the parabola, which is the equilibrium resting point, follows an upside-down copy of the U-parabola itself! This important geometric fact is shown in Fig. 7.4. The geometry does not reveal itself until we look in Fig. 7.4e at a "soft ball" that is soft enough to clearly show its gravitational shifts. A hard superball is more like Fig. 7.4b that barely shows such a small shift.

Hardball total potential is $u(y)=8y^2+y$ with a total force function $f(y)=-16y-1$ in graph units of Fig. 7.4(a-b). A medium total potential is $u(y)=y^2+y$ with a total force function $f(y)=-2y-1$ is plotted in Fig. 7.4(c-d). The latter clearly shows the equilibrium or lowest "sag" point of zero force. The softball total potential is $u(y)=(1/4)y^2+y$ with a total force function $f(y)=-(1/2)y-1$ in Fig. 7.4e. The hardball potential requires about 6 meters ($Y=-6$ or $y=-0.6$) to cancel the energy from the 30 meter fall (from $Y=30$ or $y=3$) and maximum force of about $F=10$. This is much more than the constant $F=6$ that stopped the same daredevil in 5 meters in Fig. 7.3c because a linear force has only the area under a triangle which has a factor of $\frac{1}{2}$. Here $\frac{1}{2}(F=10)(Y=-6)$ gives the necessary energy of *30 Joules*. So the AHD ruling has actually *increased* the maximum force on the daredevil! (But, only during the final milliseconds is F large.)

Note that the focus of the $U(y)$ parabola is on the y-axis because we plot gravity with $slope=1$. Can you find a geometrical a way to locate that focus given some allowed stopping distance?

Parabolic geometry of an oscillator potential subject to a uniform (or nearly uniform) force field is an important one in physics. Electronic charges pinned to an atomic potential well behave like oscillators in an electric field of a passing light wave. Generally the light wavelength of 0.5 micron ($0.5E-6m$) is several thousand times as long as the atomic radius of a few Angstrom ($1E-10m$). So the effective potential is a rigid parabola like Fig. 7.4e shifting to and fro and up and down at some frequency.

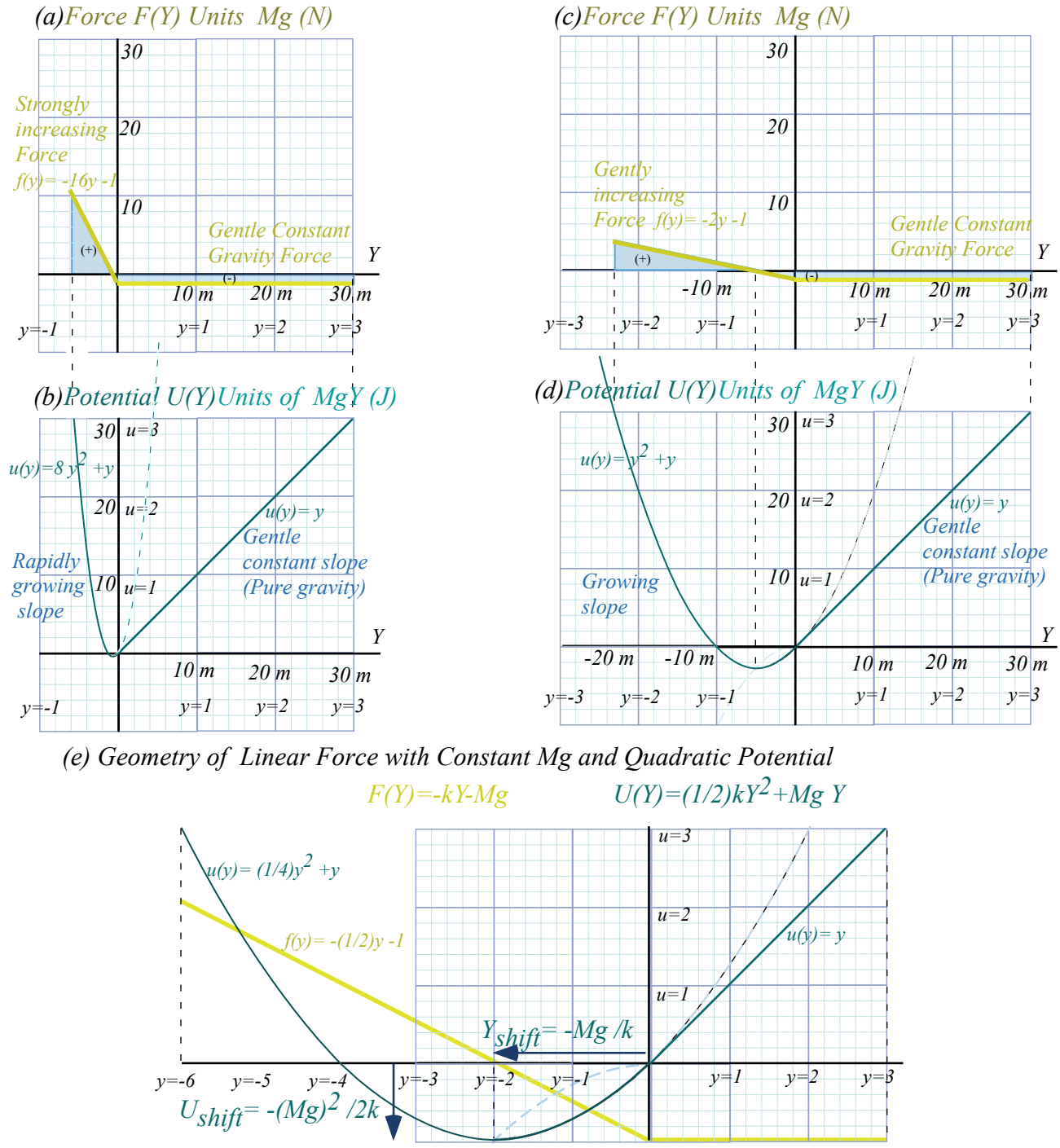

Fig. 7.4 Linear deceleration force after constant falling force. (a-b) Hard (c-d) Medium (e)Soft

As we mentioned, superball force function is non-linear; approximately $F_{ball}(y)\sim y^4$ plotted in Fig. 7.2 and Fig. 7.5 below. Compare this to the linear balloon-like force curve $F_{balloon}(y)\sim y^1$ in Fig. 7.4e above. (Recall (7.2).) $F_{balloon}(y)$ is a pair of straight lines bent at contact point $y=0$, while $F_{ball}(y)$ has a long flat region below $y=0$. For either case, the force integrals $\int F^{total}(y)dy$ and the areas they represent cancel between any two points $y=h$ and $y=y_{max}$ that have the same potential energy $U(h)=E=U(y_{max})$. If that energy is the total energy E then these points $y=h$ and $y=y_{max}$ are *classical turning points*. The mass M stops with zero KE (no speed) to turn around and fall backward or forward, respectively, into the potential valley lying between

h and y_{max}. *PE* curve $U^{total}(y)$ near bottom (y_{static}) in Fig. 7.2-5 is nearly parabolic as is $U(x)$ in Fig. 6.3. The difference for Fig. 7.4 is that *all* of the $U^{total}(y)$ curves are *perfectly* parabolic for $y<0$. (See exercise 1.7.1.)

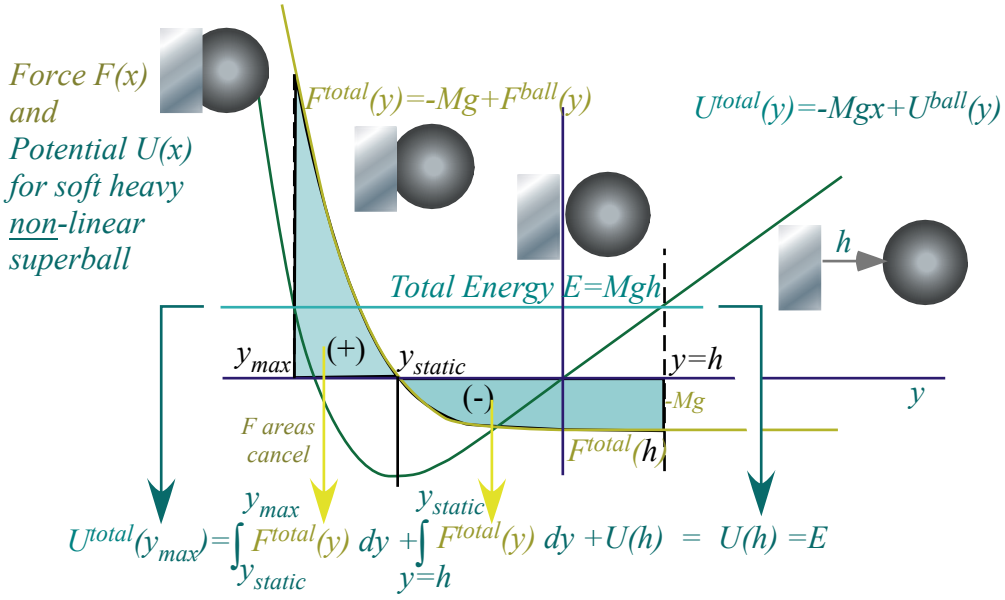

Fig. 7.5 Force and potential for soft nonlinear ($F=ky^4$) superball dropped from height h

Why super-elastic bounce?

Super-elastic bounce involving two balls was introduced way back in Fig. 4.5 and "explained" by the 2-Bang model sketched there. Is that the only explanation? Certainly not! Is it even right? Well, yes and no. Here is a chance to discuss how science works or doesn't work. It is, after all, a human endeavor. *(To err is…)*

RumpCo versus Crap Corp

Let's imagine a big scientific fight between two research groups something like real ones I've seen. We'll imagine it's about superball dynamics. On one side is a small but creative group working for the Rumpany Company® that first discovers the effect and explains it with the 2-Bang model. But their small budget limits them to things you can do cheaply with a ruler and compass.

On the other side is the huge *Crap Corporation*®. With unlimited military contracts, *CrapCorp* can afford any kind of computer or lab equipment. They hear about RumpCo's discovery and decide to develop and sell it to the Army as a bomb detonation system.

I hope you'll excuse a scatological nomenclature and contempt for shortsighted and mindless goals often associated with post-modern cash-flow-science. My allegorical objective is to encourage curiosity-driven-science that is now becoming regarded as quaint. I do believe that humans are capable of creating much more than fertilizer and should be strongly encouraged to do better. If earning gets in the way of learning, then humans do poorly. I have watched big labs in government, industry, and university die of a pernicious groupthink fueled by the *a*cquisitive rather than the *in*quisitive human drives. People lose their ability to reflect and become happy to merely genuflect. A novel *Radiance* by Carter Scholz *(Picador 2002)* is a "Star Wars" *romaine a'clef* exposing foibles of scientists at Livermore and Los Alamos.

On one side of our allegory is poor but resourceful little RumpCo full of ideas but nowhere to go. Their 2-Bang model of super-elastic bounce is simple, elegant, but appears wrong. The powerful *Crap Corp*, on the other hand, knows where it's going and what's right. It has every resource imaginable. Except wisdom.

Crap Corp's first move is to discredit RumpCo's work. They set up a computer that uses lab observed potential functions to fully analyze a *2*-ball bounce. Let's compare two competing vu-graphs side-by-side.

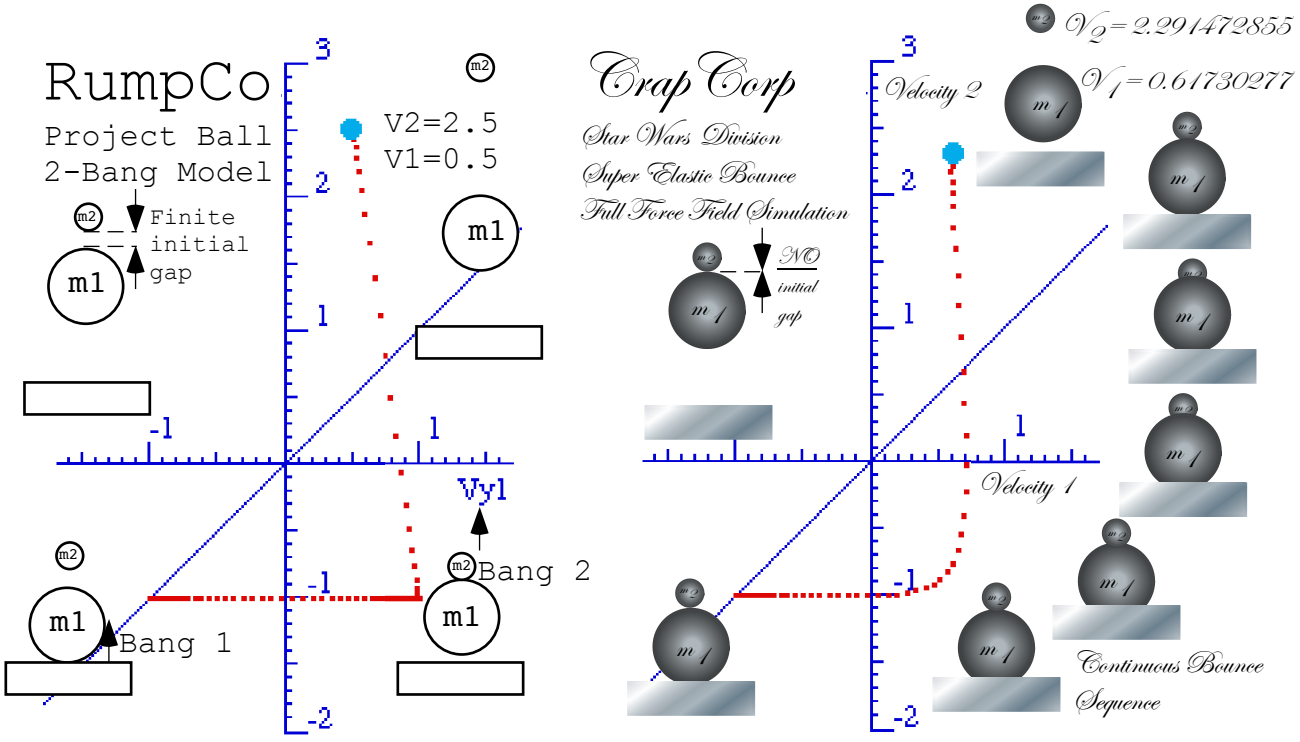

Fig. 7.6 RumpCo *theory versus* *Crap Corp*'s *simulation. (*RumpCo*) Finite initial gap (*Crap Corp*) NO gap*

One thing is clear. *Crap Corp* does fancy-schmancy vu-graphs! They resemble wedding invitations. And, while *Crap Corp*'s 10-figure precision is dubious, we note their V_1=0.62 and V_2=2.29 disagree with RumpCo's predictions (Recall Fig. 4.4.) of final v_1=0.5 and v_2=2.5 by a little. Furthermore, RumpCo uses an independent 2-ball bang model. They assume or *idealize* an initial gap separating mass m_1 from m_2 so *Bang-1* of m_1 with the floor is independent of *Bang-2* between m_1 and m_2. So v_1 and v_2 result from 2-body energy-momentum conservation. RumpCo's results are not sensitive to force functions.

Crap Corp can compute the difficult *3-body collision* between m_2 , m_1, and m_0 (the Earth) all together just like what's really happening on the floor. *Crap Corp* 's curvy V_1 *vs.* V_2 plot in Fig. 7.6 is very sensitive to each force function *F(y)* between each pair of colliding bodies. When (and *if*) *Crap Corp* values check out with experiment, they'll happily sneer at the primitive pair of straight lines in the RumpCo velocity plot.

Does RumpCo have nearly the right (v_1,v_2) for wrong reasons? Not entirely. The reason a 2-Bang model works at all is that the force function for these balls is highly *non*-linear. A quartic function $F(y)=y^4$ has a flat bottom as noted before Fig. 7.5. That allows the floor-m_1 collision to nearly finish before the m_1-m_2 bang really gets going even though the balls are in contact all during the collision.

Realizing this, the RumpCo researchers suggest that *Crap Corp* try a *linear* force $F(y)=y^1$ simulation to see if super-elastic bounce disappears. They do, it does, and the rest is history. As seen in Fig. 7.7, m_1 and m_2 bounce up in unison. It's a *pax de deux*. Super-elastic bounce goes away!

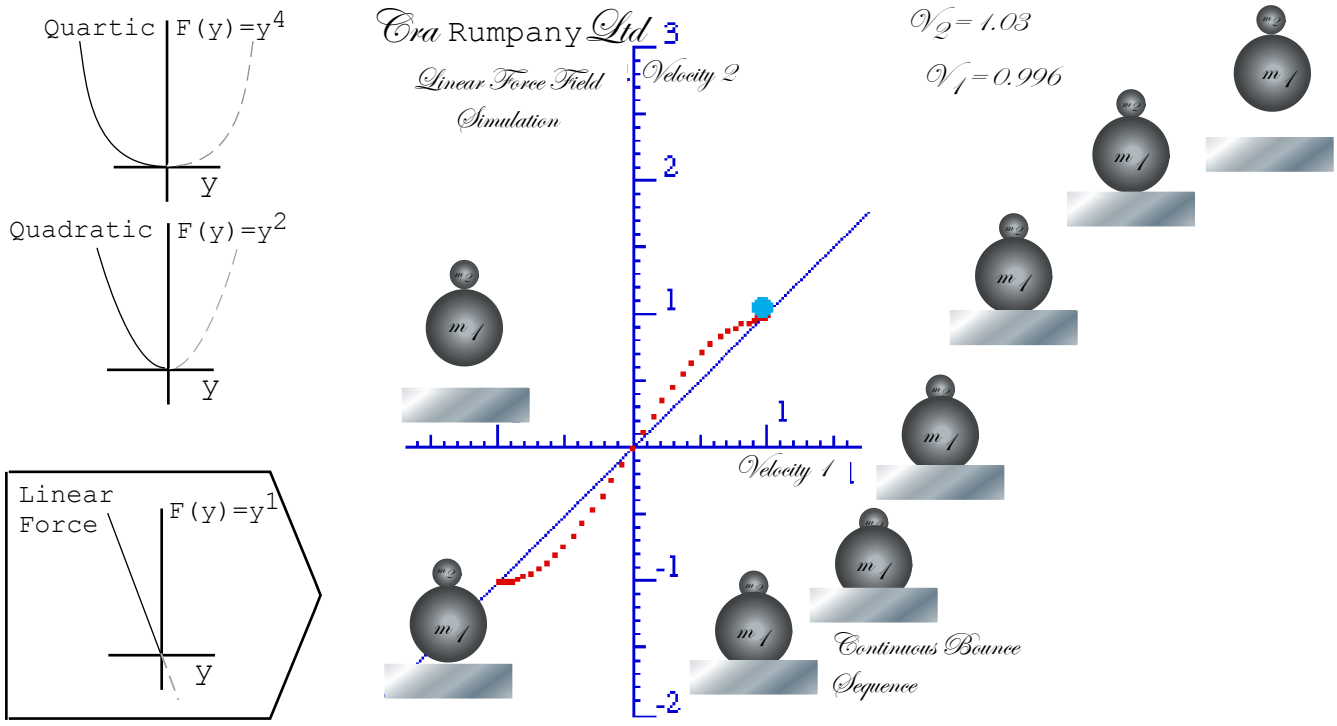

Fig. 7.7 Linear force kills super-elastic bounce. (Collaborative effort.)

The two groups decide to stop feuding and join forces. A corporate merger results in a multi-national conglomerate *Carumpany Ltd.* based in the Caymans. They lived happily ever after. (Well, sort of.)

Seatbelts and buckboards

Another important physics lesson from this section is, "Fasten your seatbelts…tightly!" To avoid great and damaging force you need to avoid non-linear force functions and fasten yourself with linear ones that can start working off your kinetic energy and momentum most immediately after a collision. The non-linear force with its "flat" region applies little or no force at first but then has to make up for its procrastination with deadly high force after it's too late. Note how nonlinear force in Fig. 7.5 finishes much higher than the linear force in Fig. 7.4. Even worse is having no seatbelt at all. That's like a very non-linear force of, say, $F(x)=kx^{100}$. It's a flat gap with a practically vertical wall waiting to crush you!

One of the most dangerous vehicles in the Wild West of the early US was the *buckboard*, a wagon with no suspension except for a set of springs right under the rider's seat. When the buckboard hit a bump it generally lived up to its name. Unfortunate riders ended up like a little m_1 superball knocked skyward by a big m_2 wagon. A safer and more comfortable ride is had in a car with a body as much heavier than the wheels and suspension as possible. So-called "Monster trucks" have the worst kind of ratio possible for stability.

Friction and all that "dirty" stuff

Slowly we have put back some of the "real-world" features of the superball collisions that our idealized "Bang-Bang" models of Ch.4 ignored in order to make the problems more easily solvable. The effects of gravity during collision have been introduced and applied to interacting zero-gap superballs. More such effects will be studied in what follows since interacting linear forces are very common in nature and there are ways to make them easily solvable, too. The oscillating neutron star in Ch. 9 provides a taste of what is to come in the study of waves and oscillation in Unit 4 and orbits in Unit 5.

But even the neutron star model neglects what is the bane of the purist physicist, the dreaded *frictional forces*. These are among the most neglected and poorly treated physical effects in physics. If anything goes wrong with a theory, we just blame it on friction! Often we have little choice in this matter.

Friction is a result of having more particles than we'd like to admit. Consider one $m_1=72$ *gram* superball. That's about a *mole* of Carbon C_6 rings and a mole has *6.02E23* (That's *Avogodro's number*.) of these C_6 molecules. So we're dealing with not *one* mass m_1 particle but an enormous heap with an unimaginably huge number *60,200,000,000,0000,000,000,000* of particles that individually are (mostly) friction-free and well behaved, but their mob-behavior is just plain abominable!

You've got to get down to at least the individual molecular level before "internal-friction" is pretty much a non-existent phenomena and pure quantum wave mechanics rules. So what we call "frictional loss" is simply the best accounting we can do of 60.2 gazillion chiseling thieves stealing bits of energy that turn up later as "heat." In conservative economics the effect is known as "supply side" or "trickle-down." Let's see if we can account for energy chiseled by just *three* thieves. (And, then we'll hire more thieves until we bankrupt the whole operation!)

Important atomic and molecular force geometry

1.1.2 A most important mechanics problems is that of atomic oscillators affected by electric fields since it is basic to all spectroscopy. A useful approximate model is potential $V^{atom}(x)=k\,x^2/2$ function of center x of charge Q where k is a spring constant of atomic polarizability. A uniform electric field E is assumed to apply a force $F=Q\cdot E$ to the charge by adding a potential $V^E(x)$ to $V^{atom}(x)$. (Give $V^E(x)=$_____ and $F^E(x)=$_____)

Consider the resulting potential $V^{total}(x)$ for an atom for unit constants $k=1$ and $Q=1$. Derive and plot the new values for equilibrium position $x^{equil}(E)$, energy $V^{equil}(E)$, dipole moment $p^{equil}(E)$. Plot $V^{total}(x)$ for field values of $E=-2,-1, 0, 1, and\ 2$.

Does charge oscillation frequency $\omega^{equil}(E)$ change? If so express in terms of $\omega^{equil}(0)$ and E?

Chapter 8 N-Body Collisions: Two's company but three's a crowd

Without knowing force and potential effects on superball collisions, it is often impossible to even approximately predict the outcome for *N=3, 4,* or more balls. But, if all *N* masses have independent one-on-one collisions with the floor, the ceiling, and each other, prediction can be done "Bang-by-Bang" as in Ch.5. Difficulty arises when three or more collide at once. Then prediction may need precise and detailed treatment of their interactive force laws. Elastic binary or one-on-one collisions in *one* dimension are solved completely by momentum conservation alone as we've done since Ch. 4. But, as we'll see, anything more complicated may require more work, and often it requires a *lot* more work!

The X3: Three-ball towers

One of the goals of *Project Ball* at USC was to optimize final velocity for superball towers with three or more balls stacked up like a pyramid as in a multi-stage rocket. One dumb idea was a cheap satellite launcher. It's dumb because, even if you could achieve *8 km/s* (See discussion in Ch. 9.), you'd burn it up in the atmosphere. (Well, OK, but on the *moon*…?)

Actually we were happy just to break the theoretical 2-ball limit of *3.0*-times-initial. (Recall discussion of the INF limit in and after Fig. 4.5.) As seen in Fig. 8.1a that is done quite easily by a 3-stage tower which achieves a velocity that is $V_3=3.41$ times initial drop-speed $(V_n(0)=1 \text{ for } n=1,2,3)$.

An even better final speed of $V_3=3.62$ is had in independent collisions caused by setting initial gaps between the falling balls as shown in Fig. 8.1(b) so each collision can be completed before the next one begins. Then the result becomes independent of the force law governing the detailed trajectory within each collision, and a geometric construction in Fig. 8.1(b), based on momentum conservation, finds velocity accurately if collisions are independent. This requires force non-linearity or large initial gaps that are enough to reduce or eliminate *N*-body contact effects for $N>2$.

Conversely, zero initial gaps often reduce the final velocity maximum below independent collision values. This is particularly true if the force law is linear as shown in Fig. 8.1(c). The 3-ball linear case comes out very much like the linear case for a 2-ball tower in Fig. 7.7. No single mass gains much speed over its neighbors. Super-elastic bounce is essentially squelched.

The American Journal of Physics† paper produced by *Project Ball* contains a discussion of attempts to optimize super-elastic bounce in towers of 3 or 4 balls. Progress was made but the theory needs work. As we will see later, this dynamics is somewhat analogous to wave motion in a varying channel. An early AJP paper†† has an analogy between a trumpet and a chain of sliding balls whose masses increase geometrically. It's also analogous to tsunami wave build-up. A rule-of-thumb is that optimum-velocity chains satisfy a geometric-mean mass relation $m_2=\sqrt{(m_1 m_3)}$ as is approximately so in Fig. 8.1. Later on, some of this technology was developed into a toy by Stirling Colgate (astrophysicist and toothpaste heir) and company.

† Class of WGH, *Am. J. Phys.* **39**, 656 (1971).

†† J. B. Hart and R. B. Herrmann *Am. J. Phys.* **36**, 46 (1968).

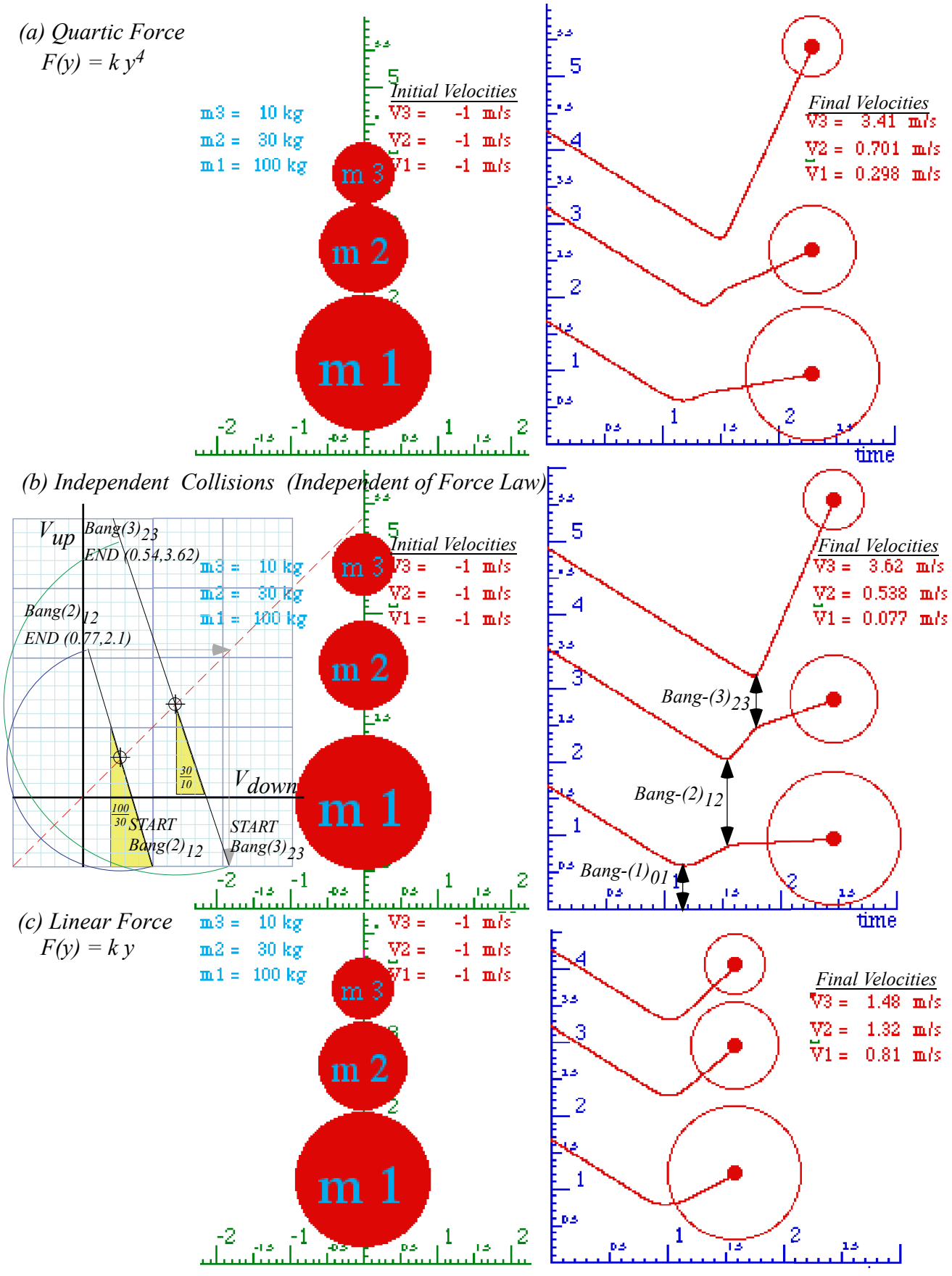

Fig. 8.1 Dropped 3-ball tower. (a) Quartic force (b) Independent (Finite gap) (c) Linear force.

Geometric properties of N-stage collisions

The 3-stage collision construction in Fig. 8.1b uses earlier construction of Fig. 4.4. It begins after the lowest mass $m_1=100$ has rebounded from the floor to the *Bang(2)$_{12}$ START* point $(V_1=1,V_2=-1)$ where it meets mass $m_2=30$ and bangs up to *Bang(2)$_{12}$ END* point $(V_1=0.77,V_2=2.1)$ on a slope $^{100}/_{30}$ line. The second velocity $(V_2=2.1)$ of mass $m_2=30$ is then transferred (See gray arrows.) to the first component of *Bang(3)$_{23}$ START* point $(V_2=2.1,V_3=-1)$. There m_2 meets mass $m_3=10$ and bangs it up to *Bang(3)$_{23}$ END* point $(V_2=0.54,V_3=3.62)$ on a slope $^{30}/_{10}$ line, giving final top m_3 velocity $V_3=3.62$.

A 4-stage collision tower sequence with nearly the same mass ratios is constructed in Fig. 8.2(a). Here each mass m_1, m_2, and m_3, is exactly 3-times the one above it, and the top mass m_4 gets the biggest boost of nearly *5.8*. Recall *Maximum Energy Transfer* (*MET*) case in Fig. 4.5 where a mass ratio of three $(m_1/m_2=3)$ leaves the lowest ball stopped $(V_1=0)$. In Fig. 8.1b m_1 is nearly stopped. $(V_1=0.077)$.

The same arrangement with a higher mass ratio $m_k/m_{k+1}=7$ is constructed in Fig. 8.2b. Here the top mass m_4 gets a boost of over *9.0*. That is a kinetic energy boost factor of $(V_4)^2=81$ and an altitude bounce of four or five hundred feet if dropped from arm's length. (Friction is being seriously neglected!)

Supernovae super-duper-elastic bounce (SSDEB)

Imagine dropping two towers like the ones in Fig. 8.2a-b from either side of a tunnel through the Earth so the two lowest m_1-masses run into each other at the center. If the resulting collisions were elastic, they could send the other masses to infinity with energy to spare! Later we see escape from Earth's surface takes only three times the energy it takes to sit there. *(Starlet escapes!)* Energy factors for a conservative *3:1*-tower are $2^2=4$, $3.5^2=12.3$, and $5.8^2=34.8$ and more than enough for a free ride to kingdom come. Astrophysical modeling of Type-II supernovae reveals just such a high speed SSDEB when a star, like a spherical layer-cake with lighter elements above heavier ones, collapses. *Boom!* It appears that most of our Earth and bodily stuff has come along on such a ride! As Carl Sagan remarked, we are of blown-up stars.

Newton's balls

Novelty stores have simple examples of multistage collisions made by hanging identical ball bearings in line as sketched in Fig. 8.2c-d. These are also common lecture demos, and they have been called "Newton's balls." That can at least elicit some giggles from otherwise boring lectures.

Few teachers explain the details of the cool pop-up-single in Fig. 8.2d. In fact, it won't work unless all the collisions are *independent*, and this requires *non*-linearity of the sphere-on-sphere force function, as we saw in Fig. 8.1. Cooler still, is an elastic *4*-ball column-bounce in Fig. 8.3c. *N*-balls need $N(N+1)/2(=10 \text{ if } N=4)$ independent bangs to get all *N* balls back with the same speed. Given this, it seems a wonder that solid objects can bounce elastically. (In fact, they cannot, quite!)

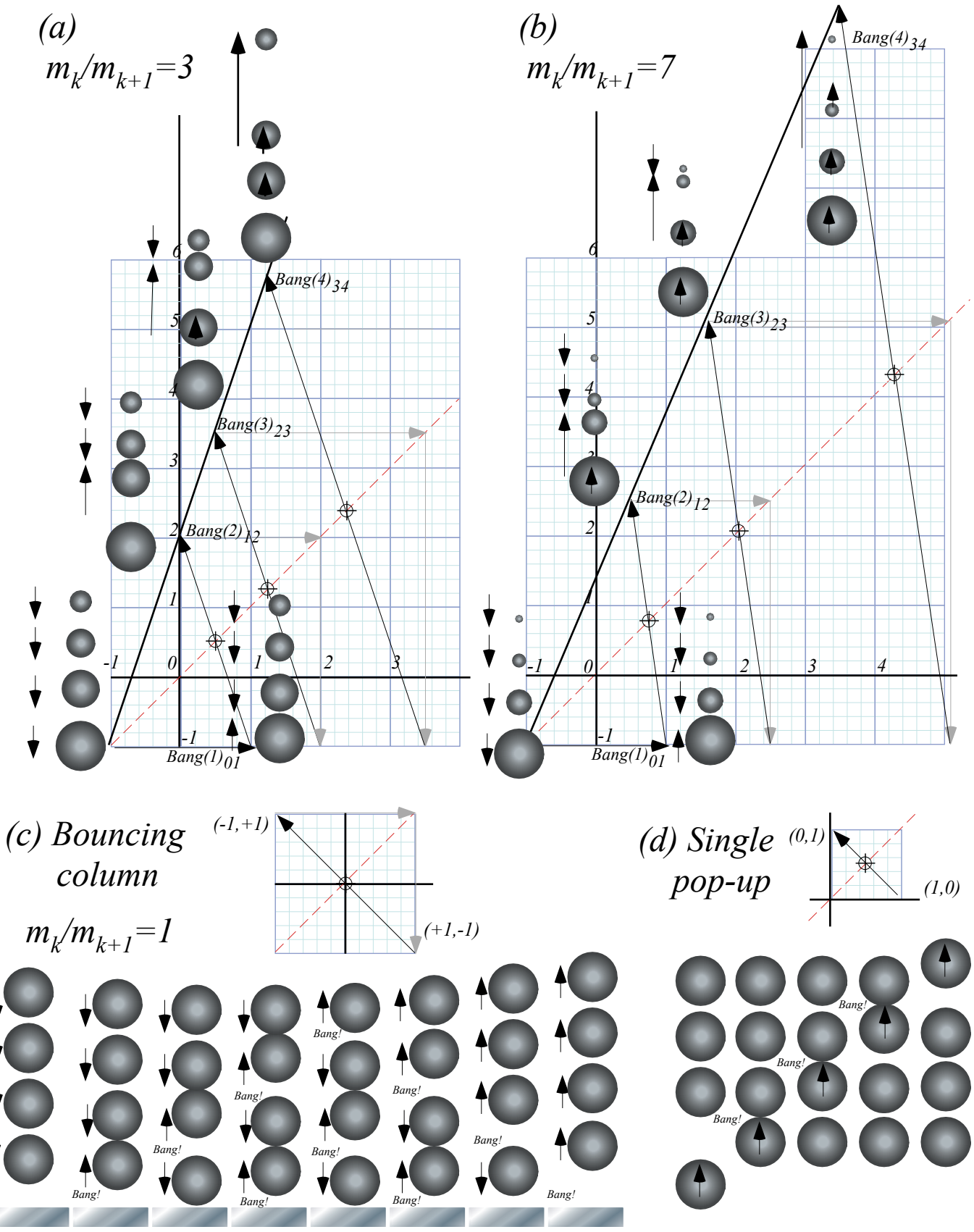

Fig. 8.2 4-ball towers. Mass-ratios m_k/m_{k+1} (a) 3, (b) 7, (c-d) 1. Independent bangs used for all.

Friction, again: Inelastic energy-momentum quadratic equations

Perhaps, you noticed that *FINAL* velocity values could be found from *INITIAL* values by two different ways. Back in Fig. 2.1 we noted an easy way using a momentum conserving straight line and a circle through $\mathbf{V}^{COM}$ from $\mathbf{v}^{IN}$ to the answer $\mathbf{v}^{FIN}$. But, Fig. 3.1 showed another way using an energy-conserving ellipse to connect $\mathbf{v}^{IN}$ to the answer $\mathbf{v}^{FIN}$. The first way uses simple linear equations and the second way uses more complex quadratic equations.

Why are there two ways? Often this means that situations exist where both are needed. Here friction or *inelastic* collisions make total kinetic energy decrease. (Recall our *60.2*-gazillion thieves? They're *baa-ck*!) Such a situation is plotted in Fig. 8.3b with the energy decrease indicated by a smaller ellipse inside the initial ellipse in Fig. 8.3a. This similar to an earlier Fig. 3.2.

The idea is that momentum conservation is still true even if the two masses are exerting sticky, energy-wasteful, forces on each other. No matter how wasteful those inter-particle forces may be, they still must obey Newton's 3rd axiom demanding equal-and-opposite forces on each other. So the final answer for $\mathbf{v}^{FIN}$ must be at an intersection of the *old* momentum line with a *new and smaller* ellipse.

However, intersecting an ellipse and a line uses a *quadratic* equation. And, in Fig. 8.3, there appear *two* solutions to the quadratic equation. One $\mathbf{u}^{FIN}$ we want is near the old energy-conserving $\mathbf{v}^{FIN}$. But, the other one that we now *don't* want is a $\mathbf{u}^{IN}$, which is nearer to the old $\mathbf{v}^{IN}$.

Let's look at a quadratic equation for u_1^{FIN}. There are two given constants *KE(u)* and MV^{COM}.

$$m_1u_1 + m_2u_2 = MV^{COM} = p_u = const. \quad (8.1) \qquad \frac{1}{2}m_1u_1^2 + \frac{1}{2}m_2u_2^2 = KE(u) = k_u \quad (8.2)$$

The COM momentum p_u in (8.1) is a constant during the entire collision. Not so for the kinetic energy k_u in (8.2). It's just a given loss parameter that is quite difficult to predict. We first solve p_u for u_2.

$$u_2 = \frac{p_u - m_1u_1}{m_2} \quad (8.4a)$$

Then we insert the u_2 result into k_u equation (8.2) to get the needed quadratic equation for just u_1.

$$\frac{1}{2}m_1u_1^2 + \frac{1}{2}m_2\left(\frac{p_u - m_1u_1}{m_2}\right)^2 = k_u \text{ or: } m_1\left(\frac{m_1+m_2}{m_2}\right)u_1^2 - 2p_u\frac{m_1}{m_2}u_1 + \frac{{p_u}^2}{m_2} - 2k_u = 0 \quad (8.4b)$$

The solution isn't pretty but its ± gives both u_1^{FIN} and u_1^{IN} shown in Fig. 8.3b.

$$u_1 = \frac{2p_u(m_1/m_2) \pm \sqrt{(2p_u)^2 - 4(m_1/m_2)(m_1+m_2)\left[\left({p_u}^2/m_2\right) - 2k_u\right]}}{2(m_1/m_2)(m_1+m_2)} = V^{COM} \pm \frac{\sqrt{{p_u}^2 - (m_1/m_2)(m_1+m_2)\left[\left({p_u}^2/m_2\right) - 2k_u\right]}}{(m_1/m_2)(m_1+m_2)}$$

(8.5a) (8.5b)

The unwanted (+) solution u_1^{IN} (given that we started with v_1^{IN}) means the two balls "wiffle" through each other. In classical physics, only u_1^{FIN} makes sense starting with v_1^{IN} and only u_1^{IN} makes sense starting with v_1^{FIN}. In quantum theory, masses can "wiffle." Then *both* solutions make sense (sort of).

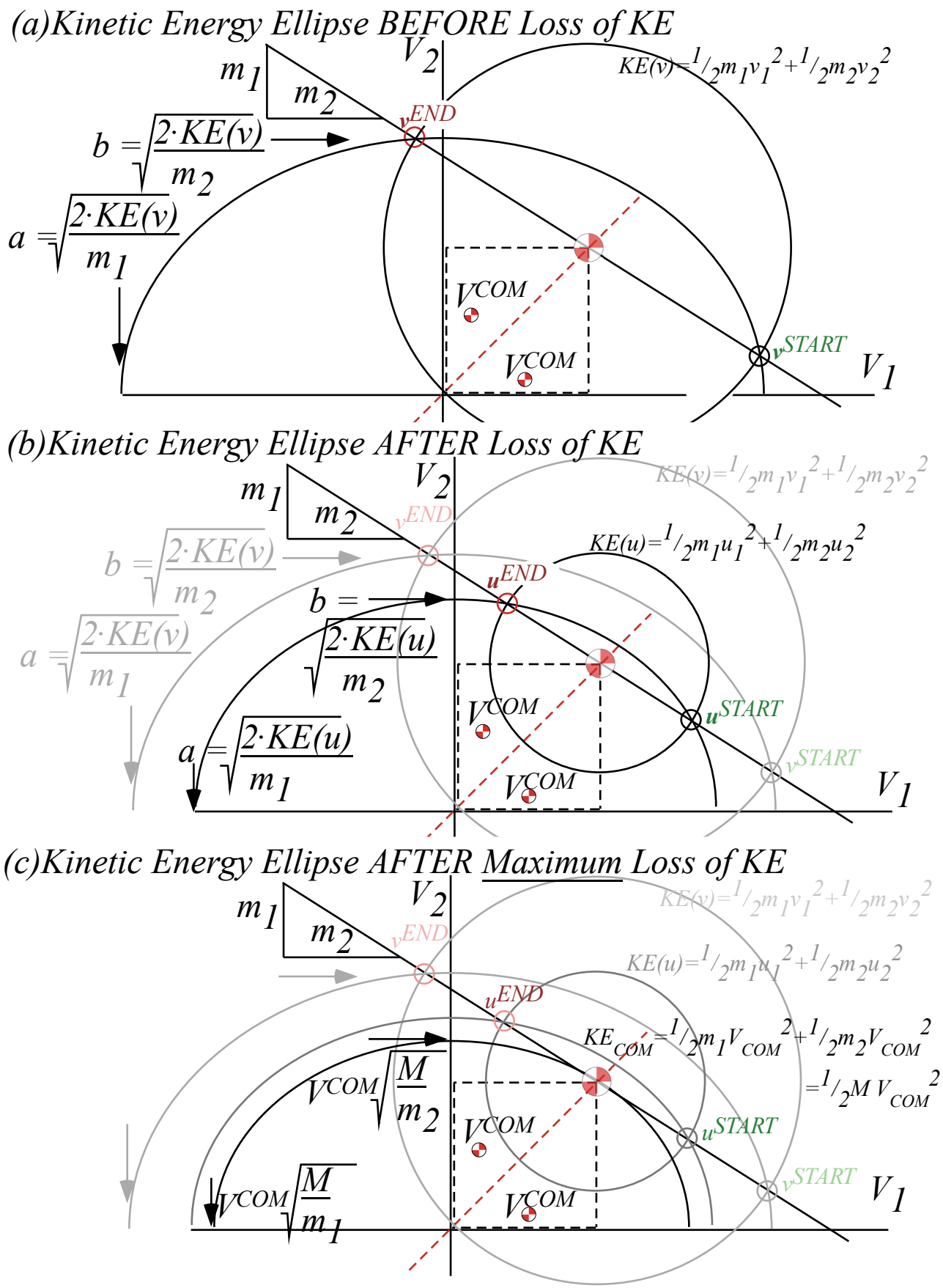

Fig. 8.3 KE-Ellipse shrinks by frictional loss. (a) Elastic (No loss). (b) Inelastic. (c) Totally inelastic.

Geometric derivation of elastic and inelastic energy ellipses

Can you do quadratic solutions (8.5) with a ruler and compass? At first this seems difficult, but the energy ellipse construction in Fig. 3.7 and geo-mean square root construction in Fig. 1.9a can be used.

As shown in Fig. 3.6, an ellipse has two radii, a *major radius a* giving x-coordinate $x=a\cos\theta$, and a *minor radius b* giving y-coordinate $y=b\sin\theta$. The Cartesian ellipse equation (3.7) is satisfied by these x and y, and polar angle parameter θ is eliminated. (x and y may switch places.)

$$\frac{x^2}{a^2}+\frac{y^2}{b^2}=1=\frac{m_1}{2\cdot KE}(V_1)^2+\frac{m_2}{2\cdot KE}(V_2)^2 \qquad (3.7)_{\text{repeated}}$$

Velocity values $x=V_1$ and $y=V_2$ have equal magnitude for initial *Bang(0)* ($V_1=-V^{IN}$, $V_2=-V^{IN}$) or *Bang(1)* ($V^{IN},-V^{IN}$), and for a totally inelastic final state ($V_1=V^{COM}$, $V_2=V^{COM}$). The geometry needed to solve for the initial elliptic radii (a^{IN}, b^{IN}) in Fig. 8.3a or totally inelastic radii (a^{COM}, b^{COM}) in Fig 8.3c is described in Fig. 8.4. Then an energy ellipse in (V_1, V_2)–space such as in Fig. 8.3b may be derived for any radii ($a^{FIN}\sqrt{R}$, $b^{FIN}\sqrt{R}$) where the *energy retention ratio* $R=KE^{FIN}/KE^{IN}$ ranges from $R=1$ down to $R_{min}=(a^{COM}/a)^2=(b^{COM}/b)^2$ as (a^{FIN}, b^{FIN}) range from initial radii (a^{IN}, b^{IN}) to totally inelastic (a^{COM}, b^{COM}) at minimum KE allowed by momentum conservation.

The roots (8.5) are two points where energy ellipse and momentum line intersect. For totally inelastic collision they coalesce and the momentum line is tangent at (V^{COM}, V^{COM}) as in Fig. 8.3c. The slope $m_1/m_2=a^2/b^2$ of the momentum line is fixed no matter how much energy is wasted. So is ellipse aspect ratio $a/b=\sqrt{(m_1/m_2)}$. Square root construction (from Fig. 1.8) finds a/b from a^2/b^2 in Fig. 8.4a-c.

The construction begins by boxing the momentum line in the 1st quadrant and doubling it using a semi-circular arc around its upper left hand corner. An extended box including the arc is drawn in Fig. 8.4b. The center of the extended box is the center of a second arc that finds the square root $\sqrt{(m_1/m_2)}$ of the momentum line slope in Fig. 8.4c that is the desired ellipse aspect ratio a/b of all possible energy ellipses for the masses m_1 and m_2. The basis of this construction is the mean geometry of Fig. 1.9a.

Location of radii a^{COM} and b^{COM} in Fig. 8.4d uses vertical and horizontal projections of pt-(V^{COM}, V^{COM}) to the $(\sqrt{(m_1/m_2)}=a/b)$-line. This is helped by the fact that pt-(V^{COM}, V^{COM}) lies on the ellipse *and* on the 45° line so that its x-coordinate $(x=a\cos\theta)$ and y-coordinate $(y=b\sin\theta)$ are equal. Thus angle parameter is $\tan^{-1}a/b=\theta$, the a/b line slope. So x and y projections of (V^{COM}, V^{COM}) onto the θ–line yield hypotenuse lengths a^{COM} and b^{COM} in Fig. 8.4d. Concentric circles of radii a^{COM} and b^{COM} let us construct the ellipse as in Fig. 3.7.

Initial pt-(V^{IN}, V^{IN}) gives initial elliptic radii a^{IN} and b^{IN} in Fig. 8.4e. Square-radii ratio $(a^{COM}/a^{IN})^2=(b^{COM}/b^{IN})^2$ or ratio $(a^{COM}b^{COM})/(a^{IN}b^{IN})$ of the two ellipse areas lets us find the lowest possible kinetic energy retention ratio R_{min}. You should prove (geometrically *and* algebraically) that minimum ratio is given as follows.

$$\sqrt{R_{\min}}=\frac{V^{COM}}{V^{IN}}=\frac{m_1-m_2}{m_1+m_2} \qquad (8.6a)$$

$$\frac{m_2}{m_1}=\frac{V^{IN}-V^{COM}}{V^{IN}+V^{COM}}=\sqrt{\frac{1-\sqrt{R_{\min}}}{1+\sqrt{R_{\min}}}} \qquad (8.6b)$$

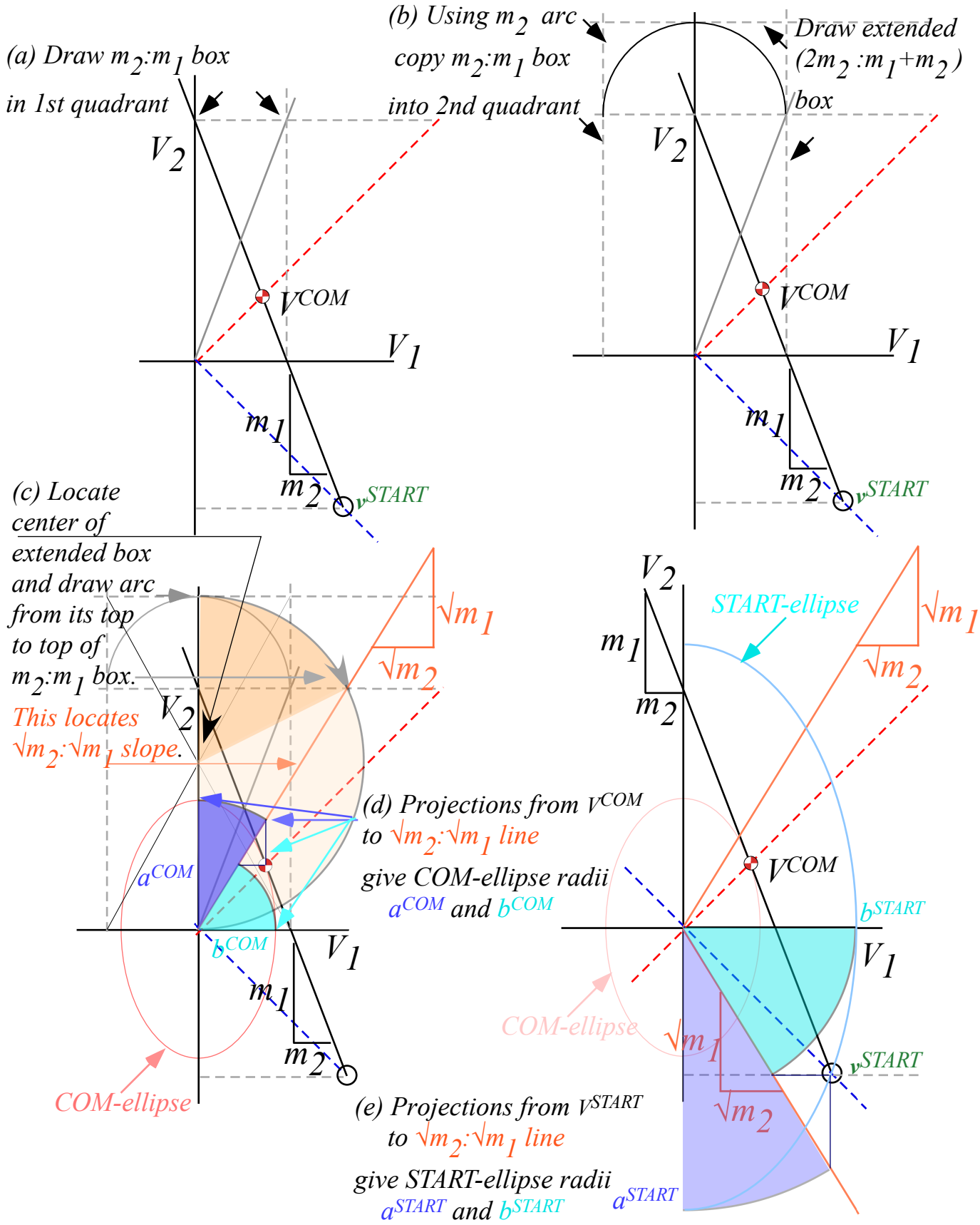

Fig. 8.4 Energy ellipse geometry. (a-c) Axes ratio $\sqrt{m_2}$:$\sqrt{m_1}$. (d) a^{COM} and b^{COM}. (e) a^{START} and b^{START}.

Ka-Runch-Ka-Runch-Ka-Runch-Ka-Runch-…:Inelastic pile-ups

N-body collisions described so far have been mostly elastic. That's not true for California freeway pile-ups. California pile-up chains start when a cell-phony driver enters a fog at 60 mph and rear-ends a vehicle or vehicles that have slowed down or stopped. Cars drive bumper-to-bumper so dozens may be involved.

Pile-up mass grows with each car added to it by a series of inelastic *"Ka-runch"* collisions like Fig. 2.1 of Ch. 2. Cars may be added to a pile-up's rear or to its front or even to both ends. Fig. 8.5 shows a single *60 mph* car piling up a line of five stationary cars and, *vice versa*, Fig. 8.6 shows a line of five *60 mph* cars piling up on a single stationary car. Each pile-up collision loses as much energy as it can while keeping momentum constant. It makes the smallest ellipse that touches the momentum line in Fig. 3.2c and Fig. 8.3c.

In each case the sequence of velocity-velocity slopes is an *arithmetic progression* *1:1*, *2:1*, *3:1*, *4:1*,… similar to velocity sequences in Fig. 6.4 and Fig. 6.5. Both have lines that intersect on a single point and inverse or complimentary slope sequence *1/1*, *1/2*, *1/3*, *1/4*,…, known as a *harmonic progression*.

The incoming car in Fig. 8.5 has momentum $P^{IN}=mv=60$ and energy $KE^{IN}=\frac{1}{2}mv^2=1800$ with $v=v^{IN}=60$. The final pile-up mass $M=6$ has the same momentum $P^{FIN}=MV=60$ but reduced velocity $V=v^{FIN}=10$ and energy $KE^{FIN}=\frac{1}{2}MV^2=300$ down by *1500* units. (These are (very) Old English units with unit mass *(m=1 ton)* cars.)

The incoming cars in Fig. 8.6 together have momentum $P^{IN}=5mv=300$ and energy $KE^{IN}=5\frac{1}{2}mv^2=9000$. The final pile-up mass $M=6$ has the same momentum $P^{FIN}=MV=300$ with increased velocity $V=v^{FIN}=50$ but reduced energy $KE^{IN}=\frac{1}{2}MV^2=7500$. The same energy deficit of *1500* units is seen in Fig. 8.5 and Fig. 8.6.

Of these two equal-energy-loss nightmares the latter is worse since it began with five times the kinetic energy and still has *7500* units to dissipate. Worse nightmares combine the two as shown in Fig. 8.7. This a particularly troubling set of nightmares since there are many possible outcomes that have different orders of combination with differing results.

How would you like to be an insurance adjustor for that one?

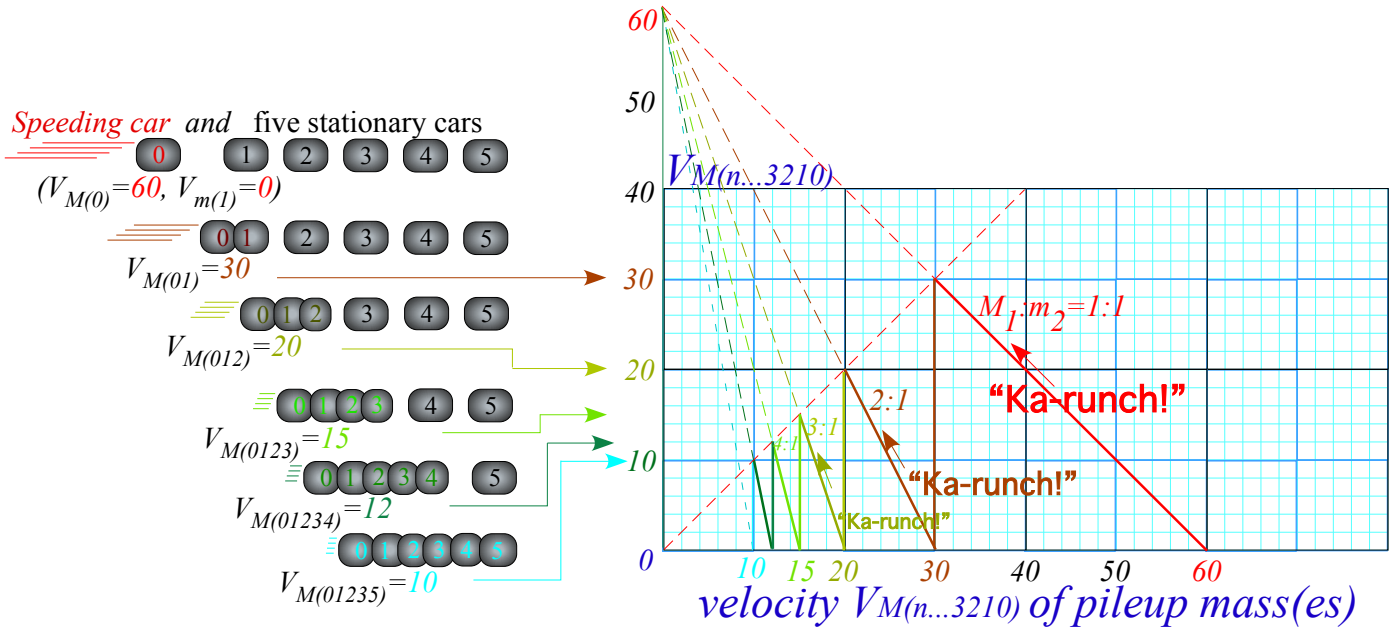

Fig. 8.5 Pile-up due to one 60 mph car hitting stationary line of five cars

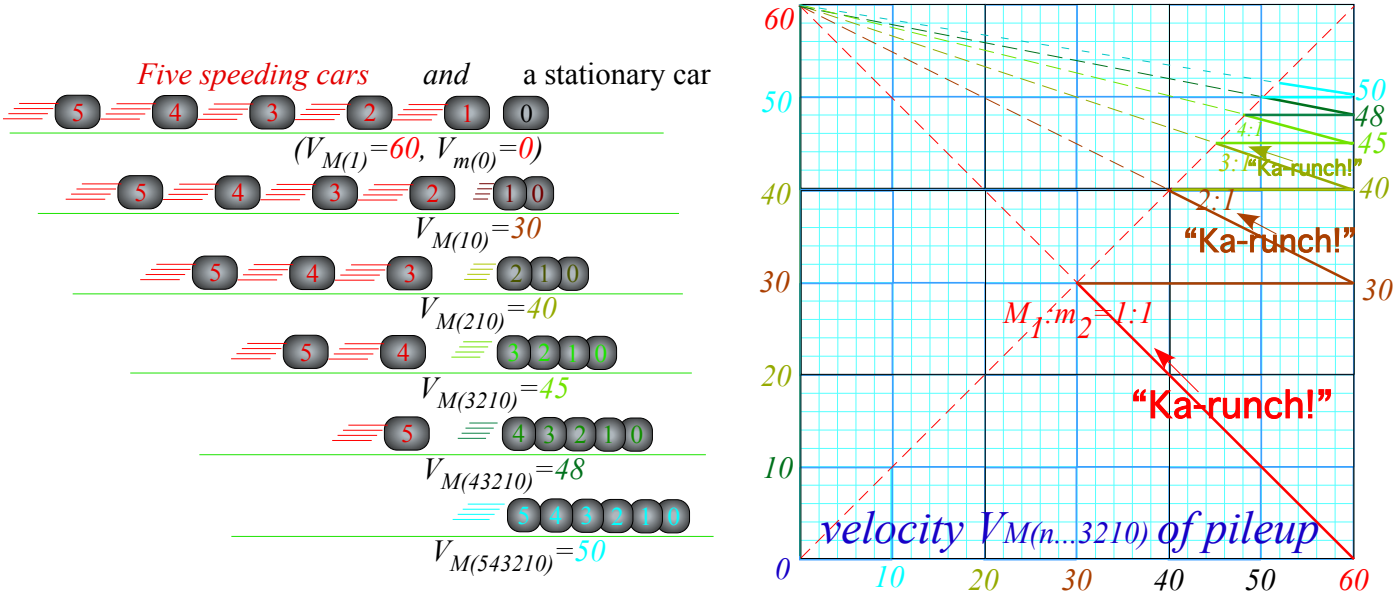

Fig. 8.6 Pile-up due to a line of five 60 mph cars hitting one stationary car

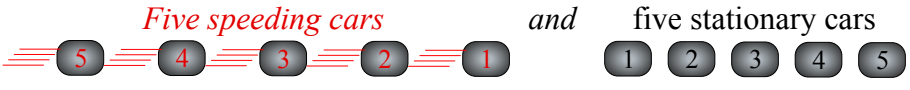

Fig. 8.7 A worse nightmare: Line of five 60 mph cars hitting five stationary cars.

Ka-pow-Ka-pow-Ka-pow-Ka-pow-…:Rocket science

An *N*-body model of rocket propulsion is made by "time-reversing" pile-ups. Let us imagine a line of $N=11$ equal $(m=1)$-masses separated by explosive charges that go *"pow!"* in just the right sequence to blow one fuel-pellet at a time backwards off the rear end of a rocket and propel the remaining rocket mass forward.

Fig. 8.8 is a velocity-velocity plot of seven such *"pow!"*-blasts after which a rocket with just three masses numbered *8*, *9*, and *10* speeds off the page to the right. Presumably, the *payload* of this rocket is the ball labeled *10* at the head of the line. For $N=11$ balls, there are ten *pow(b)*-blasts numbered by $b=0$ *to* 9.

The velocity unit in Fig. 8.8 is the relative exhaust velocity $\Delta v_e=-1$ of each *pow(b)*-blast. The 0^{th}-blast at the bottom of Fig. 8.8a starts with eleven stationary balls and blows ball-*0* away from the line of ten balls *1-2-3…8-9-10*. To conserve momentum (initially zero) the *10*-ball rocket of mass $(M=10m=10)$ has final velocity $\Delta V_M=+1/10$ to cancel momentum $\Delta P_0=m\cdot\Delta v_0=-1$ of fuel-pellet ball-*0* in a zero-sum *pow(0)*-blast.

$$m\cdot\Delta v_0+10m\cdot\Delta V_M(0)=0 \qquad (8.7a)$$

The 0^{th}-blast line begins at the origin $(V_M=0,v_e=0)$ of the V_M-v_e-plot in Fig. 8.8b and extends one unit down and $1/10^{th}$ unit right to point $(V_M(0)=1/10,v_e=-1)$. *Pow(0)*-line slope is mass ratio $(-m/M=-1/10)$. It is a COM line of a *time reversed* totally *in*elastic collision. (You might call it a *super-elastic* collision.)

The 0^{th},1^{st},2^{nd},3^{rd},…, or 9^{th} blast blows off fuel pellet-ball $b=0$, 1, 2, 3…, or 9, respectively. Each blast gives a larger rocket velocity boost $\Delta V_M(1)=1/9$, $\Delta V_M(2)=1/8$, $\Delta V_M(3)=1/7$…$\Delta V_M(b)=1/(10-b)$ since rocket mass is less by $m=1$ after each blast but the exhaust momentum impulse $m\cdot\Delta v_e=-1$ is the same each time.

$$m\cdot\Delta v_1+9m\cdot\Delta V_M(1)=0 \qquad m\cdot\Delta v_2+8m\cdot\Delta V_M(2)=0 \quad \ldots \quad m\cdot\Delta v_b+(10-b)m\cdot\Delta V_M(b)=0 \qquad (8.7b)$$

The *harmonic progression* $1/10,1/9,1/8\ldots1/5,1/4,1/3,1/2,1$ in Fig. 8.8a contains momentum impulse terms $\Delta V_M(b)$ in a *10*-term *harmonic series* $1/10+1/9+1/8\ldots1/5+1/4+1/3+1/2+1$. Rocket velocity after its b^{th} *pow (b)*-blast is a partial sum of the first $b+1$ harmonic terms. The (V_M,v_e)-plots in Fig. 8.8b show this.

0^{th}: $V(0)=1/10=0.1$ 1^{st}: $V(1)=1/10+1/9=0.211$ 2^{nd}: $V(2)=1/10+1/9+1/8=0.336$

3^{rd}: $V(3)=V(2)+1/7=0.478$ 4^{th}: $V(4)=V(3)+1/6=0.646$ 5^{th}: $V(5)=V(4)+1/5=0.846$

6^{th}: $V(6)=V(5)+1/4=1.096$ 7^{th}: $V(7)=V(6)+1/3=1.429$ 8^{th}: $V(8)=V(7)+1/2=1.929$

On its 9^{th} and final *pow(9)* the rocket is boosted by a whole unit exhaust velocity to $V(9)=V(8)+1=2.929$.

A *10*-blast rocket exceeds exhaust velocity $(|v_e|=1)$ on its 6^{th} *pow(6)*-blast with $V(6)=1.096$. This is labeled in extreme lower right hand side of Fig. 8.8b. In COM frame, exhaust mass *6* thru *9* end up moving *forward* but in rocket frame each exhaust mass leaves moving *backward* at exactly $v_e=-1$ until another blast-boost hits the rocket. Exhaust masses numbered *0-9* separate from each other and from payload mass-*10*. Total COM momentum is always zero, and so all eleven balls always "balance" at COM origin.

N-blast velocity is a *logarithm* function if *N* is large. Momentum is still conserved for each blast.

$$M\cdot\Delta V=-v_e\cdot\Delta M \quad \text{becomes:} \quad M\cdot dV=-v_e\cdot dM \quad \text{or:} \quad dV=-v_e\frac{dM}{M} \qquad (8.8a)$$

We integrate this from initial rocket mass M_{IN} to final payload M_{FIN} and from rocket V_{IN} to final V_{FIN}.

$$\int_{V_{IN}}^{V_{FIN}} dV=-v_e\int_{V_{IN}}^{M_{FIN}}\frac{dM}{M} \quad \text{becomes:} \quad V_{FIN}-V_{IN}=-v_e\left[\ln M_{FIN}-\ln M_{IN}\right]=v_e\left[\ln\frac{M_{IN}}{M_{FIN}}\right] \qquad (8.8b)$$

This is the famous *rocket equation*. (Its predictions discourage interstellar travel. See exercises.)

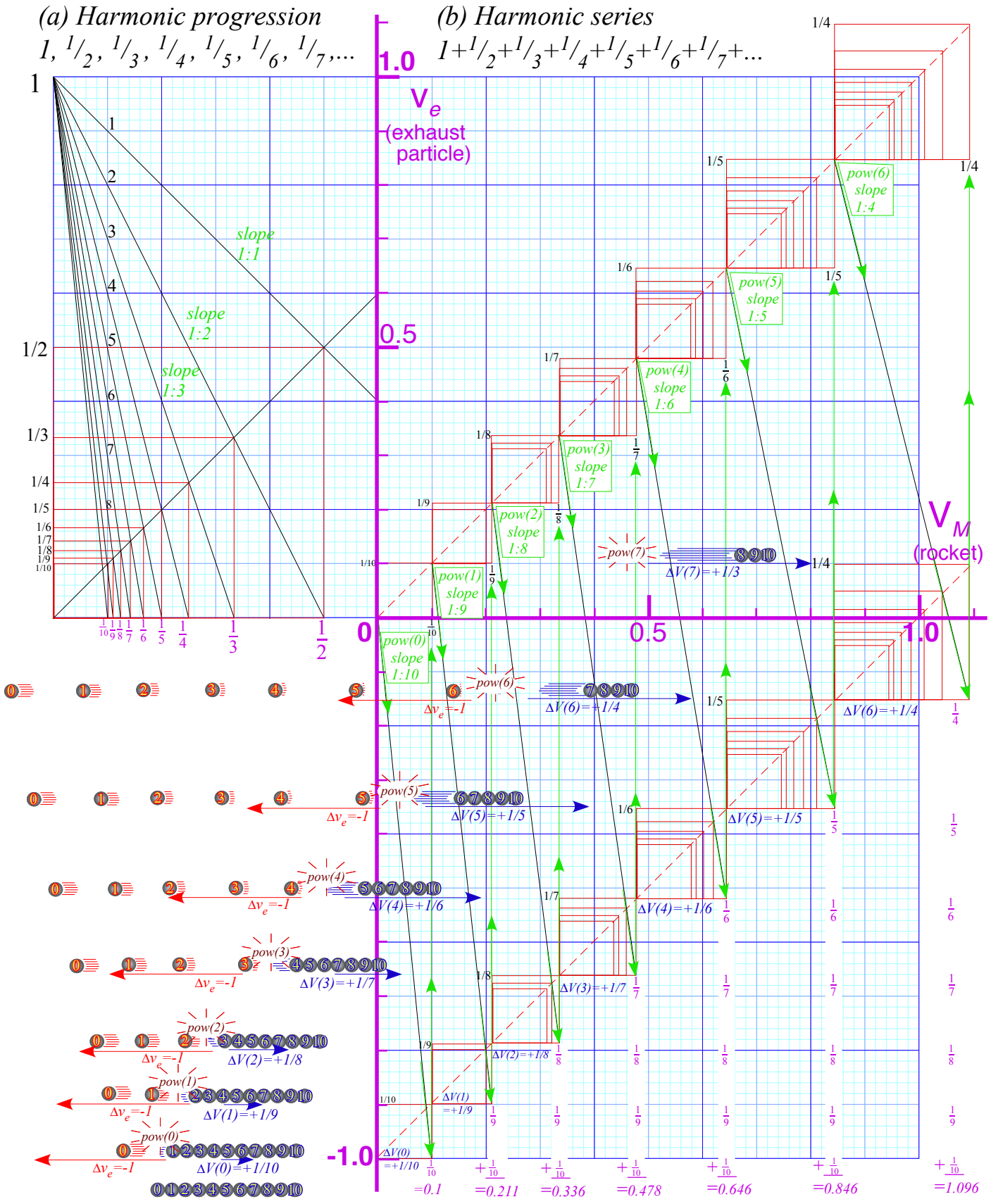

Fig. 8.8 Rocket science by harmonic series geometry.

Exercise 1.8.1 Maximum Energy Transfer (MET Limit)
Suppose each ball has just the right mass ratio with the one above it to pass on all its energy to the next in line. Construct v-v diagrams, velocity at each stage, and mass values for
(a) $N=2$, (b) $N=3$, (c) $N=4$, (d) Give algebraic formulas for general N.

Exercise 1.8.2 Absolute Maximum Velocity Limit (INF Limit)
Suppose each ball is very much larger than the one above so as to approach upper limit. Construct v-v diagrams , limiting intermediate velocity values and limiting top value for (a) $N=2$, (b) $N=3$, (c) $N=4$, (d) Give algebraic formulas for general N.

Exercise 1.8.3 Rocket Science and Backside of exponentials
Compare discrete-blast rocketry in eq.(8.7) or Fig. 8.8 with continuous-blast "rocket science" of eq.(8.8) and study logarithmic-exponential geometry of the latter.
(a) In particular, when do blasted exhaust particles end up going in the same direction as the rocket in the initial (lab) frame where the rocket starts out with zero velocity?
(b) Plot exponential $y=e^x$ and $y=\log_e x$ functions on same graph and draw tangent-triangle whose hypotenuse is tangent to a curves and intercepts x or y axes at -2, -1, 0, 1, 2,.. Give the base and altitude coordinates of the tangent point in each case.

Chapter 9 Geometry and physics of common potential fields

Physical and geometric aspects of elementary force and potential fields are introduced in this section. Most important are oscillator and Coulomb fields that will later occupy Unit 4 on resonance and Unit 5 on orbits.

Geometric multiplication and power sequences

The most common *power-law potentials* are $U(x) = Ax^2$ (*Oscillator potential*) in Fig. 9.1, $U(x) = Ax$ (*Uniform field potential*) , and $U(x) = Ax^{-1}$ (*Coulomb potential*) Fig. 9.5. Power-law potentials and force laws have simple geometric constructions. Exponential or logarithmic fields (shown in Ch. 10) do not.

Multiplicative power operations are done using a staircase of similar triangles as shown in Fig. 9.2. A geometric progression $\{1=s^0, s=s^1, s^2, s^3,...\}$ and an inverse progression $\{1=s^0, 1/s=s^{-1}, s^{-2}, s^{-3},...\}$ lie on either side of the unit stair step $1=s^0$. A slope or scale factor $s=2$ or $s=1/2$ is used in Fig. 9.2a or Fig. 9.2b. They resemble perspective drawings of school hallways. (Elementary School is (a) and High School is (b).) Each stair zigzags between slope-*1* line-*(y=x)* and slope-*s* *line-(y=s·x)* or between *line-(y=-x)* and *line-(y=x/s)*. The *line-(y=s·x)* and *line-(y=x/s)* are perpendicular or *normal* to each other. So are *line-(y=x)* and *line-(y=-x)*.

A two-step triangle in Fig. 9.1a gives each point on the oscillator potential, a parabola $y=x^2$. To find where the parabola hits vertical *line-(x=2.2)*, for example, we go up that line to the *45° line-(y=x)* and then go across to vertical *line-(x=1)*. A dashed blue line is drawn from origin thru that point to an arrow intersecting *line-(x=2.2)* at *pt-(x=2.2, y=2.2²)* on parabola-*(y=x²)*. A similar zigzag gives *pt-(x=-2, y=4)* or any point on the parabola *(y=U(x)=x²)* below.

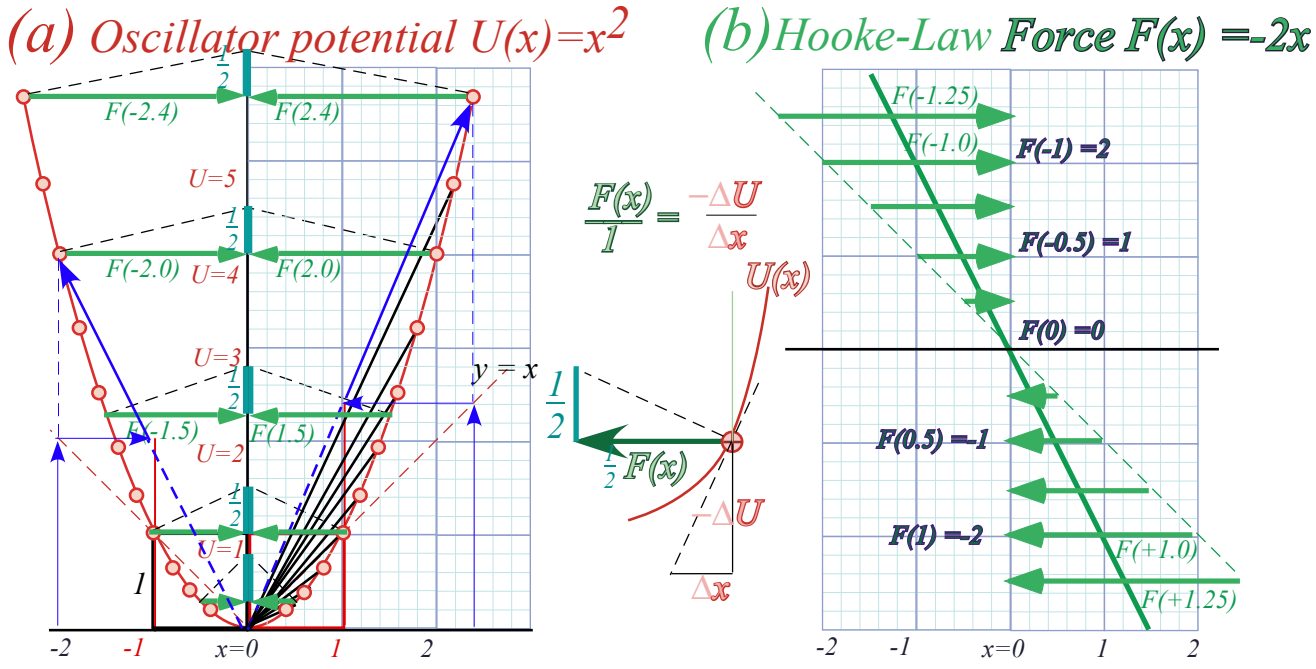

Fig. 9.1 Geometric construction of $U(x)=x^2$ potential and Hooke's force law $F(x)=-2x$.

The physicist *Force =-Slope* rule (6.9) is drawn using force triangles in Fig. 9.1a. Force is linear in x, that is, $F=-2x$, and that is minus the slope of x^2. A line of slope -2 in Fig. 9.1b plots $F(x)$. Force vector **F** scaled by $1/2$ gives a force vector shown in Fig. 9.1a equal and opposite to coordinate x. Each force triangle has base **F**/2, an altitude that is a constant $1/2$, and a hypotenuse normal to the parabola tangent. It is similar to the tangent triangle with base ΔU and altitude Δx (center of Fig.9.1) that shows *force=-slope* ($F(x)=-\frac{\Delta U}{\Delta x}$).

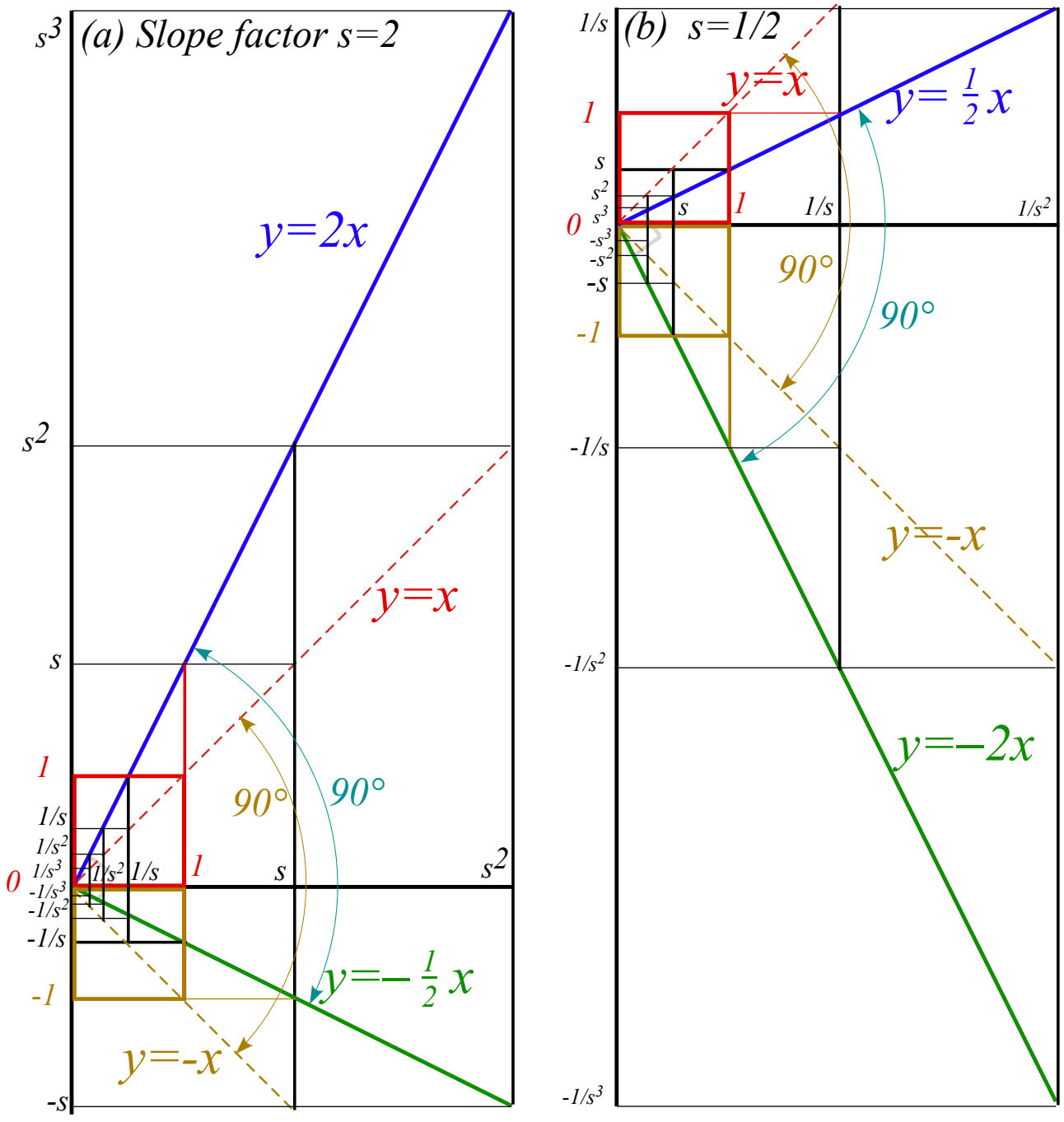

Fig. 9.2 Geometric sequences and "staircases" for slope or scale factor (a) s=2, and (b) s=1/2 .

Parabolic geometry

A parabola $U(x)=Ax^2$ has a *focal point* at $y=U=A/4$ where vertical rays meet if reflected by parabola tangents as in Fig. 9.3b. A parabolic radius is its half-width λ at the focus. For $y=x^2$ we have $\lambda=1/2$. (Note how $F(\pm 0.5)$ vectors point at the focus in Fig. 9.1a.) An old name for λ is *latus rectum*. A circle through the focus about any parabolic point will be tangent to a line called the *directrix* located at a distance λ from the focus. Focus and directrix define a parabola that passes midway between them thru the tip-point M of the parabola where its focal radius and equal distance-to-directrix both reach their minimum value λ/2.

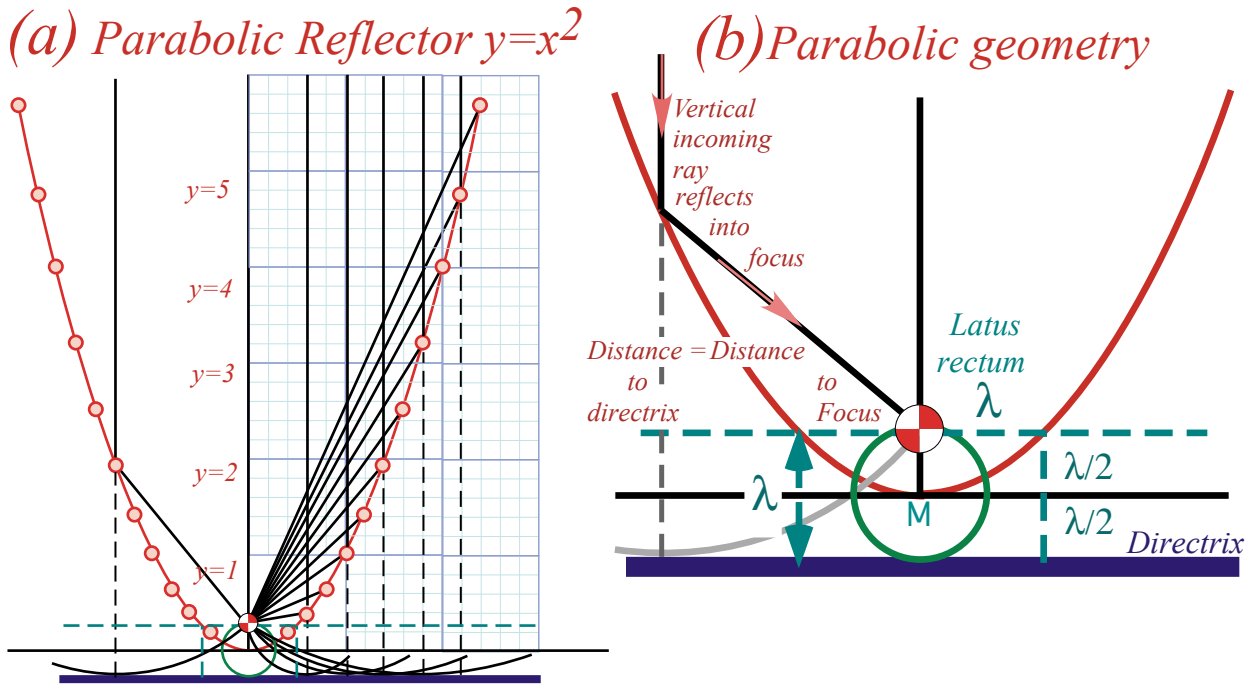

Fig. 9.3 Parabola and analytic geometry (a) Rays converging on focus. (b) λ-geometry of tangent reflection.

Directrix is a so named because it "directs" both the rays and wave phase of an optical reflector. Since the *focal radius* (length of each sloping ray line in Fig. 9.3a) equals the perpendicular *directrix distance* (length of corresponding dashed vertical line), waves are guaranteed to be plane waves. Also, the equality of angle of incidence and reflection off the parabola bisecting the dashed and solid lines, guarantees vertical parallel rays for all which leave the focus and bounce off the inside of the parabola. It also guarantees that parallel vertical rays bouncing off the *outside* will go away from the focus. Either side of a parabolic surface converts plane waves to spherical ones or *vice-versa*.

To better understand the parabola's geometric optics we draw examples of the *tangent-kite* for four different tangent slope values. The blue kite of *slope=2* in Fig. 9.4a and yellow kite of *slope=5/2* in Fig. 9.4b have equal focal radius and perpendicular distance-to-directrix forming the major iscosoles triangle of the kite. A minor iscosoles triangle (upside down in Fig. 9.4) shares a base with the major one. Their

perpendicular bisector is the tangent line. The bisection point is slope $\frac{dy}{dx}=\frac{x}{\lambda}=\frac{x}{2p}$ in units of λ as indicated by vertical arrows.

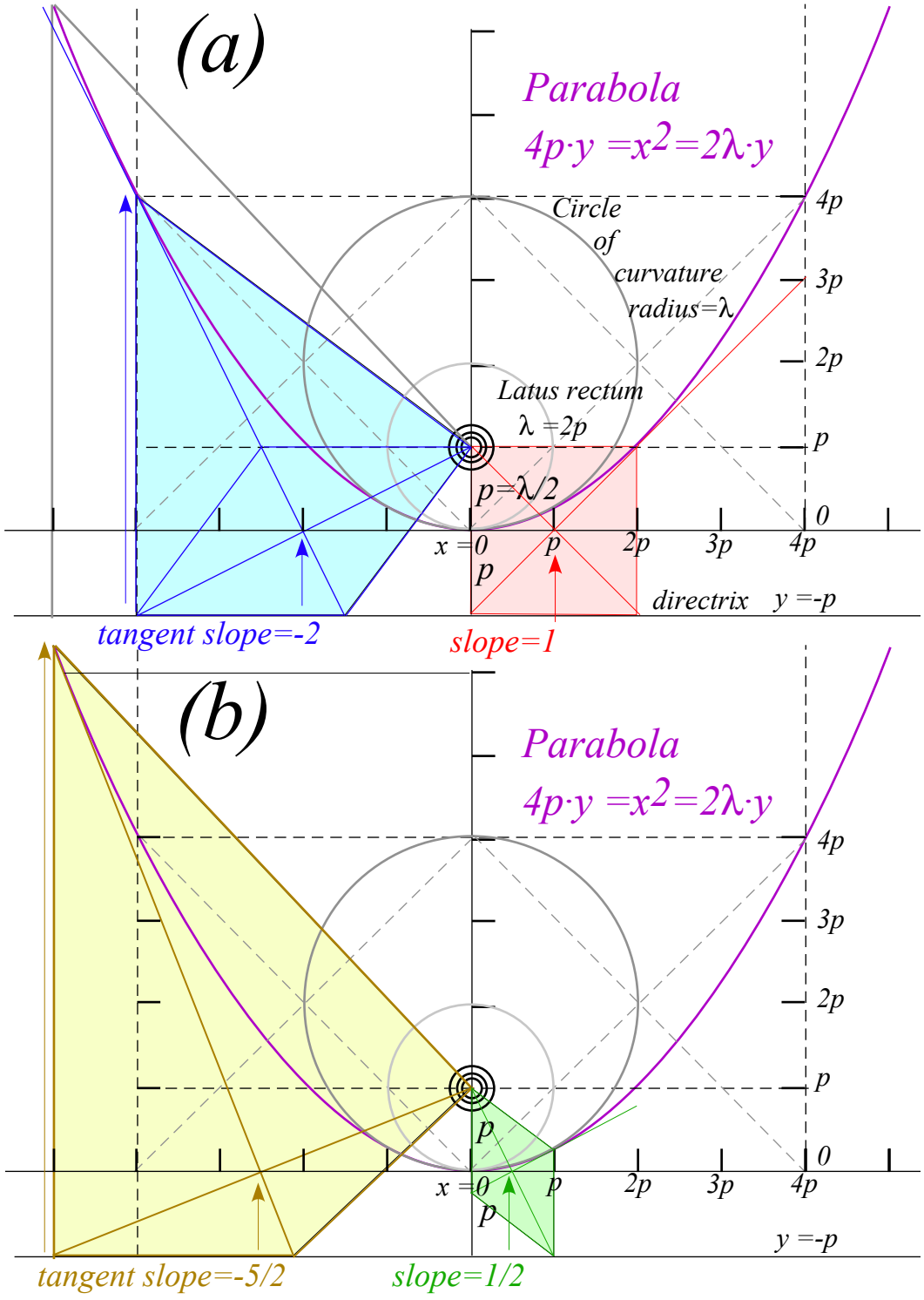

Fig. 9.4 Parabola and geometry of curvature and slope of tangent-kites.

A singular case is the red kite of *slope=1* that is square. Lesser *slope=1/2* gives a rhomboidal green kite with one side on the vertical parabolic axis instead of on the horizontal directrix. Points of *slope=±1* on the

($4py=x^2=2\lambda y$)-parabola lie on either side of its focus at distance $\lambda=2p$ from it. $\lambda=2p$ is also the (minimum) *radius of curvature* of the parabola at its tip (minimum y at $x=0$) that lies a distance $\lambda/2=p$ below the focus.

Coulomb and oscillator force fields

Our atoms and molecules depend on the electrostatic Coulomb field to have stable chemistry and biology. Like charges repel and opposites attract with a force that varies inversely with the square of distance r between them. A simple version of the electric Coulomb force law (axiom) is:

$$F(r)=\frac{1}{4\pi\varepsilon_0}\frac{qQ}{r^2}\quad where:\frac{1}{4\pi\varepsilon_0}=9{,}000{,}000{,}000\frac{Newtons\cdot meter\cdot square}{per\ square\ Coulomb} \tag{9.1}$$

The units and notation are standard but the size of this is *mind boggling*. It's nine *billion Newtons* for just two charge-units a meter apart. (To be precise it's $8.99\cdot10^9\ Nm^2/C^2$.) OK, a $1N$ is only about $\frac{1}{4}\ lb$, but are you able to hold up a billion sticks of butter? Also, you have *thousands* of Coulomb charge units in each fingertip with only a centimeter separation so add another factor of *(100)-squared*. Make that ninety *trillion* Newtons for each Coulomb or about a *million trillion* Newtons trying their darndest to blow your pinkie to bits!

But, still we're underestimating this monster force. Most of the electronic charge in the world is crammed into atoms and molecules with at most a nanometer (10^{-9} meter) across and some are an *Angstrom* (10^{-10} meter) or a tenth of a *nano*. So put on another factor of (10^{-9})-squared or million-billion trying to undo your pinkie, that's a *trillion-trillion-billion*. Does your manicurist know about this?

Sometimes these forces get loose as in a TNT blast, but usually, tiny nuclei with an equal positive charge hold down potentially rebellious electrons. Still, what's holding nuclei together? Nuclear radii are *femto*-meters (10^{-15} meter) or *Fermi*. (Note: both *fm* and *Fm* are abbreviations for $10^{-15}m=10^{-13}cm$.)

Oops! That's another factor of $(10^{-15})^2$ or another million-trillion-trillion to increase our stress level. Nuclear charge is 10^5 times more pent-up than its atomic electronic counterpart with a grand total of about a *trillion-trillion-trillion-trillion* Newtons hankering to blow up your fingertip nuclei. Cancel the manicure!

When nuclei do blow up, the result is more than 10^5 times more devastating than TNT bangs. We don't use *force* to estimate the devastation of a nuclear fission bomb or the yield of nuclear power plant fuel. Rather we use electric *potential energy*, that varies as $1/r$ not $1/r^2$. (Slope of a $U(r)=1/r$-curve is $F(r)=1/r^2$.)

$$U(r)=\frac{1}{4\pi\varepsilon_0}\frac{qQ}{r}\quad where:\frac{1}{4\pi\varepsilon_0}=9{,}000{,}000{,}000\frac{Joule}{per\ square\ Coulomb} \tag{9.2a}$$

Energy or *(Force)-times-(distance)*-unit is *Joule* or *Newton·meter (N·m)*. Like superball potential field $U(r)$ in (6.9), force $F(r)$ (9.1) is a *(-)*derivative of potential $U(r)$ that in turn is *(-)*integral of force $F(r)$. (Recall (7.5.)

$$F(r)=-\frac{dU(r)}{dr}=-\frac{qQ}{4\pi\varepsilon_0}\frac{d}{dr}r^{-1}=\frac{qQ}{4\pi\varepsilon_0}r^{-2} \tag{9.2b}$$

$$U(R)=-\int_\infty^R F(r)\cdot dr=\frac{qQ}{4\pi\varepsilon_0}r^{-1}\Big|_\infty^R=\frac{qQ}{4\pi\varepsilon_0}R^{-1} \tag{9.2c}$$

Potential nuclear energy yield is about a million times greater than for the same number of chemical energy sources since *femto*-meter nuclei are a million times smaller $(R_{NUC}\sim10^{-15})$ than *nano*-meter molecules $(R_{MOL}\sim10^{-9})$. Nuclear forces would then be a trillion times greater than typical atomic and molecular forces.

Fig. 9.5 plots attractive Coulomb force $F(r)=-1/r^2$ and potential $U(r)=-1/r$ of *negative* charge $-q$ to a *positve* $+Q$ nucleus. (Negative force points toward the $+Q$ origin $(x=0)$.) It uses zigzag geometry of Fig. 9.4.

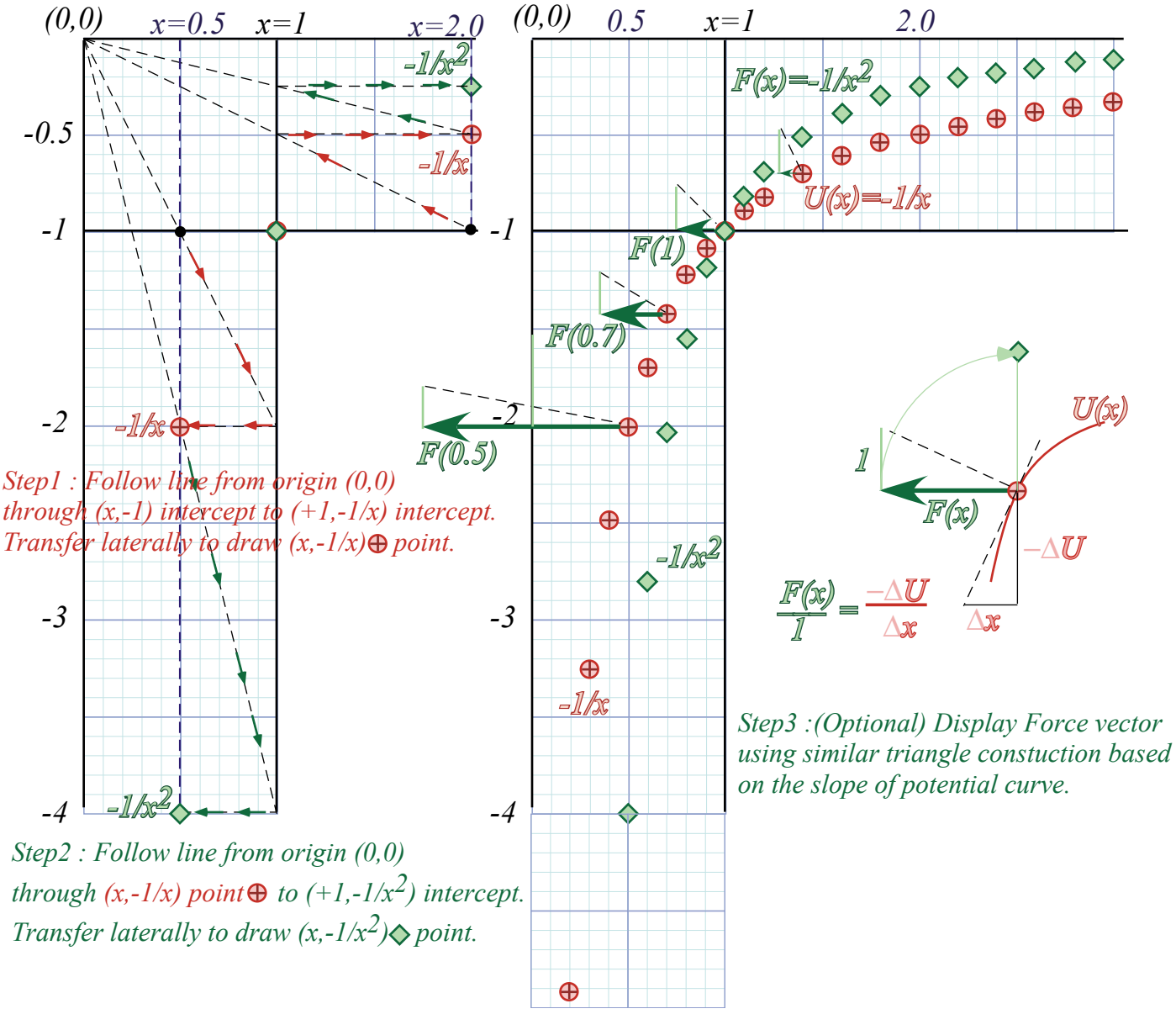

*Fig. 9.5 Attractive Coulomb force F(x) and potential U(x) curves. (**F**(x) vectors drawn at 1/4-scale.)*

Could the Coulomb $F(r)\sim 1/r^2$ force field be derived like the superball force $F(Y)\sim 1/Y^3$ in (6.10) by counting momentum bangs? Indeed, if a charge ejected a cloud of little "bang-balls" then the number of bangs scored at distance r would vary inversely with area $4\pi r^2$ of a radius r sphere. But, that idea doesn't explain very well *attraction* of a charge $+Q$ to a $-q$ or of a mass M to a mass m in Newton's gravity law.

$$F_{grav}(r) = -GMm / r^2 \text{ , where: } G=0.000000000067\ N\ m/kg^2 \qquad (9.3)$$

Gravity is universally attractive (no "negative" matter readily available) but much weaker than the electric one since G constant *6.672E-11* ($\frac{2}{3}\cdot 10^{-10}$ in *mks* units) is smaller (*by 10^{20} times!*) than the $9\cdot 10^{+9}$ in (9.2).

As of this writing it is still a mystery why these are so different. We really do not yet understand either of these forces at a fundamental level. They are still very much in the axiom box.

Tunneling to Australia: Earth gravity inside and out

Imagine $x=1$ in Fig. 9.5 is the Earth radius $R_\oplus=6.4E6m$. The $F(r)$ plot shows gravity falling off for $r>R_\oplus$ or $x>1$. But it's wrong for subterranean radii $(r<R_\oplus)$ unless Earth is compressed. $F(r)=-1/r^2$ doesn't apply everywhere unless Earth is squashed to a 10 millimeter radius "black hole." (More on this later.)

If you were to be at sub-$R_\oplus$ levels all Earth mass at radii above your radius r can be completely ignored in figuring your weight! As you might expect, you're weightless at the center ($r=0$) since the pull of all Earth's mass exactly cancels there. But, so also does your attraction to a spherical mass shell cancel anywhere inside it. One could float weightlessly anywhere therein regardless of the shell's size or weight.

Such a cancellation is a geometric peculiarity of an inverse square law. (It also underlies a Gauss law explanation of why you're safe inside a car struck by lightning.) Any direction you look inside a uniform mass shell has a mass element m whose force is cancelled by another element M behind. (See Fig. 9.6.)

The shell tangent to the m-point you're facing intersects the tangent to the M-point behind you to make an isosceles triangle whose sides make an angle Θ with your line of sight along the base. This means a narrow cone of sight will include shell mass $m=Ad^2$ at a distance d in front of you and shell mass $M=AD^2$ at a distance D directly behind you, where the angular factor $A\sim 1/\sin\Theta$ is the same for both. That assures perfect cancellation of gravity m/d^2 in front with $-M/D^2$ behind you. This applies for *all directions* in Fig. 9.6.

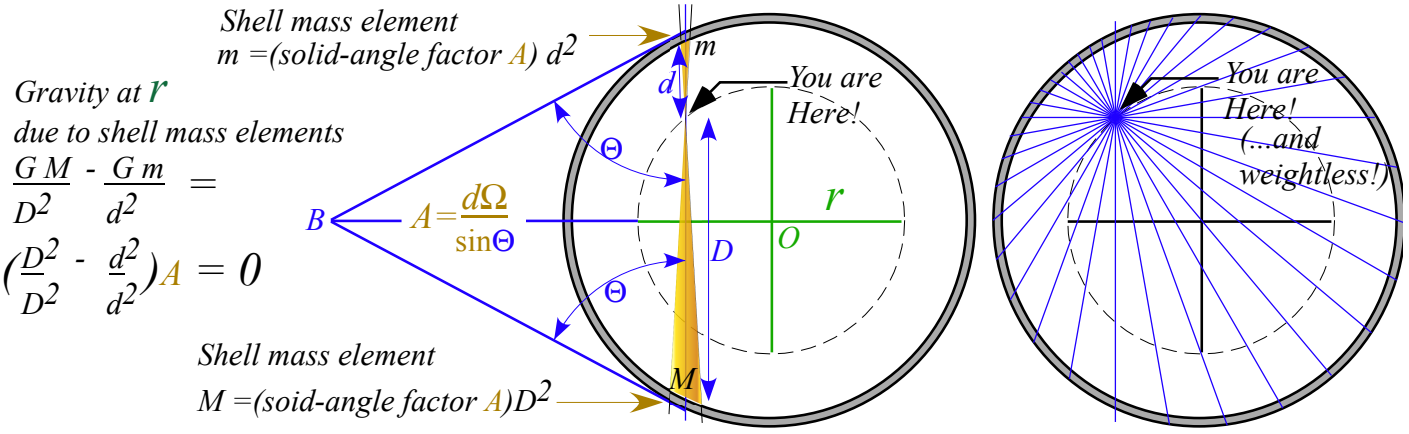

Fig. 9.6 Equal-opposite attraction. Geometry for you floating weightless inside a spherical shell.

A mass m at radius r inside Earth feels gravity attraction $GmM_</r^2$ where $M_<$ is Earth mass *inside* the radius r indicated by the dashed circle in Fig. 9.6. If Earth is uniform density ρ, then that inside-mass is $M_<=4\rho\pi r^3/3$. Force law r^{-2} cancels all but one r of the r^3 in mass $M_<$. We then get a *linear* force law.

$$F_{inside}(r)=GmM_</r^2=m(G4\pi\rho/3)\,r=mg(r/R_\oplus)=mgx \qquad (9.4a)$$

$$(\text{Earth surface gravity: } g=G R_\oplus 4\pi\rho/3=9.8ms^{-2}) \qquad (9.4b)$$

The linear force law (9.4) is like that of a harmonic oscillator in Fig. 9.1b and so the inside-Earth potential must be a parabola like Fig. 9.1a. Force $F(1)=-1$ is continuous as we cross $x=1$ and so must be the slope of potential $U(x)$ as U changes from $-1/x^2$ to parabola. Terrestrial beings such as ourselves live in a nearly-

constant-field ($\frac{dF}{dx} \sim 0$)-region near $x=1$. In Fig. 9.7 we find the potential parabola geometrically by its focal point and directrix using the tangent at $x=1$. Recall a tangent at $x=\lambda=2p$ in Fig. 9.4a has *slope=1* or *45°*. So does the parabola at $x=1$ in Fig. 9.7 below have a slope of *(+1)* and a force of *(-1)* (That's *–mg* in *mks* units.)

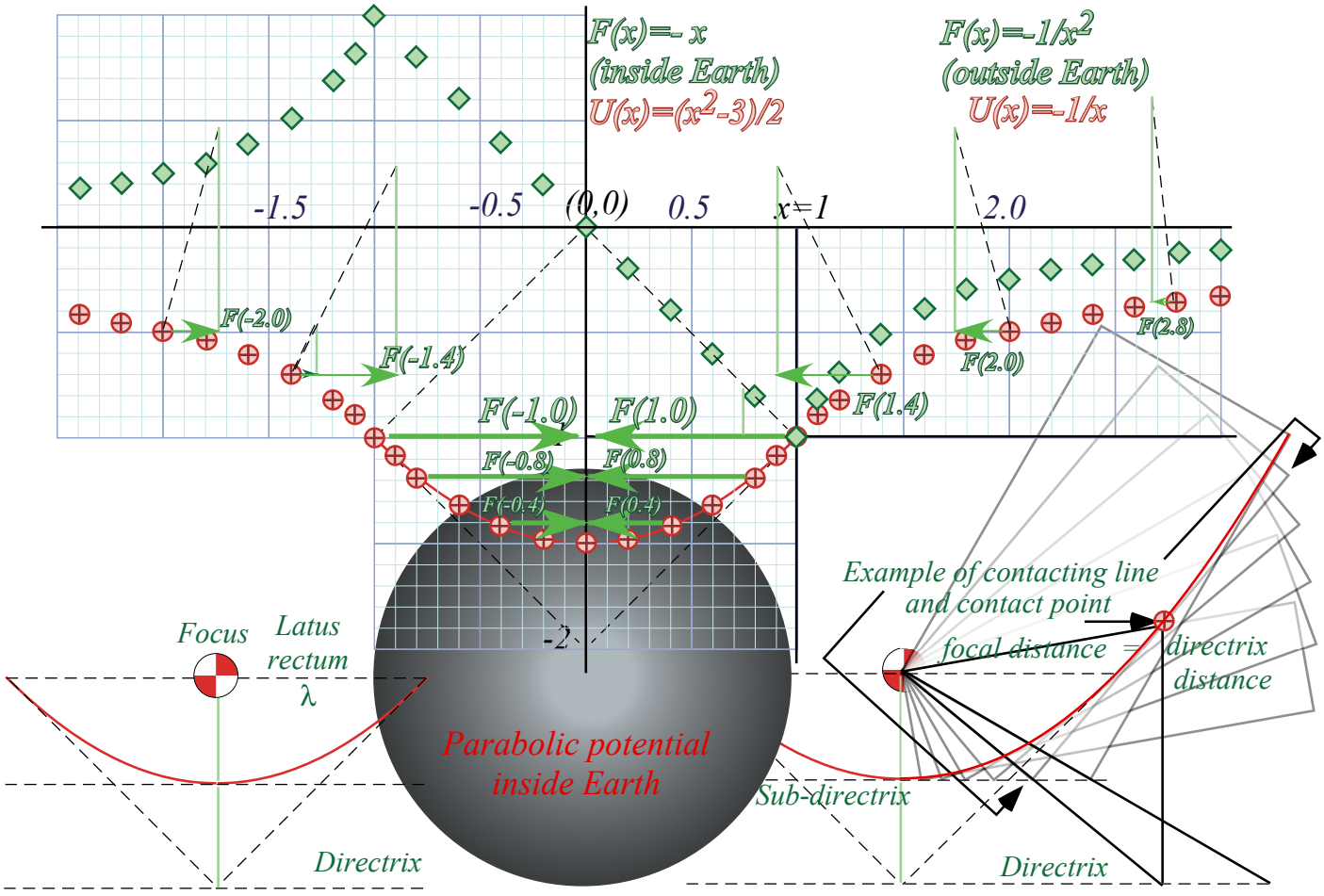

Fig. 9.7 Construction of Earth gravitational fields inside and outside.(units of x: $R_\oplus$,; F: mg; U: $mgR_\oplus$)

A parabola tangent bisects the angle between the line to the focus and the directrix drop-line as in Fig. 9.4. Twice *45°* gives *90°*. The focus is $\lambda=1.0$ units straight across and the directrix is $\lambda=1.0$ units below as shown in Fig. 9.7 (lower-left). Using this we may construct the parabola by rotating a square corner of a piece of graph paper around the focus so the corner touches a line halfway to the directrix. (We can call this half-way line the *sub-directrix*. It is the line of tangent intersections indicated by arrows in Fig. 9.4.)

The parabola so constructed is $y=x^2/2-3/2$. That is the *interior* potential $U^{IN}(x)$ $(-1<x<1)$. It meets the curve $y=-1/x$ that is the *exterior* potential $U^{EX}(x)$ $(1<x<\infty)$ at $x=1$ where they are equal ($U^{IN}(1)=-1=U^{EX}(1)$) as is slope, which is the force ($F^{IN}(1)=-1=F^{EX}(1)$). (However, the slope of the *force* curve takes a *big* jump!)

Adding a constant to a potential won't alter slope or force. We added $\frac{-3}{2}$ to $\frac{x^2}{2}$ to make it equal $\frac{-1}{x}$ at $x=1$.

To catch a falling neutron starlet

The "glue" that holds in the rebellious nuclear proton charge is called *nuclear matter*, a mix of neutrons, mesons, and their ingredients. Let's imagine a fingertip *(1cc)* of neutrons as densely packed as they are in a nucleus or neutron star and estimate how such a neutron starlet might travel through Earth. First, we find the density of nuclear matter. Let's say a nucleus of atomic weight *50* has a radius of *3 fm*, so it has *50* nucleons each with a mass $2\cdot10^{-27}kg$. (It's actually more like $1.67\cdot10^{-27}$, but roughly $2\cdot10^{-27}$.)

That is $100\cdot10^{-27}=10^{-25}\ kg$ packed into a volume of $\frac{4\pi}{3}r^3=\frac{4\pi}{3}(3\cdot10^{-15})^3\ m^3$ or about $10^{-43}\ m^3$. That gives a whopping density of $10^{-25+43}=10^{18}kg\ per\ m^3$ or a *trillion* kilograms in the size of a fingertip.

That's a pretty heavy fingertip! Its weight *mg* is ten trillion Newtons. (Well, actually 9.8 trillion Newtons. No need to exaggerate here!) In spite of this, its gravitational attraction to nearby rocks on the Earth is comparatively moderate. A $(10cm)^3$ 1kg rock would cling to the starlet with a force of about

$$F_{rock}=Gm(1kg)/r^2=100Gm=100(6.7E\text{-}11)1E12=6{,}700\ N, \qquad (m=M_{starlet}=10^{12}kg)$$

or less than a ton and small change for a starlet weighing billions of tons and cutting into the Earth like a bullet going through cotton candy. Let's see what speed it might gain falling from the surface.

Starlet energy is assumed constant since friction would be tiny compared to its enormous weight.

$$E=KE+PE=\tfrac{1}{2}mv^2+U(x)=\tfrac{1}{2}mv^2+\tfrac{1}{2}mg(x^2-3)=const. \qquad (9.5)$$

Let it be released at Earth surface *(x=1)* with zero velocity. This sets the energy constant.

$$E=\tfrac{1}{2}m0^2+\tfrac{1}{2}mg(1^2-3)=const.=-mg \qquad (9.6)$$

At Earth center *(x=0)* we solve for the velocity there. (The starlet mass *m* cancels out.)

$$E=\tfrac{1}{2}mv^2+\tfrac{1}{2}mg(0^2-3)=const.=-mg \quad \text{or: } v^2=g\,, \qquad (9.7a)$$

$$v=\sqrt{g} \quad (\text{In } mks \text{ units: } v^2=gR_\oplus\,, \text{ or : } v_0=\sqrt{(g\,R_\oplus)}=8\ km/s) \qquad (9.7b)$$

$v_0=8\ km/s$ is also Earth's minimum *orbital insertion speed*. A mass dropped down the tunnel flies with the same *x*-coordinate as one shot with the speed v_0 into circular orbit. One flies above the other and they meet each other on the other side *42* minutes later as shown in Fig. 9.8. We now show this synchrony of orbital timing holds for all pairs of starlets sent from anywhere inside the Earth!

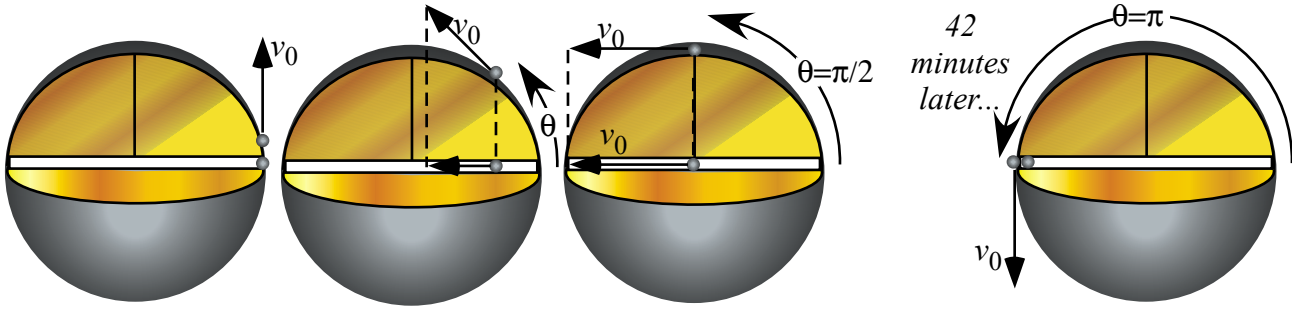

Fig. 9.8 Neutron starlet penetrates Earth as satellite orbits to meet 1/2-way around in 42 minutes.

This synchrony involves a physicist's most favored type of potential energy $U=\frac{1}{2}kx^2$. When $PE=U$ is a square like kinetic energy $KE=\frac{1}{2}mv^2$ we have a wonderful symmetry between position x and velocity v.

$$E=KE+PE=\text{const.}=\tfrac{1}{2}mv^2+\tfrac{1}{2}kx^2$$

We make any constant-sum-of-squares into a *Pythagorian relation* $1=\sin^2\theta+\cos^2\theta$ just as we did to analyze the sum (5.10) of super-ball KE. Here (9.5) is a sum $E=KE+PE$ and the constant k is starlet weight mg.

$$1=(m\,v^2/2E)+(k\,x^2/2E)=\sin^2\theta+\cos^2\theta \qquad (9.8a)$$

Position x and velocity v are then expressed in terms sine and cosine of a *phase angle* θ .

$$x=\sqrt{(2E/k)}\,\sin\theta \qquad (9.8b) \qquad v=\sqrt{(2E/m)}\,\cos\theta\ . \qquad (9.8c)$$

Velocity v is proportional to $\cos\theta$ and θ has a constant *angular velocity* $\omega=\frac{d\theta}{dt}$ so that $\theta=\omega\cdot t+\alpha$. ($\alpha=\theta_0=const.$)

$$v=\frac{dx}{dt}=\frac{dx}{d\theta}\frac{d\theta}{dt}=\frac{dx}{d\theta}\omega=\omega\sqrt{\frac{2E}{k}}\cos\theta=\sqrt{\frac{2E}{m}}\cos\theta \quad (9.9a) \qquad \textit{where:} \qquad \omega=\frac{d\theta}{dt}=\sqrt{\frac{k}{m}} \qquad (9.9b)$$

Angle θ is a polar angle in *(x,v/ω)-phasor-space* of Fig. 9.10a. *(x,v/ω)*-orbits are circular-*clockwise* ($\omega=-|\omega|$) if positive phasor v-axis is *up* and positive-x axis is to the *right*. Earth xy-orbits may be elliptical with a polar angle ϕ that can orbit either way in Fig. 9.10. Each spatial dimension x and y has a constant sub-total energy.

$$KE_{Total}=e_y+e_y \quad \textit{where:} \quad e_x=\text{const.}=\tfrac{1}{2}mv_x^2+\tfrac{1}{2}kx^2 \qquad \textit{and:} \qquad e_y=\text{const.}=\tfrac{1}{2}mv_y^2+\tfrac{1}{2}ky^2 \qquad (9.10)$$

Equal constants $(e_x=e_y)$ give the circular orbit in Fig. 9.8. Frequency ω (9.9) is independent of energy value e_x or e_y and so orbit and x-tunnel motion each have frequency $\omega=\sqrt{g}$, but tunnel motion, with same e_x but zero e_y, has half the energy. All motions of the starlet inside the Earth have the same *84*-minute period. That is a *fundamental harmonic period* of a uniform Earth and approximates behavior of the real Earth.

To depict the force vector **F** on the starlet simply draw an arrow from it to origin as in Fig. 9.9a since **F** is proportional to coordinate vector **-r**. (In Fig. 9.7, F is equal to $-r$.) It's projection on x or y-axes are the forces components driving the *84*-minute oscillations along x or y-axes. Perhaps, there is a starlet deep below us swishing out *84*-minute elliptical orbits as in Fig. 9.9b.

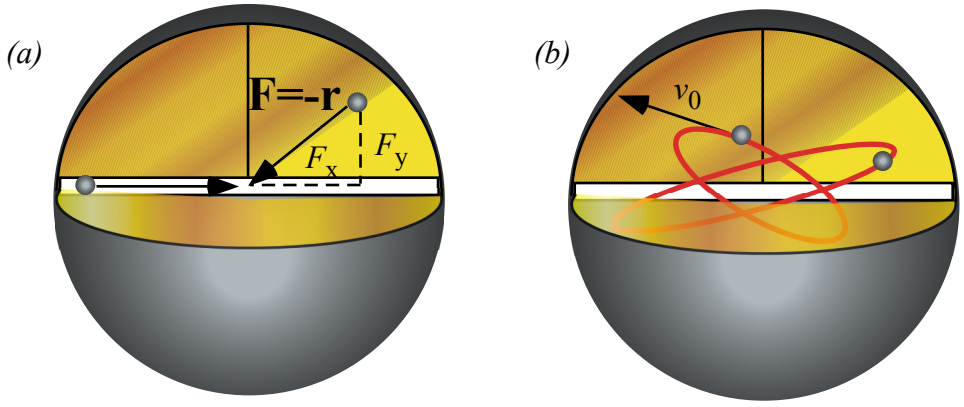

*Fig. 9.9 Force and orbits inside Earth. (a) **F** is minus the coordinate vector (b) Typical orbits.*

Starlet escapes! (In 3 equal steps)

Imagine starlet-m has decayed to where it sits at the bottom of the $U(x)=\frac{1}{2}mg(x^2-3)$ curve in Fig. 9.7. How much energy does it take for it to escape from Earth center and go back whence it came? The plot of $U(x)$ in Fig. 9.7 and discussions above suggest three equal steps of $1/2$ that bring energy $-3/2$ at $x=0$ up *zero* at $x=\infty$

Step-1 is to drag or shoot the starlet-m to the Earth's surface. That takes energy $\Delta E_1=\frac{1}{2}$. (That's $\frac{1}{2}mgR_\oplus$ in *mks* units.) Shooting radially at velocity $v_0=\sqrt{(gR_\oplus)}$ given by (9.7b) would do this first step. It would then come to rest (momentarily) at the Earth surface at $r=R_\oplus$.

Step-2 is to launch starlet-m into a minimal circular orbit from the Earth's surface. That takes dollop of energy $\Delta E_2=\frac{1}{2}$ equal to the first. (Again, that's $\frac{1}{2}mgR_\oplus$ in *mks* units.) Shooting tangentially with minimum orbital insertion velocity $v_0=\sqrt{(gR_\oplus)}$ given by (9.7b) does this second step.

Step-3 involves a final energy jump $\Delta E_3=\frac{1}{2}$ equal to each of the first two by increasing from the orbital insertion velocity $v_0=\sqrt{(gR_\oplus)}$ to the *escape velocity* V_e from Earth's surface $r=R_\oplus$.

$$V_e=v_0\sqrt{2}=\sqrt{(2gR_\oplus)}=11.3\ km/s=7\ mile/s \qquad (9.11a)$$

In terms of fundamental potential $U_{grav}(R_\oplus)=-GMm/R_\oplus$ at a planets surface $r=R_\oplus$ the escape velocity is

$$V_e=v_0\sqrt{2}=\sqrt{(2GM/R_\oplus)}\ . \qquad (9.11b)$$

Orbital threshold velocity v_0 of radius $R_\oplus$ is $\sqrt{2}=0.707$ or about *71%* of the escape velocity V_e from there.

No escape: A black-hole Earth!

By uniformly compressing Earth, we imagine extending the region of the Coulomb potential $-1/r$ in Fig. 9.5 to lower values of r while making the harmonic potential $U(r)=\frac{1}{2}kr^2$ inside the body occupy a smaller and smaller radius $R_\oplus$ and take on narrower, deeper, and more negative energy values.

The plot in Fig. 9.5 maintains its shape but we rescale to accommodate a squashed Earth. The escape velocity in (9.11b) grows as we consider a decreasing squashed-planet radius $R_\otimes$. Finally there comes a particular radius $R_\otimes$ where the escape velocity (9.11b) is the speed c of light.

$$c=\sqrt{(2GM/R_\otimes)} \qquad (9.12a)$$

That radius is called the *Schwarschild radius* or "black hole" radius since light cannot escape.

$$R_\otimes=2GM/c^2 \qquad (9.12b)$$

For the earth of mass $M_\oplus=6\cdot10^{24}\ kg$ the radius $R_\otimes$ is about nine *mm*, or the size of a fingertip. It is hard to imagine our world so squashed! Things may be collapsing all around, but please, not *that* much.

Oscillator phasor plots and elliptic orbits

The oscillator functions in (9.8) suggest a coordinate-velocity plot or *phase-space* plot. By (9.9) the phase angle $\theta=\omega t+\alpha$ is a product of angular frequency ω and time. To get a circle starting on the x-axis, we set initial phase to $\alpha=\theta_0=\pi/2$ and plot $(x= X\cos\omega t,\ v/\omega= -X\sin\omega t)$ for the "clock" or *phasor plot* in Fig. 9.10a.

So that positive *v versus x* defines its 1st quadrant, a phasor rotates *clockwise* like a clock hand so angle $\theta=-|\omega|t$ has a minus sign. (This is quite *apropos* since our clocks now *are* waves and harmonic oscillators.)

Each dimension x and y has its phasor plot as indicated by Fig. 9.10b. In other words there are four phase-space or phasor dimensions $(x\ ,\ v_x/\omega\ ,\ y\ ,\ v_y/\omega)$ being plotted. Here the frequency ω for each dimension x and y is identical due to symmetry or *isotropy* of the Earth model. But, initial phases α_x and α_y of x and y are independent. In Fig. 9.10b we set x-oscillator phase to *2* o'clock (on a 16-hour clock) and y-oscillator 2 hours ahead to *4* o'clock so the ellipse orbit is *clockwise* and have a *left-handed* symmetry. Setting x to be 2 hours ahead of y makes the same orbit but it will go *counter*-clockwise and have a *right-handed* symmetry.

The *x versus y* plot with x always two hours or *45°* behind y, is an inclined elliptical xy-orbit path in Fig. 9.10b. It might represent a typical neutron starlet path in the Earth. Or else, it might represent an optical polarization ellipse described in Unit 2. Below is a discussion of some special cases of orbit ellipses.

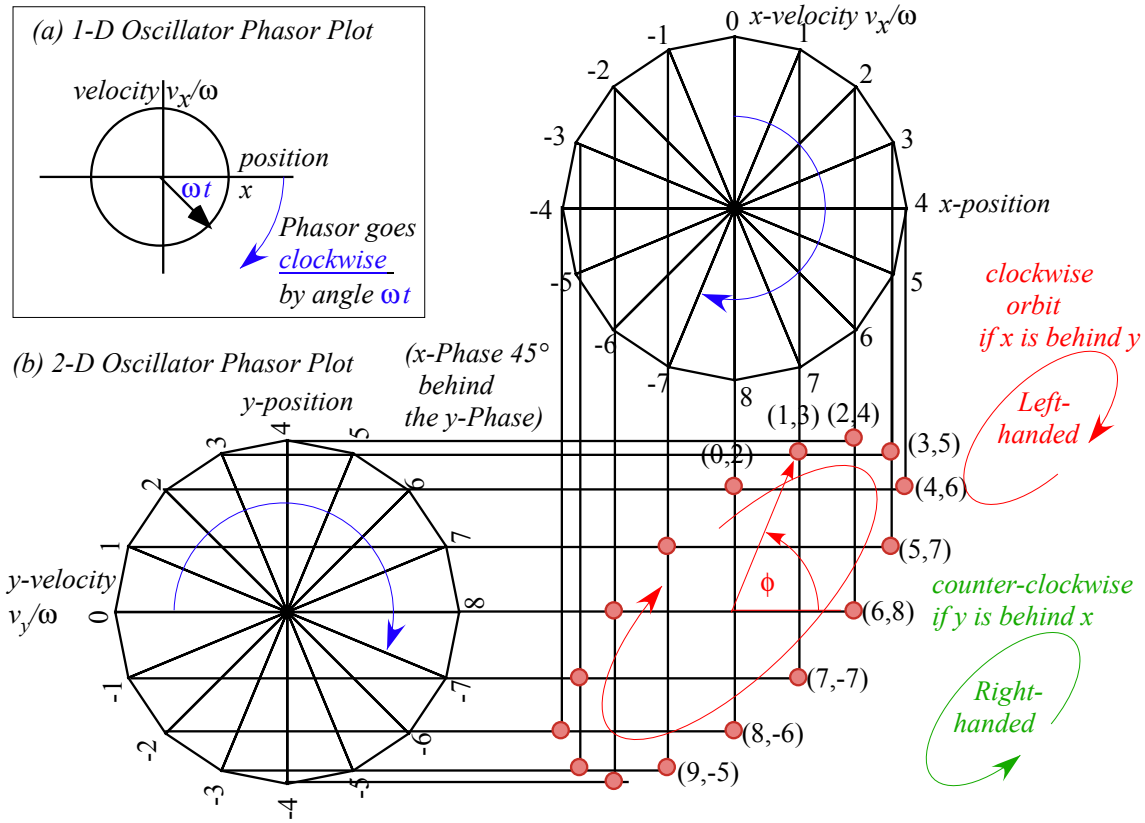

Fig. 9.10 Oscillator plots. (a) 1D-HO phasor plot. (b) Isotropic 2D-oscillator phasors and xy-path.

First we verify by algebra that orbits in Fig. 9.10 and Fig. 9.11 are ellipses. Fig. 9.11a has x running $90°$ behind y with a *relative phase lag* $\Delta\alpha=\alpha_x-\alpha_y=\pi/2$ that is *4* hours or *1/4*-period behind in phase on a *16*-hour clock. We say such a $90°$-lagging-x-motion is *in-quadrature* to y-motion. It gives an un-tilted ellipse with a left-handed orbit, and if $e_x=a=b=e_y$ then it gives a circular orbit or *left-circular polarization*. (See Fig. 9.11a on right.) For right-handed orbits x-motion and x-motion switch leads to $\Delta\alpha=\alpha_x-\alpha_y=-\pi/2$.

In-quadrature xy -motion is a *cosine* and *sine* projection on a-side and b-side of an ellipse, respectively, based on expressions (9.8).

$$x = a\cos\omega t\,, \qquad (9.13a) \qquad y = b\cos(\pi/2-\omega t) = b\sin\omega t\,. \qquad (9.13b)$$

Squaring and adding cosine and sine expressions gives a standard xy-ellipse equation.

$$x^2/a^2 + y^2/b^2 = 1 \qquad (9.13c)$$

Zero phase lag $\Delta\alpha=0$ or *in-phase* motion gives *linear* polarization in Fig. 9.11b. In the case of Fig. 9.11b where x and y-motions are *in-phase* we have

$$x = a\cos\omega\cdot t\,, \qquad (9.14a) \qquad y = b\cos\omega\cdot t\,. \qquad (9.14b)$$

Combining these two gives a trajectory that follows a straight line of slope (b/a) seen in the figure.

$$y = (b/a)\,x \qquad (9.14c)$$

Lag $\Delta\alpha=\pm\pi$ or *pi-out-of-phase* is a linear polarized motion, too.

$$x = a\cos\omega\cdot t\,, \qquad (9.15a) \qquad y = -b\cos\omega\cdot t\,. \qquad (9.15b)$$

It is simply a horizontal mirror reflection of the in-phase path.

$$y = -(b/a)\,x \qquad (9.15c)$$

In each of the figures we could imagine *three* starlets going in unison. The first starlet obeys the y-equation (9.13b) with $x=0$. The second starlet obeys the x-equation (9.13a) with $y=0$ and tunnels as in Fig. 9.8. A third starlet obeys *both* the x *and* y equations like the starlet orbiting above the tunneling one(s).

In a *linear force field* $\mathbf{F}=-k\mathbf{r}$ all Cartesian components oscillate sinusoidally at the same frequency.

$$\mathbf{F}=-k\mathbf{r} \quad \text{implies}: F_x=-kx\,,\quad F_y=-ky\,,\quad F_z=-kz \qquad (9.15)$$

Neither the coulomb field $\mathbf{F}=-k\mathbf{r}/r^3$ nor any other power-law field $\mathbf{F}=-k\mathbf{r}r^p$ is so convenient!

As shown in Unit 5, negative energy orbits in Coulomb fields are also elliptic, and elegant ruler & compass geometry gives them, too. However, Coulomb ellipses are symmetric about origin only for circular orbits. All other Coulomb orbits are *eccentric* since they orbit about an off-center *focal point* and not the ellipse center of symmetry that lies at origin (**r=0**) for any Hooke's law oscillator orbit of a starlet.

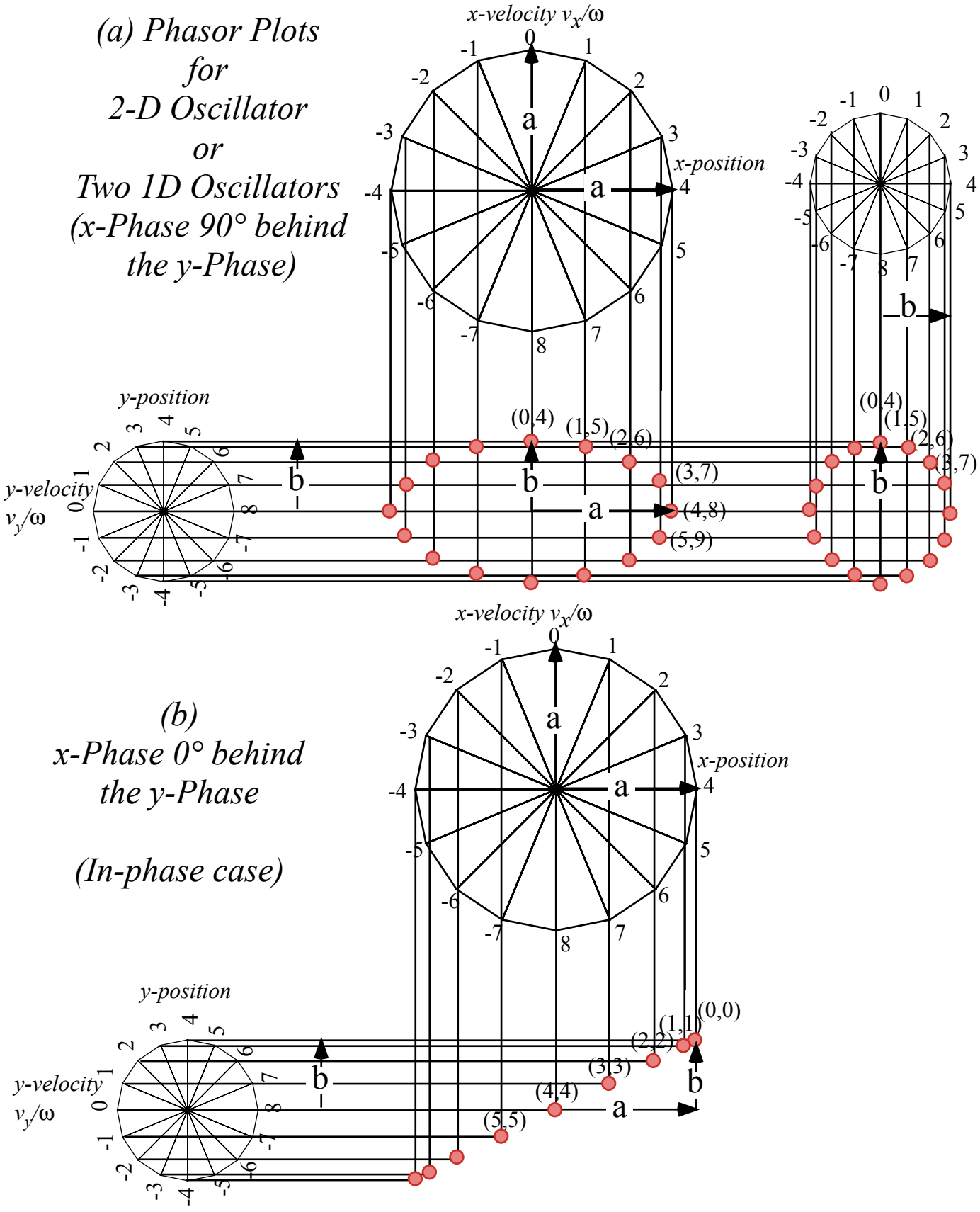

Fig. 9.11 Two 1-D oscillator phasor plots combine to give 2D-oscillator xy-trajectory.

Exercise 1.9.3. Tunnels to UK (5600 miles away as an earthworm crawls) are shown below. One high-road is a direct route. The other low-road turns around at the Earth center. Travel and turn-around are assumed frictionless and survivable. (a) How long is each trip? Discuss.

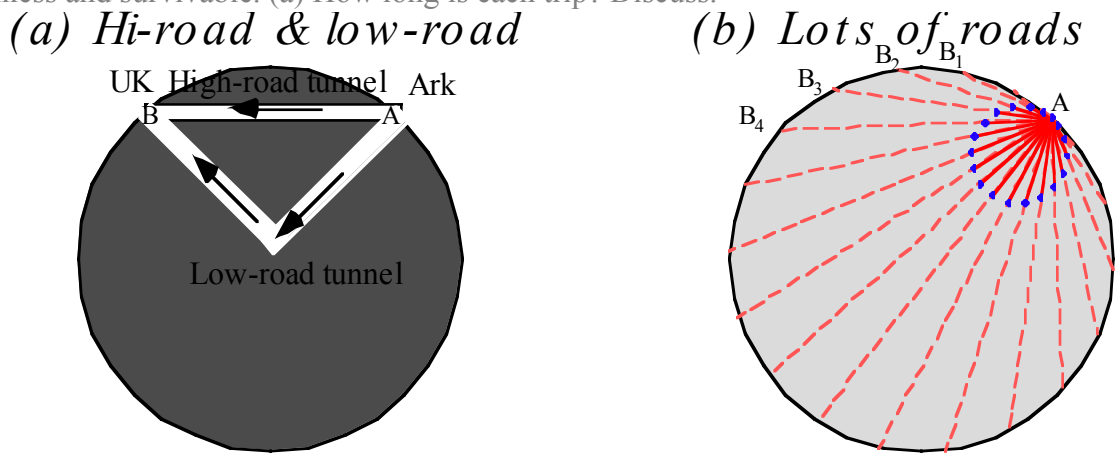

(b) A network of subways leaving Ark. at time t=0. What curve (like the dots) describe each moment?

Exercise 1.9.4. Consider competing tunnels between points *A*-to-*B* separated by $R\sqrt{2} \sim 5600$ miles (thru Earth) or $\Delta\phi = 90°$ of longitude and 6 Time Zones. The preceding problem asked you to compare the high-road or direct-route to the low-road or via-Earth-center-and-back-route. Here we consider middle-road routes such as in Fig *(a)* below. *(a)* Find the fastest 2-straight-section middle road *A*-to-*B* by geometry or algebra. How much faster is it? (Give answer for local travel:$\Delta\phi = 1°$, long distance:$\Delta\phi = 90°$ and for general $\Delta\phi$.)
(b) How long does it take to go from *A*-to-*B* on slow-roads ("V"-road and "U"-road) in Fig. (b).

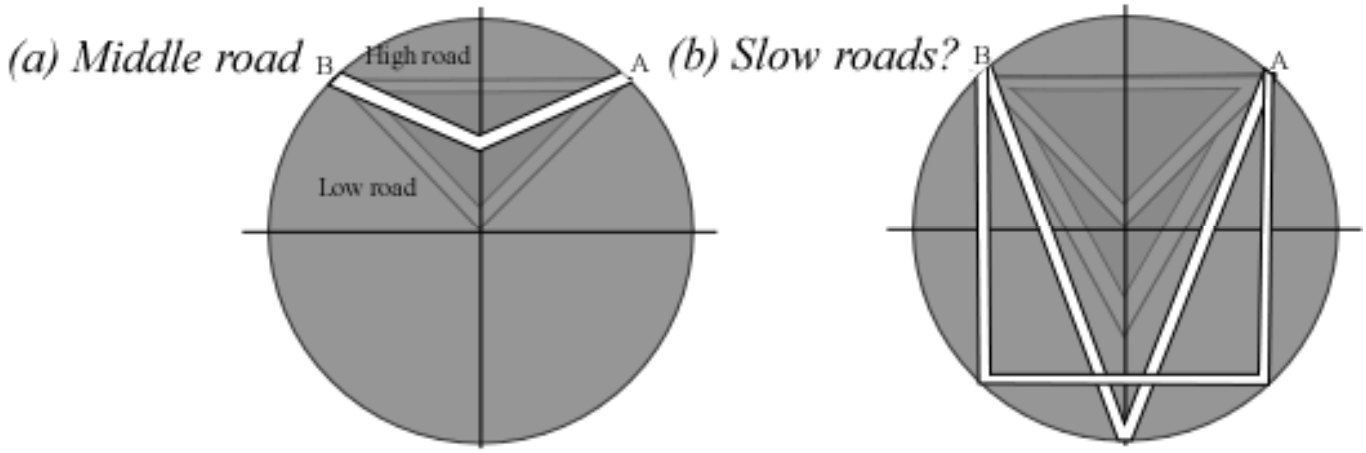

Exercise 1.9.5. Construct 24-point neutron-starlet orbits (One point for every hour assuming a 24-hour orbital period.) inside a uniform asteroid with x-component oscillation amplitude exactly *equal* to that of y and the x-component phase fixed relative to that of y as follows:
(a) x is *in phase* with y. *(b)* x is *behind* y by 1 hour. *(c)* 2 hours. *(d)* 3 hours. *(e)* 4 hours. *(f)* 5 hours. *(g)* 6 hours. *(h)* 7 hours.
Do the orbits change if we replace *behind* by *ahead* in *(a)* to *(h)*? Discuss or describe.

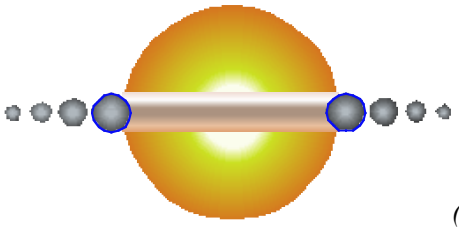

(Scale of ball-towers greatly magnified)

Super-Duper-Nova Model

1.9.6 Identical ball towers are dropped toward each other from opposite sides of Earth into a center-of-Earth tunnel. How many can bounce back up to surface and how many of those reach escape velocity for:

(a) $N=2$ case: $m_2 = 1$, $m_1=2$. (b) $N=4$ case: $m_4 = 1$, $m_3=2$, $m_2=4$, $m_1=8$.

Chapter 10 Calculus of exponentials, logarithms, and complex fields

A *logarithmic* potential curve $U=ln(y)=log_e y$ was given by (6.11). Our first example is the flip or inverse *exponential* curve $y=e^U$ since that function is so important for making the *complex phasor* $e^{-(i\omega+\Gamma)t}$.

Also, the *population growth function* $y=e^t=exp(t)$ is one of the most used if not *the* most useful of *transcendental* functions. Roughly, *transcendental* means not expressed by finite algebra or constructed by Euclid's strict rules. (However, like transcendental spirituality, it is easily *approximated*!) Later in this section we will prove that the exponential is the only function that is equal to its slope or *derivative*.

$$\frac{d}{dx}f(x)=f(x) \qquad \text{if and only if :} \qquad f(x)=e^x \qquad \text{where: } e=2.7182818... \quad (10.1)$$

In other words, if e^x is a force or potential curve then $F(x)$ and $U(x)$ are similar, in fact, identical.

$$F^{math}(x)=\frac{dU}{dx}=U(x). \text{ if and only if: } U(x)=e^x \qquad (10.2a)$$

For physicist's definition (6.9) of force, e^{-x} is the one for which potential and force are identical.

$$F^{phys}(x)=-\frac{dU}{dx}=U(x). \text{ if and only if: } U(x)=e^{-x} \qquad (10.2b)$$

For now we use these slope-function relations to construct the exponential curve approximately. Starting from origin $(x=0)$ we use the fact that any positive number to zero power is 1. $(e^0=1)$ From that point we draw a right triangle made of a unit altitude, a unit base, and a hypotenuse line of slope-1 as indicated in *Step-0* of Fig. 9.12. The hypotenuse line gives approximately the points just above and just below $x=0$. Then subsequent steps move the right triangle Δx to a point on the previously constructed line to make the next line. Since the slope is equal to the new function value, the base stays fixed at 1, but the altitude grows with the function value and makes the new line and a new point up the e^x-curve.

This approximation is a rough one. It underestimates a concave curve and overestimates convex ones because it puts the next point $x+\Delta x$ on a tangent from the previous point x. That's OK only if the curve is pretty straight and tangent slope is about the same at $x+\Delta x$. A better approximation uses the tangent halfway between neighboring tangents and extends that new slope to $x+\Delta x$ to find the next point.

Now if you rotate your $y=e^x$-graph by $90°$ you get a *logarithm* $U(y)=-ln(y)$ graph as shown in Fig. 10.1 (lower right). Each $U(y)$-curve-normal defines a unit-altitude triangle whose base is the force $F(y)=1/y$.

The story of e : A tale of great interest

Long ago banks would pay simple *interest* at some rate *r* such as *r=0.03* (3%) based on a 1 year period. You gave a principal *p(0)* to the bank and some time *t* later they would pay you *p(t)=(1+r·t)p(0)*. If you put in $1.00 at rate *r=1* (like Israel and Brazil that once had 100% intrest.) you got $2.00 at *t=1*year.

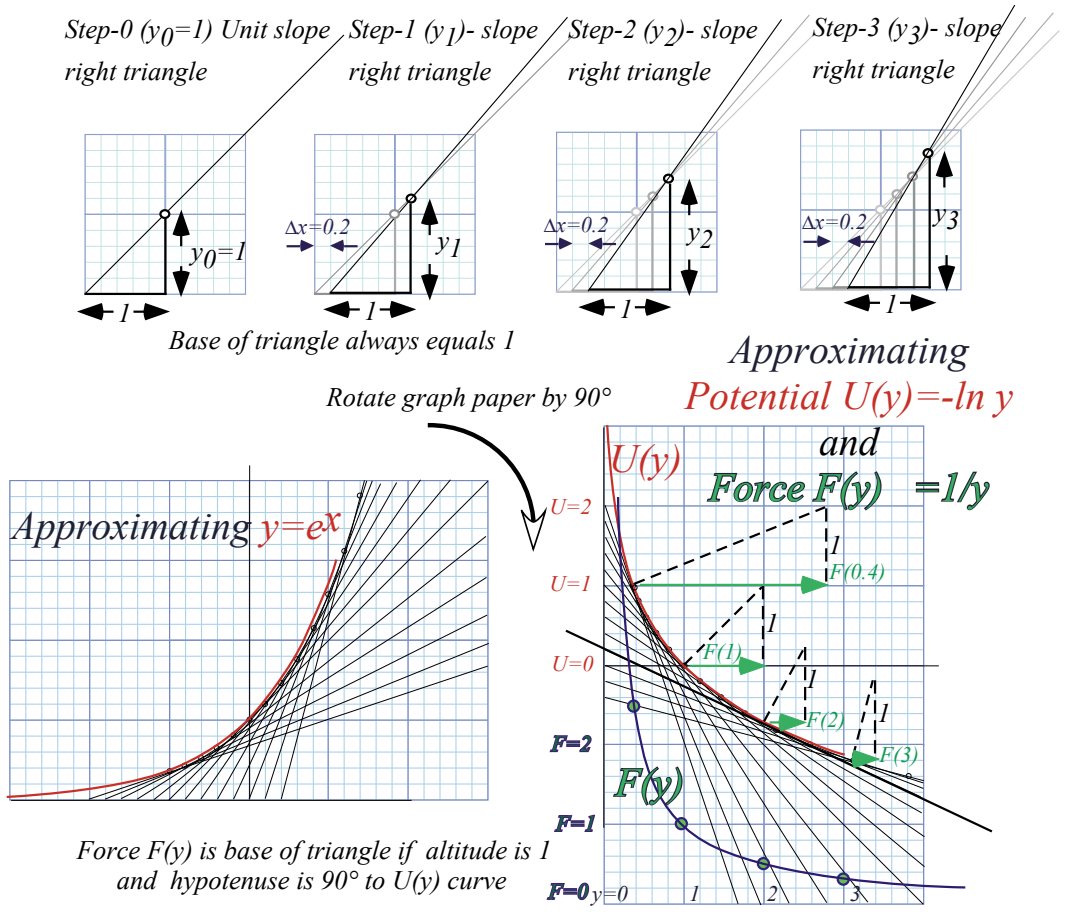

Fig. 10.1 Rough constructions (a) exponential curve $y=e^x=\exp(x)$. (b) Log potential. (c) 1/y-Force.

Later on fancy banks would pay *semester compounded* interest $p(\frac{t}{2})=(1+r\cdot\frac{t}{2})p(0)$ at the half-period $\frac{t}{2}$ and then use $p(\frac{t}{2})$ during the last half to figure final payment. Now $1.00 at rate *r=1* earns $2.25.

$$p^{\frac{1}{2}}(t)=(1+r\cdot\tfrac{t}{2})p(\tfrac{t}{2})=(1+r\cdot\tfrac{t}{2})\cdot(1+r\cdot\tfrac{t}{2})p(0)=\tfrac{3}{2}\cdot\tfrac{3}{2}\cdot 1=\tfrac{9}{4}=2.25$$

Fancier banks would pay *trimester compounded* interest $p(\frac{t}{3})=(1+r\cdot\frac{t}{3})p(0)$ at the *1/3rd*-period $\frac{t}{3}$ or 1st trimester and then use that to figure the 2nd trimester and so on. Now $1.00 at rate *r=1* earns $2.37.

$$p^{\frac{1}{3}}(t)=(1+r\cdot\tfrac{t}{3})p(2\tfrac{t}{3})=(1+r\cdot\tfrac{t}{3})\cdot(1+r\cdot\tfrac{t}{3})p(\tfrac{t}{3})=(1+r\cdot\tfrac{t}{3})\cdot(1+r\cdot\tfrac{t}{3})\cdot(1+r\cdot\tfrac{t}{3})p(0)=\tfrac{4}{3}\cdot\tfrac{4}{3}\cdot\tfrac{4}{3}\cdot 1=\tfrac{64}{27}=2.37$$

Still fancier banks would pay *quarterly*, *monthly*, *weekly*, *daily*, and so on. The race was on to give better earnings at a given interest rate *r*. Let's compare some different earnings on $1.00 at rate *r=1*. At first it looks like you gain a lot by compounding more often. Then earnings slow to a halt just shy of **$2.7**2.

$p^{\frac{1}{1}}(t)=(1+r\cdot\frac{t}{1})^1\,p(0)=\left(\frac{2}{1}\right)^1\cdot 1=\frac{2}{1}=2.00$ Monthly: $p^{\frac{1}{12}}(t)=(1+r\cdot\frac{t}{12})^{12}\,p(0)=\left(\frac{13}{12}\right)^{12}\cdot 1=2.613$

$p^{\frac{1}{2}}(t)=(1+r\cdot\frac{t}{2})^2\,p(0)=\left(\frac{3}{2}\right)^2\cdot 1=\frac{9}{4}=2.25$ Weekly: $p^{\frac{1}{52}}(t)=(1+r\cdot\frac{t}{52})^{52}\,p(0)=\left(\frac{53}{52}\right)^{52}\cdot 1=2.693$

$p^{\frac{1}{3}}(t)=(1+r\cdot\frac{t}{3})^3\,p(0)=\left(\frac{4}{3}\right)^3\cdot 1=\frac{64}{27}=2.37$ Daily: $p^{\frac{1}{365}}(t)=(1+r\cdot\frac{t}{365})^{365}\,p(0)=\left(\frac{366}{365}\right)^{365}\cdot 1=\mathbf{2.71}45$

$p^{\frac{1}{4}}(t)=(1+r\cdot\frac{t}{4})^4\,p(0)=\left(\frac{5}{4}\right)^4\cdot 1=\frac{625}{256}=2.44$ Hrly: $p^{\frac{1}{8760}}(t)=(1+r\cdot\frac{t}{8760})^{8760}\,p(0)=\left(\frac{8761}{8760}\right)^{8760}\cdot 1=\mathbf{2.718}1$

That halting point is *Euler's growth constant e=2.718281828459…* that we're after. Let's try huge numbers *(m)* of multiplications in $p^{1/m}(1)=(1+\frac{1}{m})^m$. (Get out a calculator. Rule & compass is useless now!)

$p^{1/m}(1)$ = **2.71**69239322 *for m = 1,000*
$p^{1/m}(1)$ = **2.718**1459268 *for m = 10,000*
$p^{1/m}(1)$ = **2.7182**682372 *for m = 100,000*
$p^{1/m}(1)$ = **2.71828**04693 *for m = 1,000,000* (10.3)
$p^{1/m}(1)$ = **2.7182816**925 *for m = 10,000,000*
$p^{1/m}(1)$ = **2.7182818**149 *for m = 100,000,000*
$p^{1/m}(1)$ = **2.71828182**71 *for m = 1,000,000,000*

The **solid figures** represent numbers that stay the same as we raise *m*. It's still a torturous way to find *e*. We do a *Billion (That's "B" as in "Boy!")* multiplications *($m=10^9$)* just to get 6 **solid figures** beyond **2.71**.

A better way expands binomial $e=\lim_{m\to\infty}(1+\frac{1}{m})^m$ or its power $e^{rt}=\lim_{m\to\infty}(1+\frac{1}{m})^{mr\cdot t}$ for all rates *r* and times *t*. We let *mr·t=n* and *m =n/r·t* to simplify it for huge multiplication numbers *m* or *n*.

$$e^{r\cdot t}=\lim_{m\to\infty}(1+\tfrac{1}{m})^{mr\cdot t}=\lim_{n\to\infty}(1+\tfrac{r\cdot t}{n})^n \qquad (10.4)$$

A *binomial expansion* *(See page 119)* turns exponential function $e^{r\cdot t}$ into a power series in $y=\frac{r\cdot t}{n}$ with *x=1*.

$$(x+y)^n=x^n+n\cdot x^{n-1}y+\frac{n(n-1)}{2!}x^{n-2}y^2+\frac{n(n-1)(n-2)}{3!}x^{n-3}y^3+\ldots+n\cdot xy^{n-1}+y^n$$

We actually *save* work as multiplication number *n* gets huge! ("*Huge*" means "*as close to ∞ as you like.*")

$$(1+\frac{r\cdot t}{n})^n=1+n\cdot\left(\frac{r\cdot t}{n}\right)+\frac{n(n-1)}{2!}\left(\frac{r\cdot t}{n}\right)^2+\frac{n(n-1)(n-2)}{3!}\left(\frac{r\cdot t}{n}\right)^3+\ldots$$

(Note factorials: 0!=1=1!, 2!=1·2, 3!=1·2·3, etc.)

Huge *n* makes *n(n-1)* cancel n^2, and *n(n-1)(n-2)* cancel n^3, and so on. The exponential $e^{r\cdot t}$ series is born.

$$e^{r\cdot t}=1+r\cdot t+\frac{1}{2!}(r\cdot t)^2+\frac{1}{3!}(r\cdot t)^3+\ldots=\sum_{p=0}^{o}\frac{(r\cdot t)^p}{p!} \quad (10.5a)$$

$$e=1+1+\frac{1}{2!}+\frac{1}{3!}+\ldots\frac{1}{o!}=\sum_{p=0}^{o}\frac{1}{p!} \quad (10.5b)$$

Let's try it out for *r·t=1* to evaluate *e* to order-*o*. (The *precision order o* is the power of highest term used.)

Precision order:
(o=1)-e-series = **2**.00000 =1+1
(o=2)-e-series = **2**.50000 =1+1+1/2
(o=3)-e-series = **2.**66667 =1+1+1/2+1/6
(o=4)-e-series = **2.7**0833 =1+1+1/2+1/6+1/24
(o=5)-e-series = **2.71**667 =1+1+1/2+1/6+1/24+1/120 (10.6)
(o=6)-e-series = **2.7180**5 =1+1+1/2+1/6+1/24+1/120+1/720
(o=7)-e-series = **2.71825**
(o=8)-e-series = **2.71828**

Nine terms in series (10.5) give 5-figure accuracy (10.6) and do the work of a million products in (10.3). That's a *million* reduced to 8 sums and half-dozen or so divisions. It's a *big* savings of arithmetic labor!

Derivatives, rates, and rate equations

Binomial expansions provide ways to find calculus formulas for *slope* or *velocity* introduced geometrically in Ch. 1. Soon we will do the same for *curvature* or *acceleration* and other higher order calculus concepts.

Suppose someone gives you a plot of formula like $x(t)=t^2$ or $x(t)=\sin 4t$ or an exponential plot of $x(t)=e^t$ that we just did in Fig. 10.1. You should be able to *estimate* its slope at any point from its x versus t graph. However, a binomial expansion may let you find an *exact* formula for its slope.

Consider a parabola $x(t)=t^2$ for example. Let's find the slope $\frac{\Delta x}{\Delta t}$ of a line that goes through point $x(t)$ and a point $x(t+\Delta t)=(t+\Delta t)^2$ that is a *tiny* time interval Δt later. Binomial expansion gives $\Delta x=x(t+\Delta t)-x(t)$.

$$\Delta x=x(t+\Delta t)-x(t)=(t+\Delta t)^2-t^2=t^2+2t\cdot\Delta t+(\Delta t)^2-t^2=2t\cdot\Delta t+(\Delta t)^2$$

Slope ratio $\frac{\Delta x}{\Delta t}$ follows. If Δt is *tiny* we ignore it. Then *tangent slope* $v(t)=\frac{dx}{dt}$ is the *1st derivative* of $x(t)=t^2$.

$$\frac{\Delta x}{\Delta t}=\frac{2t\cdot\Delta t+(\Delta t)^2}{\Delta t}=2t+\Delta t \qquad (10.7a) \qquad \frac{dx}{dt}=v(t)=2t=\frac{d}{dt}t^2 \qquad (10.7b)$$

This checks the geometry of parabola $2\lambda y=x^2$ in Fig. 9.4. Slope is $\frac{dy}{dx}=\frac{2x}{2\lambda}=\frac{x}{\lambda}$, twice the x-value in units of 2λ. Consider an n-power curve $x(t)=At^n$. Binomial expansion of $\Delta x=x(t+\Delta t)-x(t)$ has n terms, most in $+\ldots+$.

$$\Delta x=x(t+\Delta t)-x(t)=A(t+\Delta t)^n-At^n=At^n+Ant^{n-1}\cdot\Delta t+\ldots+A(\Delta t)^n-At^n=Ant^{n-1}\cdot\Delta t+\ldots+A(\Delta t)^n$$

If Δt is *tiny*, only *1st* term Ant^{n-1} in slope ratio $\frac{\Delta x}{\Delta t}$ is not *tiny-tiny*. That *1st* term is *1st derivative* of $x(t)=At^n$.

$$\frac{\Delta x}{\Delta t}=A\frac{nt^{n-1}\cdot\Delta t+\ldots+(\Delta t)^n}{\Delta t}=Ant^{n-1}+\ldots+A(\Delta t)^{n-1} \qquad (10.8a) \qquad \frac{dx}{dt}=v(t)=Ant^{n-1}=\frac{d}{dt}At^n \qquad (10.8b)$$

Series for $x(t)=Ae^t$ is unchanged *(for r=1)* by $\frac{d}{dt}$. It does kill term number-∞, but $\frac{1}{\infty!}r^\infty t^\infty$ is *tiny-tiny-tiny* anyway.

$$\begin{aligned}
\frac{d}{dt}e^{rt}&=\frac{d}{dt}1+\frac{d}{dt}rt+\frac{d}{dt}\frac{1}{2!}r^2t^2+\frac{d}{dt}\frac{1}{3!}r^3t^3+\frac{d}{dt}\frac{1}{4!}r^4t^4+\ldots && \text{(From (10.5a) and linearity)}\\
&=0+r+\frac{2}{2!}r^2t+\frac{3}{3!}r^3t^2+\frac{4}{4!}r^4t^3+\ldots && \text{(From (10.8b))}\\
&=0+r+r^2t+\frac{1}{2!}r^3t^2+\frac{1}{3!}r^4t^3+\ldots && \text{(Factorial n!=n·(n-1)·(n-2)·...·1)}\\
&=r\left(1+rt+\frac{1}{2!}r^2t^2+\frac{1}{3!}r^3t^3+\ldots\right)=re^{rt} && \text{(From (10.5a) again)}
\end{aligned} \qquad (10.9)$$

For 100% intrest ($r=1$), growth rate-of-Ae^t *equals* Ae^t. Otherwise, growth rate of Ae^{rt} is *proportional* to Ae^{rt}. To state that the growth rate of a function $x(t)$ equals a constant *"intrest rate"* r times current value of $x(t)$ is to write a *differential rate equation* whose "solution" is $x(t)=Ae^{rt}$. (The constant A is *"initial capital"* $A=x(0)$.)

$$\textit{Rate equation}: \quad \frac{dx}{dt}=r\cdot x(t) \quad \textit{has solution}: \quad x(t)=x(0)e^{rt} \qquad (10.10)$$

It is *Malthus's population explosion equation* for positive rate $r>0$! It is *radioactive decay equation* for $r<0$.

The binomial expansion

High school algebra courses generally contain a treatment of the *binomial theorem* that is used for our $e^{r\cdot t}$ expansion after equation (10.4). In case your course missed that (or you weren't paying attention!) we'll take a close look at this remarkable formula. The binomial algebra and related Pascal triangle geometry is the basis of so much mathematics and physics that it deserves a book chapter of its own.

First it helps to work out the first few binomial series $(x+y)^0$, $(x+y)^1$, xy^2 $(x+y)^2$, $(x+y)^3$,... by simply multiplying them together as we did for the $e^{r\cdot t}$ series that started this discussion. The first examples $(x+y)^0=1$ and $(x+y)^1=x+y$ are easy since the 0^{th} and 1^{st} powers of a number n are defined to be 1 and n, respectively. The square of a binomial is simple enough, too.

$$(x+y)^2=(x+y)\cdot(x+y)=x^2+xy+yx+y^2=x^2+2xy+y^2 \qquad (1)$$

You might find it helps to make a table of product terms to do algebraic multiplication of this sort. Just make a box and write one factor ($(x+y)$ in this case) on top and the other ($(x+y)$ again) along the left.

	x	$+y$
x	x^2	xy
$+y$	yx	y^2

$$= x^2+xy+yx+y^2 = x^2+2yx+y^2 \qquad (2)$$

The just multiply each thing on top by each thing on the left and add them up to get (1). Try it with $(x+y)^3$.

$$(x+y)^3 = \begin{array}{c|ccc} & x^2 & +2xy & +y^2 \\ \hline x & x^3 & 2x^2y & xy^2 \\ +y & yx^2 & 2y^2x & y^3 \end{array} = x^3+3x^2y+3xy^2+y^3 \qquad (3)$$

We can continue this process to get $(x+y)^4$, $(x+y)^5$,...and so forth.

$$(x+y)^4 = \begin{array}{c|cccc} & x^3 & +3x^2y & +3xy^2 & +y^3 \\ \hline x & x^4 & 3x^3y & 3x^2y^2 & xy^3 \\ +y & yx^3 & 3x^2y^2 & 3xy^3 & y^4 \end{array} = x^4+4x^3y+6x^2y^2+4xy^3+y^4 \qquad (4)$$

$$(x+y)^4 = \begin{array}{c|ccccc} & x^4 & +4x^3y & +6x^2y^2 & +4xy^3 & +y^4 \\ \hline x & x^5 & +4x^4y & +6x^3y^2 & +4x^2y^3 & +xy^4 \\ +y & yx^4 & +4x^3y^2 & +6x^2y^3 & +4xy^4 & +y^5 \end{array} = x^5+5x^4y+10x^3y^2+10x^2y^3+5xy^4+y^5 \qquad (5)$$

After awhile, you might notice a pattern in the numbers or coefficients B_{pq} of the various power terms x^py^q where the powers p and q must add up to the power $n=p+q$ of $(x+y)^n$ being calculated. These B_{pq} are called the *binomial coefficients* of x^py^q and a triangular array pattern in Fig. 1 is called *Pascal's triangle*.

This pattern is like a Ponzi scheme since every number in it except the pinnacle $B_{00}=1$ is the sum of one or two numbers that lie above it and to either side. (This sum is going on in (2) thru (5) above.) So the pinnacle position $q-p=0$ on the central vertical triangle axis ends up with the biggest number B_{pq} for each power-row $n=p+q$. At $n=p+q=10^{th}$ row, pinnacle $B_{5,5}$ accumulates 252 from 11 spots $-5<q-p<+5$.

Table 1. Binomial combinatorial coefficients up to power n=10

$B^{n=p+q}_{p,q}$	$q-p=$	−9	−8	−7	−6	−5	−4	−3	−2	−1	0	1	2	3	4	5	6	7	8	9	10
$p+q=$											1										
1										1		1									
2									1		2		1								
3								1		3		3		1							
4							1		4		6		4		1						
5						1		5		10		10		5		1					
6					1		6		15		20		15		6		1				
7				1		7		21		35		35		21		7		1			
8			1		8		28		56		70		56		28		8		1		
9		1		9		36		84		126		126		84		36		9		1	
10	1		10		45		120		210		252		210		120		45		10		1

Gamblers may recognize $B_{55}=252$ as the number of ways you can get exactly *5* x-cards and *5* y-cards from an $n=20$ card deck of *10* x-cards and *10* y-cards. More simply, $B_{55}=252$ is the number of ways to get exactly *5* heads and *5* tails from an $n=10$ coin tosses, or x^5y^5 from an $(n=10)$-power binomial.

$$(x+y)(x+y)(x+y)(x+y)(x+y)(x+y)(x+y)(x+y)(x+y)(x+y)=(x+y)^{10}=x^{10}+...252x^5y^5+...y^{10} \qquad (7)$$

As you go down the line of 10 factors $(x+y)$ you must pick x or y from each factor $(x+y)$ to make just one $(n=10)$-power term x^py^q with $n=p+q$. There are $2^{10}=1024$ such terms. (Just add up the 10^{th} row of Table 1.)

$$(1+1)^{10}=2^{10}=1^{10}+...252\cdot 1^5 1^5+...=1+10+45+120+210+252+210+120+45+10+1=1024 \qquad (8)$$

Check the other rows, too. (It's a good to know powers-of-2 in a binary age!)

$$2^2=4,\ 2^3=8,\ 2^4=16,\ 2^5=32,\ 2^6=64,\ 2^7=128,\ 2^8=256,\ 2^9=512,\ 2^{10}=1024,\ldots \qquad (9)$$

Now suppose, instead of just two things x or y, you could choose n different things $\{a,b,c,...,x,y,z,..\}$ from each of the n factors in (7). Then the number of ways you may get a given term $a\cdot b\cdot c\cdot\ldots\cdot x\cdot y\cdot z\cdot..$ having all n different things is the number $n!=n\cdot(n-1)\cdot(n-2)\cdot\ldots\cdot 2\cdot 1$ of permutations of n things. Each permutational reordering gives another equal term $(a\cdot b=b\cdot a)$.

So, $n!$ is the "*n-nomial* coefficient" for a term with n-different factors. However, if we are counting terms x^py^q like a binomial series has with only two different things, the $p!$ permutations of the x things and the $q!$ permutations of the y things do not count as new terms. Then $n!$ divided by $p!$ and $q!$ gives B_{pq}.

$$B^n_{p,q}=\frac{n!}{p!q!}=B^n_{q,p} \quad examples:\ B^{10}_{1,9}=\frac{10!}{1!9!}=10,\quad B^{10}_{2,8}=\frac{10!}{2!8!}=\frac{10\cdot 9}{2}=45,\ ...$$

This gives binomial series that follows (10.4) and the Gauss-binomial distribution plotted below.

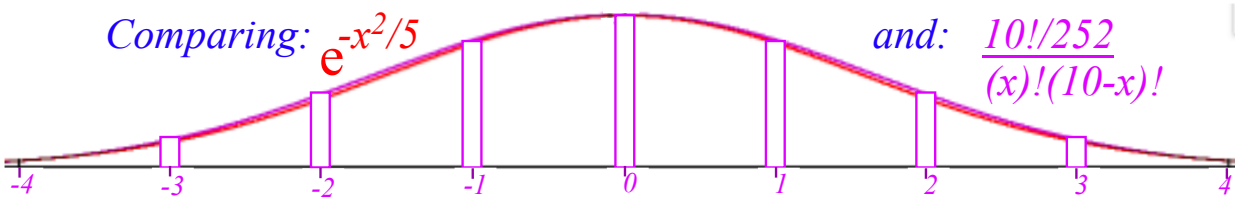

General power series approximations

Are power series like (10.5) useful for functions other than exponentials? Well, Mr. Maclaurin and Mr. Taylor thought so. Series that bear their names are *de rigeur* in good math books. (And, in this one, too!)

Let's start with a general power series like (10.5) but with arbitrary constant coefficients c_0, c_1, *etc.*

$$x(t) = c_0 + c_1 t + c_2 t^2 + c_3 t^3 + c_4 t^4 + c_5 t^5 + \ldots + c_n t^n + \qquad (10.11a)$$

We derive c_0 by setting time t to an *initial time t=0*. (Like C-programmers, we count *"uh-zero, uh-one, uh-two,.."*)

$$c_0 = x(0) \qquad (10.11b)$$

So the 0th coefficient c_0 is *initial position x(0)*. Now we use (10.8b) to find a derivative of each term.

$$v(t) = \frac{d}{dt} x(t) = 0 + c_1 + 2c_2 t + 3c_3 t^2 + 4c_4 t^3 + 5c_5 t^4 + \ldots + nc_n t^{n-1} + \qquad (10.11c)$$

Rate of change of position $x(t)$ is *velocity v(t)*. Setting $t=0$ derives c_1.

$$c_1 = v(0) \qquad (10.11d)$$

So the 1st coefficient c_1 is *initial velocity v(0)*. Now find a 2nd derivative using (10.8b).

$$a(t) = \frac{d}{dt} v(t) = 0 + 2c_2 + 2\cdot 3c_3 t + 3\cdot 4c_4 t^2 + 4\cdot 5c_5 t^3 + \ldots + n(n-1)c_n t^{n-2} + \qquad (10.11c)$$

Change of velocity $v(t)$ is *acceleration a(t)*. Set $t=0$ to get c_2.

$$c_2 = \tfrac{1}{2} a(0) \qquad (10.11d)$$

So the 2nd coefficient c_2 is half the *initial acceleration a(0)*. Now a 3rd derivative:

$$j(t) = \frac{d}{dt} a(t) = 0 + 2\cdot 3c_3 + 2\cdot 3\cdot 4c_4 t + 3\cdot 4\cdot 5c_5 t^2 + \ldots + n(n-1)(n-2)c_n t^{n-3} + \qquad (10.11e)$$

Change of acceleration $a(t)$ is *jerk j(t)*. (*Jerk* is a NASA sanctioned term!) Set $t=0$ to get c_3.

$$c_3 = \tfrac{1}{3!}\ j(0) \qquad (10.11f)$$

So the 3rd coefficient c_3 is *initial jerk j(0) over 3!* Now a 4th derivative:

$$i(t) = \frac{d}{dt} j(t) = 0 + 2\cdot 3\cdot 4c_4 + 2\cdot 3\cdot 4\cdot 5c_5 t + \ldots + n(n-1)(n-2)(n-3)c_n t^{n-4} + \qquad (10.11g)$$

Change of jerk $j(t)$ is *inauguration i(t)*. (If NASA can be silly, so can we!) Set $t=0$ to get c_4.

$$c_4 = \tfrac{1}{4!}\ i(0) \qquad (10.11h)$$

So the 4th coefficient c_4 is *initial inauguration i(0) over 4!*. Now a 5th derivative.

$$r(t) = \frac{d}{dt} i(t) = 0 + 2\cdot 3\cdot 4\cdot 5c_5 + \ldots + n(n-1)(n-2)(n-3)(n-4)c_n t^{n-5} + \qquad (10.11i)$$

Change of inauguration $i(t)$ is *revolution r(t)*. (Ooops! Politically incorrect!) Quick set $t=0$ to get c_5.

$$c_5 = \tfrac{1}{5!}\ r(0) \qquad (10.11j)$$

That's enough iterations to show the Maclaurin series of any function $x(t)$ that has decent derivatives.

$$x(t) = x(0) + v(0)t + \tfrac{1}{2!} a(0)t^2 + \tfrac{1}{3!} j(0)t^3 + \tfrac{1}{4!} i(0)t^4 + \tfrac{1}{5!} r(0)t^5 + \ldots + \tfrac{1}{n!} x^{(n)} t^n + \ldots \qquad (10.12a)$$

By "decent" we mean the non-exploding types that we can deal with. The following is a list that shows some of the notations used for the higher order derivatives discussed so far.

$$
\begin{aligned}
v(t) &= \frac{d}{dt}x(t) = \dot{x}(t) \\
a(t) &= \frac{d}{dt}v(t) = \dot{v}(t) = \frac{d^2}{dt^2}x(t) = \ddot{x}(t) \\
j(t) &= \frac{d}{dt}a(t) = \dot{a}(t) = \frac{d^2}{dt^2}v(t) = \ddot{v}(t) = \frac{d^3}{dt^2}x(t) = \dddot{x}(t) \\
i(t) &= \frac{d}{dt}j(t) = \dot{j}(t) = \frac{d^2}{dt^2}a(t) = \ddot{a}(t) = \frac{d^3}{dt^2}v(t) = \dddot{v}(t) = \frac{d^4}{dt^4}x(t) = \ddot{\dddot{x}}(t)
\end{aligned}
\qquad (10.12b)
$$

The "dot" notation writes n-derivatives of $x(t)$ by puttting n-dots over x. This may help prevent writer's cramp. But, *j-dot* looks, well, kind of jerky. It's common to use primes ($y' = \frac{dy}{dx}, y'' = \frac{d^2y}{dx^2}, etc.$) for x-derivatives.

How good is a power series (10.5) at faking $x=e^t$ beyond $t=1$listed in (10.6)? We plot various orders of approximation in Fig. 10.2. The 1st order (2-terms of (10.5a)) is just a straight line of slope 1. A 2nd order (3-term) parabola, 3rd order cubic, 4th order quartic, *etc.* each peel off $x=e^t$ in sucession. All meet at ($t=0,x=1$).

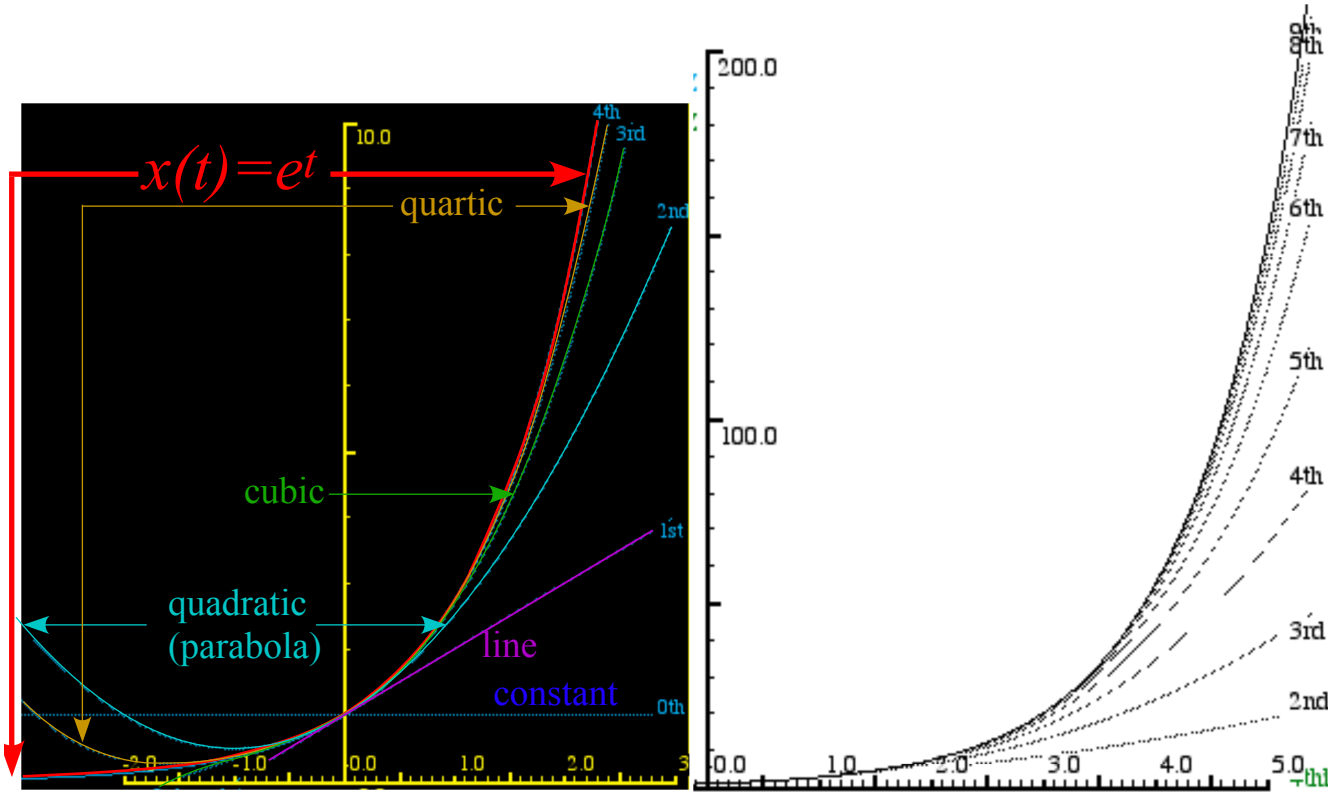

Fig. 10.2 Comparing $x=e^t$ with its n^{th}-order approximate power series.

Sine-wave power series

A severe test of power series is their ability to fake sine waves. The derivative and rate equation for the sine function $x(t)=\sin\omega t$ uses expansion $x(t+\Delta t)=\sin\omega(t+\Delta t)$. To expand $\sin(a+b)$ or $\cos(a+b)$ we use Fig. 10.3.

$$\sin(a+b)=\cos a\sin b+\sin a\cos b \qquad (10.13a) \qquad \cos(a+b)=\cos a\cos b-\sin a\sin b \qquad (10.13b)$$

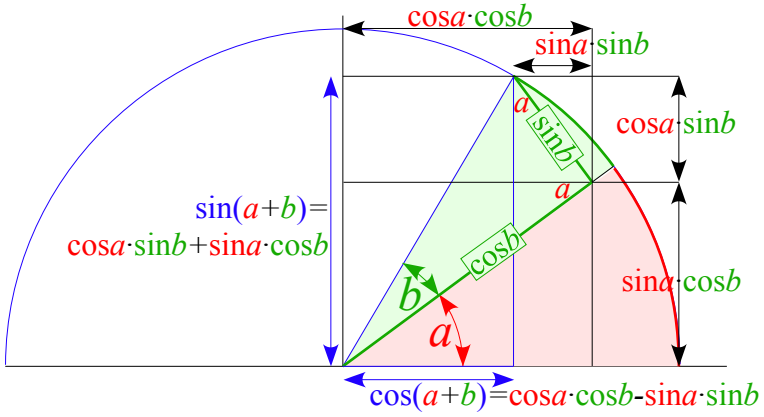

Fig. 10.3 Geometry of sine and cosine expansion identities.

Expansion of $\Delta x=x(t+\Delta t)-x(t)$ for sine or cosine is easy since $\sin\omega\cdot\Delta t=\omega\cdot\Delta t$ and $\cos\omega\cdot\Delta t=1$ for *tiny* Δt.

$$\begin{aligned}&\sin\omega(t+\Delta t)-\sin\omega\cdot t\\&=\cos\omega\cdot t\sin\omega\cdot\Delta t+\sin\omega\cdot t\cos\omega\cdot\Delta t-\sin\omega\cdot t\\&=\cos\omega\cdot t\ (\omega\cdot\Delta t)\ +\sin\omega\cdot t\ (1)\qquad -\sin\omega\cdot t\\&=(\omega\cdot\Delta t)\cos\omega\cdot t\end{aligned} \qquad (10.14a)$$

$$\begin{aligned}&\cos\omega(t+\Delta t)-\cos\omega\cdot t\\&=\cos\omega\cdot t\cos\omega\cdot\Delta t-\sin\omega\cdot t\sin\omega\cdot\Delta t-\cos\omega\cdot t\\&=\cos\omega\cdot t\ \ (1)\qquad -\sin\omega\cdot t\ (\omega\cdot\Delta t)\ -\cos\omega\cdot t\\&=-(\omega\cdot\Delta t)\sin\omega\cdot t\end{aligned} \qquad (10.14b)$$

We will need the sine and cosine slope (derivative) formulas that follow from this.

$$\frac{d}{dt}\sin\omega\cdot t=\frac{\sin\omega(t+\Delta t)-\sin\omega\cdot t}{\Delta t}=\omega\cdot\cos\omega\cdot t \qquad (10.15a)$$

$$\frac{d}{dt}\cos\omega\cdot t=\frac{\cos\omega(t+\Delta t)-\cos\omega\cdot t}{\Delta t}=-\omega\cdot\sin\omega\cdot t \qquad (10.15b)$$

A list of series coefficients $c_n=\frac{1}{n!}\frac{d^n x}{dt^n}$ in (10.12) for sine $x=\sin\omega t$ and cosine $x=\cos\omega t$ is worked out below.

$$c_0=x(0)=\sin\omega\cdot 0=0$$
$$c_1=v(0)=+\omega\cdot\cos\omega\cdot 0=+\omega$$
$$c_2=\frac{a(0)}{2!}=-\frac{\omega^2}{2!}\cdot\sin\omega\cdot 0=0$$
$$c_3=\frac{j(0)}{3!}=-\frac{\omega^3}{3!}\cdot\cos\omega\cdot 0=-\frac{\omega^3}{3!}$$
$$c_4=\frac{i(0)}{4!}=+\frac{\omega^4}{4!}\cdot\sin\omega\cdot 0=0$$
$$c_5=\frac{r(0)}{5!}=+\frac{\omega^5}{5!}\cdot\cos\omega\cdot 0=+\frac{\omega^5}{5!}$$

$$c_0=x(0)=\cos\omega\cdot 0=1$$
$$c_1=v(0)=-\omega\cdot\sin\omega\cdot 0=0$$
$$c_2=\frac{a(0)}{2!}=-\frac{\omega^2}{2!}\cdot\cos\omega\cdot 0=-\frac{\omega^2}{2!}$$
$$c_3=\frac{j(0)}{3!}=+\frac{\omega^3}{3!}\cdot\sin\omega\cdot 0=0$$
$$c_4=\frac{i(0)}{4!}=+\frac{\omega^4}{4!}\cdot\cos\omega\cdot 0=+\frac{\omega^4}{4!}$$
$$c_5=\frac{r(0)}{5!}=-\frac{\omega^5}{5!}\cdot\sin\omega\cdot 0=0$$

A sine derivative repeats after four orders: *…sin t, cos t, -sin t, -cos t, (again) sin t, cos t, -sin t, -cos t, (etc.)* .

The resulting sine and cosine series show this *repeat-after-4-pattern* of factors 0,1,0,-1 of $\frac{(\omega t)^n}{n!}$ terms.

$$\sin\omega t = 0+\omega t+0-\frac{(\omega t)^3}{3!}+0+\frac{(\omega t)^5}{5!}+0-\ldots \qquad (10.16a)$$

$$\cos\omega t = 1+0-\frac{(\omega t)^2}{2!}+0+\frac{(\omega t)^4}{4!}+0-\ldots \qquad (10.16b)$$

The sine is an *odd* function to time reversal *(sin(-t) =-sin(t))*, but cosine is *even (cos(-t) =+cos(t))*. Thus sine has only odd powers *p=1,3,5,…* of time and cosine has only even powers *p=0,2,4,….* Series plots (10.16) in Fig. 10.4 have highest power or *order o=1st,2nd,3rd,4th,etc.* Number *n* of terms is $\frac{o+1}{2}$ for sine and $\frac{o+2}{2}$ for cosine.

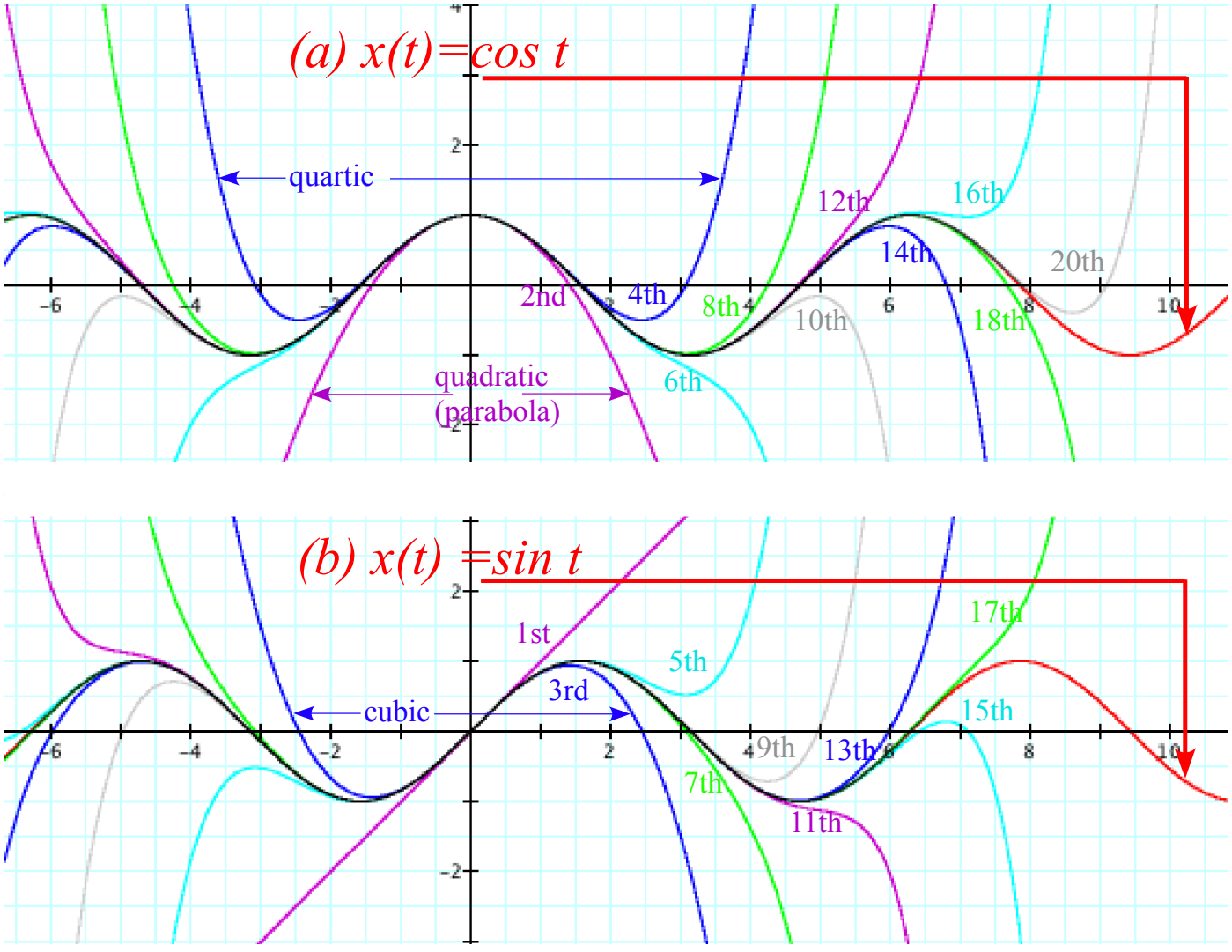

Fig. 10.4 Comparing (a) x=sin t and (b) x=cos t with their n^{th}-order approximate power series.

It takes a *9th* (for *sin t*) or *10th* (for *cos t*) order series of 5 terms to get one full oscillation with 5% or better precision. Then 10 terms gives two oscillations, and so on. Fig. 10.4 shows that precision breaks down quite explosively. Polynomials are *exponentially degrading* approximations of wave motion.

Euler's theorem and relations

Sine, cosine, and e^{rt} power series (10.16) and (10.9) lead to an 18th Century crown jewel of mathematics. It is due to a close relation of these series and the functions they represent. It is hard to imagine, but exponential intrest rate growth and simple harmonic oscillation are related. As it turns out, the relation *is* quite imaginary!

Suppose the fancy bankers really went bonkers and made interest rate r an *imaginary number* $r=i\theta$. Imaginary number $i=\sqrt{-1}$ has powers with a *repeat-after-4-pattern:* $i^0=1$, $i^1=i$, $i^2=-1$, $i^3=-i$, $i^4=1$,*etc...* It fits the pattern leading to *cos*θ and *sin*θ series (10.16). Series (10.9) with imaginary $rt=i\theta$ joins the (10.16) series.

$$e^{i\theta}=1+i\theta+\frac{(i\theta)^2}{2!}+\frac{(i\theta)^3}{3!}+\frac{(i\theta)^4}{4!}+\frac{(i\theta)^5}{5!}+\ldots \qquad \text{(From series (10.9))}$$

$$=1+i\theta-\frac{\theta^2}{2!}-i\frac{\theta^3}{3!}+\frac{\theta^4}{4!}+i\frac{\theta^5}{5!}-\ldots \qquad (i=\sqrt{-1}\ \text{imples: } i^1=i,\ i^2=-1,\ i^3=-i,\ i^4=+1,\ i^5=i,\ldots)$$

$$=\left(1-\frac{\theta^2}{2!}+\frac{\theta^4}{4!}-\ldots\right)+\left(i\theta-i\frac{\theta^3}{3!}+i\frac{\theta^5}{5!}-\ldots\right) \qquad \text{(To match series (10.16))}$$

$$e^{i\theta} = \cos\theta + i\sin\theta \qquad \textit{Euler - DeMoivre Theorem} \qquad (10.17)$$

The resulting *Euler-DeMoivre Theorem* is a beautiful identity and a very powerful tool as we shall see. First and foremost it is a *complex wave phasor function* $\psi = Ae^{-i\omega t}$ that we will use in Unit 4. (Note: $\theta=-\omega\cdot t$.)

$$\psi = Ae^{-i\omega t} = A\cos\omega t - iA\sin\omega t = \mathrm{Re}\,\psi + i\,\mathrm{Im}\,\psi = \psi_x + i\psi_y \qquad (10.18)$$

Fig. 10.5a plots $e^{i\theta}$ in the *complex plane*, a real-*vs*-imaginary graph. Fig. 10.5b shows $\psi = Ae^{-i\omega t}$ as a *complex phasor clock*. *Real part* Re$\psi=x(t)$ is position. *Imaginary part* is ω-scaled velocity Im$\psi=v(t)/\omega$. Conversion of polar-to-Cartesian (10.19a) and *vice-versa* (10.19b) is on scientific calculators. *(Recall cautions at end of Ch. 1.)*

$$\textit{Cartesian } (x,y)\textit{ form}\begin{cases}\psi_x=\mathrm{Re}\,\psi(t)=x(t)=A\cos\omega t\\ \psi_y=\mathrm{Im}\,\psi(t)=\dfrac{v(t)}{\omega}=-A\sin\omega t\end{cases} \qquad (10.19a)$$

$$\textit{Polar } (r,\theta)\textit{ form}\begin{cases}r=A=|\psi|=\sqrt{\psi_x{}^2+\psi_y{}^2}\\ \theta=-\omega t=\arctan(\psi_y/\psi_x)\end{cases} \qquad (10.19b)$$

Real part Reψ is the *"is"* (*that Clinton sought in 1997*) and Imψ is what Reψ is *"gonna-be"* in $\frac{1}{4}$-cycle (*as in "gonna be in trouble!"* A mantra, *"Imagination precedes reality by one quarter"* works here as in US corporate world.) *Euler expo-sinusoidal identities* relate cosθ, sinθ, and $e^{\pm i\theta}$. A *conjugate* ψ^* reflects i with $-i$.

$$\begin{aligned}\psi &= re^{+i\theta}=re^{-i\omega t}=r(\cos\omega t-i\sin\omega t)\\ \psi^* &= re^{-i\theta}=re^{+i\omega t}=r(\cos\omega t+i\sin\omega t)\end{aligned} \qquad (10.20a)$$

$$\begin{aligned}\cos\theta&=\tfrac{1}{2}(e^{+i\theta}+e^{-i\theta})\\ \sin\theta&=\tfrac{1}{2i}(e^{+i\theta}-e^{-i\theta})\end{aligned} \qquad (10.20b)$$

A special case is $e^{-i\pi}=-1$. (We'll also use a *real* π-exponential: $e^{-\pi}=0.04321$.) Other special cases are noted.

$$e^{-i\pi}=-1=e^{+i\pi}, \qquad e^{+i\frac{\pi}{2}}=i=-e^{-i\frac{\pi}{2}}, \qquad e^{+i\frac{\pi}{4}}=\tfrac{1}{\sqrt{2}}(1+i)=-e^{-i\frac{3\pi}{4}}=-e^{+i\frac{5\pi}{4}}. \qquad (10.21)$$

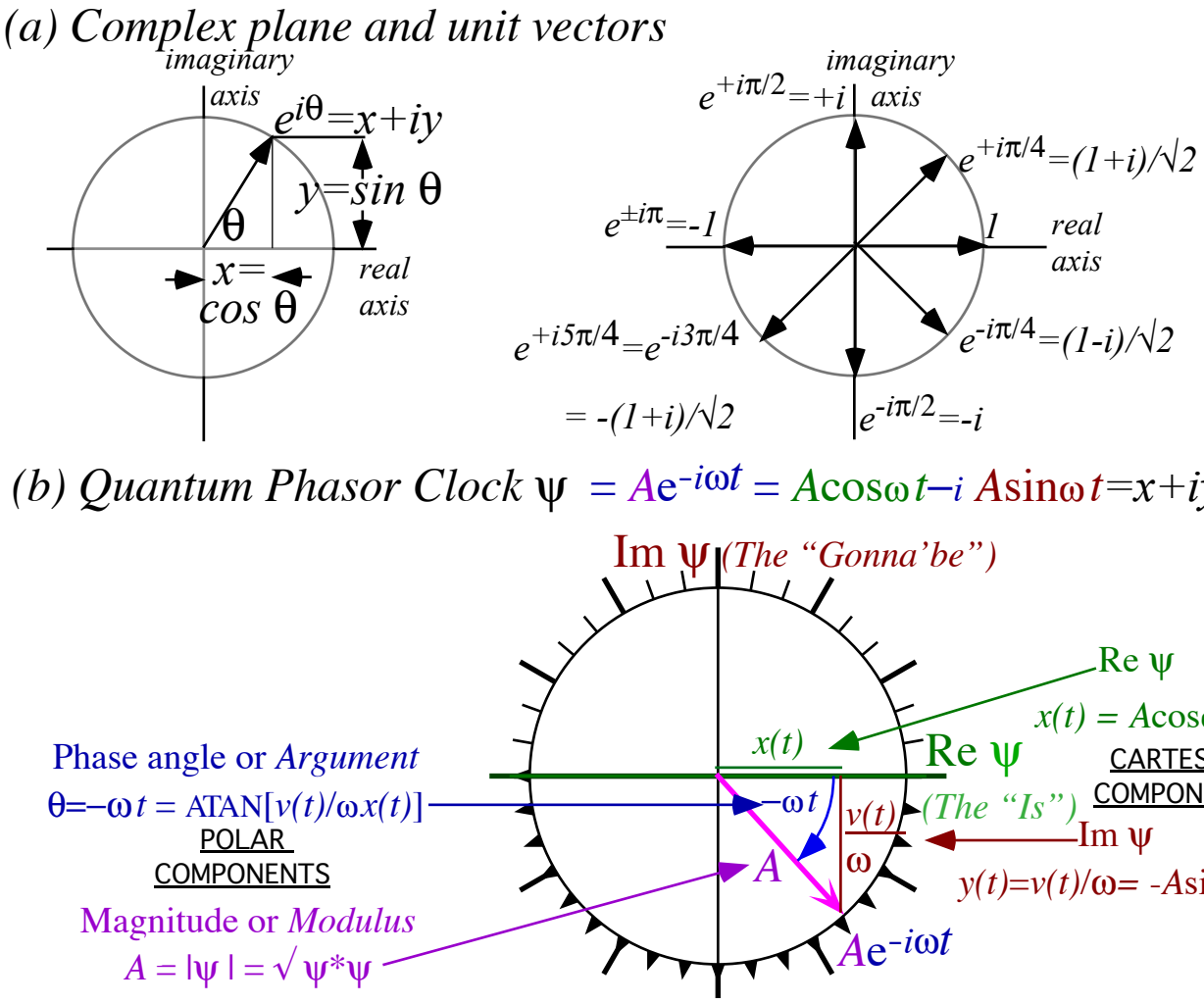

Fig. 10.5 (a) Complex plane. (b) Phasor clock. Cartesian form uses (Re ψ, Im ψ). Polar form uses (|ψ|,θ).

Wages of imaginary intrest: Phasor oscillation dynamics

By now bankers should know what happens when you use *imaginary intrest*. The accounts *oscillate* up and down and the imagineering bankers *oscillate* in and out of the slammer. (At least that was the way until 2001 when the Bush administration passed the *No Banker Left on His Behind Act* that also outlawed reality.)

Consider exponential rate equation (10.15) with negative imaginary rate $r=-i\omega$.

$$\text{Imaginary rate equation}: \quad \frac{dx}{dt} = -i\omega \cdot x(t) \quad \text{has solution}: \quad x(t) = x(0)e^{-i\omega t} \tag{10.22a}$$

It becomes a real 2^{nd} order equation if we apply the derivative operation to both sides.

$$\frac{d}{dt}\frac{dx(t)}{dt} = \frac{d^2x}{dt^2} = -i\omega \cdot \frac{d}{dt}x(t) = -i\omega \cdot (-i\omega \cdot x(t)) = -\omega^2 x(t) \tag{10.22b}$$

It is the *Newton-Hooke simple harmonic oscillator equation*, but it has the same solution as (10.19) above.

$$Newton-Hooke\ HO\ equation:\ \frac{d^2x}{dt^2}=-\omega^2x(t)\ \ has\ solution:\ x(t)=x(0)e^{-i\omega t} \tag{10.23a}$$

It combines *Newton's force law F=m·a=m ẍ* and *Hooke's force law F=-k·x*. The ω value repeats (9.9b).

$$m\frac{d^2x}{dt^2}=-k\cdot x(t)\ \ has\ angular\ frequency:\ \omega=\sqrt{\frac{k}{m}} \tag{10.23b}$$

What Good Are Complex Exponentials?

Complex Exponentials are used to describe oscillation, resonance, waves and fields. We don't use them just to be cute! Let's look at some compelling reasons for using imaginary or complex arithmetic.

Complex numbers provide "automatic trigonometry"

If you have trouble remembering trigonometric identities then this is a good reason all by itself to use complex numbers. For example, if you're taking a test and you can't remember what is cos*(a+b)*, then just factor $e^{i(a+b)}=e^{ia}e^{ib}$, expand exponentials into $e^{ia}=\cos a+i\sin a$ and multiply them out.

$$e^{i(a+b)}=e^{ia}e^{ib}$$

$$cos(a+b)+i\,sin(a+b)=(cos\,a+i\,sin\,a)\,(cos\,b+i\,sin\,b)$$

$$cos(a+b)+i\,sin(a+b)=[cos\,a\,cos\,b-sin\,a\,sin\,b]+i[sin\,a\,cos\,b+cos\,a\,sin\,b] \tag{10.24a}$$

That's two trig identities for the price of one! The real part gives the cosine relation (10.13b).

$$\cos(a+b)=[\cos a\cos b-\sin a\sin b] \tag{10.24b}$$

The imaginary part gives the sine relation (10.13a).

$$\sin(a+b)=[\sin a\cos b+\cos a\sin b]. \tag{10.24c}$$

Complex exponentials $Ae^{-i\omega t}$ tracks position and velocity using Phasor Clock.

Recall discussion of phasor diagram in Fig. 10.5b. Real and imaginary give *phase*: position and velocity.

Complex numbers add like vectors.

Physics of *wave interference* involves the addition or subtraction of oscillating signals. If the signals are represented by complex numbers then you simply add (or subtract) their Cartesian components.

$$z_{sum}=z+z'=(x+iy)+(x'+iy')=(x+x')+i(y+y')$$

$$z_{diff}=z-z'=(x+iy)-(x'+iy')=(x-x')+i(y-y')$$

Before adding, convert *z and z′* to Cartesian *(x,y)* form if given in polar form $z=re^{i\phi}$ and $z'=r'e^{i\phi'}$. Radius *r* of a vector *z* is its *magnitude* or *complex absolute value* |*z*|. Square $|z|^2$ is proportional to energy or *intensity*.

$$|z|=r=\sqrt{(x^2+y^2)}=\sqrt{([x-iy][x+iy])}=\sqrt{(z^*z)}$$

We write $|z|^2$ as product of *z* and its *complex conjugate* $z^*=x-iy=re^{-i\phi}$ to derive radius $|z_{sum}|$ of a vector sum z_{sum} or radius $|z_{diff}|$ of a difference z_{diff}. It is an easy way to get the well-known *cosine laws*.

$$|z_{SUM}|=\sqrt{(z+z')^*(z+z')}=\sqrt{\left(re^{i\phi}+r'e^{i\phi'}\right)^*\left(re^{i\phi}+r'e^{i\phi'}\right)}=\sqrt{\left(re^{-i\phi}+r'e^{-i\phi'}\right)\left(re^{i\phi}+r'e^{i\phi'}\right)}$$
$$=\sqrt{r^2+r'^2+rr'\left(e^{i(\phi-\phi')}+e^{-i(\phi-\phi')}\right)}=\sqrt{r^2+r'^2+2rr'\cos(\phi-\phi')} \tag{10.25a}$$

$$|z_{DIFF}|=\sqrt{(z-z')^*(z-z')}=\sqrt{r^2+r'^2-2rr'\cos(\phi-\phi')} \tag{10.25b}$$

Vector diagrams of sum, difference, and product of complex z and z' are shown in Fig. 10.6.

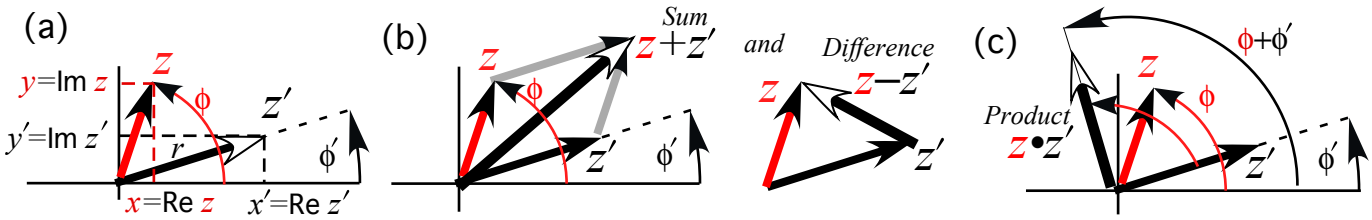

Fig. 10.6 Parallelogram diagonals are sum $z_{sum}=z+z'$ and difference $z_{diff}=z-z'$ vectors.

Complex products provide 2D rotation operations.

A product zz' of two complex numbers expressed in Cartesian form as $z = x + iy$ and $z'= x'+ iy'$ is

$$z\,z' = (x + iy)\,(x' + iy') = [xx' - yy'] + i[xy' + yx'].$$

It is simpler if the numbers are expressed in polar form as $z = r\,e^{i\phi}$ and $z' = r'\,e^{i\phi'}$.

$$z\,z' = (\,re^{i\phi}\,)(\,r'e^{i\phi'}\,) = r\,r'\,e^{i(\phi+\phi')}. \qquad (10.26)$$

Note that multiplication results in addition of exponents and a sum of polar angles. Radii multiply to give a product rr' but angles add to give a sum $(\phi+\phi')$. You might imagine z rotating vector z' by ϕ radians or that z' rotates z by ϕ' radians. Consider in detail a *rotational operator* $e^{i\phi}$ on a vector $z =(x + iy)$.

$$e^{i\phi}\cdot z = (\cos\phi + i\sin\phi)\cdot(x + iy) = x\cos\phi - y\sin\phi + i(x\sin\phi + y\cos\phi\,) \qquad (10.27a)$$

Ch. 5 *2-by-2* rotation matrix $\mathbf{R}_\phi$ (Fig. 5.3d) acts on a 2D vector $\mathbf{r}$ to give results precisely similar to $e^{i\phi}\cdot z$.

$$\mathbf{R}_{+\phi}\bullet\mathbf{r} = (x\cos\phi - y\sin\phi)\hat{\mathbf{e}}_x + (x\sin\phi + y\cos\phi)\hat{\mathbf{e}}_y \qquad (10.27b)$$

$$\begin{pmatrix}\cos\phi & -\sin\phi\\ \sin\phi & \cos\phi\end{pmatrix}\bullet\begin{pmatrix}x\\ y\end{pmatrix} = \begin{pmatrix}x\cos\phi - y\sin\phi\\ x\sin\phi + y\cos\phi\end{pmatrix} \qquad (10.27c)$$

Complex products set initial values

Phase angle $-\omega t$ of phasor $e^{-i\omega t}$ rotates clockwise with time. Multiplying $e^{-i\omega t}$ by a complex amplitude $A = |A|e^{i\rho}$ sets its phase *back* by angle ρ and its radius to $|A|$. Amplitude A is the *initial value* $x(0)=|A|e^{i\rho}$.

$$x(t)=Ae^{-i\omega t} = x(0)e^{-i\omega t} = |A|e^{i\rho}e^{-i\omega t} = |A|e^{-i(\omega t-\rho)} \qquad (10.28)$$

Such products set initial values of oscillator clocks. A positive angle ρ is a *phase lag* since it moves the phasor counter-clockwise and sets its clock back. A negative angle $\rho=-|\rho|$ gives a *phase lead*.

Complex products provide 2D "dot"(•) and "cross"(x) products.

Consider any two vectors $A=A_x+iA_y$ and $B=B_x+iB_y$ and their "star" (*)-product $A*B$.

$$\begin{aligned} A*B &= (A_x + iA_y)^*(B_x + iB_y) = (A_x - iA_y)(B_x + iB_y)\\ &= (A_xB_x + A_yB_y) + i(A_xB_y - A_yB_x) = \mathbf{A}\bullet\mathbf{B} + i\,|\,\mathbf{A}\times\mathbf{B}\,|_{Z\perp(x,y)} \end{aligned} \qquad (10.29)$$

Real part is scalar or "dot"(•) product $\mathbf{A}\bullet\mathbf{B}$. Imaginary part is vector or "cross"(×) product, but just the Z-component normal to xy-plane. To better understand this math trickery, we rewrite $A*B$ in polar form.

$$\begin{aligned} A*B &= (|A|e^{i\theta_A})^*(|B|e^{i\theta_B}) = |A|e^{-i\theta_A}|B|e^{i\theta_B} = |A||B|e^{i(\theta_B-\theta_A)}\\ &= |A||B|\cos(\theta_B-\theta_A) + i|A||B|\sin(\theta_B-\theta_A) = \mathbf{A}\bullet\mathbf{B} + i\,|\,\mathbf{A}\times\mathbf{B}\,|_{Z\perp(x,y)} \end{aligned} \qquad (10.30a)$$

This matches standard 3D definitions of dot(•) and cross(×) products in Appendix 1.A of this Unit.

$$\mathbf{A}\bullet\mathbf{B}=|A||B|\cos(\angle_A^B) \qquad |\mathbf{A}\times\mathbf{B}|=|A||B|\sin(\angle_A^B) \qquad (10.30b)$$

Expansion (10.24) of Δ-angle $a+b=\angle_A^B=\theta_B-\theta_A$ relates $re^{i\theta}$ forms (10.30) to *xy*-forms in (10.29).

$$\begin{aligned}\mathbf{A}\bullet\mathbf{B}&=|A||B|\cos(\theta_B-\theta_A) & |\mathbf{A}\times\mathbf{B}|&=|A||B|\sin(\theta_B-\theta_A)\\ &=|A|\cos\theta_A|B|\cos\theta_B+|A|\sin\theta_A|B|\sin\theta_B & &=|A|\cos\theta_A|B|\sin\theta_B-|A|\sin\theta_A|B|\cos\theta_B\\ &= A_xB_x + A_yB_y \quad (10.30c) & &= A_xB_y - A_yB_x \quad (10.30d)\end{aligned}$$

*Complex derivative contains "divergence"(∇•**F**) and "curl"(∇x**F**) of 2D vector field*

By relating *(z,z*)* to *(x=*Re*z,y=*Im*z)* we may define a *z*-derivative $\frac{df}{dz}$ and "star" *z**-derivative $\frac{df}{dz^*}$.

$$\begin{aligned}z&=x+iy & x&=\tfrac{1}{2}(z+z^*) & \frac{df}{dz}&=\frac{\partial x}{\partial z}\frac{\partial f}{\partial x}+\frac{\partial y}{\partial z}\frac{\partial f}{\partial y}=\frac{1}{2}\frac{\partial f}{\partial x}-\frac{i}{2}\frac{\partial f}{\partial y}\\ z^*&=x-iy & y&=\frac{1}{2i}(z-z^*) & \frac{df}{dz^*}&=\frac{\partial x}{\partial z^*}\frac{\partial f}{\partial x}+\frac{\partial y}{\partial z^*}\frac{\partial f}{\partial y}=\frac{1}{2}\frac{\partial f}{\partial x}+\frac{i}{2}\frac{\partial f}{\partial y}\end{aligned} \qquad (10.31)$$

Derivative chain-rule shows real part of $\frac{df}{dz}$ has 2D divergence ∇•**F** and imaginary part has curl ∇×**F**.

$$\frac{df}{dz}=\frac{d}{dz}(f_x+if_y)=\frac{1}{2}\left(\frac{\partial f}{\partial x}-i\frac{\partial f}{\partial y}\right)(f_x+if_y)=\frac{1}{2}\left(\frac{\partial f_x}{\partial x}+\frac{\partial f_y}{\partial y}\right)+\frac{i}{2}\left(\frac{\partial f_y}{\partial x}-\frac{\partial f_x}{\partial y}\right)=\frac{1}{2}\nabla\bullet\mathbf{F}+\frac{i}{2}|\nabla\times\mathbf{F}| \qquad (10.32)$$

Now we can invent *source-free 2D vector fields* that are both zero-divergence and zero-curl by taking any function *f(z)* and conjugating it (change all *i*'s to *–i*) to give *f*(z*)* for which $\frac{df^*}{dz}=0$. For example, if *f(z)=a·z* then *f*(z*)=a·z*=a(x-iy)* is not a function of *z* so it has zero *z*-derivative, hence zero ∇•**F** and zero |∇×**F**|.

F=*(F_x,F_y)=(f*_x,f*_y)=(a·x,-a·y) has zero divergence:* ∇•**F**=*0 and has zero curl:* |∇×**F**|=*0*. (10.32)

A plot of vector field **F**=*(f*_x,f*_y)* =*(a·x,-a·y)* in Fig. 10.7 shows a *divergence-free laminar (DFL)* flow field.

Complex potential ϕ *contains "scalar"(***F**=∇Φ*) and "vector"(***F**=∇x**A**) potentials*

Any DFL flow field **F** is a gradient of a *scalar potential field* Φ or a curl of a *vector potential field* **A**.

$$\mathbf{F}=\nabla\Phi \qquad \mathbf{F}=\nabla\times\mathbf{A}$$

There is a *complex potential* ϕ*(z)=*Φ*(x,y)+i*A*(x,y)* whose *z*-derivative is *f(z)* and it comes with its complex conjugate ϕ**(z*)=*Φ*(x,y)-i*A*(x,y)* whose *z**-derivative is the *f*(z*)* that we use to plot DFL flow fields **F**.

$$f(z)=\frac{d\phi}{dz} \quad (10.33a) \qquad f^*(z^*)=\frac{d\phi^*}{dz^*} \quad (10.33b)$$

Derivative $\frac{d\phi^*}{dz^*}$ by (10.31) has 2D gradient $\nabla\Phi=\begin{pmatrix}\frac{\partial\Phi}{\partial x}\\ \frac{\partial\Phi}{\partial y}\end{pmatrix}$ of scalar Φ and curl $\nabla\times\mathbf{A}=\begin{pmatrix}\frac{\partial\mathbf{A}}{\partial y}\\ -\frac{\partial\mathbf{A}}{\partial x}\end{pmatrix}$ of vector **A**.

$$\frac{d}{dz^*}\phi^*=\frac{d}{dz^*}(\Phi-i\mathbf{A})=\frac{1}{2}\left(\frac{\partial}{\partial x}+i\frac{\partial}{\partial y}\right)(\Phi-i\mathbf{A})=\frac{1}{2}\left(\frac{\partial\Phi}{\partial x}+i\frac{\partial\Phi}{\partial y}\right)+\frac{1}{2}\left(\frac{\partial\mathbf{A}}{\partial y}-i\frac{\partial\mathbf{A}}{\partial x}\right)=\frac{1}{2}\nabla\Phi+\frac{1}{2}\nabla\times\mathbf{A} \qquad (10.34)$$

Some more math trickery has "vector-**A**" be just a "*Z*-component" **A**=*A_z***e_z** *normal* to the complex *(x,y)*-plane. So **A***(x,y)=A_z(x,y)* is treated as a *single* function of *(x,y)* like scalar Φ*(x,y)*. Also, a *mathematician definition* for force field **F**=+∇Φ replaces our usual physicist's definition **F**=-∇Φ of (6.9). (No annoying *(-)*-sign now!)

To find $\phi=\Phi+iA$ we integrate $f(z)=a\cdot z$ to get ϕ and isolate real $(\mathrm{Re}\phi=\Phi)$ and imaginary $(\mathrm{Im}\phi=A)$ parts.

$$\phi = \Phi + i\ A = \int f\cdot dz = \int az\cdot dz = \tfrac{1}{2}\,az^2 = \tfrac{1}{2}\,a(x+iy)^2$$
$$= \tfrac{1}{2}\,a(x^2-y^2) + i\ axy \qquad (10.35a)$$

Note: *either* part gives the *whole* **F** field. Factors $(\frac{1}{2},\frac{1}{2})$ in (10.34) could be $(\frac{1}{3},\frac{2}{3})$ or $(\frac{1}{4},\frac{3}{4})$ or any (f,j) with $f+j=1$.

$$\nabla\Phi = \begin{pmatrix}\frac{\partial\Phi}{\partial x}\\ \frac{\partial\Phi}{\partial y}\end{pmatrix} = \begin{pmatrix}\frac{\partial}{\partial x}\frac{a}{2}(x^2-y^2)\\ \frac{\partial}{\partial y}\frac{a}{2}(x^2-y^2)\end{pmatrix} = \begin{pmatrix}ax\\ -ay\end{pmatrix} = \mathbf{F} \qquad (10.35b)$$

$$\nabla\times\mathbf{A} = \begin{pmatrix}\frac{\partial\mathbf{A}}{\partial y}\\ -\frac{\partial\mathbf{A}}{\partial x}\end{pmatrix} = \begin{pmatrix}\frac{\partial axy}{\partial y}\\ -\frac{\partial axy}{\partial x}\end{pmatrix} = \begin{pmatrix}ax\\ -ay\end{pmatrix} = \mathbf{F} \qquad (10.35c)$$

Scalar *static potential lines* $\Phi=const.$ and vector *flux potential lines* $\mathbf{A}=const.$ define a *field-net* in Fig.10.7.

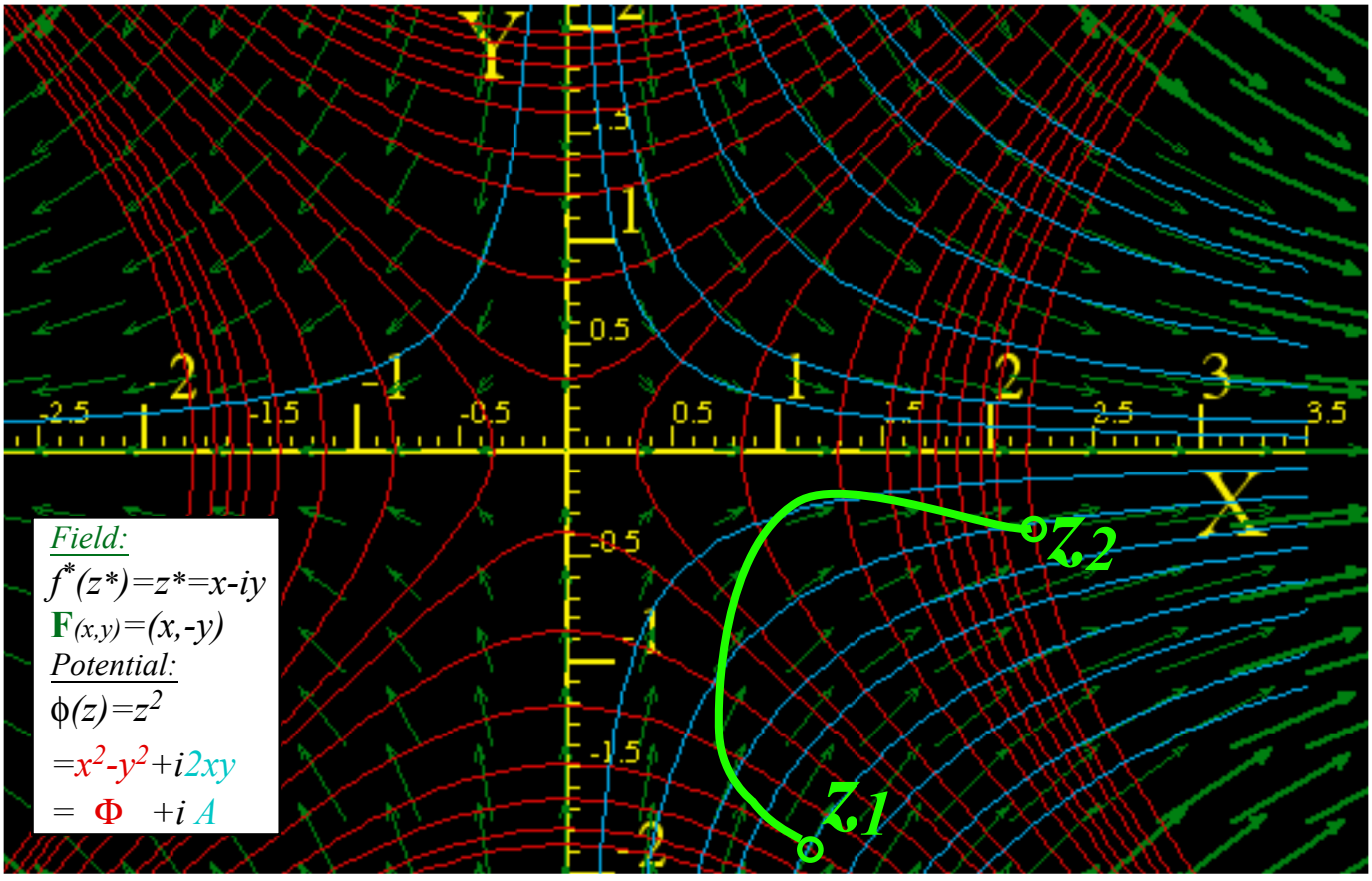

Fig.10.7 Complex field f(z)=z of **F***=(x,-y) vectors on potentials of static* $\Phi=(x^2-y^2)/2$ *and flux* $\mathbf{A}=xy$.

*Complex integrals ∫ f(z)dz count "flux"(∫***F**x**dr***) and "vorticity"(∫***F**•**dr***)*

Integral $f(z)$ (10.35a) between point z_1 and point z_2 in Fig. 10.8 is potential difference $\Delta\phi=\phi(z_2)-\phi(z_1)$ between the end-points. In DFL fields, $\Delta\phi$ is independent of the integration path $z(t)$ connecting z_1 and z_2.

$$\Delta\phi = \phi(z_2)-\phi(z_1) = \int_{z_1}^{z_2} f(z)dz = \Phi(x_2,y_2)-\Phi(x_1,y_1)+i[\mathbf{A}(x_2,y_2)-\mathbf{A}(x_1,y_1)] \qquad (10.36)$$
$$\Delta\phi = \quad \Delta\Phi \quad + i \quad \Delta\mathbf{A}$$

The real part $\Delta\Phi$ of $\Delta\phi$ is work $\int_1^2 \mathbf{F}\cdot d\mathbf{r}$ done pushing $\mathbf{r}$ *up* a hill in Fig. 10.8. (Now force $\mathbf{F}=\nabla\Phi$ points *up*-slope.) Since $\mathbf{F}=(f^*_x, f^*_y)$ is plotted using $f^*(z^*)$, we set $f(z)=(f^*(z^*))^*$ to get real and imaginary parts of $f(z)dz$.

$$\int f(z)dz = \int\left(f^*(z^*)\right)^* dz = \int\left(f^*(z^*)\right)^*\left(dx+i\,dy\right) = \int\left(f_x^*+i\,f_y^*\right)^*\left(dx+i\,dy\right) = \int\left(f_x^*-i\,f_y^*\right)\left(dx+i\,dy\right)$$

$$= \int(f_x^*dx+f_y^*dy)+i\int(f_x^*dy-f_y^*dx) \qquad (10.37)$$

$$= \int \mathbf{F}\bullet d\mathbf{r} + i\int \mathbf{F}\times d\mathbf{r}\bullet\hat{\mathbf{e}}_Z = \int \mathbf{F}\bullet d\mathbf{r} + i\int \mathbf{F}\bullet d\mathbf{r}\times\hat{\mathbf{e}}_Z$$

$$= \int \mathbf{F}\bullet d\mathbf{r} + i\int \mathbf{F}\bullet d\mathbf{S} \quad \text{where:} \quad d\mathbf{S} = d\mathbf{r}\times\hat{\mathbf{e}}_Z$$

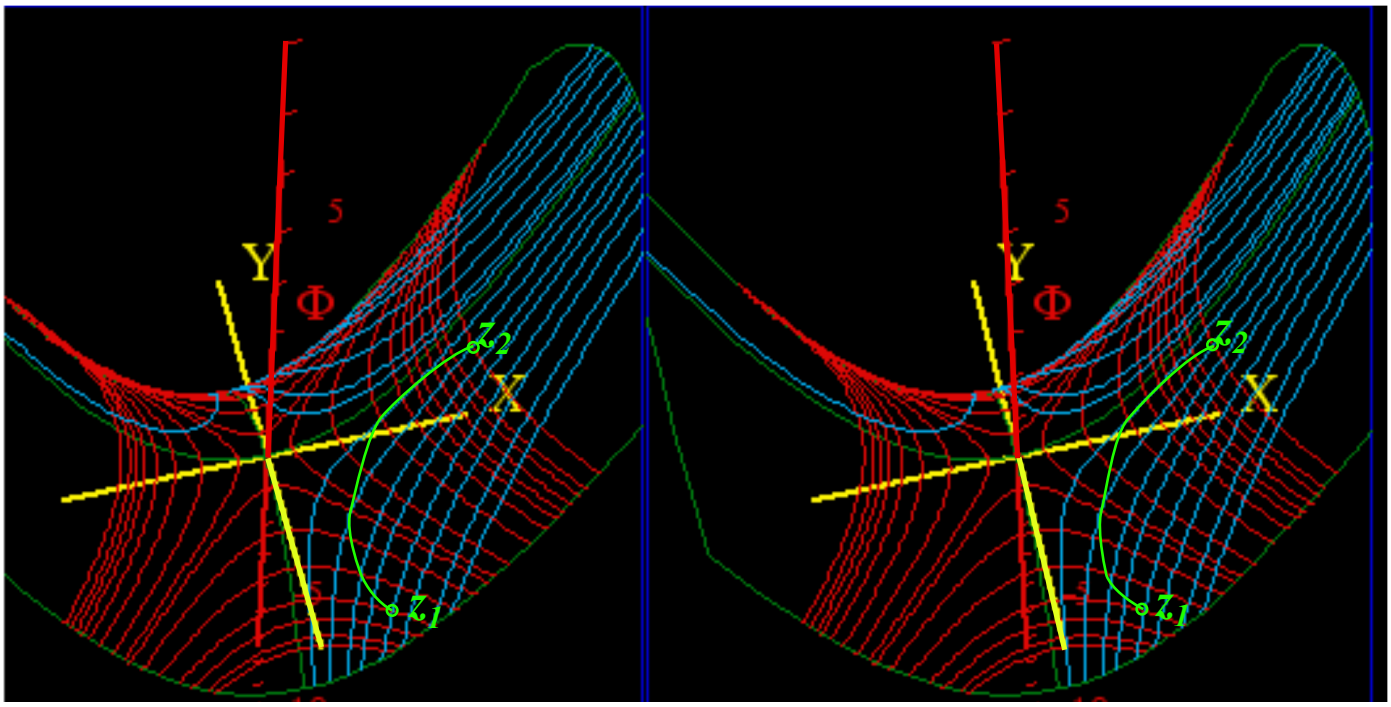

Fig. 10.8 Stereo-3D view of Fig. 10.7(ϕ(z)=z²/2) plots static potential Φ normal to xy-axes.

Real part $\int_1^2 \mathbf{F}\bullet d\mathbf{r}$ sums **F** projections *along* path vectors $d\mathbf{r}$ to get $\Delta\Phi$ in (10.36). Imaginary part $\int_1^2 \mathbf{F}\bullet d\mathbf{S} = \Delta\mathbf{A}$ sums **F** projection *across* $d\mathbf{r}$ that is, it sums *flux* thru surface elements $d\mathbf{S}=d\mathbf{r}\times\mathbf{e}_Z$ normal to $d\mathbf{r}$ to get $\Delta\mathbf{A}$.

One power-law field $f(z)=az^n$ lacks a power-law potential $\phi(z)=\frac{a}{n+1}z^{n+1}$. It is $f(z)=\frac{a}{z}=az^{-1}$. Its integral is a *logarithmic potential* $\phi(z)=a\cdot\ln(z)=a\cdot\ln(x+iy)$. (Recall (6.11).) Use $\ln(a\cdot b)=\ln(a)+\ln(b)$, $\ln(e^{i\theta})=i\theta$, and $z=re^{i\theta}$.

$$\phi(z) = \Phi + i\mathbf{A} = \int f(z)dz = \int \frac{a}{z}dz = a\ln(z) = a\ln(re^{i\theta}) = a\ln(r) + i\,a\theta \qquad (10.38)$$

Potential $a\cdot\ln(z)$ is the field of a *line of charge q* if $a=q$ is real and a *line of current J* if $a=iJ$ is imaginary. Fig. 10.9a is a diverging **F**-field of unit charge ($q=1$) and Fig. 10.9b is a curling **F**-field of unit current ($J=1$). Line charge **F**-field is like an *electric* **E**-field. Line current **F**-field is like a *magnetic* **B**-field of a wire, a *vortex*.

F-field and radial streamlines (**A**=θ =*const.*) diverge normal to equal-Φ circles *(*Φ=*r* =*const.)* in Fig. a. **F**-field and circular streamlines (**A**=*r* =*const.*) curl clockwise normal to radial equal-Φ lines *(*Φ=θ =*const.)* in Fig. b. (The clockwise *(-i)*-sense of rotation results from plotting $f^*(z^*)=-i/z^*$ as our *(*)*-convention requires.)

Stereo-3D potential plots of real-line-source field shown in Fig. 10.10a show mathematical structure of its Φ and **A** potentials that lets us compare them to imaginary-line-source potentials in Fig. 10.10b. Real

part Φ=ln*(r)* of (10.38) for real *(a=1)*-source in Fig10.10a is a surface like a *morning-glory*. Blue-(A=θ=*const.*) -streamlines stream down its throat normal to *(Φ=r =const.)* level circles.

(a) Unit Z-line-flux field f(z)=1/z *(b) Unit Z-line-vortex field f(z)=i/z*

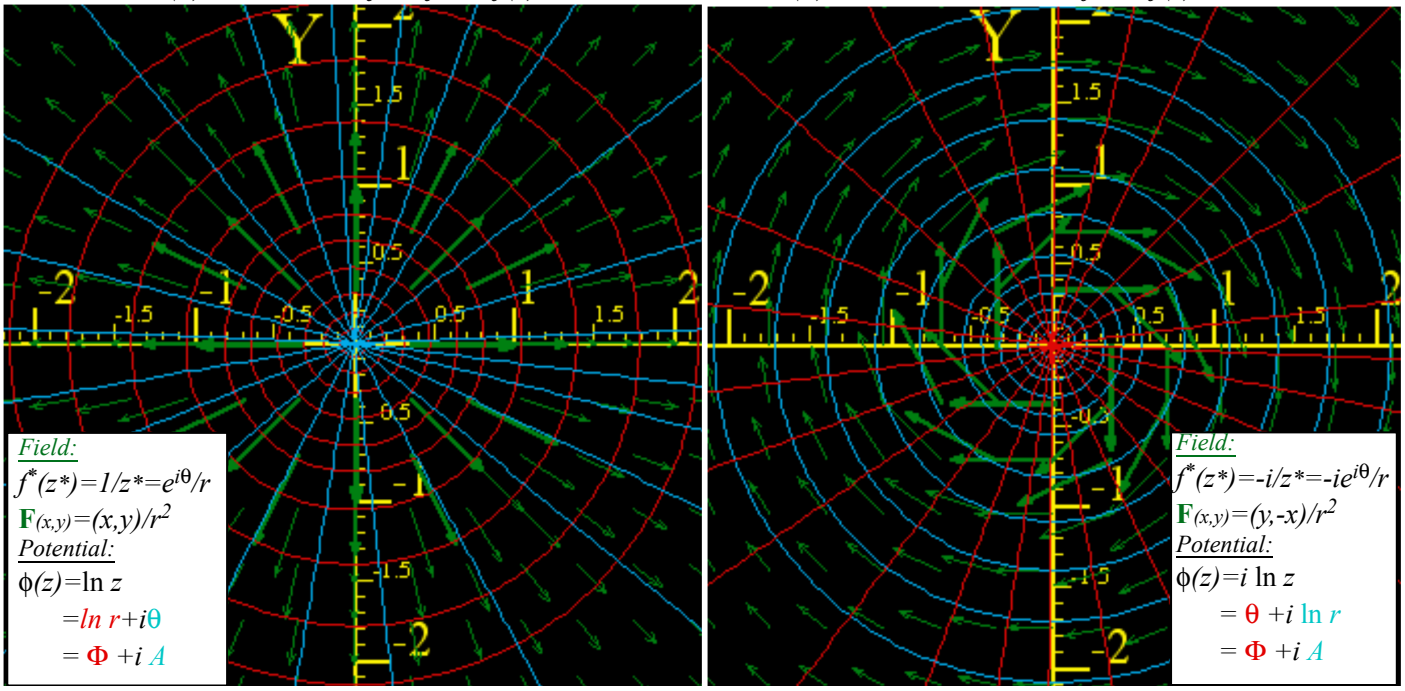

Fig. 10.9 Fields due to a unit Z-line-source normal to center. (a) Real source a=q=1. (b) Imaginary a=iJ=i.

Below that Φ-*vs*-*(x,y)*-plot is a 3D A-*vs*-*(x,y)*-plot for the same real source in Fig. 10.10a. Imaginary part A=θ of (10.38) gives radial steps that are level lines of a single helix or *helicoid*. Red-*(Φ=r =const.)*-lines stream up its spiral staircase normal to *(A=θ=const.)* steps. At the top step A=θ=π , above the –X-axis, is a "waterfall" of red lines falling by ΔA=2π straight to bottom helical step A=θ=-π. This 2π*i*-fall of complex potential φ*(z)* by Δφ=*i*ΔA=2π*i* at θ=±π equals the *loop integral* of *f(z)* from θ=-π to θ=+π.

$$\Delta\phi = i\Delta\mathbf{A} = \oint f(z)dz = \oint \frac{dz}{z} = 2\pi i \qquad (10.39)$$

Imaginary part ΔA of a loop integral counts real source (*"flux"*) since loop flux is $\mathrm{Im}\oint f(z)dz$ in (10.37). Real part $\Delta\Phi = \mathrm{Re}\oint f(z)dz = \oint \mathbf{F}\cdot d\mathbf{r}$ counts imaginary source (*"vorticity"*) since only that makes work around a loop, that is, *perpetual motion*! In Fig. 10.10b, Φ and A switch roles to make imaginary-line-source-potentials.

(a) Unit Z-line-flux field f(z)=1/z

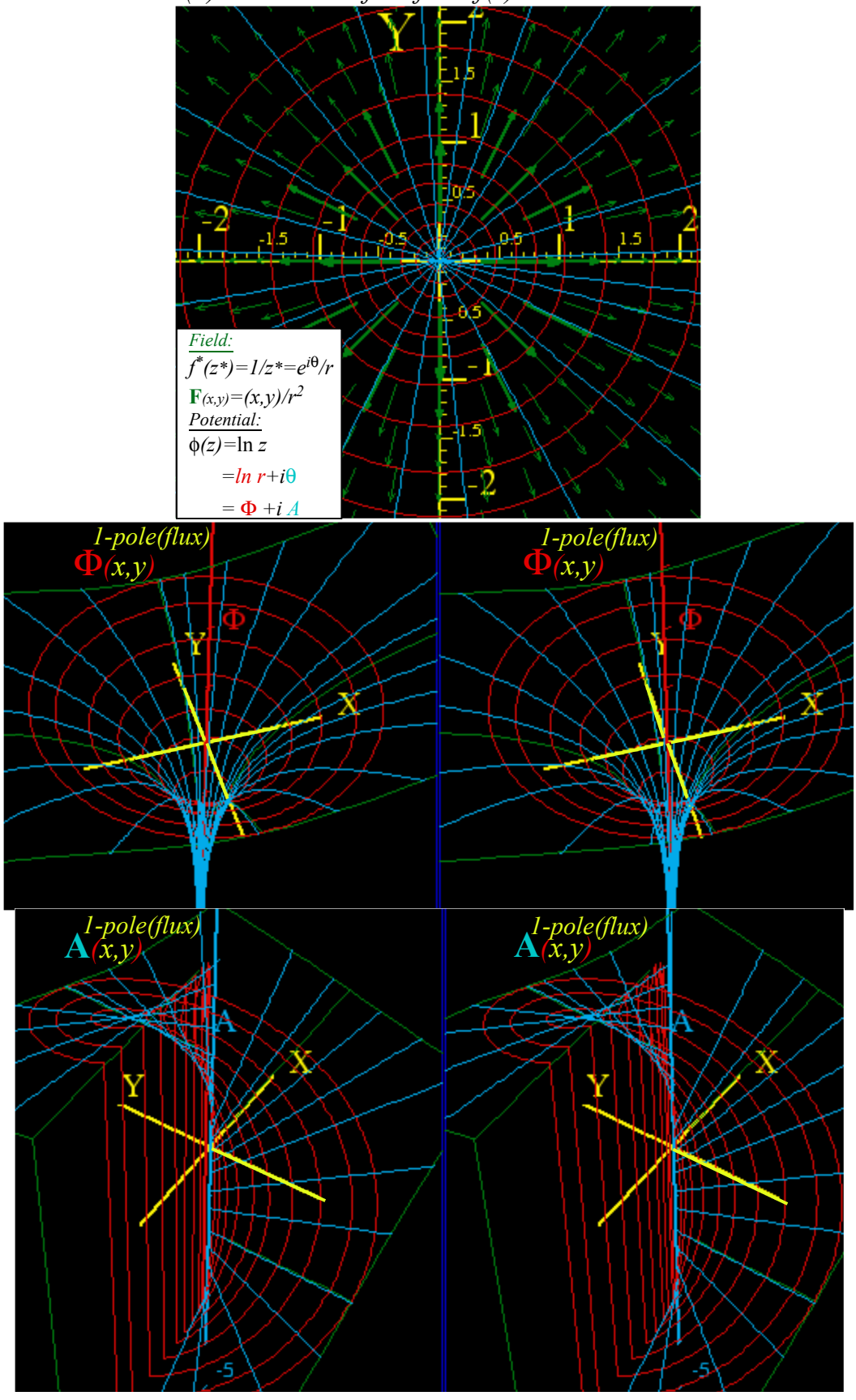

Fig. 10.10(a) Real unit line-source (a=1) with diverging **F***-field resembling* **E***-field of electric line-charge.*

(b) Unit Z-line-vortex field f(z)=i/z

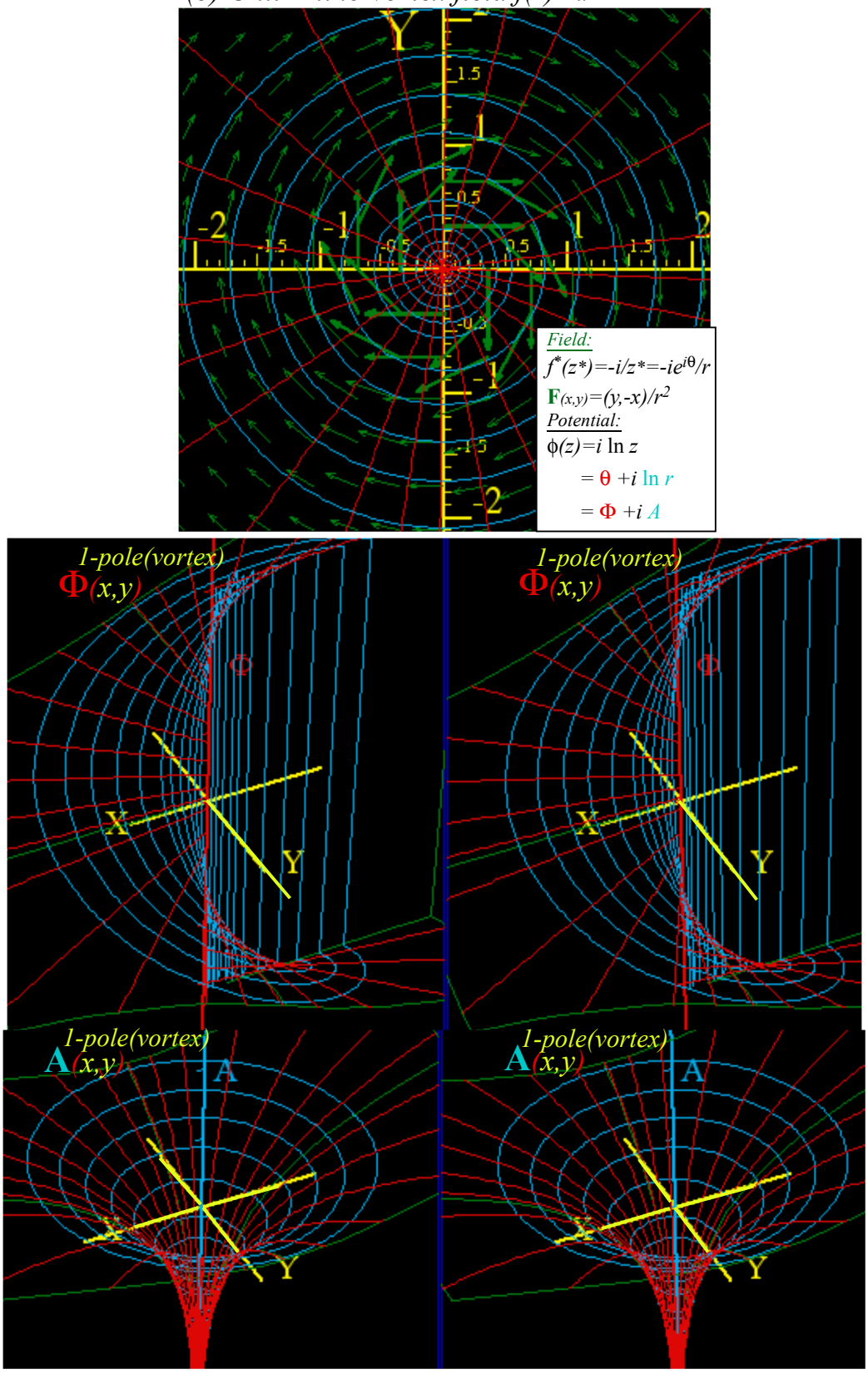

*Fig. 10.10(b) Imaginary line-source (a=i) with curling **F**-field resembling **B**-field of electric line-current.*

Complex derivatives give 2D multipole fields

Of all integer-power-law field functions $f(z)=z^n$ of z, only $a/z=az^{-1}$ has a non-power-law multi-valued integral and potential $\phi(z)=\int az^{-1}dz=a\ln z$ (10.38) and non-zero flux-work-loop integral $\oint az^{-1}dz=2\pi ia$ (10.39). This $f(z)=az^{-1}$ is a 2D line *monopole field* and $\phi(z)=a\ln z$ is its *monopole potential* of source strength a.

$$f^{1\text{-}pole}(z)=\frac{a}{z}=\frac{d\phi^{1\text{-}pole}}{dz} \qquad (10.40a) \qquad \phi^{1\text{-}pole}(z)=a\ln z \qquad (10.40b)$$

Now let these two line-sources of equal but opposite source constants $+a$ and $-a$ be located at $z=\pm\Delta/2$ thus separated by a small interval Δ. This sum (actually difference) of $f^{1\text{-}pole}$-fields is called a *dipole field*.

$$f^{dipole}(z)=\frac{a}{z+\frac{\Delta}{2}}-\frac{a}{z-\frac{\Delta}{2}}=\frac{-a\cdot\Delta}{z^2-\frac{\Delta^2}{4}} \qquad \phi^{dipole}(z)=a\ln(z-\tfrac{\Delta}{2})-a\ln(z+\tfrac{\Delta}{2})=a\ln\frac{z-\frac{\Delta}{2}}{z+\frac{\Delta}{2}}$$

If interval Δ is *tiny* and is divided out we get a *point-dipole field* $f^{2\text{-}pole}$ that is the z-derivative of $f^{1\text{-}pole}$.

$$f^{2\text{-}pole}=\frac{-a}{z^2}=\frac{df^{1\text{-}pole}}{dz}=\frac{d\phi^{2\text{-}pole}}{dz} \quad (10.\,41a) \qquad \phi^{2\text{-}pole}=\frac{a}{z}=\frac{d\phi^{1\text{-}pole}}{dz} \qquad (10.\,41b)$$

A *point-dipole potential* $\phi^{2\text{-}pole}$ (whose z-derivative is $f^{2\text{-}pole}$) is a z-derivative of $\phi^{1\text{-}pole}$. Pair (10. 41) looks like a Coulomb force (9.1) and potential (9.2) of 3D point monopoles. However, 2D dipole field (10. 41a) is quite different as is 2D potential (10. 41b) whose Φ=*const.* and $\mathbf{A}$=*const.* lines make a circle-net in Fig. 10.11.

$$\phi^{2\text{-}pole}=\frac{a}{z}=\frac{a}{x+iy}=\frac{a}{x+iy}\frac{x-iy}{x-iy}=\frac{ax}{x^2+y^2}+i\frac{-ay}{x^2+y^2}=\frac{a}{r}\cos\theta-i\frac{a}{r}\sin\theta \qquad (10.42)$$
$$=\Phi^{2\text{-}pole}+i\,\mathbf{A}^{2\text{-}pole}$$

(Note that complex $z=x+iy$ is cleared from the denominator by using $z^*=x-iy$ to give real $r^2=z^*z=x^2+y^2$.)

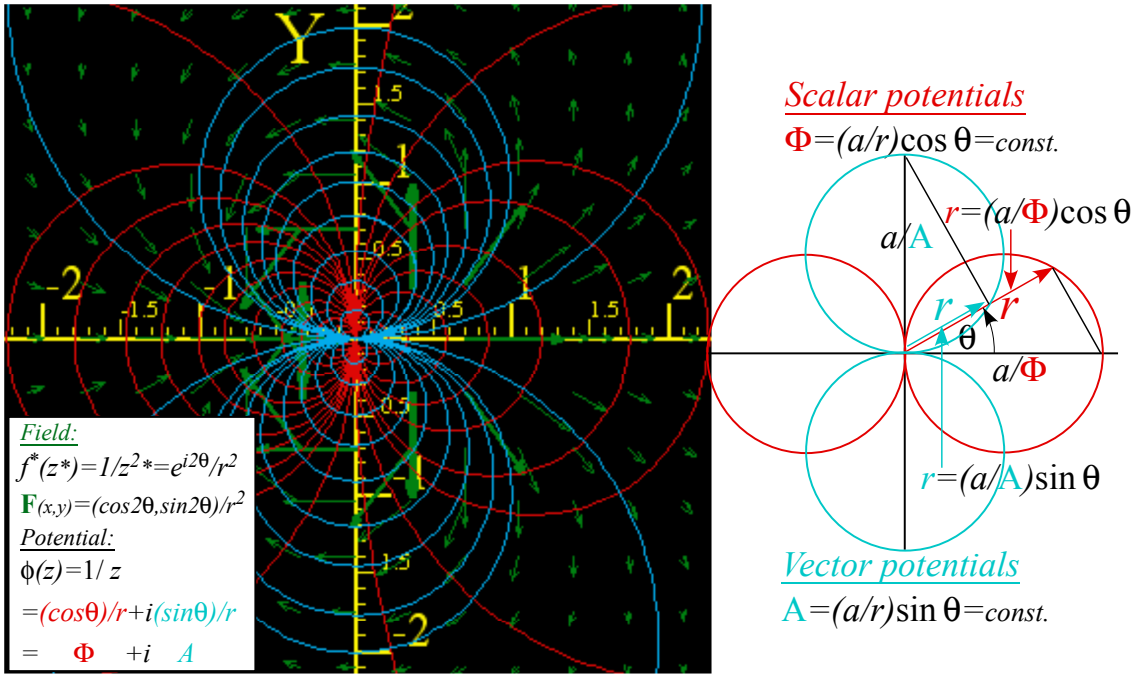

Fig. 10.11 Dipole **F***-field* $f(z)=1/z^2$ *and scalar potential (*Φ*=const.)-circles orthogonal to (*$\mathbf{A}$*=const.)-circles.*

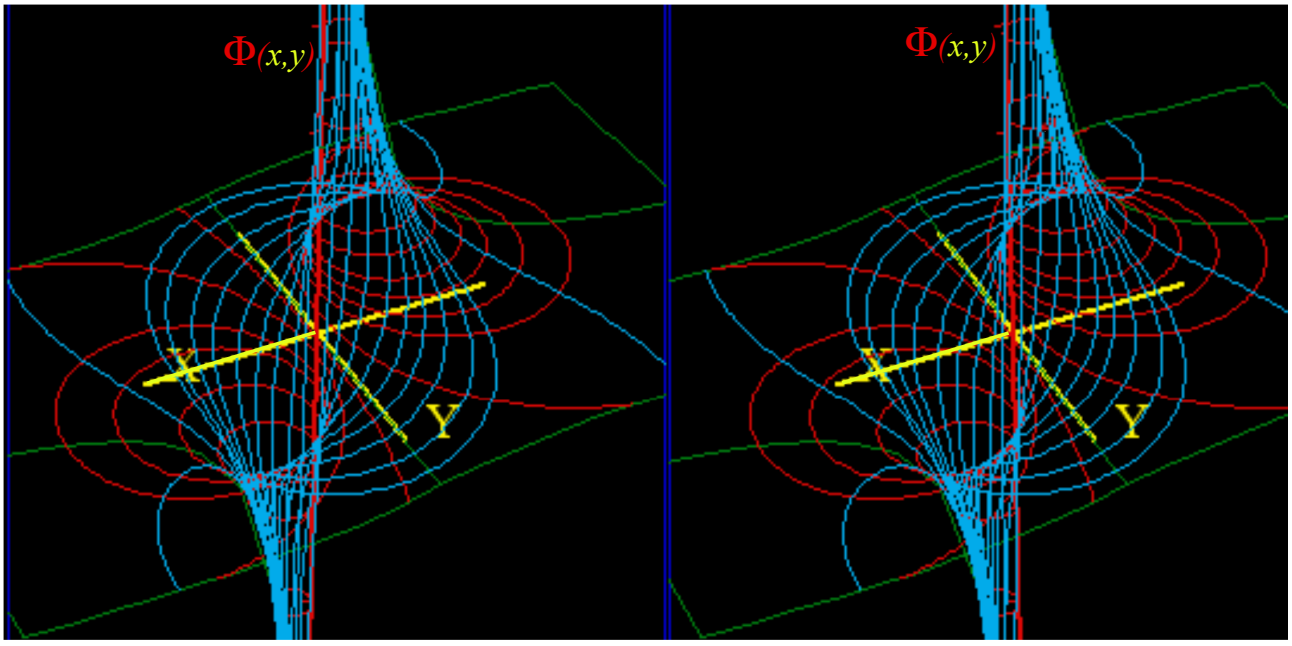

Fig. 10.12 Stereo 3D plot of dipole ϕ(z)=1/z scalar potential Φ(x,y) with A-streamlines between poles.

Complex power series are 2D multipole expansions

A *z*-derivative turns *1-pole* fields into *2-pole* fields in (10. 41). It makes a copy of *1-pole* in (10. 40) with a sign change and puts the *(-)*copy *very* near the original. What if we put a *(-)*copy of a *2-pole* near its original? Well, the result is *4-pole* or *quadrupole* field $f^{4\text{-}pole}$ and potential $\phi^{4\text{-}pole}$, each a *z*-derivative of $f^{2\text{-}pole}$ and $\phi^{2\text{-}pole}$.

$$f^{4\text{-}pole} = \frac{a}{z^3} = \frac{1}{2}\frac{df^{2\text{-}pole}}{dz} = \frac{d\phi^{4\text{-}pole}}{dz} \quad (10.43a) \qquad \phi^{4\text{-}pole} = -\frac{a}{2z^2} = \frac{1}{2}\frac{d\phi^{2\text{-}pole}}{dz} \quad (10.43b)$$

Fig. 10.13 shows *4-pole* structure. Two +∞-poles loom above Y-axis and two -∞-poles lurk below X-axis . The **F**-field vectors and their **A**-streamlines are shown running at 90° to **Φ**-equipotential lines in Fig. 10.13.

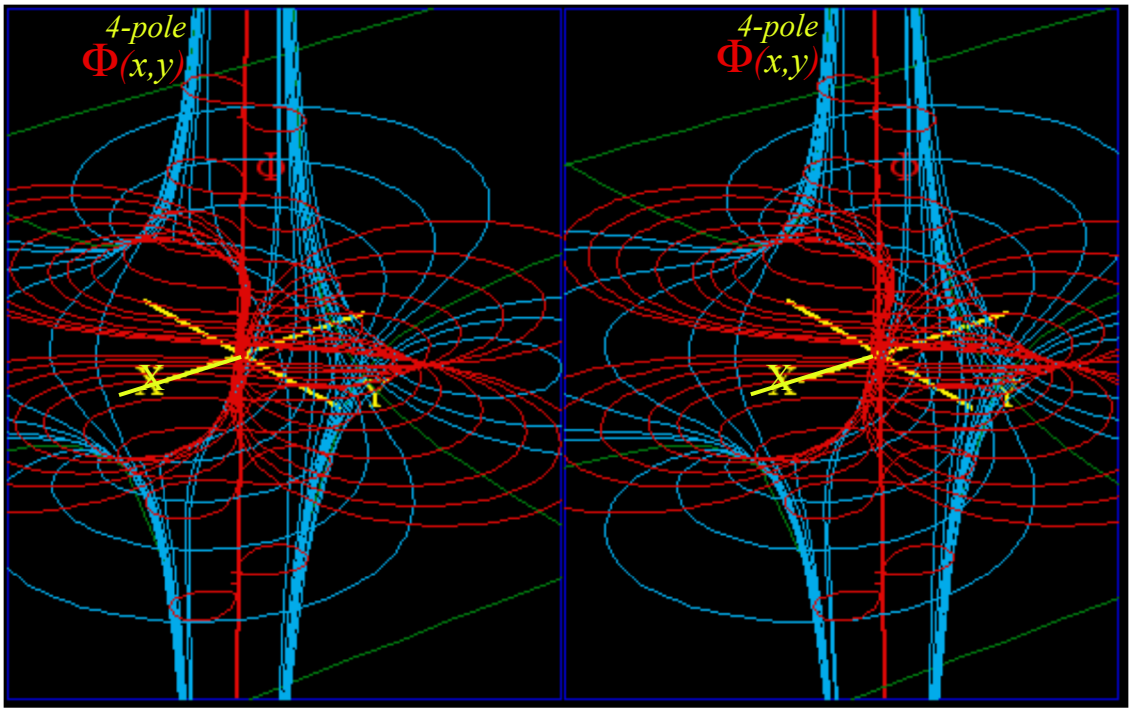

Fig. 10.13 Stereo 3D plot of quadrupole $\phi(z)=1/z^2$ scalar potential $\Phi(x,y)$ with A-streamlines between poles.

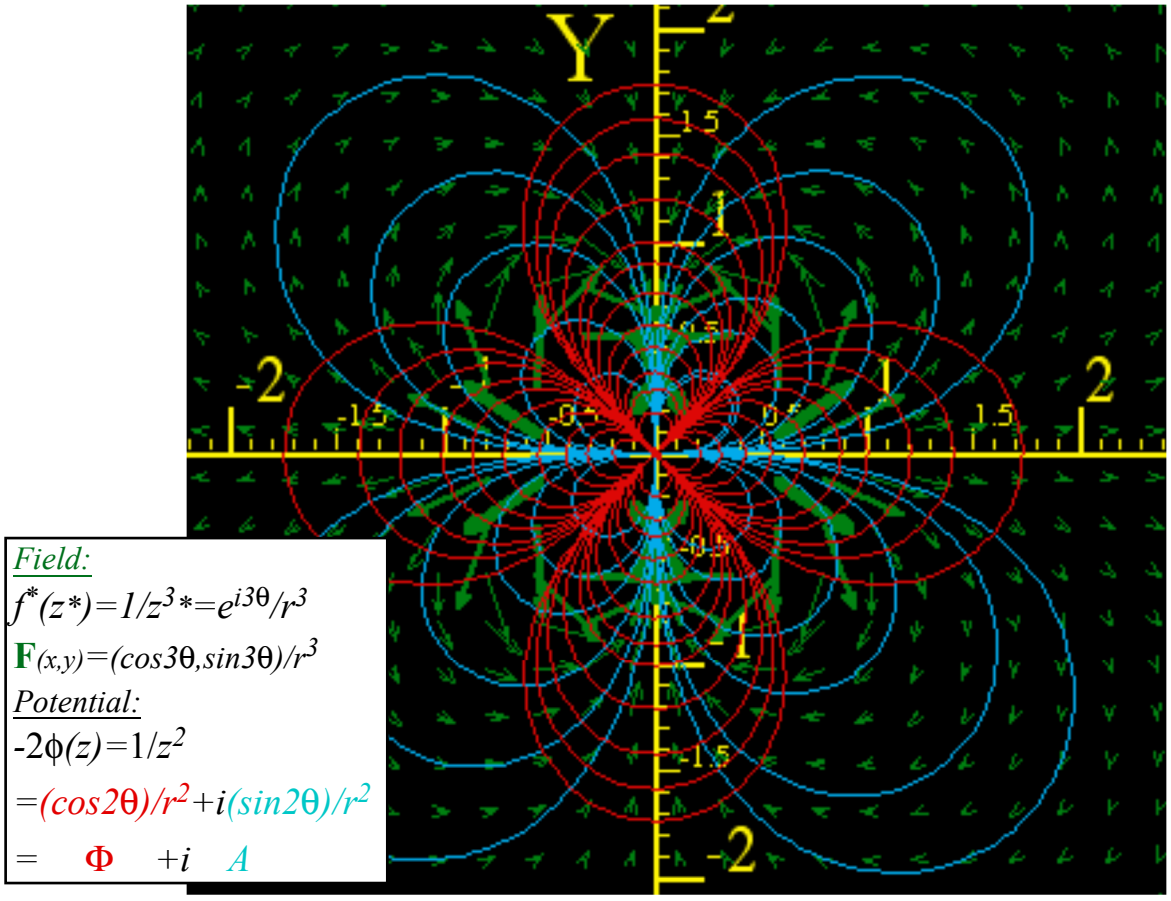

*Fig. 10.14 **F**-field $f(z)=1/z^3$ of 4-pole with scalar (Φ=const.)-equipotentials normal to (A=const.)-streamlines.*

A field $f(z)$ with sources only at origin $(z=0)$ or at infinity $(z=\infty)$ may be given by power series that generalize Maclaurin series derived in (10.11) by using both positive and negative powers $z^{\pm n}$. Series $\Sigma a_{\pm n} z^{\pm n}$ is called a *Laurent series* or *multipole expansion* (10.44) of a given complex field function $f(z)$ around $z=0$. All field terms $a_{m-1}z^{m-1}$ except *1-pole* $\frac{a_{-1}}{z}$ have potential term $a_{m-1}z^m/m$ of a 2^m-*pole* at $z=0$ $(z=\infty)$ for $m<0$ $(m>0)$.

$$\begin{aligned} f(z) &= \ldots a_{-3}z^{-3} + a_{-2}z^{-2} + a_{-1}z^{-1} + a_0 + a_1 z + a_2 z^2 + a_3 z^3 + a_4 z^4 + a_5 z^5 + \ldots \\ &\quad \cdots\ 2^2\text{-pole} \quad 2^1\text{-pole} \quad 2^0\text{-pole} \quad 2^1\text{-pole} \quad 2^2\text{-pole} \quad 2^3\text{-pole} \quad 2^4\text{-pole} \quad 2^5\text{-pole} \quad 2^6\text{-pole} \cdots \\ &\quad\ \text{at } z=0 \quad \text{at } z=0 \quad \text{at } z=0 \quad \text{at } z=\infty \quad \text{at } z=\infty \quad \text{at } z=\infty \quad \text{at } z=\infty \quad \text{at } z=\infty \quad \text{at } z=\infty \\ \phi(z) &= \ldots \frac{a_{-3}}{-2} z^{-2} + \frac{a_{-2}}{-1} z^{-1} + a_{-1}\ln z + a_0 z + \frac{a_1}{2} z^2 + \frac{a_2}{3} z^3 + \frac{a_3}{4} z^4 + \frac{a_4}{5} z^5 + \frac{a_5}{6} z^6 + \ldots \end{aligned} \tag{10.44}$$

The unique *1-pole*(2^0-*pole*)$\tilde{\phi}$term $a_{-1}\ln z$ is *not* a constant $a_{-1}z^0=a_{-1}$. (Constant$\tilde{\phi}$ has no field: $f=\frac{d\phi}{dz}=\frac{da}{dz}^{-1}=0$) Also a *1-pole* at $z=\infty$ gives zero field near $z=0$. However, a 2^1-*pole* at $z=\infty$ gives a constant field $f(z)=a_0$ near $z=0$. A quadrupole $(2^2$-*pole*$)$ at $z=\infty$ gives the linear field $f(z)=a_1 z$ shown if Fig. 10.7, but a 2^2-*pole* at $z=0$ gives the field $a_{-3}z^{-3}$ in Fig. 10.14. Octupoles $(2^3$-*poles*$)$ at $z=\infty$ (or $z=0$) give $a_2 z^2$ (or $a_{-4}z^{-4}$), and so on for $m=4,5,\ldots$

Complex 1/z gives stereographic projection

The potential $\tilde{\phi}$expansion is most useful for revealing multi-pole structure. A negative power $\tilde{\phi}$term $a_{-m-1}z^{-m}/m$ belongs to a 2^m-*pole* at $z=0$. A positive power $\tilde{\phi}$term $a_{m-1}z^m/m$ belong to a 2^m-*pole* at $z=\infty$. Pole field geometry involves mapping z-points onto a sphere so $z=0$ is its North Pole and $z=\infty$ is its South Pole in Fig. 10.15. There a *stereographic projection* maps a point $z=x+iy$ on the *z-plane* tangent to North Pole into a point $w=1/z=u+iv$ in the inverse *w-plane* tangent to the South Pole. The map geometry uses an inscribed rectangle. A pair of red unit circles $|z|=1$ and $|w|=1$ map into each other. Any point z inside the $|z|=1$ circle maps into a point w outside the $|w|=1$ circle as shown and *vice-versa* outside z maps to inside w.

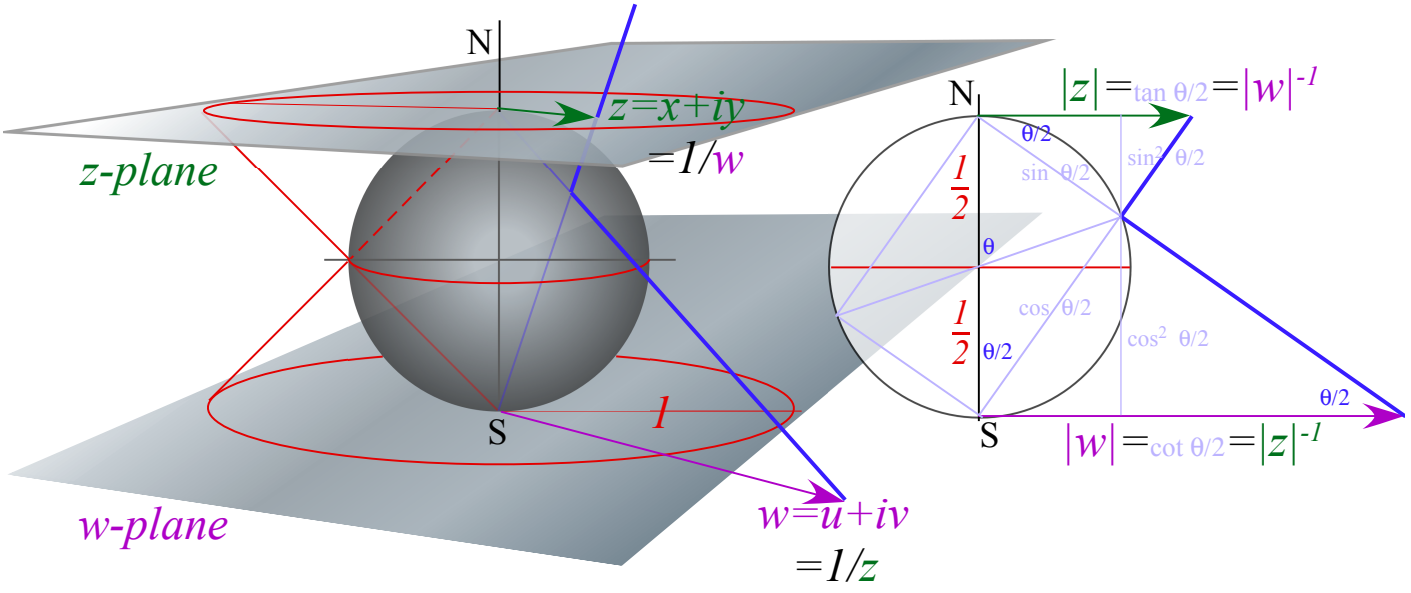

Fig. 10.15 Stereographic projection of z-plane through a unit-diameter sphere to inverse 1/z=w-plane.

Replacing z with $w=z^{-1}$ in (10.13) switches positive multi-pole-m terms in potential ϕ with negative ones.

$$\phi(z) = \ldots \frac{a_{-3}}{-2} z^{-2} + \frac{a_{-3}}{-2} z^{-2} + \frac{a_{-2}}{-1} z^{-1} + a_{-1} \ln z + a_0 z + \frac{a_1}{2} z^2 + \frac{a_2}{3} z^3 + \ldots \text{ (from (10.44))}$$

$$\phi(w) = \ldots \frac{a_{-3}}{-2} w^{-2} + \frac{a_{-3}}{-2} w^{-2} + \frac{a_{-2}}{-1} w^{-1} + a_{-1} \ln w + a_0 w + \frac{a_1}{2} w^2 + \frac{a_2}{3} w^3 + \ldots \text{(with } z=w^{-1}\text{)}$$

$$= \ldots \frac{a_2}{3} z^{-2} + \frac{a_1}{2} z^{-2} + a_0 z^{-1} - a_{-1} \ln z + \frac{a_{-2}}{-1} z + \frac{a_{-3}}{-2} z^2 + \frac{a_{-3}}{-2} z^3 + \ldots \text{(with } w=z^{-1}\text{)}$$

But, the unique monopole source term stays put with only a sign change ($\ln \frac{1}{z} = -\ln z$) as seen in Fig. 10.16a.

Constant field $f=a_0$ in (10.44) appears if there is a dipole at the South Pole and, *vice-versa*, a dipole field at the North Pole appears to be a constant field near the South Pole as seen in Fig. 10.16b.

Of all 2^m*-pole* field terms $a_{m-1}z^{m-1}$, only the $m=0$ monopole $a_{-1}z^{-1}$ has a non-zero loop integral (10.39).

$$\oint f(z)dz = \oint a_{-1} z^{-1} dz = 2\pi i a_{-1} \qquad a_{-1} = \frac{1}{2\pi i} \oint f(z)dz$$

This $m=1$*-pole* constant-a_{-1} formula is just the first in a series of Laurent coefficient expressions.

$$\cdots a_{-3} = \frac{1}{2\pi i} \oint z^2 f(z)dz \;,\; a_{-2} = \frac{1}{2\pi i} \oint z^1 f(z)dz \;,\; a_{-1} = \frac{1}{2\pi i} \oint f(z)dz \;,\; a_0 = \frac{1}{2\pi i} \oint \frac{f(z)}{z} dz \;,\; a_1 = \frac{1}{2\pi i} \oint \frac{f(z)}{z^2} dz \;,\cdots$$

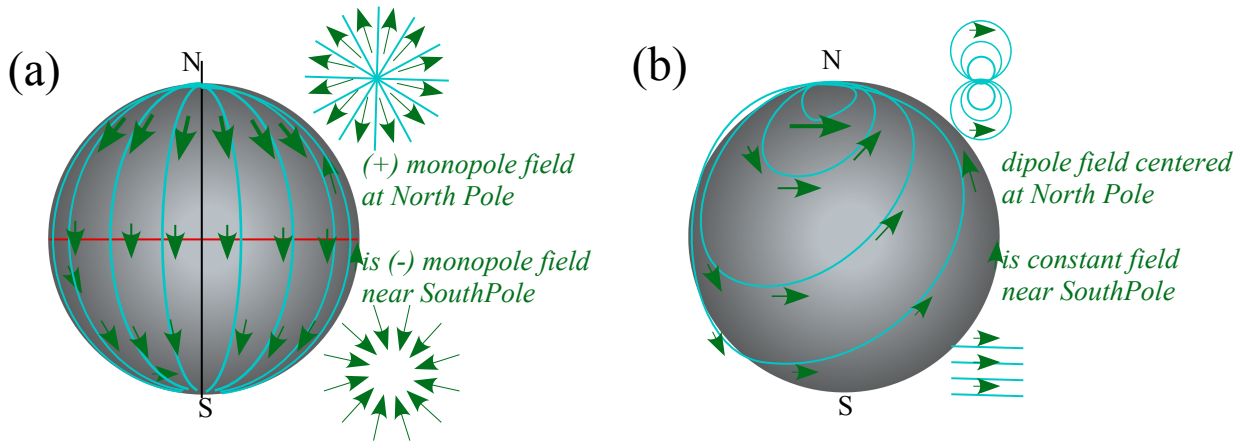

Fig. 10.16 Projective sphere view of North Pole (z=0) sources. (a) monopole (b) dipole.

Cauchy integrals

Source analysis starts with 1-pole loop integrals $\oint z^{-1}dz = 2\pi i$ or, with origin shifted $\oint (z-a)^{-1}dz = 2\pi i$.

They hold for any loop around point-*a*. A continuous function *f(z)* is just *f(a)* on a *tiny* circle around point-*a*.

$$\oint \frac{f(z)}{z-a}dz = \oint \frac{f(a)}{z-a}dz = f(a)\oint \frac{1}{z-a}dz = 2\pi i f(a) \quad (10.45a) \qquad f(a) = \frac{1}{2\pi i}\oint \frac{f(z)}{z-a}dz \quad (10.45b)$$

The *f(a)* result is called a *Cauchy integral*. Then repeated *a*-derivatives gives a sequence of them.

$$\frac{df(a)}{da} = \frac{1}{2\pi i}\oint \frac{f(z)}{(z-a)^2}dz\ ,\ \frac{d^2f(a)}{da^2} = \frac{2}{2\pi i}\oint \frac{f(z)}{(z-a)^3}dz\ ,\ \frac{d^3f(a)}{da^3} = \frac{3!}{2\pi i}\oint \frac{f(z)}{(z-a)^4}dz,\ \cdots, \frac{d^nf(a)}{da^n} = \frac{n!}{2\pi i}\oint \frac{f(z)}{(z-a)^{n+1}}dz$$

This leads to a general *Taylor-Laurent* power series expansion of function *f(z)* around point-*a*.

$$f(z) = \sum_{n=-\infty}^{\infty} a_n (z-a)^n \qquad where:\ a_n = \frac{1}{2\pi i}\oint \frac{f(z)}{(z-a)^{n+1}}dz \left(= \frac{1}{n!}\frac{d^nf(a)}{da^n} \quad for:\ n \ge 0 \right) \quad (10.45c)$$

If the function *f(z)* has no poles inside the contour then only positive powers *n>0* are needed in its expansion and the series above reduces to a Taylor series or (if *a=0*) a Maclaurin series like (10.12) derived previously. There the n^{th} expansion coefficient a_n is given by n^{th} derivative of *f(z)* as in (10.45c) above. Otherwise, negative powers are needed with coefficients given by n^{th} order pole loop integrals above.

This represents just a "tip of an iceberg" for an enormous subject of complex analysis. We shall use only tiny portions of this grand mathematical subject, and later we will consider generalizations of complex numbers to hyper-complex *quaternions* and *spinor* operators in Unit 4. This takes the analysis from a 2D framework into a 3D and 4D description that is more like the space-time we seem to live in.

Non-analytic fields: Source distributions

What kind of field do you get if there is a continuous distribution of charge or current sources? Such a field is described by non-analytic functions of z and z^*. Each field may have a non-analytic complex *potential function* $\phi(z,z^*)=\Phi(x,y)+iA(x,y)$, a non-analytic *force field function* $f(z,z^*) = f_x(x,y) + if_y(x,y)$, and a non-analytic *source function* $s(z,z^*) = \rho(x,y) + i\, I(x,y)$. The source function is a new concept which we have avoided since analytic fields are source-free except at singularities. The following source definitions are made to generalize the **f*** field equations (10.33) based on relations (10.31) and (10.32).

$$2\frac{df^*}{dz} = s^*(z,z^*) \qquad (10.46a) \qquad\qquad 2\frac{df}{dz^*} = s(z,z^*) \qquad (10.46b)$$

The complex field equations for the potentials are like (10.33) given before but with an extra factor of *2*.

$$2\frac{d\phi}{dz} = f(z,z^*) \qquad (10.47a) \qquad\qquad 2\frac{d\phi^*}{dz^*} = f^*(z,z^*) \qquad (10.47b)$$

Source equations (10.46) expand like (10.32) into a real and imaginary parts of divergence and curl terms.

$$s^*(z,z^*) = 2\frac{df^*}{dz} = \left[\frac{\partial}{\partial x} - i\frac{\partial}{\partial y}\right]\left[f_x^*(x,y)+if_y^*(x,y)\right] = \rho - i\,I\,, \quad \text{where: } f_x^* = f_x\,, \text{ and: } f_y^* = -f_y \qquad (10.48a)$$

$$= \left[\frac{\partial f_x^*}{\partial x} + \frac{\partial f_y^*}{\partial y}\right] + i\left[\frac{\partial f_y^*}{\partial x} - \frac{\partial f_x^*}{\partial y}\right] = \left[\nabla \bullet \mathbf{f}^*\right] + i\left[\nabla \times \mathbf{f}^*\right]_Z \qquad (10.48b)$$

The real part is a *Poisson* equation. The imaginary part is a *Biot-Savart* equation.

$$\nabla \bullet \mathbf{f}^* = \rho \qquad (10.48c) \qquad\qquad \nabla \times \mathbf{f}^* = -I \qquad (10.48d)$$

One describes a *scalar source* or *charge density* ρ and the second one describes a *vector source* or *current density I*. For analytic fields the sources are concentrated into singular points. Non-analytic quantities allow for sources that are spread out into continuous 2-D distributions.

The field equations (10.47) also expand into real and imaginary parts that are x and y components of vector gradient of Φ and curl of A_Z based on potential $\phi = \Phi + iA$ or $\phi^* = \Phi - iA$. Here we treat $\mathbf{A}_Z = A_Z\mathbf{e}_Z$ as a vector function of x and y normal to the complex (x,y) plane.

$$f^*(z,z^*) = 2\frac{d\phi^*}{dz^*} = \left[\frac{\partial}{\partial x} + i\frac{\partial}{\partial y}\right](\Phi - iA) = f_x^* + if_y^* \qquad (10.49a)$$

$$= \left[\frac{\partial \Phi}{\partial x} + i\frac{\partial \Phi}{\partial y}\right] + \left[\frac{\partial A}{\partial y} - i\frac{\partial A}{\partial x}\right] = \left[\nabla\Phi\right] + \left[\nabla \times \mathbf{A}_Z\right] \qquad (10.49b)$$

If the source function is non-zero then vector field **f*** may have two distinct parts, a gradient of a scalar potential called the *longitudinal field* $\mathbf{f}_\mathbf{L}^*$ and a curl of a vector potential called the *transverse field* $\mathbf{f}_\mathbf{T}^*$.

$$\mathbf{f}^* = \mathbf{f}_\mathbf{L}^* + \mathbf{f}_\mathbf{T}^* \qquad (10.50a) \qquad \mathbf{f}_\mathbf{L}^* = \nabla\Phi \qquad (10.50b) \qquad \mathbf{f}_\mathbf{T}^* = \nabla \times \mathbf{A} \qquad (10.50c)$$

For source-free analytic functions these two fields are identical. (Recall that (10.35b) equals (10.35c).) There it seems redundant to have potentials Φ and A give the same field. Here they may give quite different fields. Consider a non-analytic field $f(z) = (z^*)^2$ or $f^*(z) = z^2$. By (10.47) the source function is as follows.

$$s^*(z,z^*) = 2\frac{df^*}{dz} = 4z = 4x + i4y, \qquad (10.51)$$
$$or: \quad \rho = 4x, \quad and: \quad I = -4y.$$

The non-analytic potential function follows by integrating (10.47a) to give (10.49).

$$\phi(z,z^*)=\frac{1}{2}\int f(z)\,dz=\frac{1}{2}\int (z^*)^2\,dz=\frac{z(z^*)^2}{2}=\frac{(x+iy)(x^2-y^2-i2xy)}{2},$$
$$or:\quad \Phi=\frac{x^3+xy^2}{2},\quad and:\ A=\frac{-y^3-yx^2}{2}. \tag{10.52}$$

The longitudinal field $\mathbf{f}_\mathbf{L}^*$ is quite different from the transverse field $\mathbf{f}_\mathbf{T}^*$.

$$\mathbf{f}_\mathbf{L}^*=\nabla\Phi=\nabla\left(\frac{x^3+xy^2}{2}\right)=\begin{pmatrix}\frac{3x^2+y^2}{2}\\ xy\end{pmatrix},\quad \mathbf{f}_\mathbf{T}^*=\nabla\times\mathbf{A}=\nabla\times\left(\frac{-y^3-yx^2}{2}\mathbf{e_z}\right)=\begin{pmatrix}\frac{\partial A}{\partial y}\\ -\frac{\partial A}{\partial x}\end{pmatrix}=\begin{pmatrix}\frac{-3y^2-x^2}{2}\\ xy\end{pmatrix}. \tag{10.53}$$

The longitudinal field $\mathbf{f}_\mathbf{L}^*$ has no curl and the transverse field $\mathbf{f}_\mathbf{T}^*$ has no divergence. The sum field has both making a violent storm, indeed, as shown by a plot of $\mathbf{f}_\mathbf{L}^*+\mathbf{f}_\mathbf{T}^*$ in Fig. 10.17.

$$\mathbf{f}^*=\mathbf{f}_\mathbf{L}^*+\mathbf{f}_\mathbf{T}^*=\begin{pmatrix}\frac{3x^2+y^2}{2}\\ xy\end{pmatrix}+\begin{pmatrix}\frac{-3y^2-x^2}{2}\\ xy\end{pmatrix}=\begin{pmatrix}x^2-y^2\\ 2xy\end{pmatrix},\quad \nabla\bullet\mathbf{f}^*=\nabla\bullet\mathbf{f}_\mathbf{L}^*=4x=\rho,\quad \nabla\times\mathbf{f}^*=\nabla\times\mathbf{f}_\mathbf{T}^*=4y=-I. \tag{10.54}$$

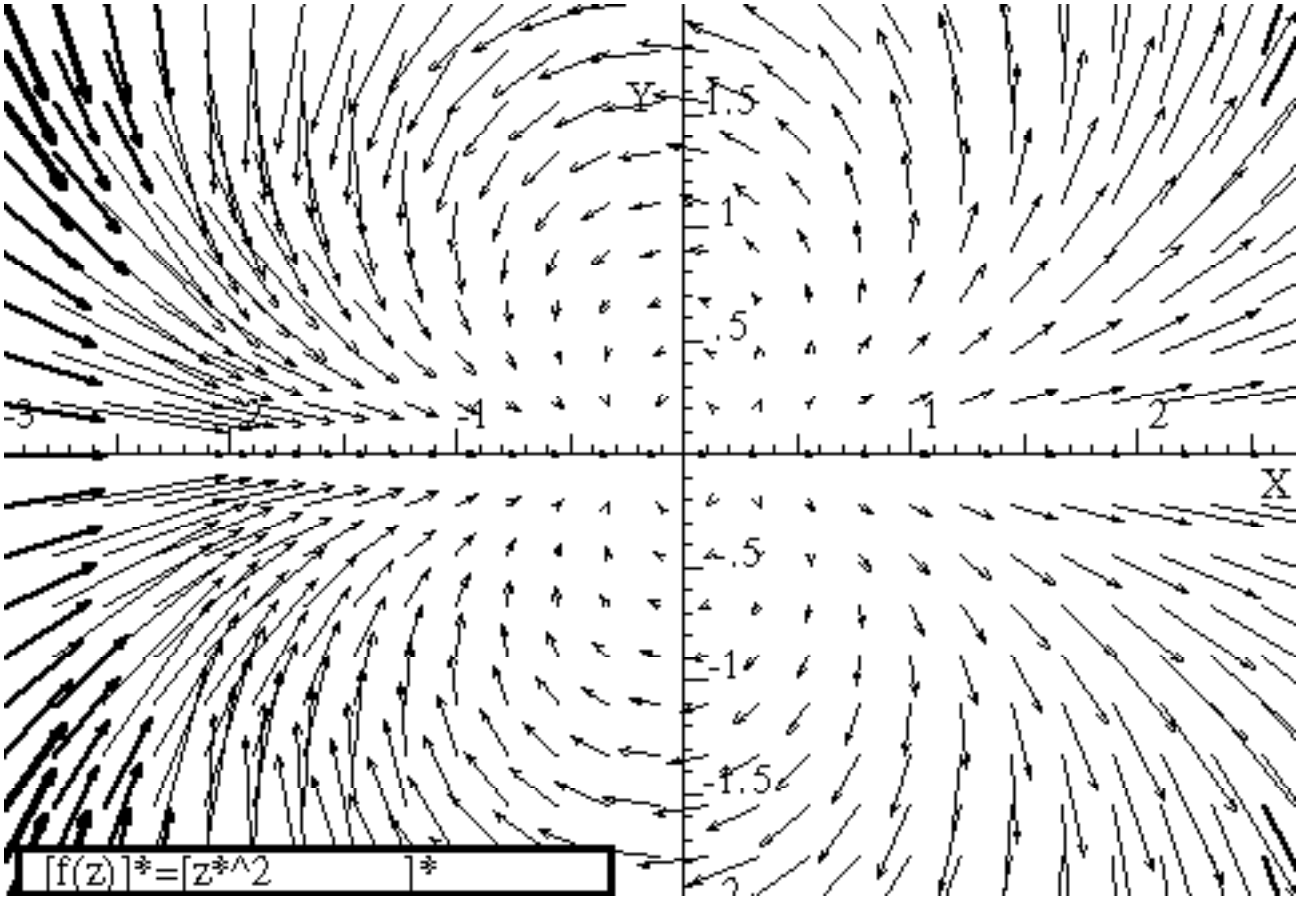

Fig.10.17 Force field vectors for non-analytic function f(z) = $(z^*)^2$

Consider a simple non-analytic field $f(z) = k{\cdot}z^*$ or $f^*(z) = k{\cdot}z$. The source function follows by (10.47).

$$s^*(z,z^*) = 2\frac{df^*}{dz} = 2k, \qquad or:\ \rho = 2k,\ \ and:\ I = 0. \tag{10.51}$$

The non-analytic potential function is found by integrating (10.47a).

$$\phi(z,z^*) = \frac{1}{2}\int f(z)dz = \frac{1}{2}\int k{\cdot}z^*\,dz = k{\cdot}\frac{z^*z}{2}, \qquad or: \quad \Phi = k{\cdot}\frac{x^2+y^2}{2},\ \ and: \quad A = 0. \tag{10.52}$$

Again, the longitudinal field is quite different from the transverse field which is zero here.

$$\mathbf{f}_\mathbf{L}^* = \nabla\Phi = \nabla\left(k{\cdot}\frac{x^2+y^2}{2}\right) = k{\cdot}\begin{pmatrix} x \\ y \end{pmatrix}, \qquad \mathbf{f}_T^* = \nabla\times\mathbf{A} = \nabla\times\left(0{\cdot}\mathbf{e_z}\right) = \begin{pmatrix} 0 \\ 0 \end{pmatrix}. \tag{10.53}$$

The result is a constant-density (that is, constant-divergence) scalar source of a linear radial force field that results from a 2D isotropic harmonic oscillator (IHO) that is like the inside-Earth potential in Fig. 9.7.

$$\nabla{\bullet}\mathbf{f}_\mathbf{L}^* = \nabla{\bullet}\begin{pmatrix} k{\cdot}x \\ k{\cdot}y \end{pmatrix} = 2k$$

A companion non-analytic field is $f(z) = ik{\cdot}z^*$ or $f^*(z) = -ik{\cdot}z$. Its source function follows.

$$s^*(z,z^*) = 2\frac{df^*}{dz} = -2ki, \qquad or:\ \rho = 0, \quad and:\ I = 2k. \tag{10.54}$$

Its non-analytic potential function is found by integrating (10.47a).

$$\phi(z,z^*) = \frac{1}{2}\int f(z)dz = \frac{i}{2}\int k{\cdot}z^*\,dz = ki\frac{z^*z}{2}, \qquad or: \quad \Phi = 0, \quad and: \quad A = k\frac{x^2+y^2}{2}. \tag{10.55}$$

Now the longitudinal field is zero and the transverse field is a constant-curl rigid rotation field.

$$\mathbf{f}_\mathbf{L}^* = \nabla\Phi = \nabla(0) = \begin{pmatrix} 0 \\ 0 \end{pmatrix}, \quad \mathbf{f}_T^* = \nabla\times\mathbf{A} = \nabla\times\left(k{\cdot}\frac{x^2+y^2}{2}{\cdot}\mathbf{e_z}\right) = \begin{pmatrix} \dfrac{\partial A}{\partial y} \\ -\dfrac{\partial A}{\partial x} \end{pmatrix} = \begin{pmatrix} k{\cdot}y \\ -k{\cdot}x \end{pmatrix}, \ \text{where:}\nabla\times\mathbf{f}_T^* = -2k. \tag{10.56}$$

A final figure (Fig. 10.18 below) shows the integral/derivative relations (10.52) to (10.56) between potential function $\phi^*(z,z^*)$, the force field $f^*(z,z^*)$, and the source field $s^*(z,z^*)$ is quite analogous to time integral/derivative relations between position $x(t)$, velocity $v(t)$, and acceleration $a(t)$ of elementary particle mechanical variables of motion.

Then acceleration-free ($a=0$) mechanics is analogous to source-free field structure ($s^*(z,z^*)=0$) that is described by *analytic* potential $\phi^*(z^*)$ and force field $f^*(z^*)$ functions described previously. Acceleration-free particle trajectories are straight lines with zero curvature, while source-free potential and force fields have zero curvature in that they obey Laplace's equation ($\nabla^2\phi = 0 = \nabla^2 f$). This is because an analytic function can only be a function $f(z)$ of z or *else* a function $f(z^*)$ of z^* and not *both* so either df/dz or df/dz^* is zero.

$$If\ \ function\ f\ is\ analytic\ then\ either\ \frac{d}{dz}f = 0 = \frac{1}{2}\left(\frac{\partial}{\partial x} - i\frac{\partial}{\partial y}\right)f \ \ or\ \ \frac{d}{dz^*}f = 0 = \frac{1}{2}\left(\frac{\partial}{\partial x} + i\frac{\partial}{\partial y}\right)f \tag{10.57}$$

((10.57) follows from (10.31).) This implies that product derivative $\frac{d}{dz^*}\frac{d}{dz}$ zeros any analytic function.

$$\frac{d}{dz^*}\frac{d}{dz}f=0=\frac{1}{4}\left(\frac{\partial}{\partial x}+i\frac{\partial}{\partial y}\right)\left(\frac{\partial}{\partial x}-i\frac{\partial}{\partial y}\right)f=\frac{1}{4}\left(\frac{\partial^2}{\partial x^2}+\frac{\partial^2}{\partial y^2}\right)f=\frac{1}{4}\nabla^2 f \tag{10.58}$$

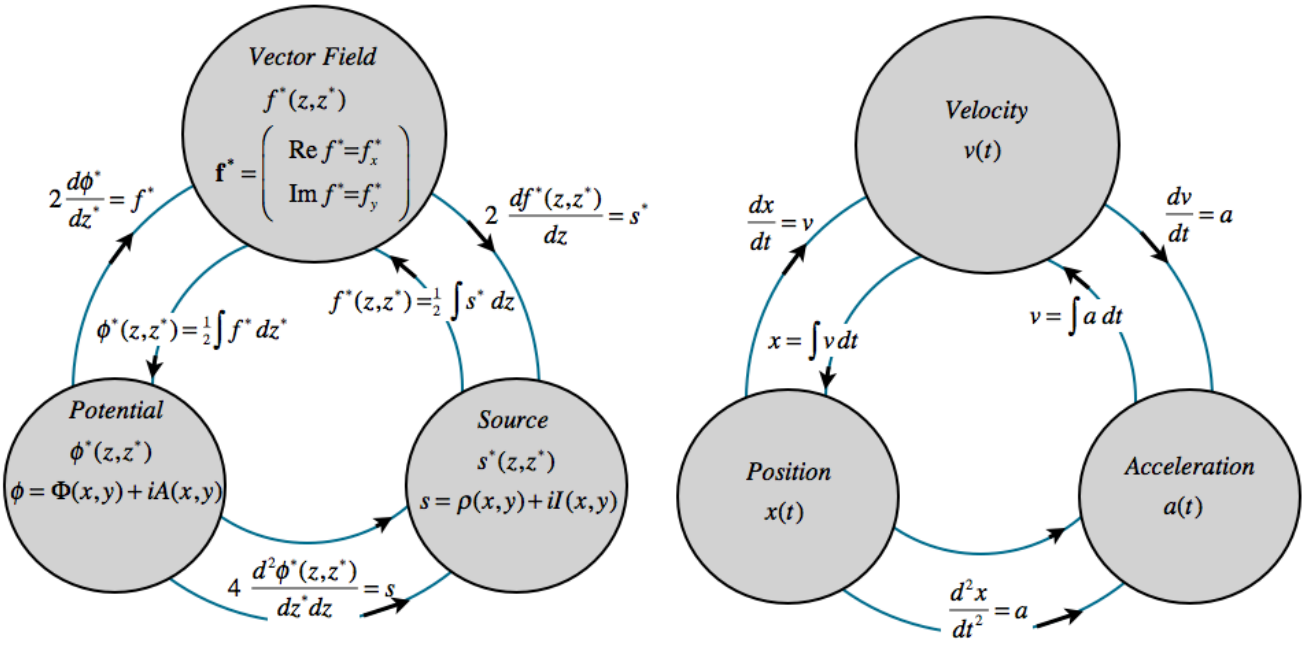

Fig.10.18 Non-analytic fields of {Potential $\phi(z,z^*)$, Force $f(z,z^*)$, *and* Source $s(z,z^*)$} are *analogous to mechanical variables* {Position $x(t)$, Velocity $v(t)$, *and* Acceleration $a(t)$}.

Having a zero df/dz^* implies relations between real Ref and imaginary Imf parts of f.

$$2\frac{d}{dz^*}f=0=\left(\frac{\partial}{\partial x}+i\frac{\partial}{\partial y}\right)(\mathrm{Re}\, f+i\,\mathrm{Im}\, f)=\left[\frac{\partial \mathrm{Re}\, f}{\partial x}-\frac{\partial \mathrm{Im}\, f}{\partial y}\right]+i\left[\frac{\partial \mathrm{Re}\, f}{\partial y}+\frac{\partial \mathrm{Im}\, f}{\partial x}\right] \tag{10.59}$$

These are the *Reimann-Cauchy* relations. These (with sign change of Imf) give results (10.34) thru (10.37).

$$\frac{\partial \mathrm{Re}\, f}{\partial x}=+\frac{\partial \mathrm{Im}\, f}{\partial y}\quad\text{and}\quad\frac{\partial \mathrm{Re}\, f}{\partial y}=-\frac{\partial \mathrm{Im}\, f}{\partial x}\quad\text{for analytic: } f(z)=\mathrm{Re}\, f+i\,\mathrm{Im}\, f \tag{10.60}$$

They apply as well to analytic force field f and potential ϕ, and cause equi-potential lines to be orthogonal to the streamlines.

Exercises

Construct dipole function geometry of Fig. 10.11.

Chapter 11. Oscillation, Rotation, and Angular Momentum

We last left the neutron starlet orbiting on an ellipse inside the Earth in Fig. 9.10 according to

$$x = a\cos\omega t \quad (9.13a)_{repeated} \qquad y = b\sin\omega t \quad (9.13b)_{repeated}$$

Here we show a Kepler construction for such an orbit that works for any ellipse. (It is like Fig. 3.6.) We also expose more geometry of velocity-velocity KE-ellipses used to introduce Lagrangian, Hamiltonian, action, and contact transformations in the following Chapter 12. That leads to more efficient ways to treat orbits.

Keplerian construction of elliptic oscillator orbits

To be historically correct, Kepler was concerned with elliptic orbits that lie *out*side of the Earth not the *in*side-Earth orbits in a linear force law $F(r) = -kr$ that we plotted. As we will show in Unit. 5, outside orbits in a Coulomb force law $F(r) = -kr^{-2}$ also have elliptic orbits, albeit with origin $r=0$ at a *focal point*. That's a little more complicated. So, we first study the easier inside-Earth orbit ellipses that have $r=0$ centered. This gives some properties of their country cousins who live well outside the city limits.

Elementary ellipse construction

Fig. 11.1 shows an easy 4-step construction for points on a *(major-radius=a, minor radius=b)*-ellipse. Note that you don't have to draw *OA* first. Pick a vertical *(AX)* or a horizontal *(BR)* line first and then find the others including the *OA* radius that goes with your choice. Given x or y, you find t or *vice versa*.

The big a-circle acts like a clock dial. The x-shadow or projection of the clock dial is $x = a\cos\omega t$ and every mass that starts at $x=a$ at zero-x-velocity will forever live in the shadow of the tip of the clock hand. This includes any ellipse with semi-major axis a, but arbitrary semi-minor axis b.

The ellipse in Fig. 11.1 has $b=1$ and $a= 2.2$. The speed of the orbiting mass can be estimated by the space between positions at equal time intervals. Speed is smaller as the mass rounds the long end of the ellipse than it is as it zips by the minor axis. In fact we shall show that it is exactly 2.2 times faster, a result that is attributed to Johannes Kepler and is the result of the *conservation of angular momentum*.

As mentioned before after Fig. 9.8, all orbits have the same period, and the mass that tunnels through the Earth center at the bottom of Fig. 11.1 has exactly the same x-equation $x = a\cos\omega t$ as the ellipse-following mass above it. They differ only in their y-equation $y = b\sin\omega t$; in the first case the tunneling mass has $b=0$. A circular orbit would have $b=a$, but its x-equation would be the same. Note how the radius vector $\mathbf{r}$ of the mass lags behind the ωt-clock-hand at first, but then at the b-axis low point (perigee) of the orbit it catches up and passes until the clock hand catches it again at the other a-axis high point (apogee or "up-ogee"). This leap-frog motion relates to one of Kepler's most famous laws and the conservation of angular momentum as will be reviewed shortly.

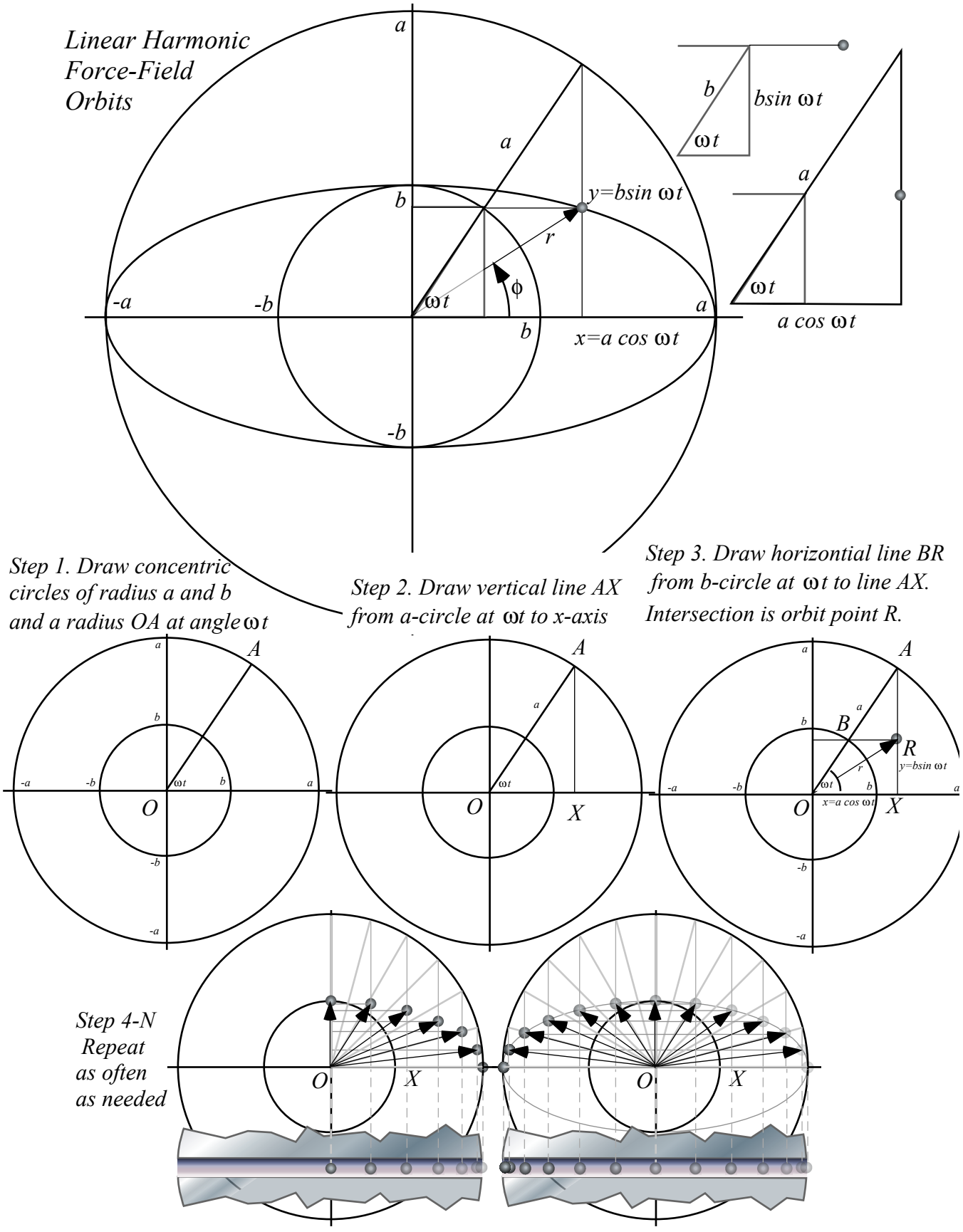

Fig. 11.1. Harmonic force-field elliptical orbit construction.

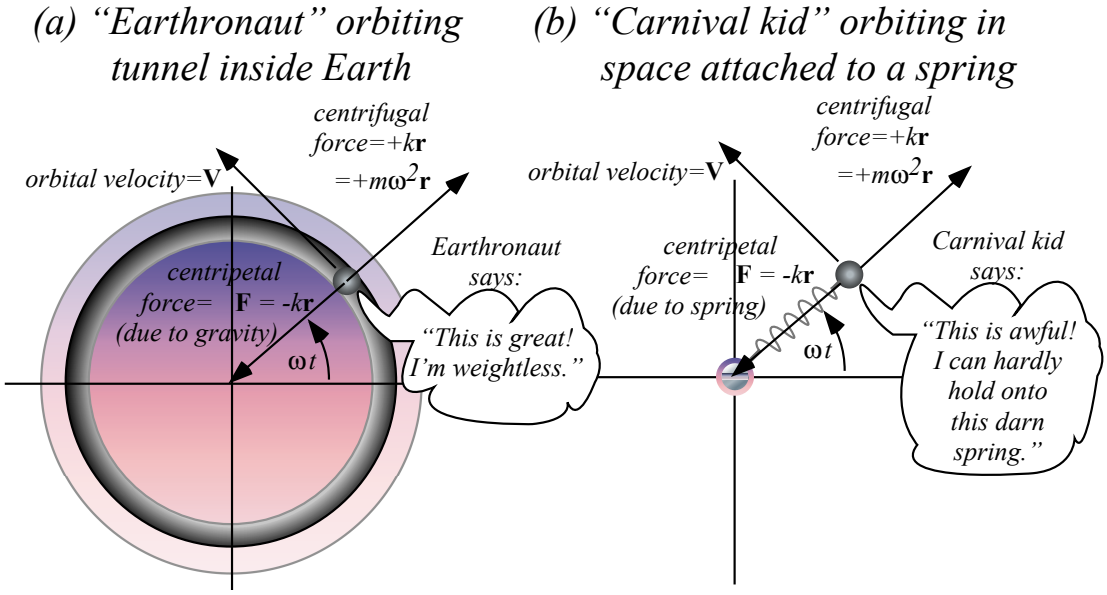

Fig. 11.2 Two different systems with identical oscillator orbits. (a) Inside Earth, (b) Mass on spring.

Orbiting versus rotating: Centripetal versus centrifugal

Imagine an "Earthronaut" orbits inside the Earth in a linear gravity field $\mathbf{F}=-k\mathbf{r}$, as sketched in Fig. 11.2(a). (Recall "starlet" in Fig. 9.9.) Let's compare to a kid rotating in a carnival ride at one end of a spring as the other end pivots frictionlessly about a fixed point. (See Fig. 11.2(b).) Each m does the same orbit, but there's a big difference. You'd notice it if *you* were the mass m.

The Earthronaut feels weightless like astronauts in orbit. But the rotating kid feels a great outward pull, a *centrifugal* or *center-fleeing* force $\mathbf{F}=+k\mathbf{r}$. Stop the rotating "carnival kid" and the centrifugal force goes away. If the kid lets go he feels weightless in space. Stop the orbiting Earthronaut and the inward tug $\mathbf{F}=-k\mathbf{r}$ by the *centripetal* or *center-pulling* force of gravity returns as the Earthronaut resumes *weighing* $mg=kr$. Earth gravity is no longer cancelled by inertial reaction force and he cannot let go of g.

An orbiting Earthronaut feels weightless because the two forces, outward centrifugal $\mathbf{F}=+k\mathbf{r}$ and inward centripetal $\mathbf{F}=-k\mathbf{r}$, cancel to zero for body mass m or any part of it. On the other hand, the carnival kid feels stretched out by two equal and opposite forces, again an outward centrifugal $\mathbf{F}=+k\mathbf{r}$ pulling the kid up opposes an inward centripetal $\mathbf{F}=-k\mathbf{r}$ provided by the spring that the kid is holding onto.

In each case, outward centrifugal $F=kr$ is due to rotation at angular rate ω around a circle of radius r at velocity $V=\omega r$. The angular rate ω is the Earth or spring oscillator frequency from (9.9) or (10.23).

$$\omega = \sqrt{\frac{k}{m}} \qquad (11.2a) \qquad \text{or:} \qquad k = m\omega^2 \qquad (11.2b)$$

Centrifugal force formulas that result are among the most famous formulas in rotational mechanics.

$$F_{centrifugal} = k\,r = m\omega^2\,r = m\,V^2/r \qquad \text{where: } V=\omega\,r \qquad (11.3a)$$

Removing the mass m gives the also-famous *centrifugal acceleration* formulas.

$$a_{centrifugal} = \omega^2 r = V^2/r \qquad \text{where: } V = \omega r \qquad (11.3b)$$

Circular curvature

A geometer likes to imagine fitting a curve by circles at each point with smaller circles fitting more curvy points. These so-called *circles of curvature* become bigger circles as a curve straightens out. A geometer-physicist does the same, but imagines driving at a constant speed V along the curve with an accelerometer to measure transverse centrifugal acceleration $a_{centrifugal}$. By (11.3b) the accelerometer reads V^2/r_{curv} *outward* from a curve if the car is rounding a circle of radius $r_{curv} = V^2/ a_{centrifugal}$ with its center that distance *inside* the curve. The $a_{centrifugal}$-reading is *inversely* proportional to *radius of curvature* for fixed *linear* velocity V, but *directly* proportional to it for fixed *angular* velocity ω.

$$r_{curv} = V^2/a_{centrifugal} = a_{centrifugal}/\omega^2 \qquad \text{where: } V = \omega r_{curv} \qquad (11.3c)$$

It is a strange but useful view of a curve! The physicist imagines riding a carnival Merry-Go-Round whose rim speed V is constant but whose radius and center keep changing! If the road straightens to veer the other way, the Merry-Go-Round center becomes infinite and reappears on the other side.

Note that road speed V is constant in the physicist's image. There's no acceleration along the road, only perpendicular to it. However, in real orbits around planets or springs, velocity V holds constant only for circular orbits or, ever so briefly, at special points on elliptical ones. One special point is a low point or *perigee*. Another is a high point or *apogee*. (Think "*ap*" means "up" in space lingo.)

An astronaut in an elliptic orbit or a mass on an elliptic oscillator orbit like Fig. 11.1 will increase speed (accelerate) as it "falls" from the high-point apogee on the x-axis toward the low-point perigee on the y-axis. Then it will decrease speed (decelerate) as it rises back to apogee. Only at apogee or perigee is the speed momentarily constant. Then, and only then, is force and acceleration *perpendicular* to the flight path. In between, the $\mathbf{F}=-k\mathbf{r}$ vector makes an angle θ with velocity $\mathbf{V}$ that is not $90°$ so the work $(dW = \mathbf{F}\bullet d\mathbf{r} = |Fdr|\cos\theta)$ or power $(P = \mathbf{F}\bullet\mathbf{V} = |FV|\cos\theta)$ is non-zero so kinetic energy varies.

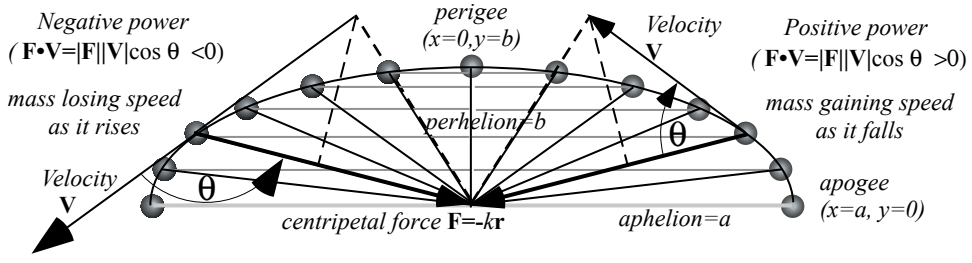

Fig. 11.3 Elliptic orbit force, velocity, and power variation.

More inertial forces: Coriolis and tidal forces

Carnival kid would feel even more forces on an elliptic orbit, though the Earthronaut may still be nearly weightless. Gravitational force is balanced by centrifugal force and, between apogee and perigee, by another kind of inertial force called the *Coriolis force* that opposes orbital velocity.

To visualize Coriolis force imagine what you would feel walking along a radial railing toward the center of a Merry-Go-Round rotating to your right as in Fig. 11.4(a). The railing pushes you left (*against* the rotation) to slow you down to zero speed when or if you get to the center of the Merry-Go-Round. The Coriolis force is proportional to your radial walking speed. Stop walking inward and all you feel is the usual centrifugal force pulling back out along the radial railing path. Walk back out and Coriolis pushes you to the right to get you up to the Merry-Go-Round rotation speed at each point.

Coriolis forces can make you dizzy and nauseous. Centrifugal force is steady as long as you are fixed to the Merry-Go-Round. But, if you just turn your head, the fluids in your inner ear get a kick perpendicular to the direction of motion and they're not used to that.

Fig. 11.4(b) shows centrifugal and Coriolis forces of an inward falling orbiting mass analogous to that of the Merry-Go-Round. The Coriolis force acts oppositely to orbital velocity **V** on the way in and then acts with **V** on the way out in Fig. 11.4(c). At apogee or perigee in Fig. 11.4(d) there is centrifugal-centripetal force but no Coriolis force since the mass momentarily stops its radial motion.

The Earthronaut may not feel centrifugal or Coriolis forces if every atom almost perfectly balances inertial force by equal and opposite gravitational force to make a feel-force-free orbit. But, "almost" is not zero! Suppose our astronaut is on a 1 kHz neutron star orbit. (That's $\omega=2000\pi$.) He (or she) is toast and jelly due to what is called *tidal force*. Only the astronaut's center-of-gravity is right on a feel-force-free elliptic orbit. For the rest that's the wrong ellipse! The poor astronaut's left and right hands (and ears and other bilateral pieces of anatomy) try to change places 2000 times per second as disparate free-fall orbits crisscross back-and-forth twice each period. *Really* barf!

The *k*-constant or spring constant for an oscillator tidal force felt by a neutron-astronaut (who will be reduced to a "neuternaut" by one orbit) is given by (11.2b).

$$k=m\omega^2= m6.28^2\ E6\ \ (N/m) \quad \text{for: } \omega=2000\pi$$

That is almost *40 million Newtons* (*10 million lbs*. or 5 *thousand tons*) for each kilogram of mass a meter off-center or *50 tons* of pressure just on a *1 cm*-sized fingertip.

Quite a number of astrophysical effects are due to tidal forces like ocean tides. The Moon presents one face because its tides due to Earth have wasted as much of its rotational energy as possible. So it's locked relative to Earth with only slight (but interesting) nutational wobbling due partly to its eccentric orbit.

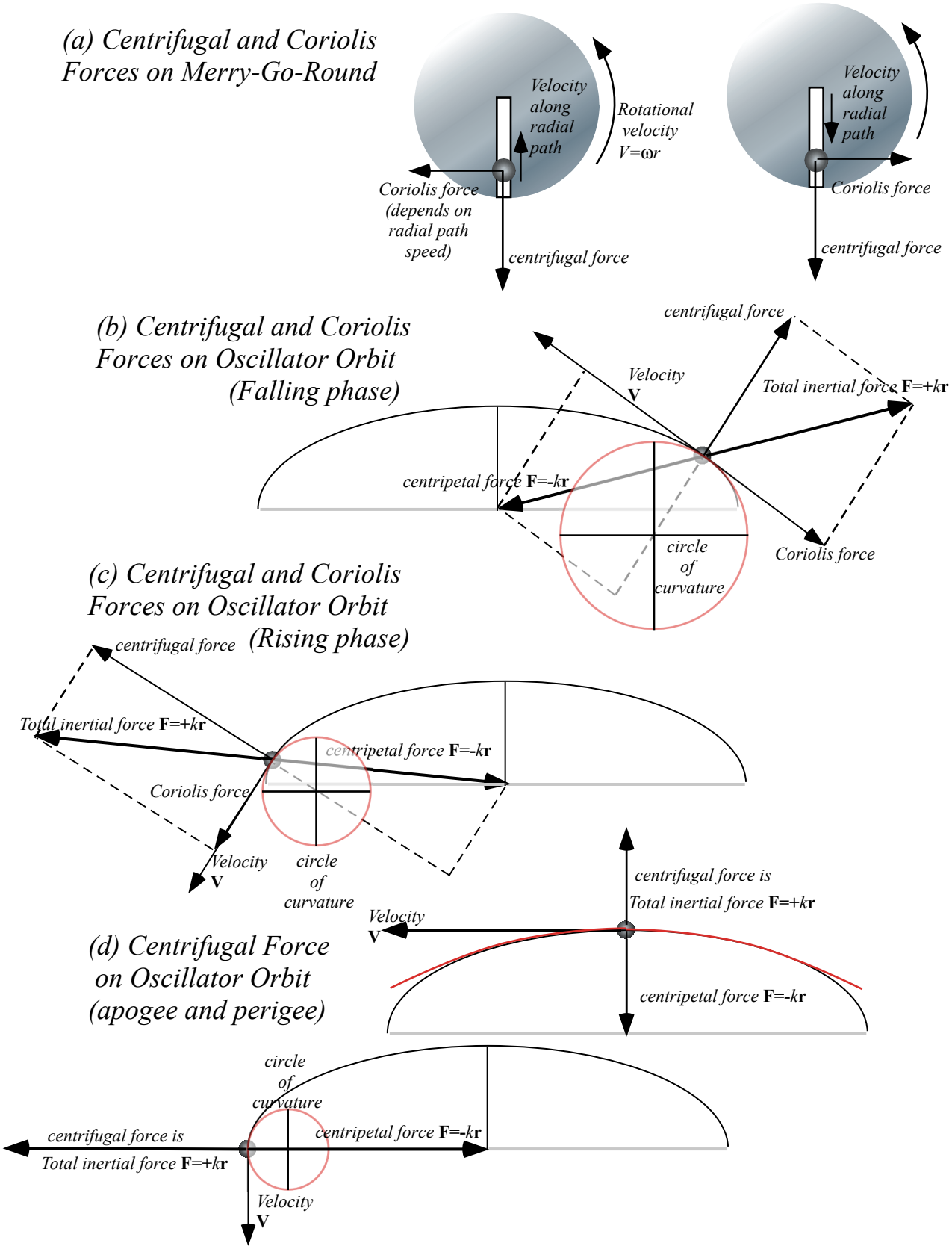

Fig. 11.4 Centrifugal and Coriolis forces. (a) Simple Merry-Go-Round. (b-d) Various orbital phases.

Vector analysis and geometry of elliptic oscillator orbit

An ellipse orbit is characterized using vectors **r**, **v**, and **F**= *m***a** that are arrows in Fig. 11.4. First, there is the location, position, or *radius vector* **r** that we found in (9.13).

$$\mathbf{r} = \begin{pmatrix} r_x \\ r_y \end{pmatrix} = \begin{pmatrix} x \\ y \end{pmatrix} = \begin{pmatrix} a\cos\omega t \\ b\sin\omega t \end{pmatrix} \tag{11.5a}$$

Second, there is the rate, speed, or *velocity vector* **v** that is a 1st time derivative $\frac{d}{dt}\begin{pmatrix}\cos\omega t\\ \sin\omega t\end{pmatrix} = \omega\begin{pmatrix}-\sin\omega t\\ \cos\omega t\end{pmatrix}$.

$$\mathbf{v} = \begin{pmatrix} v_x \\ v_y \end{pmatrix} = \begin{pmatrix} -a\omega\sin\omega t \\ b\omega\cos\omega t \end{pmatrix} = \frac{d\mathbf{r}}{dt} = \dot{\mathbf{r}} \tag{11.5b}$$

Unit-*m* force **F** is proportional to 2nd derivative (Change-of-velocity is *acceleration* **a**) and is just -ω²**r**.

$$\frac{\mathbf{F}}{m} = \mathbf{a} = \begin{pmatrix} a_x \\ a_y \end{pmatrix} = \begin{pmatrix} -a\omega^2\cos\omega t \\ -b\omega^2\sin\omega t \end{pmatrix} = \frac{d\mathbf{v}}{dt} = \dot{\mathbf{v}} = \ddot{\mathbf{r}} = \frac{d^2\mathbf{r}}{dt^2} \tag{11.5b}$$

Then the 3rd derivative (Change-of-acceleration is *jerk* **j**), is just -ω²**v**,

$$\mathbf{j} = \begin{pmatrix} j_x \\ j_y \end{pmatrix} = \begin{pmatrix} +a\omega^3\sin\omega t \\ -b\omega^3\cos\omega t \end{pmatrix} = \frac{d\mathbf{a}}{dt} = \dot{\mathbf{a}} = \ddot{\mathbf{v}} = \dddot{\mathbf{r}} = \frac{d^3\mathbf{r}}{dt^3} \tag{11.5c}$$

and finally the 4th derivative (Change-of-jerk is *inauguration* **i**), equals the **r**-vector with a scale factor ω⁴.

$$\mathbf{i} = \begin{pmatrix} i_x \\ i_y \end{pmatrix} = \begin{pmatrix} +a\omega^4\cos\omega t \\ +b\omega^4\sin\omega t \end{pmatrix} = \frac{d\mathbf{j}}{dt} = \dot{\mathbf{j}} = \ddot{\mathbf{a}} = \dddot{\mathbf{v}} = \ddddot{\mathbf{r}} = \frac{d^4\mathbf{r}}{dt^4} \tag{11.5d}$$

Linear Hooke force **F**=-*k***r** gives **F**=*m***a**=-*k***r** then **a**=-ω²**r** then **j**= -ω²**v**, and so on. The 5th derivative (Change-of-inauguration is *revolution*) is just ω⁵**v**. As plotted in Fig. 11.5, the four vectors **r**, **v**/ω, **a**/ω², and **j**/ω³ follow each other on one ellipse orbit of Fig. 11.1 taking turns to slow down then to speed up.

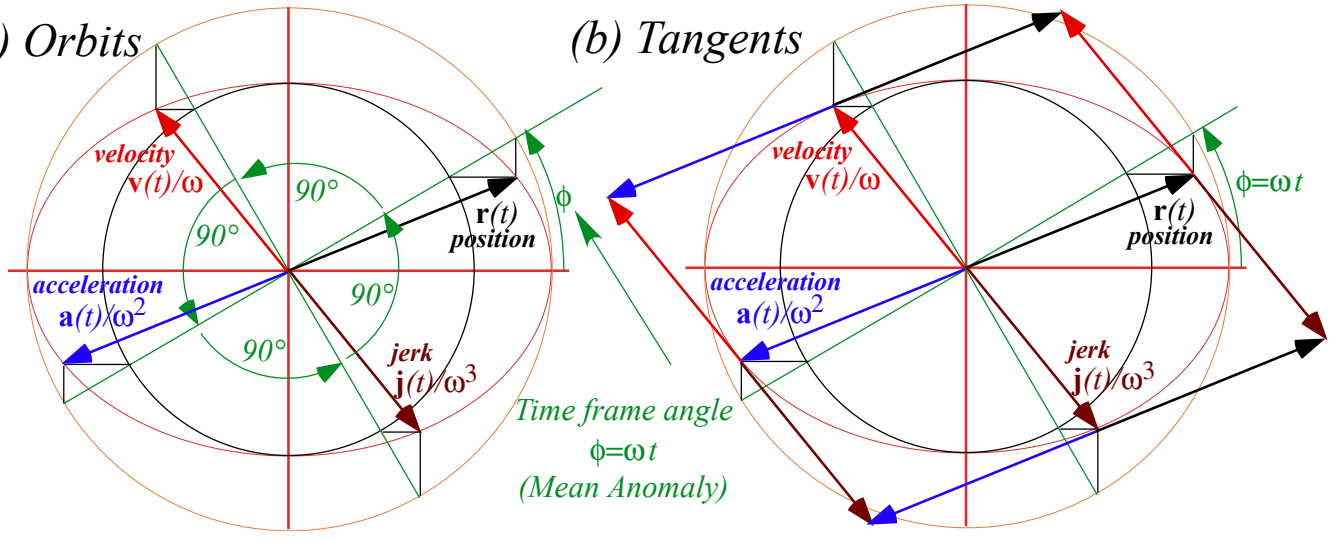

Fig. 11.5 Harmonic oscillator orbit ellipse (a) All derivatives follow same orbit. (b) Related tangents.

Each of the four vectors $\mathbf{r}$, $\mathbf{v}/\omega$, $\mathbf{a}/\omega^2$, and $\mathbf{j}/\omega^3$ in Fig. 11.5 has a time-phase angle or *mean anomaly* value $\phi=\omega t$ that is spaced at $\pi/2$ intervals ωt, $\omega t+\pi/2$, $\omega t+\pi$, and $\omega t+3\pi/2$, respectively, as listed below.

$$\mathbf{r}(t)=\begin{pmatrix} a\cos\omega t \\ b\sin\omega t \end{pmatrix} = \begin{pmatrix} a\cos\phi \\ b\sin\phi \end{pmatrix} \quad (11.6a) \qquad \frac{\mathbf{v}(t)}{\omega}=\begin{pmatrix} -a\sin\phi \\ b\cos\phi \end{pmatrix} = \begin{pmatrix} a\cos\left(\phi+\frac{\pi}{2}\right) \\ b\sin\left(\phi+\frac{\pi}{2}\right) \end{pmatrix} \quad (11.6b)$$

$$\frac{\mathbf{a}(t)}{\omega^2}=\begin{pmatrix} -a\cos\phi \\ -b\sin\phi \end{pmatrix} = \begin{pmatrix} a\cos\left(\phi+\frac{2\pi}{2}\right) \\ b\sin\left(\phi+\frac{2\pi}{2}\right) \end{pmatrix} \quad (11.6c) \qquad \frac{\mathbf{j}(t)}{\omega^3}=\begin{pmatrix} a\sin\phi \\ -b\cos\phi \end{pmatrix} = \begin{pmatrix} a\cos\left(\phi+\frac{3\pi}{2}\right) \\ b\sin\left(\phi+\frac{3\pi}{2}\right) \end{pmatrix} \quad (11.6d)$$

Matrix operations and dual quadratic forms

Ellipse equation $\frac{x^2}{a^2}+\frac{y^2}{b^2}=1$ may be written using a matrix $\mathbf{Q}=\begin{pmatrix} 1/a^2 & 0 \\ 0 & 1/b^2 \end{pmatrix}$ on position vector $\mathbf{r}=\begin{pmatrix} x \\ y \end{pmatrix}=\begin{pmatrix} x & y \end{pmatrix}$.

$$\begin{pmatrix} x & y \end{pmatrix}\bullet\begin{pmatrix} \frac{1}{a^2} & 0 \\ 0 & \frac{1}{b^2} \end{pmatrix}\bullet\begin{pmatrix} x \\ y \end{pmatrix}=1=\begin{pmatrix} x & y \end{pmatrix}\bullet\begin{pmatrix} \frac{x}{a^2} \\ \frac{y}{b^2} \end{pmatrix}=\frac{x^2}{a^2}+\frac{y^2}{b^2} \qquad \text{or:} \qquad \mathbf{r}\bullet\mathbf{Q}\bullet\mathbf{r}=1 \qquad (11.7)$$

Function $\mathbf{r}\bullet\mathbf{Q}\bullet\mathbf{r}$ is a *quadratic form QF*. *QF*'s are useful to mechanics and their powerful geometry will be demonstrated for orbit ellipses and later for KE ellipses. First note that if a matrix $\mathbf{Q}=\begin{pmatrix} 1/a^2 & 0 \\ 0 & 1/b^2 \end{pmatrix}$ acts on a radial position vector $\mathbf{r}=\begin{pmatrix} x \\ y \end{pmatrix}$ it gives a vector $\mathbf{p}$ *perpendicular* to ellipse tangent $\dot{\mathbf{r}}=\frac{d\mathbf{r}}{d\varphi}$ at $\mathbf{r}$.

$$\mathbf{p}=\mathbf{Q}\bullet\mathbf{r}=\begin{pmatrix} 1/a^2 & 0 \\ 0 & 1/b^2 \end{pmatrix}\bullet\begin{pmatrix} x \\ y \end{pmatrix}=\begin{pmatrix} x/a^2 \\ y/b^2 \end{pmatrix}=\begin{pmatrix} (1/a)\cos\phi \\ (1/b)\sin\phi \end{pmatrix} \quad \text{where:} \quad \begin{matrix} x=r_x=a\cos\phi=a\cos\omega t \\ y=r_y=b\sin\phi \ \ =b\sin\omega t \end{matrix} \qquad (11.8a)$$

$\mathbf{p}$ is perpendicular, that is, orthogonal to the velocity vector $\mathbf{v}=\dot{\mathbf{r}}$ (11.5b) as seen here and in Fig. 11.6.

$$\dot{\mathbf{r}}\bullet\mathbf{p}=0=\begin{pmatrix} \dot{r}_x & \dot{r}_y \end{pmatrix}\bullet\begin{pmatrix} p_x \\ p_y \end{pmatrix}=\begin{pmatrix} -a\sin\phi & b\cos\phi \end{pmatrix}\bullet\begin{pmatrix} (1/a)\cos\phi \\ (1/b)\sin\phi \end{pmatrix} \quad \text{where:} \quad \begin{matrix} \dot{r}_x=-a\sin\phi \\ \dot{r}_y=b\cos\phi \end{matrix} \quad \text{and:} \quad \begin{matrix} p_x=(1/a)\cos\phi \\ p_y=(1/b)\sin\phi \end{matrix} \qquad (11.8b)$$

These $\mathbf{p}$-vectors define their own ellipse $\mathbf{r}\bullet\mathbf{Q}^{-1}\bullet\mathbf{r}=1$ of an *inverse quadratic form* $Q^{-1}F$. Its radii are inverse *(1/a, 1/b)* of the original $\mathbf{Q}$-ellipse radii *(a,b)* in (11.7). The $Q^{-1}F$-ellipse is the dashed oval in Fig. 11.6.

$$\begin{pmatrix} p_x & p_y \end{pmatrix}\bullet\begin{pmatrix} a^2 & 0 \\ 0 & b^2 \end{pmatrix}\bullet\begin{pmatrix} p_x \\ p_y \end{pmatrix}=1=\begin{pmatrix} p_x & p_y \end{pmatrix}\bullet\begin{pmatrix} a^2p_x \\ b^2p_y \end{pmatrix}=a^2p_x^2+b^2p_y^2 \quad \text{or:} \quad \mathbf{p}\bullet\mathbf{Q}^{-1}\bullet\mathbf{p}=1 \qquad (11.9)$$

Inverse operation $\mathbf{Q}^{-1}\bullet\mathbf{p}$ on perpendicular $\mathbf{p}$ returns the radial position vector $\mathbf{r}$ on the Q-ellipse.

$$\mathbf{r}=\mathbf{Q}^{-1}\bullet\mathbf{p}=\begin{pmatrix} a^2 & 0 \\ 0 & b^2 \end{pmatrix}\bullet\begin{pmatrix} p_x \\ p_y \end{pmatrix}=\begin{pmatrix} a^2p_x \\ b^2p_y \end{pmatrix}=\begin{pmatrix} a\cos\phi \\ b\sin\phi \end{pmatrix} \quad \text{where:} \quad \begin{matrix} p_x=(1/a)\cos\phi \\ p_y=(1/b)\sin\phi \end{matrix} \qquad (11.10a)$$

$\mathbf{r}$ is orthogonal to the $Q^{-1}F$-ellipse tangent $\dot{\mathbf{p}}$, just as $\mathbf{p}$ is orthogonal to the QF-ellipse tangent $\dot{\mathbf{r}}$ in (11.8b).

$$\dot{\mathbf{p}}\bullet\mathbf{r}=0=\begin{pmatrix} \dot{p}_x & \dot{p}_y \end{pmatrix}\bullet\begin{pmatrix} r_x \\ r_y \end{pmatrix}=\begin{pmatrix} (-1/a)\sin\phi & (1/b)\cos\phi \end{pmatrix}\bullet\begin{pmatrix} a\cos\phi \\ b\sin\phi \end{pmatrix} \quad \text{where:} \quad \begin{matrix} \dot{p}_x=(-1/a)\sin\phi \\ \dot{p}_y=(1/b)\cos\phi \end{matrix} \quad \text{and:} \quad \begin{matrix} r_x=a\cos\phi \\ r_y=b\sin\phi \end{matrix} \qquad (11.10b)$$

Vectors **p** and **r** maintain a *unit mutual projection*, that is, dot-products **p•r** and $\dot{\mathbf{p}}\bullet\dot{\mathbf{r}}$ *always equal* 1.

$$\mathbf{p}\bullet\mathbf{r}=1=\begin{pmatrix}p_x & p_y\end{pmatrix}\bullet\begin{pmatrix}r_x\\ r_y\end{pmatrix}=\begin{pmatrix}\frac{1}{a}\cos\phi & \frac{1}{b}\sin\phi\end{pmatrix}\begin{pmatrix}a\cos\phi\\ b\sin\phi\end{pmatrix}=\mathbf{p}\bullet Q^{-1}\bullet\mathbf{p}=1=\mathbf{r}\bullet Q\bullet\mathbf{r} \qquad (11.10c)$$

Fig. 11.6b shows a geometric-algebraic symmetry where ellipse plots are scaled by geometric mean $S=\sqrt{(ab)}$ so that each scaled major radius $a_S=a/S$ is the inverse of its minor radius $b_S=b/S$ and $a_S\,b_S=1$.

$$a_S=a/S=\sqrt{(a/b)}=1/b_S \quad (11.11a) \qquad b_S=b/S=\sqrt{(b/a)}=1/a_S \quad (11.11b)$$

Then inverse ellipse $\mathbf{r}\bullet\mathbf{Q}^{-1}\bullet\mathbf{r}=1$ is an axis switch ($a_S \rightleftarrows b_S$) or 90° rotation of ellipse $\mathbf{r}\bullet\mathbf{Q}\bullet\mathbf{r}=1$ by symmetry.

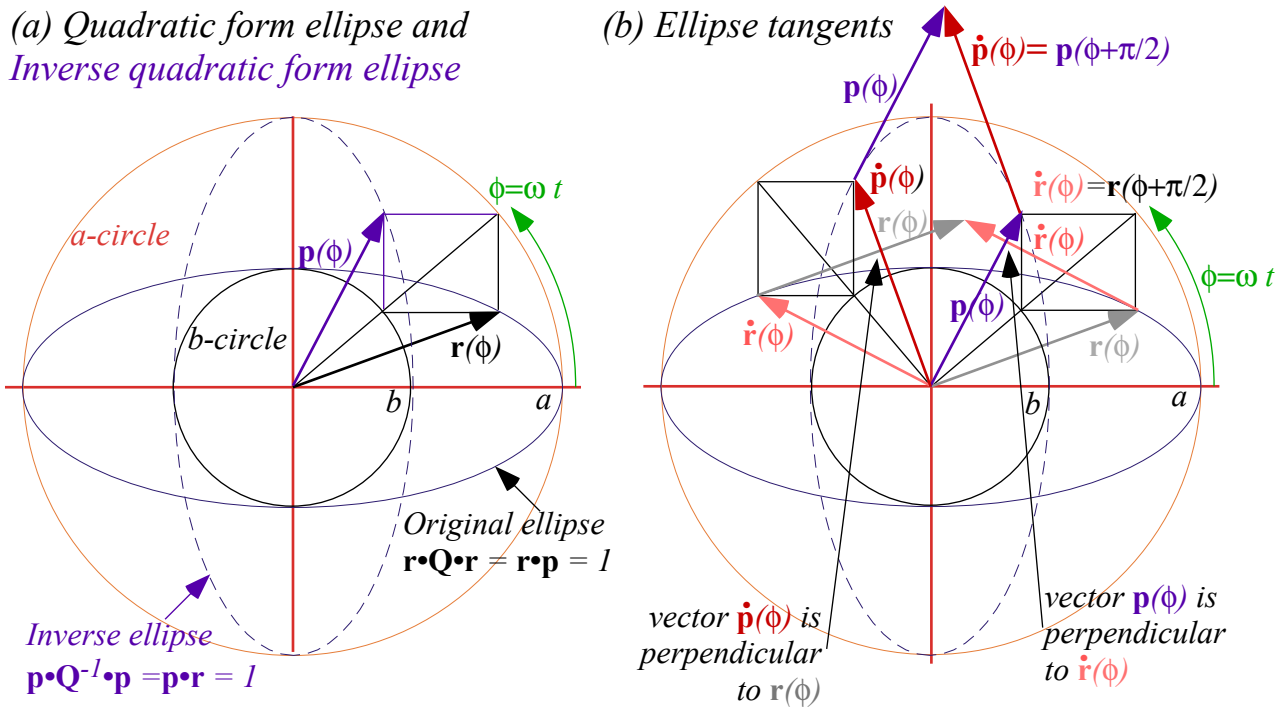

Fig. 11.6 Ellipse vectors and tangents for quadratic forms. (a) Ellipse vectors. (b) Tangent geometry.

Slope multiplication and eigenvectors

Matrix $\mathbf{R}=\begin{pmatrix}1/a & 0\\ 0 & 1/b\end{pmatrix}$ or $\mathbf{R}^{-1}=\begin{pmatrix}a & 0\\ 0 & b\end{pmatrix}$ acting on a vector $\mathbf{r}=\begin{pmatrix}x\\ y\end{pmatrix}$ multiplies its slope $\frac{y}{x}$ by a/b or b/a respectively.

$$\mathbf{R}\bullet\mathbf{r}=\begin{pmatrix}1/a & 0\\ 0 & 1/b\end{pmatrix}\begin{pmatrix}x\\ y\end{pmatrix}=\begin{pmatrix}x/a\\ y/b\end{pmatrix} \quad (11.12a) \qquad \mathbf{R}^{-1}\bullet\mathbf{r}=\begin{pmatrix}a & 0\\ 0 & b\end{pmatrix}\begin{pmatrix}x\\ y\end{pmatrix}=\begin{pmatrix}a\cdot x\\ b\cdot y\end{pmatrix} \quad (11.12b)$$

Matrix $\mathbf{Q}=\mathbf{R}^2=\begin{pmatrix}1/a^2 & 0\\ 0 & 1/b^2\end{pmatrix}$ or $\mathbf{Q}^{-1}=\mathbf{R}^{-2}=\begin{pmatrix}a^2 & 0\\ 0 & b^2\end{pmatrix}$ multiplies slope by a^2/b^2 as in (11.8a) or b^2/a^2 as in (11.10a).

$$\mathbf{Q}\bullet\mathbf{r}=\mathbf{R}^2\bullet\mathbf{r}=\begin{pmatrix}x/a^2\\ y/b^2\end{pmatrix}=\mathbf{p} \quad (11.13a) \qquad \mathbf{Q}^{-1}\bullet\mathbf{r}=\mathbf{R}^{-2}\bullet\mathbf{r}=\begin{pmatrix}a^2\cdot x\\ b^2\cdot y\end{pmatrix} \quad (11.13b)$$

Only vectors of slope *zero* or *infinity*, such as $\hat{\mathbf{a}}=\binom{1}{0}$ or $\hat{\mathbf{b}}=\binom{0}{1}$, are immune to slope-change by **R** or $\mathbf{R}^{-1}$.

$$\mathbf{R}^{-1}\bullet\hat{\mathbf{a}}=\begin{pmatrix}a & 0\\ 0 & b\end{pmatrix}\begin{pmatrix}1\\ 0\end{pmatrix}=a\begin{pmatrix}1\\ 0\end{pmatrix}=a\cdot\hat{\mathbf{a}} \quad (11.14a) \qquad \mathbf{R}^{-1}\bullet\hat{\mathbf{b}}=\begin{pmatrix}a & 0\\ 0 & b\end{pmatrix}\begin{pmatrix}0\\ 1\end{pmatrix}=b\begin{pmatrix}0\\ 1\end{pmatrix}=b\cdot\hat{\mathbf{b}} \quad (11.14b)$$

They are called *eigenvectors* of $\mathbf{R}^{-1}$ or any power $\mathbf{R}^p=\{\mathbf{R}^2=\mathbf{Q},\mathbf{R}^3,\mathbf{R}^4=\mathbf{Q}^2,\mathbf{R}^5,\mathbf{R}^6=\mathbf{Q}^3,\mathbf{R}^7,...\}$ of **R** or $\mathbf{R}^{-1}$.

$$\mathbf{R}^{-2}\bullet\hat{\mathbf{a}}=\mathbf{Q}^{-1}\bullet\hat{\mathbf{a}}=a^2\cdot\hat{\mathbf{a}} \qquad (11.15a) \qquad \mathbf{R}^{-2}\bullet\hat{\mathbf{b}}=\mathbf{Q}^{-1}\bullet\hat{\mathbf{b}}=b^2\cdot\hat{\mathbf{b}} \qquad (11.15b)$$

$$\mathbf{R}^{2}\bullet\hat{\mathbf{a}}=\mathbf{Q}\bullet\hat{\mathbf{a}}=(1/a^2)\cdot\hat{\mathbf{a}} \qquad (11.15c) \qquad \mathbf{R}^{2}\bullet\hat{\mathbf{b}}=\mathbf{Q}\bullet\hat{\mathbf{b}}=(1/b^2)\cdot\hat{\mathbf{b}} \qquad (11.15d)$$

These special vectors are operator $\mathbf{R}^p$'s own base vectors for any power p. Eigenvector is German for "*own*-vector." Base vectors $\hat{\mathbf{a}}$ and $\hat{\mathbf{b}}$ define a $\mathbf{Q}^p$-and-$\mathbf{R}^p$-ellipse's own major and minor axial directions. The axial radii a and b are the *eigenvalues* of $\mathbf{R}^{-1}$ in (11.14). Powers a^p and b^p are *eigenvalues* of $\mathbf{R}^{-p}$.

Geometric slope series

Each action of $\mathbf{R}$ (or $\mathbf{Q}$) on vector $\mathbf{r}$ grows its slope by a/b (or a^2/b^2) so it approaches eigenvector $\hat{\mathbf{b}}=\binom{0}{1}$ while $\mathbf{R}^{-1}$ and $\mathbf{Q}^{-1}$ make it approach eigenvector $\hat{\mathbf{a}}=\binom{1}{0}$. Each slope polar angle ϕ_k plotted in Fig. 11.7 is obtained from its neighbors ϕ_{k-1} and ϕ_{k+1} by inscribing a rectangle between $r=a$ and $r=b$ with its main diagonal on the ϕ_k line. Lower and upper corners on the cross-diagonal give radial position $\mathbf{r}(\phi_{k-1})$ on the Q-ellipse and perpendicular $\mathbf{p}(\phi_{k+1})$ on the Q^{-1}-ellipse, respectively, following Fig. 11.1 and (11.13).

$$\mathbf{p}(\phi_{k+1})=\mathbf{Q}\bullet\mathbf{r}(\phi_{k-1}) \qquad \text{where: } \tan(\phi_{k+1})=(a/b)^2\tan(\phi_{k-1}) \qquad (11.16)$$

For the k^{th} triad, angle $\phi_k=\omega t_k$ is the "timer" angle and polar angle of main diagonal while ϕ_{k-1} is the polar angle of radial position $\mathbf{r}(\phi_{k-1})$ and ϕ_{k+1} is the polar angle of perpendicular $\mathbf{p}(\phi_{k+1})$ to velocity $\dot{\mathbf{r}}(\phi_{k-1})=\mathbf{v}(t_k)$.

$$\mathbf{p}(\phi_{k+1})\bullet\dot{\mathbf{r}}(\phi_{k-1})=0=\dot{\mathbf{p}}(\phi_{k+1})\bullet\mathbf{r}(\phi_{k-1}) \qquad (11.17a) \qquad \mathbf{p}(\phi_{k+1})\bullet\mathbf{r}(\phi_{k-1})=1 \qquad (11.17b)$$

This restates the duality relations (11.10) for an entire sequence, part of which is shown by Fig. 11.7b.

A $\{\phi_k\}$ sequence may start on any angle but a choice $\phi_0=\pi/4$ in Fig. 11.7 gives symmetric results. Also, we may let: $ab=1$ and: $\mathbf{Q}=\begin{pmatrix} b/a & 0 \\ 0 & a/b \end{pmatrix}$ below by assuming unit scale $S=1$ in (11.11).

$$\mathbf{p}(\phi_1)=\begin{pmatrix} b\cos\phi_0 \\ a\sin\phi_0 \end{pmatrix}=\begin{pmatrix} b/\sqrt{2} \\ a/\sqrt{2} \end{pmatrix} \qquad \mathbf{p}(\phi_0)=\begin{pmatrix} b\cos\phi_{-1} \\ a\sin\phi_{-1} \end{pmatrix}=\begin{pmatrix} ab/\sqrt{a^2+b^2} \\ ab/\sqrt{a^2+b^2} \end{pmatrix} \qquad \mathbf{p}(\phi_{-1})=\begin{pmatrix} b\cos\phi_{-2} \\ a\sin\phi_{-2} \end{pmatrix}=\begin{pmatrix} a^2b/\sqrt{a^4+b^4} \\ ab^2/\sqrt{a^4+b^4} \end{pmatrix}$$

$$=\mathbf{Q}\bullet\mathbf{r}(\phi_{-1}) \quad (11.18a) \qquad =\mathbf{Q}\bullet\mathbf{r}(\phi_{-2}) \quad (11.18b) \qquad =\mathbf{Q}\bullet\mathbf{r}(\phi_{-3}) \quad (11.18c)$$

$$\mathbf{r}(\phi_{-1})=\begin{pmatrix} a\cos\phi_0 \\ b\sin\phi_0 \end{pmatrix}=\begin{pmatrix} a/\sqrt{2} \\ b/\sqrt{2} \end{pmatrix} \qquad \mathbf{r}(\phi_0)=\begin{pmatrix} a\cos\phi_1 \\ b\sin\phi_1 \end{pmatrix}==\begin{pmatrix} ab/\sqrt{a^2+b^2} \\ ab/\sqrt{a^2+b^2} \end{pmatrix} \qquad \mathbf{r}(\phi_1)=\begin{pmatrix} a\cos\phi_2 \\ b\sin\phi_2 \end{pmatrix}=\begin{pmatrix} ab^2/\sqrt{a^4+b^4} \\ a^2b/\sqrt{a^4+b^4} \end{pmatrix}$$

Triads $\{\boldsymbol{r}_{k+1},\boldsymbol{r}_k,\boldsymbol{r}_{k-1}\}$ and $\{\boldsymbol{p}_{k+1},\boldsymbol{p}_k,\boldsymbol{p}_{k-1}\}$ of vectors $\boldsymbol{r}_k=\mathbf{r}(\phi_k)$ and $\boldsymbol{p}_k=\mathbf{p}(\phi_k)$ are given for $\phi_0=\pi/4$.

$$\mathbf{p}(\phi_k)=\begin{pmatrix} b\cos\phi_{k-1} \\ a\sin\phi_{k-1} \end{pmatrix} \qquad \mathbf{r}(\phi_k)=\begin{pmatrix} a\cos\phi_{k+1} \\ b\sin\phi_{k+1} \end{pmatrix} \qquad \begin{aligned} \cos\phi_k &= b^k/\sqrt{a^{2k}+b^{2k}}=\sin\phi_{-k} \\ \cos\phi_{-k} &= a^k/\sqrt{a^{2k}+b^{2k}}=\sin\phi_k \end{aligned} \qquad (11.19)$$

Each triad $\{\boldsymbol{r}_{k+1},\boldsymbol{r}_k,\boldsymbol{r}_{k-1}\}$ easily gives the tangent $\boldsymbol{v}_{k-1}=\mathbf{v}(\phi_{k-1})=\dot{\mathbf{r}}_{k-1}$ that contacts the $\mathbf{Q}$-ellipse at $\boldsymbol{r}_{k-1}$. An arc by $\boldsymbol{r}_k$ intersects $\boldsymbol{r}_{k+1}$ where $\boldsymbol{v}_{k-1}$ is perpendicular to $\boldsymbol{r}_{k+1}$ or $\boldsymbol{p}_{k+1}=\mathbf{p}(\phi_{k+1})$. (See Fig. 11.7a and exercises.)

So far the ellipse axes line up with the Cartesian coordinate axes of a standard page. Ellipses in other bases may be rotated, and certainly an orbit of an isotropic oscillator may choose any direction for its axes. The following general 2D quadratic form gives a rotated conic section (ellipse or hyperbola).

$$\begin{pmatrix} x & y \end{pmatrix} \bullet \begin{pmatrix} A & B \\ B & C \end{pmatrix} \bullet \begin{pmatrix} x \\ y \end{pmatrix} = 1 = \begin{pmatrix} x & y \end{pmatrix} \bullet \begin{pmatrix} Ax + By \\ Bx + Cy \end{pmatrix} = Ax^2 + 2Bxy + Cy^2 \quad \text{or:} \quad \mathbf{r} \bullet \mathbf{Q} \bullet \mathbf{r} = 1 \qquad (11.20)$$

(a) Basic $\mathbf{r}_k = \mathbf{r}(\phi_k)$ *or* $\mathbf{p}_k = \mathbf{p}(\phi_k)$ *triad around* $\phi_0 = 45°$

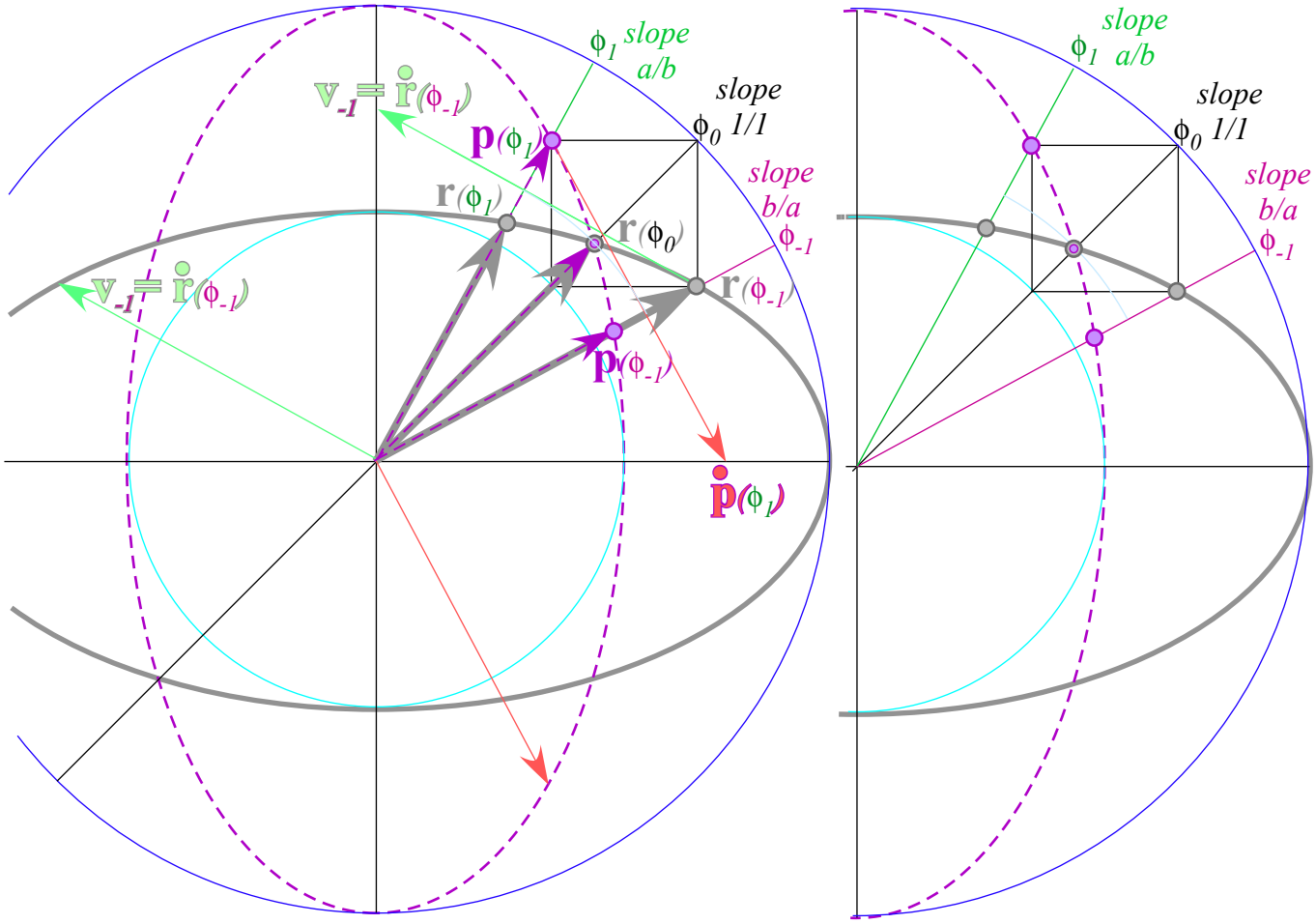

(b) Sequence of $\mathbf{r}_k = \mathbf{r}(\phi_k)$ *or* $\mathbf{p}_k = \mathbf{p}(\phi_k)$ *triads on* $\{\ldots \phi_2, \phi_1, \phi_0, \phi_{-1}, \phi_{-2}, \ldots\}$

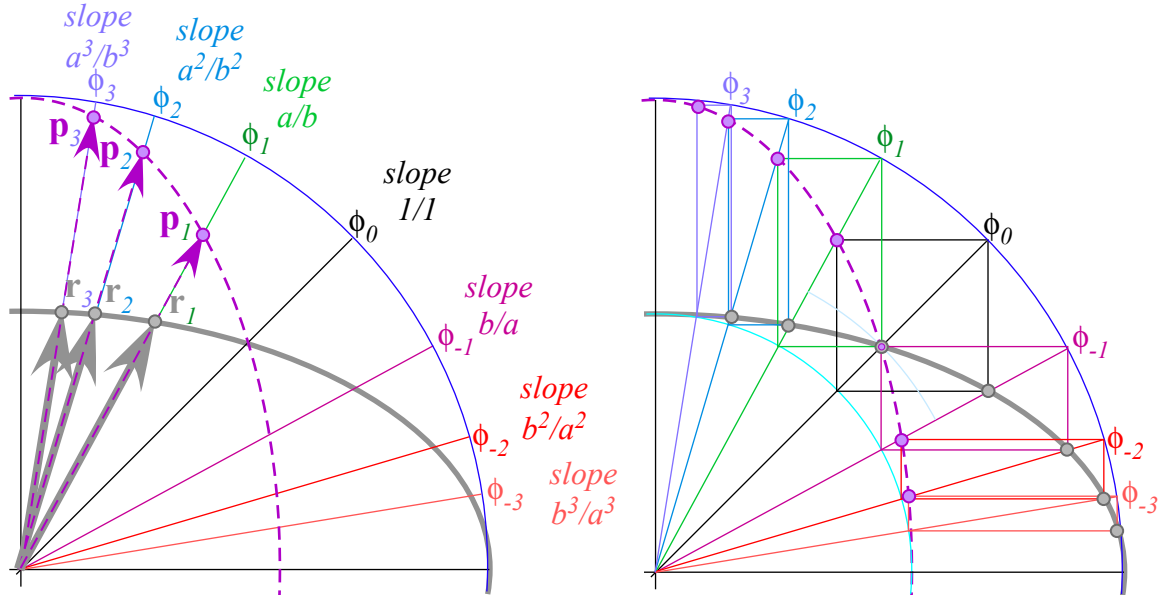

Fig. 11.7 Triad sequence geometry of radial position vector $\mathbf{r}(\phi_{n-1})$ *and tangent-perpendicular* $\mathbf{p}(\phi_{n+1})$.

However, all the relative geometric properties such as their tangent geometry are the same in all bases. It's abstract vector equation 1=**r•Q•r** looks the same in any coordinate base system, but the matrix components may include non-zero off-diagonal elements $B\neq 0$ that indicate it is a rotated ellipse.

Angular momentum and Kepler's law

The shape and rotational orientation of an isotropic oscillator orbit ellipse is constant with time. The cross product of **rxv** of position and velocity is also a constant of the motion by (11.5). (See App. 1.A.)

$$\mathbf{r}\times\mathbf{v} = r_x v_y - r_y v_x = a\cos\omega t\cdot(b\omega\cos\omega t) - a\sin\omega t\cdot(-b\omega\sin\omega t) = ab\cdot\omega \qquad (11.21)$$

The quantity $L=m$ **rxv** is called *orbital angular momentum*. It's conserved as mass m orbits.

$$L = m\,\mathbf{r}\times\mathbf{v} = m\left(r_x v_y - r_y v_x\right) = m\cdot ab\cdot\omega \qquad (11.22)$$

It means the area of **r+v** or **r-v** triangles, as discussed in Appendix 1.A, are constant on an orbit as indicated in Fig. 11.8 below. Area enclosed by **r** and **v** is proportional to the area $\pi\, ab$ of the whole orbit.

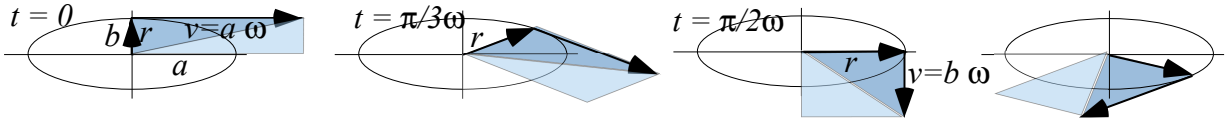

Fig. 11.8 Vector **r+v** *and* **r-v** *parallelogram and triangle areas are constant all during orbit.*

By (11.22), velocity at perigee $(x=0,y=b)$ is $v_b=L/mb=a\omega$. At apogee it slows to $v_a=L/ma=b\omega$. This is consistent with velocity formula (11.5b). Constant momentum relates to *Kepler's Law*: the radius **r**-vector sweeps the same area every second or every hour and equal time means equal area.

This is true since the triangle made of **r** and $d\mathbf{r}=\mathbf{v}\,dt$ has the same area $^1/_2\mathbf{rxv}\,dt = (L/m)dt$ for the same time interval dt. This law applies to any central force that is a function of radius r alone, not just the oscillator force $F=-k\cdot r$. This includes the Coulomb force $F=-k/r^2$, which is the only other force to have elliptical orbits that maintain their orientation.

The oscillator and Coulomb forces each have hidden symmetry beyond their Keplerian rotational isotropy that conserves angular momentum and this makes their orbits have simple geometric properties. This extra symmetry will be analyzed in units 4 and 5.

Flight of a stick: Introducing geometry of cycloids

If linear momentum and angular momentum are conserved they often do so together. As an example, we consider the flight of a rigid rod or stick in free space. Flying rods are treated in Sec. 6.4 of the rigid body

unit (Unit 6) but elementary aspects of rigid body motion are easy to derive and they display cycloid geometry that is useful for several classical mechanical phenomena. A mass m rotating on a circle of radius r with angular velocity ω has a linear tangential velocity $V=\omega\cdot r$ and kinetic energy $KE=\frac{1}{2}mV^2$. (Recall (9.10) for orbiting starlet.) An angular form is derived here again.

$$KE^{angular} = \varepsilon = \frac{1}{2}mV^2 = \frac{1}{2}mr^2\omega^2 = \frac{1}{2}I\cdot\omega^2 \qquad (11.23)$$

Circular orbiter angular momentum (from (11.22) above) takes an angular form, too.

$$P^{angular} = \Pi\cdot r = mV\cdot r = mr^2\omega = I\cdot\omega \qquad (11.24)$$

In each the point mass rotational inertia $I=mr^2$ replaces linear mass m while angular velocity ω replaces V.

A rod or lever of length ℓ rotating about one end is viewed as an integral from $r=0$ to $r=\ell$ of its mass points $dm=\rho\cdot dr$ each of infinitesimal inertia $dI=r^2dm=\rho\cdot r^2dr$. Density ρ is the rod's total mass M per length ℓ, and that is assumed to be uniform. Total inertia follows from taking the integral over its length.

$$I=\int dI=\int_0^{\ell}\rho\cdot r^2\,dr=\frac{1}{3}\rho\cdot\ell^3=\frac{1}{3}M\cdot\ell^2 \qquad \text{where: } \rho=M/\ell \qquad (11.25)$$

This inertial formula is true for two identical rods of length ℓ welded end-to-end and rotating about that point. Now mass M is that of the total system. In free space the straight welded rod will rotate naturally with constant angular velocity ω about the welded point at its center of mass and that center travels at a constant velocity V^{CM} until hit by an outside force.

Then free-space paths of each point on the rod, including its center-of-mass, are *generalized cycloids* such as are shown in Fig. 11.9. There are two dots on the rod (a red dot • and a green dot •) that follow *normal cycloids*. Each comes to a complete stop at a cycloid *cusp* (as green dot • is in the lower center of the figure) while the opposite dot is just reaching its maximum velocity (as red dot • is in the upper center of the figure). On left and (later) right sides of Fig. 11.9 is similar with rod flipped.

Imagine dot • and dot • are pieces of gum stuck to opposite sides of a tire (green circle of radius p in Fig. 11.9) rolling left-to-right along a line ("road") with rod CM point attached at tire center. A blue dot • on one end of the rod is initially above the green dot • (upper left of Fig. 11.9) while the rod's lower end has a violet dot • attached below the red dot • where the tire initially meets the road. Rod points outside tire radius (blue dot • and violet dot •) trace *curlate cycloids*. Inside points (CM and yellow dot •) trace *prolate cycloids*. The CM just follows a straight line at constant speed. Tire radius p depends on hit-height h above CM point where momentum impulse Π is delivered in Fig. 11.10. However, regardless of h, the CM point will travel at constant linear velocity $V=\Pi/M$ while the rod conserves linear momentum $\Pi=MV$.

Center of percussion, radius of gyration, and "sweet-spot"

Angular velocity ω relates to hit-height *h* factor in angular momentum $I\omega=\Lambda=\Pi h$ and to tire radius *p* where red dot • on tire comes to rest on road, and velocity $\omega\cdot p=\Pi h\cdot p/I$ due to rotation cancels velocity $V=\Pi/M$ due to translation. This gives relation $h\cdot p=I/M$. Rod inertia $I=\frac{1}{3}M\cdot\ell^2$ then gives relation $h\cdot p=\frac{1}{3}\ell^2$ between hit-height *h* and *radius p of percussion* for rod of radius ℓ. We call hit point *h* a "sweet-spot" for point P and *vice-versa*.

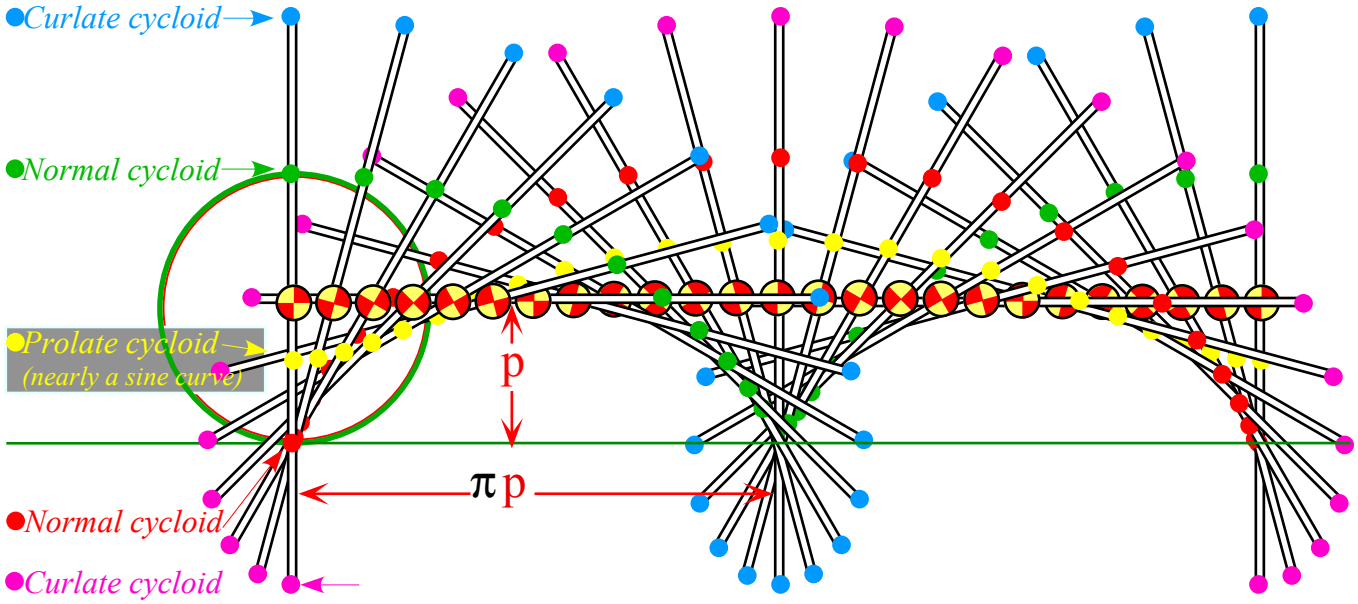

Fig. 11.9 Free flying rod of length L=2ℓ "rolls" left-to-right on "tire" of radius p.

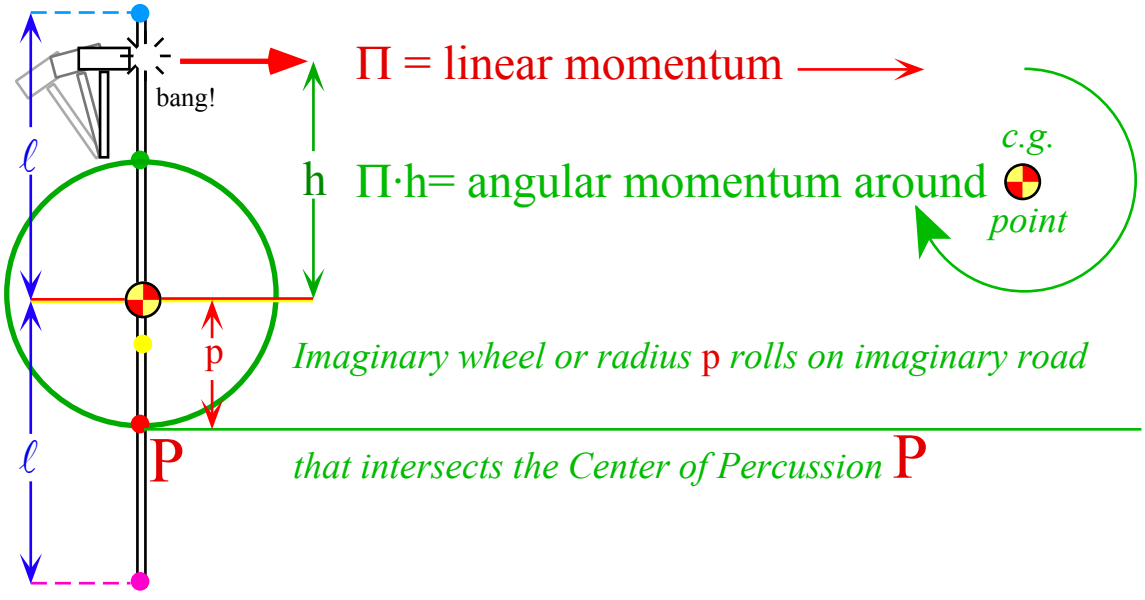

Fig. 11.10 Impulse hit-height h relates to rod radius ℓ and percussion radius p of rolling "tire."

If the hit-height h is zero then percussion radius p is infinite and all points of the rod follow straight parallel paths since there will then be zero rod rotational velocity ω and zero angular momentum $\Lambda=\Pi h$. Only linear velocity $V=\Pi/M$ would be nonzero then. If the hit-height h is equal to ℓ (the maximum practical value of h is the radius ℓ of rod) then the percussion radius is $p=\ell/3$, its minimum practical value.

Reducing h increases p proportionally. The two are equal at the value $p=\ell/\sqrt{3}=h=0.866\ell$ which is called the *radius of gyration* of the rod. Reducing hit-height h further to $\ell/2$ and $\ell/3$ increases the percussion radius p to $p=2\ell/3$ and $p=\ell$, respectively. The percussion point is where you can hold the lever and feel the very least recoil during the hit. In fact, the dynamics at a normal cycloid cusp point at radius p in Fig. 11.9 amounts to a gentle tug *along* the lever but no force perpendicular to it.

Baseball bats are made thicker at the hitting end to accommodate h and p points further from the ends than allowed by $p=h=0.866\ell$. Cricket bats, on the other hand, seem to be more like sticks.

Exercise 1.11.1

Quadratic form matrices are generally non-diagonal $\mathbf{Q}=\begin{pmatrix} A & B \\ B & D \end{pmatrix}$. If $\mathbf{Q}$ has positive eigenvalues $1/a^2$ and $1/b^2$ its form is called *positive definite* and $\mathbf{r}\bullet\mathbf{Q}\bullet\mathbf{r}=1$ gives an ellipse rotated by angle θ with radii a and b. So does $\mathbf{r}\bullet\mathbf{Q}^{-1}\bullet\mathbf{r}=1$.

(a) Derive relations between matrix parameters $\{A,B,D\}$ and ellipse parameters $\{a,b,\theta\}$. (Hint: Start with diagonal matrix and rotate it to $\mathbf{Q}'=\mathbf{R}\cdot\mathbf{Q}\cdot\mathbf{R}^{-1}$ by applying rotation transformation matrices $\mathbf{R}=\begin{pmatrix} \cos\theta & -\sin\theta \\ \sin\theta & \cos\theta \end{pmatrix}$ and $\mathbf{R}^{-1}=\begin{pmatrix} \cos\theta & \sin\theta \\ -\sin\theta & \cos\theta \end{pmatrix}$.)

(b) Show Trace$\mathbf{Q}$ and det$\mathbf{Q}$ (or Trace$\mathbf{Q}^{-1}$ and det$\mathbf{Q}^{-1}$) are invariant to θ and relate them to conserved quantities such as total energy $E=\frac{1}{2}m\dot{\mathbf{r}}\bullet\dot{\mathbf{r}}+\frac{1}{2}m\omega^2\mathbf{r}\bullet\mathbf{r}$ and orbital momentum $\ell=|m\mathbf{r}\times\dot{\mathbf{r}}|$ of isotropic 2D harmonic oscillator orbit elliptic orbit $\mathbf{r}(t)$ in (11.5). Could the energy or momentum of an isotropic 2D HO orbit depend on orientation angle θ? How or why not?

(c) Suppose $\mathbf{Q}$'s eigenvalues were $1/a^2$ and $-1/b^2$. What curve is $\mathbf{r}\bullet\mathbf{Q}\bullet\mathbf{r}=1$? Plot for $a=1=b$ and θ = 45°.

Exercise1.11.2

Recall Fig. 11.7 geometric sequence $\{\mathbf{r}_{-3},\mathbf{r}_{-2},\mathbf{r}_{-1},\mathbf{r}_0,\mathbf{r}_1,\mathbf{r}_2,\mathbf{r}_3,\ldots\}$ of ellipse radii $\mathbf{r}_k=\mathbf{r}(\phi_k)$ and perpendicular-to-tangents $\mathbf{p}_{k+2}=\mathbf{Q}\bullet\mathbf{r}_k$ defined by quadratic forms $\mathbf{r}_k\bullet\mathbf{Q}\bullet\mathbf{r}_k=1=\mathbf{p}_k\bullet\mathbf{Q}^{-1}\bullet\mathbf{p}_k$ by $\mathbf{Q}=\begin{pmatrix} b/a & 0 \\ 0 & a/b \end{pmatrix}$. (Ellipse radii had $ab=1$ and 0th sequence slope was $\tan\phi_0=1$ ($\phi_0=\pi/4$) but other values work as well.)

(a) Construct super-imposed $\mathbf{r}$-ellipse and $\mathbf{p}$-ellipse with at least seven vectors each for $a/b=2$ (done in class) and $a/b=5/4$. Give the vectors $\mathbf{r}_k$ you draw algebraically (in terms of a and b) for $-2\le k\le 2$ and check $k=2$ cases numerically with geometry.

(b) Verify duality relations: $\mathbf{r}_{k-1}\bullet\mathbf{p}_{k+1}=1$ and $\dot{\mathbf{r}}_{k-1}\bullet\mathbf{p}_{k+1}=0=\mathbf{r}_{k-1}\bullet\dot{\mathbf{p}}_{k+1}$. (For time derivatives let $\omega=1$.)

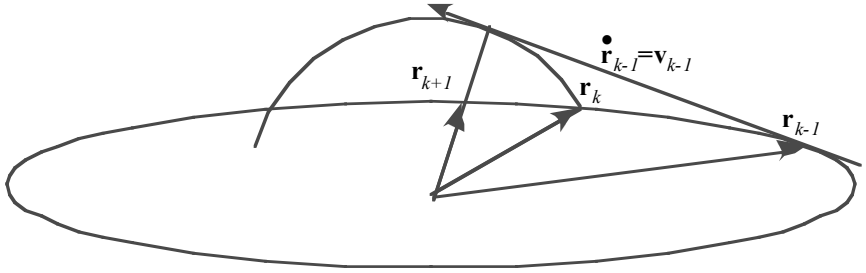

(c) The text noted that a ellipse tangent $\mathbf{v}_{k-1}=\mathbf{v}(\phi_{k-1})=\dot{\mathbf{r}}_{k-1}$ at $\mathbf{r}_{k-1}$ is also tangent to a circular arc $C_{k\ to\ k+1}$ swept by radius $|\mathbf{r}_k|$ from the tip of $\mathbf{r}_k$ to where $C_{k\ to\ k+1}$ is perpendicular the $\mathbf{r}_{k+1}$-line. Show this implies a relation

$$\mathbf{r}_{k-1}\bullet\hat{\mathbf{r}}_{k+1}=|\mathbf{r}_k|.\text{(Notation } \hat{\mathbf{r}}_{k+1} \text{ denotes unit vector: } |\hat{\mathbf{r}}_{k+1}|=1)$$

Verify this algebraically and geometrically for the case $k=-1$ and $k=0$ using vectors you have derived. Use the result to construct tangents $\mathbf{v}_k$ contacting each radius $\{\mathbf{r}_{-3}, \mathbf{r}_{-2}, \mathbf{r}_{-1}, \mathbf{r}_0, \mathbf{r}_1, \mathbf{r}_2, \mathbf{r}_3,\ldots\}$ on **r**-ellipse. Place the tangent vectors in **r**-ellipse.

Chapter 12. Velocity vs momentum functions: Lagrange vs Hamilton

Relating energy ellipses in velocity and momentum space

The ellipse in Fig. 5.1 is skinny and difficult to see. To better view multiple collisions, the v_1-v_2 axes are rescaled into "quasi-velocities" $V_k=v_k\sqrt{m_k}$ so the ellipse forms into a nice circle in Fig. 5.2.

$$KE=\tfrac{1}{2}(m_1v_1^2+m_2v_2^2)=\tfrac{1}{2}(V_1^2+V_2^2) \text{ where: } V_1=(m_1)^{1/2}v_1 \text{ and: } V_2=(m_2)^{1/2}v_2 \qquad (12.1)$$

The half-power mass scale is helpful. A full power m_k-scale converts velocity v_k to momentum p_k.

$$KE=\tfrac{1}{2}(m_1v_1^2+m_2v_2^2)=\tfrac{1}{2}\left(\frac{p_1^2}{m_1}+\frac{p_2^2}{m_2}\right) \text{ where: } p_1=m_1v_1 \text{ and: } p_2=m_2v_2 \qquad (12.2)$$

Geometry of a **p**-ellipse is just a flip of the **v**-ellipse, but there are compelling algebraic reasons for dealing with such alternative functions. In fact two of these functions have famous names attached.

Lagrangian, Estrangian, and Hamiltonian functions

An energy that is an explicit function of *velocities* is called a *Lagrangian function L=L(v_k..)*.

$$L(v_k\ldots)=\tfrac{1}{2}(m_1v_1^2+m_2v_2^2+\ldots)=L(\mathbf{v}...) \qquad (12.3)$$

An energy that is an explicit function of *momenta* is called a *Hamiltonian function H=H(p_k..)*.

$$H(p_k\ldots)=\tfrac{1}{2}\left(\frac{p_1^2}{m_1}+\frac{p_2^2}{m_2}+\ldots\right)=H(\mathbf{p}...) \qquad (12.4)$$

A compromising function like (12.1) has no famous name so we'll call it an *Estrangian E=E(V_k..)*.

$$E(V_k\ldots)=\tfrac{1}{2}(V_1^2+V_2^2+\ldots)=E(\mathbf{V}\ldots) \qquad (12.5)$$

While all these functions may have the same numerical value for a given situation, the have quite different functional dependence. To emphasize this let us write our first equations of (non)-motion.

$$\frac{\partial L}{\partial p_k}\equiv 0\equiv\frac{\partial E}{\partial p_k} \quad (12.6a) \qquad \frac{\partial H}{\partial v_k}\equiv 0\equiv\frac{\partial E}{\partial v_k} \quad (12.6b) \qquad \frac{\partial L}{\partial V_k}\equiv 0\equiv\frac{\partial H}{\partial V_k} \quad (12.6a)$$

The first two for L and H say that L has no *explicit* **p**-dependence and H has no *explicit* **v**-dependence. L may still vary if **p** varies but L is not *defined* by **p** and the same for H and **v**. Calculus distinguishes *total* derivatives $\frac{dL}{dz}$ or $\frac{dH}{dz}$ from *partial* derivatives $\frac{\partial L}{\partial z}$ or $\frac{\partial H}{\partial z}$ and begins by defining *differential chain rule* sums.

$$dL=\frac{\partial L}{\partial v_1}dv_1+\frac{\partial L}{\partial v_2}dv_2+\cdots \quad (12.7a) \qquad dH=\frac{\partial H}{\partial p_1}dp_1+\frac{\partial H}{\partial p_2}dp_2+\cdots \quad (12.7a)$$

Then L (or H) varies with any variable z such as v_k, p_k, or time t according to *derivative chain rule* sums.

$$\frac{dL}{dz}=\frac{\partial L}{\partial v_1}\frac{dv_1}{dz}+\frac{\partial L}{\partial v_2}\frac{dv_2}{dz}+\cdots \quad (12.7a) \qquad \frac{dH}{dz}=\frac{\partial H}{\partial p_1}\frac{dp_1}{dz}+\frac{\partial H}{\partial p_2}\frac{dp_2}{dz}+\cdots \quad (12.7a)$$

(Imagine *L(***v**...*)* is "married" to **v** and *H (***p**...*)* to **p**. Dots denote coordinates and time discussed later.)

Neither may use another's dependents without legal difficulty! Geometry helps clarify this below.

L, E, and H ellipse geometry

A Lagrangian ellipse plot *const.* = $L(\mathbf{v})$ in Fig. 12.1a is similar to the superball collision diagram in Fig. 5.1. It is to be compared with the corresponding Estrangian ellipse (circle) plot *const.* = $E(\mathbf{V})$ in Fig. 12.1b and the Hamiltonian ellipse plot *const.* = $H(\mathbf{p})$ in Fig. 12.1c. COM and collision line slopes are compared.

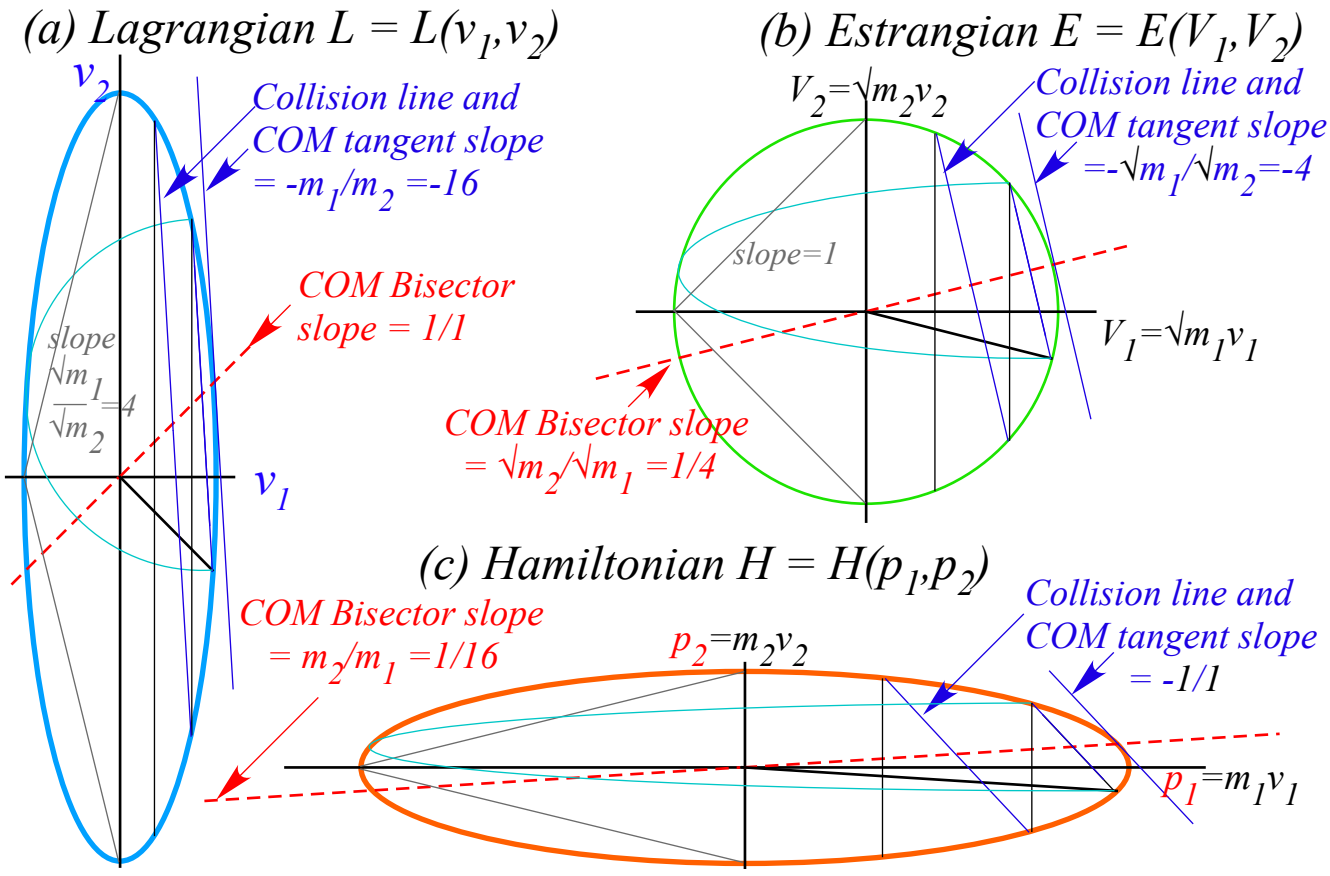

Fig. 12.1 KE ellipse functions related by scale. (a) L in velocity v_k space. (b) E in V_k. (c) H in p_k.

Functions *L*, *E*, and *H* are quadratic forms of vectors **v**, **V=R•v**, and **p=M•v=R²•v**, respectively.

$$L(\mathbf{v}) = \tfrac{1}{2}\,\mathbf{v}\bullet\mathbf{M}\bullet\mathbf{v} \quad (12.8a) \qquad E(\mathbf{V}) = \tfrac{1}{2}\,\mathbf{V}\bullet\mathbf{1}\bullet\mathbf{V} \quad (12.8b) \qquad H(\mathbf{p}) = \tfrac{1}{2}\,\mathbf{p}\bullet\mathbf{M}^{-1}\bullet\mathbf{p} \quad (12.8c)$$

The corresponding scaling matrices are powers of the root-mass matrix: $\mathbf{R}=\begin{pmatrix}\sqrt{m_1} & 0\\ 0 & \sqrt{m_2}\end{pmatrix}$

$$\mathbf{M}=\begin{pmatrix}m_1 & 0\\ 0 & m_2\end{pmatrix}=\mathbf{R}^2 \qquad \mathbf{1}=\begin{pmatrix}1 & 0\\ 0 & 1\end{pmatrix} \qquad \mathbf{M}^{-1}=\begin{pmatrix}1/m_1 & 0\\ 0 & 1/m_2\end{pmatrix}=\mathbf{R}^{-2} \quad (12.9)$$

The 2nd power rescaling $\mathbf{M}=\mathbf{R}^2$ mass matrix maps *L(v)* space (a) into Hamiltonian *H(p)* space (c).

The **p**-to-**v** tangent-normal mapping is analogous to **r**-to-**p** mapping in Fig. 11.6 as displayed in a Fig. 12.2c that overlaps parts (a) and (c) of Fig. 12.1. Velocity **v** is a **p**-space gradient operation $\nabla_p H = \mathbf{v}$ and thus normal to *H*-ellipse, and vice-versa for the normal $\mathbf{p}=\nabla_v L$ to the *L*-ellipse. Matrix notation is given, too.

$$\nabla_v L = \mathbf{p} = \frac{\partial L}{\partial \mathbf{v}} = \mathbf{M}\bullet\mathbf{v} \qquad (12.10a)$$

$$\nabla_p H = \mathbf{v} = \frac{\partial H}{\partial \mathbf{p}} = \mathbf{M}^{-1}\bullet\mathbf{p} \qquad (12.10b)$$

$$\begin{pmatrix} \frac{\partial L}{\partial v_1} \\ \frac{\partial L}{\partial v_2} \end{pmatrix} = \begin{pmatrix} p_1 \\ p_2 \end{pmatrix} = \begin{pmatrix} m_1 & 0 \\ 0 & m_2 \end{pmatrix} \begin{pmatrix} v_1 \\ v_2 \end{pmatrix} \qquad (12.10c)$$

$$\begin{pmatrix} \frac{\partial H}{\partial p_1} \\ \frac{\partial H}{\partial p_2} \end{pmatrix} = \begin{pmatrix} v_1 \\ v_2 \end{pmatrix} = \begin{pmatrix} m_1^{-1} & 0 \\ 0 & m_2^{-1} \end{pmatrix} \begin{pmatrix} p_1 \\ p_2 \end{pmatrix} \qquad (12.10d)$$

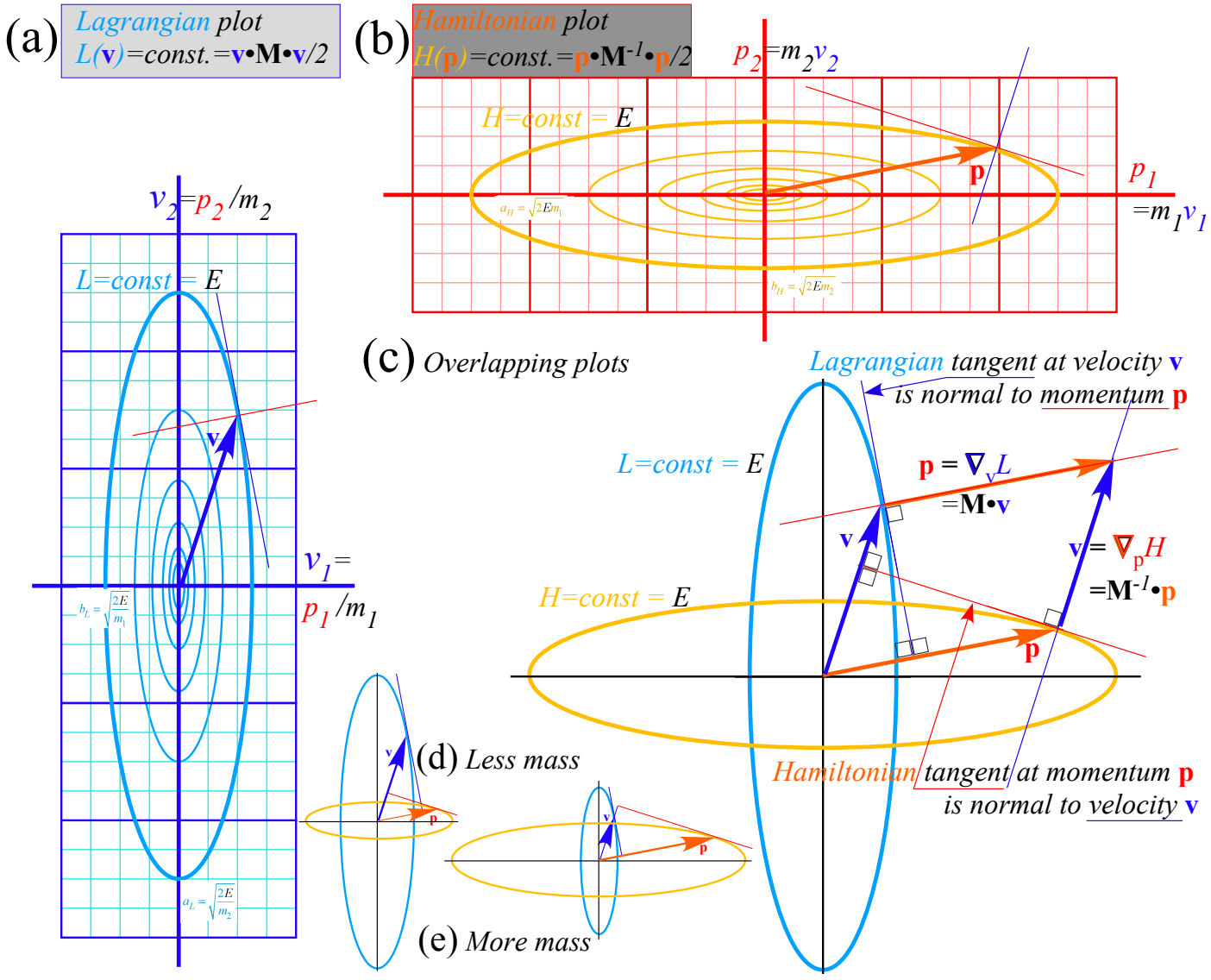

Fig. 12.2 Tangent-normal mapping between (a) Lagrangian L(v) space and (b) H(p) space.
If mass increases s-times then L-ellipse radii become s times H-ellipse radii. (d) s=1/2, (e) s=2.

Fig. 12.2 is a top view of *L*(**v**)*-vs-***v** and *H*(**p**)*-vs-***p** plots. Side views are shown and discussed below.

Legendre contact transformations

Given mapping $\mathbf{p}=\mathbf{M}\bullet\mathbf{v}$ or inverse $\mathbf{v}=\mathbf{M}^{-1}\bullet\mathbf{p}$, it might appear that either quadratic form $L(\mathbf{v})=\frac{1}{2}\mathbf{v}\bullet\mathbf{M}\bullet\mathbf{v}$ or $H(\mathbf{p})=\frac{1}{2}\mathbf{p}\bullet\mathbf{M}^{-1}\bullet\mathbf{p}$ may be written simply as $\frac{1}{2}\mathbf{v}\bullet\mathbf{p}$ or $\frac{1}{2}\mathbf{p}\bullet\mathbf{v}$. This is correct numerically but its calculus is not. Instead, it is $\mathbf{p}\bullet\mathbf{v}-\frac{1}{2}\mathbf{p}\bullet\mathbf{v}=\mathbf{p}\bullet\mathbf{v}-H$ or else $\mathbf{p}\bullet\mathbf{v}-\frac{1}{2}\mathbf{p}\bullet\mathbf{v}=\mathbf{p}\bullet\mathbf{v}-L$ that gives correct *derivatives*. This results in the *Legendre contact transformation* between *H(p)* and *L(v)* expressed by the following identical equations.

$$L(\mathbf{v})=\mathbf{p}\bullet\mathbf{v}-H(\mathbf{p}) \quad (12.11a) \qquad H(\mathbf{p})=\mathbf{p}\bullet\mathbf{v}-L(\mathbf{v}) \quad (12.11b)$$

They give correct partial derivatives with zero for $\frac{\partial L}{\partial p}$ and $\frac{\partial H}{\partial v}$ according to definitions in (12.6), as follows.

$$\frac{\partial L}{\partial \mathbf{p}}=\frac{\partial}{\partial \mathbf{p}}\mathbf{p}\bullet\mathbf{v}-\frac{\partial H}{\partial \mathbf{p}} \quad (12.12a) \qquad \frac{\partial H}{\partial \mathbf{v}}=\frac{\partial}{\partial \mathbf{v}}\mathbf{p}\bullet\mathbf{v}-\frac{\partial L}{\partial \mathbf{v}} \quad (12.12b)$$

$$0=\mathbf{v}-\frac{\partial H}{\partial \mathbf{p}} \qquad 0=\mathbf{p}-\frac{\partial L}{\partial \mathbf{v}}$$

The results are the *first Hamilton equation* and the *first Lagrange definition* (Recall (12.10). Reversing **p** and **v** derivatives gives them again in reverse order but quite consistently.

$$\frac{\partial L}{\partial \mathbf{v}}=\frac{\partial}{\partial \mathbf{v}}\mathbf{p}\bullet\mathbf{v}-\frac{\partial H}{\partial \mathbf{v}} \quad (12.12c) \qquad \frac{\partial H}{\partial \mathbf{p}}=\frac{\partial}{\partial \mathbf{p}}\mathbf{p}\bullet\mathbf{v}-\frac{\partial L}{\partial \mathbf{p}} \quad (12.12d)$$

$$=\mathbf{p}-0 \qquad =\mathbf{v}-0$$

Side-view sketches of eqs. (12.11) and (12.12) are given in Fig. 12.3a-b and Fig. 12.4a-b below.

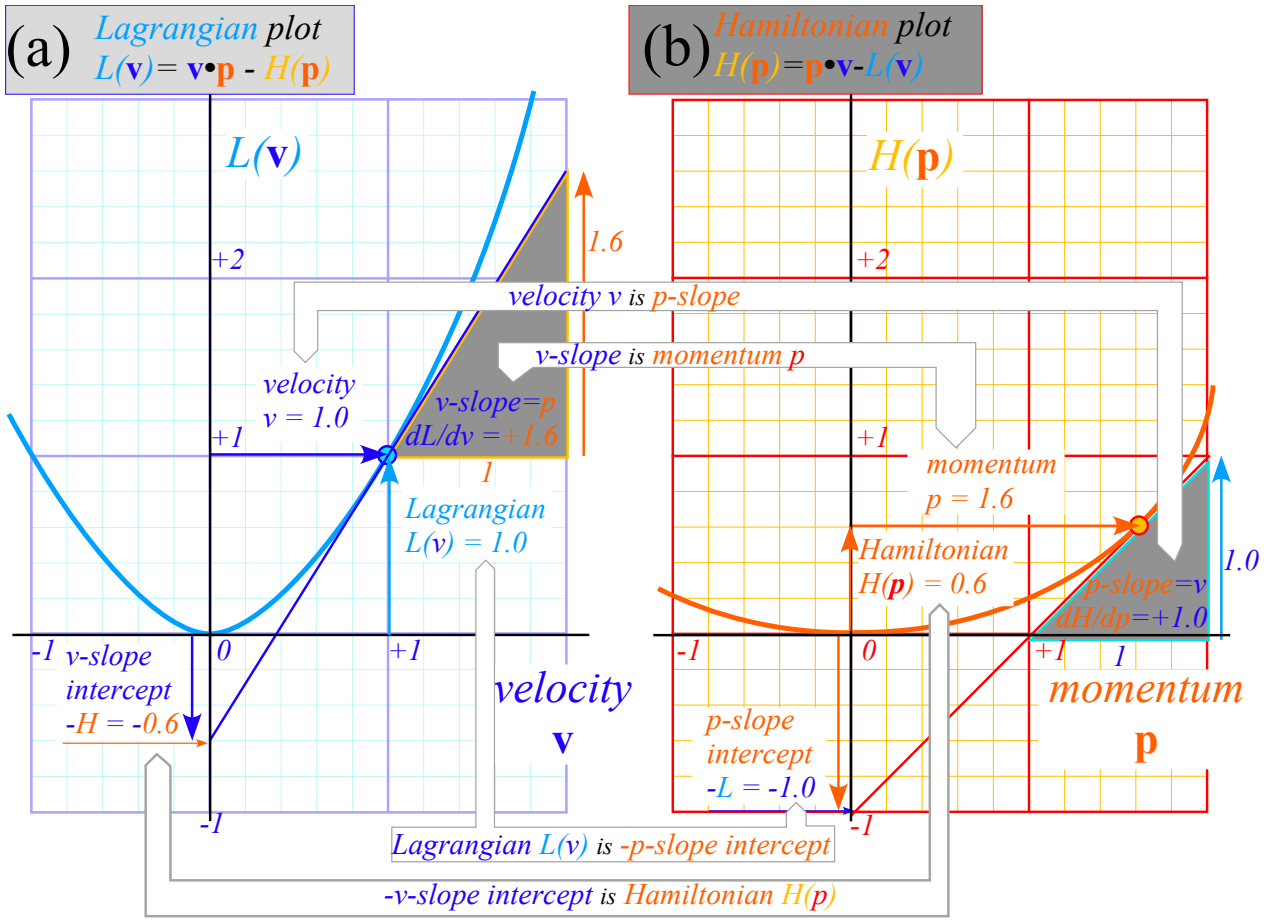

*Fig 12.3 Geometry of Legendre contact transformation relating (a) L(**v**)-vs-**v** and (b) H(**p**)-vs-**p** plots.*

Extreme geometry of contact transformations

Contact transformations are among the most enduring and fundamental ideas in either classical or modern physics. Yet few texts on these subjects explain them adequately, if at all. Most can't even tell why "contact" appears in their name. Our explanation revolves around explicit-function issues involving equations (2.12):

"*L*(**v**...) is *not* function of **p**, *H*(**p**...) is *not* function of **v**, yet *L*(**v**...), *H*(**p**...), **p**, and **v** *are all related!*"

There is method in this madness! One should learn how these ideas "contact" so much of physics.

The term "contact" refers to a line or curve *touching* or being *tangent-to* another curve. It is opposite to more common cases of *crossing* or being *secant-to* another curve (swordlike). Examples in Fig. 12.4 are based on Fig. 12.3. Lagrangian side (a) shows secant lines $L(\mathbf{v}) = p \bullet v - H$ all of slope p but decreasing intercept $-H(v_{-2}) > -H(v_{-1}) > \ldots$ tied to increasing velocity points $v_{-2} > v_{-1} > \ldots > v_0$ leading to a unique tangent to the $L(\mathbf{v})$ curve at *tangent contact point* v_0 that has a max-value $H(v_0)$ of H. At that point the Hamiltonian H has *no 1st order variation* with respect to velocity, that is, H has *zero 1st v-derivative*.

$$\frac{\partial H}{\partial v} = 0 \text{ at each point } v = \frac{\partial H}{\partial p} \text{ of } L(v) \text{ with slope } p = \frac{\partial L}{\partial v} \qquad (12.13a)$$

Thus H loses its explicit v-dependence at each tangent point but $H(p)$ *does* depend on its slope p. So also does L lose its explicit p-dependence at each tangent point but $L(v)$ *does* depend on that tangent slope v.

$$\frac{\partial L}{\partial p} = 0 \text{ at each point } p = \frac{\partial L}{\partial v} \text{ of } H(p) \text{ with slope } v = \frac{\partial H}{\partial p} \qquad (12.13b)$$

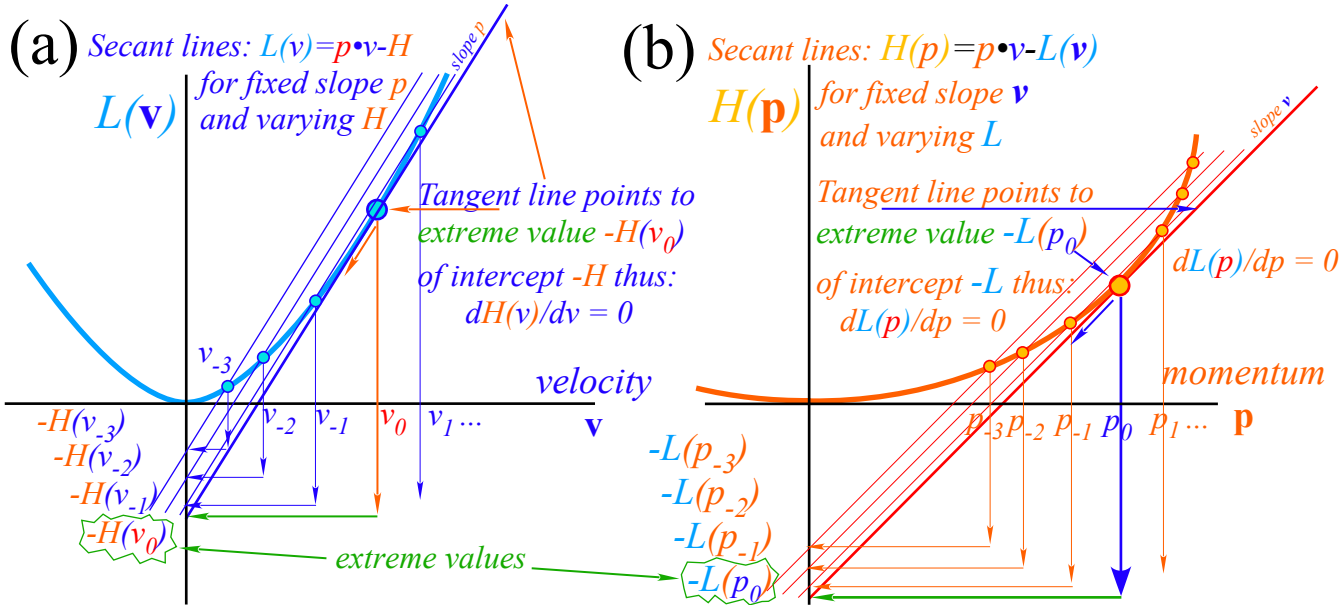

Fig 12.4 Geometry of explicit dependence. (a) $L(v)$ loses p dependence. (b) $H(p)$ loses v dependence.

Let's examine more general examples of contact mapping that help clarify its beautiful structure and utility.

General contact transformation geometry

Consider now a contact transformation that relates to some classical physics or to some modern physics while reviewing some sophomore physics. It involves the geometry of volcanic plumes on *Io* or atomic clouds rising and falling in Earth gravity as sketched in Fig. 12.5a or b, respectively. Each is modeled by a parabolic trajectory fountain in Fig. 12.5c that you may have studied in sophomore physics.

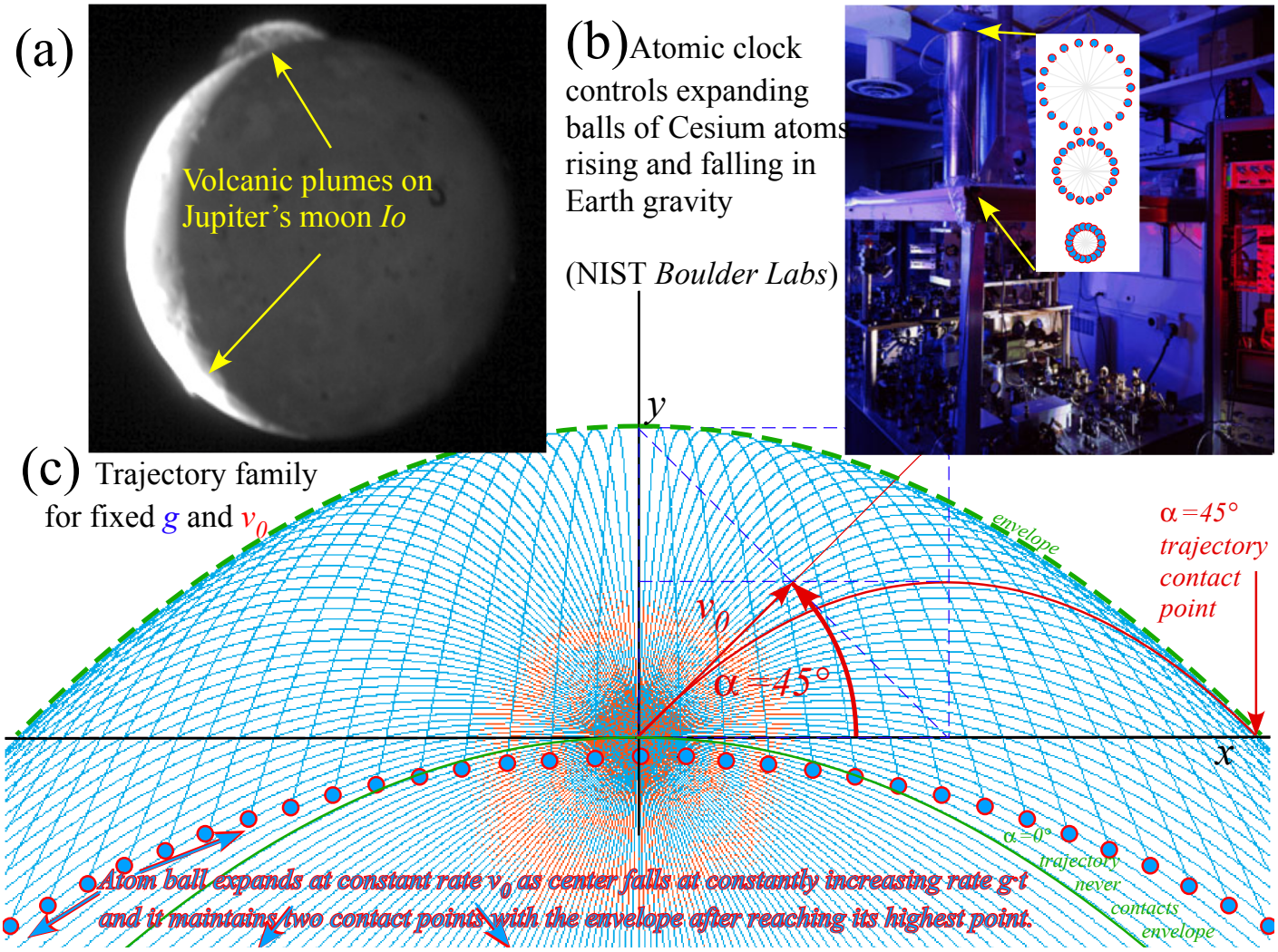

Fig. 12.5 Modeling (a) Io volcano and (b) Atomic clock by (c) trajectories of initial velocity v_0 and angle α.

Initial position *x(0)=0=y(0)* and velocity $\mathbf{v}(0)=\dot{\mathbf{x}}(0)$ below lead to a fixed-*g* trajectory $\mathbf{x}(t)=(x(t),y(t))$.

$$x(t)=(v_0\cos\alpha)t \qquad (12.14a) \qquad y(t)=(v_0\sin\alpha)t-\frac{1}{2}gt^2 \qquad (12.14b)$$

$$\dot{x}(0)=v_x(0)=v_0\cos\alpha \qquad \dot{y}(0)=v_y(0)=v_0\sin\alpha\,.$$

The *x(t)*-solution has time $t=x/(v_0\cos\alpha)$ to put in *y(t)* and get each trajectory *y(x)* plotted in Fig. 12.5c.

$$y(x)=\frac{v_0\sin\alpha}{v_0\cos\alpha}x-\frac{gx^2}{2{v_0}^2\cos^2\alpha}=x\tan\alpha-\frac{gx^2}{2{v_0}^2\cos^2\alpha}\,. \qquad (12.14c)$$

Each trajectory is a zero value of a *Contact Generating Solution* $S(v_0, \alpha : x, y)$ given by

$$S\left(v_0,\alpha:x,y\right)=-y+x\tan\alpha-\frac{gx^2}{2{v_0}^2\cos^2\alpha}=0\,. \qquad (12.15)$$

$S(v_0, \alpha : x, y)$ maps initial value point $(v_0=1, \alpha=45°)$ in Fig. 12.6 onto red trajectory curve $y(x)$ in Fig. 12.5c. A horizontal line of points (same v_0 but α varies) fills a region of $y(x)$ space with the v_0-trajectory family.

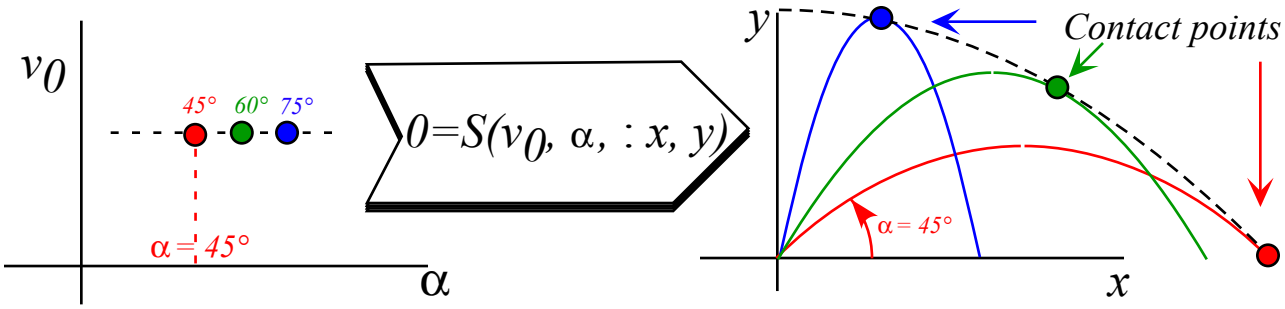

Fig. 12.6 Contact transformation maps point (v_0, α) *to trajectory of initial velocity* v_0 *and angle* α.

Envelopes of the v_0-trajectory region contain extremal *contact points* with each trajectory. Varying α at such a point does not change S so 1st α-derivative of S is zero, quite analogous to zero derivatives in (12.13).

$$\frac{\partial S\left(v_0,\alpha:x,y\right)}{\partial\alpha}=0 \qquad (12.16a)$$

$$x\frac{\partial\tan\alpha}{\partial\alpha}-\frac{gx^2}{2{v_0}^2}\frac{\partial\cos^{-2}\alpha}{\partial\alpha}=0=\frac{x}{\cos^2\alpha}-\frac{gx^2}{2{v_0}^2}\frac{2\sin\alpha}{\cos^3\alpha} \qquad (12.16b)$$

Solving this equation relates the x-value and the α-value of each contact point for a given fixed v_0.

$$\tan\alpha=\frac{{v_0}^2}{gx}\,,\quad \text{or:}\quad x=\frac{{v_0}^2}{g\tan\alpha}\,. \qquad (12.16c)$$

If you put this relation into generating function (12.15), it gives the contact envelope function $y_{env}(x)$.

$$y_{env}(x)=x\tan\alpha-\frac{gx^2}{2{v_0}^2}\left(1+\tan^2\alpha\right)\Rightarrow y_{env}(x)=x\frac{{v_0}^2}{gx}-\frac{gx^2}{2{v_0}^2}\left(1+\frac{{v_0}^4}{g^2x^2}\right)=\frac{{v_0}^2}{2g}-\frac{gx^2}{2{v_0}^2}\,. \qquad (12.17)$$

It is the dashed parabolic curve in Fig. 12.5-6 contacting each and (almost) every parabolic trajectory from above. The envelope happens to share the shape of the $(\alpha=0)$-trajectory hilited in green in Fig. 12.5. That is the single trajectory that never contacts the envelope. Do exercises to see more of this lovely geometry!

A generic general contact transformation $S(x,y:X,Y)$ shown in Fig. 12.7 maps points (x_k, y_k) in (x, y)-space into points (X_k, Y_k) in (X, Y)-space so function $y(x)$ is contact-transformed to function $Y(X)$ there. Such a transformation can occur from one curved set of points to another in the *same* space as in Huygen's wavelet view of wave propagation: each wavefront curve at one instant is a contact transform of a wavefront at another time. (Presumably, it's an *earlier* time but quantum waves *are* time reversible.) Contact transform geometry plays such a big role in connecting (contacting) classical and modern physics as we'll see.

Contact transforms are key to classical thermodynamics. For example, *internal energy U(S,V)* is defined as a function of entropy *S* and volume *V*. A new function *enthalpy H(S,P)* depends on entropy and *pressure P*. It is a Legendre transform *H(S,P)=P·V+U* of energy *U(S,V)* to new variable $P = -(\frac{\partial U}{\partial V})_S$. Except for ±signs, it's our Hamiltonian *H(p)=p·v-L(v)* from Lagrangian *L(v)* to new variable momentum $p = (\frac{\partial L}{\partial v})_x$.

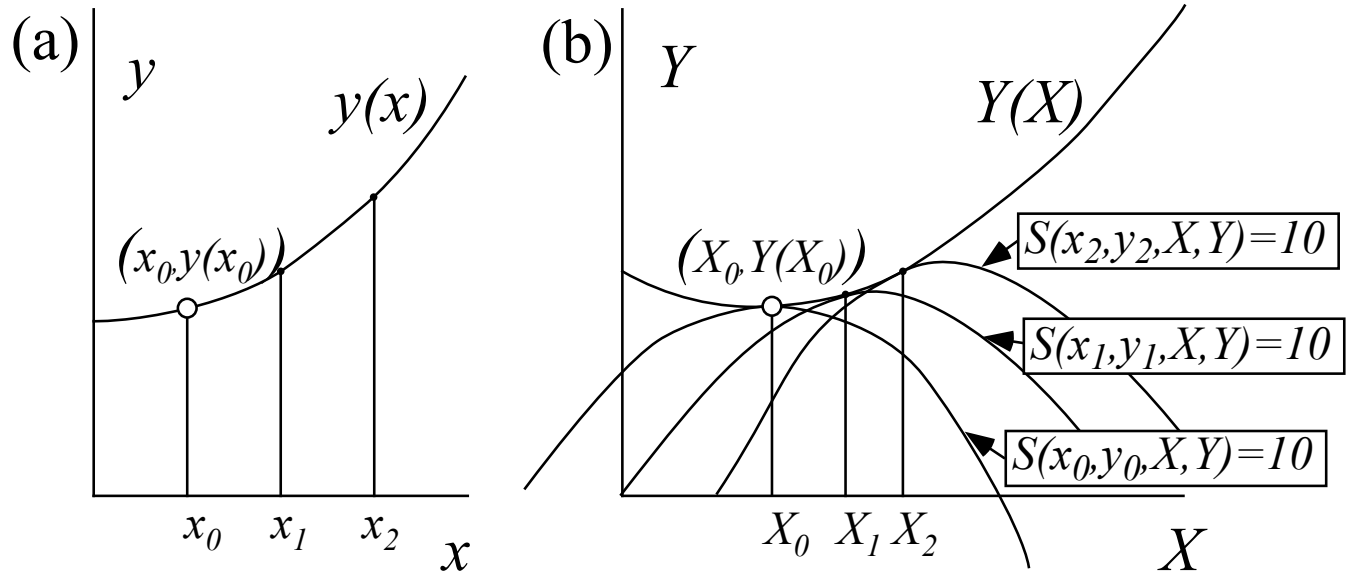

Fig. 12.7 General contact transformation S(x,y:X,Y) maps each point (x_k, y_k) to a contact point (X_k,Y_k).

Let us return briefly to the Legendre-Lagrangian-Hamiltonian relation (12.11) by comparing it's geometry in Fig. 12.8 to the generic case in Fig. 12.7. The general case makes contacts using curved tangents. Legendre uses straight line tangents and is thus easily invertible as shown below in Fig. 12.9 and before in Fig. 12.3.

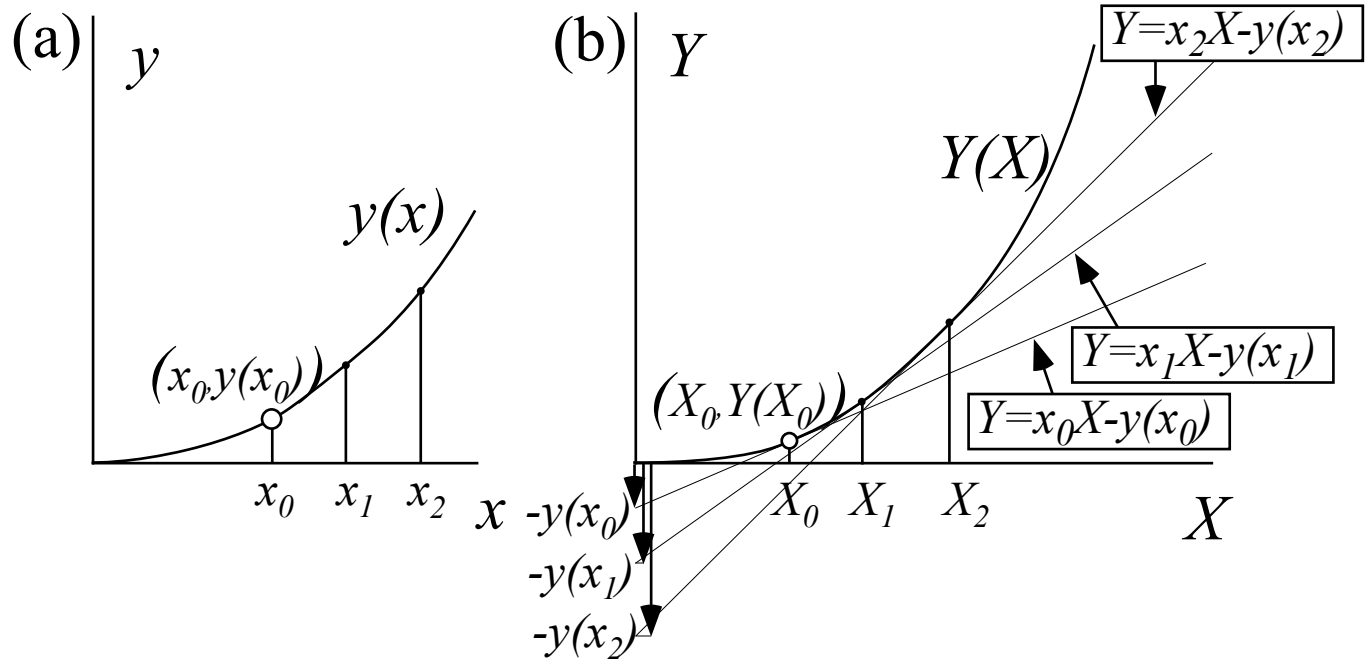

Fig. 12.8 Legendre contact transform S(x,y:X,Y) maps each point (x_k, y_k) to a contact point (X_k,Y_k).

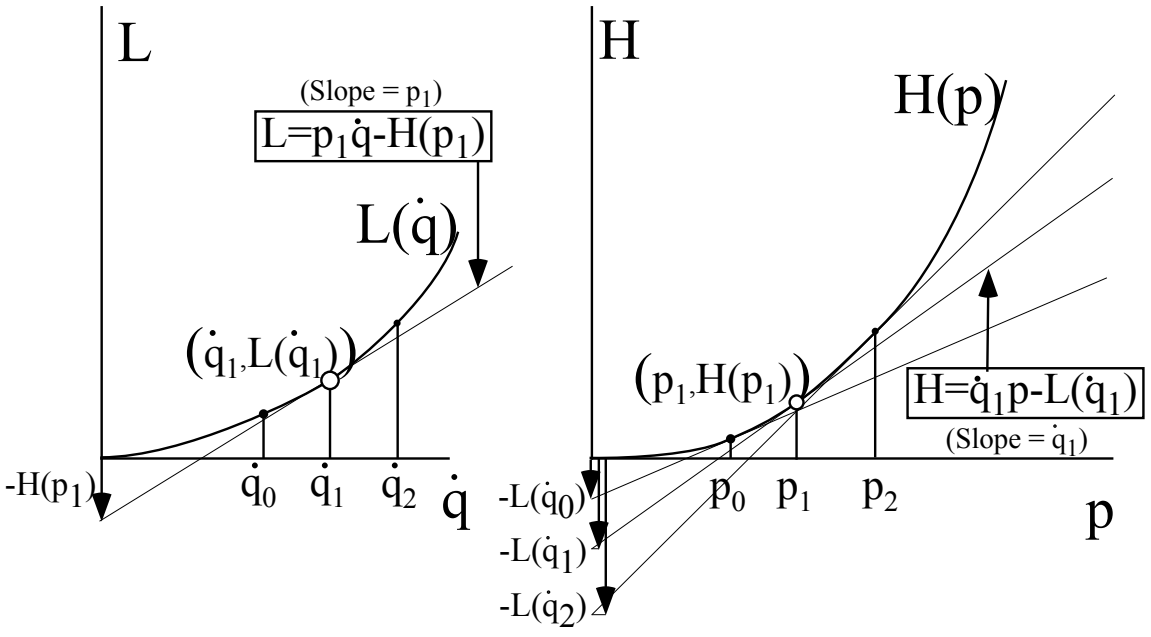

Fig. 12.9 Summary sketch of Legendre-Lagrangian-Hamiltonian geometry of Fig. 12.3 and 12.4.

The Equations of the Classical Universe (Lagrange, Hamilton, and others)

While string theorists search for an *"Equation of the Universe"*(EOTU) or a *"Theory of Everything"* (TOE) it should be noted that virtually all our modern physics, however avant-garde, has a classical foundation in Lagrangian or Hamiltonian equations. So a derivation of these all-important equations is in order. We already have deduced, mostly by symmetry and functional trickery, half of the Lagrange equations ($\frac{\partial L}{\partial \mathbf{v}}=\mathbf{p}$ in 12.12c) and half of the Hamilton equations ($\frac{\partial H}{\partial \mathbf{p}}=\mathbf{v}$ in 12.12d) for purely *kinetic* quadratic form Lagrangian $L(\mathbf{v})=\frac{1}{2}\mathbf{v}\bullet\mathbf{M}\bullet\mathbf{v}$ or Hamiltonian $H(\mathbf{p})=\frac{1}{2}\mathbf{p}\bullet\mathbf{M}^{-1}\bullet\mathbf{p}$. Needed now are the other half that add a *potential* energy $U(\mathbf{x})$ with *spatial* coordinate-$\mathbf{x}$ dependence to $L(\mathbf{v},\mathbf{x})$ and $H(\mathbf{p},\mathbf{x})$. That wrecks our nice translational symmetry and momentum conservation. Fortunately, the halves we have so far still apply. (Nature is *so* kind!) Also, the to-be-derived EOTCU *(Equations of the Classical Universe)* translate easily to "quite queer" coordinates $\{q^1, q^2,...\}$ such as polar, parabolic, hyperbolic, *etc*. that were introduced in Ch. 10 in connection with complex potential fields.

Generalized curvilinear coordinate (GCC) q^m systems are a big deal with a long history coming after (de)Cartesian coordinates x^j (or x_j) introduced in Chapter 1. GCC *super*script q^m convention that puts the index m *up* (where exponents usually go) and its notation by letter-q may seem, well, quite queer. But, such oddity can be forgiven if the q^m let us write all EOTCU in a single compact translatable form! It is based on an N-dimension differential chain relation between Cartesian coordinate (CC) differential dx^j and GCC dq^m.

$$dx^j=\frac{\partial x^j}{\partial q^m}dq^m\left(\equiv\sum_{m=1}^{N}\frac{\partial x^j}{\partial q^m}dq^m\quad\left\{\begin{matrix}\text{Defining a shorthand}\\ \text{dummy-index } m\text{-sum}\end{matrix}\right\}\right)\qquad(12.18)$$

An N-dimension sum is implied over any index repeated (like m above) to avoid writing "Sigma"-sums.

An identical linear relation exists between CC velocity $v^j \equiv \dot{x}^j$ and GCC velocity $v^m \equiv \dot{q}^m$.

$$dx^j = \frac{\partial x^j}{\partial q^m} dq^m \qquad \dot{x}^j = \frac{\partial x^j}{\partial q^m} \dot{q}^m \tag{12.19}$$

Total time-derivatives of CC (Cartesian velocity) and GCC (Generalized velocity) are denoted as follows.

$$v^j \equiv \dot{x}^j \equiv \frac{dx^j}{dt} \qquad v^m \equiv \dot{q}^m \equiv \frac{dq^m}{dt}$$

In (12.19) *Jacobian* $J_m{}^j$ matrix gives each CCC differential dx^j or velocity $\dot{x}^j$ in terms of GCC dq^m or $\dot{q}^m$.

$$J^j_m \equiv \frac{\partial x^j}{\partial q^m} = \frac{\partial \dot{x}^j}{\partial \dot{q}^m} \quad \left\{ \begin{matrix} \text{Defining } \textit{Jacobian} \\ \text{matrix component} \end{matrix} \right\} \tag{12.20a}$$

Inverse (so-called) *Kajobian* $K_j{}^m$ matrix is defined by a partial derivative that is a flip of the one for $J_m{}^j$.

$$K^m_j \equiv \frac{\partial q^m}{\partial x^j} = \frac{\partial \dot{q}^m}{\partial \dot{x}^j} \quad \left\{ \begin{matrix} \text{Defining } \textit{"Kajobian"} \\ \text{(inverse to Jacobian)} \end{matrix} \right\} \tag{12.20b}$$

Product of matrix $J_m{}^j$ and $K_j{}^m$ is a j-sum or $\partial_n q^m$ that by definition of partial derivatives, gives unit matrix.

$$K^m_j \cdot J^j_n \equiv \frac{\partial q^m}{\partial x^j} \cdot \frac{\partial x^j}{\partial q^n} = \frac{\partial q^m}{\partial q^n} = \delta^m_n = \begin{cases} 1 & if \ \ m = n \\ 0 & if \ \ m \neq n \end{cases}$$

So a $K_j{}^m$ matrix gives GCC dq^m or $\dot{q}^m$ in terms of dx^j or $\dot{x}^j$, respectively, the reverse of (12.18) or (12.19).

$$dq^m = \frac{\partial q^m}{\partial x^j} dx^j \qquad \dot{q}^m = \frac{\partial q^m}{\partial x^j} \dot{x}^j$$

GCC acceleration or *2nd* time-derivatives are a bit more complicated. We first apply $\frac{d}{dt}$ to velocity (12.19).

$$\ddot{x}^j \equiv \frac{d}{dt} \dot{x}^j = \frac{d}{dt} \left(\frac{\partial x^j}{\partial q^m} \dot{q}^m \right) = \frac{d}{dt} \left(\frac{\partial x^j}{\partial q^m} \right) \dot{q}^m + \frac{\partial x^j}{\partial q^m} \ddot{q}^m$$

Then a differential chain sum is applied to the Jacobian. Partial derivatives ∂_m and ∂_n are reversible.

$$\frac{d}{dt} \left(\frac{\partial x^j}{\partial q^m} \right) = \frac{\partial}{\partial q^n} \left(\frac{\partial x^j}{\partial q^m} \right) \frac{dq^n}{dt} = \left(\frac{\partial^2 x^j}{\partial q^n \, \partial q^m} \right) \frac{dq^n}{dt} = \left(\frac{\partial^2 x^j}{\partial q^m \, \partial q^n} \right) \frac{dq^n}{dt} = \frac{\partial}{\partial q^m} \left(\frac{\partial x^j}{\partial q^n} \frac{dq^n}{dt} \right) = \frac{\partial \dot{x}^j}{\partial q^m}$$

Velocity eq. (12.19) then equates total t-derivative of Jacobian to a partial q^m-derivative of CC velocity $\dot{x}^j$.

$$\frac{d}{dt} \left(\frac{\partial x^j}{\partial q^m} \right) = \frac{\partial \dot{x}^j}{\partial q^m} \tag{12.21}$$

This and (12.20) are two main keys to converting the Newton Second Law (Newt II) to GCC forms that apply to all classical mechanical phenomena due to any number of particles in one, two, or three dimensions. These then serve as mathematical analogies or *analogs* to modern physics of relativity and quantum theory that describe optical, nuclear, atomic, and molecular phenomena that involve bizarre wavelike behavior in unimaginably countless dimensions. Even LHC physics is glimpsed but that's still a work in progress.

Lagrange's version of Newt-II (f=Ma)

Lagrange's derivation starts with the following multidimensional CC version of Newt-II (*f=Ma*).

$$f_j = M_{jk}\, a^k = M_{jk}\, \ddot{x}^k \tag{12.22}$$

It is based upon a multidimensional CC version of kinetic energy that generalizes $\frac{1}{2}\mathbf{v}\bullet\mathbf{M}\bullet\mathbf{v}$ in (12.8).

$$T = \frac{1}{2} M_{jk}\, v^j v^k = \frac{1}{2} M_{jk}\, \dot{x}^j \dot{x}^k \quad \text{(where } M_{jk} = M_{kj} \text{ are inertia constants)} \tag{12.23}$$

Into the CC expression for differential work $dW = \mathbf{f}\bullet d\mathbf{r} = f_j dx^j$ is put the 1st GCC differential (12.19).

$$dW = f_j dx^j = f_j \left(\frac{\partial x^j}{\partial q^m} dq^m \right) = M_{jk}\, \ddot{x}^k \left(\frac{\partial x^j}{\partial q^m} dq^m \right) \tag{12.24}$$

The dq^m-sum is true term-by-term since dq^m are independent. (Sum still holds if all dq^m are zero but one.)

This gives an expression for each *generalized GCC force component* F_m defined as follows.

$$dW = f_j dx^j = F_m dq^m = f_j \frac{\partial x^j}{\partial q^m} dq^m = M_{jk}\, \ddot{x}^k \frac{\partial x^j}{\partial q^m} dq^m \tag{12.24a}$$

$$where: \quad F_m = f_j \frac{\partial x^j}{\partial q^m} = M_{jk}\, \ddot{x}^k \frac{\partial x^j}{\partial q^m} \tag{12.24b}$$

Now for Lagrange's clever end game. First set $A = M_{jk}\, \ddot{x}^k$ and $B = \frac{\partial x^j}{\partial q^m}$ with $\left[\ddot{A}B = \frac{d}{dt}\left(\dot{A}B\right) - \dot{A}\dot{B} \right]$ to get:

$$F_m = M_{jk}\, \ddot{x}^k \frac{\partial x^j}{\partial q^m} = M_{jk}\, \frac{d}{dt}\left(\dot{x}^k \frac{\partial x^j}{\partial q^m} \right) - M_{jk} \dot{x}^k \frac{d}{dt}\left(\frac{\partial x^j}{\partial q^m} \right)$$

Then convert ∂x^j to $\partial \dot{x}^j$ by (12.20a) on 1st term and (12.21) on 2nd term. Simplify by: $\left[M_{ij} v^i \frac{\partial v^j}{\partial q} = M_{ij} \frac{\partial}{\partial q} \frac{v^i v^j}{2} \right]$

$$F_m = M_{jk}\, \frac{d}{dt}\left(\dot{x}^k \frac{\partial \dot{x}^j}{\partial \dot{q}^m} \right) - M_{jk} \dot{x}^k \left(\frac{\partial \dot{x}^j}{\partial q^m} \right) = \frac{d}{dt} \frac{\partial}{\partial \dot{q}^m} \left(\frac{M_{jk} \dot{x}^k \dot{x}^j}{2} \right) - \frac{\partial}{\partial q^m} \left(\frac{M_{jk} \dot{x}^k \dot{x}^j}{2} \right)$$

The result is *Lagrange's GCC force equation* using kinetic energy (12.23).

$$F_m = \frac{d}{dt} \frac{\partial T}{\partial \dot{q}^m} - \frac{\partial T}{\partial q^m} \quad \text{where: } T = \frac{1}{2} M_{jk}\, \dot{x}^j \dot{x}^k \tag{12.25a}$$

But, Lagrange isn't done yet! If the force is conservative it's a gradient $\mathbf{F} = -\nabla U$ or in GCC: $F_m = -\frac{\partial U}{\partial q^m}$.

$$F_m = -\frac{\partial U}{\partial q^m} = \frac{d}{dt} \frac{\partial T}{\partial \dot{q}^m} - \frac{\partial T}{\partial q^m}$$

This gives *Lagrange's GCC potential equation* with a new definition for the *Lagrangian: L=T-U*.

$$0 = \frac{d}{dt} \frac{\partial L}{\partial \dot{q}^m} - \frac{\partial L}{\partial q^m} \quad \text{where: } L(\dot{q}^m, q^m) = T(\dot{q}^m, q^m) - U(q^m) \tag{12.25b}$$

Note that the potential function U cannot have any velocity ($\dot{q}^m = v^m$) dependence or else the first term of (12.25b) would be wrong. Lagrange's equations have simple forms that use *GCC momentum* p_m.

$$\frac{d}{dt}\frac{\partial L}{\partial \dot{q}^m} = \frac{\partial L}{\partial q^m} \qquad (12.25c)$$

$$\dot{p}_m \equiv \frac{dp_m}{dt} = \frac{\partial L}{\partial q^m} \quad (12.25d) \qquad p_m = \frac{\partial L}{\partial \dot{q}^m} \qquad (12.25e)$$

The first one (12.25d) is what we did *not* have when we found in (12.12c) the form $\mathbf{p} = \frac{\partial L}{\partial \mathbf{v}}$. The latter is the CC version of (12.25e) above. Pretty nice EOTCU *(Equations of the Classical Universe)* here! Let's try them out.

Consider an example of Lagrange equations in polar coordinates *($q^1 = r$, $q^2 = \phi$)* defined as follows.

$$x = x^1 = r\cos\phi\,, \qquad y = x^2 = r\sin\phi$$

First we find Jacobian and Kajobian matrices. <J> is easy to get by (12.20a). Inverting <J> gives <K>.

$$\langle J\rangle = \begin{pmatrix} \frac{\partial x^1}{\partial q^1} & \frac{\partial x^1}{\partial q^2} \\ \frac{\partial x^2}{\partial q^1} & \frac{\partial x^2}{\partial q^2} \end{pmatrix} = \begin{pmatrix} \frac{\partial x}{\partial r} = \cos\phi & \frac{\partial x}{\partial \phi} = -r\sin\phi \\ \frac{\partial y}{\partial r} = \sin\phi & \frac{\partial y}{\partial \phi} = r\cos\phi \end{pmatrix}$$

$\uparrow \mathbf{E}_1 \quad \uparrow \mathbf{E}_2 \qquad \uparrow \mathbf{E}_r \qquad \uparrow \mathbf{E}_\phi$

$$\langle K\rangle = \langle J^{-1}\rangle = \begin{pmatrix} \frac{\partial r}{\partial x} = \cos\phi & \frac{\partial r}{\partial y} = \sin\phi \\ \frac{\partial \phi}{\partial x} = \frac{-\sin\phi}{r} & \frac{\partial \phi}{\partial y} = \frac{\cos\phi}{r} \end{pmatrix} \begin{matrix} \leftarrow \mathbf{E}^r = \mathbf{E}^1 \\ \leftarrow \mathbf{E}^\phi = \mathbf{E}^2 \end{matrix} \qquad (12.26)$$

Two kinds of *quasi-unit vectors* show up. Columns of <J> are *covariant vectors* $\mathbf{E}_1 = \mathbf{E}_r$ and $\mathbf{E}_2 = \mathbf{E}_\phi$ Rows of <K> are *contravariant vectors* $\mathbf{E}^1 = \mathbf{E}^r$ and $\mathbf{E}^2 = \mathbf{E}^\phi$. They are plotted and sketched generically in Fig. 12.10.

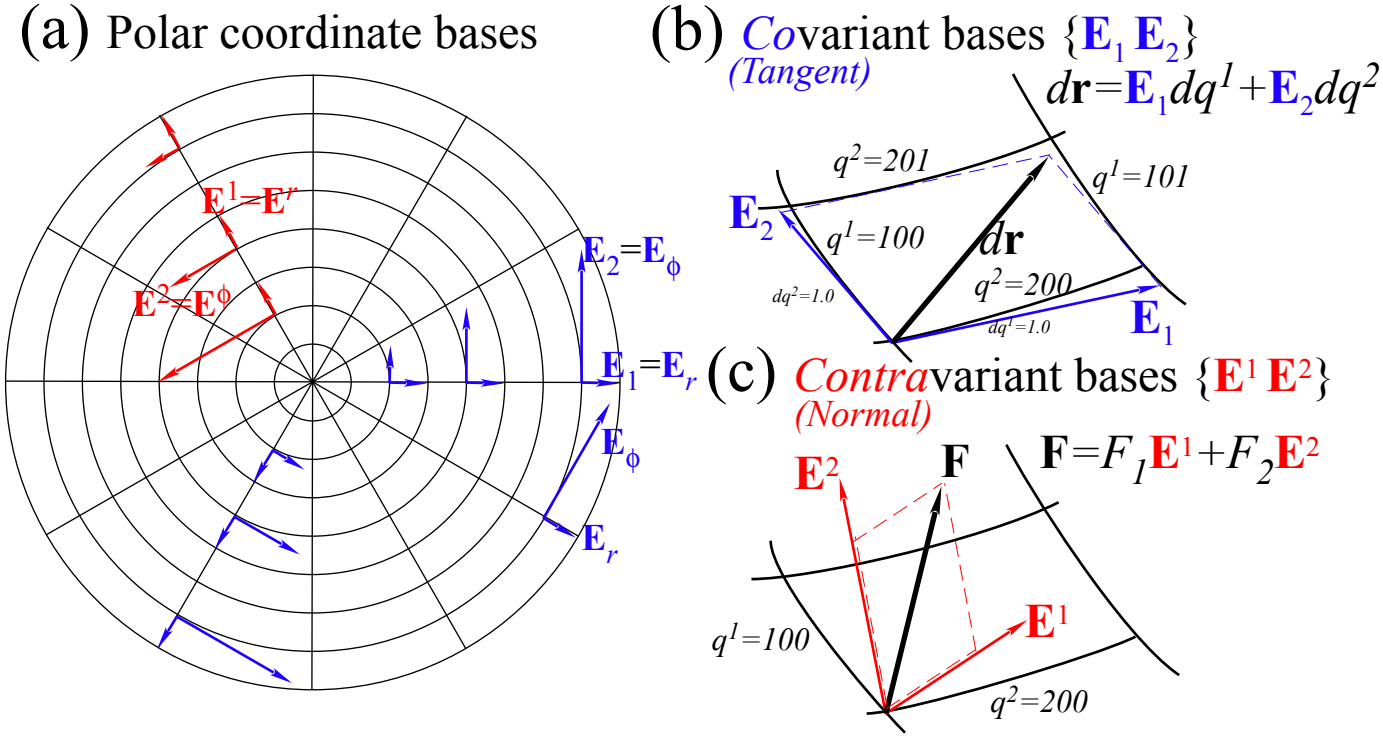

Fig. 12.10 Covariant force vector components in a polar space ($\mathbf{E}^\rho, \mathbf{E}^\phi$).

Covariant vector $\mathbf{E}_m$ is *tangent* to the q^m coordinate line of a cell wall. $\mathbf{E}_m$ *grows* as its cell grows according to the *1st* differential relation (12.18) sketched in Fig. 12.10b and rewritten here in vector notation.

$$d\mathbf{r} = \mathbf{E}_1 dq^1 + \mathbf{E}_2 dq^2 = \frac{\partial \mathbf{r}}{\partial q^1} dq^1 + \frac{\partial \mathbf{r}}{\partial q^2} dq^2 \tag{12.27}$$

Note $\mathbf{E}_2$ grows in Fig. 12.10a. $\mathbf{E}_m$ are convenient bases for *ex*tensive quantities like distance and velocity.

Contravariant vector $\mathbf{E}^m$ is *normal* to the q^m=*const*. surface or coordinate line of a cell wall. $\mathbf{E}^m$ *shrinks* as its cell side grows according to gradient relation (12.28) sketched in Fig. 12.10c.

$$\mathbf{F} = F_1 \mathbf{E}^1 + F_2 \mathbf{E}^2 = F_1 \frac{\partial q^1}{\partial \mathbf{r}} + F_2 \frac{\partial q^2}{\partial \mathbf{r}} = F_1 \nabla q^1 + F_2 \nabla q^2 \tag{12.28}$$

$\mathbf{E}^m$ are convenient bases for *in*tensive quantities like force and momentum.

Polar coordinates are orthogonal, but GCC $\mathbf{E}_m$ and $\mathbf{E}^m$ are at home in more exotic non-orthogonal manifolds and provide mutually orthonormal dual bases with GCC orthogonality relations. (Prove this!)

$$\mathbf{E}^m \bullet \mathbf{E}_n = \delta^m{}_n = \begin{cases} 1 \; if \; m = n \\ 0 \; if \; m \neq n \end{cases} \tag{12.30a}$$

Scalar products $\mathbf{E}_m \bullet \mathbf{E}_n$ give *co*variant *metric* g_{mn}*-tensor* matrix and similarly $\mathbf{E}^m \bullet \mathbf{E}^m$ gives *contra*-g^{mn}.

$$\mathbf{E}_m \bullet \mathbf{E}_n = g_{mn} \tag{12.30b}$$

$$\mathbf{E}^m \bullet \mathbf{E}^n = g^{mn} \tag{12.30c}$$

GCC version for 1-free-particle Lagrangian $L=\frac{1}{2}M\mathbf{v}\bullet\mathbf{v}$ involves g_{mn} factors using (12.27) and (12.30b).

$$L(\mathbf{v}) = \tfrac{1}{2}M\mathbf{v}\bullet\mathbf{v} = \tfrac{1}{2}M\dot{\mathbf{r}}\bullet\dot{\mathbf{r}} = \tfrac{1}{2}M(\mathbf{E}_m\dot{q}^m)\bullet(\mathbf{E}_n\dot{q}^n) = \tfrac{1}{2}M(g_{mn}\dot{q}^m\dot{q}^n) = L(\dot{q}^m) \tag{12.31}$$

Polar coordinate metric tensors follow from (12.26). g_{mn} and g^{mn} are diagonal (orthogonal) mutual inverses.

$$\begin{pmatrix} g_{rr} & g_{r\phi} \\ g_{\phi r} & g_{\phi\phi} \end{pmatrix} = \begin{pmatrix} \mathbf{E}_r \bullet \mathbf{E}_r & \mathbf{E}_r \bullet \mathbf{E}_\phi \\ \mathbf{E}_\phi \bullet \mathbf{E}_r & \mathbf{E}_\phi \bullet \mathbf{E}_\phi \end{pmatrix} = \begin{pmatrix} 1 & 0 \\ 0 & r^2 \end{pmatrix} \qquad \begin{pmatrix} g^{rr} & g^{r\phi} \\ g^{\phi r} & g^{\phi\phi} \end{pmatrix} = \begin{pmatrix} \mathbf{E}^r \bullet \mathbf{E}^r & \mathbf{E}^r \bullet \mathbf{E}^\phi \\ \mathbf{E}^\phi \bullet \mathbf{E}^r & \mathbf{E}^\phi \bullet \mathbf{E}^\phi \end{pmatrix} = \begin{pmatrix} 1 & 0 \\ 0 & 1/r^2 \end{pmatrix}$$

The resulting polar-coordinate Lagrangian and its covariant momentum p_m expressions (12.25e) follow.

$$L(\dot{r},\dot{\phi}) = \tfrac{1}{2}M(\dot{r}^2 + r^2\dot{\phi}^2) \qquad p_r = \frac{\partial L}{\partial \dot{r}} = M\dot{r} \qquad p_\phi = \frac{\partial L}{\partial \dot{\phi}} = Mr^2\dot{\phi} \tag{12.32}$$

p_r is radial linear momentum. p_ϕ is angular momentum complete with moment of inertia Mr^2. A potential $U(r,\phi)$ turns the Lagrangian into $L=T-U(r,\phi)$ of (12.25b). Momentum t-derivatives (12.25d) follow.

$$L(\dot{r},\dot{\phi}) = \tfrac{1}{2}M(\dot{r}^2 + r^2\dot{\phi}^2) - U(r,\phi) \qquad \begin{aligned} \dot{p}_r &= \frac{\partial L}{\partial r} = Mr\dot{\phi}^2 - \frac{\partial U}{\partial r} \\ &= M\ddot{r} \end{aligned} \qquad \begin{aligned} \dot{p}_\phi &= \frac{\partial L}{\partial \phi} = -\frac{\partial U}{\partial \phi} \\ &= Mr^2\ddot{\phi} + 2Mr\dot{r}\dot{\phi} \end{aligned} \tag{12.33}$$

Note how centrifugal force $Mr\dot{\phi}^2$ and Coriolis force $2Mr\dot{r}\dot{\phi}$ are derived so easily by Lagrange GCC. Also, if potential is radial-isotropic (no ϕ-dependence) then angular momentum is a conserved constant.

$$\dot{p}_\phi = 0 \Rightarrow p_\phi = \ell = const. \tag{12.35}$$

Lagrange GCC is elegant and powerful. So is Hamiltonian GCC and, as we'll see, it's more conservative!

Hamilton's version of Newt-II (f=Ma)

A GCC *Hamiltonian H(p,q)* uses *momenta* and coordinates as independent variables rather than generalized *velocities* and coordinates employed by *Lagrangian* $L(q,\dot{q})$. The total time derivative of L is

$$\dot{L}\left(q,\dot{q},t\right)=\frac{dL}{dt}=\frac{\partial L}{\partial q^m}\frac{dq^m}{dt}+\frac{\partial L}{\partial \dot{q}^m}\frac{d\dot{q}^m}{dt}+\frac{\partial L}{\partial t}.$$

Here we leave open the possibility that the Lagrangian may have *explicit* time dependence and a non-zero *partial t*-derivative. (Think of a mad scientist dialing up the force field as the experiment progresses.)

The Lagrange equations (12.25) let us insert momentum p_m and its time derivative $\dot{p}_m$ into (12.36).

$$\begin{aligned}\dot{L}\left(q,\dot{q},t\right)=\frac{dL}{dt}&=\dot{p}_m\frac{dq^m}{dt}+p_m\frac{d\dot{q}^m}{dt}+\frac{\partial L}{\partial t}\\ &=\frac{dL}{dt}=\ \frac{d}{dt}\left(p_m\dot{q}^m\right)\qquad+\frac{\partial L}{\partial t}\end{aligned}$$

A derivative identity $\dot{p}\frac{dq}{dt}+p\frac{d\dot{q}}{dt}=\frac{d}{dt}\left(p\dot{q}\right)$ lets us collect the two pq terms. Reordering gives a total t-derivative of a GCC version of a form ($H(\mathbf{p})=\mathbf{p}\bullet\mathbf{v}-L(\mathbf{v})$) first encountered in (12.11b). That's the GCC *Hamiltonian H(p,q)*.

$$\frac{d}{dt}\left(p_m\dot{q}^m-L\right)=-\frac{\partial L}{\partial t}=\frac{dH}{dt}\quad where: H=p_m\dot{q}^m-L \qquad (12.36a)$$

The momentum side (12.12) of Hamilton's equations follows. So does the other (coordinate) side (12.36c).

$$\frac{\partial H}{\partial p_m}=\dot{q}^m \qquad (12.36b) \qquad\qquad \frac{\partial H}{\partial q^m}=0-\frac{\partial L}{\partial q^m}=-\dot{p}_m \qquad (12.36c)$$

To get (12.36b) we apply $\frac{\partial}{\partial p}$ to H. (Recall $\frac{\partial L}{\partial p}=0$.) To get (12.36c) we apply $\frac{\partial}{\partial q}$ to H. (Recall $\frac{\partial L}{\partial q}=\dot{p}$ (12.25d).)

The Hamiltonian function has an unusual property. Its *total* time derivative equals its *partial* time derivative. If H lacks *explicit* time dependence it is a *conserved* constant. (Imagine our mad scientist asleep at the dial!) That constant is energy. To show this, apply metric definition (12.31) of T in $L=T-U$.

$$H=p_m\dot{q}^m-L=\left(Mg_{mn}\dot{q}^n\right)\dot{q}^m-\left(T-V\right)=Mg_{mn}\dot{q}^m\dot{q}^n-\left(\tfrac{1}{2}Mg_{mn}\dot{q}^m\dot{q}^n\right)+V \qquad (12.37a)$$

$$H=\tfrac{1}{2}Mg_{mn}\dot{q}^m\dot{q}^n+V=T+V\equiv E \qquad (\text{Numerically correct ONLY!}) \qquad (12.37b)$$

$$H=\frac{1}{2M}g^{mn}p_mp_n+V=T+V\equiv E \qquad (\text{Formally and Numerically correct}) \qquad (12.37c)$$

So, the *Hamiltonian* is the sum of kinetic energy T and potential U which is the *total energy* $E=T+U$. Equations (3.12.5) amount to the *conservation of total energy* if L and H are *not explicit* functions of time.

Note that we use the *co*variant metric g_{mn} for the velocity **v**-dependent Lagrangian, but the inverse *contra*variant metric g^{mn} comes into play for the momentum **p**-dependent Hamiltonian. Seem like so much formalistic foo-foo? Perhaps. But, just wait until Unit 8 where we develop the relativistic and quantum mechanical versions of this. Then this "formalism" will morph into the most sublimely gorgeous geometry that you have ever imagined!

Variational calculus of Lagrangian mechanics

Here is a funny way to derive Lagrange's equations. It involves something called *variational calculus*.

Variational calculus finds extreme (minimum or maximum) values to entire integrals such as

$$S(q)=\int_{t_0}^{t_1} dt\; L\big(q(t),\dot{q}(t),t\big). \qquad (12.38)$$

Here the curve $q(t)$ can vary at each time t. If $S(q)$ was a simple function like $S(q)=q^2-4q$ we would find zeros of its derivative $dS/dq=(2q-4)=0$ at $q=2$ and be done. However, here $S(q)$ is a *functional*, that is, a function $\int dt\, L(q,\dot{q},t)$ of entire functions $q(t)$ and t-derivative $\dot{q}(t)$ either of which can be varied arbitrarily at any point between limits t_0 and t_1 of the dependent time integration variable as shown in Fig. 12.11. (Again, we allow the possibility that $L(q,\dot{q},t)$ may have explicit t-dependence, too.)

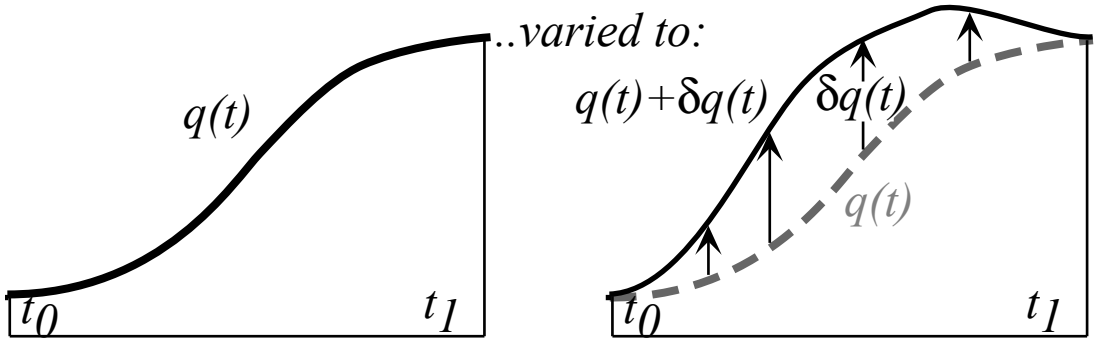

Fig. 12.11 Variation of functional curve or trajectory path from q(t) to $q(t)+\delta q(t)$

An arbitrary but small variation function $\delta q(t)$ is allowed at every point t in the figure along the curve except at the end points t_0 and t_1. There we demand it not vary at all.

$$\delta q(t_0)=0=\delta q(t_1) \qquad (12.39)$$

The variant $\delta q(t)$ changes integral (12.38) according to a first order Taylor series.

$$S(q+\delta q)=\int_{t_0}^{t_1} dt\left[L(q,\dot{q},t)+\frac{\partial L}{\partial q}\delta q+\frac{\partial L}{\partial \dot{q}}\delta\dot{q}\right] \quad \text{where: } \delta\dot{q}=\frac{d}{dt}\delta q \qquad (12.40)$$

Replacing $\frac{\partial L}{\partial \dot{q}}\delta\dot{q}$ with $\frac{d}{dt}\left(\frac{\partial L}{\partial \dot{q}}\delta q\right)-\frac{d}{dt}\left(\frac{\partial L}{\partial \dot{q}}\right)\delta q$ gives a sum of two and then three integrals.

$$S(q+\delta q)=\int_{t_0}^{t_1} dt\left[L(q,\dot{q},t)+\frac{\partial L}{\partial q}\delta q-\frac{d}{dt}\left(\frac{\partial L}{\partial \dot{q}}\right)\delta q\right]+\int_{t_0}^{t_1} dt\,\frac{d}{dt}\left(\frac{\partial L}{\partial \dot{q}}\delta q\right)$$

$$=\int_{t_0}^{t_1} dt\; L(q,\dot{q},t)+\int_{t_0}^{t_1} dt\left[\frac{\partial L}{\partial q}-\frac{d}{dt}\left(\frac{\partial L}{\partial \dot{q}}\right)\right]\delta q+\left(\frac{\partial L}{\partial \dot{q}}\delta q\right)\Big|_{t_0}^{t_1}$$

The third term vanishes according to (12.40). This leaves the following first order variation δS.

$$\delta S=S(q+\delta q)-S(q)=\int_{t_0}^{t_1} dt\left[\frac{\partial L}{\partial q}-\frac{d}{dt}\left(\frac{\partial L}{\partial \dot{q}}\right)\right]\delta q$$

If integral S is an extremum its first order variation δS must be zero for all $\delta q(t)$ even the case where $\delta q(t)$ is only non-zero at only one tiny t-interval. Thus the δS integrand must be zero everywhere.

$$\delta S = 0 \Rightarrow \frac{d}{dt}\left(\frac{\partial L}{\partial \dot{q}}\right) - \frac{\partial L}{\partial q} = 0 \qquad (12.41a)$$

The result is an *Euler-Lagrange equation*. It is a 1-dimensional version of GCC Lagrange equation (12.25c)

$$\frac{d}{dt}\left(\frac{\partial L}{\partial \dot{q}}\right) = \frac{\partial L}{\partial q} \qquad (12\text{-}41b)$$

We may just as well demand extreme (actually *minimum*) values for multi-dimensional Lagrange integrals.

$$S(q) = \int_{t_0}^{t_1} dt\ L\left(q^m(t), \dot{q}^m(t), t\right). \qquad (12.38)_{N\text{-}dim}$$

The result is the N-dimensional Lagrange equations (12.25) derived from Newt-II. But, why should Newt-II make the integral of Lagrangian minimum? Something weird underlies classical laws! Henri Poincare recognized early on that a new physics (modern physics) must be hiding down there.

Poincare's invariant, quantum phase, and action

The Legendre relation (12.11a) becomes *Poincare's invariant differential* if $\mathbf{v} = \frac{d\mathbf{r}}{dt}$ has dt cleared.

$$L dt = \mathbf{p}\bullet\mathbf{v} \cdot dt - H \cdot dt = \mathbf{p}\bullet d\mathbf{r} - H \cdot dt \qquad (12.42a)$$

It is also the time differential dS of *action* $S = \int L\, dt$ whose time derivative is rate L of *quantum phase*.

$$dS = L dt = \mathbf{p}\bullet d\mathbf{r} - H \cdot dt \quad \text{where:} \quad L = \frac{dS}{dt} \qquad (12.42b)$$

In Unit 2 we find *DeBroglie law* $\mathbf{p}=\hbar\mathbf{k}$ and *Planck law* $H=\hbar\omega$ that, if conserved, give a quantum plane wave:

$$\psi(\mathbf{r},t) = e^{iS/\hbar} = e^{i(\mathbf{p}\bullet\mathbf{r} - H\cdot t)/\hbar} = e^{i(\mathbf{k}\bullet\mathbf{r} - \omega\cdot t)} \qquad (12.42c)$$

Time-independent or Hamilton's *reduced action* is the spatial integral $S_H = \int \mathbf{p}\bullet d\mathbf{r}$. Classical trajectories minimize action integrals S and S_H according to *Least Action Principles* like (12.41).

Huygen's principle: "Proof" of classical axioms and path integrals

Enveloping curves generated by contact transformations like (12.15) or Fig. 12.7 are closely related to *Huygen's principle* of wave optics. This also applies to quantum waves of matter. Suppose a hypothetical action function $S_H(\mathbf{r}_0 : \mathbf{r})$ generates the curves $S_H(\mathbf{r}_0 : \mathbf{r})=10,\ 20,$ and 30 as sketched in Fig. 12.12.

Now imagine the same generator acts starting from two points $\mathbf{r}_{10}$ and $\mathbf{r}'_{10}$ on the $S_H(\mathbf{r}_0 : \mathbf{r})=10$ wave front thereby generating two sets of intermediate wave fronts: $S_H(\mathbf{r}_{10} : \mathbf{r})=10$ and $S_H(\mathbf{r}'_{10} : \mathbf{r})=10$ around each of these two points. All points on these curves represent a total accumulation of $20\ J{\cdot}s$ of action since leaving $\mathbf{r}_0$, but only for select points like $\mathbf{r}_{20}$ and $\mathbf{r}'_{20}$ is $20\ J{\cdot}$ the *least* action that can be accumulated after leaving $\mathbf{r}_0$. All other points have a more direct route from $\mathbf{r}_0$ that is cheaper than $20\ J{\cdot}s$.

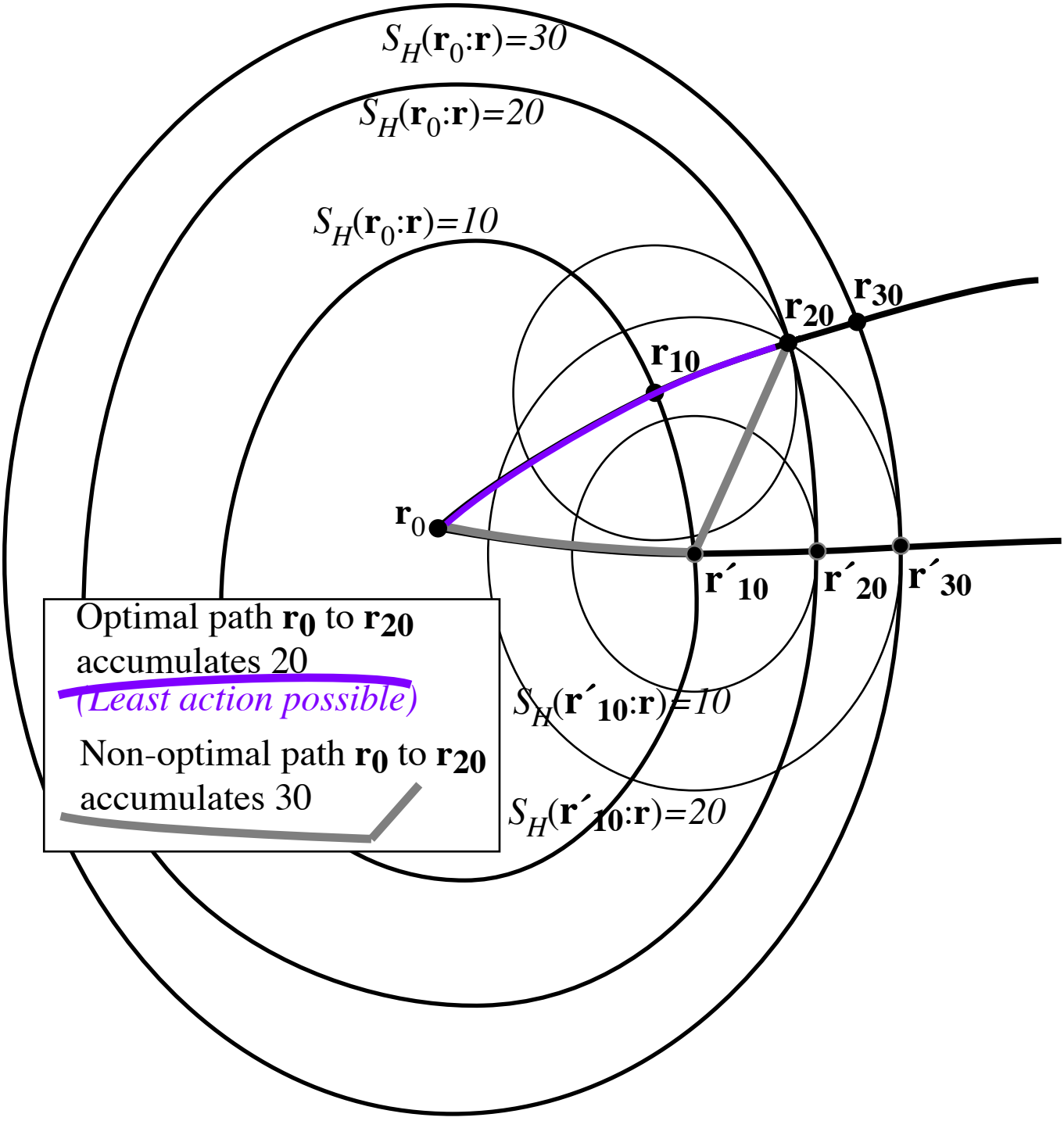

Fig. 12.12 Comparison of paths and wave fronts for discussion of Huygen's principle.

These special points $\mathbf{r}=\mathbf{r}_{20}$ and $\mathbf{r}=\mathbf{r}'_{20}$ of least action are just the contacting ones that lie on the envelope curve $S_H(\mathbf{r}_0 : \mathbf{r})=20$. They also lie on optimal (least action) trajectory paths from $\mathbf{r}_0$ which have never failed to follow the undeviating "straight-and-narrow" paths determined by Lagrange equations.

What makes these paths appear to follow the classical Lagrange equations? Why do they appear to optimize their action so faithfully? Huygens knew the answer in the 1600's, at least for rays of light. The key

word here is "appear" since neither light waves nor matter waves originally have any intention of following a straight and narrow path!

Quite the contrary, every point on a Huygen's wave front broadcasts a continuum of deviant wave fronts in the form of the intermediate "wavelet" ovals such as $S_H(\mathbf{r}_{10} : \mathbf{r})=10$ and $S_H(\mathbf{r}'_{10} : \mathbf{r})=10$ in Fig. 12.12. But, for each of these non-optimal deviant "rascals" there are thousands more neighboring "rascals" whose actions vary linearly with deviation so that non-extreme action paths end up canceling each other by destructive interference of the varying phases due to deviant actions. No honor amongst "rascals" here!

Only for those optimal paths of stationary action (and therefore, stationary phase) do the phases add constructively, and it is only for these that quantum wave intensity or classical presence appears to exist most of the time in a classical world of enormous action. All paths are possible to varying degrees and exist in some sense, but only the optimal ones make their presence known and generally do so while obeying quite precisely the classical equations of motion.

In a sense, this constitutes an evolutionary proof of Newton's "laws" or at least justification of Newton's axioms in the case of high action or the classical limit. The classical world appears to be a result of a continual process of natural selection of waves!

However, the situation is different for systems with discrete or limited number of paths as in the case of low action or when wavelength is comparable to the size of a system. Then the classical myth is likely to disintegrate like Dracula out of his coffin at dawn! Now matter how dearly we believe in our precisely machined gears and fine particles there comes a time and place where the classical equations part company with new reality that appears with increasingly clever and precise experimental evidence.

Nevertheless, the classical apparatus is far too well developed to die forever, and it rises to assist the newly appointed quantum paradigm in what is called semi-classical approximation theory. The role of generating action functions $S(\mathbf{r}_0,t_0 : \mathbf{r},t)$ and $S_H(\mathbf{r}_0 : \mathbf{r})$ is taken over in quantum theory by amplitudes, wavefunctions, or matrix elements such as the amplitude $\langle \mathbf{r},t|\,\mathbf{r}_0,t_0\rangle$ of time-evolution and or the transition-overlap amplitude $\langle \mathbf{r} \mid \mathbf{r}_0 \rangle$. Here, $|\langle \mathbf{B} \mid \mathbf{A} \rangle|^2$ is the probability for a state-**A** to become state-**B** if forced to make a choice. Bracket $\langle \mathbf{B} \mid \mathbf{A} \rangle$ is called a *probability amplitude*; past-to-future is read right-to-left like Hebrew. Probability amplitudes may be approximated by semi-classical relations similar to (12.42c).

$$\left\langle \mathbf{r}_1,t_1\middle|\mathbf{r}_0,t_0\right\rangle = e^{i\,S\left(\mathbf{r}_0,t_0:\mathbf{r}_1,t_1\right)/\hbar} \quad (12.43a) \qquad \left\langle \mathbf{r}_1\middle|\mathbf{r}_0\right\rangle = e^{i\,S_H\left(\mathbf{r}_0:\mathbf{r}_1\right)/\hbar} \quad (12.43b)$$

Restating Huygen's principle with semiclassical amplitudes gives a *completeness* or *closure* relation.

$$\sum_{\mathbf{r}'}\left\langle \mathbf{r}_1\middle|\mathbf{r}'\right\rangle\left\langle \mathbf{r}'\middle|\mathbf{r}_0\right\rangle \cong \sum_{\mathbf{r}'} e^{i\left(S_H\left(\mathbf{r}_0:\mathbf{r}'\right)+S_H\left(\mathbf{r}':\mathbf{r}_1\right)\right)/\hbar} = e^{i\,S_H\left(\mathbf{r}_0:\mathbf{r}_1\right)/\hbar} = \left\langle \mathbf{r}_1\middle|\mathbf{r}_0\right\rangle \quad (12.44)$$

Intermediate **r**'-path sums, as in Fig. 12.12, cancel by phase variation except on the optimal stationary-action path $\mathbf{r}_1 \leftarrow \mathbf{r}_0$. The sum over phase factors from **r**'-paths is well approximated by the amplitude for the stationary optimal path. Methods for summing over all paths of significant importance (including deviant ones) are called *Feynman path integration techniques*. This is a difficult chore since “all paths...” are a tangled uncountably infinite mess. Often, the extra effort needed to count them is not needed.

Bohr quantization

Bohr quantization requires quantum phase $S_H/\hbar$ in amplitude (12.44) to be an integral multiple υ of 2π after a closed loop integral $S_H(\mathbf{r}_0:\mathbf{r}_0)=\int_{r_0}^{r_0}\mathbf{p}\bullet d\mathbf{r}$. The integer υ (υ = *0, 1, 2,...*) is a *quantum number*.

$$1=\langle\mathbf{r}_0|\mathbf{r}_0\rangle=e^{iS_H(\mathbf{r}_0:\mathbf{r}_0)/\hbar}=e^{i\Sigma_H/\hbar}=1 \quad \text{for: } \Sigma_H=2\pi\hbar\upsilon=h\upsilon \qquad (12.45)$$

A colorful way to display action and its Bohr quantization is to numerically integrate Hamilton's equations and Lagrangian *L* and color the trajectory according to the current accumulated value of action.

$$S_H(\mathbf{0}:\mathbf{r})=S_p(\mathbf{0},0:\mathbf{r},t)+Ht=\int_0^t L\,dt+Ht\,. \qquad (12.46)$$

The hue should represent the phase angle $S_H(\mathbf{0}:\mathbf{r})/\hbar$ *modulo* 2π as, for example, *0=red, π/4=orange, π/2=yellow, 3π/4=green, π=cyan* (opposite of red), *5π/4=indigo, 3π/2=blue, 7π/4=purple, and 2π=red* (full color circle). Interpolating action on a palette of *32* colors is enough precision for low quanta.

The colored paths display a confused gray mess if phases fail to interfere constructively. But, for select quantizing values of energy, there appear striking patterns of colors when Bohr quantization makes phases interfere constructively. Patterns are outlines of spatial quantum wave amplitudes (12.43b).

$$\langle\mathbf{r}_1|\mathbf{r}_0\rangle=e^{iS_H(\mathbf{r}_0:\mathbf{r}_1)/\hbar} \qquad (12.43)_{repeated}$$

Heller and Davis first tried this *color-quantization* technique on a CRAY-*Dicomed* film system in 1983.

A quantizing example for a 2-dimensional oscillator using the *ColorU(2)* program is shown in Fig. 11.13. Viewing this in gray-scale is possible since only two hues actually survive: *red*, representing a phase of *0*, and *cyan*, representing a phase of *π*. The example is a standing wave mode in *(x,y)*-coordinate space, so the only possible wave amplitude is *±1*, that is, complimentary hues *red* and *cyan* which appear as light and dark gray in a gray scale portrait. Remaining colors pile up on nodal lines with so many phases interfering to destroy the amplitude. A time-dependent action *S(**0**, 0 : **r**, t)* (12.43a) gives time-dependent moving waves such as the snapshot in Fig. 11.14 of a quantum fountain discussed after Fig. 12.5. Wave animation is done by shift the computer color wheel by the time-dependent phase angle $H\cdot T/\hbar=\omega\cdot T$ in (12.46).

$$\langle\mathbf{r}_1,t_1|\mathbf{r}_0,t_0\rangle=e^{iS(\mathbf{r}_0,t_0:\mathbf{r}_1,t_1)/\hbar}=e^{iS_H(\mathbf{r}_0:\mathbf{r}_1)/\hbar-i\omega\cdot T} \quad \text{where: } T=t_1-t_0, \text{ and: } H=\hbar\omega \qquad (12.46)$$

A moving wave has a *quantum phase velocity* found by setting *S=const.* or $dS(\mathbf{0},0:\mathbf{r},t)=0=\mathbf{p}\bullet d\mathbf{r}-Hdt$.

$$\mathbf{V}_{phase}=\frac{d\mathbf{r}}{dt}=\frac{H}{\mathbf{p}}=\frac{\omega}{\mathbf{k}} \qquad (12.47)$$

This is quite the opposite of classical particle velocity which is *quantum group velocity*.

$$\mathbf{V}_{group}=\frac{d\mathbf{r}}{dt}=\frac{\partial H}{\partial\mathbf{p}}=\frac{\partial\omega}{\partial\mathbf{k}} \qquad (12.48)$$

By making two of the entries in the phase-color palette to be black-and-white it is possible to display a wave front line which will march in step with the other hues in the palette.

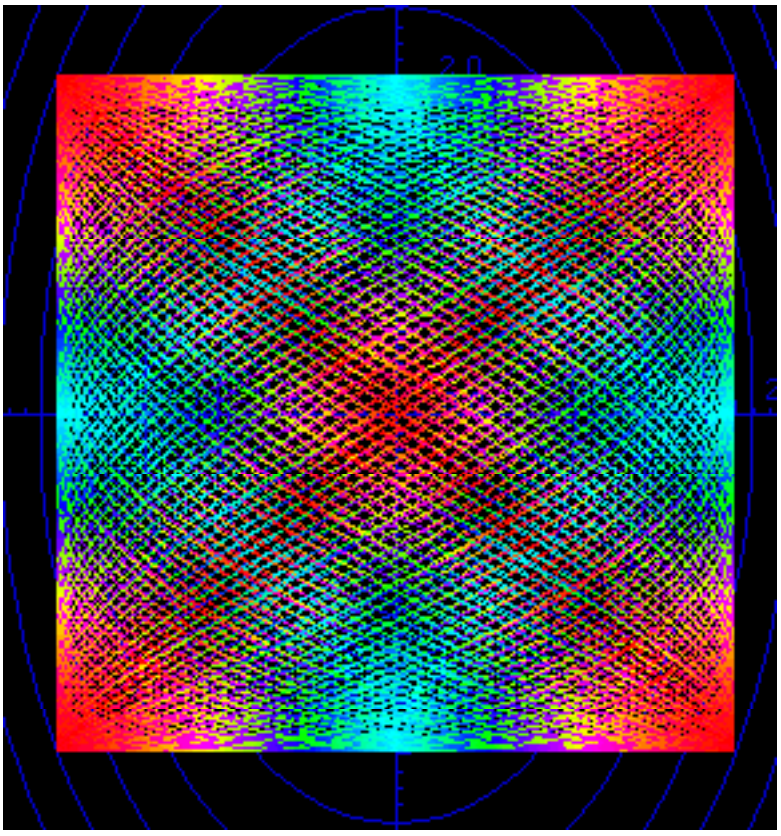

Fig. 12.13 Phase-color 2-dimensional harmonic oscillator paths showing (2,2) quantum wave function.

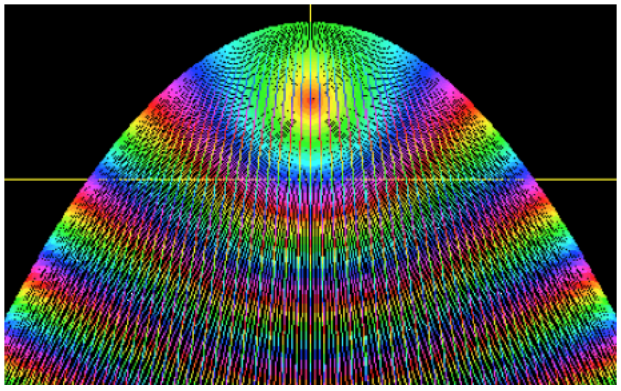

Fig. 12.14 Phase-color trajectory paths showing quantum wave fronts of moving wave.

A sequence of quantum wavefronts underlying the quantum fountain are drawn in Fig. 12.15 for three different values of reduced action S_H. This is equivalent to taking snapshots at different times. As classical momentum approaches zero at the top of Fig. 12.15b, the S wave phase speed diverges to infinity. Then two "cat ears" are created and race out along the top of the classical envelope in Fig. 12.15c and then slow down as the classical momentum **p** again picks up. High **p** in Fig. 12.15 means high gradient $\nabla S_H = \mathbf{p}$ so the S_H contours are closer together. S fronts move from one $S_H = n2\pi$ contour to the next $S_H = (n+1)2\pi$ contour at frequency $\omega = H/\hbar$ so large **p** means slow going. Note that the lower regions of each contour in Fig. 12.15 are slower than upper regions; quite the opposite of the classical particle “ball” in Fig. 12.5. The two "cat ears" move out and down rapidly until, like Lewis Carroll's Cheshire cat, nothing remains but its smile!

Dynamics of phase and group velocity are keys to relativity and quantum theory as shown in Unit 8.

Fig. 12.15 Constant S_H contours for iso-energetic trajectory family are normal to trajectory paths.

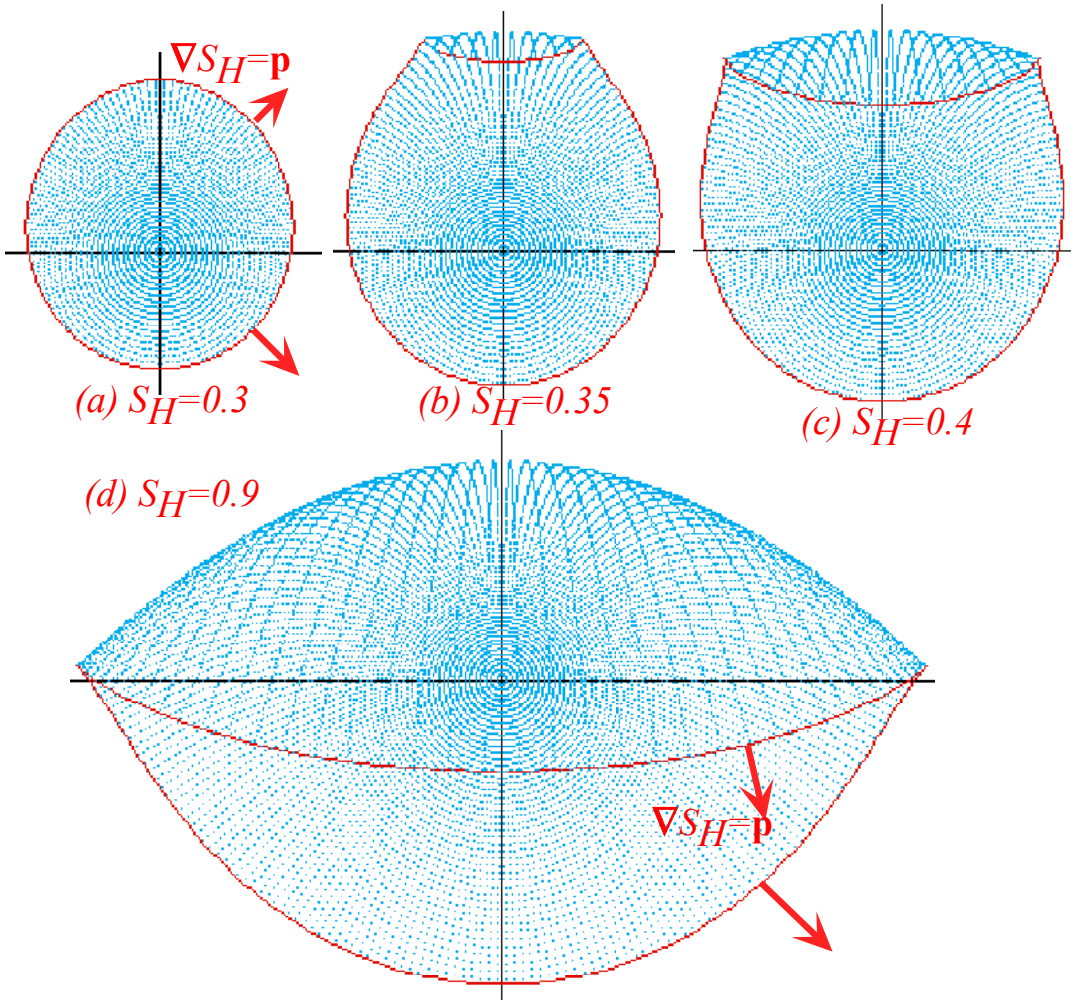

16th Century carving on St. Wifred's in Grappenhall

From Alice's Adventures in Wonderland by Lewis Carrol (1865)

St. Nicolas carving

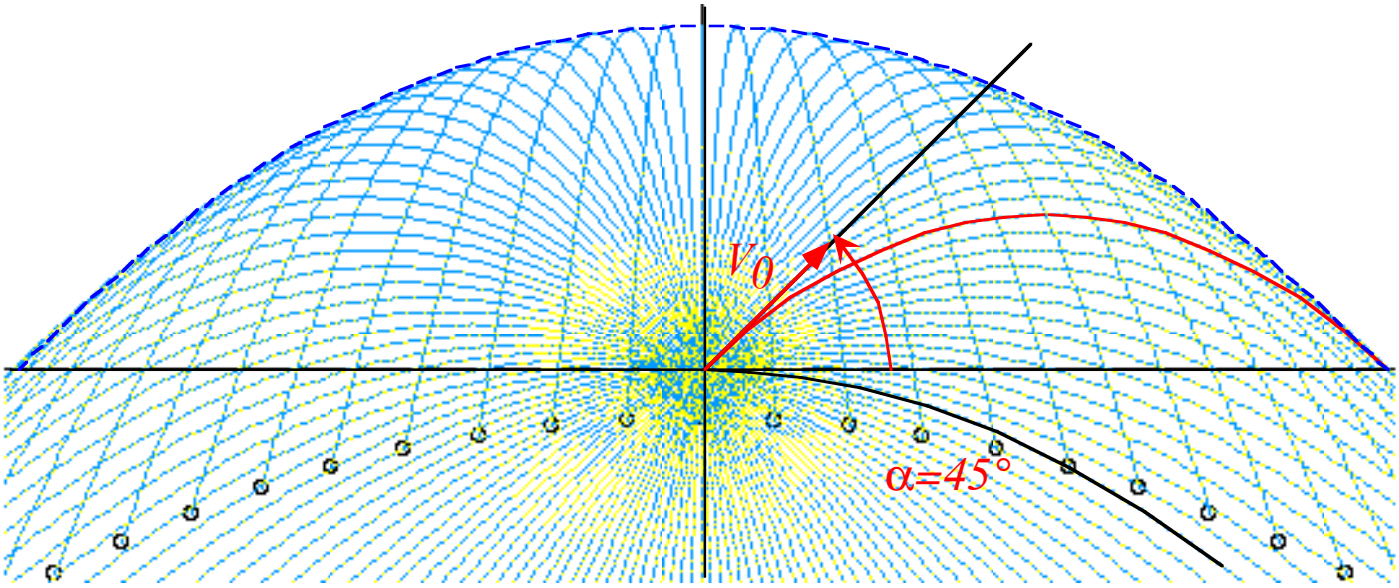

The volcanoes of Io and NIST atomic fountain

1.12.1. A fountain spraying water in many directions at equal speed appears to form a parabola of revolution whose cross-section is plotted above. You see this also in photos of volcanoes on Jupter's moon Io. Let's model this with a ***Bang!*** of equal-initial-speed v_0 particles ejected from origin in uniform gravity g vacuum and develop geometry of parabolic trajectories and their envelope. Key questions: *"What curve or "blast wave" do the particles form at each moment of time?"* and *"Is the envelope, in fact, parabolic?"*

(a) First describe how observers see the trajectories behave if they are riding in a well-shielded free-falling elevator frame-(x',y') that passes the origin point at the moment of ejection.

(b) Meanwhile, in the lab (x,y)-frame, describe the parabolic fragment trajectories as a function of the initial elevation angle α for each fragment. Give equations for the focal point of each parabola and describe what curve these foci form (the *focus-locus*). (See if you can do it without peeking at Ch. 12.)

(c) Construct examples of parabolas with their focus-locus and find a relation between the focal point and the contact point for each parabolic path with the envelope. *Is the envelope parabolic?* and, if so, *where is its focus?* Construct drawings of $\alpha=30°$ and $\alpha=45°$ paths and "blast wave" at the moment each path contacts the envelope.

Problem for a volcanolgist (or baseball outfielder)

1.12.2. Suppose you are on the x-axis some distance from the origin where a baseball (or volcano rock) is thrown up and toward you so it appears to move straight up the y-axis like an imaginary elevator that is at the line-of-sight projection of baseball (or rock) onto y-axis. Elevator motion indicates if you are in position to catch the ball (or be clobbered by the rock) or whether the object will fly over or fall short. Describe apparent elevator velocity and/or acceleration that distinguishes the three cases, particularly the middle one.

1.12.3. Suppose a neutron starlet enters a pocket of U^{235} at position $\mathbf{r}(0)$ and goes *Bang!* The U^{235} detonates and blasts off pieces of starlet that each fly away with the same initial speed $|\mathbf{v}(0)|=1$ (we assume) but various velocities $\mathbf{v}(0)=(0,1)$, $(\frac{1}{\sqrt{2}},\frac{1}{\sqrt{2}})$, $(0,1)$, $(\frac{1}{\sqrt{2}},\frac{-1}{\sqrt{2}})$, *etc.* (Units use the usual geometric $\omega=1$ scaling.)

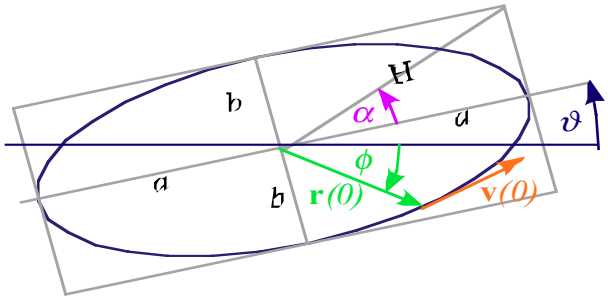

The short answer problems concern the resulting orbits of equal mass starlet pieces inside the Earth.

Do the starlet blast orbits conserve values for any physical quantities such as (Yes or No) initial speed $|\mathbf{v}|$?__, momentum $|\mathbf{p}|$?__, angular momentum ℓ?__, KE?__, PE?__, total Energy E?__ .

Do the starlet blast orbits conserve values for some geometric quantities such as (Yes or No) a?__, b?__ , r?__ , H?__, ϕ?__, ϑ?__, α?__. (See sketch of general ellipse orbit above.)

For whichever it is possible, give $|\mathbf{v}|$, $|\mathbf{p}|$, ℓ, KE, PE, or E in terms of a, b, H, ϑ or α. Note if any correspond to particular geometrical length or area that characterizes an orbit.

Do the starlet blast orbits share equal values for any physical quantities such as (Yes or No)

Average momentum p?__, angular momentum ℓ?__, average KE?__, average PE?__, total E?__ .

Do the starlet blast orbits share equal values for some geometric quantities such as (Yes or No) a?__, b?__ , H?__, ϕ?__, ϑ?__, α?__. (See sketch of general ellipse orbit above.)

Geometric orbit and envelope constructions

Using the graph on the attached page, do the following for initial position vector $\mathbf{r}(0)=(1,0)$:

(a) Construct the orbit for initial $\mathbf{v}(0)=(0,1)$ in part (a) of the graph.

(b) Construct the orbit for initial $\mathbf{v}(0)=(1,0)$ in part (b) of the graph.

(c) Construct the orbit for initial $\mathbf{v}(0)=(\frac{1}{\sqrt{2}},\frac{1}{\sqrt{2}})$ in part (c) of the graph.

(d) Construct the orbit for initial $\mathbf{v}(0)=(\frac{-1}{\sqrt{2}},\frac{1}{\sqrt{2}})$ in part (c) of the graph.

(e) There is a "blast wavefront" or locus of starlet pieces that expands with each instant of time. Using whatever means you like, plot points of this curve for $t/\tau_{period}= 1/12, 2/12, 3/12,$ and $4/12$.

(f) There is a constant contacting curve that envelops all orbits with $\mathbf{r}(0)=(1,0)$ and $|\mathbf{v}(0)|=1$. Construct this enveloping boundary for $|\mathbf{v}(0)|=1$. How does the envelope vary with initial speed $|\mathbf{v}(0)|$?

(g) See if you can deduce a relation between the focal point(s) and the contact point(s) for each elliptic path with the envelope. *Is the envelope also elliptic?* If so, *where are its foci?*

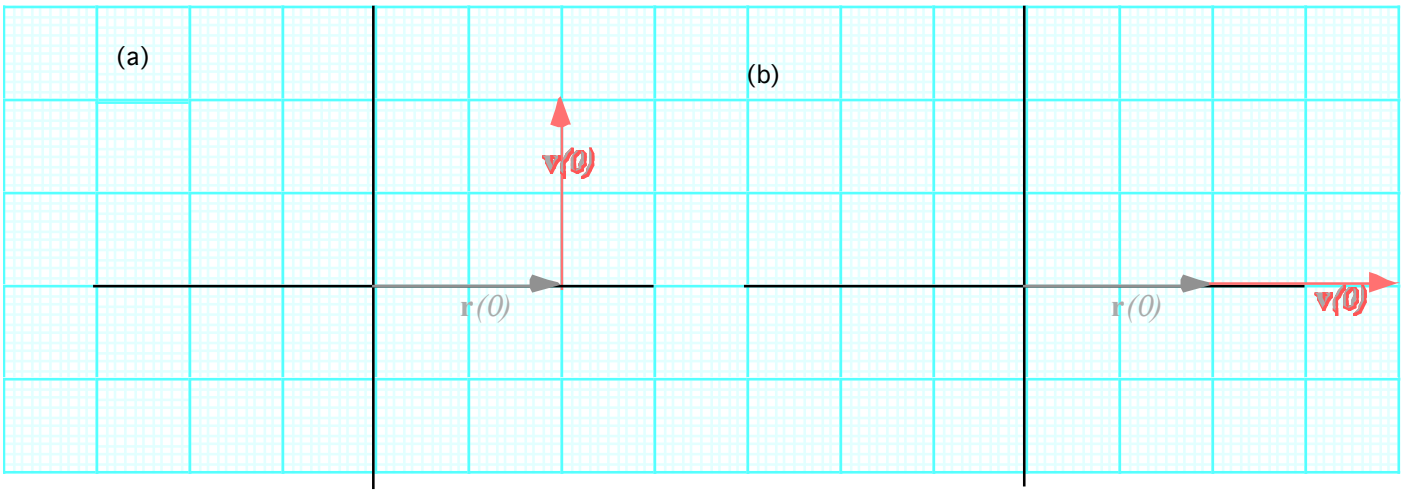
(a)
v(0)
r(0)
(b)
r(0)
v(0)

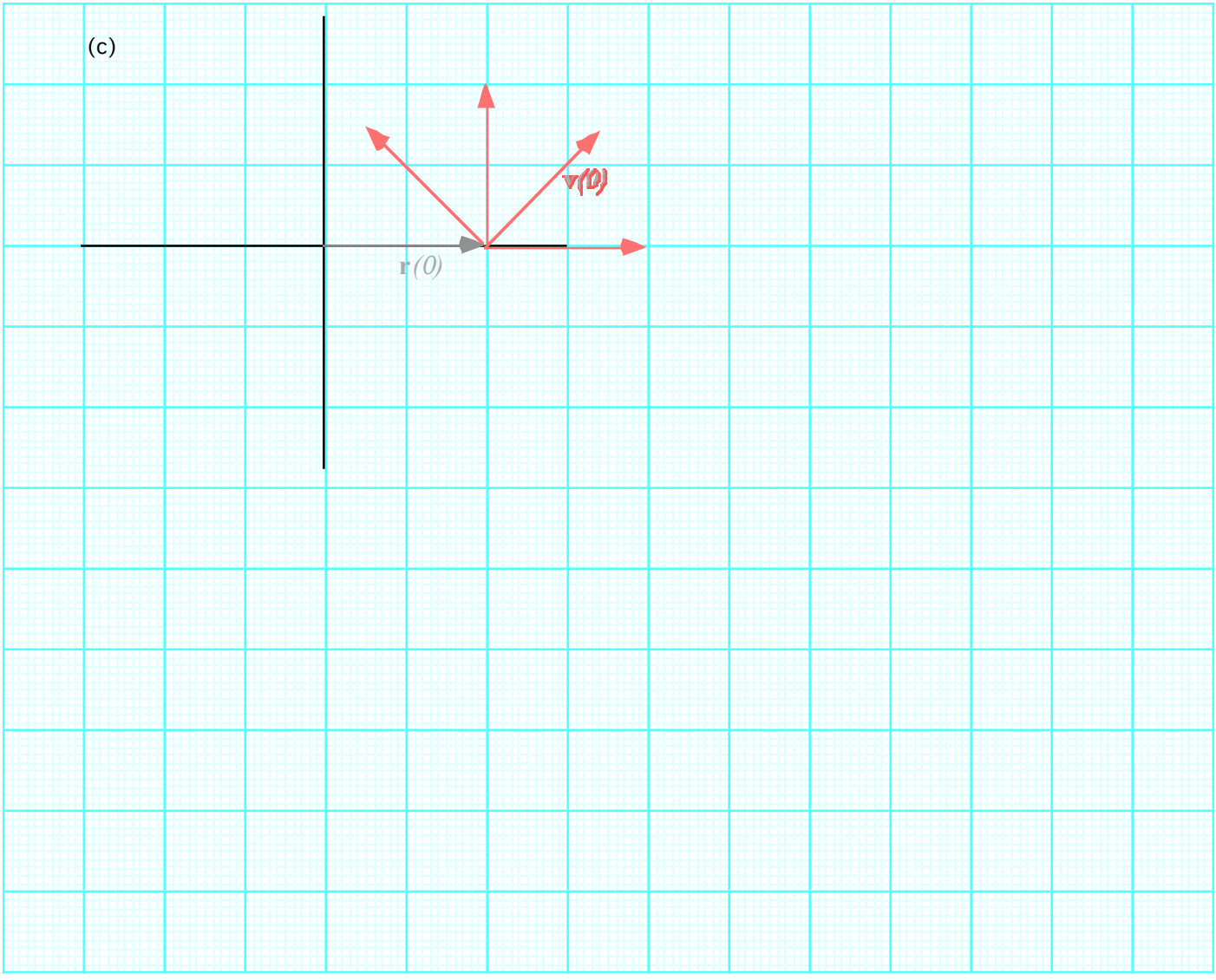
(c)
v(0)
r(0)

Appendix 1.A Vector product geometry and Levi-Civita ε_{ijk}

Vectors have *relative* projections onto each other. Components *x*, *y*, or *z* are projections of **r** onto unit **i**, **j**, and **k**. Power **F•v** $=Fv\cos\theta$ is a *dot product* cosine projection of **F** on **v**. Coriolis $a=|\boldsymbol{\omega}\times\mathbf{v}|=w v\sin\theta$ is a sine-like transverse projection called the *cross product*. Product **A•B** (or |**AxB**|) is cosine (or sine) of a relative angle (θ_B-θ_A) times length factor *AB* shown in Fig. 1.A.1. Also, recall complex products in (10.30).

The cosine or dot-projection may be given in Cartesian lab components $(A_x=A\cos\phi_A)\ A_y=A\sin\phi_A)$.

$$A\bullet B = AB\cos(\phi_B-\phi_A)=A\cos\phi_A B\cos\phi_B + A\sin\phi_A B\sin\phi_B = A_xB_x + A_yB_y \qquad (1.A.1a)$$

The sine or cross-projection has a somewhat different or "crossed-up" form.

$$A\times B = AB\sin(\phi_B-\phi_A)=A\cos\phi_A B\sin\phi_B - A\sin\phi_A B\cos\phi_B = A_xB_y - A_yB_x \qquad (1.A.1b)$$

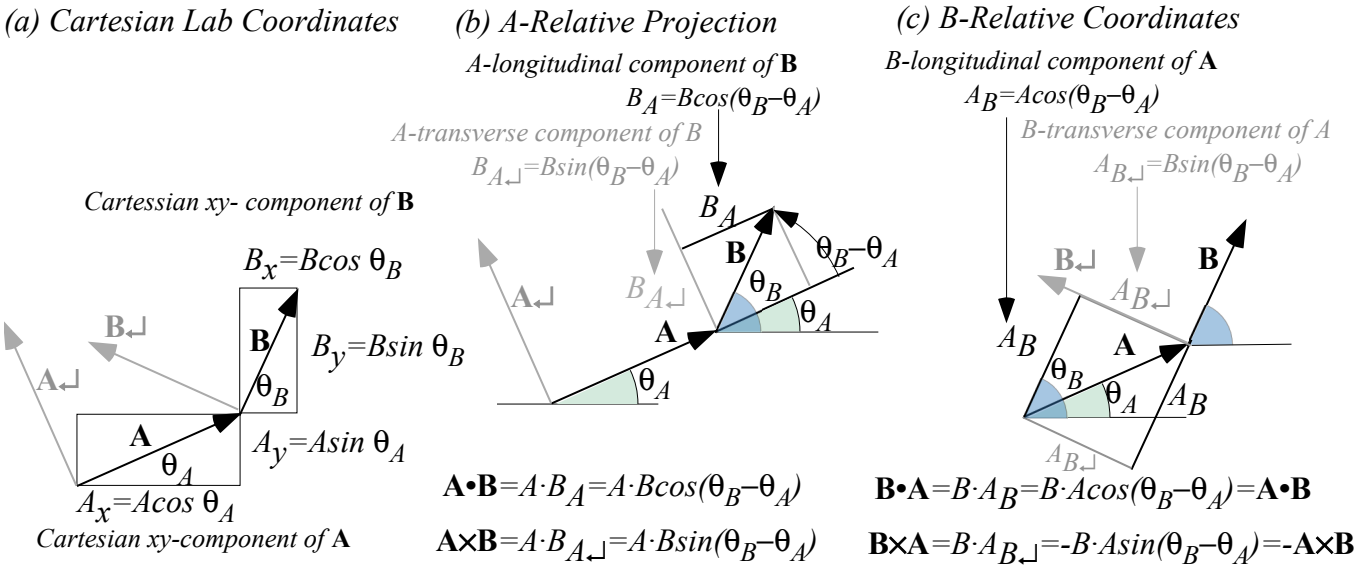

Fig. 1.A.1 Vector component geometry (a) Lab-relative. (b) A-relative. (c) B-relative.

Here **A•B** and **AxB** are numbers or *scalars*. Full **AxB** definition ((1.A.4b) below) is a vector perpendicular to both **A** and **B**. (In Fig. 1.A.1, it would stick out of the page.) Also it happens that **AxB** is the area of the vector parallelogram and $^1/_2$**AxB** is the area of the **A+B** or **A-B** triangle as shown in Fig. 1.A.2.

In Fig. 1.A.1b vector **B** refers to axes made of vector **A** and its perpendicular copy $\mathbf{A}_\perp$ and *vice-versa* in Fig. 1.A.1(c). Dot products are *reflexive* (**A•B** = **B•A**). However, cross products must be *anti-reflexive* (**AxB** =**-BxA**) since the $\mathbf{B}_\perp$ vector is in a negative direction relative to **A** in Fig. 1.A.1(c). One way to display the relation between the pair *(***A**, $\mathbf{A}_\perp$*)* and the pair *(***B**, $\mathbf{B}_\perp$*)* is in a *rotation matrix*.

$$\begin{pmatrix} A_B & A_{B\perp} \\ A_{\perp B} & A_{\perp B_\perp} \end{pmatrix} = \begin{pmatrix} \cos\theta_{BA} & -\sin\theta_{BA} \\ \sin\theta_{BA} & \cos\theta_{BA} \end{pmatrix} = \begin{pmatrix} B_A & B_{A\perp} \\ B_{\perp A} & B_{\perp A_\perp} \end{pmatrix}^{-1} = \begin{pmatrix} \cos\theta_{BA} & \sin\theta_{BA} \\ -\sin\theta_{BA} & \cos\theta_{BA} \end{pmatrix}^{-1} \qquad (1.A.2)$$

Algebraic definitions of **A•B** and **AxB** are based on the symmetric *Kronecker function* δ_{ij} and the totally *anti*-symmetric *Levi-Civita function* ε_{ijk} defined as follows.

$$\delta_i^j = \delta_{ij} = \begin{cases} 1 \text{ if: } i = j \\ 0 \text{ if: } i \neq j \end{cases} \quad (1.A.3a) \qquad \varepsilon^{ijk} = \varepsilon_{ijk} = \begin{cases} +1 \text{ if } \{ijk\} \text{ is EVEN permutation of } \{123\}, \\ -1 \text{ if } \{ijk\} \text{ is ODD permutation of } \{123\}, \\ 0 \qquad\qquad\qquad\qquad \text{otherwise.} \end{cases} \quad (1.A.3a)$$

These are fundamental to tensor analysis and exterior calculus that will be introduced in Unit 3.
They also define scalar **A•B** and vector **AxB** products in useful ways for fast computer logic, as follows.

$$\mathbf{A} \bullet \mathbf{B} = \sum_{i=1}^{3}\sum_{j=1}^{3} \delta_{ij} A_i B_j = \sum_{i=1}^{3} A_i B_i \quad (1.A.4a) \qquad \left(\mathbf{A} \times \mathbf{B}\right)_k = \sum_{i=1}^{3}\sum_{j=1}^{3} \varepsilon_{ijk} A_i B_j = \sum_{i=1}^{3}\sum_{j=1}^{3} \varepsilon_{kij} A_i B_j \quad (1.A.4b)$$

The notation $C_k = (\mathbf{C})_k$ denotes the k^{th} component of a vector **C**.

Determinants and triple products

Levi-Civita sums define the *determinant detU* of a matrix U_{ij}. An *expansion by minors* is shown here.

$$\det U = \begin{vmatrix} U_{11} & U_{12} & U_{13} \\ U_{21} & U_{22} & U_{23} \\ U_{31} & U_{32} & U_{33} \end{vmatrix} = \sum_{i,j,k} \varepsilon_{ijk} U_{1i} U_{2j} U_{3k} = U_{11} \begin{vmatrix} U_{22} & U_{23} \\ U_{32} & U_{33} \end{vmatrix} - U_{12} \begin{vmatrix} U_{21} & U_{23} \\ U_{31} & U_{33} \end{vmatrix} + U_{13} \begin{vmatrix} U_{21} & U_{22} \\ U_{31} & U_{32} \end{vmatrix} \quad (1.A.5)$$

A *triple vector product* ***AxB•C*** is such a determinant made from a matrix of three vector components.

$$\mathbf{A} \bullet \mathbf{B} \times \mathbf{C} = \begin{vmatrix} A_1 & A_2 & A_3 \\ B_1 & B_2 & B_3 \\ C_1 & C_2 & C_3 \end{vmatrix} = \sum_{i,j,k} \varepsilon_{ijk} A_i B_j C_k = A_1 \begin{vmatrix} B_2 & B_3 \\ C_2 & C_3 \end{vmatrix} - A_2 \begin{vmatrix} B_1 & B_3 \\ C_1 & C_3 \end{vmatrix} + A_3 \begin{vmatrix} B_1 & B_2 \\ C_1 & C_2 \end{vmatrix} \quad (1.A.6a)$$

$$= A_1 \left(\mathbf{B} \times \mathbf{C}\right)_1 + A_2 \left(\mathbf{B} \times \mathbf{C}\right)_2 + A_3 \left(\mathbf{B} \times \mathbf{C}\right)_3 \quad (1.A.6b)$$

Minor expansion (1.A.5) is a (•)-product of **A** with (×)-product vector **BxC**. Base area |**BxC**| times altitude (**A** projected onto normal **BxC**) equals the parallelepiped volume enclosed by **A**, **B**, and **C**.

Anti-symmetric ε-forms let us generalize geometry from 2-and 3-dimensions to *N*-dimensions. Advanced mechanics has *many* dimensions. One mole ($6 \cdot 10^{23}$ particles) has at least $6 \cdot 10^{23}$ dimensions and two or three times that if the atoms move in 2D or 3D. So ε-forms are necessary!

Products of anti-symmetric ε-forms reduce to symmetric δ-forms by a *LeviCivita identity*.

$$\sum_{k=1}^{3} \varepsilon_{ijk} \varepsilon_{mnk} = \delta_{im}\delta_{jn} - \delta_{in}\delta_{jm} = \sum_{k=1}^{3} \varepsilon_{kij} \varepsilon_{kmn} \quad (1.A.7)$$

A triple-cross-product formula $\mathbf{A} \times (\mathbf{B} \times \mathbf{C}) = (\mathbf{A} \bullet \mathbf{C})\mathbf{B} - (\mathbf{A} \bullet \mathbf{B})\mathbf{C}$ is a first application.

$$\left(\mathbf{A} \times (\mathbf{B} \times \mathbf{C})\right)_i = \sum_{j,k}^{3} \varepsilon_{ijk} A_j (\mathbf{B} \times \mathbf{C})_k = \sum_{j,k,m,n}^{3} \varepsilon_{ijk} \varepsilon_{mnk} A_j B_m C_n = \sum_{j,m,n}^{3} (\delta_{im}\delta_{jn} - \delta_{in}\delta_{jm}) A_j B_m C_n$$

$$= \sum_{n}^{3} A_n B_i C_n - \sum_{m}^{3} A_m B_m C_i = (\mathbf{A} \bullet \mathbf{C})\left(\mathbf{B}\right)_i - (\mathbf{A} \bullet \mathbf{B})\left(\mathbf{C}\right)_i$$

The LC-identity (1.A.7) reduces each sum over *k* to dot-product terms.

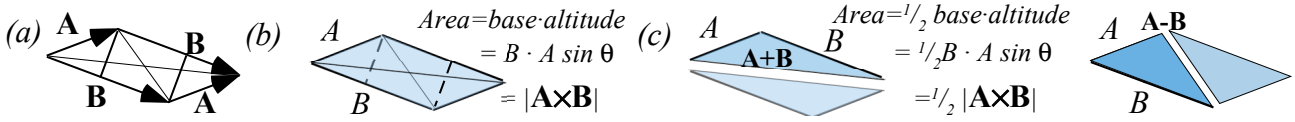

Fig. 1.A.2 Cross-product and area of (a)-(b) Parallelogram, (c) Sum triangle, (d) Difference triangle.

Operator products

The Levi-Civita ε-identity is helpful for unraveling operator products. One example is the expressions for magnetic force $\mathbf{v}\times\mathbf{B}$ where field $\mathbf{B}$ is a curl $\nabla\times\mathbf{A}$ of vector potential $\mathbf{A}$ that occurs in Unit 2 Ch. 8.

$$\mathbf{F}/e=\mathbf{v}\times\mathbf{B}=\mathbf{v}\times\left(\nabla\times\mathbf{A}\right)$$

Index notation for the double-cross product is the following. Note ε-symmetry gives: $\varepsilon_{ijk}=\varepsilon_{kij}=-\varepsilon_{ikj}$

$$\left[\mathbf{v}\times\left(\nabla\times\mathbf{A}\right)\right]_k=\left[\varepsilon_{ijk}v_i\left(\nabla\times\mathbf{A}\right)_j\right]_k=\varepsilon_{\bar{i}\bar{j}k}\varepsilon_{ab\bar{j}}v_{\bar{i}}\left(\partial_a A_b\right)$$

Here the *dummy-index-convention* sums any indices repeated on *one* side of the equation such as i, j, a, and b above. Applying the Levi-Civita ε-identity reduces the equation.

$$\begin{aligned}\left[\mathbf{v}\times\left(\nabla\times\mathbf{A}\right)\right]_k&=\varepsilon_{kij}\varepsilon_{abj}v_i\left(\partial_a A_b\right)=(\delta_{ka}\delta_{ib}-\delta_{kb}\delta_{ia})v_i\left(\partial_a A_b\right)\\&=\delta_{ka}\delta_{ib}v_i\left(\partial_a A_b\right)-\delta_{kb}\delta_{ia}v_i\left(\partial_a A_b\right)\\&=\quad v_b\left(\partial_k A_b\right)\quad -v_a\left(\partial_a A_k\right)\\&=\quad \left(\partial_k A_b\right)v_b\quad -v_a\left(\partial_a A_k\right)\\&=\partial_k\left(A_b v_b\right)-\left(\partial_k v_b\right)A_b-v_a\left(\partial_a A_k\right)\end{aligned}$$

This is converted back to Gibbs's **bold** vector notation that involves *tensors* like $\nabla\mathbf{A}$ and $\nabla\mathbf{v}$.

$$\mathbf{v}\times\left(\nabla\times\mathbf{A}\right)=\left(\nabla\mathbf{A}\right)\bullet\mathbf{v}-\mathbf{v}\bullet\nabla\mathbf{A}$$

Again, tensor index notation helps to distinguish $\left(\nabla\mathbf{A}\right)\bullet\mathbf{v}$, $\mathbf{v}\bullet\left(\nabla\mathbf{A}\right)$, and $\nabla(\mathbf{A}\bullet\mathbf{v})=(\nabla\mathbf{A})\bullet\mathbf{v}+(\nabla\mathbf{v})\bullet\mathbf{A}$.

$$\left[\left(\nabla\mathbf{A}\right)\bullet\mathbf{v}\right]_k=\frac{\partial A_j}{\partial x_k}v_j=(\partial_k A_j)v_j \qquad \left[\mathbf{v}\bullet\left(\nabla\mathbf{A}\right)\right]_k=v_j\frac{\partial A_k}{\partial x_j}=(v_j\partial_j A_k)$$

$$\left[\nabla(\mathbf{A}\bullet\mathbf{v})\right]_k=\left[(\nabla\mathbf{A})\bullet\mathbf{v}+(\nabla\mathbf{v})\bullet\mathbf{A}\right]_k$$
$$\partial_k\left(A_b v_b\right)=\left(\partial_k v_b\right)A_b-\left(\partial_k v_a\right)A_a$$

However, in Newtonian mechanics the position $\mathbf{r}$ and velocity $\dot{\mathbf{r}}=\mathbf{v}$ have *no explicit dependence* and so all $\mathbf{r}$-partial derivative of $\mathbf{v}$ (or vice-versa) are identically zero.

$$\frac{\partial v^j}{\partial x^k}\equiv\partial_k v^j\equiv 0\ \ \textit{implies :}\ \ \nabla\mathbf{v}=\frac{\partial\mathbf{v}}{\partial\mathbf{r}}=\mathbf{0}\quad(\textit{for Newtonian mechanics})$$

Then the double-cross product reduces as follows.

$$\mathbf{v}\times\left(\nabla\times\mathbf{A}\right)=\left(\nabla\mathbf{A}\right)\bullet\mathbf{v}-\mathbf{v}\bullet\nabla\mathbf{A}=\nabla(\mathbf{A}\bullet\mathbf{v})-(\nabla\mathbf{v})\bullet\mathbf{A}-\mathbf{v}\bullet\nabla\mathbf{A}\left(=\nabla(\mathbf{A}\bullet\mathbf{v})-0-\mathbf{v}\bullet\nabla\mathbf{A}\ \textit{for mechanics}\right)$$

Try using ε-identities to reduce $\nabla\times\left(\nabla\times\mathbf{A}\right)$, $\nabla\times\left(\mathbf{A}\times\mathbf{B}\right)$, $\nabla\bullet\left(\nabla\times\mathbf{A}\right)$, and $\nabla\bullet\left(\mathbf{A}\times\mathbf{B}\right)$.

Unit 1 References